NEW ANTIMICROBIAL PEPTIDES FROM BACTERIA/INVERTEBRATE OBLIGATE SYMBIOTIC ASSOCIATIONS

EDITED BY: András Fodor, Eustachio Tarasco, Selcuk Hazir, David Clarke and Adler Ray Dillman

PUBLISHED IN: Frontiers in Microbiology

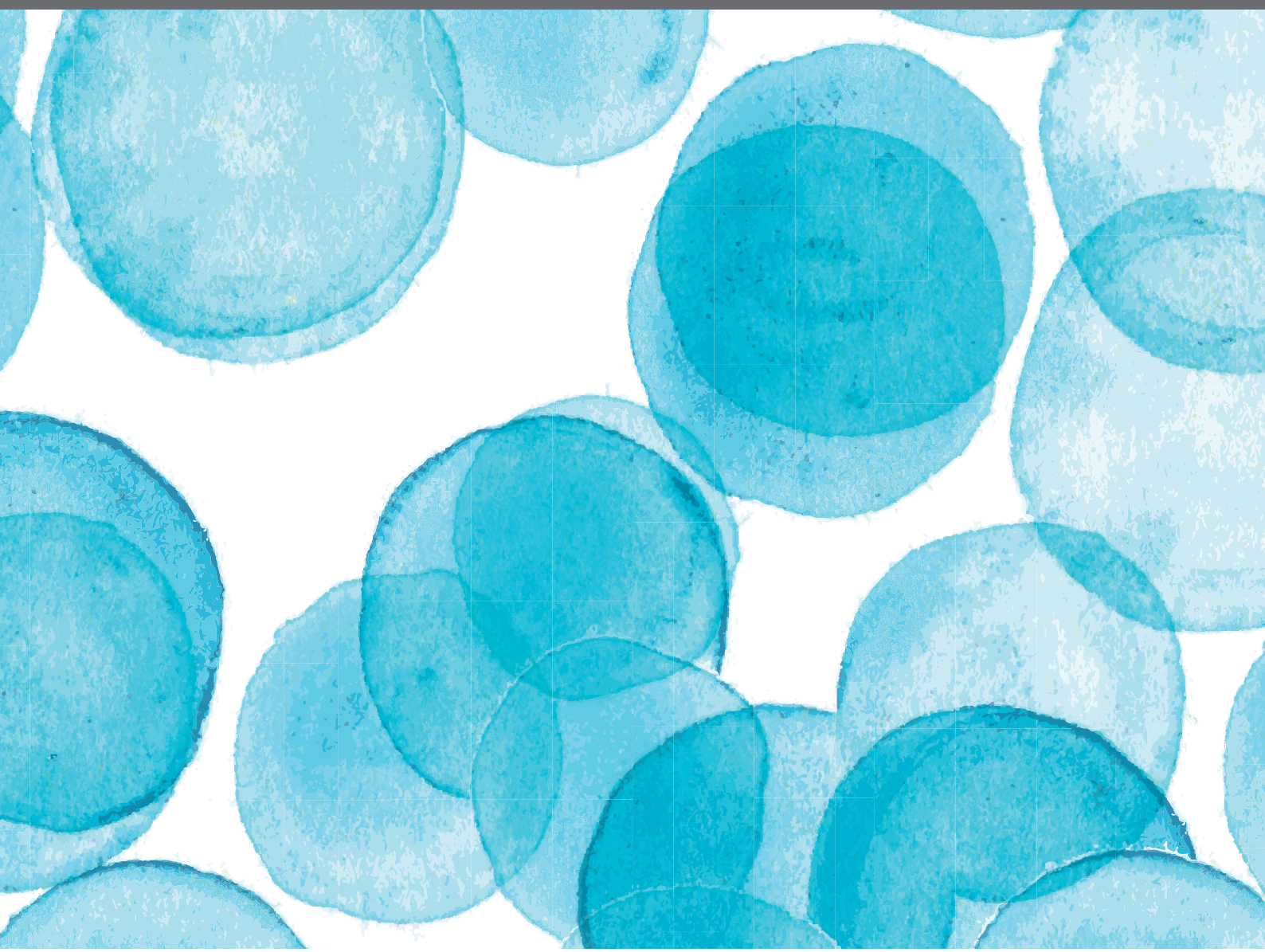

frontiers Research Topics

ISSN 1664-8714
ISBN 978-2-88974-793-1
DOI 10.3389/978-2-88974-793-1

About Frontiers

Frontiers is more than just an open-access publisher of scholarly articles: it is a pioneering approach to the world of academia, radically improving the way scholarly research is managed. The grand vision of Frontiers is a world where all people have an equal opportunity to seek, share and generate knowledge. Frontiers provides immediate and permanent online open access to all its publications, but this alone is not enough to realize our grand goals.

Frontiers Journal Series

The Frontiers Journal Series is a multi-tier and interdisciplinary set of open-access, online journals, promising a paradigm shift from the current review, selection and dissemination processes in academic publishing. All Frontiers journals are driven by researchers for researchers; therefore, they constitute a service to the scholarly community. At the same time, the Frontiers Journal Series operates on a revolutionary invention, the tiered publishing system, initially addressing specific communities of scholars, and gradually climbing up to broader public understanding, thus serving the interests of the lay society, too.

Dedication to Quality

Each Frontiers article is a landmark of the highest quality, thanks to genuinely collaborative interactions between authors and review editors, who include some of the world's best academicians. Research must be certified by peers before entering a stream of knowledge that may eventually reach the public - and shape society; therefore, Frontiers only applies the most rigorous and unbiased reviews.
Frontiers revolutionizes research publishing by freely delivering the most outstanding research, evaluated with no bias from both the academic and social point of view. By applying the most advanced information technologies, Frontiers is catapulting scholarly publishing into a new generation.

What are Frontiers Research Topics?

Frontiers Research Topics are very popular trademarks of the Frontiers Journals Series: they are collections of at least ten articles, all centered on a particular subject. With their unique mix of varied contributions from Original Research to Review Articles, Frontiers Research Topics unify the most influential researchers, the latest key findings and historical advances in a hot research area! Find out more on how to host your own Frontiers Research Topic or contribute to one as an author by contacting the Frontiers Editorial Office: frontiersin.org/about/contact

NEW ANTIMICROBIAL PEPTIDES FROM BACTERIA/INVERTEBRATE OBLIGATE SYMBIOTIC ASSOCIATIONS

Topic Editors:
András Fodor, University of Szeged, Hungary
Eustachio Tarasco, University of Bari Aldo Moro, Italy
Selcuk Hazir, Adnan Menderes University, Turkey
David Clarke, University College Cork, Ireland
Adler Ray Dillman, University of California, Riverside, United States

Citation: Fodor, A., Tarasco, E., Hazir, S., Clarke, D., Dillman, A. R., eds. (2022). New Antimicrobial Peptides From Bacteria/Invertebrate Obligate Symbiotic Associations. Lausanne: Frontiers Media SA. doi: 10.3389/978-2-88974-793-1

Table of Contents

04 ***Editorial: New Antimicrobial Peptides From Bacteria/Invertebrate Obligate Symbiotic Associations***
András Fodor, David J. Clarke, Adler R. Dillman, Eustachio Tarasco and Selcuk Hazir

07 ***Nematode-Associated Bacteria: Production of Antimicrobial Agent as a Presumptive Nominee for Curing Endodontic Infections Caused by* Enterococcus faecalis**
Hicran Donmez Ozkan, Harun Cimen, Derya Ulug, Sebastian Wenski, Senem Yigit Ozer, Murat Telli, Neriman Aydin, Helge B. Bode and Selcuk Hazir

18 ***From Worms to Drug Candidate: The Story of Odilorhabdins, a New Class of Antimicrobial Agents***
Emilie Racine and Maxime Gualtieri

28 ***Mygalin: An Acylpolyamine With Bactericidal Activity***
Abraham Espinoza-Culupú, Elizabeth Mendes, Hector Aguilar Vitorino, Pedro Ismael da Silva and Monamaris Marques Borges

42 ***Potent Chimeric Antimicrobial Derivatives of the* Medicago truncatula *NCR247 Symbiotic Peptide***
Sándor Jenei, Hilda Tiricz, János Szolomájer, Edit Tímár, Éva Klement, Mohamad Anas Al Bouni, Rui M. Lima, Diána Kata, Mária Harmati, Krisztina Buzás, Imre Földesi, Gábor K. Tóth, Gabriella Endre and Éva Kondorosi

52 ***Spätzle Homolog-Mediated Toll-Like Pathway Regulates Innate Immune Responses to Maintain the Homeostasis of Gut Microbiota in the Red Palm Weevil,* Rhynchophorus ferrugineus *Olivier (Coleoptera: Dryophthoridae)***
Abrar Muhammad, Prosper Habineza, Xinghong Wang, Rong Xiao, Tianliang Ji, Youming Hou and Zhanghong Shi

64 ***Unexplored Arsenals of Legume Peptides With Potential for Their Applications in Medicine and Agriculture***
Rui M. Lima, Salome Kylarová, Peter Mergaert and Éva Kondorosi

72 **Bacteriocins: *An Overview of Antimicrobial, Toxicity, and Biosafety Assessment by* in vivo *Models***
Diego Francisco Benítez-Chao, Angel León-Buitimea, Jordy Alexis Lerma-Escalera and José Rubén Morones-Ramírez

90 ***Antimicrobial Peptides: Novel Source and Biological Function With a Special Focus on Entomopathogenic Nematode/Bacterium Symbiotic Complex***
Surajit De Mandal, Amrita Kumari Panda, Chandran Murugan, Xiaoxia Xu, Nachimuthu Senthil Kumar and Fengliang Jin

106 ***A Novel Antimicrobial Peptide Sparamosin$_{26–54}$ From the Mud Crab* Scylla paramamosain *Showing Potent Antifungal Activity Against* Cryptococcus neoformans**
Yan-Chao Chen, Ying Yang, Chang Zhang, Hui-Yun Chen, Fangyi Chen and Ke-Jian Wang

125 ***Identification and Antifungal Mechanism of a Novel Actinobacterium* Streptomyces huiliensis *sp. nov. Against* Fusarium oxysporum *f. sp. cubense Tropical Race 4 of Banana***
Dengfeng Qi, Liangping Zou, Dengbo Zhou, Miaoyi Zhang, Yongzan Wei, Lu Zhang, Jianghui Xie and Wei Wang

frontiers in Microbiology

EDITORIAL
published: 08 March 2022
doi: 10.3389/fmicb.2022.862198

Editorial: New Antimicrobial Peptides From Bacteria/Invertebrate Obligate Symbiotic Associations

András Fodor[1,2]*, *David J. Clarke*[3], *Adler R. Dillman*[4], *Eustachio Tarasco*[5,6] and *Selcuk Hazir*[7]

[1] Department of Genetics, Eötvös University, Budapest, Hungary, [2] Department of Genetics, University of Szeged, Szeged, Hungary, [3] School of Microbiology and APC Microbiome Ireland, University College Cork, Cork, Ireland, [4] Department of Nematology, University of California, Riverside, Riverside, CA, United States, [5] Department of Soil, Plant and Food Sciences, University of Bari "Aldo Moro", Bari, Italy, [6] Institute for Sustainable Plant Protection of CNR, Bari, Italy, [7] Department of Biology, Faculty of Arts and Sciences, Adnan Menderes University, Aydin, Turkey

Keywords: multidrug resistance (MDR), antimicrobial peptide (AMP), non-ribosomal templated peptides (NRP), non-ribosomal peptide synthetases (NRPS), EPN/EPB symbiosis, Legume/Rhizobium symbiosis, QSAR

Editorial on the Research Topic

OPEN ACCESS

Edited and reviewed by:
Takema Fukatsu,
National Institute of Advanced Industrial Science and Technology (AIST), Japan

***Correspondence:**
András Fodor
fodorandras@yahoo.com

Specialty section:
This article was submitted to Microbial Symbioses, a section of the journal Frontiers in Microbiology

Received: *25 January 2022*
Accepted: *31 January 2022*
Published: *08 March 2022*

Citation:
Fodor A, Clarke DJ, Dillman AR, Tarasco E and Hazir S (2022) Editorial: New Antimicrobial Peptides From Bacteria/Invertebrate Obligate Symbiotic Associations. Front. Microbiol. 13:862198. doi: 10.3389/fmicb.2022.862198

Editorial: New Antimicrobial Peptides From Bacteria/Invertebrate Obligate Symbiotic Associations

Antimicrobial multidrug resistance (MDR) of the different types in prokaryotic and eukaryotic pathogenic organisms is an enormous challenge of clinical, veterinary, and plant pathogenic significance (Fodor et al., 2020). Antimicrobial peptides (AMPs) have demonstrated great potential against MDR pathogens. AMPs are polyamide molecules with an ester, thioester, or otherwise modified backbone (Ötvös and Wade, 2014). AMPs are pivotal to host defense and are widely conserved across the plant and animal kingdoms. Moreover, AMPS are often produced in prokaryote/eukaryote symbiotic associations where they bridge the innate and the adaptive immune system and provide optimal conditions for symbiosis. Efforts to maximize human benefits from AMPs antimicrobial activity include identification, quantitative structure/activity relation (QSAR) analysis of natural AMPs and derivatives (Loza et al., 2020), followed by designing, optimizing, synthesizing, and screening analogs (Fodor et al., 2020).

This Research Topic (RT) was designed as a platform for publications from separate trends in AMP research, focusing on ribosomal templated and non-ribosomal templated (NRP) AMP molecules, respectively. NRP-AMPs are synthesized via multi-enzyme thiol-template mechanisms mediated by two specific enzymes (non-ribosomal peptide synthetases (NRPS) and/or fatty acid synthase (FAS)-related polyketide synthases, PKS) (Fuchs et al., 2014; Wenski et al., 2020), encoded by biosynthetic gene clusters (BGC) (Wenski et al., 2019). In total, 10 of the 16 submitted manuscripts were accepted, of which five are reviews and five are original research papers that appeared in Frontiers Microbiology.

One review highlights new sources of AMPs and the design of peptidomimetic antimicrobial agents that can complement the defects of therapeutic peptides that have been used as a template (De Mandal et al.).

A potential source of novel NRP-AMPs is the entomopathogenic nematode/bacterium (EPN/EPB) symbiotic associations (Clarke, 2020; Tarasco and De Luca, 2021), where the prokaryotic partners (Xenorhabdus or Photorhabdus) provide optimized pathobiome conditions for the symbiosis (Ogier et al., 2020). Another of the reviews describes the history of the odilorhabdin (ODL, AMP NOSO-502), "from worms" to the current preclinical trials for the treatment of multidrug-resistant Gram-negative infections in hospitalized patients (Racine and Gualtieri). An original comparative study using the cell-free culture media of seven different EPB species indirectly proved that the NRP-AMP fabclavine (Fuchs et al., 2012, 2014; Gualtieri et al., 2012) is a presumptive nominee for curing the endodontic infections caused by MDR E. faecalis. In this study, fabclavine production was linked to a specific BGC by promoter exchange (Ozkan et al.).

In Legume/Rhizobium associations the plant directs its symbiont toward irreversible terminal differentiation, via actions of symbiosis-specific AMP-like ribosomal-templated peptides (but bacterial BacA is also required for terminal differentiation). Thus, a virulence factor of pathogenesis and effectors of innate immunity were adapted in symbiosis for the benefit of the plant partner (Kereszt et al., 2011). One review (Lima et al.) describes nodule specific cysteine-rich (NCR) legume peptides, which are exclusively produced in the symbiotic cells, and reported that those having 4–6 conserved cysteines and highly diverse amino acid sequences comprise a variety of anionic, neutral, and cationic peptides with antimicrobial activities against both bacteria and fungi. One original research article deals with two of the ∼700 AMPs (NCR247 and NCR335) that exert strong antimicrobial activity on various pathogenic (including ESKAPE) bacteria. Some chimeric derivatives obtained by fusion of NCR247C with other peptide fragments proved even more efficient (Jenei et al.).

Three original research articles deal with novel AMPs obtained from Arthropoda. Mygalin (a spermidine analog) is a synthetic acylpolyamine derived from the spider Acanthoscurria gomesiana, exerting anti-Gram-negative activity with underlying mechanisms involving ROS generation and chelation of iron ions (Espinoza-Culupú et al.). Sparamosin (from mud crab Scylla paramamosain) is a peptide of 54 amino acids that contains a signal peptide. The antimicrobial activity of the synthetic mature peptide (sparamosin 26–54) exerts antimicrobial activity against a wide range of prokaryotic and eukaryotic pathogens, and anti-biofilm activity with underlying mechanisms involving ROS generation without any reported cytotoxic effects on mammalian cells (Chen et al.). Spätzle (Spz) is a dimeric ligand that responds to bacterial and fungal infections in arthropods by inducing AMP secretion. The Toll-like signaling pathway not only mediates innate immunity but modulates the homeostasis of gut microbiota (Muhammad et al.)

To date, Fusarium cannot be controlled either chemically or biologically. One original research article reported that Streptomyces huiliensis sp. nov. SCA2-4T has strong antifungal activity and genomic analysis identified 51 putative biosynthetic gene clusters of secondary metabolites. Furthermore, 10 gene clusters are involved in the biosynthesis of antimicrobial metabolites, as a biological control agent (Qi et al.). Bacteriocins are narrow spectral antimicrobial peptides that are effective against closely related competitors and have a significant drug potential. One review summarizes research efforts on biosafety of aspects of this subject (DiegoBenítez-Chao et al.).

This group of articles highlights the search for the discovery of novel AMPs that have the potential for combatting MDR pathogens *in vitro* and/or *in vivo*.

AUTHOR CONTRIBUTIONS

AF suggested the idea and conception of initiating that RT and then drew the conclusions allowed to write the first version of this Editorial, which, however, has not ever been materialized in the absence of the strong help of DC, who gave the most professional, formatting, and linguistic-grammar helps. DC and AD own that large scale of overlapping knowledge which made them capable of editing and handling the most MSs coming from different areas to our RT, and they provided the important add-valued to his Editorial. The special knowledge and professional skill of ET and EH were indispensably essential for the right evaluations of EPN/EPB-related papers from the aspect of the scope.

ACKNOWLEDGMENTS

We thank the contributing authors for their submissions and the reviewers for their time. We also thank Dr. Rustam Aminov for handling this Research Topic.

REFERENCES

Clarke, D. J. (2020). Photorhabdus: a tale of contrasting interactions. *Microbiology* 166, 335–348. doi: 10.1099/mic.0.000907

Fodor, A., Abate, B. A., Deák, P., Fodor, L., Gyenge, E., Klein, M. G., et al. (2020). Multidrug Resistance (MDR) and collateral sensitivity in bacteria, with special attention to genetic and evolutionary aspects and to the perspectives of antimicrobial peptides-a review. *Pathogens* 9, 522. doi: 10.3390/pathogens9070522

Fuchs, S. W., Grundmann, F., Kurz, M., Kaiser, M., and Bode, H. B. (2014). Fabclavines: bioactive peptide-polyketide-polyamino hybrids from Xenorhabdus. *Chembiochem* 15, 512–516. doi: 10.1002/cbic.201300802

Fuchs, S. W., Sachs, C. C., Kegler, C., Nollmann, F. I., Karas, M., and Bode, H. B. (2012). Neutral loss fragmentation pattern-based screening for arginine-rich natural products in Xenorhabdus and Photorhabdus. *Anal. Chem.* 84, 6948–6955. doi: 10.1021/ac300372p

Gualtieri, M., Villain-Guillot, P., Givaudan, A., and Pages, S. (2012). *Nemaucin is an antibiotic produced by entomopathogenic Xenorhabdus cabanillasii*. Patent No: WO2012085177A1. Washington, DC: U.S. Patent and Trademark Office. Available online at: https://patentimages.storage.googleapis.com/38/d2/9c/fd8c0cec65b7fc/WO2012085177A1.pdf

Kereszt, A., Mergaert, P., Maróti, G., and Kondorosi, E. (2011). Innate immunity effectors and virulence factors in symbiosis. *Curr. Opin. Microbiol.* 14, 76–81. doi: 10.1016/j.mib.2010.12.002

Loza, E., Sarciaux, M., Ikaunieks, M., Katkevics, M., Kukosha, T., Trufilkina, N., et al. (2020). Structure-activity relationship studies on the inhibition of the bacterial translation of novel Odilorhabdins analogues. *Bioorg. Med. Chem.* 28, 115469. doi: 10.1016/j.bmc.2020.115469

Ogier, J. C., Pagès, S., Frayssinet, M., and Gaudriault, S. (2020). Entomopathogenic nematode-associated microbiota: from monoxenic paradigm to pathobiome. *Microbiome* 8, 25. doi: 10.1186/s40168-020-00800-5

Ötvös, L. Jr., and Wade, J. D. (2014). Current challenges in peptide-based drug discovery. *Front. Chem.* 2, 62. doi: 10.3389/fchem.2014.00062

Tarasco, E., and De Luca, F. (2021). Biological control and insect pathology. *Insects* 12, 291. doi: 10.3390/insects12040291

Wenski, S. L., Cimen, H., Berghaus, N., Fuchs, S. W., Hazir, S., and Bode, H. B. (2020). Fabclavine diversity in *Xenorhabdus* bacteria. *Beilstein J. Org. Chem.* 16, 956. doi: 10.3762/bjoc.16.84

Wenski, S. L., Kolbert, D., Grammbitter, G. L. C., and Bode, H. B. (2019). Fabclavine biosynthesis in *X. szentirmaii*: shortened derivatives and characterization of the thioester reductase FclG and the condensation domain-like protein FclL. *J. Ind. Microbiol. Biotechnol.* 46, 565–572. doi: 10.1007/s10295-018-02124-8

Conflict of Interest: The authors declare that the research was conducted in the absence of any commercial or financial relationships that could be construed as a potential conflict of interest.

Publisher's Note: All claims expressed in this article are solely those of the authors and do not necessarily represent those of their affiliated organizations, or those of the publisher, the editors and the reviewers. Any product that may be evaluated in this article, or claim that may be made by its manufacturer, is not guaranteed or endorsed by the publisher.

frontiers in Microbiology

ORIGINAL RESEARCH
published: 22 November 2019
doi: 10.3389/fmicb.2019.02672

Nematode-Associated Bacteria: Production of Antimicrobial Agent as a Presumptive Nominee for Curing Endodontic Infections Caused by *Enterococcus faecalis*

Hicran Donmez Ozkan[1], Harun Cimen[2], Derya Ulug[2], Sebastian Wenski[3], Senem Yigit Ozer[1], Murat Telli[4], Neriman Aydin[4], Helge B. Bode[3] and Selcuk Hazir[2]**

[1]Department of Endodontics, Faculty of Dentistry, Adnan Menderes University, Aydin, Turkey, [2]Department of Biology, Faculty of Arts and Sciences, Adnan Menderes University, Aydin, Turkey, [3]Molekulare Biotechnologie, Fachbereich Biowissenschaften, Buchmann Institute for Molecular Life Sciences (BMLS), Goethe Universität Frankfurt Biozentrum, Frankfurt am Main, Germany, [4]Department of Microbiology, Faculty of Medicine, Adnan Menderes University, Aydin, Turkey

OPEN ACCESS

Edited by:
Fabian Cieplik, University Medical Center Regensburg, Germany

Reviewed by:
Daniel Manoil, Karolinska University Hospital, Sweden
Prasanna Neelakantan, The University of Hong Kong, Hong Kong

***Correspondence:**
Hicran Donmez Ozkan
hicran.donmez@adu.edu.tr
Selcuk Hazir
selcuk.hazir@gmail.com

Specialty section:
This article was submitted to Antimicrobials, Resistance and Chemotherapy, a section of the journal Frontiers in Microbiology

Received: *28 June 2019*
Accepted: *04 November 2019*
Published: *22 November 2019*

Citation:
Donmez Ozkan H, Cimen H, Ulug D, Wenski S, Yigit Ozer S, Telli M, Aydin N, Bode HB and Hazir S (2019) Nematode-Associated Bacteria: Production of Antimicrobial Agent as a Presumptive Nominee for Curing Endodontic Infections Caused by Enterococcus faecalis. Front. Microbiol. 10:2672. doi: 10.3389/fmicb.2019.02672

Xenorhabdus and/or *Photorhabdus* bacteria produce antibacterial metabolites to protect insect cadavers against food competitors allowing them to survive in nature with their nematode host. The effects of culture supernatant produced by *Xenorhabdus* and *Photorhabdus* spp. were investigated against the multidrug-resistant dental root canal pathogen *Enterococcus faecalis.* The efficacy of seven different cell-free supernatants of *Xenorhabdus* and *Photorhabdus* species against *E. faecalis* was assessed with overlay bioassay and serial dilution techniques. Additionally, time-dependent inactivation of supernatant was evaluated. Among the seven different bacterial species, *X. cabanillasii* produced the strongest antibacterial effects. Loss of bioactivity in a phosphopantetheinyl transferase-deficient mutant of *X. cabanillasii* indicated that this activity is likely based on non-ribosomal peptide synthetases (NRPSs) or polyketide synthases (PKSs). Subsequent *in silico* analysis revealed multiple possible biosynthetic gene clusters (BGCs) in the genome of *X. cabanillasii* including a BGC homologous to that of zeamine/fabclavine biosynthesis. Fabclavines are NRPS-derived hexapeptides, which are connected by PKS-derived malonate units to an unusual polyamine, also PKS-derived. Due to the known broad-spectrum bioactivity of the fabclavines, we generated a promoter exchange mutant in front of the fabclavine-like BGC. This leads to over-expression by induction or a knock-out by non-induction which resulted in a bioactive and non-bioactive mutant. Furthermore, MS and MS^2 experiments confirmed that *X. cabanillasii* produces the same derivatives as *X. budapestensis*. The medicament potential of 10-fold concentrated supernatant of induced fcl promoter exchanged *X. cabanillasii* was also assessed in dental root canals. Calcium hydroxide paste, or chlorhexidine gel, or fabclavine-rich supernatant was applied to root canals. Fabclavine-rich supernatant exhibited the highest inactivation efficacy of ≥ 3 $\log_{10}$ steps CFU reduction, followed by calcium hydroxide paste (≤ 2 $\log_{10}$ step). The mean percentage of *E. faecalis*-free dental root canals after treatment was

63.6, 45.5, and 18.2% for fabclavine, calcium hydroxide, and chlorhexidine, respectively. Fabclavine in liquid form or preferably as a paste or gel formulation is a promising alternative intracanal medicament.

Keywords: endodontic infections, *Enterococcus faecalis*, fabclavine, *Photorhabdus*, *Xenorhabdus*

INTRODUCTION

Enterococcus faecalis is a species of the Enterococci that is associated with humans as part of the microbiota of the gastrointestinal system. However, the bacterium sometimes is an opportunistic human pathogen (Karchmer, 2000). *E. faecalis* is the most common etiological agent of human enterococcal infections (Kayaoglu and Orstavik, 2004). Moreover, this bacterium can exist as a nosocomial infection and result in mortalities surpassing 50% in some immunocompromised and cancer patients (Schmidt-Hieber et al., 2007; Arias and Murray, 2012).

In dentistry, *E. faecalis* is linked to persistent periradicular lesions with major endodontic infections and persistent infections of the root canal (Sanchez-Sanhueza et al., 2015). Eradication of *E. faecalis* is challenging because it creates a biofilm, utilizes diverse compounds as energy sources, and survives extreme environmental conditions (Gilmore et al., 2002; Tendolkar et al., 2003). These characteristics contribute to bacterial tenacity and virulence in tooth infections (Stojicic et al., 2010).

The number of bacterial cells can be reduced by shaping of the root canal with mechanical instrumentation and irrigation with antimicrobial agents. However, these techniques are inept in adequately eliminating *E. faecalis* due to the complex anatomy of the root canal system (Stuart et al., 2006; Vianna and Gomes, 2009; Asnaashari et al., 2017). Accordingly, intracanal treatment is recommended for lowering the number of bacteria before filling the root canal (Bystrom et al., 1985). Calcium hydroxide ($Ca(OH)_2$) pastes and chlorhexidine (CHX) gels are commonly used as intracanal medicaments (Siqueira and de Uzeda, 1997; Tervit et al., 2009).

Even though CHX and $Ca(OH)_2$ are regular intracanal medicaments in endodontic therapy, previous studies have revealed that *E. faecalis* can still persist (Orstavik and Haapasalo, 1990; Heling et al., 1992; Evans et al., 2002; Delgado et al., 2010). Moreover, an effective antibiotic to decolonize patients with antibiotic-resistant *E. faecalis* is unknown or unavailable. The health care concern posed by *E. faecalis* stresses the pressing urgency for new approaches for decolonization and therapeutic treatment. The discovery of novel antibiotics or antibacterial agents can serve as alternatives for *E. faecalis* suppression. The most important antibacterial sources in nature are viruses (Suttle, 1994; Fuhrman, 1999), fungi (Brian and Hemming, 1947; Zhang et al., 2012), bacteria (Kirkup, 2006; Gillor and Ghazaryan, 2007; Newman and Cragg, 2016), and plants (Cowan, 1999). Various fungi and bacteria produce antimicrobial compounds as secondary metabolites to compete with other organisms. Among bacteria, research over the past three decades has shown that the genera *Photorhabdus* and *Xenorhabdus* produce antimicrobial compounds that may have potential use against an array of bacterial pathogens (Boemare and Akhurst, 2006; Shi and Bode, 2018).

Xenorhabdus and *Photorhabdus* species are insect pathogenic bacteria that are symbiotically associated with nematodes in the families Steinernematidae and Heterorhabditidae, respectively (Hazir et al., 2003). These entomopathogenic nematodes (EPNs) with their bacteria are obligate, lethal parasites of soil insects. The symbiotic organisms have many positive attributes such as safety to humans and nontarget organisms and ease of mass production (Fodor et al., 2017).

The nematode-killed insect is protected from secondary invasion by contaminating organisms that allow the nematodes to develop in the cadaver. The protection is provided by *Photorhabdus* and *Xenorhabdus* by the production of a variety of small antibiotic molecules. For example, *Xenorhabdus* spp. synthesize a variety of secondary metabolites including antimicrobials made of linear and cyclic peptides (Bode, 2009; Shi and Bode, 2018). To date, the compounds examined from *X. bovienii, X. nematophila,* and *X. cabanillasii*, are indole, xenorhabdin, xenocoumacin, PAX peptides, and cabanillasin with antibacterial, antifungal, or both activities (Gu et al., 2009; Hazir et al., 2016). It was stated that *Photorhabdus* species also generate antimicrobial compounds including isopropylstilbenes and the β-lactam carbapenem (Webster et al., 2002). Some of these compounds especially from *P. temperata* and *P. luminescens* subsp. *luminescens* are known to have antibiotic properties. The trans-stilbenes and anthraquinone pigments were detected as antibacterial (Boemare and Akhurst, 2006). These findings of antimicrobial compounds have attracted considerable interest for pharmaceutical and agronomic purposes (Webster et al., 2002; Hazir et al., 2016). It is known that different species/strains of *Xenorhabdus* and *Photorhabdus* produce various antimicrobial compounds. Hence, we hypothesized that some species of *Xenorhabdus* and/or *Photorhabdus* spp. produce active compound(s) in their secondary metabolites that will inhibit the growth of antibiotic-resistant *E. faecalis*. Accordingly, we tested this hypothesis with seven different supernatants of *Xenorhabdus* and *Photorhabdus* species against antibiotic-resistant *E. faecalis* with *in vitro* antibacterial tests. Subsequently, the medicament potential of the antibacterial compound obtained from the most effective species was compared with CHX and $Ca(OH)_2$ against *E. faecalis* in root canals.

MATERIALS AND METHODS

Source of Bacteria and Supernatant Preparation

Antibiotic activity of seven bacterial isolates of *Xenorhabdus* and *Photorhabdus* was tested against *E. faecalis*. The nematode species and strains from which each tested bacterial species

or subspecies was isolated is presented in **Supplementary Table S1**. Henceforth, we will refer to all isolates as bacterial species even though we recognize that *P. luminescens* includes two subspecies (*luminescens* and *laumondii*).

Bacterial isolates were recovered from nematode-infected *Galleria mellonella* (Lepidoptera: Pyralidae) larva (Kaya and Stock, 1997). *Xenorhabdus* and *Photorhabdus* bacteria have phase-changing capabilities when cultured *in vitro*. Phase-I is associated with nematodes and produces toxins, enzymes, antibiotics, etc. that provide better support for nematode growth in insect cadavers, whereas phase-II occurs spontaneously under unfavorable conditions or long incubation periods (Leclerc and Boemare, 1991; Boemare, 2002). Thus, we used only phase-I of each of the bacterial isolates as observed by their distinctive colony and cell morphology on NBTA (nutrient agar 31 g/L, bromothymol blue 25 mg/L, and 2,3,5-triphenyl tetrazolium chloride 40 mg/L) plates and by a catalase test. After isolating the phase-I bacterium, each isolate was stored at −80°C until further use (Boemare and Akhurst, 2006).

To conduct the experiments, each bacterial isolate was streaked onto a NBTA plate and after 24 h, a loopful of bacterial cells was transferred to 100 ml of Tryptic Soy Broth (TSB) (Difco, Detroit, MI) in an Erlenmeyer flask. Because the optimum time for antibiotic production is 120–144 h (Furgani et al., 2008), cultures were incubated at 28°C and 150 rpm for 144 h (Hazir et al., 2016). Later on, supernatants were obtained from the centrifuged bacterial culture at 4°C and 20,000 *g* for 15 min. To eliminate all bacterial cells, the supernatants were filtered through a 0.22-µm Millipore filter (Thermo scientific, NY). Each cell-free supernatant was stored at 4°C in sterile falcon tubes (Corning, NY) and used within 2 weeks.

Pathogen Cultures

Multidrug-resistant *Enterococcus faecalis* V583 (ATCC 700802) was used for the experiments. The strain was grown overnight in Trypticase Soy broth (TSB) (Merck) (Awori et al., 2016) and the bacterial stock suspension was kept at −80°C (Boemare and Akhurst, 2006).

Antibacterial Activity of Different *Photorhabdus* and *Xenorhabdus* Spp. Against *Enterococcus faecalis*

Overlay Bioassay

Cell-to-cell competition of test bacteria with the antibiotic producer colony on a solid media (slightly modified method of Furgani et al., 2008) was used for the antibacterial test. The overlay bioassay permitted us to assess the efficacy of different species of antibiotic producing *Xenorhabdus* and *Photorhabdus* spp. against *E. faecalis* by measuring the inactivation zones. *Xenorhabdus* and *Photorhabdus* cultures were prepared by inoculating a loopful of bacteria from NBTA plate into 50 ml of TSB and incubating them at 150 rpm and 28°C in an incubator overnight. A 5-µl bacterial sample from the overnight culture was transferred onto the center of Mueller Hinton Agar (MHA) (Merck) plates. The bacteria were incubated for 5 days at 28°C (Furgani et al., 2008). For preparation of overnight *E. faecalis* culture, *E. faecalis* was inoculated in 50 ml of TSB medium and incubated at 37°C and 150 rpm. A volume of 100 µl of the pathogen culture (44×10^8 CFU/ml) was added to 3.5 ml of soft agar (0.6% w/v) at 45–50°C, which was then poured into the test plates where the *Xenorhabdus* or *Photorhabdus* colony had been growing. To prevent bacterial expansion on agar media, the propagated *Xenorhabdus* or *Photorhabdus* colony was left under UV light for 5 min before layering the mixture of *E. faecalis* and soft agar over the plate. After the solidification of soft agar, the petri dishes were incubated for 48 h at 37°C. The zone diameter around the colony of antibiotic-producing cells was measured in two directions perpendicular to each other and the average was taken (Mattigatti et al., 2012). Each bacterial species had 10 replicates and the experiment was conducted three times.

Antibacterial Activity of Cell-Free *Xenorhabdus* or *Photorhabdus* Supernatants

The cell-free supernatants of all species of *Xenorhabdus* and *Photorhabdus* listed in **Supplementary Table S1** were tested against *E. faecalis*. Different proportions (1, 5, 10, 20, 30, 40, 50, and 100%) of supernatants containing bacterial metabolites were tested for inactivation of growth of *E. faecalis*. For each proportion (1, 5, 10, 20, 30, 40, 50, and 100%), filtrated supernatants were incorporated on a *v/v* basis into test tubes with 2 ml of sterile Mueller Hinton Broth (MHB) (Merck) (Gualtieri et al., 2012). According to supernatant proportions, the same amount of MHB was discarded before adding bacterial supernatant (for example, for 5%, 0.1 ml supernatant was incorporated into 1.9 ml of MHB). A volume of 10 µl of a culture of *E. faecalis* (44×10^8 CFU/ml) incubated overnight was pipetted into the test tubes containing MHB and cell-free supernatants. There were positive and negative control groups. Positive control included MHB and *E. faecalis*, whereas the negative control was only cell-free supernatant. The tubes were incubated in the shaker incubator at 150 rpm and 37°C for 48 h. Following the incubation period, bacterial growth was evaluated visually to determine maximum inhibiting dilutions (MIDs; according to Furgani et al., 2008, we used the term "dilution" not concentration]. The MID is the maximum supernatant dilution that yields no visible growth. In each series of tubes, the last tube with clear supernatant was considered to be without any growth and was assumed to give the MID value. Turbidity in the tubes indicated growth of *E. faecalis*. Visual evaluations were made independently by three examiners and a consensus opinion was agreed upon (Furgani et al., 2008; Aarati et al., 2011). An aliquot of 100 µl was taken from each tube where no bacterial growth had been observed visually and was transferred to the blood-agar medium (5% sheep blood) to determine maximum bactericidal dilution (MBD). After streaking the subsamples on the blood-agar medium, the petri dishes were incubated at 37°C for 48 h to verify total inactivation. The smaller the MID or MBD values, the stronger the antibiotic production obtained (Furgani et al., 2008). National Committee

for Clinical Laboratory Standart Institute (CLSI) recommended procedures were used for MID and MBD determination.

Three replicates were used for each supernatant proportion and the experiment was conducted three times.

Time-Dependent Inactivation of Cell-Free Supernatant

Depending on the results of the experiment on overlay bioassay and the MID and MBD values, bacterial supernatant that produced the maximum antibacterial activity (*X. cabanillasii* supernatant) was used to determine the time to inactivation of *E. faecalis*. This was done by using 25 ml of sterile TSB mixed with 25 ml of cell-free supernatant of *X. cabanillasii* in a 100-ml flask. A 0.5-ml aliquot of *E. faecalis* from an overnight culture (44×10^8 CFU/ml) was transferred to the 50% supernatant, and afterward the flask was incubated at 37°C at 150 rpm. On a 2-h basis from 0 to 16 h, a 10-µl subsample was pipetted from the flask and spread on a blood agar. Plates were incubated for 48 h at 37°C. Three replicates were used and the experiment was conducted three times.

Identification of Bioactive Antibacterial Compound

To determine the bioactive compound, promoter exchanged mutants of *X. cabanillasii* were generated and matrix assisted laser desorption/ionization-mass spectrometry (MALDI-MS) and MALDI-MS^2 experiments were performed.

Generation of Deletion and Promoter Exchange Mutants in *Xenorhabdus cabanillasii*

Due to the phosphopantetheinyl transferase (PPTase)-dependence of NRPS- and PKS-derived secondary metabolites, we deleted the responsible gene in *X. cabanillasii*. This should lead to a loss of production and bioactivity in the mutant if the compound is NRPS- or PKS-derived.

Deletion of the phosphopantetheinyl transferase (Xcab_04003) in *X. cabanillasii* was performed by double homologous recombination. About 1,000 bps were amplified by PCR with the primers SW305_Xcab_LF_fw (5′-CGATCCTCTAGAGTCGACCTGCAGTGTATAGGTCATAGCGCATTTTCC-3′) and SW306_Xcab_LF_rv (5′-TTTCATCTCTTATTTTGTTGTTCTTGGGTATTGTTCG-3′) for the upstream and SW307_Xcab_RF_fw (5′-TACCCAAGAACAACAAAATAAGAGATGAAAACCCCGG-3′) and SW308_Xcab_RF_rv (5′-GAGAGCTCAGATCTACGCGTTTCATATGGGTTTTAGCCCAATCTTATGCC-3′) for the downstream regions. Both were integrated by Hot Fusion assembly into the *Pst*I/*Nde*I digested deletion vector pDS132 and transformed into *E. coli* ST18 (Fu et al., 2014). The plasmid pDS132 containing the *sacB* gene and a kanamycin resistance cassette. *X. cabanillasii* was conjugated with *E. coli* ST18 and insertion mutants were selected on kanamycin-supplemented LB agar plates. The second homologous recombination was then enforced by cultivation on sucrose-supplemented LB agar plates, which is toxic due to the SacB conversion.

Promoter exchange in front of the fcl-homologous gene cluster was performed upstream of the *fclC*-like gene (Xcab_02060) in *X. cabanillasii*. The first 1,000 bps of Xcab_02060 were amplified by the primers SW128_Xcab_fw (5′-TTTGGGCTAACAGGAGGCTAGCATATGACCAAGACGTATTTTTTGCATG-3′) and SW129_Xcab_rv (5′-TCTGCAGAGCTCGAGCATGCACATTTTACCTGCCCTTCCAGACG-3′) and cloned into the PCR-amplified vector pCEP_kan by Hot Fusion assembly (Fu et al., 2014; Bode et al., 2015). After transformation, positive *E. coli* S17 clones were confirmed by restriction, conjugated with *X. cabanillasii,* and insertion mutants selected on kanamycin-supplemented LB agar plates (**Supplementary Table S2**). Successfully generated deletion and promoter exchange mutants were verified by colony PCR and analyzed by MALDI-MS.

Identification of Antibacterial Compound by MALDI-MS and MALDI-MS^2

Cultures for MALDI-MS measurements were prepared with 10 ml of lysogeny broth media supplemented with kanamycin (50 µg/ml) if appropriate, inoculated with 400 µl of a preculture, and incubated at 30°C for 72 h with shaking. Induced promoter exchange mutants were additionally supplemented with 0.2% L-arabinose (Bode et al., 2015). Liquid cultures were spotted on a steel target with a volume of 0.3 µl mixed with 0.25 µl of 1:10 diluted ProteoMass Normal Mass Calibration Mix (Sequazyme™ Peptide Mass Standards Kit) for internal calibration and 0.9 µl of alpha-Cyano-4-hydroxycinnamic acid (CHCA) matrix (3 mg/ml in 75% acetonitrile, 0.1% trifluoroacetic acid). After air-drying, the sample spot was washed with 5% formic acid and mixed again with 0.6 µl of CHCA. Cell MALDI measurements were performed with a MALDI LTQ Orbitrap XL (Thermo Fisher Scientific, Inc., Waltham, MA) instrument with a nitrogen laser at 337 nm in FTMS scan mode with 100 shots per measurement in a mass range of 350–1,500 m/z with high resolution. MALDI-MS^2 experiments were performed in CID-mode using ITMS scan mode with the following parameters: Normalized collision energy, 28; Act. Q, 0.250; and Act. Time (ms), 30.0. Data were analyzed using Qual Browser version 2.0.7 (Thermo Fisher Scientific, Inc., Waltham, MA).

Testing the Antibacterial Activity of *Xenorhabdus cabanillasii* Mutant Strains

Antibacterial activity of 5-day-old cell-free supernatants of wild-type, pptase deletion mutant, induced (with arabinose) and non-induced (without arabinose) *fclC* promoter exchange mutant of *X. cabanillasii* was tested with agar-well diffusion bioassay as described before. Each petri dish included four wells and each well was filled with 70 µl of one of the cell-free *X. cabanillasii* supernatants. After the incubation period for 48 h at 37°C, the inactivation zones (mm) on plates were measured (Mattigatti et al., 2012). Five replicates were used and the experiment was conducted three times.

Medicament Potential of the Antibacterial Compound in Dental Root Canals

One-day-old cell-free supernatant of induced *fcl*C mutant strain of *X. cabanillasii* was concentrated 10-fold using an evaporator and tested in dental root canals. Recently extracted human mandibular premolars were collected from patients who signed a patients' consent protocol (2016/1052) approved by Adnan Menderes University, Local Ethical Committee. Soft tissue remnants and calculus were removed from the external root surfaces by using a periodontal scaler. Periapical radiographs were taken from both buccolingual and mesiodistal directions to determine the teeth that have a straight single root canal. Next, a dental operating microscope (Leica M320) was used to select the teeth with no resorption, defect, or cracks. According to these criteria, 44 mandibular premolar teeth with curvature less than 5° and 15–18 mm long were selected (Schneider, 1971; Pladisai et al., 2016). The roots were sectioned using a diamond disk, perpendicular to the long axis into samples 13 mm long from the cementoenamel junction to the apical root end (Pladisai et al., 2016). A single endodontist removed the pulp tissue and checked the canal patency with a #10 stainless steel K-File (Mani Inc. Tochigi, Japan) until it was visible at the apical foramen. Working length was set at 1 mm short of this length. Then root canals were instrumented with Protaper Next rotary system (Dentsply, Ballaigues, Switzerland) up to X3 (0.30 mm tip with 7% taper) by the same endodontist in a crown-down manner, at a rotational speed of 300 rpm and 200 g/cm torque. Root canals were washed with 2 ml of 5% NaOCl using a 27-gauge notched-tip irrigation needle (Ultradent, UT, USA) between each instrument. At the end of the instrumentation, a final flush was applied using a sequence of 5 ml of 17% EDTA and 5 ml of 5% NaOCl to remove the smear layer, followed by 5 ml of 10% sodium thiosulfate and 5 ml of sterile distilled water (Sasanakul et al., 2019). Finally, specimens were dried with paper points. All teeth were sterilized in an autoclave (121°C for 15 min) before using in the experiments (Alves et al., 2013; Zan et al., 2013).

A 10-µl aliquot of *E. faecalis* from an overnight culture adjusted to 5×10^5 CFU/ml (Ardizzoni et al., 2009) was placed in the root canals of 44 teeth using a sterile micropipette. The teeth were placed individually in 2-ml capacity sterile centrifuge tubes containing 1 ml of BHI broth and incubated for 21 days at 37°C. This is to allow bacteria to penetrate the dentinal tubules and biofilm formation (Pladisai et al., 2016). The media were replaced with sterile BHI every other day (Sasanakul et al., 2019).

After the incubation period, the teeth were embedded in the silicone impression material to create a closed-end channel (Tay et al., 2010). Then, to imitate the final irrigation process before medicament applications in clinical conditions, the specimens were irrigated with 3 ml of 17% EDTA, 3 ml of 5% NaOCl, 3 ml of 10% sodium thiosulfate, and 3 ml of sterile distilled water, respectively. The root canals were subsequently dried with paper points and they were randomly divided into four groups (n = 11 specimens per group).

The root canals of the first and second groups were filled with $Ca(OH)_2$ paste (Ultracal XS, Ultradent Products Inc., USA) and 2% CHX gluconate gel (Gluco-Chex, Cerkamed, Poland) by using a Lentulo spiral (Dentsply-Maillefer), respectively. The root canals in the third group were filled with 10-fold concentrated supernatant of *fclC*-induced *X. cabanillasii* with the help of a sterile syringe. The remaining 11 teeth were filled with sterile BHI medium and this served as the control group. Coronal access of the teeth was closed with parafilm. After the treatments, silicon impression material around the specimens was removed and it was placed in 2-ml sterile centrifuge tubes containing BHI medium individually. The tubes were incubated aerobically at 37°C for 7 days. The media were replaced with sterile BHI every other day.

At the end of experimental period, a ProTaper X3 rotary instrument was used for 20 s to remove CHX gel and Ca(OH)2 paste. For the neutralization of Ca(OH)2, 3 ml of 5% citric acid, and for CHX gel, the mixture of 0.3% L-α-Lecithin and 3% Tween 80 were used. Then both medicament groups were irrigated with 3 ml of physiological saline (Pektas et al., 2013). The specimens in supernatant applied and control group were treated with 6 ml of sterile physiological saline.

The remaining bacteria in the root canals and inner dentins were collected by shaving the root canal walls with a No. 4 Peeso reamer (Dentsply-Maillefer). The collected dentin chips were transferred to 0.5 ml of BHI medium in Eppendorf tube and vortexed vigorously. Then, 50-µl sample was streaked on blood-agar plates. The plates were incubated at 37°C for 48 h and the colonies on blood agar were counted and inferred as colony forming units (CFUs).

Statistical Analysis

SPSS 25.0 (IBM Corp., Chicago, IL, USA) package program with a level of significance set at 0.05 was used. Differences in antibacterial effects of the supernatants were compared with one-way ANOVA and the means separated using Tukey's test. The data of time-dependent CFU reduction and medicament potential of the antibacterial compound in dental root canals were shown as medians, including 25 and 75% quartiles. In these results, horizontal dotted, solid, and dashed lines represent reductions of 2, 3, and 5 $\log_{10}$ steps CFU, respectively. Medians on or below these lines exhibit bacterial killing efficacy of 99% (2 $\log_{10}$), 99.9% (3 $\log_{10}$), and 99.999 (5 $\log_{10}$) (Boyce and Pittet, 2002).

RESULTS

Antibacterial Activity of Different *Xenorhabdus* and *Photorhabdus* Spp. Against *Enterococcus faecalis*

Overlay Bioassay

The antibiotic production of *Xenorhabdus* and *Photorhabdus* against *E. faecalis* differed significantly among species (F = 527.73; df = 6, 202; $p < 0.001$) (**Figure 1**). *Xenorhabdus cabanillasii* had the most pronounced inactivation (50.4 mm) and *X. bovienii* and *P. luminescens laumondii* the lowest (**Figure 1**).

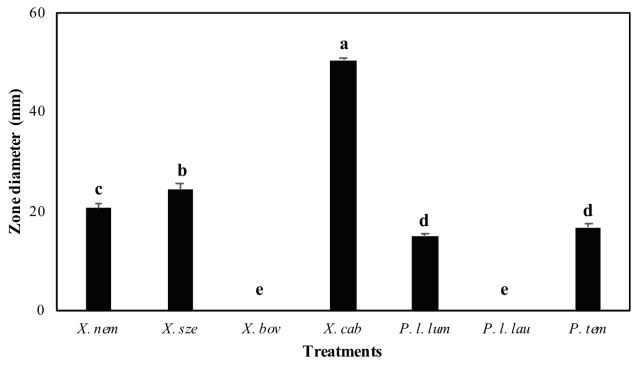

FIGURE 1 | Inactivation zones (mm) resulting from overlay experiments using species of *Xenorhabdus* and *Photorhabdus* against *Enterococcus faecalis*. X. nem, *Xenorhabdus nematophilus*; X. sze, *X. szentirmaii*; X. bov, *X. bovienii*; X. cab, *X. cabanillasii*; P. l. lum, *Photorhabdus luminescens luminescens*; P. l. lau, *P. luminescens laumondii*; P. tem, *P. temperata*. Means indicated by the different lower-case letters on the bars are significantly different ($p < 0.05$).

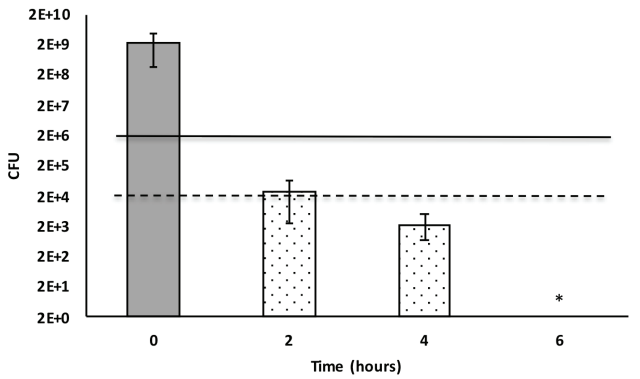

FIGURE 2 | Time-dependent inactivation of *Enterococcus faecalis* cells incubated in 50% *Xenorhabdus cabanillasii* supernatant. Data in this figure are shown as CFU medians with 25 and 75% quartiles. Solid and dashed lines represent reductions of ≥3 and ≥ 5 $\log_{10}$ steps CFU, respectively. * indicates reduction below detection limit.

Antibacterial Activity of Cell-Free *Xenorhabdus* or *Photorhabdus* Supernatants

All *Photorhabdus* and *X. bovienii* supernatants caused inactivation (based on lack of visible growth; MID) when undiluted supernatants were used (**Supplementary Table S3**). *Xenorhabdus nematophila* and *X. szentirmaii* caused inactivation at 20 and 40% proportions of supernatant including cultures, respectively. The greatest inactivation was achieved by *X. cabanillasii,* which showed inactivation even at a 1% concentration of supernatant. After the transfer of samples where no visually bacterial growth was observed on the blood-agar media, *E. faecalis* colonies were observed even at undiluted supernatants (100%) of *X. nematophila*, *X. bovienii,* and all *Photorhabdus* species (**Supplementary Table S3**). *Xenorhabdus szentirmaii* exhibited complete inactivation (MBD) only at 100% supernatant concentration. Similar to the visual inactivation results, we observed that the 5% supernatant of *X. cabanillasii* eliminated all cells of *E. faecalis* (**Supplementary Table S3**). *Enterococcus faecalis* proliferated in all positive controls, whereas no bacterial growth was observed in the negative control groups.

Time-Dependent Inactivation of Cell-Free Supernatant

Bacterial culture media that included 50% *X. cabanillasii* supernatant showed inactivation starting from the time of the first subsample (2 h after inoculation) and the number of colonies of *E. faecalis* gradually decreased over time. The supernatant killed 99.999% of the bacteria after 2 h. Complete inactivation of *E. faecalis* occurred 6 h after the inoculation (**Figure 2**).

Testing the Antibacterial Activity of *Xenorhabdus cabanillasii* Mutant Strains

Wild-type and induced *fclC* promoter exchange mutant of *X. cabanillasii* supernatants exhibited average of 18 (±1.4) and 17.5 (±0.8) mm zone diameters, respectively. But, there was no inactivation circle around the wells of Δ*pptase* and non-induced *fclC* mutants (**Figure 3**).

Identification of Bioactive Antibacterial Compound Produced by *Xenorhabdus cabanillasii*

Since the Δ*pptase* mutant showed no more bioactivity (**Figure 3**), it can be postulated that the responsible compound is generated by a non-ribosomal peptide synthetase (NRPS) or a polyketide synthase (PKS). *In silico* analysis of the *X. cabanillasii* genome revealed multiple potential NRPS- and PKS-BGCs. Due to the known broad-spectrum bioactivity of zeamine/fabclavine, we focused on the fcl-homologous BGC (Fuchs et al., 2014; Masschelein et al., 2015a,b). We performed a promoter exchange in front of the first essential biosynthesis gene *fclC* and observed that the bioactive antibacterial compound is produced by this BGC (**Figure 3**) (Wenski et al., 2019). High-resolution MALDI-MS comparison revealed that the active compounds are the fabclavines Ia, Ib, IIa, and IIb, which were previously described for *X. budapestensis* DSM 16342 (**Figure 4**) as confirmed by the fragmentation pattern of signal 1302.92 (IIb) (**Supplementary Table S4** and **Supplementary Figure S1**).

Medicament Potential of the Antibacterial Compound in Dental Root Canals

Fabclavine-rich supernatant exhibited the highest inactivation efficacy of ≥3 $\log_{10}$ steps CFU reduction, followed by calcium hydroxide paste (≤2 $\log_{10}$ step) (**Figure 5**).

If we considered no tolerance to any bacterial growth in root canals (even one cell), the fabclavine-rich supernatant completely eradicated *E. faecalis* in 63.6% of the treated teeth. The mean percentage of *E. faecalis*-free dental root canals after treatment was 45.5% for $Ca(OH)_2$ and 18.2% for CHX. The median number of colonies were 0, 10, and 20 for fabclavine-rich supernatant, $Ca(OH)_2$, and CHX, respectively. However, number of colonies in the control group was 1,120 CFU (**Figure 5**).

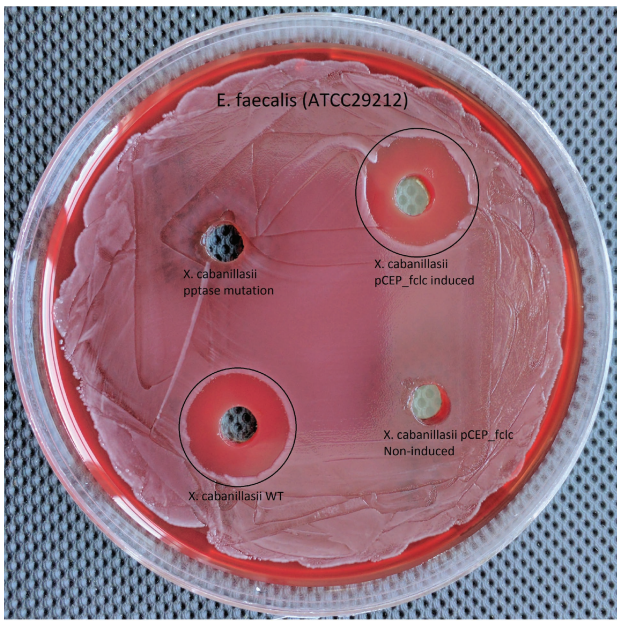

FIGURE 3 | Comparison of wild-type, Δ*pptase*, pCEP-*fclC* induced, and pCEP-*fclC* non-induced mutant of *X. cabanillasii* against *Enterococcus faecalis*.

DISCUSSION

Our data showed that there were significant variations among the seven bacterial species in the production of effective antibacterial compounds against multidrug-resistant *E. faecalis*. Overall, the supernatant of *X. cabanillasii* exhibited the greatest inhibitory and bactericidal effect followed by supernatants of *X. nematophila* and *X. szentirmaii*. On the other hand, supernatants of *X. bovienii* and *P. luminescens laumondii* did not display any antibacterial efficacy against *E. faecalis*. Prior studies have reported variations among *Xenorhabdus* or *Photorhabdus* species (or strains) in the production of antimicrobial metabolites, and the efficacy of metabolites differed depending on the target organisms (Furgani et al., 2008; Fodor et al., 2010; Hazir et al., 2016). Furgani et al. (2008) reported that *X. cabanillasii* and *X. szentirmaii* produced larger diameter inhibitory zones than *X. nematophila* and *X. bovienii* against the primary mastitis pathogens *Staphylococcus aureus*, *Klebsiella pneumoniae*, and *Escherichia coli* when a cell-to-cell competition bioassay was conducted. In another study, *X. szentirmaii* produced a larger inhibitory zone (73.7 mm) than *X. cabanillasii* (60.7 mm) against Gram positive *S. aureus* (Fodor et al., 2010). However, in our overlay bioassay, cell-free supernatant of *X. cabanillasii* resulted in an inactivation zone of 50.4 mm, whereas

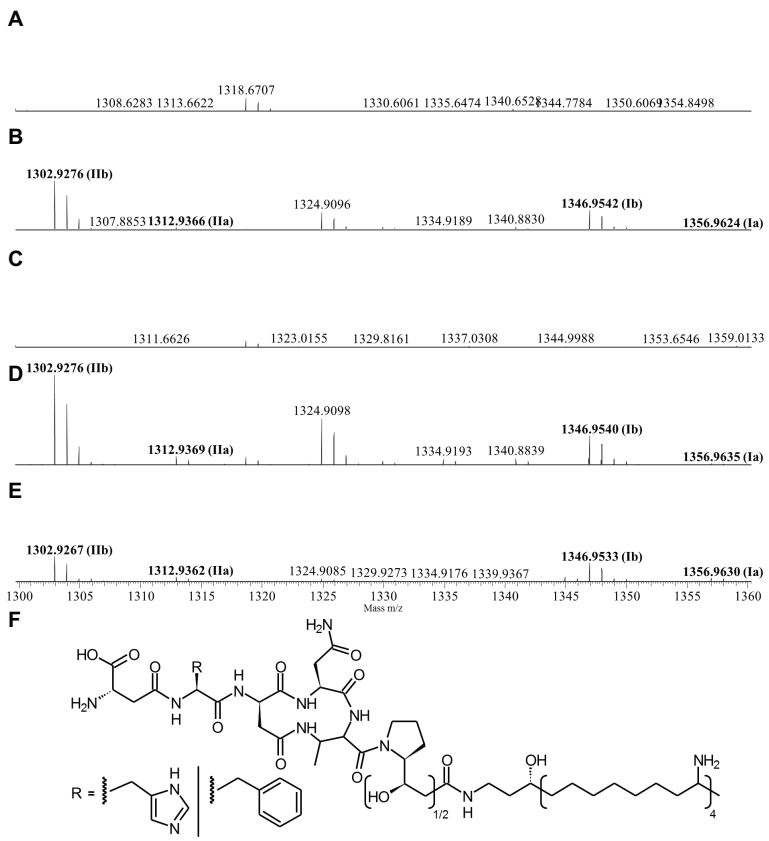

FIGURE 4 | High-resolution MALDI-MS data of liquid cultures of *X. cabanillasii* Δ*ppt* **(A)**, *X. cabanillasii* JM26 WT **(B)**, *X. cabanillasii* P_{Bad}-*fclC* (non-induced) **(C)**, *X. cabanillasii* P_{Bad}-*fclC* (induced) **(D)**, *X. budapestensis* DSM 16342 **(E)**, and the corresponding fabclavine derivatives **(F)**. Highlighted in bold are signals that correspond with identified fabclavines in *X. budapestensis* (Fuchs et al., 2014). Cultures were grown for 72 at 30°C. MALDI-MS measurement was internally calibrated.

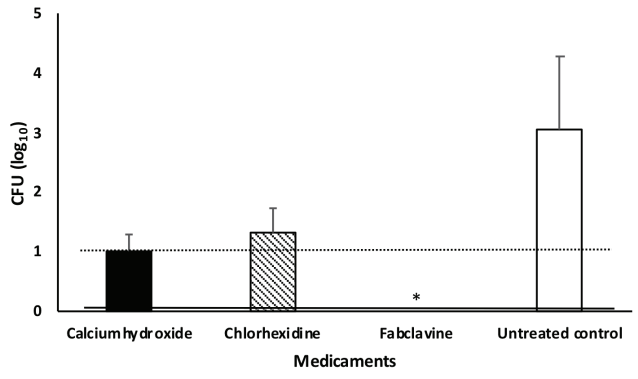

FIGURE 5 | Median number of *Enterococcus faecalis* colony after treating dental root canals with different medicaments. Data were shown as CFU medians. Dotted and solid lines represent reductions of ≥2 and ≥ 3 log_{10} steps CFU, respectively. * indicates reduction below detection limit.

X. szentirmaii exhibited an inactivation zone of 24.4 mm with *E. faecalis*. This discrepancy probably can be attributed to differences in the target organisms, or possibly strain differences in *X. szentirmaii* and *X. cabanillasii* used in the two different studies.

Previous studies demonstrated that *Xenorhabdus* and *Photorhabdus* secrete antimicrobial compounds (Furgani et al., 2008; Fodor et al., 2010; Hazir et al., 2016). Furgani et al. (2008) and Gualtieri et al. (2012) observed antibiotic activity when used not only as the purified antimicrobial compound, but also the cell-free supernatants of *Xenorhabdus* spp. Similarly, we observed antibacterial activity and determined MID and MBD values of *Xenorhabdus* and *Photorhabdus* in cell-free supernatants. The best MID and MBD values against *E. faecalis* were obtained from *X. cabanillasii* supernatant. Concentrations of 1 and 5% of *X. cabanillasii* supernatant were sufficient to inhibit bacterial growth (MID) and completely eliminate *E. faecalis* (MBD), respectively. Gualtieri et al. (2012) determined MBC values as the lowest concentration of antibiotic that resulted in 0.1% survival in the subculture. But we aimed for the complete inactivation of *E. faecalis* to prevent its re-colonization in the dental root canal. Therefore, our MBD values were designated according to full eradication. Our data clearly demonstrated that *X. cabanillasii* produce bactericidal molecule(s) rather than one with bacteriostatic effects, whereas other *Xenorhabdus* and *Photorhabdus* spp. tested in our study showed only a bacteriostatic effect.

To restrict the quantity of potential biosynthesis gene clusters responsible for the bactericidal compound, we compared the WT and Δ*pptase* mutant of *X. cabanillasii*. The loss of bioactivity of the Δ*pptase* mutant suggested the antibacterial compound against *E. faecalis* to be a natural product dependent on a PPTase as it is the case for typical NRPS- or PKS-derived natural products. Different biosynthetic gene clusters are known for *X. cabanillasii*, which could produce potential bioactive compounds like PAX-peptides, rhabdopeptides, or fabclavines (Tobias et al., 2017). The bioactivity of the mutant strain with a promoter exchange in front of the fabclavine-homologous gene cluster indeed confirmed that the bioactive compounds are fabclavines (Fuchs et al., 2014; Fodor et al., 2017). Biochemically, they are derived from a NRPS that produces a hexapeptide, which is elongated with one or two malonate units by a PKS and connected with an unusual polyamine (Fuchs et al., 2014; Wenski et al., 2019). Furthermore, our MALDI-MS and MS^2 experiments confirmed that the fabclavines produced by *X. cabanillasii* are identical to the already described derivatives of *X. budapestensis* (Fuchs et al., 2014). It was reported that fabclavines Ia and Ib had a broad-spectrum bioactivity against different organisms such as *Micrococcus luteus, Escherichia coli, Bacillus subtilis*, *Saccharomyces cerevisiae, Trypanosoma cruzi, T. brucei,* and *Plasmodium falciparum* (Fuchs et al., 2014). Tobias et al. (2017) stated that except for *Photorhabdus asymbiotica* that might produce a shortened fabclavine derivative, other *Photorhabdus* species do not produce fabclavines, which were more widespread in *Xenorhabdus* strains. These data can explain why none of our tested *Photorhabdus* showed antibacterial efficacy against *E. faecalis*.

The success of endodontic treatment depends mainly on the complete inactivation of the infecting microorganisms from the root canal and prevention of reinfection. However, it is known that conventional root canal irrigants have limited action inside dentinal tubules beyond which viable bacteria are present (Gu et al., 2009). Our control data also showed that the irrigation of root canal with conventional irrigants (EDTA and NaOCl) was not enough to eradicate *E. faecalis* from dentinal tubules. Therefore, the use of intracanal medicaments between appointments is suggested for complete inactivation of bacteria before filling root canals (Bystrom et al., 1985; Pektas et al., 2013). Over the years, a number of synthetic antimicrobial agents have been employed as endodontic irrigants and medicaments against *E. faecalis*. Because of toxic and harmful side effects of common antibacterial agents and the increased antibiotic resistance to antimicrobial agents, a search for alternative agents that are non-toxic, affordable, and effective is needed.

Calcium hydroxide and CHX gel are known as the most effective intracanal medicaments and commonly used in dental practices (Haapasalo and Orstavik, 1987; Evans et al., 2003; Lakhani et al., 2017). However, they are not sufficient for the complete inactivation of *E. faecalis* from root canals in all cases (Siqueira, 2001; Evans et al., 2003; Mozayeni et al., 2014). The results of our study showed that 9 and 5 of 11 teeth treated with CHX and $Ca(OH)_2$ were still contaminated with *E. faecalis*, respectively. Fabclavine-rich supernatant of *X. cabanillasii* exhibited more antimicrobial efficacy than CHX and $Ca(OH)_2$ in root canals with complete inactivation from 7 of 11 teeth. Furthermore, $Ca(OH)_2$ and CHX are formulated as paste and gluconate gel, respectively, to provide longer and better contact with microorganisms in root canals, whereas bacterial supernatant was in liquid form. This could be a possible reason why we did not obtain complete eradication in the root canals of all teeth (even though *X. cabanillasii* supernatant exhibited very strong bactericidal activity). We observed that some of the supernatant filled in root canal run off from the apex. Thus, it might be that the antibacterial compound does not reach *E. faecalis* hidden deep in the dentinal tubules. Accordingly, it will be useful to test the efficacy of formulated fabclavine-rich supernatant in future studies.

Fabclavines show very strong antimicrobial effects against both prokaryotic and eukaryotic pathogens and therefore they might

also display adverse effects to host cells (Fuchs et al., 2014; Fodor et al., 2017; Tobias et al., 2017).

Our data clearly revealed that the fabclavine in the supernatant of *X. cabanillasii* has strong antibacterial activity against *E. faecalis*. Here we used fabclavine-rich supernatant as intracanal medicament for simplicity and it was highly effective against multidrug-resistant *E. faecalis*. Fabclavines might not display equivalent efficiencies against all bacterial species especially in primary endodontic infections which are polymicrobial. In this type of situation, they can be combined with other antibiotics which would lead to synergistic effects on pathogens while simultaneously reducing the potential adverse side effects (Fuchs et al., 2014).

We also compared the efficacy of cell-free supernatant of *X. cabanillasii* against multidrug-resistant V583 (ATCC 700802), antibiotic susceptible (ATCC 29212) and a clinic isolate (obtained from root canal of a patient) of *E. faecalis* using overlay bioassay method and there was no difference among the zone diameters (data were not shown in the manuscript). This indicates that the antibacterial mechanism of fabclavine derivatives has a different mode of action than commonly used traditional antibiotics. Based on the structural similarities to the (pre-)zeamines, we assume a similar mode of action (Masschelein et al., 2015a). Zeamines also show a broad-spectrum bioactivity against a wide variety of organisms, which is probably caused by a membrane disruptive mode of action (Masschelein et al., 2015b).

In conclusion, the data of the induced and non-induced fabclavine promoter exchange mutants clearly show that fabclavine derivatives are bioactive compounds responsible for the bactericidal effect. Although commonly used synthetic intracanal medicaments CHX gel and $Ca(OH)_2$ paste do not eradicate infected root canals in all cases, they are commonly used as medicaments in root canals. Instead, purified and formulated fabclavine derivatives have a great potential to be used as intracanal medicament against dental root canal infections. Further studies with fabclavine-rich derivatives at different concentrations, different formulations and combine applications with other medicaments are needed to test against potential root canal pathogens in *in vitro* and *in vivo* bioassays. Of course one must determine the toxicity of fabclavines against eukaryotic cells at the applied concentration, since they also show some bioactivity against cell lines (Fuchs et al., 2014). However, the large number of fabclavine derivatives found in other *Xenorhabdus* strains might enable the identification of more specific derivatives with less toxicity.

Though *Enterococcus faecalis* is a commensal organism of humans, it is the third most common pathogen isolated from human bloodstream infections (Karchmer, 2000). It can also cause endocarditis; meningitis; and nosocomial, urinary tract, and wound infections (Kau et al., 2005). The efficacy of fabclavine derivatives obtained from *X. cabanillasii* can also be evaluated against these infections in the future.

DATA AVAILABILITY STATEMENT

All datasets generated for this study are included in the article/**Supplementary Material**.

ETHICS STATEMENT

The studies involving human participants were reviewed and approved by Adnan Menderes University, Local Ethical Committee. The patients/participants provided their written informed consent to participate in this study.

AUTHOR CONTRIBUTIONS

SH and HD designed the research. HD, HC, DU, and MT carried out the research, collected the data, and contributed to data analyses. HB and SW generated promoter exchanged mutant strains. NA and SY assisted with the experiments. SH and HB wrote the paper. All authors discussed the results and commented on the manuscript.

FUNDING

This work was financially supported by Aydin Adnan Menderes University (project number DHF-19009) and work in the Bode lab was supported by an ERC advanced grant under grant agreement no. 835108.

ACKNOWLEDGMENTS

We appreciate Dr. Harry K. Kaya from the University of California, Davis-USA, and Dr. David Shapiro-Ilan from USDA-ARS, SEA SE Fruit and Tree Nut Research Unit, Byron-USA, for editing the manuscript.

SUPPLEMENTARY MATERIAL

The Supplementary Material for this article can be found online at: https://www.frontiersin.org/articles/10.3389/fmicb.2019.02672/full#supplementary-material

REFERENCES

Aarati, N., Ranganath, N. N., Soumya, G. B., Kishore, B., and Mithun, K. (2011). Evaluation of antibacterial and anticandidal efficacy of aqueous and alcoholic extract of neem (*Azadirachta indica*) an in vitro study. *Int. J. Res. Ayurveda Pharm.* 2, 230–235.

Alves, F. R., Neves, M. A., Silva, M. G., Roças, I. N., and Siqueira, J. F. Jr. (2013). Antibiofilm and antibacterial activities of farnesol and xylitol as potential endodontic irrigants. *Braz. Dent. J.* 24, 224–229. doi: 10.1590/0103-6440201302187

Ardizzoni, A., Blasi, E., Rimoldi, C., Giardino, L., Ambu, E., Righi, E., et al. (2009). An *in vitro* and *ex vivo* study on two antibiotic-based endodontic irrigants: a challenge to sodium hypochlorite. *New Microbiol.* 32, 57–66.

Arias, C. A., and Murray, B. E. (2012). The rise of the enterococcus: beyond vancomycin resistance. *Nat. Rev. Microbiol.* 10, 266–278. doi: 10.1038/nrmicro2761

Asnaashari, M., Ashraf, H., Rahmati, A., and Amini, N. (2017). A comparison between effect of photo-dynamic therapy by LED and calcium hydroxide therapy for root canal disinfection against *Enterococcus faecalis*: a randomized controlled trial. *Photodiagn. Photodyn. Ther.* 17, 226–232. doi: 10.1016/j.pdpdt.2016.12.009

Awori, R. M., Nganga, P. N., Nyongesa, L. N., Amugune, N. O., and Masiga, D. (2016). Mursamacin: a novel class of antibiotics from soil-dwelling roundworms of Central Kenya that inhibits methicillin-resistant *Staphylococcus aureus*. *F1000Res* 5, 2431–2439. doi: 10.12688/f1000research.9652.1

Bode, H. B. (2009). Entomopathogenic bacteria as a source of secondary metabolites. *Curr. Opin. Chem. Biol.* 13, 224–230. doi: 10.1016/j.cbpa.2009.02.037

Bode, E., Brachmann, A. O., Kegler, C., Simsek, R., Dauth, C., Zhou, Q., et al. (2015). Simple "on-demand" production of bioactive natural products. *ChemBioChem* 16, 1115–1119. doi: 10.1002/cbic.201500094

Boemare, N. (2002). "Biology, taxonomy and systematics of *Photorhabdus* and *Xenorhabdus*" in *Entomopathogenic nematology*. ed. R. Gaugler (UK: CABI Publishing), 35–56.

Boemare, N. E., and Akhurst, R. J. (2006). "The genera *Photorhabdus* and *Xenorhabdus*" in *The prokaryotes*. eds. M. Dworkin, S. Falkow, E. Rosenberg, K. H. Schleifer, and E. Stackebrandt (New York: Springer Science + Business Media Inc.), 451–494.

Boyce, J. M., and Pittet, D. (2002). Guideline for hand hygiene in health-care settings: recommendations of the healthcare infection control practices advisory committee and the HICPAC/SHEA/APIC/IDSA hand hygiene task force. *Infect. Control Hosp. Epidemiol.* 23, 3–40.

Brian, P. W., and Hemming, H. G. (1947). Production of antifungal and antibacterial substances by fungi; preliminary examination of 166 strains of fungi imperfecti. *J. Gen. Microbiol.* 1, 158–167. doi: 10.1099/00221287-1-2-158

Bystrom, A., Claesson, R., and Sundqvist, G. (1985). The antibacterial effect of camphorated paramonochlcorophenol, camphorated phenol and calcium hydroxide in the treatment of infected root canals. *Endod. Dent. Traumatol.* 1, 170–175. doi: 10.1111/j.1600-9657.1985.tb00652.x

Cowan, M. M. (1999). Plant products as antimicrobial agents. *Clin. Microbiol. Rev.* 12, 564–582. doi: 10.1128/CMR.12.4.564

Delgado, R. J., Gasparoto, T. H., Sipert, C. R., Pinheiro, C. R., Moraes, I. G., Garcia, R. B., et al. (2010). Antimicrobial effects of calcium hydroxide and chlorhexidine on *Enterococcus faecalis*. *J. Endod.* 36, 1389–1393. doi: 10.1016/j.joen.2010.04.013

Evans, M. D., Baumgartner, J. C., Khemaleelakul, S. U., and Xia, T. (2003). Efficacy of calcium hydroxide: chlorhexidine paste as an intracanal medication in bovine dentin. *J. Endod.* 29, 338–339. doi: 10.1097/00004770-200305000-00005

Evans, M., Davies, J. K., Sundqvist, G., and Figdor, D. (2002). Mechanisms involved in the resistance of *Enterococcus faecalis* to calcium hydroxide. *Int. Endod. J.* 35, 221–228. doi: 10.1046/j.1365-2591.2002.00504.x

Fodor, A., Fodor, A. M., Forst, S., Hogan, J. S., Klein, M. G., Lengley, K., et al. (2010). Comparative analysis of antibacterial activities of *Xenorhabdus* species on related and non-related bacteria *in vivo*. *J. Microbiol. Antimicrob.* 2, 36–46.

Fodor, A., Makrai, L., Fodor, L., Venekei, I., Husveth, F., Pal, L., et al. (2017). Anti-coccidiosis potential of autoclaveable antimicrobial peptides from *Xenorhabdus budapestensis* resistant to proteolytic (pepsin, trypsin) digestion based on *in vitro* studies. *Microbiol. Res. J. Int.* 22, 1–17. doi: 10.9734/MRJI/2017/38516

Fu, C., Donovan, W. P., Shikapwashya-Hasser, O., Ye, X., and Cole, R. H. (2014). Hot fusion: an efficient method to clone multiple DNA fragments as well as inverted repeats without ligase. *PLoS One* 9:e115318. doi: 10.1371/journal.pone.0115318

Fuchs, S. W., Grundmann, F., Kurz, M., Kaiser, M., and Bode, H. B. (2014). Fabclavines: bioactive peptide-polyketide-polyamino hybrids from *Xenorhabdus*. *ChemBioChem* 15, 512–516. doi: 10.1002/cbic.201300802

Fuhrman, J. A. (1999). Marine viruses and their biogeochemical and ecological effects. *Nature* 399, 541–548. doi: 10.1038/21119

Furgani, G., Böszörmenyi, E., Fodor, A., Mathe-Fodor, A., Forst, S., Hogan, J. s., et al. (2008). *Xenorhabdus* antibiotics: a comparative analysis and potential utility for controlling mastitis caused by bacteria. *J. Appl. Microbiol.* 104, 745–758. doi: 10.1111/j.1365-2672.2007.03613.x

Gillor, O., and Ghazaryan, L. (2007). Recent advances in bacteriocin application as antimicrobials. *Recent Pat. Antiinfect. Drug Discov.* 2, 115–122. doi: 10.2174/157489107780832613

Gilmore, M. S., Clewell, D. B., Courvalin, P., Dunny, G. M., Murray, B. E., and Rice, L. B. (2002). *The enterococci: Pathogenesis, molecular biology, and antibiotic resistance*. Washington DC: ASM Press, 439.

Gu, L. S., Kim, J. R., Ling, J., Choi, K. K., Pashley, D. H., and Tay, F. R. (2009). Review of contemporary irrigant agitation techniques and devices. *J. Endod.* 35, 791–804. doi: 10.1016/j.joen.2009.03.010

Gualtieri, M., Villain-Guillot, P., Givaudan, A., and Pages, S. (2012). Nemaucin, an antibiotic produced by entomopathogenic *Xenorhabdus cabanillasii*. Google Patents.

Haapasalo, M., and Orstavik, D. (1987). *In vitro* infection and disinfection of dentinal tubules. *J. Dent. Res.* 66, 1375–1379.

Hazir, S., Kaya, H. K., Stock, S. P., and Keskin, N. (2003). Entomopathogenic nematodes (Steinernematidae and Heterorhabditidae) for biocontrol of soil pests. *Turk. J. Biol.* 27, 181–202.

Hazir, S., Shapiro-Ilan, D. I., Bock, C. H., Hazir, C., Leite, L. G., and Hotchkiss, M. W. (2016). Relative potency of culture supernatants of *Xenorhabdus* and *Photorhabdus* spp. on growth of some fungal phytopathogens. *Eur. J. Plant Pathol.* 146, 369–381. doi: 10.1007/s10658-016-0923-9

Heling, M., Steinberg, D., Kenig, S., Gavrilovich, I., Sela, M. N., and Friedman, M. (1992). Efficacy of a sustained-release device containing chlorhexidine and $Ca(OH)_2$ in preventing secondary infection of dentinal tubules. *Int. Endod. J.* 25, 20–24. doi: 10.1111/j.1365-2591.1992.tb00944.x

Karchmer, A. W. (2000). Nosocomial bloodstream infections: organisms, risk factors, and implications. *Clin. Infect. Dis.* 31, 139–143. doi: 10.1086/314078

Kau, A. L., Martin, S. M., Lyon, W., Hayes, E., Caparon, M. G., and Hultgren, S. J. (2005). *Enterococcus faecalis* tropism for the kidneys in the urinary tract of C57BL/6J mice. *Infect. Immun.* 73, 2461–2468. doi: 10.1128/IAI.73.4.2461-2468.2005

Kaya, H. K., and Stock, S. P. (1997). "Techniques in nematology" in *Manual of techniques in insect pathology*. ed. L. A. Lacey (San Diego: Academic Press), 281–324.

Kayaoglu, G., and Orstavik, D. (2004). Virulence factors of *Enterococcus faecalis*: relationship to endodontic disease. *Crit. Rev. Oral Biol. Med.* 15, 308–320. doi: 10.1177/154411130401500506

Kirkup, B. C. Jr. (2006). Bacteriocins as oral and gastrointestinal antibiotics: theoretical considerations, applied research, and practical applications. *Curr. Med. Chem.* 13, 3335–3350. doi: 10.2174/092986706778773068

Lakhani, A. A., Sekhar, K. S., Gupta, P., Tejolatha, B., Gupta, A., Kashyap, S., et al. (2017). Efficacy of triple antibiotic paste, moxifloxacin, calcium hydroxide and 2% chlorhexidine gel in elimination of *E. faecalis*: an in vitro study. *J. Clin. Diagn. Res.* 11, 6–9. doi: 10.7860/JCDR/2017/22394.9132

Leclerc, M. C., and Boemare, N. (1991). Plasmids and phase variations in *Xenorhabdus* spp. *Appl. Environ. Microbiol.* 57, 2597–2601.

Masschelein, J., Clauwers, C., Awodi, U. R., Stalmans, K., Vermaelen, W., Lescrinier, E., et al. (2015a). A combination of polyunsaturated fatty acid, nonribosomal peptide and polyketide biosynthetic machinery is used to assemble the zeamine antibiotics. *Chem. Sci.* 6, 923–929. doi: 10.1039/c4sc01927j

Masschelein, J., Clauwers, C., Stalmans, K., Nuyts, K., De Borggraeve, W., Briers, Y., et al. (2015b). The zeamine antibiotics affect the integrity of bacterial membranes. *Appl. Environ. Microbiol.* 81, 1139–1146. doi: 10.1128/AEM.03146-14

Mattigatti, S., Ratnakar, P., Moturi, S., varma, S., and Rairam, S. (2012). Antimicrobial effect of conventional root canal medicaments vs. propolis against *Enterococcus faecalis*, *Staphylococcus aureus* and *Candida albicans*. *J. Contemp. Dent. Pract.* 13, 305–309. doi: 10.5005/jp-journals-10024-1142

Mozayeni, M. A., Haeri, A., Dianat, O., and Jafari, A. R. (2014). Antimicrobial effects of four intracanal medicaments on *Enterococcus faecalis*: an in vitro study. *Iran. Endod. J.* 9, 195–198.

Newman, D. J., and Cragg, G. M. (2016). Natural products as sources of new drugs from 1981 to 2014. *J. Nat. Prod.* 79, 629–661. doi: 10.1021/acs.jnatprod.5b01055

Orstavik, D., and Haapasalo, M. (1990). Disinfection by endodontic irrigants and dressings of experimentally infected dentinal tubules. *Endod. Dent. Traumatol.* 6, 142–149. doi: 10.1111/j.1600-9657.1990.tb00409.x

Pektas, B. A., Yurdakul, P., Gülmez, D., and Görduysus, Ö. (2013). Antimicrobial effects of root canal medicaments against *Enterococcus faecalis* and *Streptococcus mutans*. *Int. Endod. J.* 46, 413–418. doi: 10.1111/iej.12004

Pladisai, P., Ampornaramveth, R. S., and Chivatxaranukul, P. (2016). Effectiveness of different disinfection protocols on the reduction of bacteria in *Enterococcus faecalis* biofilm in teeth with large root canals. *J. Endod.* 42, 460–464. doi: 10.1016/j.joen.2015.12.016

Sanchez-Sanhueza, G., González-Rocha, G., Dominguez, M., and Bello-Toledo, H. (2015). *Enterococcus* spp. isolated from root canals with persistent chronic apical periodontitis in a Chilean population. *Braz. J. Oral. Sci.* 14, 240–245. doi: 10.1590/1677-3225v14n3a13

Sasanakul, P., Ampornaramveth, R. S., and Chivatxaranukul, P. (2019). Influence of adjuncts to irrigation in the disinfection of large root canals. *J. Endod.* 45, 332–337. doi: 10.1016/j.joen.2018.11.015

Schmidt-Hieber, M., Blau, I. W., Schwartz, S., Uharek, L., Weist, K., Eckmanns, T., et al. (2007). Intensified strategies to control vancomycin-resistant enterococci in immunocompromised patients. *Int. J. Hematol.* 86, 158–162. doi: 10.1532/IJH97.E0632

Schneider, S. W. (1971). A comparison of canal preparations in straight and curved root canals. *Oral Surg. Oral Med. Oral Pathol.* 32, 271–275. doi: 10.1016/0030-4220(71)90230-1

Shi, Y. M., and Bode, H. B. (2018). Chemical language and warfare of bacterial natural products in bacteria–nematode–insect interactions. *Nat. Prod. Rep.* 35, 309–335. doi: 10.1039/C7NP00054E

Siqueira, J. F. Jr. (2001). Aetiology of root canal treatment failure: why well-treated teeth can fail. *Int. Endod. J.* 34, 1–10. doi: 10.1046/j.1365-2591.2001.00396.x

Siqueira, J. F. Jr., and de Uzeda, M. (1997). Intracanal medicaments: evaluation of the antibacterial effects of chlorhexidine, metronidazole, and calcium hydroxide associated with three vehicles. *J. Endod.* 23, 167–169. doi: 10.1016/S0099-2399(97)80268-3

Stojicic, S., Zivkovic, S., Qian, W., Zhang, H., and Haapasalo, M. (2010). Tissuse dissolution by sodium hypochlorite: effect of concentration, temperature, agitation and surfactant. *J. Endod.* 36, 1558–1562. doi: 10.1016/j.joen.2010.06.021

Stuart, C. H., Schwartz, S. A., Beeson, T. J., and Owatz, C. B. (2006). *Enterococcus faecalis*: its role in root canal treatment failure and current concepts in retreatment. *J. Endod.* 32, 93–98. doi: 10.1016/j.joen.2005.10.049

Suttle, C. A. (1994). The significance of viruses to mortality in aquatic microbial communities. *Microb. Ecol.* 28, 237–243. doi: 10.1007/BF00166813

Tay, F. R., Gu, L. S., Schoeffel, G. J., Wimmer, C., Susin, L., Zhang, K., et al. (2010). Effect of vapor lock on root canal debridement by using a side-vented needle for positive-pressure irrigant delivery. *J. Endod.* 36, 745–750. doi: 10.1016/j.joen.2009.11.022

Tendolkar, P. M., Baghdayan, A. S., and Shankar, N. (2003). Pathogenic *Enterococci*: new developments in the 21st century. *Cell. Mol. Life Sci.* 60, 2622–2636. doi: 10.1007/s00018-003-3138-0

Tervit, C., Paquette, L., Torneck, C. D., Basrani, B., and Friedman, S. (2009). Proportion of healed teeth with apical periodontitis medicated with two percent chlorhexidine gluconate liquid: a case-series study. *J. Endod.* 35, 1182–1185. doi: 10.1016/j.joen.2009.05.010

Tobias, N. J., Heinrich, A. K., Eresmann, H., Wright, P. R., Neubacher, N., and Backofen, R. (2017). *Photorhabdus*-nematode symbiosis is dependent on *hfq*-mediated regulation of secondary metabolites. *Environ. Microbiol.* 19, 119–129. doi: 10.1111/1462-2920.13502

Vianna, M. E., and Gomes, B. P. (2009). Efficacy of sodium hypochlorite combined with chlorhexidine against *Enterococcus faecalis* in vitro. *Oral Surg. Oral Med. Oral Pathol. Oral Radiol Endod.* 107, 585–589. doi: 10.1016/j.tripleo.2008.10.023

Webster, J. M., Chen, G., Hu, K., and Li, J. (2002). "Bacterial metabolites" in *Entomopathogenic nematology*. ed. R. Gaugler (London: CABI International), 9–114.

Wenski, S. L., Kolbert, D., Grammbitter, G. L. C., and Bode, H. B. (2019). Fabclavine biosynthesis in *X. szentirmaii*: shortened derivatives and characterization of the thioester reductase FclG and the condensation domain-like protein FclL. *J. Ind. Microbiol. Biotechnol.* 46, 565–572. doi: 10.1007/s10295-018-02124-8

Zan, R., Hubbezoglu, I., Ozdemir, A. K., Tunc, T., Sumer, Z., and Alici, O. (2013). Antibacterial effect of different concentration of boric acid against *Enterococcus faecalis* biofilms in root canal. *Marmara Dent. J.* 2, 76–80.

Zhang, X. Y., Bao, J., Wang, G. H., He, F., Xu, X. Y., and Qi, S. H. (2012). Diversity and antimicrobial activity of culturable fungi isolated from six species of the South China Sea gorgonians. *Microb. Ecol.* 64, 617–627. doi: 10.1007/s00248-012-0050-x

Conflict of Interest: The authors declare that the research was conducted in the absence of any commercial or financial relationships that could be construed as a potential conflict of interest.

frontiers in Microbiology

REVIEW
published: 18 December 2019
doi: 10.3389/fmicb.2019.02893

From Worms to Drug Candidate: The Story of Odilorhabdins, a New Class of Antimicrobial Agents

*Emilie Racine and Maxime Gualtieri**

Nosopharm, Nîmes, France

A major issue currently facing medicine is antibiotic resistance. No new class of antibiotics for the treatment of Gram-negative infections has been introduced in more than 40 years. We screened a collection of *Xenorhabdus* and *Photorhabdus* strains in the quest to discover new structures that are active against the most problematic multidrug-resistant bacteria. These species are symbiotic bacteria of entomopathogenic nematodes and their life cycle, the richness of the bacteria's genome in non-ribosomal peptide synthetase (NRPS) and polyketide synthase (PKS) genes, and their propensity to produce secondary metabolites with a large diversity of chemical structures make them a good starting point to begin an ambitious drug discovery program. Odilorhabdins (ODLs), a novel antibacterial class, were identified from this campaign. These compounds inhibit bacterial translation by binding to the small ribosomal subunit at a site not exploited by current antibiotics. Following the development of the total synthesis of this family of peptides, a medicinal chemistry program was started to optimize their pharmacological properties. NOSO-502, the first ODL preclinical candidate was selected. This compound is currently under preclinical development for the treatment of multidrug-resistant Gram-negative infections in hospitalized patients.

Keywords: Odilorhabdins, antimicrobial agent, *Xenorhabdus*, translation inhibitor, cationic peptide

OPEN ACCESS

Edited by:
András Fodor,
University of Szeged, Hungary

Reviewed by:
John D. Wade,
The University of Melbourne, Australia
Adler Ray Dillman,
University of California, Riverside, United States
Eva Kondorosi,
Biological Research Centre (MTA), Hungary
David Clarke,
University College Cork, Ireland

***Correspondence:**
Maxime Gualtieri
m.gualtieri@nosopharm.com

Specialty section:
This article was submitted to Antimicrobials, Resistance and Chemotherapy, a section of the journal Frontiers in Microbiology

Received: *07 October 2019*
Accepted: *02 December 2019*
Published: *18 December 2019*

Citation:
Racine E and Gualtieri M (2019) From Worms to Drug Candidate: The Story of Odilorhabdins, a New Class of Antimicrobial Agents. Front. Microbiol. 10:2893. doi: 10.3389/fmicb.2019.02893

INTRODUCTION

The efforts of the pharmaceutical industry to generate new highly potent antibiotics with novel mechanisms of action have weakened dramatically over the last three decades for economic, scientific, or strategic reasons, resulting in the decline of the discovery of new classes of antibacterials. The rapid emergence of resistant bacteria combined with the absence of new drugs has led clinicians to a therapeutic impasse, especially in intensive care units. It is thus urgent to find new antibiotic chemical scaffolds to renew the current therapeutic arsenal. Natural products have historically been of crucial importance in the identification and development of antibacterial agents (Clardy et al., 2006). Indeed, most antibiotics in clinical use or advanced development come from secondary metabolites that were originally isolated from bacteria or fungi, such as penicillin, isolated from the fungus *Penicillium*, or tetracycline found in the soil-dwelling bacteria *Streptomyces aureofaciens*. Historically, *Actinomycetes* have been the most important source for the discovery of new antibiotics. Many drugs used today in clinical practice originate from metabolites produced by *Actinomycetes*, (Genilloud, 2017) such as chloramphenicol (producing strain: *Streptomyces venezuelae*),

daptomycin (*Streptomyces roseoporus*), erythromycin (*Saccharopolyspora erythraea*), gentamicin (*Micromonospora purpurea*), lincomycin (*Streptomyces lincolnensis*), rifamycin (*Amycolatopsis mediterranei*), streptomycin (*Streptomyces griseus*), tetracycline (*S. aureofaciens*), and vancomycin (*Amycolatopsis orientalis*). Although *Actinomycetes* are still one of the most important sources for novel structures, (Genilloud, 2017) it is equally important to explore new underexploited microbial bioresources, as shown by the recent characterization of two highly promising antibiotics with novel mechanisms of action. Teixobactin was isolated from uncultured *Eleftheria terrae*, (Ling et al., 2015) and Odilorhabdins (ODLs) from *Xenorhabdus nematophila* (Pantel et al., 2018).

Xenorhabdus AND *Photorhabdus*: IMPORTANT STRAINS FOR THE DISCOVERY OF NEW ANTIBACTERIALS

The genera *Xenorhabdus* and *Photorhabdus* of the *Enterobacteriaceae* family are mutualistically associated with entomopathogenic nematodes. These bacteria have a fascinating life cycle (**Figure 1**) that requires the production of a great diversity of antibacterial and antifungal compounds (Dreyer et al., 2018). The bacteria-nematode pair infects and kills insects. *Xenorhabdus* or *Photorhabdus* bacteria then establish suitable conditions for the reproduction of the nematode by providing nutrients and protecting the insect corpse from environmental predators, such as bacteria and fungi. *Xenorhabdus* and *Photorhabdus* offer many advantages for anti-infective drug discovery. First, they produce novel and undescribed antimicrobial molecules with original chemical structures. This feature is genetically supported by the high content of non-ribosomal peptide synthetase (NRPS) and polyketide synthase (PKS) genes in their genomes (Tobias et al., 2017). NRPS and PKS enzymes or hybrids thereof are responsible for the biosynthesis of complex secondary metabolites via the combinatorial assembly of simple blocks, such as amino acids, acetate, or propionate. Then, antimicrobial compounds produced by *Xenorhabdus* and *Photorhabdus* interact with the biological matrices of the dead insect but are not toxic for the nematode. These properties represent a natural primary filter for compound drugability and safety in eukaryotic organisms. Finally, these genera are an underestimated and neglected source of novel bioactive compounds and thus constitute a promising source for undisclosed and unpatented molecules.

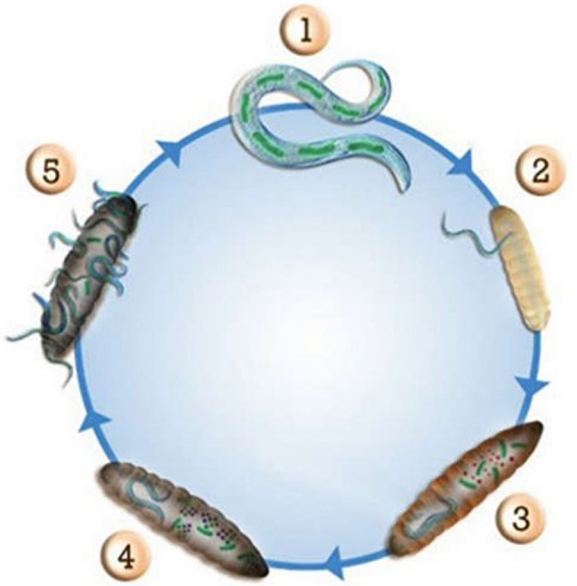

FIGURE 1 | Life cycle of entomopathogenic nematodes and their symbiotic bacteria in insect larvae. (1) *Photorhabdus* or *Xenorhabdus* bacteria live in the intestine of the host nematode; (2) The host nematode infects an insect; (3) *Photorhabdus* or *Xenorhabdus* bacteria are released within the insect and produce compounds to kill it; (4) *Photorhabdus* or *Xenorhabdus* bacteria produce a set of antibiotic molecules to prevent microbial competitors of the environment to degrade the corpse of the insect; (5) The nematode and the bacteria use the biomass of the insect as nutrients to reproduce. *Photorhabdus* or *Xenorhabdus* bacteria recolonize the nematode that will emerge from the corpse of the insect.

DISCOVERY OF ODILORHABDINS

Most bacteria do not express their full genomic potential under laboratory growth conditions or when using classic culture media and some secondary metabolites may not be produced. Multiple strategies to increase metabolite production have been described. A simple approach consists of culturing bacterial strains in various media and altering various cultivation parameters, such as temperature, salinity, flask shape, and aeration. A second approach is based on a published study showing that mutations in the RNA polymerase of various *Actinomycetes* strains are effective in enhancing the production of new antibiotics by activating biosynthetic gene clusters, which are "silent" or poorly expressed in wild type strains (Tanaka et al., 2013). This strategy has been applied to *Xenorhabdus* and *Photorhabdus* strains by the cultivation of selected clones resistant to rifamycins, an antibiotic family known to generate characteristic mutations on the RNA polymerase β subunit. Finally, a third approach, based on cocultivation of the strain of interest with multiple microbial strains (e.g., *Streptomyces abikoensis*, *Streptomyces glomeroaurantiacus*, *Alteromonas macleodii*, *Micromonospora aurantiaca*, *Stenotrophomonas terrae*, *Bacillus subtilis*, *Staphylococcus aureus*, and *Sphingomonas aquatilis*) has been used for antibiotic production and is well documented in the literature (Ueda and Beppu, 2017). For example, biphenomycin C was produced by *Streptomyces griseorubiginosus* and converted to the active antibiotic in a coculture with *Pseudomonas maltophilia* (Ezaki et al., 1993). In another example, alchivemycin A was only produced when *Streptomyces lividans* was in direct contact with bacteria producing mycolic acid (Onaka et al., 2011).

These three strategies were applied to *Xenorhabdus* and *Photorhabdus* bacteria and the supernatants of 150 cultured strains were screened for the presence of antibacterial activity.

Active supernatants were fractionated by high-performance liquid chromatography (HPLC). Antibacterial, antifungal, and cytotoxic activities of the obtained fractions were measured to select those showing only antibacterial activity to avoid potentially cytotoxic compounds. The isolation and identification of ODLs from one of these fractions followed a traditional protocol, including isolation/purification by HPLC and molecular mass determination by mass spectrometry. A total of three antibacterial metabolites were characterized from the culture supernatant of *X. nematophila* strain CNCM I-4530. These compounds were named NOSO-95A (MW: 1,296 Da), NOSO-95B (MW: 1,280 Da), and NOSO-95C (MW: 1,264 Da) (Pantel et al., 2018). The molecular masses of ODLs were compared with those in the antibiotic mass bank to confirm their novelty. ODLs have a wide antibacterial activity spectrum that includes Gram-negative and Gram-positive bacteria. NOSO-95A was shown to have activity against many resistant strains with limited treatment options, such as carbapenem-resistant *Enterobacteriaceae* (CRE) or methicillin-resistant *Staphylococcus aureus* (MRSA) (Gualtieri et al., 2013; Pantel et al., 2018). At the same time, NOSO-95A did not show any cytotoxic effect on human HepG2 cell line, even at concentrations up to 128 μg/mL which exceeds the typical MICs for *Escherichia coli*, *Klebsiella pneumoniae*, and *S. aureus* by 16-, 32-, and 128-fold, respectively. NOSO-95A showed bactericidal activity against *K. pneumoniae* and *S. aureus*. These encouraging results prompted us to continue the characterization of NOSO-95A. Its *in vivo* efficacy was evaluated in a mouse septicemia model with *S. aureus*. All NOSO-95A-treated mice survived up to the end of the study (120 h) at a dose of 2.5 mg/kg. These data show the high potential of ODLs as a new class of antibiotic.

STRUCTURAL DETERMINATION AND IDENTIFICATION OF THE BIOSYNTHETIC GENE CLUSTER

The chemical structure of NOSO-95A, solved by nuclear magnetic resonance (NMR) and LC-MS/MS fragmentation analysis, revealed ODLs to be representative of a new chemical class of antibiotics (**Figure 2**) (Pantel et al., 2018). NOSO-95A is a 10-mer linear cationic peptide containing four proteinogenic and six non-standard amino acids: (2S,3S)-α,γ-diamino β-hydroxybutyric acid (Dab(βOH) at positions 2 and 3, D-ornithine (D-Orn) at position 5, Z-α,β–dehydroarginine (Dha) at position 9, (5S)-5-hydroxylysine (Dhl) at positions 8 and 10, and a functionalized secondary amide at the C-terminal position [α,δ–diamino butane (Dbt)]. NOSO-95B and C differ from NOSO-95A by the substitution of Dhl at position 10 (NOSO-95B) or at positions 8 and 10 (NOSO-95C) by a lysine (**Figure 2**). We developed the synthesis of all diastereoisomers of the three non-standard amino acids, Dab(βOH), Dha, and Dhl, and elucidated the stereochemistry of each chiral center of NOSO-95A by the advanced Marfey's method (Bhushan and Brückner, 2004). Orn was found to be the only amino acid of R configuration while all other chiral centers were of S configuration. At the same time that the current study was being conducted, we identified the biosynthetic NRPS gene cluster (Pantel et al., 2018). This step was necessary for the production of ODLs and related analogs by engineering NRPS module enzymes. This strategy was used for daptomycin, a cyclic lipopeptide antibiotic used for the treatment of infections caused by *S. aureus* (Nguyen et al., 2010). We identified four large NRPS-coding genes in the genome of the producer *X. nematophila* as the putative biosynthetic gene cluster using anti-SMASH, a secondary metabolite gene cluster prediction software. Inactivation of the first gene of the cluster abolished production of all three ODLs, confirming that the cluster is responsible for their production (Pantel et al., 2018). Two of the non-standard amino acids, Dab(βOH) and Dha, were not commercially available and were required for the total synthesis of NOSO-95C. We developed their synthesis on a multi-gram scale and reported the first total synthesis of NOSO-95C (Sarciaux et al., 2018). The ^{1}H NMR and LC-MS spectra and antibacterial activity of the natural and synthetic peptides were similar.

STRUCTURE-ACTIVITY RELATIONSHIPS AND SELECTION OF A PRECLINICAL CANDIDATE

Based on these encouraging results and with a validated synthetic method, we initiated a medicinal chemistry program on NOSO-95C to study the structure-activity relationships (SAR) of ODLs with the objective to better understand the role of each amino acid for the antibacterial activity and the inhibition of bacterial translation (Sarciaux et al., 2018). Before starting this study, the inhibition of bacterial translation was identified as the principal mode of action of ODLs. We evaluated the antibacterial activity of analogs against *Enterobacteriaceae* (*E. coli* and *K. pneumoniae*) and their potential to inhibit bacterial translation to help drive preliminary SAR studies. First, alanine scanning (Ala scan) was performed. This consists of replacing each amino acid by an alanine to evaluate the impact of lateral chains on biological activity. This strategy has been previously used to decipher the SAR of various antibacterial peptides, such as an analog of teixobactin, (Parmar et al., 2017) and feglymycin (Hänchen et al., 2013). Removal of the lateral chain of Lys1, His7, Lys8, Lys10, or Dbt11 had little or no impact on the antibacterial activity of NOSO-95C and inhibition of translation. Replacing Dab(βOH)3 by alanine resulted in a four-fold gain in antibacterial activity and in the same level of inhibition of bacterial translation than that of NOSO-95C. A better passage through the bacterial membrane could explain the improvement of antibacterial activity while conserving the same level of inhibition of translation (**Figure 3**). Significant decreases of both antibacterial activity and inhibition of the translation were observed when substituting Dab(βOH)2 and D-Orn5 (**Figure 3**). As shown later on using X-ray crystallography, the lateral chains of these two amino acids interact directly with the bacterial ribosome (Pantel et al., 2018). Substitution of Gly4, Pro6, and Dha9 by an alanine should have a strong effect on the secondary structure of the peptide. Indeed, the antibacterial activity of

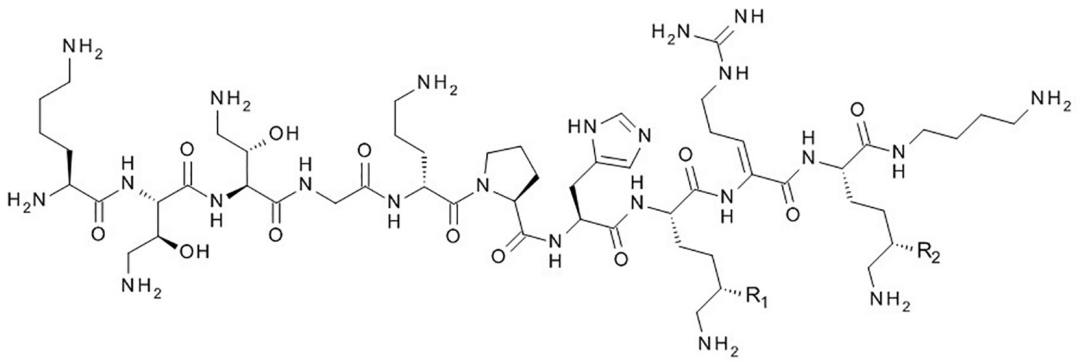

NOSO-95A : R1 = OH, R2 = OH
NOSO-95B: R1 = H, R2 = OH
NOSO-95C : R1 = H, R2 = H

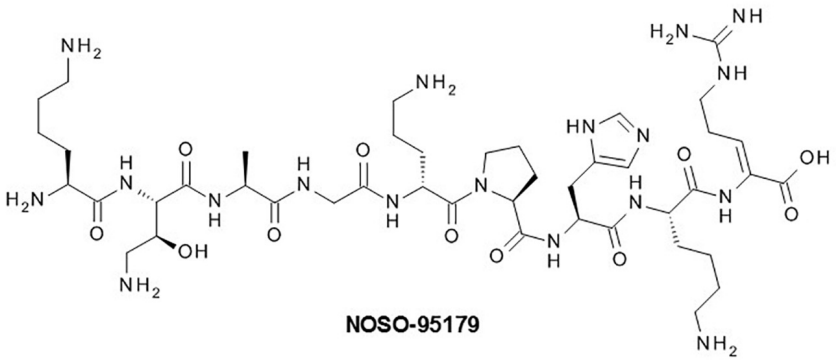

NOSO-95179

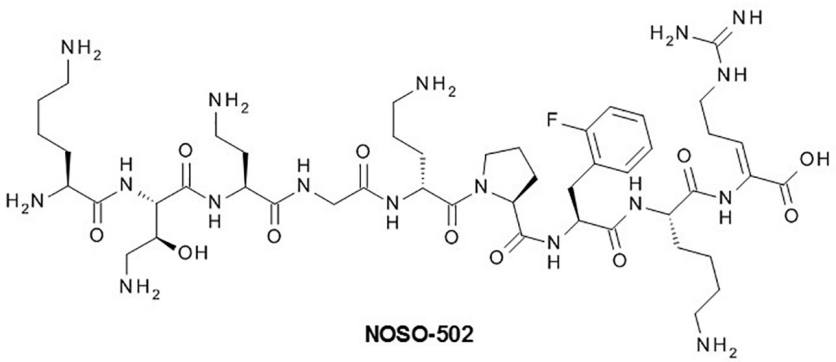

NOSO-502

FIGURE 2 | Chemical structures of NOSO-95A, B, and C, NOSO-95179 and NOSO-502.

these analogs and the inhibition of translation were strongly reduced with the exception of the analog in which Pro6 was replaced by Ala, for which activity was conserved on *E. coli* while measuring a five-fold decrease of the inhibition of translation. This could be explained by a more flexible structure, making it easier for this analog to cross the bacterial membranes. We next investigated the effect of modifying the lateral chain of Dab(βOH)2 and Dha9. First, the hydroxyl group of Dab(βOH)2 was removed resulting in a strong decrease of both antibacterial activity and inhibition of translation. The same deleterious effect was observed when Dab(βOH)2 was replaced by allo-threonine (AlloThr) or Ser to study the influence of the amine function of the lateral chain. Influence of substitution of the lateral chain of Dha9 and removal of the double bond was next investigated by introducing dehydroamino butyric acid (DhAbu), L- or D-Arg. These substitutions had a limited impact, unlike substitution by alanine, meaning that either the double bond or the guanidine moiety is needed for efficient antibacterial activity and inhibition

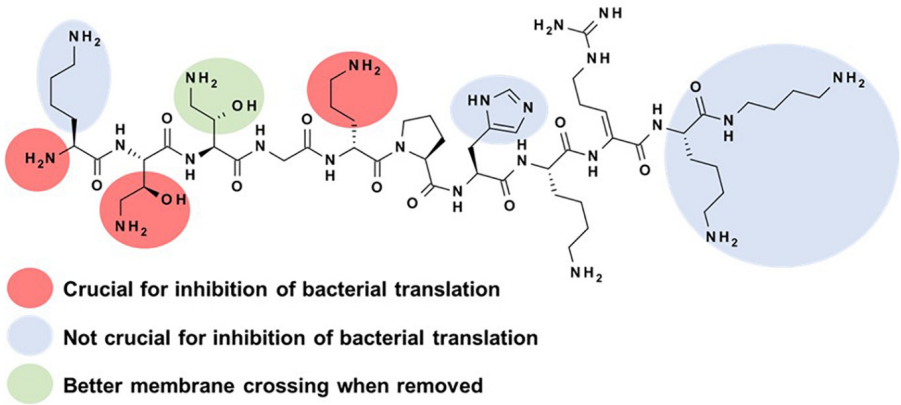

FIGURE 3 | Structure-activity relationships for the inhibition of bacterial translation by NOSO-95C.

of translation. Finally, truncation of amino acids from the N- and C-terminal position of the peptide was tested to find the shortest active sequence. Removing amino acids from C-terminal part up to Lys10 (included) led to structures with almost identical *in vitro* antibacterial efficacy and slightly better inhibition of bacterial translation compare to parent compound (**Figure 3**). Importance of Dha9 was confirmed by the strong decrease of antibacterial activity and inhibition of the translation of the analog in which this amino acid was removed. Reduction of the peptidic chain from the N-terminal side was then investigated. Removal of the first amino acid or both Lys1 and Dab(βOH)2 was detrimental for both antibacterial efficacy and inhibition of translation. The key role of the N-terminal amine function for the binding to the ribosome was later confirmed by co-crystallization studies.

The combination of best modifications and of the shorter active sequence led to NOSO-95179 identified as a lead compound showing promising *in vitro* and *in vivo* antibacterial activity against *Enterobacteriaceae* (including CRE) and low toxicity (Pantel et al., 2018; Sarciaux et al., 2018). This compound was used as the starting point for a lead-optimization campaign. The object of this final drug discovery phase was to maintain the favorable properties of the lead compound while improving on any deficiencies. One important objective was to enhance *in vitro* antibacterial activity and *in vivo* efficacy. Five hundred analogs were synthesized and evaluated using assays similar to those performed during the previous stage (MIC determination against a panel of referenced strains, cytotoxicity against the HepG2 cell line, and inhibition of bacterial translation). None of the compounds displayed cytotoxic activity and the 10% with the best antibacterial activity and inhibition of bacterial translation were selected and examined for extended microbiological properties (MIC against a large panel of bacterial strains displaying different resistance profiles, bactericidal kinetics, and frequency of resistance), and ADME-tox properties (blood stability, acute toxicity in the mouse, and hemolytic properties). The pharmacokinetic (PK) properties, plasma protein binding, and efficacy in a murine sepsis infection model of 40 selected analogs were then assessed. Finally, the properties of the 10 best analogs were compared using a large panel of tests, including pharmacology, ADME, and safety toxicology studies. Analogs with modifications at both the Ala3 and His7 positions showed a combination of good *in vitro* activity and improved *in vivo* efficacy through favorable PK profiles, leading to increased exposure. Among these analogs, NOSO-502 showed the best profile and was selected as a promising candidate (**Figure 2**) (Racine et al., 2018). MIC of NOSO-502 ranges from 0.5 to 4 μg/ml against *Enterobacteriaceae* type strains and CRE strains expressing carbapenemase belonging to classes A, B, and D of the Ambler classification. This compound retains excellent activity against strains resistant to colistin, a last resort antibiotic used to treat multidrug-resistant bacterial infections, through expression of mobile colistin resistance (mcr) genes or mutations in mgrB, PmrAB, PhoPQ genes. In addition, NOSO-502 has a low potential for resistance development (Racine et al., 2018). It is effective in mouse models of serious hospital-acquired infections (sepsis, complicated urinary tract infection (UTI), lung infection) and provides significant protection against *E. coli* and *K. pneumoniae*, the highest-incidence hospital pathogens in complicated intra-abdominal infection (IAI) and UTI. Interestingly, NOSO-502 was effective against an *E. coli* strain that expresses the metallo-β-lactamase NDM-1 and is resistant to other major antibiotic classes. Although nephrotoxicity and cardiotoxicity are associated with many antibiotics, NOSO-502 exhibited a good safety profile based on data from *in vitro* nephrotoxicity, cardiotoxicity, genotoxicity, or cytotoxicity standard studies. AUC/MIC was selected as the PK/PD index that shows the highest correlation with the antibacterial effect of NOSO-502 in a murine thigh infection model (Zhao et al., 2018). These data combined with human PK exposure and MIC distribution will be helpful in determining an appropriate dosing-regimen for future clinical studies.

MECHANISM OF ACTION

Deciphering the mechanism of action of a new antibacterial compound is crucial for a drug discovery and development program. However, it is often a complicated process, for which

various strategies have been described (Farha and Brown, 2016). We initially investigated the mode of action of ODLs by assessing the effect of the compound on the incorporation of radiolabeled precursors into four major biosynthetic pathways (protein, RNA, DNA, or peptidoglycan synthesis) of *E. coli* cells. These experiments demonstrated that bacterial protein synthesis is the main target of ODLs. In accordance with this conclusion, we showed that ODLs inhibit the production of a protein in an *E. coli* cell-free transcription-translation system with an IC_{50} in the same range as that of known ribosome-targeting antibiotics, such as chloramphenicol and spectinomycin (Pantel et al., 2018). Target identification was conducted by selecting resistant mutants carrying alterations in the drug-target site. As ODLs interfere with protein synthesis, one of the putative targets was the ribosome, which is the major target for antibacterials. The ribosome is a supramolecular enzyme which translates genetic information into proteins. In bacteria, it is composed of two subunits, a small 30S and large 50S subunit, which join to form a 70S ribosome. Each subunit is composed of proteins and ribosomal RNA (rRNA). In wild type *E. coli*, seven copies of the rRNA operon are present in the chromosome. An *E. coli* strain in which six of the seven rRNA operons had been deleted was used to increase the chances of selecting resistant strains with mutations in the rRNA. Whole-genome sequencing of the selected ODL-resistant clones showed that almost all the mutants carried mutations in the 16S rRNA gene of the small ribosomal subunit, clustered in the vicinity of the decoding center (DC) (Pantel et al., 2018). The DC of the ribosome performs messenger RNA (mRNA) translation and provides the fidelity of the codon/anticodon interactions, along with performing mRNA translocation during protein biosynthesis.

The crystal structure of a 70S ribosome associated with ODLs confirmed that this new class of antibiotic interacts with the small ribosomal subunit (30S) by forming multiple hydrogen bonds with 16S rRNA residues of helices 31, 32, and 34 (h31, h32, and h34) (Pantel et al., 2018). This binding site is at a site distinct from those of other inhibitors that target the 30S ribosomal subunit, such as aminoglycosides, tuberactinomycins (viomycin, capreomycin), edeine, pactamycin, tetracycline, and negamycin (**Table 1**). The tetracycline and negamycin sites are closest to the site of ODL binding but do not overlap with that of ODLs. Moreover, ODL-resistant clones are not resistant to other clinically used ribosomal inhibitors. These results were crucial for carrying the development of ODLs forward. In this binding site, ODLs simultaneously interact with the 16S rRNA and the anticodon loop of the transfer RNA (tRNA) in the A-site, suggesting that the drug may increase the affinity of the aminoacyl tRNA for the ribosome. The predictable consequence is constrained progression of the ribosome along the mRNA and decreased fidelity of translation. We analyzed the effect of ODLs on translocation using a toe-printing assay. This method allows the determination of interactions between ribosomes or ribosomal subunits and mRNA. At lower concentrations, ODLs induced amino acid misincorporation by reducing the accuracy of decoding, whereas at higher concentrations they interfered with translocation. This mode of translation inhibition that is dependent on the drug concentration is similar to that described for aminoglycosides and negamycin. However, these antibiotics achieve this effect via different mechanisms. Aminoglycosides interact exclusively with the 16S rRNA and increase tRNA affinity by stabilizing a conformation of the 16S rRNA that interacts with the tRNA anticodon (Demirci et al., 2013). In contrast, negamycin and ODLs establish direct contacts with the A-site tRNA, but they interact at different sites (Pantel et al., 2018). Antimicrobial peptides (AMPs) that target the ribosome are rare. Indeed, most AMPs are mostly known for their disruptive effects on bacterial membranes (e.g., polymyxin B, gramicidin, LL-37, and melittin). Only nine classes interact with the bacterial ribosome, of which five, including ODLs, interact with the small ribosomal subunit (Polikanov et al., 2018). The binding site on the 30S ribosomal and mode of action of ODLs are different from the four other classes (**Figure 4**). Edeine (EDE), a pentapeptide amide produced by *Bacillus brevis*, and GE81112, a tetrapeptide produced by some *Streptomyces* species, target the translation initiation phase. EDE inhibits the formation of the 30S pre-initiation complex and prevents the formation of a competent 70S initiation complex, whereas GE81112 induces conformational changes of the 30S subunit, preventing its joining with the 50S subunit to form the 70S initiation complex (Dinos et al., 2004; Brandi et al., 2006). Similarly to ODLs, dityromycin (DIT) and tuberactinomycins (TUBs) inhibit translocation at the elongation phase, but by different mechanisms. DIT, a cyclic peptide produced by *Streptosporangium cinnabarum*, interacts with the 30S ribosomal protein S12 and inhibits translocation by preventing EF-G from adopting the final state necessary for translocation of the tRNAs and mRNA on the small subunit (Bulkley et al., 2014). TUBs, cyclic pentapeptides produced by various *Streptomyces* species, bind at the interface between the 30S and 50S subunits and act by trapping the ribosome in an intermediate state on the translocation pathway (Ly et al., 2010). The targets of the four classes of AMPs that target the 50S ribosomal subunit are mostly clustered around the peptidyl transferase center (PTC), where the peptide bond is formed. Streptogramins, a class produced by *Streptomyces* species, prevent correct positioning of tRNAs into the PTC, making peptide-bond formation impossible (Schmeing et al., 2005). Klebsazolicin, produced by *K. pneumoniae*, obstructs the ribosomal exit tunnel and blocks elongation of the

TABLE 1 | Binding site on the 30S ribosomal subunit of various antibiotics.

Antibiotic	Binding site on the 30S and 50S ribosomal subunit	References
ODLs	h31, h32, h34	Pantel et al., 2018
Aminoglycosides	h44	Wilson, 2009
Neomycin	h44, H69	Wang et al., 2012
Tuberactinomycins	h44 and H69	Stanley et al., 2010
Edeine	h24, h28, h44, h45	Pioletti et al., 2001
Pactamycin	h23, h24	Brodersen et al., 2000
Tetracycline	h31, h34	Brodersen et al., 2000
Negamycin	h34	Polikanov et al., 2014

h: helix of the 30S subunit; H: helix of the 50S subunit.

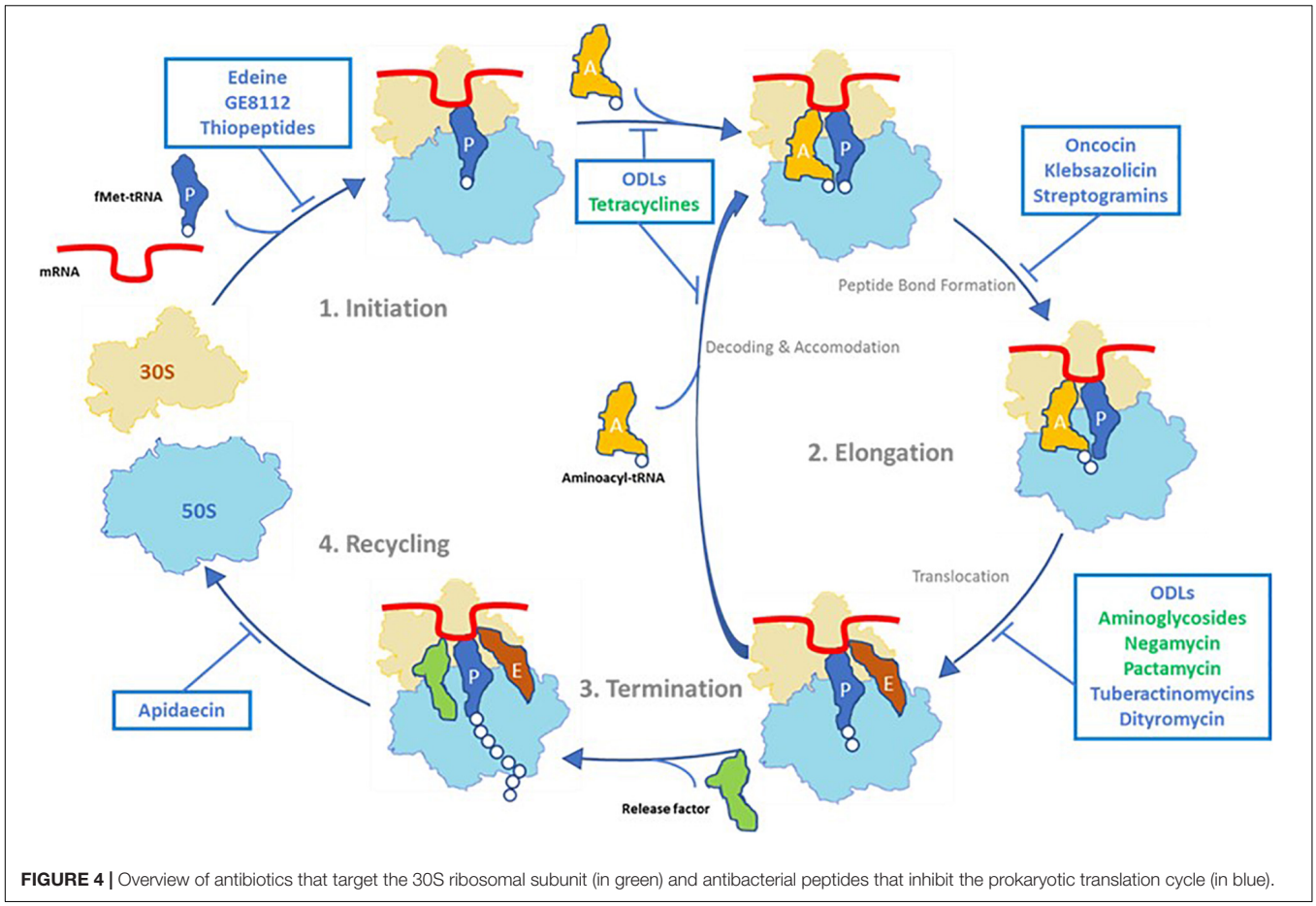

FIGURE 4 | Overview of antibiotics that target the 30S ribosomal subunit (in green) and antibacterial peptides that inhibit the prokaryotic translation cycle (in blue).

nascent peptide (Metelev et al., 2017). Proline-rich antimicrobial peptides (PrAMPs) have been found in insects, crustaceans, and mammals. Oncocins, the best-characterized type I PrAMPs, bind within the ribosomal exit tunnel in a reverse orientation relative to the nascent polypeptide chain, preventing transition into the elongation phase of translation (Roy et al., 2015). The apidaecin derivative Api137 blocks translation termination by trapping release factors (Florin et al., 2017). Finally, thiopeptide antibiotics GE2270A and thiostrepton inhibit translation by interacting with the translation factor EF-Tu or directly with the ribosome. Thiopeptides binding site on the large ribosomal subunit overlaps the IF2, EF-Tu, and EF-G translation factors' binding site (Bagley et al., 2005).

ANTIBIOTICS THAT ARE ACTIVE AGAINST CARBAPENEM-RESISTANT *Enterobacteriaceae* (CRE) IN DEVELOPMENT OR RECENTLY APPROVED

In 2013, CRE, *Clostridium difficile*, and *Neisseria gonorrhoeae* bacteria were identified by the Centers for Disease Control and Prevention (CDC) as urgent drug-resistant threats, confirming the need to rapidly develop new antibiotic scaffolds active against these pathogens (Centers for Disease Control and Prevention, 2013).The urgent need to find new therapies against CRE was recently confirmed by the WHO (Tacconelli et al., 2018). Carbapenems are broad-spectrum β-lactam antibiotics considered to be the last treatment option for infections caused by multidrug-resistant pathogens. However, their use has been compromised due to the increasing prevalence of CRE infections in hospitals. CRE have become increasingly resistant to last-resort antibiotics and cause a range of healthcare-associated infection, such as pneumonia (HABP/VABP), UTI, IAI, and bloodstream infection (BSI) (Sheu et al., 2019). Numerous outbreaks of hospital acquired infections due to CRE were reported in different regions of the world (Tzouvelekis et al., 2012; van Duin and Doi, 2017). Recent reports show that the mortality of patients with CRE infections is three times higher than for patients with similar susceptible infections (Martin et al., 2018). In 2013, the CDC evaluated that CRE (*E. coli* and *K. pneumoniae*) were responsible of 9,300 nosocomial infections in the United States and caused the deaths of approximately 600 people (Centers for Disease Control and Prevention, 2013). The main mechanism responsible for carbapenem resistance among *Enterobacteriaceae* is the production of a carbapenemases, which are β-lactamase enzymes that efficiently break down carbapenem antibiotics. Many carbapenemases belonging to

Ambler classes A, B, and D of β-lactamases have been described in *Enterobacteriaceae*. Optimal treatment for serious infections due to CRE is yet to be determined, but current treatment often involves the use of gentamicin, tigecycline, colistin, and amikacin, alone or in combination with each other antibiotics and carbapenems (Martin et al., 2018). In such infections, resistance to carbapenems is associated with high levels of resistance to other antibiotics [e.g., colistin (22.6%), gentamicin (43.5%), tigecycline (15.2%)] (Trecarichi and Tumbarello, 2017). Furthermore, certain therapies, such as colistin, gentamicin, or amikacin, are associated with an increased risk of nephrotoxicity. These observations highlight the importance of the development of new therapeutic options to obtain more positive outcomes in CRE infections, especially compounds from new classes of antibiotic with original mode of action to limit the risk of cross-resistance.

NOSO-502 or other ODL analogs could be one such novel therapy. Indeed, this new family of antibiotics is active against CRE isolates producing β-lactamases belonging to Ambler classes A, B, C, and D and also exhibiting resistance to gentamicin, amikacin, polymyxin B, or tigecycline. The vast majority of agents recently approved or still in development are the result of modifications of existing agents (**Table 2**). They cannot generally overcome multiple existing resistance mechanisms. Furthermore, none of the recently approved antimicrobials are effective against all classes of carbapenemases, unlike ODLs, with the exception of eravacycline, (Livermore et al., 2016) an antibiotic of the tetracycline class approved by the United States Food and Drug Administration (FDA) in 2018 for the treatment of complicated IAI. The combination of ceftazidime + avibactam (Avycaz®) was approved by the FDA in 2015 and by the European Medicines Agency in 2016 for the treatment of cUTI and cIAI. It is active against isolates producing class A and D carbapenemases but does not cover metallo-β-lactamases like NDM-1, VIM, or IMP (Falcone and Paterson, 2016). The combination of meropenem + vaborbactam (Vabomere®), approved by the FDA in 2017 for the treatment of cUTI (including acute pyelonephritis), cIAI, and HABP/VABP, is only active against class A carbapenemase-producing strains (KPC) within the CRE group (Castanheira et al., 2017). Plazomicin is an aminoglycoside that was approved in June 2018 for the treatment of cUTI (including pyelonephritis) caused by *E. coli*, *K. pneumoniae*, *Enterobacter cloacae*, and *Proteus mirabilis*. As other aminoglycosides, its activity is not affected by resistance mechanisms to other antibiotic classes, such as β-lactamases and carbapenemases, including metallo-β-lactamases. However, it has been shown that the class B metallo-β-lactamase NDM-1 is frequently co-expressed with 16S ribosomal RNA methyltransferases and plazomicin, like all aminoglycosides, is inactive against strains that express these enzymes (Serio et al., 2019). Other drug candidates to address these resistance issues are currently under clinical development but all belong to existing classes of antibiotics (β-lactams, β-lactamase inhibitors combined with β-lactams, tetracyclines, aminoglycosides, fosfomycins and polymyxins). Nevertheless cefiderocol, a siderophore cephalosporin, (Kohira et al., 2015) and the combinations aztreonam-avibactam or cefepim-zidebactam appear to be promising options to treat such infections (Sader et al., 2017a,b).

TABLE 2 | Antibiotics active against carbapenem-resistant *Enterobacteriaceae* (CRE) in development or recently approved by the FDA.

Product	Company	Antibacterial class	Status
Ceftazidime + avibactam	Allergan/Pfizer	βL	Approved by FDA in 2015
Vabomere	Melinta	βL-βLI	Approved by FDA in 2017
Plazomicin	Achaogen	Aminoglycoside	Approved by FDA in 2018
Eravacycline	Tetraphase	Tetracycline	Approved by FDA in 2018
Imipenem + cilastatin + relebactam	Merck & Co.	βL-βLI	Phase 3
Aztreonam + avibactam	Pfizer	βL-βLI	Phase 3
ZTI-01	Nabriva	Fosfomycin	Phase 3
Cefiderocol	Shionogi	Siderophore-βL	Phase 3
LYS228	Boston pharmaceuticals	Monobactam	Phase 2
AIC499	AiCuris	βL	Phase 1
Cefepime + Zidebactam	Wockhardt Ltd.	βL-βLI	Phase 1
GSK3342830	GlaxoSmithKline	Siderophore-βL	Phase 1
SPR741	Spero	Polymyxin	Phase 1
TP-6076	Tetraphase	Tetracycline	Phase 1

βL: beta-lactam, βLI: beta-lactamase inhibitors.

CONCLUSION

The need for new antibiotic classes is exceedingly urgent. In this context, ODLs are a promising option to treat some of the most problematic multidrug-resistant Gram-negative infections. This is one more example of the importance of preserving biodiversity as a source of future drugs.

AUTHOR CONTRIBUTIONS

Both authors listed have made a substantial, direct and intellectual contribution to the work, and approved it for publication.

FUNDING

This work received financial support from OSEO and the Languedoc-Roussillon region under grant agreement A1010014J and from the DGA under grant agreement 122906117. The research leading to these results also received support from the Innovative Medicines Initiative Joint Undertaking under grant agreement 115583, the resources of which are composed of financial contributions from the European Union Seventh Framework Program (FP7/2007-2013) and in-kind contributions of EFPIA companies.

REFERENCES

Bagley, M., Dale, J., Merritt, E., and Xiong, X. (2005). Thiopeptide antibiotics. *Chem. Rev.* 105, 685–714. doi: 10.1021/cr0300441

Bhushan, R., and Brückner, H. (2004). Marfey's reagent for chiral amino acid analysis: a review. *Amino Acids* 27, 231–247. doi: 10.1007/s00726-004-0118-0

Brandi, L., Fabbretti, A., La Teana, A., Abbondi, M., Losi, D., Donadio, S., et al. (2006). Specific, efficient, and selective inhibition of prokaryotic translation initiation by a novel peptide antibiotic. *Proc. Natl. Acad. Sci. U.S.A.* 103, 39–44. doi: 10.1073/pnas.0507740102

Brodersen, D. E., Clemons, W. M., Carter, A. P., Morgan-Warren, R. J., Wimberly, B. T., and Ramakrishnan, V. (2000). The structural basis for the action of the antibiotics tetracycline, pactamycin, and hygromycin B on the 30S ribosomal subunit. *Cell* 103, 1143–1154. doi: 10.1016/s0092-8674(00)00216-6

Bulkley, D., Brandi, L., Polikanov, Y. S., Fabbretti, A., O'Connor, M., Gualerzi, C. O., et al. (2014). The antibiotics dityromycin and GE82832 bind protein S12 and block EF-G-catalyzed translocation. *Cell Rep.* 6, 357–365. doi: 10.1016/j.celrep.2013.12.024

Castanheira, M., Huband, M. D., Mendes, R. E., and Flamm, R. K. (2017). Effect of the β-Lactamase inhibitor vaborbactam combined with meropenem against serine carbapenemase-producing *Enterobacteriaceae*. *Antimicrob. Agents Chemother.* 61, 5454–5458. doi: 10.1128/AAC.00711-16

Centers for Disease Control and Prevention, (2013). *Antibiotic Resistance Threats in the United States*. Atlanta, GA: Centers for Disease Control and Prevention.

Clardy, J., Fischbach, M. A., and Walsh, C. T. (2006). New antibiotics from bacterial natural products. *Nat. Biotechnol.* 24, 1541–1550. doi: 10.1038/nbt1266

Demirci, H., Murphy, F. T., Murphy, E., Gregory, S. T., Dahlberg, A. E., and Jogl, G. (2013). A structural basis for streptomycin-induced misreading of the genetic code. *Nat. Commun.* 4, 1355–1362. doi: 10.1038/ncomms2346

Dinos, G., Wilson, D. N., Teraoka, Y., Szaflarski, W., Fucini, P., Kalpaxis, D., et al. (2004). Dissecting the ribosomal inhibition mechanisms of edeine and pactamycin: the universally conserved residues G693 and C795 regulate P-site RNA binding. *Mol. Cell* 13, 113–124. doi: 10.1016/s1097-2765(04)00002-4

Dreyer, J., Malan, A. P., and Dicks, L. M. T. (2018). Bacteria of the genus *Xenorhabdus*, a novel source of bioactive compounds. *Front. Microbiol.* 9:3177. doi: 10.3389/fmicb.2018.03177

Ezaki, M., Shigematsu, N., Yamashita, M., Komori, T., Umehara, K., and Imanaka, H. (1993). Biphenomycin C, a precursor of biphenomycin a in mixed culture. *J. Antibiot.* 46, 135–140. doi: 10.7164/antibiotics.46.135

Falcone, M., and Paterson, D. (2016). Spotlight on ceftazidime/avibactam: a new option for MDR Gram-negative infections. *J. Antimicrob. Chemother.* 71, 2713–2722. doi: 10.1093/jac/dkw239

Farha, M. A., and Brown, E. D. (2016). Strategies for target identification of antimicrobial natural products. *Nat. Prod. Rep.* 33:66880. doi: 10.1039/c5np00127g

Florin, T., Maracci, C., Graf, M., Karki, P., Klepacki, D., Berninghausen, O., et al. (2017). An antimicrobial peptide that inhibits translation by trapping release factors on the ribosome. *Nat. Struct. Mol. Biol.* 24, 752–757. doi: 10.1038/nsmb.3439

Genilloud, O. (2017). *Actinomycetes*: still a source of novel antibiotics. *Nat. Prod. Rep.* 34, 1203–1232. doi: 10.1039/c7np00026j

Gualtieri, M., Villain-Guillot, P., Givaudan, A., and Pages, S. (2013). *Novel Peptide Derivates as Antibiotics. EP11183034.5 & US61/540.085*. Patent WO20130 45600 (A1).

Hänchen, A., Rausch, S., Landmann, B., Toti, L., Nusser, A., and Süssmuth, R. D. (2013). Alanine scan of the peptide antibiotic feglymycin: assessment of amino acid side chains contributing to antimicrobial activity. *Chembiochem* 14, 625–632. doi: 10.1002/cbic.201300032

Kohira, N., West, J., Ito, A., Ito-Horiyama, T., Nakamura, R., Sato, T., et al. (2015). *In Vitro* Antimicrobial activity of a siderophore cephalosporin, S-649266, against *Enterobacteriaceae* clinical isolates, including carbapenem-resistant strains. *Antimicrob. Agents Chemother.* 60, 729–734. doi: 10.1128/AAC.01695-15

Ling, T. T., Schneider, T., Peoples, A. J., Spoering, L., Engels, I., and Conlon, B. P. (2015). A new antibiotic kills pathogen without detectable resistance. *Nature* 22, 455–459. doi: 10.1038/nature14098

Livermore, D. M., Mushtaq, S., Warner, M., and Woodford, N. (2016). *In Vitro* activity of eravacycline against carbapenem-resistant *Enterobacteriaceae* and *Acinetobacter baumannii*. *Antimicrob. Agents Chemother.* 60, 3840–3844. doi: 10.1128/AAC.00436-16

Ly, C. T., Altuntop, M. E., and Wang, Y. (2010). Single-molecule study of viomycin's inhibition mechanism on ribosome translocation. *Biochemistry* 49, 9732–9738. doi: 10.1021/bi101029g

Martin, A., Fahrbach, K., Zhao, Q., and Lodise, T. (2018). Association between carbapenem resistance and mortality among adult, hospitalized patients with serious infections due to *Enterobacteriaceae*: results of a systematic literature review and meta-analysis. *Open Forum Infect. Dis.* 5:ofy150. doi: 10.1093/ofid/ofy150

Metelev, M., Osterman, I. A., Ghilarov, D., Khabibullina, N. F., Yakimov, A., Shabalin, K., et al. (2017). Klebsazolicin inhibits 70S ribosome by obstructing the peptide exit tunnel. *Nat. Chem. Biol.* 13, 1129–1136. doi: 10.1038/nchembio.2462

Nguyen, K. T., He, X., Alexander, D. C., Li, C., Gu, J. Q., Mascio, C., et al. (2010). Genetically engineered lipopeptide antibiotics related to A54145 and daptomycin with improved properties. *Antimicrob. Agents Chemother.* 54:140413. doi: 10.1128/AAC.01307-09

Onaka, H., Mori, Y., Igarashi, Y., and Furumai, T. (2011). Mycolic acid-containing bacteria induce natural-product biosynthesis in *Streptomyces species*. *Appl. Environ. Microbiol.* 77, 400–406. doi: 10.1128/AEM.01337-10

Pantel, L., Florin, T., Dobosz-Bartoszek, M., Racine, E., Sarciaux, M., Serri, M., et al. (2018). Odilorhabdins, antibacterial agents that cause miscoding by binding at a new ribosomal site. *Mol Cell* 70, 83–94. doi: 10.1016/j.molcel.2018.03.001

Parmar, A., Iyer, A., Prior, S. H., Lloyd, D. G., Tze Leng Goh, E., Vincent, C. S., et al. (2017). Teixobactin analogues reveal enduracididine to be non-essential for highly potent antibacterial activity and lipid II binding. *Chem. Sci.* 8:8183. doi: 10.1039/c7sc03241b

Pioletti, M., Schlünzen, F., Harms, J., Zarivach, R., Glühmann, M., Avila, H., et al. (2001). Crystal structures of complexes of the small ribosomal subunit with tetracycline, edeine and IF3. *EMBO J.* 2001:182939. doi: 10.1093/emboj/20.8.1829

Polikanov, Y. S., Aleksashin, N. A., Beckert, B., and Wilson, D. N. (2018). The mechanisms of action of ribosome-targeting peptide antibiotics. *Front. Mol. Biosci.* 5:48. doi: 10.3389/fmolb.2018.00048

Polikanov, Y. S., Szal, T., Jiang, F., Gupta, P., Matsuda, R., Shiozuka, M., et al. (2014). Negamycin interferes with decoding and translocation by simultaneous interaction with rRNA and tRNA. *Mol. Cell* 56, 541–550. doi: 10.1016/j.molcel.2014.09.021

Racine, E., Nordmann, P., Pantel, L., Sarciaux, M., Serri, M., Houard, J., et al. (2018). *In Vitro* and *in Vivo* characterization of NOSO-502, a novel inhibitor of bacterial translation. *Antimicrob. Agents Chemother.* 62:e1016-18. doi: 10.1128/AAC.01016-18

Roy, R. N., Lomakin, I. B., Gagnon, M. G., and Steitz, T. A. (2015). The mechanism of inhibition of protein synthesis by the proline-rich peptide oncocin. *Nat. Struct. Mol. Biol.* 22, 466–469. doi: 10.1038/nsmb.3031

Sader, H. S., Castanheira, M., Streit, J. M., Duncan, L. R., and Flamm, R. K. (2017a). Cefepime-Zidebactam (WCK 5222) activity tested against gram-negative organisms causing bloodstream infections worldwide. *Open Forum Infect. Dis.* 4, S374–S375.

Sader, H. S., Mendes, R. E., Pfaller, M. A., Shortridge, D., Flamm, R. K., and Castanheira, M. (2017b). Antimicrobial activities of aztreonam-avibactam and comparator agents against contemporary (2016) clinical *Enterobacteriaceae* isolates. *Antimicrob. Agents Chemother.* 62:e01856-17. doi: 10.1128/AAC.01856-17

Sarciaux, M., Pantel, L., Midrier, C., Serri, M., Gerber, C., Marcia de Figueiredo, R., et al. (2018). Total synthesis and structure-activity relationships study of odilorhabdins, a new class of peptides showing potent antibacterial activity. *J. Med. Chem.* 61, 7814–7826. doi: 10.1021/acs.jmedchem.8b00790

Schmeing, T. M., Huang, K. S., Strobel, S. A., and Steitz, T. A. (2005). An induced-fit mechanism to promote peptide bond formation and exclude hydrolysis of peptidyl-tRNA. *Nature* 438, 520–524. doi: 10.1038/nature04152

Serio, A. W., Keepers, T., and Krause, K. M. (2019). Plazomicin is active against metallo-β-lactamase-producing *Enterobacteriaceae*. *Open Forum Infect. Dis.* 6:ofz123. doi: 10.1093/ofid/ofz123

Sheu, C. C., Chang, Y. T., Lin, S. Y., Chen, Y. H., and Hsueh, P. R. (2019). Infections caused by carbapenem-resistant *Enterobacteriaceae*: an update on therapeutic options. *Front. Microbiol.* 10:80. doi: 10.3389/fmicb.2019.00080

Stanley, R. E., Blaha, G., Grodzicki, R. L., Strickler, M. D., and Steitz, T. A. (2010). The structures of the anti-tuberculosis antibiotics viomycin and capreomycin bound to the 70S ribosome. *Nat. Struct. Mol. Biol.* 17, 289–293. doi: 10.1038/nsmb.1755

Tacconelli, E., Carrara, E., Savoldi, A., Harbarth, S., Mendelson, M., Monnet, D. L., et al. (2018). Discovery, research, and development of new antibiotics: the WHO priority list of antibiotic-resistant bacteria and tuberculosis. *Lancet Inf. Dis.* 18, 318–327. doi: 10.1016/S1473-3099(17)30753-3

Tanaka, Y., Kasahara, K., Hirose, Y., Murakami, K., Kugimiya, R., and Ochi, K. (2013). Activation and products of the cryptic secondary metabolite biosynthetic gene clusters by rifampin resistance (rpoB) mutations in actinomycetes. *J. Bacteriol.* 195, 2959–2970. doi: 10.1128/JB.00147-13

Tobias, N. J., Wolff, H., Djahanschiri, B., Grundmann, F., Kronenwerth, M., Shi, Y. M., et al. (2017). Natural product diversity associated with the nematode symbionts *Photorhabdus* and *Xenorhabdus*. *Nat. Microbiol.* 2, 1676–1685. doi: 10.1038/s41564-017-0039-9

Trecarichi, E. M., and Tumbarello, M. (2017). Therapeutic options for carbapenem-resistant *Enterobacteriaceae* infections. *Virulence* 8, 470–484. doi: 10.1080/21505594.2017.1292196

Tzouvelekis, L. S., Markogiannakis, A., Psichogiou, M., Tassios, P. T., and Daikos, G. L. (2012). Carbapenemases in *Klebsiella pneumoniae* and other *Enterobacteriaceae*: an evolving crisis of global dimensions. *Clin. Microbiol. Rev.* 25, 682–707. doi: 10.1128/CMR.05035-11

Ueda, K., and Beppu, T. (2017). Antibiotics in microbial coculture. *J. Antibiot.* 70, 361–365. doi: 10.1038/ja.2016.127

van Duin, D., and Doi, Y. (2017). The global epidemiology of carbapenemase-producing *Enterobacteriaceae*. *Virulence* 8, 460–469. doi: 10.1080/21505594.2016.1222343

Wang, L., Pulk, A., Wasserman, M. R., Feldman, M. B., Altman, R. B., Cate, J. H., et al. (2012). Allosteric control of the ribosome by small-molecule antibiotics. *Nat. Struct. Mol. Biol.* 19, 957–963. doi: 10.1038/nsmb.2360

Wilson, D. N. (2009). The A-Z of bacterial translation inhibitors. *Crit. Rev. Biochem. Mol. Biol.* 44, 393–433. doi: 10.3109/10409230903307311

Zhao, M., Lepak, A. J., Marchillo, K., VanHecker, J., and Andes, D. (2018). *In Vivo* pharmacodynamic characterization of a novel odilorhabdin antibiotic, NOSO-502, against *Escherichia coli* and *Klebsiella pneumoniae* in a murine thigh infection model. *Antimicrob. Agents Chemother.* 62:e01067-18. doi: 10.1128/AAC.01067-18

Conflict of Interest: MG is a founder and shareholder of Nosopharm. ER and MG are employees of Nosopharm.

frontiers in Microbiology

ORIGINAL RESEARCH
published: 10 January 2020
doi: 10.3389/fmicb.2019.02928

Mygalin: An Acylpolyamine With Bactericidal Activity

*Abraham Espinoza-Culupú[1,2], Elizabeth Mendes[2], Hector Aguilar Vitorino[3], Pedro Ismael da Silva Jr.[4] and Monamaris Marques Borges[2]**

[1] Ph.D. Program in Biotechnology, University of São Paulo, São Paulo, Brazil, [2] Bacteriology Laboratory, Butantan Institute, São Paulo, Brazil, [3] Institute of Marine and Environmental Technology, University of Maryland Center for Environmental Science, Columbus Center, Baltimore, MD, United States, [4] Laboratory for Applied Toxinology (LETA), Butantan Institute, São Paulo, Brazil

Inappropriate use of antibiotics favors the selection and spread of resistant bacteria. To reduce the spread of these bacteria, finding new molecules with activity is urgent and necessary. Several polyamine analogs have been constructed and used to control microorganisms and tumor cells. Mygalin is a synthetic acylpolyamine, which are analogs of spermidine, derived from the hemolymph of the spider *Acanthoscurria gomesiana*. The effective activity of polyamines and their analogs has been associated with their structure. The presence of two acyl groups in the Mygalin structure may give this molecule a specific antibacterial activity. The aim of this study was to identify the mechanisms involved in the interaction of Mygalin with *Escherichia coli* to clarify its antimicrobial action. The results indicated that Mygalin exhibits intense dose and time-dependent bactericidal activity. Treatment of *E. coli* with this molecule caused membrane rupture, inhibition of DNA synthesis, DNA damage, and morphological changes. The esterase activity increased along with the intracellular production of reactive oxygen species (ROS) after treatment of the bacteria with Mygalin. In addition, this molecule was able to sequester iron and bind to LPS. We have shown that Mygalin has bactericidal activity with underlying mechanisms involving ROS generation and chelation of iron ions that are necessary for bacterial metabolism, which may contribute to its microbicidal activity. Taken together, our data suggest that Mygalin can be explored as a new alternative drug with antimicrobial potential against Gram-negative bacteria or other infectious agents.

Keywords: acylpolyamine, Mygalin, oxidative stress, *E. coli*, antimicrobial, biomolecule

OPEN ACCESS

Edited by:
Adler Ray Dillman, University of California, Riverside, United States

Reviewed by:
Autar Krishen Mattoo, Agricultural Research Service (USDA), United States
Taku Takahashi, Okayama University, Japan

****Correspondence:***
Monamaris Marques Borges
monamaris.borges@butantan.gov.br

Specialty section:
This article was submitted to Antimicrobials, Resistance and Chemotherapy, a section of the journal Frontiers in Microbiology

Received: *12 July 2019*
Accepted: *05 December 2019*
Published: *10 January 2020*

Citation:
Espinoza-Culupú A, Mendes E, Vitorino HA, da Silva PI Jr and Borges MM (2020) Mygalin: An Acylpolyamine With Bactericidal Activity. Front. Microbiol. 10:2928. doi: 10.3389/fmicb.2019.02928

INTRODUCTION

There is a constant need for new antibiotics due to the rapid development of antibiotic resistance. Extensive and prolonged use and inappropriate prescribing of antibiotics favor rapid selection of resistant microorganisms. This resistance is multifactorial but is associated with poor hygiene and often a delay in the diagnosis of bacterial infections. Each year, microorganisms develop sophisticated and complex mechanisms to circumvent the antibiotics in use, resulting

in serious and prolonged life-threatening infections (Laxminarayan et al., 2013). The urgency for developing new antibiotics is evident as infectious diseases are one of the leading causes of mortality worldwide, especially in hospital settings (Fair and Tor, 2014; Ventola, 2015). It is estimated that by 2050, approximately 10 million people will die due to antimicrobial resistance (O'Neil, 2014). The pharmaceutical industry has reduced investments in research on new antibiotics due to economic issues since these companies seek an immediate financial return, and this research is carried out over long periods. Diverse natural products in this therapeutic class have been presented as alternatives for meeting new targets, since such products provide novel and diverse chemicals, aiding in the control of microorganisms (Bush, 2004; Brown and Wright, 2016). Natural polyamines are a group of endogenous cationic compounds that differ in the number of amine groups inserted into the molecule. Putrescine is a diamine, while spermidine and spermine contain three and four amino groups, respectively. The differences in these clusters generate different functions between these molecules and are associated with broad biological functions. These molecules can control cell proliferation and differentiation and regulate protein synthesis and gene expression as they can interact with portions of DNA and RNA (Igarashi and Kashiwagi, 2010), promoting conformational changes in the structure and function of these molecules (Panagiotidis et al., 1995). The largest fraction of polyamines present in eukaryotic cells and *Escherichia coli* was found in complexed RNA (Igarashi and Kashiwagi, 2010). Polyamines also modulate intracellular signals (Huang et al., 2005) and immune functions, depending on their nature (Zhang et al., 1997; Haskó et al., 2000). In addition, these molecules have been shown to bind and alter DNA and RNA (Pegg, 2016). In infections by pathogenic microorganisms, polyamines regulate virulence gene expression (Jelsbak et al., 2012), modify bacterial resistance to oxidative stress (Ha et al., 1998; Chattopadhyay et al., 2003), interfere with biofilm formation (Patel et al., 2006) and response to antibiotics depending on the characteristics of the bacterial structure and the antimicrobial agent (Kwon and Lu, 2007). In *E. coli*, these molecules may control membrane permeability by blocking purine channels (Dela Vega and Delcour, 1996), while synthetic polyamine analogs increase membrane permeability by disruption of LPS integrity (Yasuda et al., 2004). However, the molecular mechanisms involved in these events are mostly unknown. Mygalin is a synthetic molecule originally isolated from hemocytes of the spider *Acanthoscurria gomesiana* and is characterized as a bis-acylpolyamine N1, N8-bis (2,5-dihydroxybenzoyl) spermidine of 417 Da (Pereira et al., 2007). This molecule also does not promote cytotoxicity of murine splenocytes and interferes with innate immunity (Mafra et al., 2012). Polyamines play an important role in the pathogenesis and control of some infections (Blanchet et al., 2016) and evidence suggests an association between the structure and microbicidal activity of some polyamine analogs (Balakrishna et al., 2006). Our aim was to analyze the mechanisms involved in the microbicidal activity of Mygalin using *E. coli* as a model to explore the potential of this compound for the development of a new alternative antibiotic.

MATERIALS AND METHODS

Chemicals and Reagents

Antibiotics (ciprofloxacin, gentamicin, and ampicillin), 2,5-dihydroxybenzoic acid (gentisic acid), spermidine, HBTU, EDTA, DNTB, DAPI, propidium iodide (PI), carboxyfluorescein diacetate assay (CFDA), Triton X-100, LPS from *E. coli* serotype:0111:B4 and agarose were purchased from Sigma Chemical Co. (St. Louis, MO, United States), and CM-H2DCFDA was purchased from Thermo Fisher Scientific (Waltham, MA, United States).

Synthesis of Mygalin

Mygalin was synthesized at the Center for Research on Toxins, Immune-Response and Cell Signaling (CeTICS – CEPID), Laboratory for Applied Toxinology (LETA) – Butantan Institute and provided by Dr. Pedro Ismael da Silva Jr. Mygalin was synthesized according to the classical method of peptide chemistry (Atherton, 1989). Briefly, the synthesis was carried out in HBTU solution (Knorr et al., 1989) for the esterification of the carboxyl group of gentisic acid and thus permitting the formation of one carboxamide by formal condensation of two primary amino groups from spermidine with a carboxylic group of two molecules of gentisic acid (2,5-dihydroxybenzoic acid). Data is available on the Ontology of Chemical Entities of Biological Interest (ChEBI) database as Mygalin (CHEBI:64901) (EBI, 2014).

Bacterial Strain, Culture Condition and Antibacterial Assay

All tests were performed with *E. coli* DH5α. The bacterial culture was grown at 37°C using 10 mL of Luria-Bertani broth (Kasetty et al., 2011) in a shaker incubator at 180 rpm, and 100 μL of culture grown overnight was reinoculated in 20 mL of Luria-Bertani broth and allowed to grow to the initial log phase OD_{620} of 0.3 (10^8 cells/mL). Then, 10^5 cells/mL were diluted 1:10 in 100 μL of M9 (minimal medium). The antimicrobial activity of the drugs was determined in 96-well microplates containing serial dilutions of Mygalin. The plates were then incubated in a shaker incubator at 180 rpm at 37°C and were protected from light, and the minimum inhibitory concentration (MIC) was determined after 18 h. H_2O_2 was used as the positive control of the reaction. Plates were prepared in triplicate, and light was excluded during the experiments. To assess the intrinsic property of Mygalin, 10^7 cells/mL were individually treated with two concentrations of Mygalin and H_2O_2 (0.5 and 1 mM), 1 mM spermidine and 2,5-dihydroxybenzoic acid in PBS at 37°C for 18 h (Kumar et al., 2011).

Cell Viability Assay With Resazurin-Assay and CFU Definition

Bacterial viability was determined by two methods: counting the colony forming units (CFU) and the resazurin test (Riss et al., 2004; Sarker et al., 2007). For the resazurin test, plates containing 10^4 cells/mL were incubated at 37°C and protected from light for 18 h, and 20 μL of resazurin solution (0.2 mg/mL) was added

thereafter. The reaction was incubated for 2 h, and the color change was monitored (blue, indicating non-viable and purple or pink, indicating viable) and measured at 550 and 595 nm.

Mechanism of Action of Mygalin Against *E. coli*

To study the mechanism of action of Mygalin, we examined the action against DNA, membrane integrity, protein synthesis, ROS generation and ferrous ion-chelating activity.

DNA Oxidative Damage

Bacterial DNA damage was evaluated by two different methods: using pure DNA from *E. coli* DH5α incubated with the drug (*in vitro* effects) and DNA isolated from drug-treated bacteria (*in vivo* effects). The reaction product was analyzed by alkaline electrophoresis gel (Drouin et al., 1996).

In vitro Assay

For this assay, the DNA was purified using the Wizard® Genomic DNA Purification Kit. To assess the effect of pH on the drug activity against purified bacterial DNA, 1 μg of DNA was incubated for 2 h with Mygalin or spermidine (0.25; 0.5 and 1 mM) in buffers with different pH values (citrate pH 3.6, phosphate, pH 7.2 and bicarbonate-carbonate, pH 10.6). As a positive control of DNA damage, the Fenton reaction was used, where 1 μL of FeSO4 (1 mM), 1 μL of 2% v/v H_2O_2, and 3 μL of Milli-Q water were mixed in a total reaction volume of 15 μL (Cheng et al., 2013). In another assay, to rule out the presence of DNases in the samples, Mygalin was treated with DNase inhibitors such as sodium citrate (100 mM) and EDTA (100 mM) (Kolarevic et al., 2014) or subjected to physical damage by heating at 75°C for 15 min and incubate with 1 μg of DNA. To assess the effect of spermidine on the protection of DNA the reaction was incubated for 2 h with spermidine (0.5 and 1 mM) and Mygalin (0.25; 0.5 and 1 mM). The treated DNA was used as a template to amplify the ICD (Isocitrate dehydrogenase) house-keeping gene using the primers F: 5′-ATGGAAAGTAAAGTAGTTGTTCCGGCACA-3′ and R 5′-GGACGCAGCAGGATCTGTT-3′ (Wirth et al., 2006). After treatment, equal amounts of DNA or PCR products were mixed with alkaline charge buffer, loaded into a 1% agarose gel under alkaline conditions at 70 V, and then stained with gelRed™ (Biotinun). All DNA images were obtained with an electronic documentation system (UVITEC, Cambridge).

In vivo Assay

Bacteria in the exponential growth phase (10^6 CFU/mL) were incubated with Mygalin (0.5 and 1 mM), spermidine (1 mM) or H_2O_2 (0.5 and 1 mM) at 37°C for 5 and 18 h. After the incubation, the cultures were centrifuged at 13,000 rpm. The pellet was washed once with PBS, and DNA was isolated with the Wizard® Genomic DNA Purification Kit. Equal amounts of DNA sample were mixed with alkaline buffer as described above.

In another assay, to visualize DNA fragmentation, bacterial cultures treated for 18 h with Mygalin or H_2O_2 were permeabilized with ethanol and stained with DAPI. These samples were fixed on a slide with 1% agarose and visualized by confocal microscopy (Kumar et al., 2011).

Inhibitory Effect of Mygalin on DNA Synthesis as Determined by Filamentation Assay

The inhibitory effect of Mygalin on DNA synthesis was evaluated by the *E. coli* filamentation assay described by Alfred et al. (2013) with a slight modification. Log phase bacteria (10^8 cells/mL) were cultured at 37°C in M9 medium and treated with Mygalin (0.5 mM) or ciprofloxacin (0.5 mM) for 3 h. A total of 20 μL of the sample was placed on a glass slide, air-dried and stained with Gram staining. The cells were visualized by light microscopy (1000×). All assays were performed in triplicate.

Action on Membrane Integrity and Esterase Activity in *E. coli*

To evaluate the damage caused by Mygalin to the cell membrane, *E. coli* (10^8 CFU/mL) were cultured with Mygalin (0.5 mM) or ampicillin (0.5 mM) for 5 h and then washed and suspended in 50 mM phosphate buffer, pH 7.0. Then, the bacteria were incubated with PI at a final concentration of 60 μM and kept in the dark for 15 min (Nocker et al., 2011). Then, 20 μL of sample was added to a slide with 1% agarose, the slide was covered with a coverslip, and the membrane integrity was analyzed by confocal microscopy. For the esterase activity assay, untreated bacteria and those treated with the drugs for 4 h were washed once in PBS and suspended in 50 mM phosphate buffer. A total of 180 μL of bacterial suspension was placed on black COSTAR® 96-well microplates with the addition of 20 μL of CFDA (250 μM). The samples were incubated for 30 min in the dark, and fluorescence was measured at 485/535 nm excitation/emission wavelengths (Nocker et al., 2011; Hyldgaard et al., 2015).

Determination of Reactive Oxygen Species (ROS)

For this assay, one milliliter of *E. coli* (10^6 cells/mL) obtained in the exponential growth phase was washed with PBS and resuspended in 1 mL of 50 mM phosphate buffer. The mixtures were treated or not treated with Mygalin (0.25 and 0.5 mM) or H_2O_2 (0.25, 0.5, and 1 mM) for 15 min at room temperature. After that, CM-H2DCFDA (1 μM) was added. Subsequently, 100 μL of the bacteria were transferred to black 96-well microplates (Dong et al., 2015), and the fluorescence was measured every 30 min using a PerkinElmer Victor 3™ 1420 Multilabel Counter Fluorometer with 485/535 nm excitation/emission wavelengths.

Mygalin-LPS Interactions

The LPS from *E. coli* serotype: 0111: B4 was prepared in water endotoxin-free, and 50 μL of LPS solution (10, 20, 40, 80,160, 320, and 640 ng/mL) was incubated with a fixed concentration of Mygalin (500 μM) for 1 h at 37°C. The interaction between Mygalin and LPS was determined by monitoring the change in the absorbance of Mygalin, using 2 μL of each sample in a NanoVue Plus™ spectrophotometer (GE Healthcare Life

Science) with a Pathlength of 0.5 mm. The plates containing the samples were prepared in triplicate, and light was excluded during the experiments. The blank was endotoxin-free water (Lakshminarayanan et al., 2016).

Glutathione (GSH) Levels and Protein Profile

Escherichia coli (10^9 cells/mL) were treated with Mygalin, ciprofloxacin, and gentamicin for 18 h, then centrifuged at 13,000 rpm for 5 min, thoroughly washed three times with PBS. Next, the cells were resuspended in 250 μL of lysis buffer (25 mM Tris–HCl, pH 7.5, 100 mM NaCl, 2.5 mM EDTA, 20 mM NaF, 1 mM Na3VO4, 0.5% Triton X-100 and 1 mM PMSF). The cells were sonicated on ice for five cycles of 20 s at 50 W power and allowed to rest for 1 min on the HD 2070 ultrasonic homogenizer. The cell lysate suspension was centrifuged at 4°C and 14,000 rpm for 10 min. The recovered supernatant was used to quantify the protein level using a Pierce™ BCA Protein Assay Kit (Thermo Scientific, Waltham, MA, United States). To measure glutathione (GSH) levels, Ellman's reagent was used (Ellman, 1959); 25 μg of protein was added into 96-well microplates containing 50 μL of solution (50 nM GR, 50 mM Tris–HCl (pH 7.5), 200 μM NADPH, 1 mM EDTA, 1 mM DTNB) (Zou et al., 2017). The plates were read after 15 min of incubation at room temperature at 412 nm. The GSH levels were estimated after determination of the protein levels. Cell lysates were placed in SDS gel loading buffer at 90°C for 10 min and then separated with 10% polyacrylamide gel electrophoresis (SDS-PAGE), as described by Laemmli (1970). Equal amounts of protein were loaded per lane. Protein separation was performed at 4°C for 1.5 h at 100 V in a Hoefer miniVE (Amersham Biosciences). Proteins were visualized by Coomassie Blue Staining.

Ferrous Ion-Chelating Activity

The ferrous ion-chelating activity of Mygalin was investigated according to Baccan et al. (2012) and Vitorino et al. (2015) with ferric nitrilotriacetate. Fe(NTA) was prepared by the titration of 70 mM NTA to pH 7.0 with NaOH, followed by the addition of solid FAS (ferric ammonium sulfate) to attain a final iron concentration of 20 mM, and the solution was heated in a water bath for 1 h. Aliquots of 10 μL of 2 μM Fe(NTA) in HBS/Chelex were transferred to a flat, transparent 96-well microplate and treated with 10 μL of Mygalin (0–1000 μM), followed by 180 μL of a mixture of 50 μM DHR and ascorbic acid (40 μM) in Milli-Q water. The kinetic curve was registered with excitation/emission wavelengths of 485/520 nm at 25°C for 40 min. The slopes (F min^{-1}, where F stands for arbitrary fluorescence units), calculated from 15–40 min, were then plotted against the chelator concentration. The experiment was conducted in quadruplicate.

Statistical Analysis

All results were analyzed using Student's *t*-test and one-way ANOVA, and the difference between groups was determined by the Tukey–Kramer test or Dunnett's multiple comparisons analyzed by the GraphPad Prism 7 program (Graph Pad, San Diego, California). The data were considered statistically significant at $p < 0.05$, and the results represent the mean and standard error of the mean (±SEM) from at least three independent experiments.

RESULTS

Chemical Structure of Mygalin and Effect of Mygalin on *E. coli* Viability

To explore the microbicidal activity of Mygalin, the *E. coli* DH5α model was used. **Figure 1A** shows the chemical structure of Mygalin (Pereira et al., 2007) compared with spermidine including the presence of two acyl groups, which can be used to differentiate between these molecules. To evaluate the effect of Mygalin on *E. coli* viability (**Figure 1B**), a fixed number of bacteria were treated for 6 and 18 h, and the number of colonies formed (CFU) was counted on LB agar plates after 6 and 24 h of incubation. Bacterial treatment for 6 h reduced the bacterial viability (CFU) compared to the control containing spermidine and gentisic acid, both used for Mygalin synthesis. The reduction was more apparent over 18 h of treatment with 0.5 mM Mygalin treatment showing greater effects than 1 mM H_2O_2, which was used as a positive control. The specificity of the reaction was confirmed since the treatment with spermidine or gentisic acid had no effect on the viability of the bacteria, with CFU values similar to the control without treatment.

Interaction of Mygalin With DNA

In vitro Model

Polyamines bind to nucleic acids, causing their condensation (Feuerstein et al., 1991). Since Mygalin is an acylpolyamine analog of spermidine, this led us to study DNA as its first target. Initially, we evaluated whether pH influences the action of Mygalin against bacterial DNA. Three buffers with different pH values (3.6, 7, and 10.6) were used to dilute the Mygalin. We confirmed, using alkaline electrophoresis gel, that the effect of Mygalin (0.25–1 mM) includes oxidative DNA damage (**Figure 2A**). This effect occurred in a variable pH range from acidic to alkaline, as highlighted in the figure (red box). The same assay performed with spermidine (**Figure 2B**) did not cause any DNA damage. The Fenton reaction was used as a positive control of DNA damage (yellow box). We observed that this reaction was neutralized, differing from that observed with Mygalin at the alkaline pH (**Figures 2A,B**). Another assay was performed to rule out the presence of external DNase (**Figure 3A**), it was shown that the addition of the DNase inhibitor did not alter the DNA damage caused by Mygalin, unlike the DNA samples treated with DNases alone. This result indicates that the breakdown of DNA was caused by treatment with Mygalin. **Figure 3B**, shows that the addition of spermidine (0.5 and 1 mM) protected DNA samples treated with Mygalin at doses below 0.5 mM. However, this effect was not observed with Mygalin (1 mM) or the Fenton reaction (positive control), confirming that high concentrations of Mygalin causes irreversible damage.

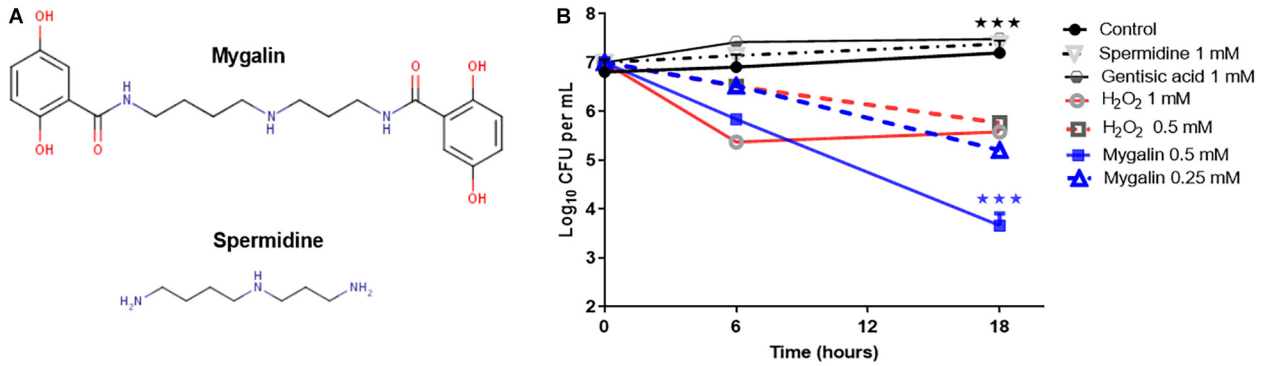

FIGURE 1 | Structure of Mygalin and time-killing curves for *Escherichia coli* DH5α. **(A)** Structural difference between Mygalin and spermidine. **(B)** Bacteria (10^7 CFU/mL) were grown in M9 medium and diluted to 10^3 in 100 μL, as described in the section "M&M," then incubated at 37°C for 6 and 18 h with or without the indicated concentrations of Mygalin (0.5 and 0.25 mM), spermidine (1 mM), gentisic acid (1 mM), and H_2O_2 (0.5 and 1 mM). Viable cell counts were determined by measuring the number of colony forming units (CFU) after 24 h. Data represent ±SEM of three independent experiments (***$p < 0.001$).

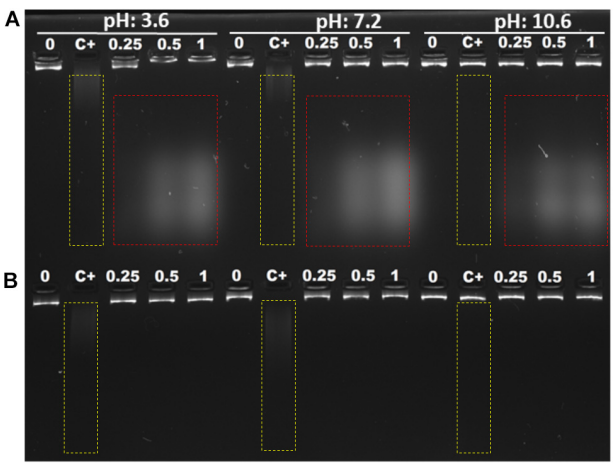

FIGURE 2 | Interaction of *E. coli* genomic DNA with Mygalin and spermidine. A total of 1 μg of DNA was incubated with different amounts of Mygalin **(A)** and spermidine **(B)** (0.25, 0.5, and 1 mM) in three buffers: citrate buffer, pH: 3.6; phosphate buffer, pH: 7.2; and bicarbonate-carbonate buffer, pH: 10.6 at 37°C for 2 h. The reaction mixtures were applied to 1% alkaline agarose gel and stained with gelRed™. The positive control of DNA damage was FeSO4 + H_2O_2, the integrity of DNA was analyzed in agarose gels, and the images were acquired using an electronic documentation system (UVITEC, Cambridge). The figure is representative of two independent experiments with similar results.

In vivo Model

To further examine the ability of Mygalin to promote DNA damage, we used viable bacteria obtained in the exponential phase of growth to confirm the effect of previous *in vitro* assays. Bacteria were cultured with Mygalin (0.5 and 1 mM) for 5 and 18 h and later washed with PBS, and the pellet was used to extract the genomic DNA. The DNA was analyzed by electrophoresis under alkaline conditions (**Figure 4**). After 5 h incubation with Mygalin, there was a marked reduction in genomic DNA, which accentuated at 18 h, when DNA was no longer visualized. In bacteria treated with the same concentration of H_2O_2, the effect was less pronounced, while spermidine did not cause any DNA damage. This confirms the previous data from *in vitro* assays, showing that the treatment of *E. coli* with Mygalin promotes DNA damage differing from that observed with spermidine.

DNA Labeling After Treatment With Mygalin

DAPI is a fluorescent dye that selectively binds DNA to form a strong fluorescent DNA-DAPI complex with high specificity. When DAPI is intercalated into cellular DNA, it fluoresces and DAPI has been widely used to evaluate DNA structural damage. This approach was used to confirm the bacterial DNA damaging effects of Mygalin. In this assay, bacteria treated with or without Mygalin (0.5 mM) or H_2O_2 as a positive control were permeabilized and stained with DAPI and analyzed by confocal microscopy. **Figure 5** shows that untreated bacteria (**Figure 5A**) were completely stained, demonstrating the integrity of the DNA. However, those treated with either Mygalin (**Figure 5B**) or H_2O_2 (**Figure 5C**) did not show extensive staining due to DAPI not being intercalated with the double strand of the damaged DNA. These data reinforce the idea that Mygalin causes oxidative damage in bacterial DNA.

Inhibition of DNA Synthesis *in vivo* by Mygalin Using *E. coli* Filamentation Assay

Another approach used to determine the interference of this compound on *E. coli* DNA was inhibition of DNA synthesis using the filamentation assay (Alfred et al., 2013). To test if Mygalin uses this system, the bacteria were treated for 3 h with 0.5 mM of Mygalin (**Figure 6B**) or ciprofloxacin (**Figure 6C**) as a positive control and their morphology and filament formation were compared with those of untreated cells (**Figure 6A**) by light microscopy (**Figure 6**). The results showed that treatment with Mygalin or ciprofloxacin interfered with cell division, resulting in long bacterial filaments when compared to untreated cells. These

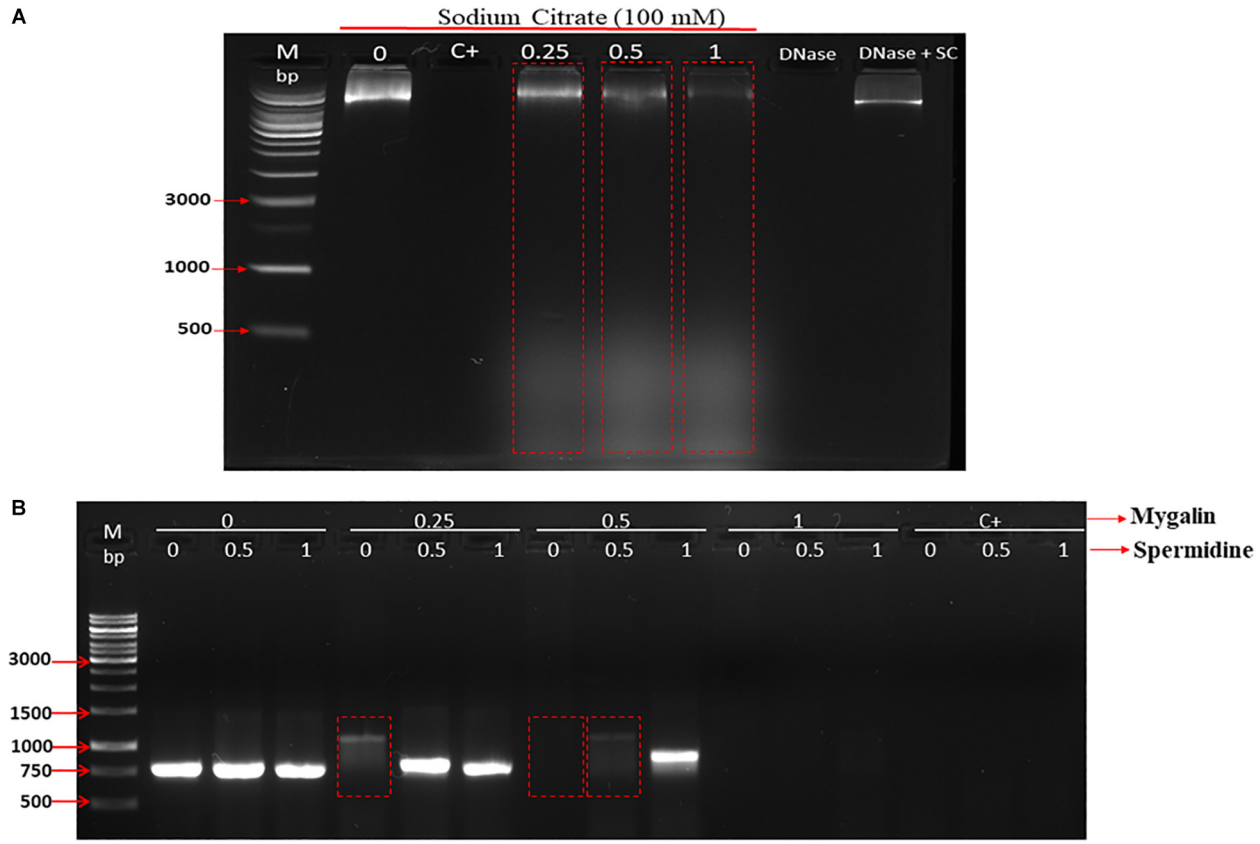

FIGURE 3 | Effect of addition of DNase inhibitor and spermidine protection on oxidative damage: **(A)** Gel electrophoresis, of DNA treated with Mygalin (0.25, 0.5, and 1 mM) in the presence of the DNase inhibitor (sodium citrate 100 mM). Controls: untreated DNA (0), Fenton reaction (C+), sodium citrate (SC). **(B)** PCR of Mygalin-treated DNA (0.25, 0.5, and 1 mM) plus spermidine (0.5 and 1 mM). Controls: untreated DNA (0), Fenton reaction (C+), Ladder Gene Ruler 1 Kb (M).

results indicate that Mygalin and ciprofloxacin can bind to DNA, inhibiting DNA synthesis *in vivo*.

Action of Mygalin on Cell Membrane and Esterase Activity

In addition to DNA damage, antimicrobial drugs can act on several other mechanisms, including disrupting the cell membrane (Epand et al., 2016). To test the effect of Mygalin on the *E. coli* membrane, bacteria were cultured for 5 h in the absence (a) or presence of 0.5 mM of Mygalin (b) or 0.5 mM of ampicillin (c) and a PI uptake assay was used to measure membrane permeability changes under confocal microscopy (**Figure 7A**). The results indicate that untreated bacteria were impermeable to PI, while *E. coli* treated with Mygalin or ampicillin showed PI uptake, visualized as cells with red staining. This suggests that Mygalin can promote cell membrane rupture in *E. coli*. To monitor this membrane change, the intracellular esterase activity was assayed using the CFDA. If the membrane breaks, fluorochrome diffuses into the cells being cleaved, and a highly fluorescent product is released that corresponds to esterase activity (Hong et al., 2015). The treatment of *E. coli* for 4 h with 0.25 and 0.5 mM of Mygalin increased the dose-dependent esterase level, which was four times higher than that of the untreated control, while ampicillin (0.25 mM) increased the activity more than ten-fold. These results confirm that Mygalin damages the bacterial cell membrane (**Figure 7B**).

Effect of Mygalin on the Glutathione Level and Protein Profile in *E. coli*

Glutathione has several functions, including a role in the metabolism of peroxides, inactivation of free radicals, and maintenance of oxidation-reduction potential, in addition to participating in reactions involving the synthesis of proteins (Smirnova and Oktyabrsky, 2005). We evaluated whether Mygalin could act on other molecular targets such as proteins; for this, we quantified the levels of GSH in *E. coli* following treatment with Mygalin, ciprofloxacin or gentamicin. Treatment with Mygalin and ciprofloxacin produced similar results, reducing the GSH level by 17%. However, GSH was more markedly reduced with gentamicin, with a reduction of approximately 50% (**Figure 8A**). Due to the low reduction in GSH levels with Mygalin, the influence of this molecule on protein profile expression was investigated (**Figure 8B**). There were no significant differences in the protein profile between untreated bacteria (1) or bacteria treated with Mygalin (2) or ciprofloxacin (3). However, with

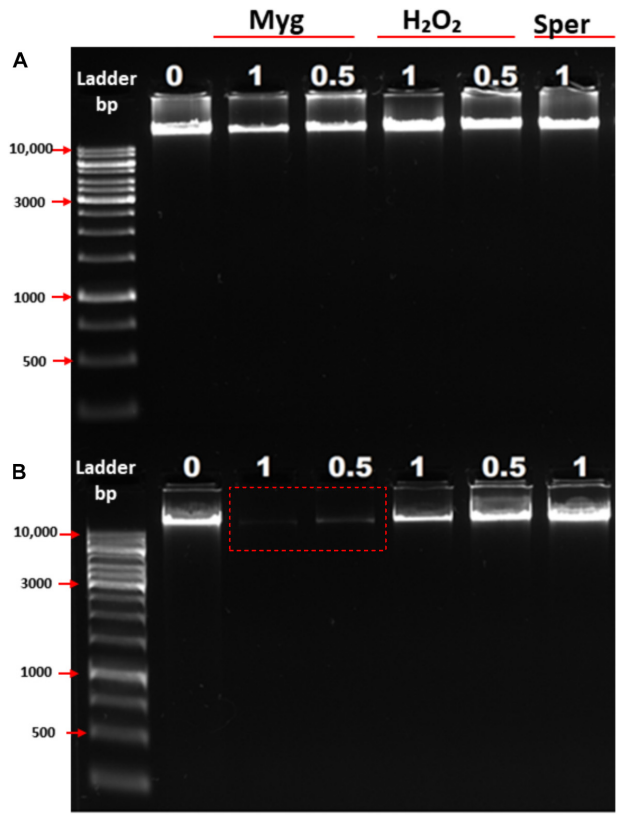

FIGURE 4 | Effect of Mygalin, hydrogen peroxide and spermidine on the integrity of *E. coli* DNA. Bacteria (10^6 CFU/mL) in the log phase were treated with or without 0.5 and 1 mM of Mygalin, H_2O_2 or spermidine (1 mM) for 5 **(A)** and 18 h **(B)** at 37°C. DNA was isolated using the Wizard® Genomic DNA Purification Kit. DNA samples (1 μL) from each group were analyzed in 1% alkaline agarose gel and stained with gelRed™. Myg = Mygalin, Sper = spermidine, H_2O_2 = hydrogen peroxide. The figure is representative of three independent experiments with similar results.

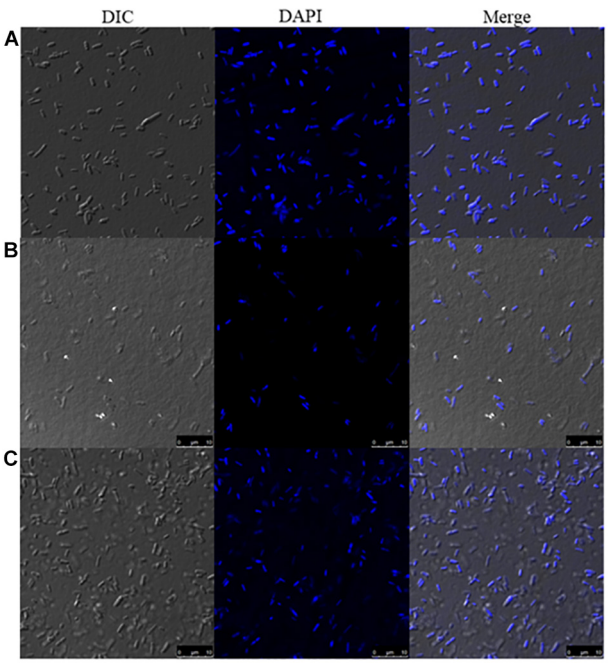

FIGURE 5 | Confocal microscopy of Mygalin-treated *E. coli* stained with DAPI or subjected to DNA fragmentation. Bacteria (10^6 CFU/mL) untreated **(A)** or treated for 18 h with **(B)** Mygalin (0.5 mM) or **(C)** H_2O_2 (0.5 mM) as a control were permeabilized with ethanol and stained with DAPI (3 μM). Confocal microscopy was used to visualize DNA fragmentation. DIC = Differential Interference Contrast.

gentamicin (4), the protein profile and GSH levels were as previously described. These data suggest that the microbicidal effect of Mygalin involves, in addition to the generation of ROS, other mechanisms already common to antibiotics, since GSH reduction is associated with ROS generation (Belenky et al., 2015).

Contribution of Mygalin to ROS Generation

The results of this study showed that Mygalin altered the permeability of the *E. coli* membrane, causing DNA damage. The intrinsic mechanisms used by this molecule to cause *E. coli* death are unknown. One of the common mechanisms of bacterial death caused by antibiotics is the oxidative damage generated by free radicals derived from oxygen, known as ROS (Kohanski et al., 2010). Thus, we investigated whether treatment of *E. coli* with Mygalin induced ROS generation (**Figure 9**). Bacteria were grown to the exponential phase, and Mygalin (0.25 and 0.5 mM) or H_2O_2 control (0.25–1 mM) was added to the cultures. ROS production was monitored for 210 min by reading the fluorescence after adding the fluorophore CM-H2DCFDA (Dong et al., 2015). As shown, the addition of Mygalin to *E. coli* cultures progressively increased the level of ROS between 60 and 210 min of incubation, regardless of the concentration used. These levels were higher than those of the H_2O_2 (0.25–1 mM) treatment. These data suggest that one of the possible mechanisms used by Mygalin to promote DNA damage and death of *E. coli* is the generation of intracellular ROS. Similar results were obtained with *E. coli* treated with norfloxacin and ampicillin (Dwyer et al., 2014) using the same fluorophore.

Interaction of Mygalin With LPS

Mygalin exerts microbicidal activity against Gram-negative bacteria only (Pereira et al., 2007), which contain LPS as their main component with major biological activity. It was previously shown that polyamine analogs can neutralize LPS *in vitro* (Miller et al., 2005). Based on this, 0.5 mM Mygalin was incubated with LPS, and the available free Mygalin level was analyzed by spectrophotometry (**Figure 10**). The incubation of Mygalin with LPS caused a reduction in the absorbance as a function of the increase in the LPS concentration, indicating an interaction between the molecules. Similar results were described with peptides incubated with LPS (Lakshminarayanan et al., 2016; Sinha et al., 2017). Our data suggest that Mygalin may interact

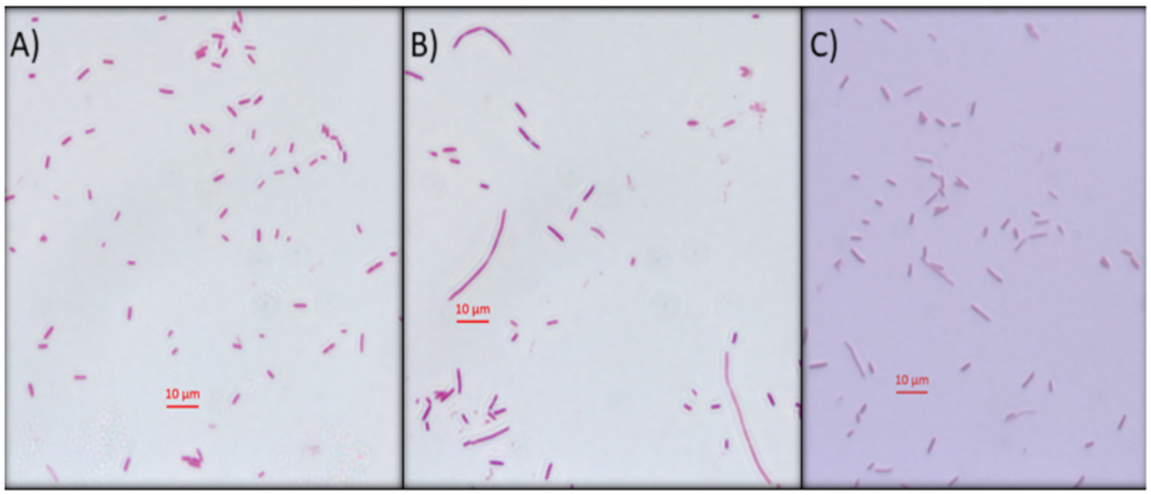

FIGURE 6 | *Escherichia coli* filamentation assay as indicative of DNA inhibition by Mygalin. **(A)** Untreated *E. coli* (10^6 CFU/mL) or **(B)** *E. coli* (10^6 CFU/mL) treated for 3 h with 0.5 mM of Mygalin **(B)** or ciprofloxacin **(C)** were stained by Gram stain. Light microscopy (magnification 1000×) was used for cell division and filament formation analysis. Scale 10 µm.

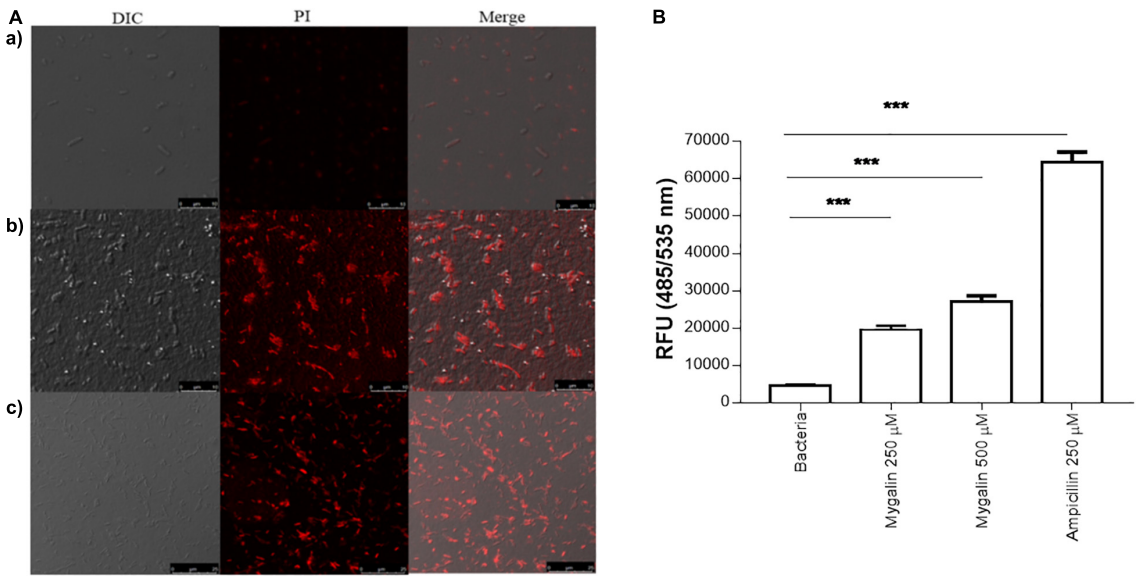

FIGURE 7 | Effect of Mygalin on membrane integrity measured by propidium iodide uptake and esterase activity of *E. coli*. **(A)** Propidium iodide uptake. **(a)** Untreated *E. coli* (10^8 CFU/mL) or *E. coli* treated with 0.5 mM Mygalin or **(b)** 0.5 mM ampicillin **(c)** as a positive control were incubated for 5 h at 37°C, fixed in agarose and observed by confocal microscopy. Bacteria in red are indicative of dead or membrane-damaged cells. **(B)** Effect of Mygalin on the esterase activity of *E. coli*. Bacteria (10^8 CFU/mL) were treated with Mygalin (250 and 500 µM) or ampicillin (250 µM) for 4 h and stained with CFDA. The fluorescence intensity was read at 485/535 nm. The results represent the fluorescence intensity and are reported as relative fluorescence units (RFU). Data represent ±SEM of three independent experiments (***$p < 0.001$).

with LPS, and this would justify its action only against Gram-negative rather than Gram-positive bacteria.

Analysis of the Iron Chelating Activity of Mygalin

The fact that Mygalin is a ROS generating molecule and has structural similarity with siderophore H4-4-LICAM (Raines et al., 2013) suggests that this molecule can function as an iron chelator. Under physiological conditions, labile Fe can generate ROS in the presence of low concentrations of ascorbate. We investigated whether Mygalin could have iron chelating activity because iron is one of the most important metals and is involved in the process of oxidative stress (Halliwell and Gutteridge, 1984). Bacteria were treated with Mygalin (0–1000 µM) followed by the addition of the DHR

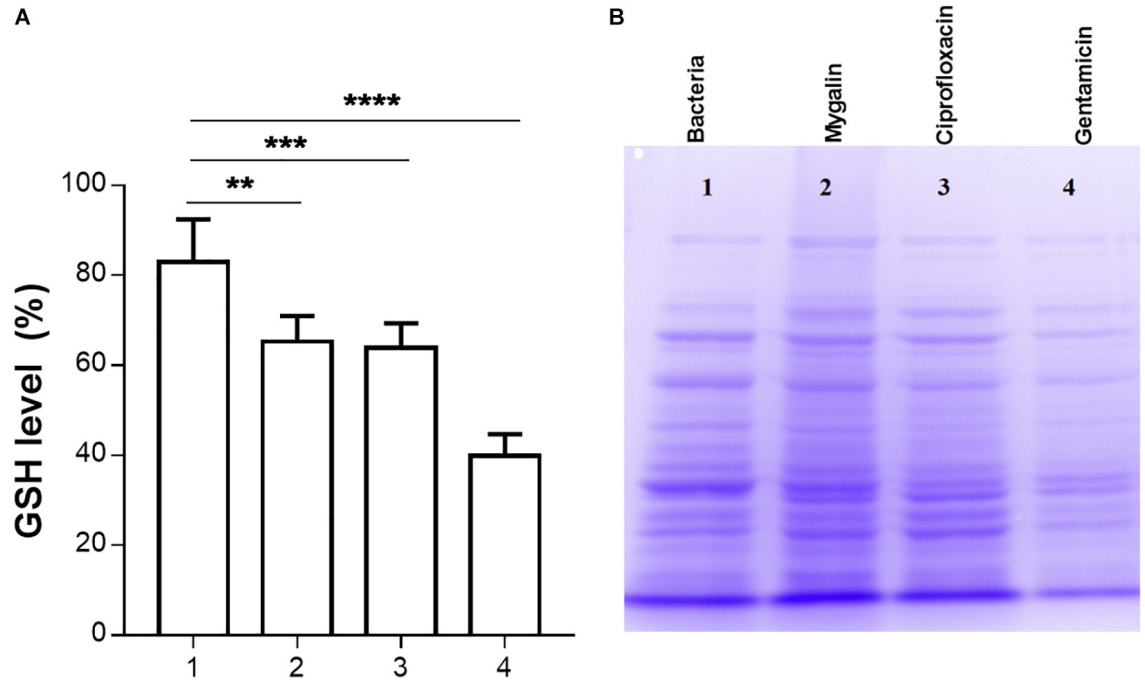

FIGURE 8 | Effect of Mygalin on intracellular GSH levels and protein profile. Bacteria (10^9 CFU/mL) were treated or not treated for 18 h, sonicated and centrifuged and the supernatant was used to measure intracellular GSH and perform protein profile analysis. **(A)** GSH was determined in untreated *E. coli* lysate (1) or that treated with 0.5 mM Mygalin (2), ciprofloxacin (3) or gentamicin (4). GSH levels were defined after the comparison between the control and treated groups using the DTNB reduction assay. **(B)** Electrophoretic protein profile (SDS-PAGE) from the *E. coli* lysate supernatant exposed to the treatments mentioned above. Proteins were visualized by Coomassie brilliant blue staining. Data represent ±SEM of three independent experiments. Statistical significance using Dunnett's multiple comparisons test comparing untreated and treated groups. $^{**}p < 0.01$ and $^{***}p < 0.001$.

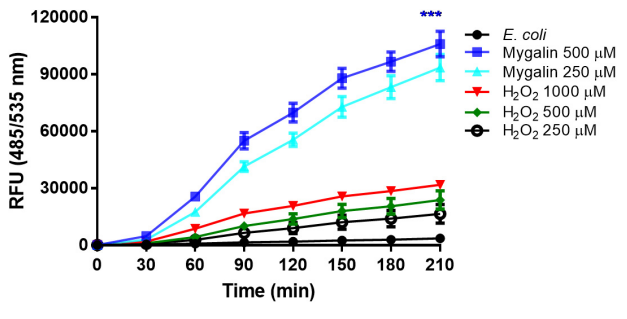

FIGURE 9 | Influence of Mygalin on intracellular ROS generation. The presence of ROS in *E coli* (10^6 CFU/mL) due to treatment with Mygalin (250 and 500 μM) or H_2O_2 (0.25, 0.5, and 1 mM), as a positive control, was studied by measuring the fluorescence of CM-H2DCFDA after 15 min of treatment. RFU = Relative Fluorescence Units. These data represent the mean (±SEM) of three independent experiments ($^{***}p < 0.001$).

probe. When the chelator binds to the metal, ROS generation is interrupted, decreasing DHR oxidation. We observed that the addition of increasing concentrations of Mygalin (0–1000 μM) to the system reduced the oxidation of DHR (**Figure 11B**), which was reflected in the reduction of the spectrum absorption of this molecule due to its association with Fe (**Figure 11A**).

DISCUSSION

Bacterial drug resistance is a concerning public health problem. The World Health Organization (World Health Organization [WHO], 2001) has encouraged research into the search for new drugs and vaccines to increase the effectiveness of treatment and reduce resistance to antibiotics. It is necessary to find new therapeutic strategies by combining products or defining new target molecules with microbicidal activity. Polyamines participate in the control of virulence genes in microorganisms but have been neglected regarding their bactericidal activity. Several polyamine analogs were constructed, showing significant effector activity alone or in combination with other drugs against tumors (Nair et al., 2007) and bacteria resistant to antibiotics (Blanchet et al., 2016). However, the contribution of analogs to the control of infections is limited. We explored the mechanisms involved in the microbicidal activity of Mygalin using the *E. coli* model *in vitro* as a strategy to evaluate the use of antimicrobial agents. Synthetic Mygalin results from the association of spermidine with gentisic acid, having two acyl groups in its structure. Individually, none of these compounds showed bactericidal activity. This suggests that the microbicidal activity could be attributed to the acyl group present in the structure of Mygalin. This effect was dose-dependent and started after 5 h of contact and was stronger than that of 1 mM H_2O_2. Studies relating the activity and structure of spermine analogs

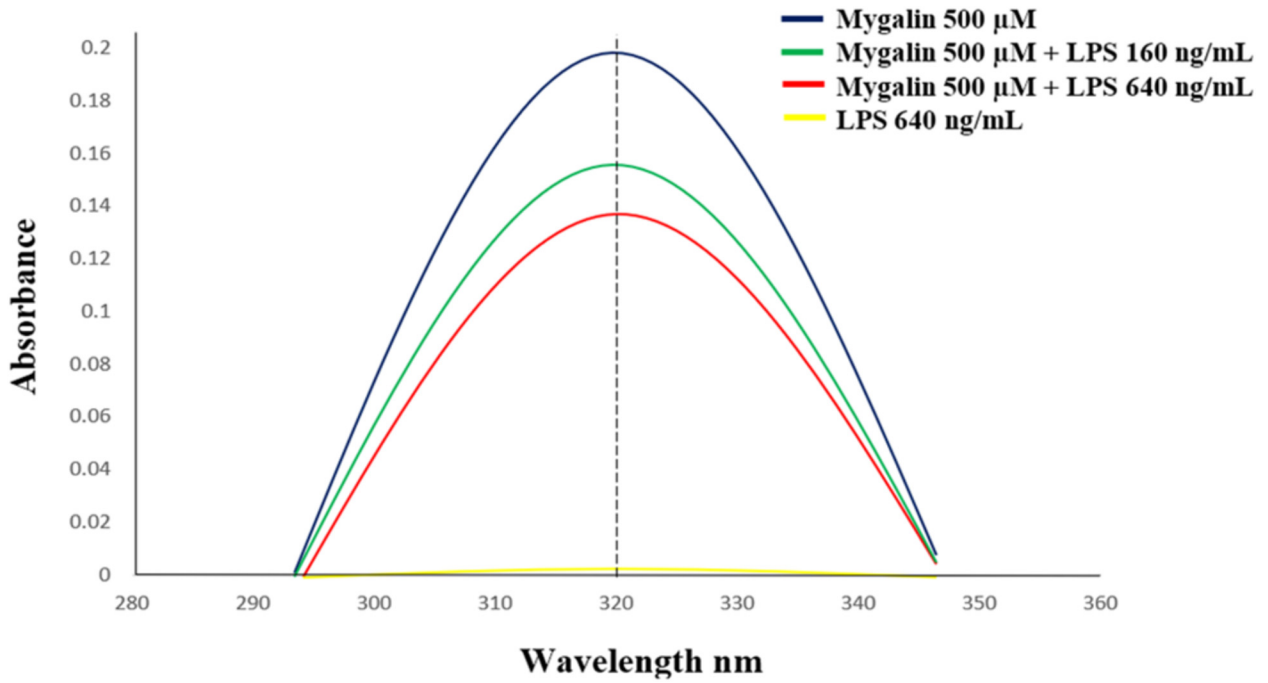

FIGURE 10 | Interaction between Mygalin and LPS. The Mygalin (500 µM)-LPS (160–640 ng/mL) interaction assay was performed after incubation for 1 h at 37°C. The change in absorbance of Mygalin (320 nm) was monitored using a NanoVue Plus™ spectrophotometer according to M&M. A decrease in absorbance intensity in LPS-Mygalin compared to Mygalin alone indicated binding to LPS. The figure is representative of three independent experiments with similar results.

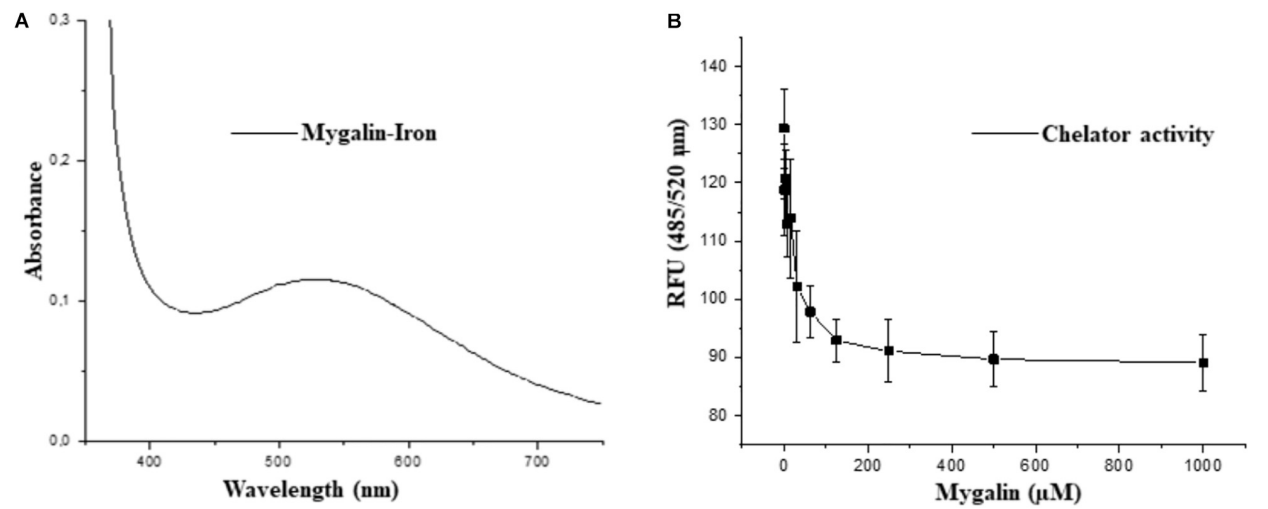

FIGURE 11 | Iron-chelating activity of Mygalin. **(A)** UV-Vis spectrum of 5 mM iron II-Mygalin in water at 25°C after 24 h. Spectrum shows a maximum wavelength at 524 nm. **(B)** The chelating effect of Mygalin (0–1000 µM) on the rate of dihydrorhodamine hydrochloride (DHR) oxidation catalyzed by iron/ascorbate in water at 25°C. The kinetics curve was recorded on a fluorometer with 485/520 nm excitation/emission wavelengths at 25°C for 40 min. The results are the average of quadruplicates. RFU = Relative Fluorescence Units. The figure is representative of three independent experiments with similar results.

have shown a strong relationship between acyl chain length and antimicrobial potency, suggesting that these analogs could be used to improve the effectiveness of conventional antibiotics (Balakrishna et al., 2006). One of the mechanisms of action of bactericidal drugs is DNA damage due to their fragmentation or protein interaction activities (Kohanski et al., 2007, 2010). The vast majority of the effects of polyamines are associated with their interaction with DNA and RNA (Igarashi and Kashiwagi, 2010). The effect of Mygalin on DNA fragmentation was investigated, and our *in vitro* and *in vivo* data showed that the treatment of genomic or purified DNA from a bacterial culture with Mygalin promoted DNA breakdown. This effect was independent of the

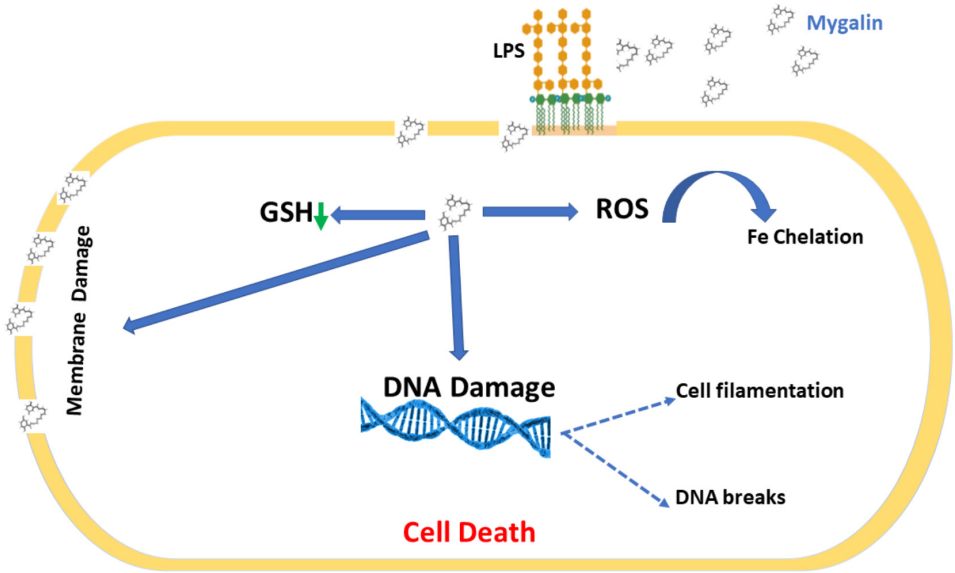

FIGURE 12 | Proposed mechanism for Mygalin action. Mygalin binds to LPS in the outer cell membrane of Gram-negative bacteria; this leads to the rupture of the cell membrane and entry of the drug into the cell, which induces the production of intracellular ROS in the initial hours of cell contact. This leads to the breakdown of bacterial DNA, preventing cell division and inducing bacterial death.

pH used in the reactions. In contrast, spermidine did not induce any DNA damage, proving its protective effect (Douki et al., 2000; von Deutsch et al., 2005) and anti-oxidant activity (Tkachenko and Fedotova, 2007; Terui et al., 2018). This shows that both molecules have distinct effects in relation to their action on DNA. The degradation of DNA caused by the treatment of bacteria with Mygalin was independent of DNase since the addition of the enzyme inhibitors did not alter the DNA damage caused by Mygalin. Treatement of *E. coli* with antibiotics promotes oxidative stress and spermidine reduces this effect (Tkachenko et al., 2012), therefore it was analyzed whether this effect could occur when DNA was treated with Mygalin. Our data showed that the addition of spermidine protected DNA samples treated with Mygalin at doses below 0.5 mM. However, this effect did not occur with Mygalin (1 mM) or in the Fenton reaction (positive control), confirming that high concentrations of Mygalin cause irreversible DNA damage. Antimicrobial drugs, as well as antibiotics, have several mechanisms of action (Epand et al., 2016). Factors that influence bacterial viability, such as alteration of cell permeability, release of intracellular components, inactivation of metabolic pathways, inhibition of bacterial growth by chelation of nutrients and metals (Kohanski et al., 2010), were explored to identify the action of Mygalin against *E. coli*. We observed by confocal microscopy that bacteria treated with Mygalin or H_2O_2 incorporated DAPI dye, showing that this acylpolyamine can induce DNA damage. In another analysis, the ability of Mygalin to disrupt the cellular membranes of *E. coli* was evidenced since the treated bacteria incorporated PI, similar to that visualized with ampicillin. DNA damage has been described in the treatment of bacteria with antibiotics (Kohanski et al., 2010), toxic metals (Espirito Santo et al., 2011) and antimicrobial peptides (Farkas et al., 2017; Diaz-Roa et al., 2019), which led to bacterial death. Inhibition of DNA synthesis was confirmed by light microscopy (Alfred et al., 2013) during the treatment of *E. coli* with Mygalin and ciprofloxacin, a high bacterial stress-inducing antibiotic (Goswami et al., 2006). This treatment interfered with the cell division cycle of the bacteria and induced the formation of filamentous bacteria. Before *E. coli* divides, several proteins are organized for "Z-ring" assembly, including the FtsZ protein (filament-forming protein), which is essential for cell division and viability of *E. coli* (Addinall et al., 1996). Studies suggest that FtsZ assembly inhibition can be used for the development of drugs against pathogenic bacteria (Wang et al., 2003), as proposed by Rai et al. (2008), who used curcumin to inhibit *Bacillus subtilis* cell division by disrupting the "Z-ring." Future investigations will be conducted to analyze whether Mygalin also utilizes this mechanism. The esterase enzyme is involved in both ester hydrolysis and lipid peroxidation. An increased esterase level is an indication of drug-induced cell membrane and DNA damage. Treatment of *E. coli* with Mygalin increased fluorescence emission in a dose-dependent manner similar to ampicillin. Therefore, Mygalin can break up the *E. coli* outer membrane, facilitating DNA damage. GSH is essential for redox system regulation and protection against oxidative stress in all cells. The presence of antioxidant mechanisms is necessary to limit the intracellular levels of these compounds. GSH reductase is one of the systems that controls free radical formation and oxidative damage to protect cells against environmental stress (Smirnova and Oktyabrsky, 2005). We observed a slight reduction in GSH reductase levels during the treatment of *E. coli* with Mygalin, without altering the protein profile. This differed from the results of gentamicin treatment, in which there was intense reduction of enzyme and protein profile change in relation to those of the control. Therefore, in addition

to Mygalin breaking down the cell membrane and promoting DNA damage, this drug also alters the synthesis of enzymes that participate in the control of oxidative stress in *E. coli*. High levels of free radicals in the intracellular environment can contribute to all of these forms of damage. The presence of intracellular ROS in cells due to treatment with Mygalin was confirmed. There was an intense increase in the level of ROS, which was greater than that observed with 1 μM H_2O_2 and proportional to incubation time. Our results indicated that Mygalin promotes DNA damage and the death of *E. coli* through the generation of high intracellular ROS levels, which may contribute to the damage found in previous tests. These considerations support the involvement of ROS in Mygalin-induced *E. coli* death as with certain antibiotics (Dwyer et al., 2014). Previous tests conducted in our laboratory showed that the addition of catalase, thiourea or spermidine to Mygalin-treated *E. coli* cultures recovered bacterial viability by 80% (manuscript in preparation), confirming the importance of the ROS mechanism in *E. coli* death. Experiments with other strains and species of bacteria are being performed in our laboratory to confirm that Mygalin treatment and ROS generation is a common mechanism for killing other bacteria. It was suggested that the microbicidal effect of Mygalin extends to Gram-negative bacteria only (Pereira et al., 2007). LPS is the predominant structural component of the outer membrane of Gram-negative bacteria and is responsible for the death of patients with septic shock in addition to causing intense inflammatory activity (Raetz and Whitfield, 2002). The possible interaction of Mygalin with LPS showed that there was an interaction between these two molecules, partially explaining its action against Gram-negative bacteria. Other drugs, such as curcumin and antimicrobial peptides, have the same ability to interact with LPS, reducing their activity (Lakshminarayanan et al., 2016; Sinha et al., 2017). The presence of chelating metals can interfere with *E. coli* metabolism, leading to its death. The ability of Mygalin to sequester important nutrients for bacterial metabolism was analyzed, and we found a dose-dependent reduction in oxidation of the DRH probe. This means that Mygalin can sequester iron and alter *E. coli* metabolism. The chemical structure of Mygalin resembles that of siderophores. These compounds have the function of solubilizing and capturing iron II for use in bacterial metabolism. A new polyamine, Vulnibactin, which contains siderophore activity, was isolated from *Vibrio vulnificus* by Okujo et al. (1994). This polyamine has two acyl groups similar to Mygalin. This evidence indicates that an increase in intracellular ROS in *E. coli* and reduced iron bioavailability may contribute to Mygalin-induced *E. coli* death. In conclusion, we describe some effector mechanisms of Mygalin, an acylpolyamine, as a new molecule with a microbicidal effect against *E. coli* DH5α. The mechanism of action involves bacterial membrane permeability changes, DNA damage, and ROS generation. In addition, Mygalin chelates iron and binds to LPS. Our data showed that the increase in intracellular ROS associated with iron sequestration and DNA damage in response to Mygalin treatment may be responsible for the death of *E. coli*. Taken together, our data suggest that Mygalin must be explored as a new alternative drug with antimicrobial potential against Gram-negative bacteria and other infectious agents. Based on our results, we propose a mechanism of action of Mygalin, as shown in **Figure 12**. Studies are underway to confirm these effects and the consequences of this oxidative stress on other bacterial groups and biofilm formation. The most interesting point of this study is that this molecule does not promote cytotoxicity in eukaryotic cells and may interfere with the innate immune response, another aspect that is being explored.

DATA AVAILABILITY STATEMENT

The raw data supporting the conclusions of this article will be made available by the authors, without undue reservation, to any qualified researcher.

AUTHOR CONTRIBUTIONS

AE-C, PS, and MB carried out the study design, conducted the study, and wrote the manuscript. EM and HV helped with the experiments.

FUNDING

This work was supported by the São Paulo Research Foundation (FAPESP) Grants No. 2013/11212-9 and 2014/04307-6, FAPESP/CeTICS – Grant No. 2013/07467-1, the Brazilian National Council for Scientific and Technological Development (CNPq) – Grant No. 472744/2012-7 and the Ph.D. Scholarship by CONCYTEC-FONDECYT Institution of Peruvian State (N092-2016), and the Butantan Foundation.

ACKNOWLEDGMENTS

We are grateful for the collaboration of Dr. Breno Esposito (Institute of Chemistry of USP), Dr. Maristela Camargo (Institute of Biomedical Sciences/USP) for the suggestions, and Dr. Alexandre Seixas de Souza (Laboratory of Cellular Biology, Butantan Institute) for support with photos taken with the confocal microscope LSM: Confocal TCS SP8, Leica, Germany.

REFERENCES

Addinall, S. G., Bi, E., and Lutkenhaus, J. (1996). FtsZ ring formation in fts mutants. *J. Bacteriol.* 178, 3877–3884. doi: 10.1128/jb.178.13.3877-3884.1996

Alfred, R. L., Palombo, E. A., Panozzo, J. F., and Bhave, M. (2013). The antimicrobial domains of wheat puroindolines are cell-penetrating peptides with possible intracellular mechanisms of action. *PLoS One* 8:e75488. doi: 10.1371/journal.pone.0075488

Atherton, E. (1989). *Solid Phase Peptide Synthesis: A Practical Approach*. Oxford: Oxford University Press.

Baccan, M. M., Chiarelli-Neto, O., Pereira, R. M. S., and Espósito, B. P. (2012). Quercetin as a shuttle for labile iron. *J. Inorg. Biochem.* 107, 34–39. doi: 10.1016/j.jinorgbio.2011.11.014

Balakrishna, R., Wood, S. J., Nguyen, T. B., Miller, K. A., Kumar, E. S., Datta, A., et al. (2006). Structural correlates of antibacterial and membrane-permeabilizing activities in acylpolyamines. *Antimicrob. Agents Chemother.* 50, 852–861. doi: 10.1128/AAC.50.3.852-861.2006

Belenky, P., Jonathan, D. Y., Porter, C. B., Cohen, N. R., Lobritz, M. A., Ferrante, T., et al. (2015). Bactericidal antibiotics induce toxic metabolic perturbations that lead to cellular damage. *Cell Rep.* 13, 968–980. doi: 10.1016/j.celrep.2015.09.059

Blanchet, M., Borselli, D., and Brunel, J. M. (2016). Polyamine derivatives: a revival of an old neglected scaffold to fight resistant gram-negative bacteria? *Future Med. Chem.* 8, 963–973. doi: 10.4155/fmc-2016-0011

Brown, E. D., and Wright, G. D. (2016). Antibacterial drug discovery in the resistance era. *Nature* 529, 336–343. doi: 10.1038/nature17042

Bush, K. (2004). Antibacterial drug discovery in the 21st century. *Clin. Microbiol. Infect.* 10, 10–17. doi: 10.1111/j.1465-0691.2004.1005.x

Chattopadhyay, M. K., Tabor, C. W., and Tabor, H. (2003). Polyamines protect *Escherichia coli* cells from the toxic effect of oxygen. *Proc. Natl. Acad. Sci. U.S.A.* 100, 2261–2265. doi: 10.1073/pnas.2627990100

Cheng, N., Wang, Y., Gao, H., Yuan, J., Feng, F., Cao, W., et al. (2013). Protective effect of extract of Crataegus pinnatifida pollen on DNA damage response to oxidative stress. *Food Chem. Toxicol.* 59, 709–714. doi: 10.1016/j.fct.2013.07.015

Dela Vega, A. L., and Delcour, A. H. (1996). Polyamines decrease *Escherichia coli* outer membrane permeability. *J. Bacteriol.* 178, 3715–3721. doi: 10.1128/jb.178.13.3715-3721.1996

Diaz-Roa, A., Espinoza-Culupu, A., Torres-Garcia, O., Borges, M. M., Avino, I. N., Alves, F. L., et al. (2019). Sarconesin II, a new antimicrobial peptide isolated from sarconesiopsis magellanica excretions and secretions. *Molecules* 24:E2077. doi: 10.3390/molecules24112077

Dong, T. G., Dong, S., Catalano, C., Moore, R., Liang, X., and Mekalanos, J. J. (2015). Generation of reactive oxygen species by lethal attacks from competing microbes. *Proc. Natl. Acad. Sci. U.S.A.* 112, 2181–2186. doi: 10.1073/pnas.1425007112

Douki, T., Bretonniere, Y., and Cadet, J. (2000). Protection against radiation-induced degradation of DNA bases by polyamines. *Radiat. Res.* 153, 29–35. doi: 10.1667/0033-7587(2000)153%5B0029:parido%5D2.0.co;2

Drouin, R., Gao, S., and Holmquist, G. P. (1996). "Agarose gel electrophoresis for DNA damage analysis," in *Technologies for Detection of DNA Damage and Mutations*, ed. G. P. Pfeifer (Boston, MA: Springer US), 37–43. doi: 10.1007/978-1-4899-0301-3_3

Dwyer, D. J., Belenky, P. A., Yang, J. H., Macdonald, I. C., Martell, J. D., Takahashi, N., et al. (2014). Antibiotics induce redox-related physiological alterations as part of their lethality. *Proc. Natl. Acad. Sci. U.S.A.* 111, E2100–E2109. doi: 10.1073/pnas.1401876111

EBI, (2014). *mygalin (CHEBI:64901)*. Available: https://www.ebi.ac.uk/chebi/chebiOntology.do;jsessionid%20%20%20%20%20%20%20=B1BFCEEC37C25C521045F2ECC47DCEA6?chebiId=64901 (accessed May 11, 2019).

Ellman, G. L. (1959). Tissue sulfhydryl groups. *Arch. Biochem. Biophys.* 82, 70–77. doi: 10.1016/0003-9861(59)90090-6

Epand, R. M., Walker, C., Epand, R. F., and Magarvey, N. A. (2016). Molecular mechanisms of membrane targeting antibiotics. *Biochim. Biophys. Acta Biomembr.* 1858, 980–987. doi: 10.1016/j.bbamem.2015.10.018

Espirito Santo, C., Lam, E. W., Elowsky, C. G., Quaranta, D., Domaille, D. W., Chang, C. J., et al. (2011). Bacterial killing by dry metallic copper surfaces. *Appl. Environ. Microbiol.* 77, 794–802. doi: 10.1128/AEM.01599-10

Fair, R. J., and Tor, Y. (2014). Antibiotics and bacterial resistance in the 21st century. *Perspect. Med. Chem.* 6, 25–64. doi: 10.4137/PMC.S14459

Farkas, A., Maróti, G., Kereszt, A., and Kondorosi, É (2017). Comparative analysis of the bacterial membrane disruption effect of two natural plant antimicrobial peptides. *Front. Microbiol.* 8:51. doi: 10.3389/fmicb.2017.00051

Feuerstein, B. G., Williams, L. D., Basu, H. S., and Marton, L. J. (1991). Implications and concepts of polyamine-nucleic acid interactions. *J. Cell. Biochem.* 46, 37–47. doi: 10.1002/jcb.240460107

Goswami, M., Mangoli, S. H., and Jawali, N. (2006). Involvement of reactive oxygen species in the action of ciprofloxacin against *Escherichia coli*. *Antimicrob. Agents Chemother.* 50, 949–954. doi: 10.1128/aac.50.3.949-954.2006

Ha, H. C., Sirisoma, N. S., Kuppusamy, P., Zweier, J. L., Woster, P. M., and Casero, R. A. (1998). The natural polyamine spermine functions directly as a free radical scavenger. *Proc. Natl. Acad. Sci. U.S.A.* 95, 11140–11145. doi: 10.1073/pnas.95.19.11140

Halliwell, B., and Gutteridge, J. M. (1984). Oxygen toxicity, oxygen radicals, transition metals and disease. *Biochem. J.* 219, 1–14. doi: 10.1042/bj2190001

Haskó, G., Kuhel, D. G., Marton, A., Nemeth, Z. H., Deitch, E. A., and Szabó, C. (2000). Spermine differentially regulates the production of interleukin-12 p40 and interleukin-10 and suppresses the release of the T helper 1 cytokine interferon-gamma. *Shock* 14, 144–149. doi: 10.1097/00024382-200014020-00012

Hong, J., Guan, W., Jin, G., Zhao, H., Jiang, X., and Dai, J. (2015). Mechanism of tachyplesin I injury to bacterial membranes and intracellular enzymes, determined by laser confocal scanning microscopy and flow cytometry. *Microbiol. Res.* 170, 69–77. doi: 10.1016/j.micres.2014.08.012

Huang, Y., Pledgie, A., Casero, R. A. Jr., and Davidson, N. E. (2005). Molecular mechanisms of polyamine analogs in cancer cells. *Anticancer. Drugs* 16, 229–241. doi: 10.1097/00001813-200503000-00002

Hyldgaard, M., Mygind, T., Piotrowska, R., Foss, M., and Meyer, R. L. (2015). Isoeugenol has a non-disruptive detergent-like mechanism of action. *Front. Microbiol.* 6:754. doi: 10.3389/fmicb.2015.00754

Igarashi, K., and Kashiwagi, K. (2010). Modulation of cellular function by polyamines. *Int. J. Biochem. Cell Biol.* 42, 39–51. doi: 10.1016/j.biocel.2009.07.009

Jelsbak, L., Thomsen, L. E., Wallrodt, I., Jensen, P. R., and Olsen, J. E. (2012). Polyamines are required for virulence in *Salmonella enterica* serovar *Typhimurium*. *PLoS One* 7:e36149. doi: 10.1371/journal.pone.0036149

Kasetty, G., Papareddy, P., Kalle, M., Rydengard, V., Morgelin, M., Albiger, B., et al. (2011). Structure-activity studies and therapeutic potential of host defense peptides of human thrombin. *Antimicrob. Agents Chemother.* 55, 2880–2890. doi: 10.1128/aac.01515-10

Knorr, R., Trzeciak, A., Bannwarth, W., and Gillessen, D. (1989). New coupling reagents in peptide chemistry. *Tetrahedron Lett.* 30, 1927–1930. doi: 10.1016/S0040-4039(00)99616-3

Kohanski, M. A., Dwyer, D. J., and Collins, J. J. (2010). How antibiotics kill bacteria: from targets to networks. *Nat. Rev. Microbiol.* 8, 423–435. doi: 10.1038/nrmicro2333

Kohanski, M. A., Dwyer, D. J., Hayete, B., Lawrence, C. A., and Collins, J. J. (2007). A common mechanism of cellular death induced by bactericidal antibiotics. *Cell* 130, 797–810. doi: 10.1016/j.cell.2007.06.049

Kolarevic, A., Yancheva, D., Kocic, G., and Smelcerovic, A. (2014). Deoxyribonuclease inhibitors. *Eur. J. Med. Chem.* 88, 101–111. doi: 10.1016/j.ejmech.2014.07.040

Kumar, A., Pandey, A. K., Singh, S. S., Shanker, R., and Dhawan, A. (2011). Engineered ZnO and TiO(2) nanoparticles induce oxidative stress and DNA damage leading to reduced viability of *Escherichia coli*. *Free Radic. Biol. Med.* 51, 1872–1881. doi: 10.1016/j.freeradbiomed.2011.08.025

Kwon, D.-H., and Lu, C.-D. (2007). Polyamine effects on antibiotic susceptibility in bacteria. *Antimicrob. Agents Chemother.* 51, 2070–2077. doi: 10.1128/aac.01472-06

Laemmli, U. K. (1970). Cleavage of structural proteins during the assembly of the head of bacteriophage T4. *Nature* 227, 680–685. doi: 10.1038/227680a0

Lakshminarayanan, R., Tan, W. X., Aung, T. T., Goh, E. T., Murugananthan, N., Li, J., et al. (2016). Branched peptide, B2088, disrupts the supramolecular organization of lipopolysaccharides and sensitizes the gram-negative bacteria. *Sci. Rep.* 6:25905. doi: 10.1038/srep25905

Laxminarayan, R., Duse, A., Wattal, C., Zaidi, A. K. M., Wertheim, H. F. L., Sumpradit, N., et al. (2013). Antibiotic resistance—the need for global solutions. *Lancet Infect. Dis.* 13, 1057–1098. doi: 10.1016/S1473-3099(13)70318-9

Mafra, D. G., da Silva, P. I. Jr, Galhardo, C. S., Nassar, R., Daffre, S., Sato, M. N., et al. (2012). The spider acylpolyamine Mygalin is a potent modulator of innate immune responses. *Cell Immunol.* 275, 5–11. doi: 10.1016/j.cellimm.2012.04.003

Miller, K. A., Suresh Kumar, E. V., Wood, S. J., Cromer, J. R., Datta, A., and David, S. A. (2005). Lipopolysaccharide sequestrants: structural correlates of activity and toxicity in novel acylhomospermines. *J. Med. Chem.* 48, 2589–2599. doi: 10.1021/jm049449j

Nair, S. K., Verma, A., Thomas, T. J., Chou, T. C., Gallo, M. A., Shirahata, A., et al. (2007). Synergistic apoptosis of MCF-7 breast cancer cells by 2-methoxyestradiol and bis(ethyl)norspermine. *Cancer Lett.* 250, 311–322. doi: 10.1016/j.canlet.2006.10.027

Nocker, A., Caspers, M., Esveld-Amanatidou, A., Van Der Vossen, J., Schuren, F., Montijn, R., et al. (2011). Multiparameter viability assay for stress profiling applied to the food pathogen Listeria monocytogenes F2365. *Appl. Environ. Microbiol.* 77, 6433–6440. doi: 10.1128/AEM.00142-11

Okujo, N., Saito, M., Yamamoto, S., Yoshida, T., Miyoshi, S., and Shinoda, S. (1994). Structure of vulnibactin, a new polyamine-containing siderophore from *Vibrio vulnificus*. *Biometals* 7, 109–116. doi: 10.1007/BF00140480

O'Neil, J. (2014). *Antimicrobial Resistance: Tackling a Crisis for the Health and Wealth of Nations*. London: Review on Antimicrobial Resistance.

Panagiotidis, C. A., Artandi, S., Calame, K., and Silverstein, S. J. (1995). Polyamines alter sequence-specific DNA-protein interactions. *Nucleic Acids Res.* 23, 1800–1809. doi: 10.1093/nar/23.10.1800

Patel, C. N., Wortham, B. W., Lines, J. L., Fetherston, J. D., Perry, R. D., and Oliveira, M. A. (2006). Polyamines are essential for the formation of plague biofilm. *J. Bacteriol.* 188, 2355–2363. doi: 10.1128/JB.188.7.2355-2363.2006

Pegg, A. E. (2016). Functions of polyamines in mammals. *J. Biol. Chem.* 291, 14904–14912. doi: 10.1074/jbc.R116.731661

Pereira, L. S., Silva, P. I., Miranda, M. T. M., Almeida, I. C., Naoki, H., Konno, K., et al. (2007). Structural and biological characterization of one antibacterial acylpolyamine isolated from the hemocytes of the spider *Acanthocurria gomesiana*. *Biochem. Biophys. Res. Commun.* 352, 953–959. doi: 10.1016/j.bbrc.2006.11.128

Raetz, C. R. H., and Whitfield, C. (2002). Lipopolysaccharide endotoxins. *Annu. Rev. Biochem.* 71, 635–700. doi: 10.1146/annurev.biochem.71.110601.135414

Rai, D., Singh, J. K., Roy, N., and Panda, D. (2008). Curcumin inhibits FtsZ assembly: an attractive mechanism for its antibacterial activity. *Biochem. J.* 410, 147–155. doi: 10.1042/BJ20070891

Raines, D. J., Moroz, O. V., Wilson, K. S., and Duhme-Klair, A.-K. (2013). Interactions of a periplasmic binding protein with a tetradentate siderophore mimic. *Angew. Chem. Int. Ed.* 52, 4595–4598. doi: 10.1002/anie.201300751

Riss, T. L., Moravec, R. A., Niles, A. L., Duellman, S., Benink, H. A., Worzella, T. J., et al. (2004). "Cell viability assays," in *Assay Guidance Manual*, eds G. S. Sittampalam, N. P. Coussens, K. Brimacombe, A. Grossman, M. Arkin, D. Auld, et al. (Rockville: Bethesda).

Sarker, S. D., Nahar, L., and Kumarasamy, Y. (2007). Microtitre plate-based antibacterial assay incorporating resazurin as an indicator of cell growth, and its application in the in vitro antibacterial screening of phytochemicals. *Methods* 42, 321–324. doi: 10.1016/j.ymeth.2007.01.006

Sinha, S., Zheng, L., Mu, Y., Ng, W. J., and Bhattacharjya, S. (2017). Structure and interactions of a host defense antimicrobial peptide thanatin in lipopolysaccharide micelles reveal mechanism of bacterial cell agglutination. *Sci. Rep.* 7:17795. doi: 10.1038/s41598-017-18102-6

Smirnova, G. V., and Oktyabrsky, O. N. (2005). Glutathione in bacteria. *Biochemistry* 70, 1199–1211. doi: 10.1007/s10541-005-0248-3

Terui, Y., Yoshida, T., Sakamoto, A., Saito, D., Oshima, T., Kawazoe, M., et al. (2018). Polyamines protect nucleic acids against depurination. *Int. J. Biochem. Cell Biol.* 99, 147–153. doi: 10.1016/j.biocel.2018.04.008

Tkachenko, A. G., Akhova, A. V., Shumkov, M. S., and Nesterova, L. Y. (2012). Polyamines reduce oxidative stress in *Escherichia coli* cells exposed to bactericidal antibiotics. *Res. Microbiol.* 163, 83–91. doi: 10.1016/j.resmic.2011.10.009

Tkachenko, A. G., and Fedotova, M. V. (2007). Dependence of protective functions of *Escherichia coli* polyamines on strength of stress caused by superoxide radicals. *Biochemistry* 72, 109–116. doi: 10.1134/S0006297907010130

Ventola, C. L. (2015). The antibiotic resistance crisis: part 1: causes and threats. *P T* 40, 277–283.

Vitorino, H. A., Mantovanelli, L., Zanotto, F. P., and Esposito, B. P. (2015). Iron metallodrugs: stability, redox activity and toxicity against *Artemia salina*. *PLoS One* 10:e0121997. doi: 10.1371/journal.pone.0121997

von Deutsch, A. W., Mitchell, C. D., Williams, C. E., Dutt, K., Silvestrov, N. A., Klement, B. J., et al. (2005). Polyamines protect against radiation-induced oxidative stress. *Gravit. Space Biol. Bull.* 18, 109–110.

Wang, J., Galgoci, A., Kodali, S., Herath, K. B., Jayasuriya, H., Dorso, K., et al. (2003). Discovery of a small molecule that inhibits cell division by blocking FtsZ, a novel therapeutic target of antibiotics. *J. Biol. Chem.* 278, 44424–44428. doi: 10.1074/jbc.M307625200

Wirth, T., Falush, D., Lan, R., Colles, F., Mensa, P., Wieler, L. H., et al. (2006). Sex and virulence in *Escherichia coli*: an evolutionary perspective. *Mol. Microbiol.* 60, 1136–1151. doi: 10.1111/j.1365-2958.2006.05172.x

World Health Organization [WHO], (2001). *WHO Global Strategy For Containment of Antimicrobial Resistance*. Geneva: WHO.

Yasuda, K., Ohmizo, C., and Katsu, T. (2004). Mode of action of novel polyamines increasing the permeability of bacterial outer membrane. *Int. J. Antimicrob. Agents* 24, 67–71. doi: 10.1016/j.ijantimicag.2004.01.006

Zhang, M., Caragine, T., Wang, H., Cohen, P. S., Botchkina, G., Soda, K., et al. (1997). Spermine inhibits proinflammatory cytokine synthesis in human mononuclear cells: a counterregulatory mechanism that restrains the immune response. *J. Exp. Med.* 185, 1759–1768. doi: 10.1084/jem.185.10.1759

Zou, L., Lu, J., Wang, J., Ren, X., Zhang, L., Gao, Y., et al. (2017). Synergistic antibacterial effect of silver and ebselen against multidrug-resistant Gram-negative bacterial infections. *EMBO Mol. Med.* 9, 1165–1178. doi: 10.15252/emmm.201707661

Conflict of Interest: The authors declare that the research was conducted in the absence of any commercial or financial relationships that could be construed as a potential conflict of interest.

frontiers in Microbiology

ORIGINAL RESEARCH
published: 21 February 2020
doi: 10.3389/fmicb.2020.00270

Potent Chimeric Antimicrobial Derivatives of the *Medicago truncatula* NCR247 Symbiotic Peptide

Sándor Jenei[1†], Hilda Tiricz[1†], János Szolomájer[2], Edit Tímár[1], Éva Klement[3], Mohamad Anas Al Bouni[1], Rui M. Lima[1], Diána Kata[4], Mária Harmati[3], Krisztina Buzás[3,5], Imre Földesi[4], Gábor K. Tóth[2,6], Gabriella Endre[1] and Éva Kondorosi[1]**

[1] Institute of Plant Biology, Biological Research Centre, Szeged, Hungary, [2] Department of Medical Chemistry, University of Szeged, Szeged, Hungary, [3] Institute of Biochemistry, Biological Research Centre, Szeged, Hungary, [4] Department of Laboratory Medicine, University of Szeged, Szeged, Hungary, [5] Department of Oral Biology and Experimental Dental Research, University of Szeged, Szeged, Hungary, [6] MTA-SZTE Biomimetic Systems Research Group, University of Szeged, Szeged, Hungary

OPEN ACCESS

Edited by:
David Clarke, University College Cork, Ireland

Reviewed by:
Dennis Ken Bideshi, California Baptist University, United States
Jose María Vinardell, University of Seville, Spain

***Correspondence:**
Gabriella Endre
endre.gabriella@brc.hu
Éva Kondorosi
kondorosi.eva@brc.hu;
eva.kondorosi@gmail.com

[†] *These authors have contributed equally to this work*

Specialty section:
This article was submitted to Antimicrobials, Resistance and Chemotherapy, a section of the journal Frontiers in Microbiology

Received: *15 November 2019*
Accepted: *06 February 2020*
Published: *21 February 2020*

Citation:
Jenei S, Tiricz H, Szolomájer J, Tímár E, Klement É, Al Bouni MA, Lima RM, Kata D, Harmati M, Buzás K, Földesi I, Tóth GK, Endre G and Kondorosi É (2020) Potent Chimeric Antimicrobial Derivatives of the Medicago truncatula NCR247 Symbiotic Peptide. Front. Microbiol. 11:270. doi: 10.3389/fmicb.2020.00270

In Rhizobium-legume symbiosis, the bacteria are converted into nitrogen-fixing bacteroids. In many legume species, differentiation of the endosymbiotic bacteria is irreversible, culminating in definitive loss of their cell division ability. This terminal differentiation is mediated by plant peptides produced in the symbiotic cells. In *Medicago truncatula* more than ∼700 nodule-specific cysteine-rich (NCR) peptides are involved in this process. We have shown previously that NCR247 and NCR335 have strong antimicrobial activity on various pathogenic bacteria and identified interaction of NCR247 with many bacterial proteins, including FtsZ and several ribosomal proteins, which prevent bacterial cell division and protein synthesis. In this study we designed and synthetized various derivatives of NCR247, including shorter fragments and various chimeric derivatives. The antimicrobial activity of these peptides was tested on the ESKAPE bacteria; *Enterococcus faecalis*, *Staphylococcus aureus*, *Klebsiella pneumoniae*, *Acinetobacter baumannii*, *Pseudomonas aeruginosa*, and *Escherichia coli* as a member of *Enterobacteriaceae* and in addition *Listeria monocytogenes* and *Salmonella enterica*. The 12 amino acid long C-terminal half of NCR247, NCR247C partially retained the antimicrobial activity and preserved the multitarget interactions with partners of NCR247. Nevertheless NCR247C became ineffective on *S. aureus*, *P. aeruginosa*, and *L. monocytogenes*. The chimeric derivatives obtained by fusion of NCR247C with other peptide fragments and particularly with a truncated mastoparan sequence significantly increased bactericidal activity and altered the antimicrobial spectrum. The minimal bactericidal concentration of the most potent derivatives was 1.6 μM, which is remarkably lower than that of most classical antibiotics. The killing activity of the NCR247-based chimeric peptides was practically instant. Importantly, these peptides had no hemolytic activity or cytotoxicity on human cells. The properties of these NCR derivatives make them promising antimicrobials for clinical use.

Keywords: antimicrobial peptides, plant symbiotic nodule-specific cysteine-rich peptides, NCR247, ESKAPE bacteria, modes of antimicrobial activity, killing kinetics, bacterial targets, antibiotics

INTRODUCTION

The world-wide spread of antibiotic resistant bacteria and the increasing mortality rate by untreatable microbial infections make the development of new antibiotics with novel modes of actions and less prone to development of resistance extremely urgent. Plant peptides, produced only in Rhizobium bacterium-legume symbiosis, in the symbiotic cells of root nodules, represent a rich source of so far unexplored biological activities and antimicrobial agents. The infected nodule cells contain thousands of bacteria that are encapsulated by plasma membrane derived vesicles, forming organelle-like structures, called symbiosomes. In the host cells the bacteria adapt to the intracellular life-style, microaerobic conditions and differentiate progressively into nitrogen-fixing bacteroids. In many legumes, this differentiation process is irreversible, and manifested by extreme cell growth, altered morphology and physiology, genome amplifications and definitive loss of cell division potential (Kondorosi et al., 2013). We described this terminal differentiation process first in *Medicago truncatula* and demonstrated that it is controlled by the host plant (Mergaert et al., 2006). We discovered an entirely new peptide family which has evolved only in those legumes where the endosymbionts' differentiation is terminal (Mergaert et al., 2003; Van de Velde et al., 2010). In *M. truncatula,* ∼700 genes code for nodule specific cysteine rich NCR peptides (Montiel et al., 2017; de Bang et al., 2017). The *NCR* genes usually consist of two exons; the first coding for a relatively conserved signal peptide, while the second one for the mature peptide. The mature NCR peptides exhibit extreme differences in their physicochemical properties due to their highly divergent amino acid compositions and sequence where only the position of 4 or 6 cysteines and a few neighboring amino acids is conserved. The NCR peptides enter the endoplasmic reticulum during their translation where the signal peptidase complex cleaves the signal peptide and the mature peptides reach the symbiosomes via the Golgi transport vesicles. NCR peptides can interact with the bacterial cell envelope, the bacterial membranes and with specific targets in the bacterial cytosol by entering the cells.

NCR247, which is the smallest peptide of the NCR family, is composed of 24 amino acids, four of which are cysteines. This cationic peptide (pI 10.15) is a self-penetrating peptide entering the bacterial cytosol without pore formation, which has exceptionally high protein binding ability and interacts with many bacterial proteins (Farkas et al., 2014). It binds to the conserved cell division protein FtsZ and abolishes the FtsZ ring formation and thereby bacterial cell division. NCR247 interacting with many ribosomal proteins inhibits translation but also downregulates the transcription of ribosomal genes. Accordingly, treatment of various pathogenic bacteria with synthetic NCR247 provoked efficient killing of many of them (Tiricz et al., 2013).

In this work, we studied the antimicrobial activity of NCR247 and its derivatives on the most problematic ESKAPE bacteria, *Enterococcus faecalis*, *Staphylococcus aureus*, *Klebsiella pneumoniae*, *Acinetobacter baumannii*, *Pseudomonas aeruginosa*, and *Escherichia coli* as well as *Listeria monocytogenes* and *Salmonella enterica*. We tested which region of NCR247 is responsible for the antibacterial activity and how this activity and antimicrobial spectrum can be further enhanced by fusion with neutral or other antimicrobial peptide (AMP) fragments. We show that the designed chimeric peptides act very fast and in at least as low or even lower concentrations than levofloxacin (Lvx) and orders of magnitude lower concentrations than carbenicillin (Cb). None of the five potent chimeric peptides provoked hemolysis of human erythrocytes or killed human cells, which makes them very promising antimicrobial candidates.

MATERIALS AND METHODS

Bacterial Strains

The pathogenic bacterial strains obtained from the ATCC (United States) and NCTC (National Collection of Type Cultures – England) were the Gram-positive: *Enterococcus faecalis* (ATCC 29212), *Staphylococcus aureus* (HNCMO112011), *Listeria monocytogenes* (ATCC 19111) and the Gram-negative: *Pseudomonas aeruginosa* (ATCC 27853), *Escherichia coli* (ATCC 8739), *Salmonella enterica* (ATCC 13076), *Klebsiella pneumoniae* (NCTC 13440), *Acinetobacter baumannii* (ATCC 17978).

Antimicrobial Activity in 20 mM Potassium-Phosphate Buffer, pH 7.4 (PPB)

Overnight bacterial cultures grown in LB were diluted and grown to OD_{600} = 0.2–0.6 at 37°C with shaking. After harvesting and washing bacteria in PPB, the suspensions were adjusted to OD_{600} = 0.1 corresponding to $\sim 10^7$ bacteria/mL. Antimicrobial activity of the peptides and the antibiotics was determined in PPB in 96 well microplates using 10 μL bacterial suspension and 90 μL of the 2-fold serial dilutions of peptides or antibiotics. Peptides were tested from 25 μM to 0.125 μM whereas the antibiotics; carbenicillin (Cb) from Duchefa Biochemie (Prod.No. C0109.0025) and levofloxacin (Lvx) from Sigma-Aldrich (Prod.No. 28266-10MG-F) from 10.24 mM to 0.1 μM. The microplates were incubated for 3 h at 37°C with 250 rpm shaking and then 5 μl from each sample was placed on LB agar and the growth of bacteria was monitored after overnight incubation at 37°C. The lowest concentration of the antimicrobial agents, which completely eliminated viable bacteria was the minimal bactericidal concentration (MBC).

Antimicrobial Activity in Mueller Hinton Broth (MHB)

Ca^{2+} and Mg^{2+} can inhibit the antimicrobial activity of cationic peptides, therefore the MBC and MIC values were also determined in MHB, which unlike PPB contains divalent cations and allows growth of bacteria. Bacteria were grown and prepared similarly except that bacteria were resuspended in MHB. 10 μl of bacteria OD_{600} = 0.1, supplemented with 45 μl MHB and 45 μl of 2-fold dilution series of peptides, were cultivated for 3 and 20 h at 37°C with shaking. Optical density of each sample was measured (Hidex Sense Microplate Reader with Plate Reader Software version 5064) and 5 μl was placed on LB

TABLE 1 | List of antimicrobial peptides.

Code	Name	Amino acid sequence	pI
A	NCR247	RNGCIVDPRCPY**QQCRRPLYCRRR**	10.15
B	**NCR247C**	**QQCRRPLYCRRR**	11.50
C	**NCR247C**-StrepII	**QQCRRPLYCRRR***WSHPQFEK*	11.05
D	X1-**NCR247C**	RPLNFKMLRFWGQ**QQCRRPLYCRRR**	11.99
E	X1-**NCR247C**-StrepII	RPLNFKMLRFWGQ**QQCRRPLYCRRR***WSHPQFEK*	11.80
F	**NCR247C**-X2	**QQCRRPLYCRRR**KALAALAKKIL	11.55
G	**NCR247C**-X2-StrepII	**QQCRRPLYCRRR**KALAALAKKIL*WSHPQFEK*	11.40
H	X2-**NCR247C**	KALAALAKKIL**QQCRRPLYCRRR**	11.65
I	X2	KALAALAKKIL	10.98
J	Transportan	GWTLNSAGYLLGKINLKALAALAKKIL	10.77

agar plates after 3 and 20 h treatment. The minimal inhibitory concentration (MIC) corresponded to the lowest concentration, which inhibited growth.

Chemical Synthesis of Peptides

The antimicrobial peptides (AMPs) listed in **Table 1** were synthesized according to the standard procedure of the solid-phase peptide synthesis (SPPS) by using an automatic peptide synthesizer (CEM Liberty Blue) with TentaGel S RAM resin (loading of amino groups −0.23 mmol/g). The applied chemistry utilized the Fmoc amino protecting group and diisopropylcarbodiimide/oxyma coupling with a fivefold excess of reagents. Removal of the fluorenyl-9-methoxycarbonyl (Fmoc) group was carried out with 10% piperazine and 0.1 mol 1-hydroxy-benzotriazole (HOBt) dissolved in 10% ethanol and 90% DMF in two cycles. After completion of the synthesis, peptides were detached from the resin with a 95:5 (v/v) trifluoroacetic acid (TFA)/water mixture containing 3% (w/v) dithiothreitol (DTT) and 3% (w/v) triisopropylsilane (TIS) at room temperature (RT) for 3 h. The resin was removed by filtration and the peptides were precipitated by the addition of ice cold diethyl ether. Next, the precipitate was filtered, dissolved in water and lyophilized. The crude peptides were analyzed and purified by reverse-phase high-performance liquid chromatography (RP-HPLC). Peptides were purified using a C18 column with a solvent system of (A) 0.1% (v/v) TFA in water and (B) 80% (v/v) acetonitrile and 0.1% TFA (v/v) in water at a flow rate of 4.0 mL/min. The absorbance was detected at 220 nm. The appropriate fractions were pooled and lyophilized. Purity of the peptides was characterized by analytical RP-HPLC at a flow rate of 1.0 mL/min. The identity of the peptides was verified by ESI-MS using Waters SQ detector.

Identification of the Interacting Bacterial Partners of NCR247C-X2-StrepII

Logarithmic phase *E. coli* bacteria (OD_{600} = 0.6) grown in LB were harvested by centrifugation, washed and re-suspended in PPB. Separation of the membrane and cytosolic proteins was done by ultracentrifugation according to Sandrini et al. (2014). Briefly, bacteria were sonicated and large debris removed by centrifugation. The membrane proteins (pellet) and the cytoplasmic proteins (supernatant) were separated by ultracentrifugation of the supernatant at 110000 *g* for 10 min at 4°C. NCR247C-X2-StrepII (peptide G, **Table 1**) or StrepII was added at 0.02 mM concentration to the membrane or cytosolic protein extract. These protein samples were incubated together with Strep-Tactin Sepharose beads (IBA Lifesciences Cat.No. 2-1201-010) for 90 min with gentle shaking on ice. Affinity chromatography of protein complexes was carried out according to the manual. Briefly, after the incubation, each column was washed seven times with washing buffer (100 mM Tris–HCl pH 8.0, 150 mM NaCl, 1 mM EDTA) and the bound proteins were eluted with elution buffer (100 mM Tris–HCl pH 8.0, 150 mM NaCl, 1 mM EDTA, 2.5 mM desthiobiotin). The 2nd and 3rd elution fractions (E2, E3) were separated with electrophoresis on 4–20% precast denaturing gel (Bio-Rad Laboratories Cat.No. 456-1093) and visualized with silver staining. Proteins were identified from E3 with mass spectrometry. Guanidine hydrochloride was added to the elution fractions to a final concentration of 6 M. The disulfide bridges were reduced by 10 mM Tris(2-carboxyethyl)phosphine (TCEP), then free sulfhydryls modified by 20 mM *S*-methyl methanethiosulfonate (MMTS). After dilution of the samples 0.5 μg trypsin was added for an overnight digestion at 37°C. The digests were desalted on Varian OMIX C18 tips and dried. An aliquot of the digests was subjected to LC-MS/MS analysis on an Orbitrap Fusion Lumos Tribrid (Thermo Fisher Scientific) mass spectrometer on-line coupled to a Waters M-Class UPLC using HCD fragmentation. The peak lists generated by Protein Discoverer (v1.4.) were subjected to database search using Protein Prospector (v5.22.0) against *E. coli* entries in the Uniprot.2019.6.12 database (1618419 entries).

Hemolysis and Cytotoxicity Assays

To evaluate possible side effects of the NCR247-based peptides, hemolysis and cytotoxicity assays were performed. Human blood was purchased from the Regional Blood Centre in Szeged. The use of human blood for the hemolysis assay has been authorized by the Regional Hungarian Ethics Committee and approved by the Ethics Review Sector of DG RTD (European Commission) in connection with EK's ERC AdG SymBiotics. The cells from 1.2 mL of EDTA-blood were centrifuged at 1500 × *g* for 1 min and washed several times in TBS buffer (10 mM Tris, pH = 7.2, 150 mM NaCl) until the supernatant became colorless. The cells were then resuspended in 12 mL TBS buffer. 100 μL of

this cell suspension was incubated with 100 μL of the peptides at 100 and 25 μM. Samples were incubated for 1 h at 37°C, and after centrifugation of the cells at 1500 *g* for 1 min, the supernatants were transferred into sterile 96-well plates and the hemoglobin release was measured at OD_{560} (Multiskan FC microplate reader, Thermo Fisher Scientific). Melittin (Bachem) at 50 μg/mL and TBS without peptides were used as positive and negative controls, respectively. Relative hemolytic activity (RHA) of each peptide was calculated as follows: (Compound OD_{560} −TBS OD_{560}) × 100/(Melittin OD_{560} −TBS OD_{560}).

The cytotoxicity of peptides X1-NCR247C and NCR247C-X2 was determined against the human melanoma A375 cells with XTT cell proliferation assay kit (PanReac Applichem) and a benchtop microplate reader (Multiskan RC, Thermo Labsystems) according to the manufacturers' instructions. A375 human melanoma cell line was obtained from ATCC and maintained in DMEM (Lonza) supplemented by 10% FBS (Euroclone) in a humidified incubator at 37°C and 5% CO_2. A375 cells were seeded to 96-well plates (4,000 cells/well) and treated with the peptides for 72 h. Cells without peptides served as negative control and the blank sample was the medium. Reduction of the tetrazolium salt XTT by the viable cells to the orange colored compounds of formazan was measured at OD_{450}. The XTT assay was performed in three biological repeats.

TABLE 2 | Minimal bactericidal concentrations (MBC; in μM) of the studied peptides and antibiotics against different pathogens after 3 h of treatment in PPB.

Peptides/ Antibiotics	*E. f.*	*S. a.*	*K. p.*	*A. b.*	*P. a.*	*E. c.*	*L. m.*	*S. e.*
A	>25	6.3	>25	12.5	3.1	6.3	>25	25
B	>25	>25	>25	25	25	6.3	>25	>25
C	>25	6.3	>25	25	6.3	6.3	>25	>25
D	6.3	3.1	12.5	3.1	3.1	3.1	3.1	1.6
E	12.5	3.1	6.3	3.1	3.1	3.1	3.1	3.1
F	25	3.1	6.3	3.1	3.1	1.6	1.6	1.6
G	12.5	1.6	3.1	1.6	3.1	1.6	3.1	1.6
H	3.1	3.1	6.3	3.1	3.1	3.1	3.1	3.1
I	>25	25	>25	25	6.3	>25	25	>25
J	3.1	3.1	3.1	1.6	3.1	3.1	3.1	1.6
Cb	5120	640	>10240	5120	10240	1280	80	640
Lvx	160	2.5	320	20	1.3	5.0	320	1.3

E. f., Enterococcus faecalis; S. a., Staphylococcus aureus; K. p., Klebsiella pneumoniae; A. b., Acinetobacter baumannii; P. a., Pseudomonas aeruginosa; E. c., Escherichia coli; L. m., Listeria monocytogenes; S. e., Salmonella enterica. Cb, carbenicillin; Lvx, levofloxacin.

RESULTS

NCR247 and Its Derivatives Are Potent Killers of Pathogenic Bacteria

Previously we have shown bactericidal activity of the synthetic NCR247 peptide in PBS on several human and plant pathogen bacteria (Tiricz et al., 2013). Our present work is focused on the activity of NCR247 and its various derivatives (**Table 1**) on the ESKAPE strains as well as on *L. monocytogenes* and *S. enterica*. Bacterial cultures were treated with 2-fold dilution series of synthetic NCR247 (peptide A, **Table 1**) starting with 25 μM concentration. The minimal bactericidal concentration (MBC) was the lowest concentration of the tested molecules where no viable bacteria remain after the treatment and therefore the growth of bacteria could not be detected (**Table 2**). The killing activity of NCR247 was the strongest with a MBC of 3.1 μM on *P. aeruginosa* while the MBC was 6.3 μM in the case of *S. aureus* and *E. coli*, 12.5 μM for *A. baumannii* and 25 μM for *S. enterica*. *K. pneumoniae*, and *L. monocytogenes* were resistant at 25 μM to NCR247 (peptide A, **Table 2**).

Then we tested which region of NCR247 is responsible for the antimicrobial properties. From the 24 amino acid long NCR247, the 12 amino acid long N-terminal and the 12 amino acid long C-terminal halves were synthetized. The N-terminal part (RNGCIVDPRCPY) was inactive on the tested bacteria, while the C-terminal part (peptide B: NCR247C, **Table 1**) retained the antimicrobial activity of NCR247 on *E. coli* (peptide B, **Table 2**) but was ineffective to kill the other bacteria at 25 μM concentration.

The synthetic, reduced and even the oxidized forms of NCR247 seems to be unstructured (Shabab et al., 2016). However, it cannot be excluded that NCR247 might be properly folded by interacting with the bacterial membranes, which may not be possible if the peptide is only 12 amino acid long. Therefore, we synthetized derivatives of the NCR247C peptide adding either C- or N-terminal extension. First, the neutral, 8 amino acid long StrepII tag (WSHPQFEK) was added to the C terminus (peptide C: NCR247C-StrepII, **Table 1**). The StrepII was chosen because in our previous study this tag did not harm the antimicrobial activity of NCR247 and it was used for pull down experiments to identify its bacterial targets (Farkas et al., 2014). NCR247C-StrepII became more active than NCR247C killing in addition to *E. coli*, *S. aureus*, and *P. aeruginosa* (peptide C, **Table 2**).

Then the N-terminus of NCR247C was extended with 13 amino acids (X1) deriving from the cationic N-terminal part of the unusual double size NCR335 which part lacks cysteines and characteristics of NCRs but increased the pI from 10.15 to 11.99 (peptide D, **Table 1**). This chimeric peptide (X1-NCR247C) turned out to be very effective on *S. enterica* (MBC 1.6 μM), *S. aureus*, *A. baumannii*, *P. aeruginosa*, *E. coli*, and *L. monocytogenes* (MBC 3.1 μM) and became able to kill *E. faecalis* (MBC 6.3 μM) and *K. pneumoniae* (MBC 12.5 μM) (peptide D, **Table 2**). Addition of StrepII to the C terminus of X1-NCR247C (peptide E: X1-NCR247C-StrepII, **Table 1**) slightly improved the bactericidal property against *K. pneumoniae* but became somewhat less efficient against *E. faecalis* and *S. enterica* (peptide E, **Table 2**).

Thereupon, we investigated how attachment of another AMP at the C- or N-terminus of NCR247C could influence the bactericidal efficiency and spectrum. We used the KALAALAKKIL sequence (peptide I: X2, **Table 1**) from the membranolytic, anti-cancer mastoparan peptide toxin from wasp venom (INLKALAALAKKIL), which is also present in the C-terminus of the 27 amino acid long cell-penetrating cationic peptide, transportan (peptide J: Transportan, **Table 1**) (Pooga et al., 1998). Attachment of KALAALAKKIL to the C-terminus

of NCR247C (peptide F: NCR247C-X2, **Table 1**) reduced the MBC to 1.6 μM in the case of *E. coli*, *L. monocytogenes*, and *S. enterica* (peptide F, **Table 2**). Further elongation of NCR247C-X2 with StrepII (peptide G: NCR247C-X2-StrepII, **Table 1**) made this derivative even more effective against *S. aureus* and *A. baumannii* (MBC 1.6 μM) (peptide G, **Table 2**). Addition of X2 to the N-terminal of NCR247C (peptide H: X2-NCR247C, **Table 1**) drastically increased the killing of *E. faecalis* and was the most active one (MBC 3.1 μM) among all tested peptide derivatives (peptide H, **Table 2**). X2 alone was incomparably less active on all tested bacteria (peptide I, **Table 2**). On the other hand transportan effectively killed all bacteria with MIC in the range of 1.6–3.1 μM (peptide J, **Table 2**).

The Antimicrobial Potential of NCR247 Based Peptides Is Comparable to Third-Generation Antibiotics

To evaluate the effectiveness of these peptides compared to antibiotics, we determined the MBC values of two antibiotics under the same experimental conditions, after 3 h treatments in PPB. One of them was the classical bactericidal antibiotic carbenicillin, belonging to the carboxypenicillin subgroup of the penicillins. The other one was levofloxacin, a third-generation, fluoroquinolone antibiotic. The MBCs of both antibiotics showed great variations on the tested bacteria (**Table 2**). Carbenicillin, except for *L. monocytogenes*, was required in the range of 640 – 10240 μM while levofloxacin was active at 1.25 – 320 μM, comparable to the chimeric NCR247C derivatives. Levofloxacin was particularly effective against *P. aeruginosa*, *S. enterica*, and *S. aureus* but the MBCs against *K. pneumoniae*, *L. monocytogenes*, and *E. faecalis* were one or two orders of magnitude higher than that of the chimeric NCR peptides.

The time dependence of bacterial killing was a further question, which act faster: the peptides or the antibiotics? The kinetics of bacterial killing was studied on *S. aureus*, *A. baumannii*, and *E. coli* treated with MBC of each antimicrobial molecule (peptide or antibiotic) (**Figure 1** and **Supplementary Table S1**). All chimeric peptides (D-H) killed all tested bacteria either instantly or within 5 min. The killing by NCR247 and its short derivatives (A-C) was slower but they eliminated *E. coli* in 20 min and *A. baumannii* in 30 min while viable cell number of *S. aureus* was only slightly reduced in line with insensitivity of *S. aureus* to the A–C peptides. Carbenicillin and levofloxacin exhibited a much more protracted killing effect than the NCR247-based peptides with large numbers of viable cells at 60 min (**Supplementary Table S1**). Based on this data, it is clear that particularly the chimeric peptides (D-H) kill bacteria much faster than the tested antibiotics.

Bactericidal Activity of the Chimeric NCR247 Based Peptides Is Maintained in Mueller Hinton Broth

Antimicrobial activity of cationic peptides is generally attenuated by the presence of divalent cations and higher salt concentrations (Hancock and Sahl, 2006). Therefore we determined the MBC and the minimal inhibitory concentration (MIC) values of all peptides (A-J) in MHB used for the cultivation of *S. aureus*, *A. baumannii*, and *E. coli* (**Table 3**). Peptides A-C, corresponding to NCR247, NCR247C and NCR247C-StrepII were ineffective against the three bacteria cultivated for 3 or 20 h at 25 μM concentration. Growth inhibition was only detectable in the case of A: NCR247 at 25 μM on *E. coli* cultivated for 20 h. Unlike A-C, the D-H peptides retained their activity in MHB. Action of D and E was, however, slowed down, as their MBC values were significantly higher at 3 h than at 20 h. In contrast, the MBC values of peptides F, G and H were identical or almost the same at 3 and 20 h. Moreover in line with fast action of these peptides, the MIC and MBC values were practically identical.

The Chimeric Peptide G: NCR247C-X2-StrepII Interacts With Many *E. coli* Proteins

Peptide G was one of the most active chimeric peptides, which via its StrepII tag attached to the C-terminus of NCR247C-X2, was used in pull-down experiments for the isolation of

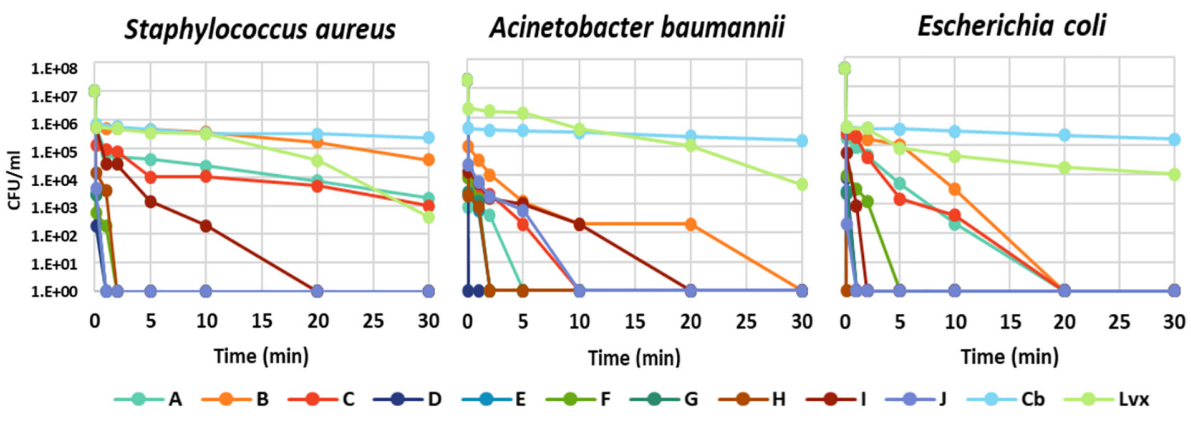

FIGURE 1 | Time-kill kinetic analysis of antibiotics and the designed peptides. The number of colony forming units (CFU) is shown at 0.0, 0.1, 1, 2, 5, 10, 20, and 30 min of treatment.

TABLE 3 | Minimal bactericidal concentrations (MBC) and minimal inhibitory concentrations (MIC) of the studied peptides in Mueller Hinton Broth on selected pathogens.

	(A)			(B)			(C)		
	S. a.	*A. b.*	*E. c.*	*S. a.*	*A. b.*	*E. c.*	*S. a.*	*A. b.*	*E. c.*
A	> 25	> 25	> 25	>25	>25	>25	>25	>25	25
B	> 25	> 25	> 25	>25	>25	>25	>25	>25	>25
C	> 25	> 25	> 25	>25	>25	>25	>25	>25	>25
D	25	6.3	12.5	3.1	3.1	3.1	3.1	3.1	3.1
E	25	12.5	25	6.3	6.3	6.3	6.3	6.3	6.3
F	3.1	3.1	3.1	3.1	3.1	3.1	3.1	3.1	3.1
G	6.3	3.1	3.1	6.3	3.1	3.1	3.1	3.1	3.1
H	6.3	6.3	6.3	3.1	3.1	6.3	3.1	3.1	6.3
I	> 25	> 25	> 25	>25	>25	>25	>25	25	>25
J	6.3	3.1	6.3	3.1	3.1	6.3	3.1	3.1	3.1

(A) *MBC (μM) – 3 h treatment,* ***(B)*** *MBC (μM) – 20 h treatment, and* ***(C)*** *MIC (μM) – 20 h treatment. S. a., Staphylococcus aureus; A. b., Acinetobacter baumannii; E. c., Escherichia coli.*

the interacting bacterial proteins. Cytosolic and membrane fractions of *E. coli* were incubated with NCR247C-X2-StrepII or with StrepII, serving as a control for identification of proteins binding to the StrepII tag. The protein complexes were purified with affinity chromatography using Strep-Tactin Sepharose beads and the eluted proteins were identified with mass spectrometry (MS) (**Supplementary Table S2**) and visualized by gel electrophoresis and silver staining (**Figure 2**). Numerous cytosolic proteins showed interaction with NCR247C-X2. They were predominantly ribosomal proteins that corresponded to the full list of ribosomal proteins identified previously as binding partners of NCR247-StrepII in the symbiotic partner *Sinorhizobium meliloti* (Farkas et al., 2014). These proteins ordered from the highest number of peptide counts by the MS analysis were the followings: L15, S5, S7, L4, L2, L9, L17, S4, L1, L3, L22, S9, S6, S13, S14, S3, L16, S19, L18, L13, L10, S18, S12, S28 (**Supplementary Table S2**). In addition, factors involved in ribosome maturation or RNA degradation (DeaD, Rne, Pnp, Hfq, Rnr, RhlE), in translation (InfC), in transcriptional and translational control (HupB, IhfA, IhfB, CsrA, RmF) including the RNA polymerase subunits (RpoA, RpoB, RpoC) were present in the NCR247C-X2-StrepII complexes (**Figure 3A**). FtsZ, a major binding partner of NCR247 and essential for the formation of the Z-ring and cell division, was represented with low peptide counts in the cytosolic fraction, indicating that the N-terminal half of NCR247 might contribute to the strong FtsZ binding. Similarly to FtsZ, MinD septum site-determining protein was detected with low peptide counts (**Figure 3A**).

There were fewer interacting partners in the membrane fraction (**Supplementary Table S2**) that were outer membrane components (LpoA, OmpA, OmpF, OmpW, RodZ, DacC, RcsF, BamA), inner membrane components (ElaB, AtpA, AtpD, AtpF, HemX, RodZ, FtsH, NuoA) and various efflux pumps (AcrA-TolC-MacA, MdtE) pumping out the toxic substances or antibiotics (**Figure 3B**).

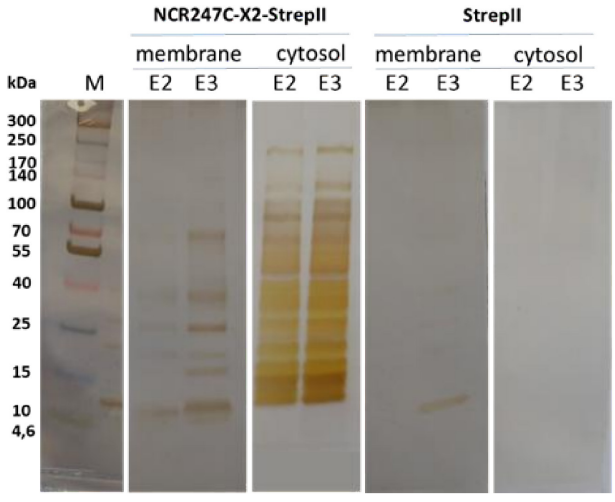

FIGURE 2 | SDS-gel electrophoresis of proteins eluted from Strep-Tactin Sepharose column. E2, E3: 2nd and 3rd elution fractions. M: molecular weight markers.

The NCR247-Based Peptides Have No Cytotoxicity Against Human Cells

Many antibiotics have severe side effects and cytotoxicity; therefore it was important to test how these plant peptides affect the integrity and viability of human cells. One of the simplest and essential assays is to measure hemolysis of erythrocytes. Hemolysis of human erythrocytes by A–J at 100 and 25 μM concentrations was measured and compared to the effect of melittin, an AMP from honey bee venom that induces complete hemolysis at 50 μg/mL. Blood cells without AMPs in TBS buffer served as negative control (**Table 4**). Only transportan showed hemolytic activity, which was 95.6 and 38.6% of the melittin provoked hemolysis at 100 and 25 μM, respectively. Interestingly, the truncated form (I) of the membranolytic mastoparan lost its hemolytic activity. Only the chimeric peptides F-H provoked negligible hemolysis at 100 μM. At 25 μM only peptide G had a slight and insignificant hemolytic activity.

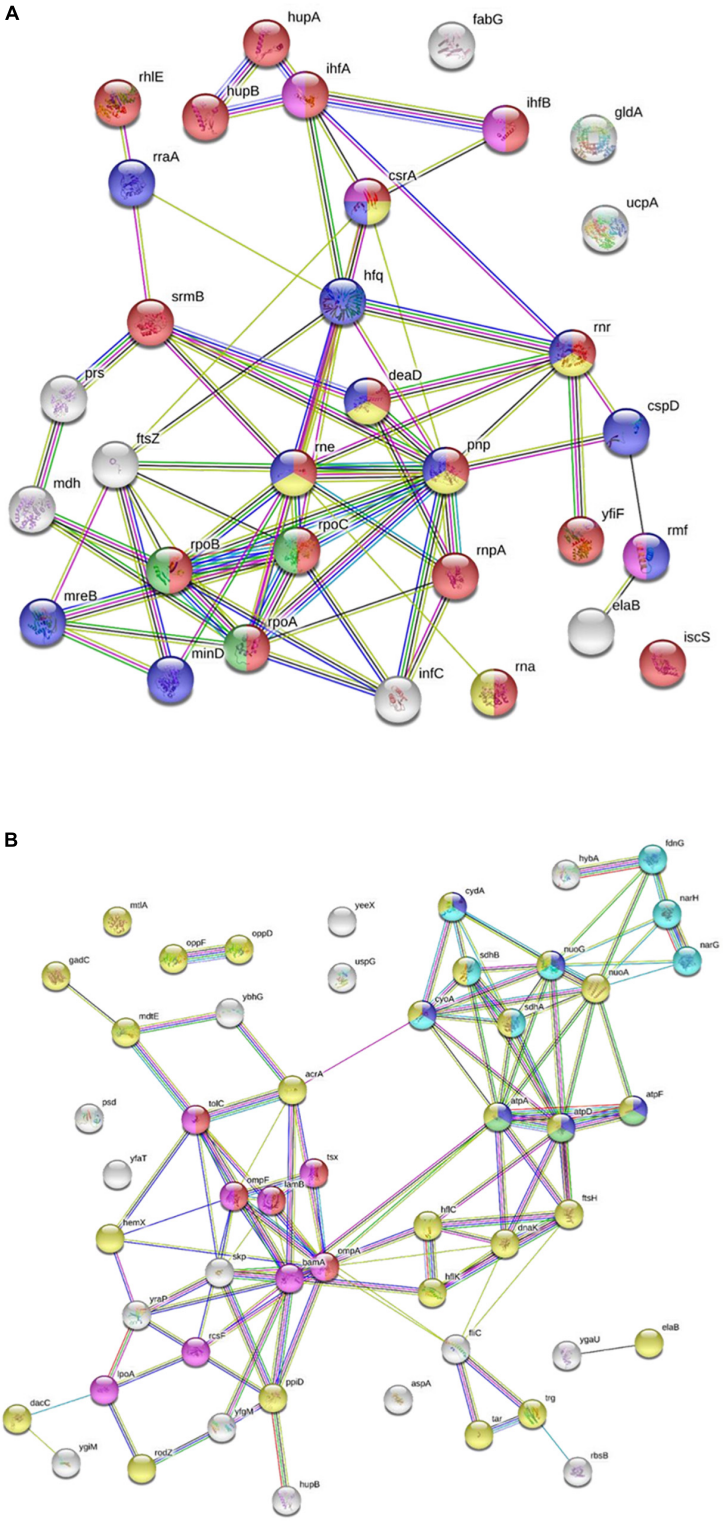

FIGURE 3 | Interaction of NCR247C-X2-StrepII with *Escherichia coli* cytosolic and membrane proteins. **(A)** STRING representation of the cytosolic interacting proteins excluding the ribosomal proteins and other proteins involved in translation. The color of nodes indicates the following functions: red, RNA metabolic process; yellow, RNA catabolic process; blue, negative regulators; green, RNA polymerase; purple, translation regulation. The connecting lines indicate the interactions. **(B)** STRING representation of the interacting membrane proteins. Protein functions are indicated with different colors. The color of nodes indicate different functions: blue, ATP metabolic process; magenta, electron transport chain; red, porin activity; green, proton transport; yellow, inner membrane component and purple, outer membrane components.

TABLE 4 | NCR247 and its derivatives do not provoke hemolysis.

AMP 100 μM	OD_{560} AVE ± SD	RHA%	AMP 25 μM	OD_{560} AVE ± SD	RHA%
A	0.02 ± 0.004	1.75	**A**	0.01 ± 0.008	0.88
B	0.01 ± 0.002	0.88	**B**	0.01 ± 0.002	0.88
C	0.02 ± 0.002	1.75	**C**	0.02 ± 0.000	1.75
D	0.04 ± 0.019	3.51	**D**	0.02 ± 0.017	1.75
E	0.04 ± 0.008	3.51	**E**	0.02 ± 0.001	1.75
F	0.08 ± 0.033	7.02	**F**	0.02 ± 0.012	1.75
G	0.13 ± 0.004	11.40	**G**	0.07 ± 0.002	6.14
H	0.07 ± 0.004	6.14	**H**	0.02 ± 0.002	1.75
I	0.02 ± 0.004	1.75	**I**	0.01 ± 0.001	0.88
J	1.09 ± 0.004	95.61	**J**	0.44 ± 0.131	38.60
Melittin	1.14 ± 0.364	100	**Melittin**	1.14 ± 0.364	100

Desintegration of red blood cells treated with 100 and 25 μM of AMPs A-J and melittin (50 μg/ml) was measured at OD_{560}. Average OD_{560} ± standard deviation (OD_{560}AVE ± SD) and the relative hemolytic activities (RHA) are presented in % of the 100% hemolytic effect of melittin.

In addition we tested the cytotoxicity of peptides X1-NCR247C and NCR247C-X2 on the viability of A375 human melanoma cells using the XTT cell proliferation assay (**Figure 4**). Conversion of XTT to formazan by metabolically active cells did not show differences between the control and the X1-NCR247C treated samples. Similarly NCR247C-X2 exhibited no cytotoxicity up to 12.5 μM, though slight decrease of the viable cell number was observed at 25 μM, which concentration is significantly higher than the MBC values. These data indicate that X1-NCR247C and NCR247C-X2 in the range of MBCs do not affect the viability and proliferation of this cell culture.

DISCUSSION

Based on the definitive loss of cell division ability of the nitrogen fixing bacteroids in *M. truncatula* root nodules, it is expected that at least a fraction of the ∼700 NCR peptides can inhibit bacterial cell division and act as antimicrobial agents *in vitro*. Indeed, in our previous studies we have shown the bactericidal action of several cationic NCR peptides (Van de Velde et al., 2010; Tiricz et al., 2013; Farkas et al., 2014; Mikuláss et al., 2016; Farkas et al., 2017; Farkas et al., 2018). Among them, the mode of action is the best known for NCR247 (Haag et al., 2012; Farkas et al., 2014; Penterman et al., 2014; Arnold et al., 2017). This peptide has numerous advantageous properties, it acts very fast, it has extreme protein binding ability and has many bacterial targets in the cytosol, by binding to FtsZ it abolishes bacterial cell division and by interacting with many ribosomal proteins it inhibits protein synthesis. Due to its multi hit mechanism, the probability of development of resistant bacteria against NCR247 is very low. A further advantage is that NCR247 is not cytotoxic for human cells.

In this work we show that NCR247 is capable of killing several, but not all of the most problematic bacteria causing incurable infections. Therefore, we aimed to further improve its bactericidal properties. Testing the antimicrobial activity of the synthetic N-terminal and C-terminal halves of NCR247 revealed that antimicrobial activity resided mostly in the C-terminal region (NCR247C). While the positive charge of the AMPs is essential for killing, in the case of NCR247C the increased positive charge (pI = 11.50) did not result in the improvement of the antimicrobial activity or the antimicrobial spectrum compared to NCR247 (pI = 10.15). NCR247C had even a much weaker antimicrobial activity which may be due to the lack of its proper folding as a result of its short length and/or to its failure to interact with the bacterial membranes. Adding the neutral StrepII tag to the NCR247C peptide improved slightly the antibacterial properties. Extending the N-terminus of NCR247C with the 13 amino acid long cationic peptide from NCR335 (D) increased the pI to 11.99 and resulted in significantly lower MBCs (1.6–12.5 μM) and broader spectrum; killing all the eight bacterium strains. Addition of the truncated mastoparan (lacking the first three N-terminal amino acids) either to the N- or the C-terminus of the NCR247C (F, H) increased in similar extent the antimicrobial properties. Further prolongation of the chimeric peptides with the StrepII tag (G) increased even more the activity reaching 1.6–3.1 μM of MBC on all bacteria except for *E. faecalis* (MBC 12.5 μM). The killing by the chimeric peptides was instant (approx. 0.1 min) or very fast (max 5 min) while the complete killing by the levofloxacin required more than 60 min and the carbenicillin acted even slower. In addition to the antibiotics' slower killing kinetics, very high doses (up to 10240 μM) were required from carbenicillin for the elimination of the tested bacteria. The MBC values of levofloxacin was more comparable to chimeric peptides (D-H), acting on *S. aureus*, *A. baumannii*, *P. aeruginosa*, *E. coli*, and *S. enterica* in the same concentration range but being somewhat less active on *K. pneumoniae* and *L. monocytogenes* and *E. faecalis*. Importantly the chimeric peptides maintained their activity also in Mueller Hinton Broth where cationic AMPs are usually inactivated by the presence of bivalent cations (Ca^{2+}, Mg^{2+}), which prevent their interaction with the bacterial membranes (Hancock and Sahl, 2006).

In the chimeric peptide G, the advantageous properties of NCR247C and mastoparan were combined and the StrepII tag in addition made possible the identification of the interacting partners in *E. coli* using pull-down experiments coupled to mass spectrometry. NCR247 showed strong interaction

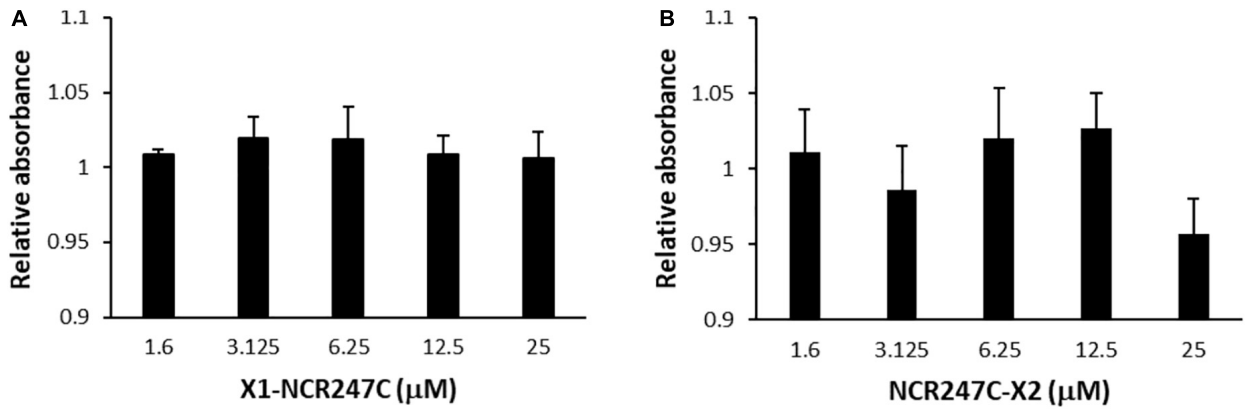

FIGURE 4 | Viability of human melanoma cell line A375 treated with **(A)** X1-NCR247C or **(B)** NCR247C-X2. Relative absorbance values represent the viability compared to untreated cells. Bar graphs represent mean ± SD values.

with many ribosomal proteins, FtsZ and GroEL of the symbiotic bacterium partner *Sinorhizobium meliloti* (Farkas et al., 2014). The hybrid G peptide interacted with many *E. coli* proteins. Ribosomal proteins represented the large majority of cytosolic partners in agreement with the list of ribosomal proteins interacting with NCR247 and confirmed that NCR247C is responsible for binding of ribosomal proteins. Even if NCR247 has an extreme protein binding ability, it is unlikely that all these proteins are primary partners. Nevertheless, interaction with a few ribosomal proteins can be sufficient to inhibit translation and prevent the development of resistance. Already several ribosome-targeting peptide antibiotics are known which interact with different subunits, various ribosomal proteins and can effect initiation, elongation cycle, termination and recycling during protein synthesis (Polikanov et al., 2018). However, none of these peptides have such a broad interaction with the translation machinery as the NCR247-based peptides.

FtsZ was detected among the binding partners of peptide G, however, FtsZ was identified with lower peptide counts; nevertheless the interaction with FtsZ and MinD might collectively contribute to abolishment of bacterial cell division. Interestingly, GroEL playing essential roles in symbiosis was not found among the *E. coli* binding partners.

Mastoparan is a membranolytic 14-residue peptide toxin, which interacts with membranes and adopts amphipathic α-helical structure in lipid environment, capable of penetrating biological membranes and causing permeabilization of both bacterial and mammalian membranes culminating in cell lysis (Moreno and Giralt, 2015; Irazazabal et al., 2016). Unexpectedly, by the loss of the first three amino acids, the truncated mastoparan (X2) did not provoke hemolysis but accordingly lost much of its antimicrobial activity. Fusing X2 with NCR247C provoked synergistic effect, greatly improving the antimicrobial efficacy. The pull down with NCR247C-X2-StrepII identified several outer membrane and inner membrane components that probably bind to the X2 region of the chimeric peptide. Among them are various efflux pumps, pumping out the toxic substances or antibiotics (Amaral et al., 2014). Attachment of X1 to NCR247C enhanced similarly the antimicrobial properties.

In summary, we successfully designed and generated from the symbiotic antimicrobial plant peptide NCR247 several chimeric peptides with fast killing action, low MBC values, and numerous bacterial targets without toxicity on human cells. These peptides represent an extremely promising novel generation of highly powerful antimicrobial candidates.

DATA AVAILABILITY STATEMENT

All datasets generated for this study are included in the article/**Supplementary Material**.

AUTHOR CONTRIBUTIONS

Antimicrobial tests were done by SJ, ET, MA, and RL. HT and ÉKl performed the pull down experiments and identification of bacterial interacting proteins. Hemolytic assays were done by DK and IF and the cytotoxicity test by MH and KB. Peptides were designed by GT, ÉKo, and GE, and synthesized by JS and GT. Experiments were designed and evaluated by ÉKo, GE, SJ, and GT. ÉKo wrote the manuscript.

FUNDING

Research has been supported by the Hungarian National Office for Research, Development and Innovation (NKFIH) through the grants GINOP 2.3.2-15-2016-00014 Evomer and GINOP 2.3.2-15-2016-00015 I-KOM, GINOP-2.3.2-15-2016-00001, GINOP-2.3.2-15-2016-00020; and by the ERC Advanced Grant 269067 "SymBiotics," the NKFIH Frontline Research project KKP129924 and the Balzan research grant to ÉKo; as well as by grants TUDFO/47138-1/2019-ITM FIKP and 20391-3/2018/FEKUSTRAT to GT.

SUPPLEMENTARY MATERIAL

The Supplementary Material for this article can be found online at: https://www.frontiersin.org/articles/10.3389/fmicb.2020.00270/full#supplementary-material

TABLE S1 | Killing kinetics of the studied AMPs and antibiotics at their respective MBC. **Figure 1** is based on these data from 0 to 30 min.

TABLE S2 | Interacting partners of NCR247C-X2-StrepII and the control StrepII peptide identified in the cytosolic and membrane fractions of *Escherichia coli*.

REFERENCES

Amaral, L., Martins, A., Spengler, G., and Molnar, J. (2014). Efflux pumps of Gram-negative bacteria: what they do, how they do it, with what and how to deal with. *Front. Pharmacol.* 4:168. doi: 10.3389/fphar.2013.00168

Arnold, M. F. F., Shabab, M., Penterman, J., Boehme, K. L., Griffitts, J. S., and Walker, G. C. (2017). Genome-wide sensitivity analysis of the microsymbiont Sinorhizobium meliloti to symbiotically important, defensin-like host peptides. *mBio* 8, e1060–e1017. doi: 10.1128/mBio.01060-17

de Bang, T. C., Lundquist, P. K., Dai, X., Boschiero, C., Zhuang, Z., Pant, P., et al. (2017). Genome-wide identification of medicago peptides involved in macronutrient responses and nodulation. *Plant. Physiol.* 175, 1669–1689. doi: 10.1104/pp.17.01096

Farkas, A., Maróti, G., Durgo, H., Györgypál, Z., Lima, R. M., Medzihradszky, K. F., et al. (2014). *Medicago truncatula* symbiotic peptide NCR247 contributes to bacteroid differentiation through multiple mechanisms. *Proc. Natl. Acad. Sci. U.S.A.* 111, 5183–5188. doi: 10.1073/pnas.1404169111

Farkas, A., Maróti, G., Kereszt, A., and Kondorosi, E. (2017). Comparative analysis of the bacterial membrane disruption effect of two natural plant antimicrobial peptides. *Front. Microbiol.* 8:51. doi: 10.3389/fmicb.2017.00051

Farkas, A., Pap, B., Kondorosi, E., and Maróti, G. (2018). Antimicrobial activity of NCR plant peptides strongly depends on the test assays. *Front. Microbiol.* 9:2600. doi: 10.3389/fmicb.2018.02600

Haag, A. F., Kerscher, B., Dall'Angelo, S., Sani, M., Longhi, R., Baloban, M., et al. (2012). Role of cysteine residues and disulfide bonds in the activity of a legume root nodule-specific, cysteine-rich peptide. *J. Biol. Chem.* 287, 10791–10798. doi: 10.1074/jbc.M111.311316

Hancock, R. E. W., and Sahl, H. G. (2006). Antimicrobial and host-defense peptides as new anti-infective therapeutic strategies. *Nat. Biotechnol.* 24, 1551–1557. doi: 10.1038/nbt1267

Irazazabal, L. N., Porto, W. F., Ribeiro, S. M., Casale, S., Humblot, V., Ladram, A., et al. (2016). Selective amino acid substitution reduces cytotoxicity of the antimicrobial peptide mastoparan. *Biochim. Biophys. Acta.* 1858, 2699–2708. doi: 10.1016/j.bbamem.2016.07.001

Kondorosi, E., Mergaert, P., and Kereszt, A. (2013). A paradigm for endosymbiotic life: cell differentiation of *Rhizobium* bacteria provoked by host plant factors. *Annu. Rev. Microbiol.* 67, 611–628. doi: 10.1146/annurev-micro-092412-155630

Mergaert, P., Nikovics, K., Kelemen, Z., Maunoury, N., Vaubert, D., Kondorosi, A., et al. (2003). A novel family in *Medicago truncatula* consisting of more than 300 nodule-specific genes coding for small, secreted polypeptides with conserved cysteine motifs. *Plant Physiol.* 132, 161–173. doi: 10.1104/pp.102.018192

Mergaert, P., Uchiumi, T., Alunni, B., Evanno, G., Cheron, A., Catrice, O., et al. (2006). Eukaryotic control on bacterial cell cycle and differentiation in the Rhizobium-legume symbiosis. *Proc. Natl. Acad. Sci. U.S.A.* 103, 5230–5235. doi: 10.1073/pnas.0600912103

Mikuláss, K. R., Nagy, K., Bogos, B., Szegletes, Z., Kovács, E., Farkas, A., et al. (2016). Antimicrobial nodule-specific cysteine-rich peptides disturb the integrity of bacterial outer and inner membranes and cause loss of membrane potential. *Ann. Clin. Microbiol. Antimicrob.* 15:43. doi: 10.1186/s12941-016-0159-8

Montiel, J., Downie, J. A., Farkas, A., Bihari, P., Herczeg, R., Bálint, B., et al. (2017). Morphotype of bacteroids in different legumes correlates with the number and type of symbiotic NCR peptides. *Proc. Natl. Acad. Sci. U.S.A.* 114, 5041–5046. doi: 10.1073/pnas.1704217114

Moreno, M., and Giralt, E. (2015). Three valuable peptides from bee and wasp venoms for therapeutic and biotechnological use: melittin, apamin and mastoparan. *Toxins* 7, 1126–1150. doi: 10.3390/toxins7041126

Penterman, J., Abo, R. P., De Nisco, N. J., Arnold, M. F., Longhi, R., Zanda, M., et al. (2014). Host plant peptides elicit a transcriptional response to control the *Sinorhizobium meliloti* cell cycle during symbiosis. *Proc. Natl. Acad. Sci. U.S.A.* 111, 3561–3566. doi: 10.1073/pnas.1400450111

Polikanov, Y. S., Aleksashin, N. A., Beckert, B., and Wilson, D. N. (2018). The mechanisms of action of ribosome-targeting peptide antibiotics. *Front. Mol. Biosci.* 5:48. doi: 10.3389/fmolb.2018.00048

Pooga, M., Hällbrink, M., Zorko, M., and Langel, U. (1998). Cell penetration by transportan. *FASEB J.* 12, 67–77. doi: 10.1096/fasebj.12.1.67

Sandrini, S. M., Haigh, R., and Freestone, P. P. P. (2014). Fractionation by ultracentrifugation of gram negative cytoplasmic and membrane proteins. *Bio Protocol.* 4:e1287. doi: 10.21769/BioProtoc.1287

Shabab, M., Arnold, M. F., Penterman, J., Wommack, A. J., Bocker, H. T., Price, P. A., et al. (2016). Disulfide cross-linking influences symbiotic activities of nodule peptide NCR247. *Proc. Natl. Acad. Sci. U. S. A.* 113, 10157–10162. doi: 10.1073/pnas.1610724113

Tiricz, H., Szucs, A., Farkas, A., Pap, B., Lima, R. M., Maróti, G., et al. (2013). Antimicrobial nodule-specific cysteine-rich peptides induce membrane depolarization-associated changes in the transcriptome of *Sinorhizobium meliloti*. *Appl. Environ. Microbiol.* 79, 6737–6746. doi: 10.1128/AEM.01791-13

Van de Velde, W., Zehirov, G., Szatmari, A., Debreczeny, M., Ishihara, H., Kevei, Z., et al. (2010). Plant peptides govern terminal differentiation of bacteria in symbiosis. *Science* 327, 1122–1126. doi: 10.1126/science.1184057

Conflict of Interest: The authors declare that the research was conducted in the absence of any commercial or financial relationships that could be construed as a potential conflict of interest.

frontiers in Microbiology

ORIGINAL RESEARCH
published: 25 May 2020
doi: 10.3389/fmicb.2020.00846

Spätzle Homolog-Mediated Toll-Like Pathway Regulates Innate Immune Responses to Maintain the Homeostasis of Gut Microbiota in the Red Palm Weevil, *Rhynchophorus ferrugineus* Olivier (Coleoptera: Dryophthoridae)

Abrar Muhammad[1,2], Prosper Habineza[1,2], Xinghong Wang[3], Rong Xiao[1,2], Tianliang Ji[1,2], Youming Hou[1,2] and Zhanghong Shi[1,2]**

[1] State Key Laboratory of Ecological Pest Control for Fujian and Taiwan Crops, Fujian Agriculture and Forestry University, Fuzhou, China, [2] Fujian Provincial Key Laboratory of Insect Ecology, College of Plant Protection, Fujian Agriculture and Forestry University, Fuzhou, China, [3] Guizhou Institute of Biology, Guizhou Academy of Sciences, Guiyang, China

Spätzle (Spz) is a dimeric ligand that responds to the Gram-positive bacterial or fungal infection by binding Toll receptors to induce the secretion of antimicrobial peptides. However, whether the Toll-like signaling pathway mediates the innate immunity of *Rhynchophorus ferrugineus* to modulate the homeostasis of gut microbiota has not been determined. In this study, we found that a Spz homolog, RfSpätzle, is a secretory protein comprising a signal peptide and a conservative Spz domain. RT-qPCR analysis revealed that *RfSpätzle* was significantly induced to be expressed in the fat body and gut by the systemic and oral infection with pathogenic microbes. The expression levels of two antimicrobial peptide genes, *RfColeoptericin* and *RfCecropin*, were downregulated significantly by *RfSpätzle* knockdown, indicating that their secretion is under the regulation of the *RfSpätzle*-mediated signaling pathway. After being challenged by pathogenic microbes, the cumulative mortality rate of *RfSpätzle*-silenced individuals was drastically increased as compared to that of the controls. Further analysis indicated that these larvae possessed the diminished antibacterial activity. Moreover, *RfSpätzle* knockdown altered the relative abundance of gut bacteria at the phylum and family levels. Taken together, these findings suggest that *RfSpätzle* is involved in RPW immunity to confer protection and maintain the homeostasis of gut microbiota by mediating the production of antimicrobial peptides.

Keywords: *Rhynchophorus ferrugineus*, Spätzle, toll pathway, antimicrobial peptides, gut microbiota

OPEN ACCESS

Edited by:
David Clarke,
University College Cork, Ireland

Reviewed by:
Ioannis Eleftherianos,
The George Washington University, United States
Justin Maire,
The University of Melbourne, Australia

****Correspondence:***
Youming Hou
ymhou@fafu.edu.cn
Zhanghong Shi
shizh@fafu.edu.cn

Specialty section:
This article was submitted to Microbial Symbioses, a section of the journal Frontiers in Microbiology

Received: *08 September 2019*
Accepted: *08 April 2020*
Published: *25 May 2020*

Citation:
Muhammad A, Habineza P, Wang X, Xiao R, Ji T, Hou Y and Shi Z (2020) Spätzle Homolog-Mediated Toll-Like Pathway Regulates Innate Immune Responses to Maintain the Homeostasis of Gut Microbiota in the Red Palm Weevil, Rhynchophorus ferrugineus Olivier (Coleoptera: Dryophthoridae). Front. Microbiol. 11:846. doi: 10.3389/fmicb.2020.00846

INTRODUCTION

Spätzle (Spz), a dimeric ligand of the Toll receptor, binds the Toll receptor to initiate the secretion of antimicrobial peptides via activating the immune signaling pathway (Lemaitre and Hoffmann, 2007). In invertebrates, genomic studies have revealed that different invertebrate species have various numbers of Spz gene copies. For example, *Drosophila melanogaster* has six *Spz* isoforms (*Dm*Spz1–6) (Parker et al., 2001), while *Aedes aegypti* (Shin et al., 2006), black tiger shrimp *Peneaus monodon* (Boonrawd et al., 2017), and white shrimp *Litopenaeus vannamei* (Wang et al., 2012) have three Spz proteins. However, only one *Spz* gene, *MrSpz*, was identified from the freshwater prawn *Macrobrachium rosenbergii* (Vaniksampanna et al., 2019). Furthermore, previous evidence indicated that *Bm*Spz1 of *Bombyx mori* (Wang et al., 2007), *Ms*Spz1 in *Manduca sexta* (An et al., 2010), and *Ap*Spz in oak silkworm *Antheraea pernyi* (Sun et al., 2016) were markedly induced by microbial infection to activate their immune responses. In *D. melanogaster*, the Spz-mediated Toll pathway has been well determined to mediate the synthesis of antimicrobial peptides, such as *drosomycin* (Weber et al., 2003; Valanne et al., 2011; Stokes et al., 2015), and activate the cellular immunity (Hultmark, 2003).

Insects harbor diverse species of symbiotic microorganisms in their guts that strongly affect host physiological traits, including nutrition metabolism (Wong et al., 2014; Janssen and Kersten, 2015; Muhammad et al., 2017; Hebineza et al., 2019), detoxification (Engel and Moran, 2013), protection from natural enemies (Kim et al., 2015; Park et al., 2018), growth and development (Blatch et al., 2010; Wong et al., 2014; Hebineza et al., 2019), mating and foraging behavior (Ami et al., 2010), and gut homeostasis (Engel and Moran, 2013; Douglas, 2015). However, the exact mechanism by which these insect hosts modulate the intensity of gut immunity to maintain the homeostasis of gut microbiota is still poorly understood outside *D. melanogaster*. In *D. melanogaster*, it is well-known that gut epithelial cells can secrete antimicrobial peptides and reactive oxygen species (ROS), which provide colonization resistance to non-commensal bacteria (Ha et al., 2005; Ryu et al., 2008; Lee et al., 2017). The production of these two immune effectors is under the control of the IMD (immune deficiency) pathway and dual oxidase (DUOX) signaling system, respectively (Lemaitre and Hoffmann, 2007; Ryu et al., 2008; Lee et al., 2017; Lin et al., 2018). Moreover, the IMD pathway has been shown to control the excessive proliferation of residential gut microbiota, as the IMD mutant exhibited an increased gut bacterial load (Guo et al., 2014). Intestinal immunity is regulated to maintain the homeostasis of the gut microbiota. For instance, a number of recognition proteins, including *PGRP-LB*, *PGRP-SC1a*, *PGRP-SC1b*, and *PGRP-SC2*, negatively regulate the IMD signaling pathway due to their amidase activity, degrading gut bacteria-derived peptidoglycan to avoid the excessive production of immune effectors in gut epithelial cells (Bischoff et al., 2006; Zaidman-Rémy et al., 2006; Paredes et al., 2011; Guo et al., 2014; Dawadi et al., 2018; Maire et al., 2018, 2019). Additionally, negative regulation can also be achieved by the regulator PIRK, interacting with *PGRP-LC*, *PGRP-LE*, and *Imd* to prevent excessive activation of the IMD signaling pathway (Aggarwal and Silverman, 2008).

To the best of our knowledge, the interactions between the gut microbiota and host immune system in many insects are far from well understood. Red palm weevil (RPW), *Rhynchophorus ferrugineus* (Olivier) (Coleoptera: Dryophthoridae), is an immensely destructive pest for palm plants in China and other tropical countries (Ju et al., 2011; Shi et al., 2014; Al-Dosary et al., 2016). The RPW gut is colonized by a complex gut bacterial community that is involved in the degradation of plant polysaccharides to impact host nutrition metabolism (Jia et al., 2013; Tagliavia et al., 2014; Montagna et al., 2015; Muhammad et al., 2017; Hebineza et al., 2019). Interestingly, RPW also houses an intracellular symbiont, *Nardonella*, within a specialized organ, the bacteriome (Hosokawa et al., 2015). *Nardonella* provides its host with tyrosine, which is used for cuticle synthesis and hardening (Anbutsu et al., 2017). Recently, we found that RfPGRP-LB acts as a negative immunity regulator to inhibit the chronic activation of the immune response by degrading peptidoglycan (Dawadi et al., 2018). It has also been found that weevil *pgrp-lb* prevents endosymbiont-released immunological molecules from escaping the bacteriocytes to chronically activate host systemic immunity (Maire et al., 2019). Furthermore, an NF-κB-like transcription factor, RfRelish, has been demonstrated to mediate the intestinal immunity to modulate the homeostasis of the RPW gut microbiota (Xiao et al., 2019). However, the role of the Spz-mediated Toll-like pathway in RPW immunity has not been determined. In this study, a Spz homolog, *RfSpätzle*, was characterized and its role in modulating the composition of the RPW gut microbiota was determined. Our evidence indicated that the *RfSpätzle*-mediated Toll signaling pathway regulates the synthesis of antimicrobial peptides to confer the protection against microbial infection and modulates the proportion of RPW gut bacteria.

MATERIALS AND METHODS

Insect Rearing

The RPW laboratory population was established and maintained by adults trapped in the Pingtan District (119°32′ E, 25°31′ N) of Fuzhou city, Fujian Province and Jinshan campus of Fujian Agriculture and Forestry University (119°30′ E, 26°08′ N). RPW individuals were fed with sugarcane stems in an incubator (Saifu ZRX-260, Ninbo Experimental Instrument Co. Ltd., China) at 27 ± 1°C, 75 ± 5% relative humidity, and a photoperiod of 24 h dark for larvae and 12 h light/12 h dark for adults (Muhammad et al., 2017).

Full-Length cDNA Cloning and Sequence Analysis of *RfSpätzle*

The fourth instar RPW larvae were dissected in a sterilized dish plate containing 2 ml of phosphate buffered saline (PBS, NaCl 137 mM, KCl 2.7 mM, Na_2HPO_4 10 mM, K_2HPO_4 2 mM, pH 7.2). Three guts were pooled as replicates and homogenized with a tissue lyser (Ningbo Scientz BioTech.

Company Limited, China). Total RNA was extracted with TRIzol Reagent (Invitrogen, Carlsbad, CA, United States) following the manufacturers' instructions. RNA concentration and integrity were determined with NanoDrop2000 (Thermo Fisher Scientific Inc., Waltham, MA) and 1% agarose gel electrophoresis, respectively. The cDNA template was prepared with the TransScript® All-in-One First Strand cDNA Synthesis Kit (Takara Bio Inc., Dalian, China). The core sequence of *RfSpätzle* was cloned with a pair of specific primers (**Table 1**). The 25-μl PCR mix consisted of 1 μl of cDNA, 12.5 μl of 2 × TaqPCR mix, 1 μl each of forward and reverse primer (10 μM) and 9.5 μl of RNase-free water. Thermal conditions were set as follows: the initial denaturation at 95°C for 2 min followed by 35 cycles at 95°C for 30 s, 60°C for 30 s, 72°C for 1 min, and a final extension at 68°C for 7 min. PCR products were confirmed by 1% agarose gel electrophoresis. The full cDNA length of *RfSpätzle* was obtained through rapid amplification of cDNA ends (RACE), which was completed by nested PCR with a SMARTer® RACE kit (Takara Bio Inc., Dalian, China) according to manufacturer guidelines. PCR products were purified with an EasyPure® Quick Gel Extraction Kit (TransGen Biotech, Beijing, China). Subsequently, the purified PCR products were ligated into the p*EASY*® -T1 cloning vector (TransGen Biotech, Beijing, China). The full cDNA sequence of *RfSpätzle* was analyzed with ExPASY tool[1] to determine its open reading frame (ORF). Conservative domains of RfSpätzle were predicted with running the SMART program[2].

TABLE 1 | Primer sequences used in this study.

Primer	Sequence (5′–3′)
Confirmatory PCR	
RfSpätzle-F	GAAGAGGACGAAGACGACAA
RfSpätzle-R	GAACGTGTCGCTGTAGAGGT
For cDNA cloning using RACE analysis	
3 R outer (*RfSpätzle*-F)	GCGAACATCCCGACCATTAT
5 R inner (*RfSpätzle*-R)	TCACCACGTACATCCAGTTTC
3 R inner (*RfSpätzle*-F)	CGTGGCATTGAACGGTTATTC
5 R outer (*RfSpätzle*-R)	GTATTTCGACGTGAGAGGATGT
For dsRNA synthesis	
dsRNA-SPZ-F	**TAATACGACTCACTATAGGG**CCGTGT ACATTCCAAAGCCT
dsRNA-SPZ-R	**TAATACGACTCACTATAGGG**GATTCG GGCATATTCACCAC
dsRNA-eGFP-F	**TAATACGACTCACTATAGGG**AGACAG TGCTTCAGCCGCTAC
dsRNA-eGFP-R	**TAATACGACTCACTATAGGG**AGAGTT CACCTTGATGCCGTTC
For RT-qPCR	
RfSpätzle-F	ACCCGTGTACATTCCAAAGC
RfSpätzle -R	TAGTTGGATTGCACGAGCTG
RfAttacin-F	TGGTTCTGGTGCCCAAGTGA
RfAttacin-R	GCCATAACGATTCTTGTTGGAGTA
RfCecropin-F	CAGAAGCTGGTTGGTTGAAGA
RfCecropin-R	GCAACACCGACATAACCCTGA
RfDefensin-F	TTCGCCAAACTTATCCTCGTG
RfDefensin-R	GGGTGCTTCGTTATCAACTTCC
RfColeoptericin-F	TCGTGGTTTCTACCATGTTCACT
RfColeoptericin-R	TCAGCTAAAACCTGATCTTGGA
Rfβ-actin-F	CCAAGGGAGCCAAGCAATT
Rfβ-actin-R	CGCTGATGCCCCTATGTATGT

The bold letters represent the T7 promoter which is added to the specific primers.

Multiple Sequence Alignments and Phylogenetic Analysis of *RfSpätzle*

BLASTX[3] was run to find the annotated Spz sequences from other insect species for the following multiple alignments. These Spz sequences were retrieved from the NCBI database. Multiple sequence alignments were performed with the Clustal Omega Program[4]. Phylogenetic analysis was completed with MEGA 5.05.

Expression Profile of *RfSpätzle* Across Different Tissues and Its Transcriptional Response to Microbial Infection

The healthy fourth instar larvae were dissected for collecting various tissues, including head, epidermis, hemolymph, fat body and gut, to determine the expression profile of *RfSpätzle*. Three larvae were dissected as a replicate and each treatment comprised four replicates. Total RNA was extracted from the tissues with TRIzol Reagent (Invitrogen, Carlsbad, CA, United States). Total RNA (1 μg) was used to synthesize cDNA with a Thermo Fisher Scientific Verso cDNA Kit (Thermo Fisher Scientific, United States). To detect the transcript abundance of *RfSpätzle*, RT-qPCR was performed with FastStart Universal SYBR Green Master (Roche, United States) with a 20-μl reaction system, including 1 μl of cDNA and 125 nM specific primers. *Rfβ-Actin* was employed as the internal reference gene. The qPCR reactions were completed with the following thermal cycling conditions: denaturation at 95°C for 10 min, 40 cycles of 95°C for 15 s, amplification at 60°C for 1 min, and with a dissociation step. The $2^{-\Delta\Delta Ct}$ method was used to calculate the relative expression level of our target genes.

To investigate the potential role of *RfSpätzle* in RPW immunity, its transcriptional response to microbial infection was examined. Systemic and oral infections were established with injecting or feeding Gram-positive bacteria *Staphylococcus aureus* and Gram-negative bacteria *Escherichia coli* DH5α as described by Dawadi et al. (2018). *Bacillus thuringiensis* is a biological control agent against RPW larvae (Pu et al., 2017). *Beauveria bassiana* was also used as fungal challenge and cultured on potato dextrose agar (PDA) for 2 weeks at 25°C. The conidial concentration of *B. bassiana* (1×10^8 spores/ml) was determined with a Neubauer hemocytometer as described by Hussain et al. (2016). Fat bodies and guts of the microbe-challenged larvae were obtained at different time points (6, 12, and 24 h). To detect the transcript changes of *RfSpätzle* by microbial challenge, RT-qPCR was performed as described above.

[1]http://www.expasy.org/

[2]http://www.smart.embl-heidelberg

[3]https://blast.ncbi.nlm.nih.gov/Blast.cgi

[4]https://www.ebi.ac.uk/Tools/msa/clustalo/

Functional Analysis of *RfSpätzle* by RNAi

To investigate the function of *RfSpätzle* in RPW immunity, the RNAi technique was used to silence this target gene. Following the manufacturer's protocols, the MEGA script® RNAi Kit (Thermo Fisher Scientific, United States) was used to synthesize *RfSpätzle* and eGFP dsRNA. In this study, eGFP dsRNA was employed as the control for our RNAi experiments. dsRNA (1 μg) was injected into the body cavity of fourth instar larvae. According to our previous investigations (Dawadi et al., 2018; Xiao et al., 2019), fat bodies, and guts were dissected 48 h after dsRNA delivery to verify RNAi efficiency by RT-qPCR.

Effect of *RfSpätzle* Knockdown on the Survival Ability of RPW Larvae

To evaluate the effect of *RfSpätzle* knockdown on the survival rate of RPW larvae, 48 h after the delivery of dsRNA, *RfSpätzle*-silenced individuals were challenged with entomopathogenic bacteria, *B. thuringiensis* strain HA (Pu et al., 2017). Five microliters of bacterial suspension (1.0×10^8 CFU/ml) or the same volume of sterile PBS (as control) was injected into the hemocoel of the fourth instar larvae (n = 30) and the survival rate was monitored every 6 h. The effect of *RfSpätzle* knockdown on the survival rate was determined with the Kaplan–Meier Log Rank survival test (IBM SPSS Statistics 22.0).

Effect of *RfSpätzle* Knockdown on the Gut Bacterial Composition of RPW

To reveal the impact of *RfSpätzle* knockdown on gut bacterial load and composition, guts were aseptically pulled out from RPW larvae at 48 h after dsRNA delivery and homogenized. Three larvae were dissected as a replicate and each treatment comprised at least three replicates. After serial dilution, gut homogenate was spread on LB agar plates and incubated for 16 h at 37°C as described by Dawadi et al. (2018). The number of colony-forming units (CFUs) of gut bacteria from the treated insects was counted. Furthermore, gut homogenate was processed for extracting total bacterial genomic DNA as described by Muhammad et al. (2017). Additionally, a blank DNA extraction was conducted as explained above but without any gut samples in each replicate. The bacterial 16S rRNA hypervariable region (V3–V4) was amplified with gene-specific primers 338F 5′-ACTCCTACGGGAGGCAGCAG-3′ and 5′-GGACTACHVGGGTWTCTAAT-3′. In the negative control, an equal volume of sterilized ddH_2O was used as the template to check for laboratory contamination. No target PCR products were detected by 1% agarose gel electrophoresis in any negative controls. The sequencing was completed with the Majorbio I-Sanger (China) Illumina MiSeq platform. The OTUs (operational taxonomic units) were clustered at the similarity threshold of 97% with the Usearch program (version 7.0[5]). Taxonomic analysis was performed with RDP Classifier[6] against the Bacteria database (Silva: Release128[7] and Greengene: Release 13.5[8]) at the confidence threshold of 0.7. The sequencing data were processed and analyzed with the methods as described by Muhammad et al. (2017) and Dawadi et al. (2018). Briefly, beta diversity analysis of RPW gut bacteria was completed through principal coordinate analysis (PCoA) and principal component analysis (PCA). ANOSIM (analysis of similarity) and DEseq analysis were employed to detect the differences in the gut bacterial community between the two groups.

[5]http://drive5.com/uparse/

[6]http://rdp.cme.msu.edu/

[7]http://www.arb-silva.de

[8]http://greengenes.secondgenome.com/

RESULTS

Molecular Characterization of *RfSpätzle*

The full-length cDNA sequence of *RfSpätzle* is 1865 bp long with a 1270-bp ORF that encodes a putative protein of 353 amino acids (**Figure 1A**), comprising an N-terminal signal peptide and a Spz domain of 97 amino acids at the C-terminus (**Figure 1B**). The presence of the Spz domain indicated that RfSpätzle is a

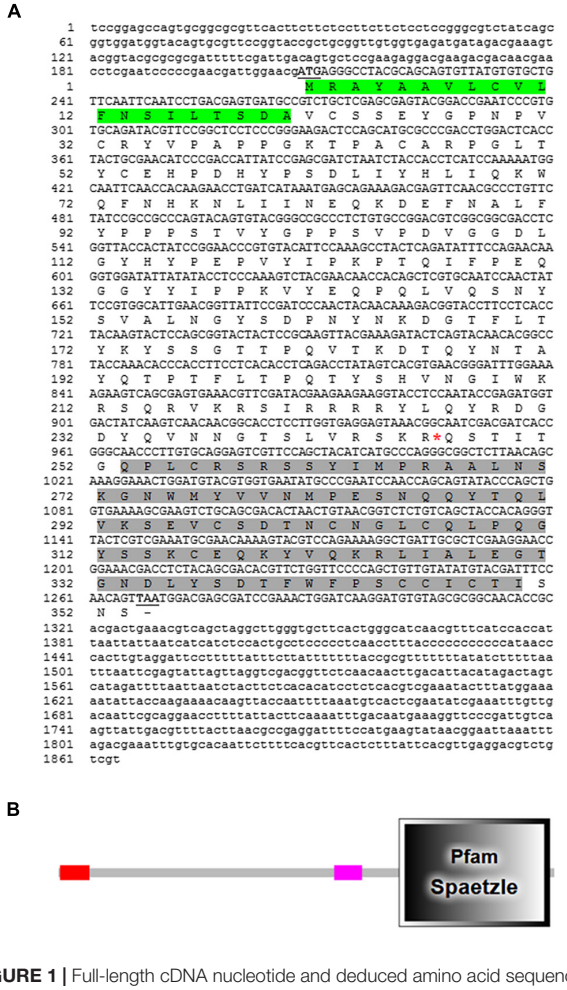

FIGURE 1 | Full-length cDNA nucleotide and deduced amino acid sequence of *RfSpätzle* **(A)** and schematic representation of the conserved functional domains in its deduced polypeptide sequence **(B)**. The start and stop codons are underlined and shown in bold letters. The signal peptide is shaded in green, and the conserved domain is dark gray. In the schematic representation, the signal peptide and Spätzle (Spz) domain are shown with the red and dark gray rectangles, respectively.

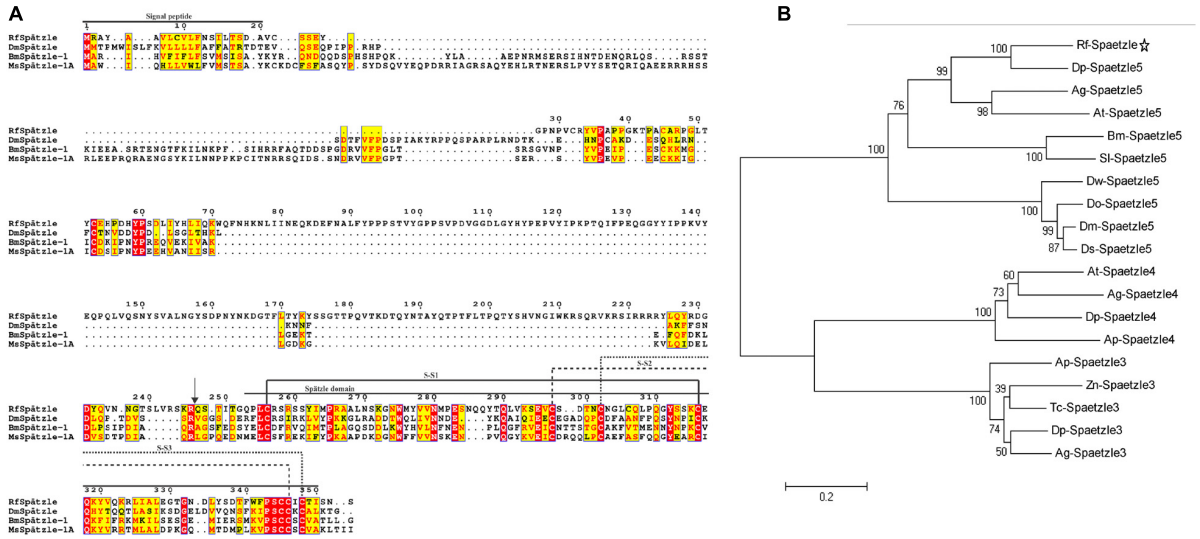

FIGURE 2 | Multiple alignments **(A)** and phylogenetic analysis **(B)** of *Rf*Spätzle with other **Spz** proteins. The arrow indicates the predicted cleavage site in RfSpätzle. The maximum likelihood (ML) method of MEGA 5.05 was employed to construct the phylogenetic tree of Spz sequences with 5000 bootstrap replicates. The following Spz were retrieved for our phylogenetic analysis: Bm-Spaetzle 5 [*Bombyx mori* AMR08002.1], Sl-Spaetzle 5 [*Spodoptera litura* XP_022816314.1], Zn-Spaetzle 3 [*Zootermopsis nevadensis* XP_021922319.1], Dm-Spaetzle 5 [*Drosophila melanogaster* NP_647753.1], Ds-Spaetzle 5 [*Drosophila serrata* XP_020809778.1], Do-Spaetzle 5 [*Drosophila obscura* XP_022208379.1], Dw-Spaetzle 5 [*Drosophila willistoni* XP_002062599.1], Dp-Spaetzle 3 [*Dendroctonus ponderosae* XP_019758543.1], Ag-Spaetzle 3 [*Anoplophora glabripennis* XP_018561823.2], Tc-Spaetzle 3 [*Tribolium castaneum* NP_001153625.1], Ap-Spaetzle 3 [*Agrilus planipennis* XP_025831835.1], Dp-Spaetzle 4 [*Dendroctonus ponderosae* XP_019771425.1], At-Spaetzle 4 [*Aethina tumida* XP_019880911.1], Ap-Spaetzle 4 [*Agrilus planipennis* XP_018325475.1], Ag-Spaetzle 4 [*Anoplophora glabripennis* XP_018575280.1], Dp spaetzle 5 [*Dendroctonus ponderosae* XP_019764273.1], Ag-Spaetzle 5 [*Anoplophora glabripennis* XP_018568892.1], and At-Spaetzle 5 [*Aethina tumida* XP_019879590.1].

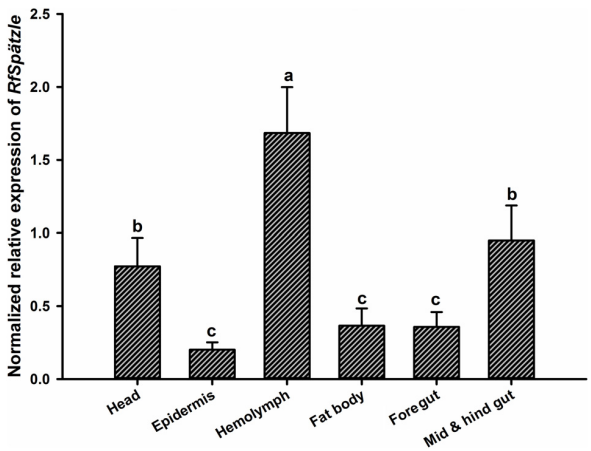

FIGURE 3 | Expression level of *RfSpätzle* in various tissues of healthy RPW larvae was quantified by RT-qPCR. The expression level of *RfSpätzle* was normalized to the *Rfβ-actin* gene. Different letters represent the significance, which was determined by Tukey's HSD (Honest Significant Difference) test at $P < 0.05$. The data are shown as the mean ± SD of four independent replicates.

member of the Spz family, mediating the Toll signaling pathway by binding the Toll receptors. The calculated mass and isoelectric point of this mature proSpätzle are 40,122.18 Da and 8.81. The putative activation cleavage site is located after VRSKR246 in pro-RfSpätzle, implying that pro-RfSpätzle might be activated by a clip-domain serine proteinase with trypsin-like specificity via limited proteolysis immediately after Arg^{246} (Jang et al., 2006; Wang et al., 2007; An et al., 2010). Interestingly, some residues, including six cysteines, two prolines, and one glutamine, are conserved in four insect species (**Figure 2A**). It has been confirmed that these six conserved cysteines are crucial to disulfide formation and fold stability of the neurotrophin-like cysteine knot (CK) structural motif (Jang et al., 2006; An et al., 2010). Moreover, most Spz members have an orphan cysteine before Cys5, which can establish an intermolecular linkage with its counterpart in another subunit to form a disulfide-linked homodimer (Hoffmann et al., 2008; Wang and Zhu, 2009; An et al., 2010). Furthermore, when 19 Spz sequences were taken into consideration for phylogenetic analysis, these sequences were split into three distinct clusters (Spz3, Spz4, and Spz5, **Figure 2B**). The inclusion of *RfSpätzle* in the same branch as *Drosophila* Spz-5, exhibiting a bootstrap value of 100, indicates that *RfSpätzle* is an ortholog of *Drosophila* Spz-5.

Expression Profile of *RfSpätzle* Across Different Tissues and Its Response to the Challenge of Pathogenic Microbes

RT-qPCR analysis showed that *RfSpätzle* was constitutively expressed in the tested tissues at significantly different levels (ANOVA: $F_{5,18} = 45.11$, $P < 0.001$) (**Figure 3**). The expression level of *RfSpätzle* in the hemolymph and gut was 8.38- and 5.00-fold higher than that in the epidermis. *RfSpätzle* was significantly induced in the fat body and gut upon the systemic and oral

pathogenic challenge of *S. aureus*, *E. coli*, and *B. bassiana* as compared to the controls (**Figures 4**, **5**). These results suggest that *RfSpätzle* might mediate the systemic and gut immune responses to fight against microbial intruders.

RfSpätzle Knockdown Impaired the Immune Response Against Pathogen Invasion

Compared to the controls, the expression levels of *RfSpätzle* in the fat body and gut were significantly reduced by 83.23 and 69.26% at 48 h after dsRNA injection (*t* test for fat body: $t = -8.95$, df = 6, $P < 0.001$; gut: $t = -2.92$, df = 6, $P < 0.05$) (**Figure 6**). After being challenged by *B. thuringiensis*, *Rf* Spätzle-silenced individuals (dsSPZ) succumbed significantly faster than their counterparts ($P < 0.05$, **Figure 7**). Further investigations revealed that *RfSpätzle* silencing led to the significant downregulation of *RfColeoptericin* (*t* test for fat body: $t = -4.18$, df = 6, $P = 0.006$; gut: $t = -2.77$, df = 6, $P < 0.05$) and *RfCecropin* (*t* test for fat body: $t = -3.34$, df = 6, $P < 0.05$; gut: $t = -2.83$, df = 6, $P < 0.05$) in fat body and gut, but the expression level of *RfDefensin* (*t* test for fat body: $t = -8.95$, df = 6, $P = 0.06$; gut: $t = -1.55$, df = 6, $P = 0.17$) and *RfAttacin* (*t* test for fat body: $t = -1.05$, df = 6, $P = 0.33$; gut: $t = -2.92$, df = 6, $P = 0.70$) was not affected by *RfSpätzle* knockdown (**Figures 8A,B**). These findings suggested that *RfSpätzle* mediates the expression of these two antimicrobial

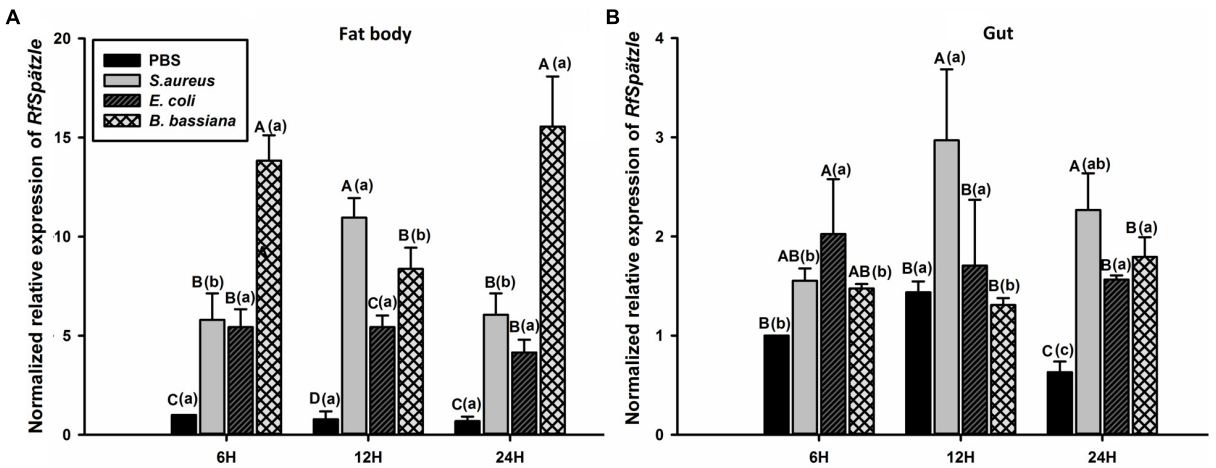

FIGURE 4 | Transcriptional response of *RfSpätzle* in fat body **(A)** and gut **(B)** of RPW larvae after the systemic challenge of microbial pathogens at different time points. The expression level of *RfSpätzle* was normalized to the *Rf*β-*actin* gene. Uppercase letters indicate significant differences across all pathogen-challenged samples at the same point, while the lowercase letters represent the significance of the same treatment across different time points. The significance was determined by Tukey's HSD test at $P < 0.05$. The data are shown as the mean ± SD of three independent replicates.

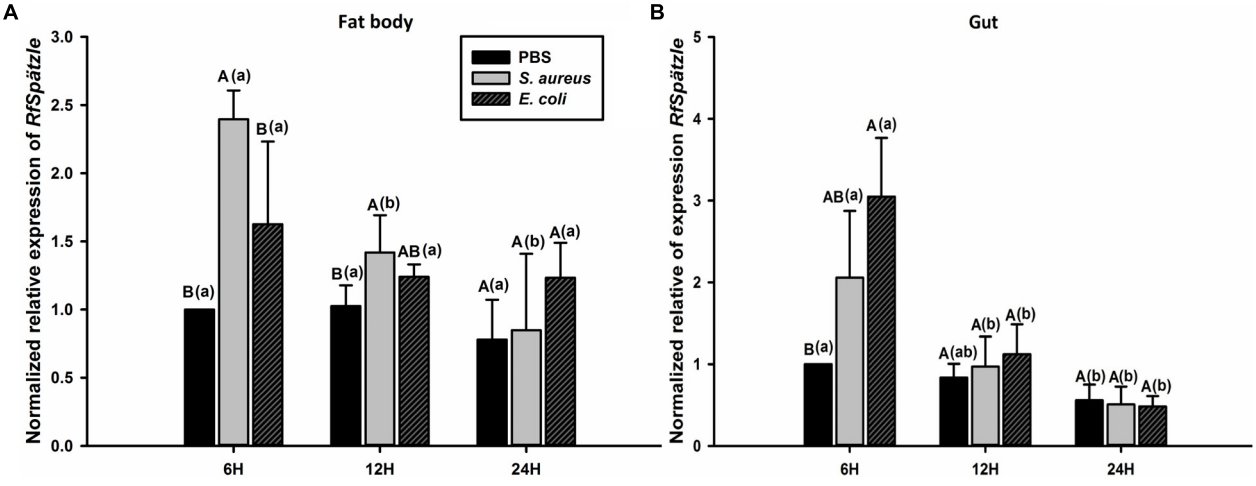

FIGURE 5 | Transcriptional response of *RfSpätzle* in fat body **(A)** and guts **(B)** of RPW larvae at different time points after being orally infected by *S. aureus* and *E. coli*. The expression level of *RfSpätzle* was normalized to the *Rf*β-*actin* gene. Uppercase letters indicate significant differences across the different challenged samples at the same time point, while the lowercase letters represent the significance of the same treatment across different time points. The significance was detected by Tukey's HSD test at $P < 0.05$. The data are shown as the mean ± SD of three independent replicates.

peptide genes (*RfColeoptericin* and *RfCecropin*) to confer RPW protection against the pathogen invasion.

RfSpätzle Knockdown Altered the Community Structure of RPW Gut Microbiota

The role of the *RfSpätzle*-mediated Toll-like pathway in regulating the composition and proportion of RPW gut bacteria was determined. Comparative analysis of the gut bacterial load showed a numerically higher number of CFUs in the *RfSpätzle*-silenced individuals although no significance was detected (*t* test: $t = -1.22$, df = 16, $P = 0.24$) (**Figure 9**). Bacterial 16S rRNA-based high-throughput sequencing yielded 431,163 reads. At the 97% similarity threshold, these reads were binned into 414 OTUs, which contained 243 OTUs from the dseGFP group and 171 OTUs from the dsSPZ group. Seventy OTUs were shared between the two groups (**Supplementary Figure S1**). Diversity analysis revealed that the community diversity (Shannon and Simpson) and species richness (ACE, Chao, and Sobs) did not vary significantly between the two groups (**Table 2** and **Supplementary Figure S2**). Proteobacteria and Tenericutes represented the bulk (95%) of the RPW gut microbiota, while the relative abundance of Bacteroidetes and Firmicutes was less than 5%. At the family level, the microbiota was dominated (>98%) by Enterobacteriaceae, Entomoplasmataceae, Pseudomonadaceae, Acetobacteraceae, Porphyromonadaceae, Spiroplasmataceae, and Enterococcaceae. ANOSIM analysis revealed that no significance was determined in the RPW gut bacterial community between the two groups ($P = 0.75$). However, the relative abundance of gut bacteria at different taxonomic levels was altered by *Rf* Spätzle silencing. For example, the percentage of Proteobacteria (*t* test: $t = 4.12$, df = 4, $P < 0.05$) in *RfSpätzle*-silenced RPW larvae was decreased by 20% compared to that of controls, while the relative abundance of Tenericutes (*t* test: $t = -5.27$, df = 4, $P < 0.05$) was increased to 23.86% by *RfSpätzle* knockdown (**Figure 10A**). Similarly, the relative abundance of Acetobacteraceae (*t* test: $t = 3.84$, df = 4, $P < 0.05$) was significantly less than that of controls. However, Entomoplasmataceae (*t* test: $t = -4.71$, df = 4, $P < 0.05$) represented a higher percentage of *Rf* Spätzle-silenced RPW larvae (**Figure 10B**). At the OTU level, DEseq analysis revealed that the abundance of OTU306 (Cellulomonadaceae, G^+), OTU279 (Gallionellaceae, G^-), and OTU283 (*Ferriphaselus*, G^-) was significantly increased while that of OTU200 (*Acetobacterium*, G^+) was decreased by *RfSpätzle* silencing (**Supplementary Table S1**). Collectively, these data indicated that *RfSpätzle* knockdown can cause some significant changes in the proportion of RPW gut bacteria, suggesting that the Spz -mediated Toll-like pathway is involved in modulating the homeostasis of the RPW gut microbiota.

DISCUSSION

Recently, the immune responses of RPW larvae to some biocontrol agents, including the entomopathogenic nematode *Steinernema carpocapsae* (Mastore et al., 2014), bacteria (Shi et al., 2014), and fungi (Hussain et al., 2016), have been investigated.

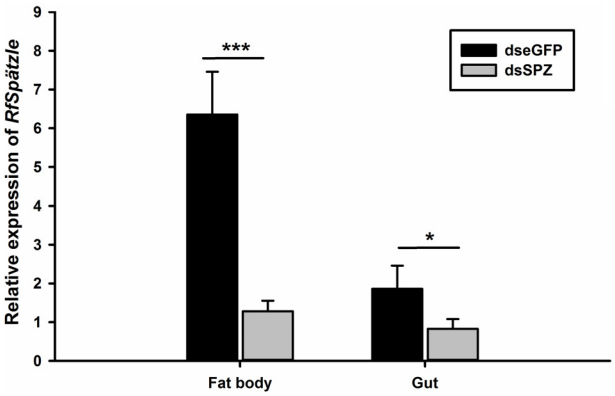

FIGURE 6 | Verification of the *RfSpätzle* RNAi efficiency in the fat body and gut of the fourth instar RPW larvae 48 h after dsRNA injection. The data are shown as the mean ± SD of four independent replicates. The significant differences were determined by an independent sample *t* test (*$P < 0.05$ and ***$P < 0.001$).

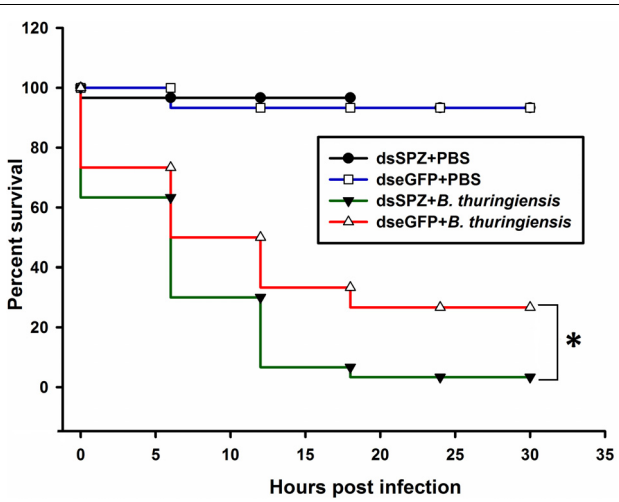

FIGURE 7 | Survival rate of *RfSpätzle*-silenced individuals after being challenged by the pathogenic bacteria *Bacillus thuringiensis* strain HA. Survival analysis was performed with Kaplan-Meir survival log rank (Mantel-Cox) test (*$P < 0.05$). The experiment was repeated three times with 30 fourth instar larvae from each cohort.

However, the underlying molecular mechanisms conferring RPW larvae to ward off the microbial pathogens have not been fully elucidated. In this work, a homolog of *D. melanogaster* Spz, *RfSpätzle*, was first cloned and characterized from *R. ferrugineus*. *RfSpätzle* encodes a protein that consists of two typical conserved functional domains, a signal peptide and a Spz domain. Multiple sequence comparisons showed that a putative activation cleavage site of *RfSpätzle* is directly after R^{246}, suggesting that an activating proteinase could cleave pro-*RfSpätzle* after this specific Arg to release the activated form of *RfSpätzle*. Interestingly, seven Cys residues, which are found in nearly all known Spz cysteine-knot domains, were also found in the C-terminal active cystine-knot domain of *Rf* Spätzle. These data suggested that *Rf* Spätzle is a

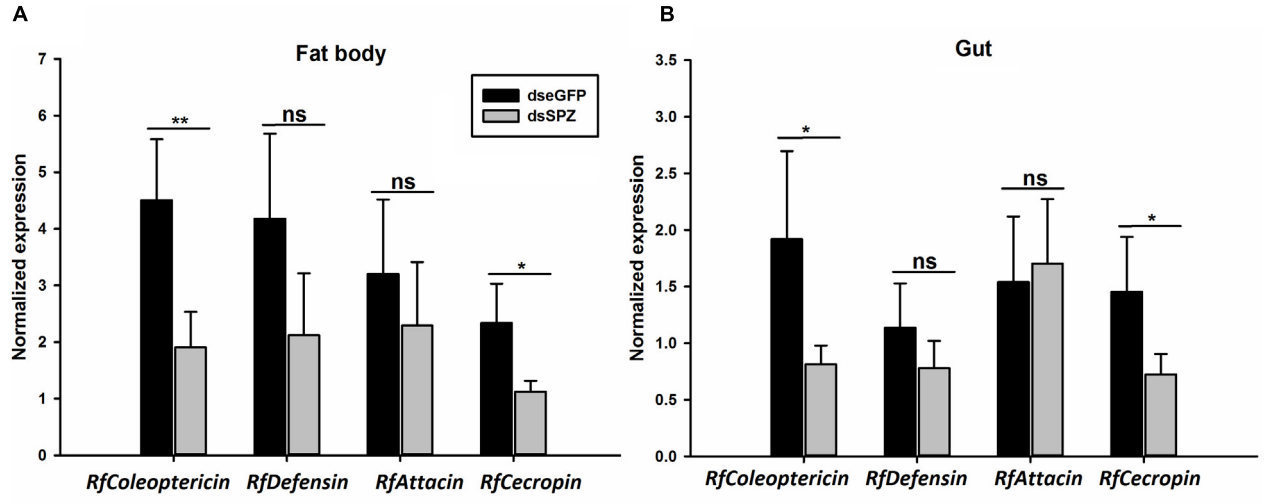

FIGURE 8 | Effects of *RfSpätzle* knockdown on the transcript abundance of four antimicrobial peptide genes, *RfColeoptericin*, *RfDefensin*, *RfAttacin*, and *RfCecropin* in the fat body **(A)** and gut **(B)** of the fourth instar RPW larvae 48 h after dsRNA delivery. The data are shown as the mean ± SD of four independent replicates. The significant differences were detected with an independent sample *t* test (ns, non-significant, $P > 0.05$, $^{*}P < 0.05$, and $^{**}P < 0.01$).

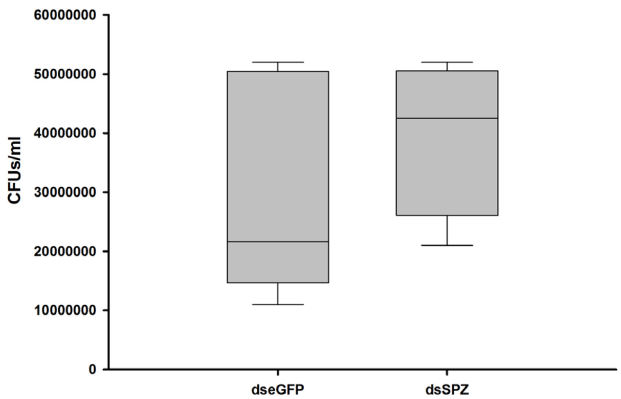

FIGURE 9 | Impact of *RfSpätzle* silencing on the gut bacterial load of RPW larvae.

TABLE 2 | Community diversity and richness of microbiota associated with the guts of control (dseGFP) and Spz knockdown (dsSPZ) RPW individuals.

		Community diversity		Community richness		
Sample ID	**Reads**	**Shannon**	**Simpson**	**ACE**	**Chao**	**Sobs**
dseGFP-1	52,972	1.4	0.39	55.1	53.0	49
dseGFP-2	50,724	0.8	0.68	168.1	66.5	41
dseGFP-3	51,848	1.1	0.52	43.7	40.1	38
dsSPZ-1	57,258	1.0	0.47	71.5	50.8	41
dsSPZ-2	57,296	1.1	0.51	81.5	76.1	72
dsSPZ-3	51,553	1.2	0.38	40.0	37.0	34

secretory cysteine-knot protein. Moreover, the conserved features of this protein implied that the *RfSpätzle* homodimer can be formed via intermolecular Cys-Cys disulfide bonds to activate the immune signaling pathway (Ferrandon et al., 2007; An et al., 2010; Zhong et al., 2012; Vaniksampanna et al., 2019).

RfSpätzle is constitutively expressed at different levels in all tested tissues of RPW larvae. The expression level of *RfSpätzle* was significantly higher in gut and hemolymph compared to other tissues, indicating that it might be involved in the systemic and gut immunity of RPW larvae. Moreover, the challenge of *S. aureus*, *E. coli*, and *B. bassiana* strongly induced the expression of *RfSpätzle* in the fat body and gut of RPW larvae. Additionally, we found that *RfSpätzle*-silenced individuals were more vulnerable to pathogenic infection than controls. Further analysis confirmed that *RfSpätzle* silencing resulted in the significant downregulation of *RfColeoptericin* and *RfCecropin*, suggesting that *RfSpätzle* knockdown could compromise RPW innate immunity. Interestingly, the secretion of cecropin is IMD-dependent in *D. melanogaster* (Önfelt Tingvall et al., 2001), and coleoptericins have been shown to be IMD-dependent in the cereal weevil *Sitophilus* (Maire et al., 2018). Recently, a similar role of the Spz gene was also revealed in shrimp *Litopenaeus vannamei* (Yuan et al., 2017), the black tiger shrimp *P. monodon* (Boonrawd et al., 2017), and freshwater prawn *M. rosenbergii* (Vaniksampanna et al., 2019). It is known that *D. melanogaster* Spz, an extracellular ligand of the Toll receptor, is required to activate the production of antimicrobial peptides via the Toll pathway (Valanne et al., 2011). Collectively, these data indicate that RfSpätzle can mediate the secretion of some antimicrobial peptides of RPW larvae to defend against microbial intruders.

The gut microbiota has been confirmed to profoundly affect host physiological fitness, including development, nutrition metabolism, and immunity, in many metazoan animals (Muhammad et al., 2017; Zheng et al., 2017; Kamareddine et al., 2018; Hebineza et al., 2019). Importantly, the healthy homeostasis of gut microbiota is critical for proper growth and

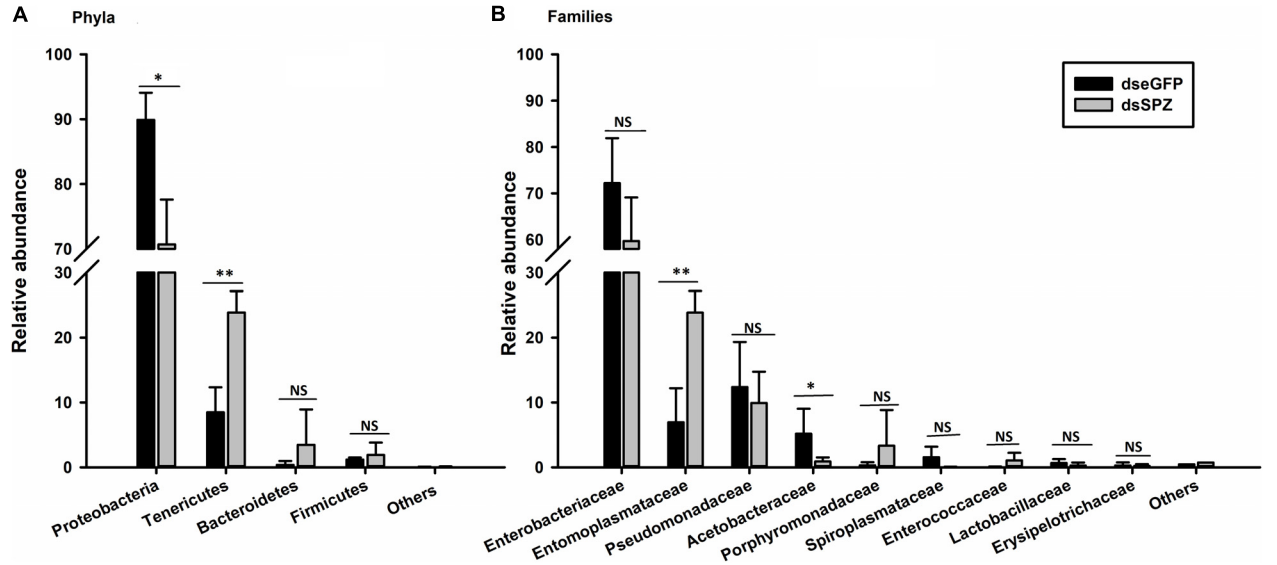

FIGURE 10 | Influence of *RfSpätzle* silencing on the relative abundance of gut bacteria at the phylum **(A)** and family **(B)** levels. The data are shown as the mean ± SD of three independent replicates. The significant differences were detected with an independent sample *t* test (ns, non-significant, $P > 0.05$, $^{*}P < 0.05$, and $^{**}P < 0.01$).

development of the host. However, the exact mechanisms by which animals tolerate the commensal bacteria while eliminating the transient pathogenic bacteria are still not well understood. In *D. melanogaster*, it is well-known that dual oxidase-mediated ROS production and the IMD pathway play vital roles in regulating the homeostasis of gut microbiota (Ryu et al., 2008; Lee et al., 2017). More recently, the *RfRelish*-mediated IMD-like pathway has been determined to be involved in modulating the homeostasis of RPW gut bacteria (Dawadi et al., 2018; Xiao et al., 2019). Insect immune responses are mainly under the control of two signaling pathways, the Toll and IMD pathways (Hetru and Hoffmann, 2009). However, the Toll pathway does not mediate local gut immunity in *D. melanogaster* (Davis and Engström, 2012). Previously, our transcriptome analysis found the essential elements for the Toll signaling pathway, including SPs, Spz-like proteins, Toll receptors, Tube-1, MyD88, TRAF, and Cactus, in the RPW gut (Muhammad et al., 2019). In the present investigation, we found that the expression levels of *RfSpätzle* and some antimicrobial peptides were drastically induced in the fat body and gut upon microbial infection. Specifically, it was found that the relative abundance of some gut bacteria in RPW larvae was significantly altered by *RfSpätzle* knockdown. The expression levels of antimicrobial peptides in the gut, *RfColeoptericin* and *RfCecropin*, were also reduced by *RfSpätzle* silencing. Antimicrobial peptides are one of the vital effectors to maintain insect-microbe symbiosis (Ryu et al., 2008; Login et al., 2011; Vigneron et al., 2012; Masson et al., 2015; Lee et al., 2017; Dawadi et al., 2018; Zaidman-Rémy et al., 2018; Xiao et al., 2019). Consequently, our data suggested that the *RfSpätzle*-mediated Toll-like signaling pathway could regulate the proportion of RPW gut bacteria by mediating the synthesis of antimicrobial peptides. To the best of our knowledge, this report is the first to reveal the possible role of the Spz-mediated Toll-like pathway in regulating the homeostasis of insect gut microbiota. However, *RfSpätzle* knockdown only differentially affected the relative abundance of four OTUs, including gram-positive and gram-negative bacteria, suggesting that the effects of the Toll-like signaling pathway on gut bacterial composition are highly limited and non-specific. It has been revealed that the majority of RPW gut bacteria are Gram-negative (Muhammad et al., 2017). This finding might explain the dominant role of the IMD-like pathway in maintaining the homeostasis of RPW gut bacteria.

It has been well defined that many weevils are associated with the γ-proteobacterial endosymbiont lineage *Nardonella*, which produces tyrosine for host cuticle formation and hardening (Hosokawa et al., 2015; Anbutsu et al., 2017). Although the weevil–*Nardonella* coevolution has lasted more than 100 million years, *Nardonella* infections in a number of weevil lineages have been lost or replaced by different bacterial lineages (Lefèvre et al., 2004; Conord et al., 2008). Therefore, although we still did not find *Nardonella* in RPW populations of our country in this study, it would be worthwhile to intensively investigate the presence of *Nardonella* in other beetle species to uncover the strikingly dynamic aspect of the endosymbiotic evolution in insects. The topic of insect immunity preserving endosymbionts and controlling their load and location while keeping the ability to cope with potential environmental infections by microbial intruders is highly interesting. Recently, the IMD-like pathway has been confirmed to mediate the control of *Sodalis pierantonius* in the bacteriome of *Sitophilus* spp. (Maire et al., 2018). However, whether the Toll pathway is involved in modulating the endosymbionts in bacteriome has not been determined. Moreover, the IMD and Toll pathways in hemipterans and other arthropods might be intertwined to target wider and overlapping

arrays of microbes (Nishide et al., 2019). Therefore, further studies can detect whether there is any crosstalk between the IMD and Toll signaling pathways in this pest to regulate the homeostasis of RPW gut bacteria.

CONCLUSION

In conclusion, we determined that *RfSpätzle* is involved in the innate immunity of RPW by mediating the secretion of the antimicrobial peptides *RfColeoptericin* and *RfCecropin*. The *Rf* Spätzle-mediated Toll-like signaling pathway not only confers protection against pathogen invasion but may also modulate the proportion of some gut bacteria.

DATA AVAILABILITY STATEMENT

The datasets generated for this study can be found in the NCBI database and the submission number of our sequence data is SAMN11959955-11959960.

AUTHOR CONTRIBUTIONS

ZS conceived and designed the research. ZS and YH provided the reagents. AM, PH, RX, and TJ completed the experiments. AM, XW, and ZS analyzed the data. ZS and AM prepared the manuscript. All authors have read and approved the final manuscript.

FUNDING

This work was supported by the National Natural Science Foundation of China (31470656), the National Key Research and Development Project of China (2017YFC1200605), and the Natural Science Foundation of Fujian Province (2018J01705).

SUPPLEMENTARY MATERIAL

The Supplementary Material for this article can be found online at: https://www.frontiersin.org/articles/10.3389/fmicb.2020.00846/full#supplementary-material

FIGURE S1 | Bacterial OTUs (operational taxonomic units) were recovered from the control insects (dseGFP) and *RfSpätzle*-silenced individuals (dsSPZ). Venn diagram indicates the unique and shared OTUs between the two groups.

FIGURE S2 | Principal coordinate analysis of the phylogenetic β-diversity matrix obtained starting from the OTU table. The explained variance is as follows: 62.71% 1st component, 27.53% 2nd component.

TABLE S1 | Effect of *RfSpätzle* knockdown on the reads number of OTUs between the two groups.

REFERENCES

Aggarwal, K., and Silverman, N. (2008). Positive and negative regulation of the *Drosophila* immune response. *BMB Rep.* 41, 267–277. doi: 10.5483/bmbrep.2008.41.4.267

Al-Dosary, N. M. N., Al-Dobai, S., and Faleiro, J. R. (2016). Review on the management of red palm weevil *Rhynchophorus ferrugineus* Olivier in date palm *Phoenix dactylifera* L. emirates. *J. Food Agri.* 28:34. doi: 10.9755/ejfa.2015-10-897

Ami, E. B., Yuval, B., and Jurkevitch, E. (2010). Manipulation of the microbiota of mass-reared mediterranean fruit flies *Ceratitis capitata* (Diptera: Tephritidae) improves sterile male sexual performance. *ISME J.* 4, 28–37. doi: 10.1038/ismej.2009.82

An, C., Jiang, H., and Kanost, M. R. (2010). Proteolytic activation and function of the cytokine Spätzle in the innate immune response of a lepidopteran insect, *Manduca sexta*. *FEBS J.* 277, 148–162. doi: 10.1111/j.1742-4658.2009.07465.x

Anbutsu, H., Moriyama, M., Nikoh, N., Hosokawa, T., Futahashi, R., Tanahashi, M., et al. (2017). Small genome symbiont underlies cuticle hardness in beetles. *Proc. Natl. Acad. Sci. U.S.A.* 114, E8382–E8391. doi: 10.1073/pnas.1712857114

Bischoff, V., Vignal, C., Duvic, B., Boneca, I. G., Hoffmann, J. A., and Royet, J. (2006). Downregulation of the *Drosophila* immune response by peptidoglycan recognition proteins SC1 and SC2. *PLoS Pathog.* 2:e14. doi: 10.1371/journal.ppat.0020014

Blatch, S. A., Meyer, K. W., and Harrison, J. F. (2010). Effects of dietary folic acid level and symbiotic folate production on fitness and development in the fruit fly *Drosophila melanogaster*. *Fly* 4, 312–319. doi: 10.4161/fly.4.4.13258

Boonrawd, S., Mani, R., Ponprateep, S., Supungul, P., Masrinoul, P., Tassanakajon, A., et al. (2017). Characterization of PmSp?tzle 1 from the black tiger shrimp *Peneaus monodon*. *Fish Shellf. Immunol.* 65, 88–95. doi: 10.1016/j.fsi.2017.04.005

Conord, C., Depres, L., Vallier, A., Balmand, S., Miquel, C., Zundel, S., et al. (2008). Long-term evolutionary stability of bacterial endosymbiosis in curculionoidea: additional evidence of symbiont replacement in the Dryophthoridae family. *Mol. Biol. Evol.* 25, 859–868. doi: 10.1093/molbev/msn027

Davis, M. M., and Engström, Y. (2012). Immune response in the barrier epithelia: lessons from the fruit fly *Drosophila melanogaster*. *J. Innate Immun.* 4, 273–283. doi: 10.1159/000332947

Dawadi, B., Wang, X., Xiao, R., Muhammad, A., Hou, Y., and Shi, Z. (2018). PGRP-LB homolog acts as a negative modulator of immunity in maintaining the gut-microbe symbiosis of red palm weevil, *Rhynchophorus ferrugineus* Olivier. *Dev. Comp. Immunol.* 86, 65–77. doi: 10.1016/j.dci.2018.04.021

Douglas, A. E. (2015). Multiorganismal insects: diversity and function of resident microorganisms. *Annu. Rev. Entomol.* 60, 17–34. doi: 10.1146/annurev-ento-010814-020822

Engel, P., and Moran, N. A. (2013). The gut microbiota of insects - diversity in structure and function. *FEMS Microbiol. Rev.* 37, 699–735. doi: 10.1111/1574-6976.12025

Ferrandon, D., Imler, J.-L., Hetru, C., and Hoffmann, J. A. (2007). The *Drosophila* systemic immune response: sensing and signalling during bacterial and fungal infections. *Nature Rev. Immunol.* 7:862. doi: 10.1038/nri2194

Guo, L., Karpac, J., Tran, S. L., and Jasper, H. (2014). PGRP-SC2 promotes gut immune homeostasis to limit commensal dysbiosis and extend lifespan. *Cell* 156, 109–122. doi: 10.1016/j.cell.2013.12.018

Ha, E.-M., Oh, C.-T., Bae, Y. S., and Lee, W.-J. (2005). A direct role for dual oxidase in *Drosophila* gut immunity. *Science* 310, 847–850. doi: 10.1126/science.1117311

Hebineza, P., Muhammad, A., Ji, T., Xiao, R., Yin, X., Hou, Y., et al. (2019). The promoting effect of gut microbiota on growth and development of red palm weevil, *Rhynchophorus ferrugineus* Olivier (Coleoptera: Dryophthoridae) by modulating nutritional metabolism. *Front. Microbiol.* 10:1212. doi: 10.3389/fmicb.2019.01212

Hetru, C., and Hoffmann, J. A. (2009). NF-κB in the immune response of *Drosophila*. *Cold Spring Harb. Perspect. Biol.* 1:a000232. doi: 10.1101/cshperspect.a000232

Hoffmann, A., Funkner, A., Neumann, P., Juhnke, S., Walther, M., Schierhorn, A., et al. (2008). Biophysical characterization of refolded *Drosophila* Spätzle, a cystine knot protein, reveals distinct properties of three isoforms. *J. Biol. Chem.* 283, 32598–32609. doi: 10.1074/jbc.M801815200

Hosokawa, T., Koga, R., Tanaka, K., Moriyama, M., Anbutsu, H., and Fukatsu, T. (2015). *Nardonella* endosymbionts of Japanese pest and non-pest weevils (Coleoptera: Curculionidae). *Appl. Entomol. Zool.* 50, 223–229.

Hultmark, D. (2003). Drosophila immunity: paths and patterns. *Curr. Opin. Immunol.* 15, 12–19. doi: 10.1016/s0952-7915(02)00005-5

Hussain, A., Rizwan-ul-Haq, M., Al-Ayedh, H., and AlJabr, A. M. (2016). Susceptibility and immune defence mechanisms of *Rhynchophorus ferrugineus* (Olivier)(Coleoptera: Curculionidae) against entomopathogenic fungal infections. *Int. J. Mol. Sci.* 17:1518. doi: 10.3390/ijms17091518

Jang, I.-H., Chosa, N., Kim, S.-H., Nam, H.-J., Lemaitre, B., Ochiai, M., et al. (2006). A Spätzle-processing enzyme required for toll signaling activation in *Drosophila* innate immunity. *Dev. Cell* 10, 45–55. doi: 10.1016/j.devcel.2005.11.013

Janssen, A. W., and Kersten, S. (2015). The role of the gut microbiota in metabolic health. *J. Fed. Am. Soc. Exp. Biol.* 29, 3111–3123.

Jia, S., Zhang, X., Zhang, G., Yin, A., Zhang, S., Li, F., et al. (2013). Seasonally variable intestinal metagenomes of the red palm weevil (*Rhynchophorus ferrugineus*). *Environ. Microbiol.* 15, 3020–3029. doi: 10.1111/1462-2920.12262

Ju, R., Wang, F., Wan, F., and Li, B. (2011). Effect of host plants on development and reproduction of *Rhynchophorus ferrugineus* (Olivier) (Coleoptera: Curculionidae). *J. Pest Sci.* 84, 33–39. doi: 10.1007/s10340.010.0323.4

Kamareddine, L., Robins, W. P., Berkey, C. D., Mekalanos, J. J., and Watnick, P. I. (2018). The *Drosophila* immune deficiency pathway modulates enteroendocrine function and host metabolism. *Cell Metabol.* 28, 449–462. doi: 10.1016/j.cmet.2018.05.026

Kim, J. K., Lee, J. B., Huh, Y. R., Jang, H. A., Kim, C-H., Yoo, J. W., et al. (2015). *Burkholderia* gut symbionts enhance the innate immunity of host *Riptortus pedestris*. *Dev. Comp. Immunol.* 53, 265–269. doi: 10.1016/j.dci.2015.07.006

Lee, J.-H., Lee, K.-A., and Lee, W.-J. (2017). Microbiota, gut physiology, and insect immunity. *Adv. Insect Physiol.* 52, 111–138. doi: 10.1016/bs.aiip.2016.11.001

Lefèvre, C., Charles, H., Vallier, A., Delobel, B., Farrell, B., and Heddi, A. (2004). Endosymbiont phylogenesis in the dryophthoridae weevils: evidence for bacterial replacement. *Mol. Biol. Evol.* 21, 965–973. doi: 10.1093/molbev/msh063

Lemaitre, B., and Hoffmann, J. (2007). The host defense of *Drosophila melanogaster*. *Annu. Rev. Immunol.* 25, 697–743. doi: 10.1146/annurev.immunol.25.022106.141615

Lin, J., Xia, X., Yu, X.-Q., Shen, J., Li, Y., Lin, H., et al. (2018). Gene expression profiling provides insights into the immune mechanism of *Plutella xylostella* midgut to microbial infection. *Gene* 647, 21–30. doi: 10.1016/j.gene.2018.01.001

Login, F. H., Balmand, S., Vallier, A., Vincent-Monégat, C., Vigneron, A., Weiss-Gayet, M., et al. (2011). Antimicrobial peptides keep insect endosymbionts under control. *Science* 334, 362–365. doi: 10.1126/science.1209728

Maire, J., Vincent-Monégat, C., Balmand, S., Vallier, A., Hervé, M., Masson, F., et al. (2019). Weevil pgrp-lb prevents endosymbiot TCT dissemination and chronic host systemic immune activation. *Proc. Natl. Acad. Sci. U.S.A.* 116, 5623–5632. doi: 10.1073/pnas.1821806116

Maire, J., Vincent-Monégat, C., Masson, F., Zaidman-Rémy, A., and Heddi, A. (2018). An IMD-like pathway mediates both endosymbiont control and host immunity in the cereal weevil *Sitophilus* spp. *Mcirobiome* 6:6. doi: 10.1186/s40168-017-0397-9

Masson, F., Vallier, A., Vigneron, A., Balmand, S., Vincent-Monégat, C., Zaidman-Rémy, L., et al. (2015). Systemic infection generates a local-like immune response of the bacteriome organ in insect symbiosis. *J. Innate Immunol.* 7, 290–301. doi: 10.1059/000368928

Mastore, M., Ariza, V., Manachini, B., and Brivio, M. (2014). Modulation of immune responses of *Rhynchophorus ferrugineus* (Insecta: Coleoptera) induced by the entomopathogenic nematode *Steinernema carpocapsae* (Nematoda: Rhabditida). *Insect Sci.* 22, 748–760. doi: 10.1111/1744-7917.12141

Montagna, M., Chouaia, B., Mazza, G., Prosdocimi, E. M., Crotti, E., Mereghetti, V., et al. (2015). Effects of the diet on the microbiota of the red palm weevil (Coleoptera: Dryophthoridae). *PLoS One* 10:e0117439. doi: 10.1371/journal.pone.0117439

Muhammad, A., Fang, Y., Hou, Y., and Shi, Z. (2017). The gut entomotype of red palm weevil *Rhynchophorus ferrugineus* Olivier (Coleoptera: Dryophthoridae) and their effect on host nutrition metabolism. *Front. Microbiol.* 8:2291. doi: 10.3389/fmicb.2017.02291

Muhammad, A., Prosper, H., Ji, T., Hou, Y., and Shi, Z. (2019). Intestinal microbiota confer protection by priming the immune systme of red palm weevil *Rhynchophorus ferrugineus* Olivier (Coleoptera: Dryophthoridae). *Front. Physiol.* 10:1303. doi: 10.3389/fphys.2019.01303

Nishide, Y., Kageyama, D., Yokoi, K., Jouraku, A., Tanaka, H., Futahashi, R., et al. (2019). Functional crosstalk across IMD and Toll pathways: insight into the evolution of incomplete immune cascades. *Proc. R. Soc. B.* 286:20182207. doi: 10.1098/rspb.2018.2207

Önfelt Tingvall, T., Roos, E., and Engström, Y. (2001). The *imd* gene is required for local Cecropin expression in *Drosophila* barrier epithelia. *EMBO Rep.* 2, 239–243. doi: 10.1093/embo-reports/kve048

Paredes, J. C., Welchman, D. P., Poidevin, M., and Lemaitre, B. (2011). Negative regulation by amidase PGRPs shapes the *Drosophila* antibacterial response and protects the fly from innocuous infection. *Immunity* 35, 770–779. doi: 10.1016/j.immuni.2011.09.018

Park, K-E., Jang, S. H., Lee, J., Lee, S. A., Kikuchi, Y., Seo, Y-S., et al. (2018). The roles of antimicrobial peptide, rip-thanatin, in the midgut of Riptortus pedestris. *Dev. Comp. Immunol.* 78, 83–90. doi: 10.1016/j.dci.2017.09.009

Parker, J. S., Mizuguchi, K., and Gay, N. J. (2001). A family of proteins related to Spätzle, the toll receptor ligand, are encoded in the *Drosophila* genome. *Proteins* 45, 71–80. doi: 10.1002/prot.1125

Pu, Y., Ma, T., Hou, Y., and Sun, M. (2017). An entomopathogenic bacterium strain, *Bacillus thuringiensis*, as a biological control agent against the red palm weevil, *Rhynchophorus ferrugineus* (Coleoptera: Curculionidae). *Pest Manag. Sci.* 73, 1494–1502. doi: 10.1002/ps.4485

Ryu, J.-H., Kim, S.-H., Lee, H.-Y., Bai, J. Y., Nam, Y.-D., Bae, J.-W., et al. (2008). Innate immune homeostasis by the homeobox gene caudal and commensal-gut mutualism in *Drosophila*. *Science* 319, 777–782. doi: 10.1126/science.1149357

Shi, Z. H., Lin, Y. T., and Hou, Y. M. (2014). Mother-derived trans-generational immune priming in the red palm weevil, *Rhynchophorus ferrugineus* olivier (Coleoptera, Dryophthoridae). *Bull. Entomol. Res.* 104, 742–750. doi: 10.1017/S0007485314000583

Shin, S. W., Bian, G., and Raikhel, A. S. (2006). A toll receptor and a cytokine, Toll5A and Spz1C, are involved in toll anti-fungal immune signaling in the mosquito *Aedes aegypti*. *J. Biol. Chem.* 281, 39388–39395. doi: 10.1074/jbc.M608912200

Stokes, B. A., Yadav, S., Shokal, U., Smith, L., and Eleftherianos, I. (2015). Bacterial and fungal pattern recognition receptors in homologous innate signaling pathways of insects and mammals. *Front. Microbiol.* 6:19. doi: 10.3389/fmicb.2015.00019

Sun, Y., Jiang, Y., Wang, Y., Li, X., Yang, R., Yu, Z., et al. (2016). The toll signaling pathway in the chinese oak silkworm, *Antheraea pernyi*: innate immune responses to different microorganisms. *PLoS One* 11:e0160200. doi: 10.1371/journal.pone.0160200

Tagliavia, M., Messina, E., Manachini, B., Cappello, S., and Quatrini, P. (2014). The gut microbiota of larvae of *Rhynchophorus ferrugineus* Oliver (Coleoptera: Curculionidae). *BMC Microbiol.* 14:136. doi: 10.1186/1471-2180-14-136

Valanne, S., Wang, J.-H., and Rämet, M. (2011). The *Drosophila* toll signaling pathway. *J. Immunol.* 186, 649–656. doi: 10.4049/jimmunol.1002302

Vaniksampanna, A., Longyant, S., Charoensapsri, W., Sithigorngul, P., and Chaivisuthangkura, P. (2019). Molecular isolation and characterization of a spätzle gene from *Macrobrachium rosenbergii*. *Fish Shellf. Immunol.* 84, 441–450. doi: 10.1016/j.fsi.2018.10.015

Vigneron, A., Charif, D., Vincent-Monégat, C., Vallier, A., Gavory, F., Wincker, P., et al. (2012). Host gene response to endosymbiont and pathogen in the cereal weevil *Sitophilus oryzae*. *BMC Microbiol.* 12(Suppl.):S14. doi: 10.1186/1471-2180-12-S1-S14

Wang, P., Liang, J., Gu, Z., Wan, D., Weng, S., Yu, X., et al. (2012). Molecular cloning, characterization and expression analysis of two novel Tolls (LvToll2 and LvToll3) and three putative Spätzle-like Toll ligands (LvSpz1–3) from *Litopenaeus vannamei*. *Dev. Comp. Immunol.* 36, 359–371. doi: 10.1016/j.dci.2011.07.007

Wang, Y., Cheng, T., Rayaprolu, S., Zou, Z., Xia, Q., Xiang, Z., et al. (2007). Proteolytic activation of pro-spätzle is required for the induced transcription of antimicrobial peptide genes in *Lepidopteran* insects. *Dev. Comp. Immunol.* 31, 1002–1012. doi: 10.1016/j.dci.2017.01.001

Wang, Y., and Zhu, S. (2009). Evolutionary and functional epitopes of the Spätzle protein: new insights into activation of the toll receptor. *Cell. Mol. Life Sci.* 66, 1595–1602. doi: 10.1007/s00018-009-9028-3

Weber, A. N., Tauszig-Delamasure, S., Hoffmann, J. A., Lelièvre, E., Gascan, H., Ray, K. P., et al. (2003). Binding of the *Drosophila* cytokine Spätzle to Toll is direct and establishes signaling. *Nat. Immunol.* 4:794. doi: 10.1038/ni955

Wong, A. C., Dobson, A. J., and Douglas, A. E. (2014). Gut microbiota dictates the metabolic response of *Drosophila* to diet. *J. Exp. Biol.* 217, 1894–1901. doi: 10.1242/jeb.101725

Xiao, R., Wang, X., Xie, E., Ji, T., Li, X., Muhammad, A., et al. (2019). An IMD-like pathway mediates the intestinal immunity to modulate the homeostasis of gut microbiota in *Rhynchophorus ferrugineus* Olivier (Coleoptera: Dryophthoridae). *Dev. Comp. Immunol.* 97, 20–27. doi: 10.1016/j.dci.2019.03.013

Yuan, K., Yuan, F., Weng, S., He, J., and Chen, Y. (2017). Identification and functional characterization of a novel Spätzle gene in *Litopenaeus vannamei*. *Dev. Comp. Immunol.* 68, 46–57. doi: 10.1016/j.dci.2016.11.016

Zaidman-Rémy, A., Hervé, M., Poidevin, M., Pili-Floury, S., Kim, M.-S., Blanot, D., et al. (2006). The *Drosophila* amidase PGRP-LB modulates the immune response to bacterial infection. *Immunity* 24, 463–473. doi: 10.1016/j.immuni.2006.02.012

Zaidman-Rémy, A., Vigneron, A., Weiss, L. B., and Heddi, A. (2018). Whant can a weevil teach a fly, and reciprocally? Interaction of host immune systems with endosymbionts in *Glossina* and *Sitophilus*. *BMC Microbiol.* 18(Suppl. 1):150. doi: 10.1186/s12866-018-1278-5

Zheng, H., Powell, J. E., Steele, M. I., Dietrich, C., and Moran, N. A. (2017). Honeybee gut microbiota promotes host weight gain via bacterial metabolism and hormonal signaling. *Proc. Natl. Acad. Sci. U.S.A.* 114, 4775–4780. doi: 10.1073/pnas.1701819114

Zhong, X., Xu, X., Yi, H., Lin, C., and Yu, X. (2012). A Toll-Spätzle pathway in the tobacco hornworm, *Manduca sexta*. *Insect Biochem. Mol. Biol.* 42, 514–524. doi: 10.1016/j.ibmb.2012.03.009

Conflict of Interest: The authors declare that the research was conducted in the absence of any commercial or financial relationships that could be construed as a potential conflict of interest.

frontiers in Microbiology

MINI REVIEW
published: 18 June 2020
doi: 10.3389/fmicb.2020.01307

Unexplored Arsenals of Legume Peptides With Potential for Their Applications in Medicine and Agriculture

Rui M. Lima[1†], Salome Kylarová[1†], Peter Mergaert[2] and Éva Kondorosi[1]*

[1] Institute of Plant Biology, Biological Research Centre, Szeged, Hungary, [2] Université Paris-Saclay, CEA, CNRS, Institute for Integrative Biology of the Cell (I2BC), Gif-sur-Yvette, France

During endosymbiosis, bacteria live intracellularly in the symbiotic organ of their host. The host controls the proliferation of endosymbionts and prevents their spread to other tissues and organs. In Rhizobium-legume symbiosis the major host effectors are secreted nodule-specific cysteine-rich (NCR) peptides, produced exclusively in the symbiotic cells. NCRs have evolved in the Inverted Repeat Lacking Clade (IRLC) of the *Leguminosae* family. They are secreted peptides that mediate terminal differentiation of the endosymbionts, forming polyploid, non-cultivable cells with increased membrane permeability. NCRs form an extremely large family of peptides, which have four or six conserved cysteines but otherwise highly diverse amino acid sequences, resulting in a wide variety of anionic, neutral and cationic peptides. *In vitro*, many synthetic NCRs have strong antimicrobial activities against both Gram-negative and Gram-positive bacteria, including the ESKAPE strains and pathogenic fungi. The spectra and minimal bactericidal and anti-fungal concentrations of NCRs differ, indicating that, in addition to their charge, the amino acid composition and sequence also play important roles in their antimicrobial activity. NCRs attack the bacteria and fungi at the cell envelope and membrane as well as intracellularly, forming interactions with multiple essential cellular machineries. NCR-like peptides with similar symbiotic functions as the NCRs also exist in other branches of the *Leguminosae* family. Thus, legumes provide countless and so far unexplored sources of symbiotic peptides representing an enormous resource of pharmacologically interesting molecules.

Keywords: *Medicago truncatula*, nodule-specific cysteine-rich peptide (NCR), antimicrobial peptide (AMP), antibacterial activity, antifungal activity, ESKAPE bacteria, multifunctional roles

OPEN ACCESS

Edited by:
David Clarke,
University College Cork, Ireland

Reviewed by:
Miriam L. Gifford,
University of Warwick,
United Kingdom
Florent Masson,
Swiss Federal Institute of Technology
Lausanne, Switzerland

****Correspondence:***
Éva Kondorosi
eva.kondorosi@gmail.com

† These authors have contributed equally to this work

Specialty section:
This article was submitted to Antimicrobials, Resistance and Chemotherapy, a section of the journal Frontiers in Microbiology

Received: *28 March 2020*
Accepted: *22 May 2020*
Published: *18 June 2020*

Citation:
Lima RM, Kylarová S, Mergaert P and Kondorosi É (2020) Unexplored Arsenals of Legume Peptides With Potential for Their Applications in Medicine and Agriculture. Front. Microbiol. 11:1307. doi: 10.3389/fmicb.2020.01307

INTRODUCTION

Legumes are particular because they can form symbiosis with nitrogen fixing bacteria, which convert the atmospheric nitrogen into ammonia and satisfy the nitrogen need of the host plant (Graham and Vance, 2003). The symbiotic rhizobium partners are soil-dwelling alpha- or beta-proteobacteria, which are present intracellularly in the symbiotic organ, the root nodule, and are called bacteroids. The bacteroid-containing nodule cells become polyploid, grow to an extreme size, and host thousands of bacteroids (Kondorosi et al., 2013). In many legumes, the nitrogen

fixing bacteroids are similar to cultured bacteria, which can change their lifestyle reversibly between the free-living and symbiotic states. In IRLC legumes or in certain legumes from the Dalbergioid clade, the bacteroids undergo an irreversible, terminal differentiation. This terminal differentiation is associated with definitive loss of cell division potential, changes in the membrane composition and permeability, cell growth from moderate to extreme sizes coupled to genome amplification, altered cell morphology (Mergaert et al., 2006; Montiel et al., 2017), and more efficient nitrogen fixation (Oono and Denison, 2010). To accomplish this, legumes have evolved a spectacular arsenal of antimicrobial peptides (AMPs) which are targeted to the bacteroids and provoke their differentiation (Mergaert, 2018; Roy et al., 2020). In the IRLC legumes, the NCR peptides, while in Dalbegioids, the convergently evolved NCR-like peptides represent the vast majority of these host effectors (Van de Velde et al., 2010; Czernic et al., 2015; Montiel et al., 2017; Trujillo et al., 2019).

The *NCR* genes are expressed in the symbiotic nodule cells but in different subsets at sequential stages of the differentiation process (Maunoury et al., 2010; Guefrachi et al., 2014). Immunogold localization and proteome of isolated bacteroids demonstrated undoubtably the presence of NCR peptides in the bacteroids (Van de Velde et al., 2010; Durgo et al., 2015). NCRs are present in all members of the IRLC, but the size and composition of the family vary dramatically among the species from 7 up to ∼700 NCRs (Montiel et al., 2017). In line with the complexity of the NCR family, the morphotype of bacteroids can be swollen, spherical, elongated or both elongated, and branched in different legumes (Montiel et al., 2017).

THE STRUCTURE OF NCR AND NCR-LIKE PEPTIDES AND THEIR RELATEDNESS TO DEFENSINS

There are ∼700 *NCR* genes in the model legume *Medicago truncatula*. The *NCR* genes are usually composed of two exons; the first one codes for a relatively conserved signal peptide while the second one for a highly diverse mature peptide, which contains four or six cysteine residues in conserved positions (Alunni et al., 2007). In 95% of the NCRs, the length of the mature peptides varies between 24 and 65 amino acids but it is mostly 35–50 amino acid long in the majority of NCRs. **Figure 1A** shows graphical representation of amino acids in multiple alignment of the mature NCR and NCR-like sequences with Jalview version 2.11.0 (Waterhouse et al., 2009) and Clustal X version 2.1 (Larkin et al., 2007) where the height of letters indicates the relative frequency of amino acids at each position (Crooks et al., 2004). Beside the cysteines, only a few amino acids are present in >60% of NCRs, such as the aspartic acid (D) in front of the second cysteine (C_2) and between C_1 and C_2, or proline (P) after C_2. Due to the high diversity of amino acid composition, the isoelectric points (pI) of the *M. truncatula* NCR peptides vary between 3.5 and 11.25. In *M. truncatula*, 35% of the NCRs are anionic, 23% neutral and 42% cationic and almost equal numbers of genes code for NCRs with four and six cysteines. The high sequence variation also applies to these subgroups. As illustrated for the cationic (pI > 9) NCRs, the presence of the positively charged amino acids (K/R) is characteristic before C_2 and in front of C_3 and C_4 in NCR 4Cs and 6Cs, respectively. Moreover, threonine (T) is frequent after C_1X in NCR 4Cs but not in the 6Cs.

The cysteines are essential for the symbiotic, *in planta* functions as replacement of a single cysteine with serine resulted in the inactivation of the *Medicago*-specific NCR169 peptide (Horváth et al., 2015). Formation of disulfide bridges between the conserved cysteines could be important structural and functional elements of the NCR peptides. The disulfide bridges can be formed in the endoplasmic reticulum (ER) where enzymes controlling the oxidation of cysteines into disulfide bonds, such as the protein disulfide isomerase and ER oxidoreductin 1, are strongly upregulated (Mergaert et al., 2003; Roux et al., 2014). On the other hand, the symbiotic cells also produce symbiosis-specific thioredoxins that are co-targeted with the NCRs to the cytosol of bacteroids and can reduce the disulfide bonds of NCR peptides (Ribeiro et al., 2017). These observations suggest that NCRs are oxidized in the ER but are reduced within the bacteroids at least partially (Alloing et al., 2018). Accordingly, the redox state of the NCR peptides could represent a further level of complexity in regulating their activites.

The role of cysteines and disulfide bridges was primarily studied in the smallest, 24 amino acid long NCR247 using chemically synthetized peptides and the symbiotic bacterium partner *Sinorhizobium meliloti* in various bioassays. Exchanging the four cysteines for serines (NSR247), altering the position of the disulfide bridges, breaking the bridges by reduction ($NCR247_{red}$) or omitting the cysteines, all affected but to a different extent the peptides' activities and stability (Haag et al., 2012; Shabab et al., 2016). The disulfide bonds in NCR044 produced in the yeast *Pichia pastoris* were confirmed between C1–C4 and C2–C3, while the three dimensional structure of this peptide was found to be largely dynamic and disordered (Velivelli et al., 2020).

The NCR-like peptides in Dalbergioid legumes, like *Aeschynomene afraspera* and *Aeschynomene indica* are distinct from the IRLC NCRs but play similar roles in provoking terminal differentiation of bacteroids (Czernic et al., 2015). The mature NCR-like peptides are ∼50 amino acid long and have six or eight conserved cysteines and a tryptophan (W) (**Figure 1A**). These sequences are less divergent and several amino acids are present at >60% frequency at given positions. The NCR-like peptides are anionic or neutral except for two mildly cationic ones.

NCRs and NCR-like peptides resemble defensins, the largest group of plant innate immunity effectors (Sathoff and Samac, 2018). Defensins are also secreted peptides with a length of approximately 45–54 amino acids and 8 or 10 conserved cysteines forming disulfide bonds (Parisi et al., 2019). In spite of variations in the primary sequence, the 3D structure of defensins is conserved. Plant defensins have a γ-core motif ($GXCX_{3-9}C$) that is a hallmark related to their antimicrobial properties (Yount and Yeaman, 2004). Interestingly, the γ-core motif is also present in the majority of NCR-like peptides (**Figure 1A**).

Both the *NCR* and *NCR-like* genes might have originated from an ancestral defensin type gene by gene duplications and fast

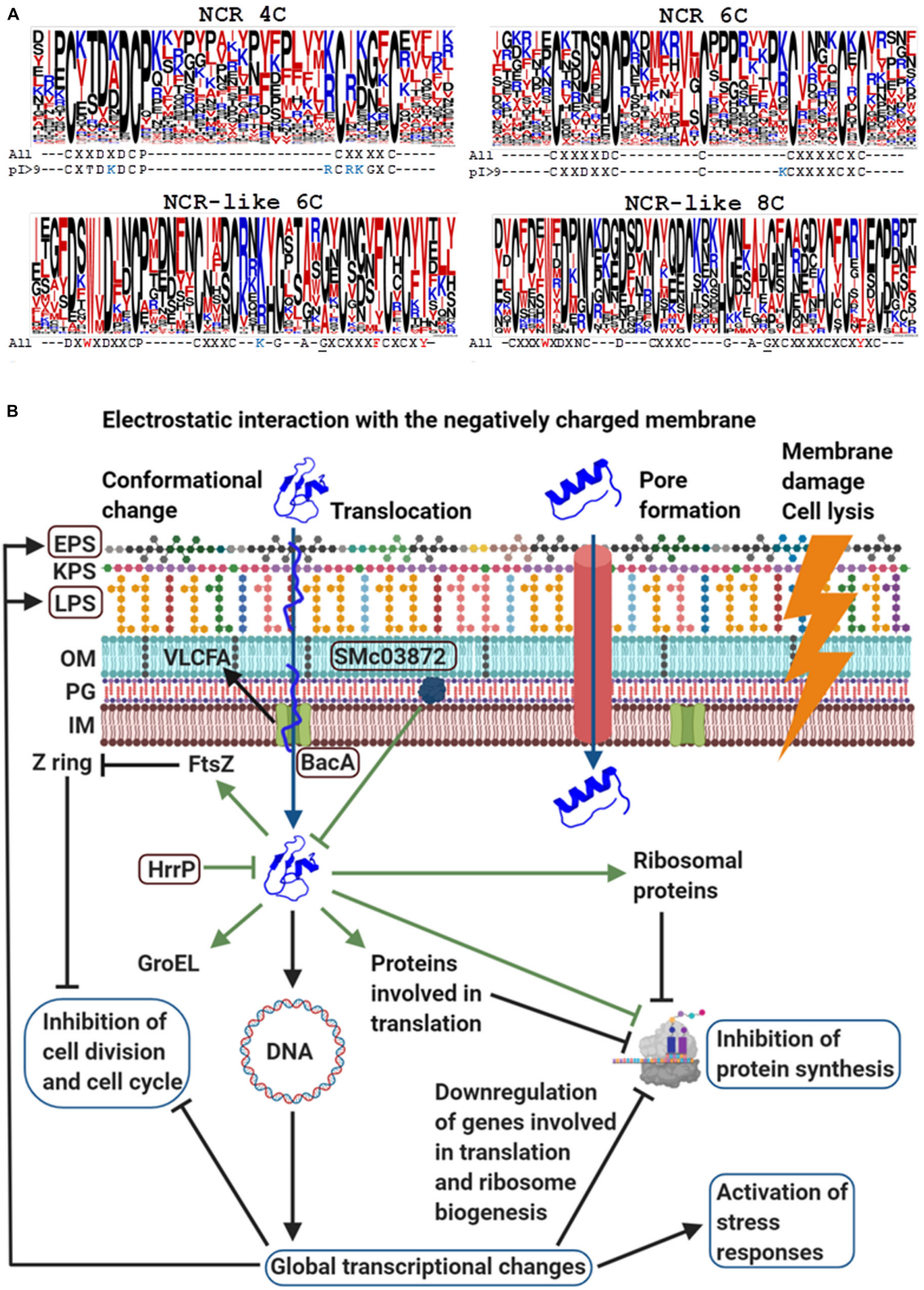

FIGURE 1 | The structure of NCRs, NCR-like peptides **(A)** and the mode of actions of cationic NCRs **(B)**. **(A)** Frequency of amino acids and conserved patterns of cysteines in the mature *M. truncatula* NCRs and NCR-like peptides from Dalbergioid legumes. The height of letters in the stacks indicates the relative frequency of

(Continued)

FIGURE 1 | Continued
each amino acid at that position. Color code of amino acids: blue, positively charged (KR) residues; red, hydrophobic (AFILMV) and amphipathic (WY) residues; black, all other amino acids. The underlined G residue in the NCR-like peptides marks the beginning of the γ-core motif. **(B)** The mode of actions of cationic NCRs based on the example of NCR247 (Created with BioRender.com). NCRs can interact with the bacterial membranes and enter the cytosol with or without pore formation or cause membrane damages and cell lysis. Intracellularly NCRs provoke global transcriptional changes and interact with numerous bacterial proteins that collectively affect essential cellular functions. The framed proteins BacA, HrrP, SMc03872, and polysaccharides EPS and LPS protect the symbiotic bacterium partner from the killing action of NCRs.

diversification. The NCR gene family evolution is probably driven by a continuous adaptation to diversifying rhizobium symbionts. In *M. truncatula*, *NCR* genes are present on all chromosomes, and beside long distance duplications, local duplications form small clusters of *NCR* genes. Since many *NCRs* are in the vicinity of transposable elements, transposons might have been involved in the multiplication of *NCR* genes (Satgé et al., 2016).

SYMBIOTIC ROLES OF *M. truncatula* NCR PEPTIDES

In the very young symbiotic nodule cells where the endosymbionts multiply, only a few non-cationic *NCR* genes are expressed. When the endosymbiont population reaches a certain density, the endosymbionts enter the differentiation process starting with cell division arrest and cell enlargement (Kondorosi et al., 2013). Changes also occur in the cell envelope and the increased membrane permeability can facilitate the exchange of metabolites between the plant and bacterium. If the differentiation process is incomplete, there is no nitrogen fixation.

One of the major tasks of the NCR peptides is to inhibit and permanently abolish the bacterial cell division. Treatment of *S. meliloti* cultures *in vitro* with synthetic NCRs revealed that cationic peptides like NCR035, NCR055, or NCR247 provoke increased membrane permeability, cell elongation, DNA amplification, and kill ultimately the bacteria (Van de Velde et al., 2010). The mode of action of NCR247 is the best studied one (**Figure 1B**). Its activation in the nodules coincides with the start of bacteroid differentiation; with cell division arrest and elongation of bacteroids (Farkas et al., 2014). Treatment of *S. meliloti* cultures with 5 μM NCR247 damaged the integrity of bacterial membranes and led to cell death (Farkas et al., 2014; Mikuláss et al., 2016). Cysteines also contribute to the antimicrobial activity of NCR247 and the reduced form is the most effective (Haag et al., 2012; Shabab et al., 2016). NCR247 as well as other cationic NCR peptides provoke formation of outer membrane vesicles (Montiel et al., 2017) but NCR247 at sublethal 1.5 μM concentration, enters the cytosol without pore formation (Farkas et al., 2014).

Treatment of log phase *S. meliloti* cultures or synchonized cells with sublethal concentrations of the reduced and the oxidized forms of NCR247 provoked global transcriptional changes affecting 14–15% of the protein coding sequences (Tiricz et al., 2013; Penterman et al., 2014). Besides general stress response activation, nearly half of the cell cycle genes were affected including critical regulators, such as *dnaA*, *gcrA*, *ctrA* and those involved in septum formation and cell division. Genes involved in translation and particularly in ribosome biogenesis were downregulated. Expression of genes involved in transcriptional regulation, membrane modifications and transport were perturbed.

The Boman index (indicating the protein binding potential) of NCR247 is one of the highest among all known proteins and indeed it possesses extreme protein binding ability (Farkas et al., 2014). Half of the ribosomal proteins and numerous proteins involved in different stages of translation were present in the NCR247 complexes leading to the inhibition of protein synthesis. Its interaction with FtsZ prevented the Z-ring formation and thereby septum assembly and bacterial cell division. Interestingly NCR035, another cationic NCR peptide coexpressed with NCR247, binds to the septum, suggesting that the host plant employs multiple peptides to interfere with specific biological processes, such as the bacterial cell division. NCR247 interacts also with the GroEL chaperone, which is essential for the differentiation of symbiotic cells though it is unknown how the binding of NCR247 affects GroEL functions. Treatment of *S. meliloti* cultures with the most cationic peptide, NCR335, resulted, similarly, in rapid downregulation of genes involved in basic cellular functions, such as transcription-translation and energy production, as well as upregulation of genes involved in stress and oxidative stress responses and membrane transport (Tiricz et al., 2013).

While cationic NCRs exhibited toxicity *in vitro* for rhizobia, none of the tested anionic peptides, except for NCR211 affected the survival of rhizobia (Kim et al., 2015). At present it is unkown how NCR211 and the non-cationic NCR-like peptides exert antimicrobial properties.

In the nodule cells, the rhizobia are viable and are likely to be exposed to lower concentrations of NCRs than those used in the *in vitro* assays. Moreover, the bacteria have evolved various mechanisms against the toxicity of NCRs. BacA is essential for the survival of bacteroids in *M. truncatula* (Haag et al., 2011). BacA is an ABC transporter protein, which promotes uptake and translocation of NCRs from the membrane to the cytosol that might diminish the membrane damage and keep the bacteria alive (Guefrachi et al., 2015; Barrière et al., 2017). Components of the cell envelope also provide protection, such as lipopolysaccharides (LPS) together with the BacA mediated synthesis of very long chain fatty acids (VLCFA), high molecular weight succinoglycans in the exopolysaccharide (EPS) layer and other membrane constituents (Arnold et al., 2017, 2018; Montiel et al., 2017). Proteolytic degradation of NCRs by the bacterial HrrP and SMc03872 represents another level of resistance (Price et al., 2015; Arnold

et al., 2017) though the oxidized forms are more stable (Shabab et al., 2016).

ANTIBACTERIAL SPECTRUM OF NCRs

Cationic NCRs are in many respects similar to membrane-permeabilizing cationic antimicrobial peptides whose net charge ranges from +2 to +9 and facilitaties their interaction with the negatively charged bacterial membranes. Most antibacterial tests have been carried out with NCR247 (net charge +6) and NCR335 (net charge +14) which were classified with four and two different AMP prediction tools as AMPs, respectively (Farkas et al., 2017). NCR335 is unusual because it is 64 amino acid long and only its C-terminal half carries the conserved cysteine pattern of NCRs. The antimicrobial activity of chemically synthetized NCRs has been tested against a broad panel of Gram-negative (*Escherichia coli*, *Salmonella enterica*, *Pseudomonas aeruginosa*, *Pseudomonas syringae* pv. *tomato*, *Xanthomonas campestris*, *Agrobacterium tumefaciens*, *Chlamydia trachomatis*) and Gram-positive (*Bacillus megaterium*, *Bacillus cereus*, *Bacillus subtilis*, *Listeria monocytogenes*, *Staphylococcus aureus*, *Clavibacter michiganensis*) bacteria, including diverse human/animal and plant pathogens. The peptides, added to 10^7, bacteria for 3 h, killed to various extent all these tested bacteria resulting in their complete elimination or decrease in the number of surviving cells from one to several orders of magnitude, depending on the strain and the peptide (Tiricz et al., 2013; Balogh et al., 2014). In general, cationic NCR peptides with pI >9.0 seem to have antibacterial activities, however, their antimicrobial spectrum was only partially overlapping indicating that in addition to their positive charge, their amino acid composition and primary sequence also contribute to the strength and spectrum of antibacterial activities. Due to the multiple bacterial targets of NCRs, there is little chance for development of resistance against them.

ANTIBACTERIAL POTENTIAL OF NCR247-BASED CHIMERIC PEPTIDES IS COMPARABLE TO THIRD GENERATION ANTIBIOTICS

Skin and soft tissue infections are mainly caused by ESKAPE bacteria which are resistant to most antibiotics (Pfalzgraff et al., 2018). Based on the different mode of action and broad spectrum of NCRs it is conceivable that they may also be able to kill these resistant pathogens. The antibacterial activity of chemically synthesized NCR247 and NCR247-derivatives was investigated against ESKAPE strains (*Enterococcus faecalis*, *S. aureus*, *Klebsiella pneumoniae*, *Acinetobacter baumannii*, *P. aeruginosa*) and *E. coli, L. monocytogenes*, and *S. enterica* (Jenei et al., 2020; **Table 1**). The minimal bactericidal concentration of NCR247 was 3.1 μM against *P. aeruginosa* and 6.3 μM against *S. aureus* and *E. coli* while killing of the other bacteria required higher concentrations. The C-terminal half of NCR247 (NCR247C) retained its activity on *E. coli* but lost its effectiveness on other bacteria. To improve its antimicrobial properties, NCR247C was fused with $NCR335_{7-19}$ (X1) or $mastoparan_{4-14}$ (X2) deriving from the 14 amino acid long mastoparan, a membranolytic peptide toxin from wasp venom. Each of these chimeric peptides possessed higher antibacterial efficacy and affected the antimicrobial spectrum. In the case of X1-NCR247C

TABLE 1 | The amino acid sequence of NCR247 and its derivatives (A) and the minimal bactericidal concentrations (MBCs) of these peptides and antibiotics (in μM) on different pathogens (B) (from Jenei et al., 2020).

(A)	Name	Amino acid sequence
	NCR247	RNGCIVDPRCPY**QQCRRPLYCRRR**
	NCR247C	**QQCRRPLYCRRR**
	X1 ($NCR335_{7-19}$)-**NCR247C**	RPLNFKMLRFWGQ**QQCRRPLYCRRR**
	NCR247C-**X2** ($Mastoparan_{4-14}$)	**QQCRRPLYCRRR**KALAALAKKIL
	X2 ($Mastoparan_{4-14}$)-**NCR247C**	KALAALAKKIL**QQCRRPLYCRRR**
	X2 ($Mastoparan_{4-14}$)	KALAALAKKIL

(B)								
Peptides/Antibiotics	***E. f.***	***S. a.***	***K. p.***	***A. b.***	***P. a.***	***E. c.***	***L. m.***	***S. e.***
NCR247	>25	**6.3**	>25	12.5	**3.1**	**6.3**	>25	25
NCR247C	>25	> 25	>25	25	25	**6.3**	>25	> 25
X1-NCR247C	**6.3**	**3.1**	12.5	**3.1**	**3.1**	**3.1**	**3.1**	**1.6**
NCR247C-X2	25	**3.1**	**6.3**	**3.1**	**3.1**	**1.6**	**1.6**	**1.6**
X2-NCR247C	**3.1**	**3.1**	**6.3**	**3.1**	**3.1**	**3.1**	**3.1**	**3.1**
X2	>25	25	>25	25	**6.3**	>25	25	>25
Cb	5120	640	>10,240	5120	10240	1280	80	640
Lvx	160	**2.5**	320	20	**1.3**	**5.0**	320	**1.3**

E. f., Enterococcus faecalis; S. a., Staphylococcus aureus; K. p., Klebsiella pneumoniae; A. b., Acinetobacter baumannii; P. a., Pseudomonas aeruginosa; E. c., Escherichia coli; L. m., Listeria monocytogenes; S. e., Salmonella enterica. Cb, carbenicillin; Lvx, levofloxacin. MBCs below 10 μM are in bold.

the minimal bactericidal concentrations (MBC) varied between 1.6 and 12.5 μM. C- or N-terminal fusion of NCR247C with X2 made the chimeric peptides very effective on most strains at 1.6 and 3.1 μM MBCs. The MBCs of these chimeric derivatives were much lower than that of the classical antibiotic carbenicillin, and were comparable or even more effective than levofloxacin, a third generation antibiotic (Jenei et al., 2020).

The killing activity of the NCR247-based chimeric peptides occurred within 0.1–5 min. While the antimicrobial activity of cationic peptides is generally attenuated by the presence of divalent cations and higher salt concentrations (Hancock and Sahl, 2006), the bactericidal activity of these chimeric peptides was maintained in Mueller Hinton broth. Importantly, these peptides did not have hemolytic activity or cytotoxicity on human cells (Jenei et al., 2020).

ANTIFUNGAL ACTIVITY OF NCRs

The relatedness of NCRs to antimicrobial peptides, particularly to plant defensins protecting the plants mostly against fungal infections suggests that NCRs also have antifungal activity. Among 19 NCR peptides with pI ranging from 3.61 to 11.22, nine with pI >9.5 inhibited the growth and the survival of both the yeast and filamentous forms of *Candida albicans*, one of the most common opportunistic human pathogens (Ördögh et al., 2014). The minimal fungicidal concentrations of the most effective peptides (NCR335, NCR044) were between 1 and 3 μM. Treatment of *C. albicans*-infected vaginal epithelial cells with NCR335, NCR247, or NCR192 for 3 h prevented epithelial cell death induced by *C. albicans*. The concentrations required for killing the fungus did not affect survival of human cells. The anticandidal activity of NCR peptides was achieved by permeabilization of the fungal membrane and interactions with multiple intracellular targets. Cationic NCR peptides were also active on *Aspergillus niger, Candida crusei, Candida parapsilosis, Fusarium graminearum*, *Rhizopus stolonifer var. stolonifer*, however, their antifungal spectrum and efficacity varied indicating that, similarly, to the bactericidal action, in addition to the pI, the amino acid sequence also contributes to the antifungal properties (Kondorosi-Kuzsel et al., 2010). NCR044 exhibited strong fungicidal activity against the plant pathogen *Botrytis cinerea* and several *Fusarium* species (Velivelli et al., 2020). The inhibitory concentration of NCR044 varied between 0.52 and 1.93 μM. NCR044 interacts with the *B. cinerea* cell wall and the membrane phospholipids, then it translocates to the cytoplasm and localizes to the nucleolus. It provokes production of reactive oxygen species and might interfere with protein synthesis. Thus, both the antibacterial and the antifungal activities of NCRs rely on multistep actions. In lettuce leaves and rose petal assays, NCR044 provided resistance to *B. cinerea*. These findings together with the economical production of NCR044 in *P. pastoris* paves the way to use NCRs in agriculture for plant protection (Velivelli et al., 2020).

CONCLUSION

Antimicrobial resistance is a global healthcare threat. Many people die from incurable infections and with the lack of appropriate antibiotics we might return to the pre-antibiotic era. AMPs represent a new hope with their rapid killing and broad spectrum activity against multidrug resistant (MDR) pathogens. AMPs, like the cationic NCRs, are multifunctional. They can interact with the membranes with or without membrane permeabilization and intracellularly they can affect transcription, translation, enzyme activities causing ultimately microbial death (Mwangi et al., 2019). A few AMPs with potent activity against MDR species are in clinical use like colistin, one of the last-resort drugs (Pfalzgraff et al., 2018; Mwangi et al., 2019). Toxicity of AMPs is, however, a major drawback and many AMPs are limited to topical application. To the 3011 AMPs in the antimicrobial peptide database (Wang, 2020), legumes can add several ten thousands of natural AMPs produced in the symbiotic cells. Legumes are mostly edible plants and NCRs are apparently not toxic for human cells while many of them kill pathogenic bacteria and fungi very effectively with multi-target actions. In laboratory conditions, NCRs or their derivatives, such as various chimeric peptides have similar or even superior antimicrobial properties than third generation antibiotics. Exploring their potential might help to fight against existing and unforeseen bacterial, fungal and possibly viral infections both in medicine and agriculture.

AUTHOR CONTRIBUTIONS

ÉK conceptualized the manuscript. RL and SK analyzed the peptide sequences and provided the **Figure 1**. All authors contributed to the manuscript.

FUNDING

This work was supported by the Hungarian National Office for Research, Development and Innovation (NKFIH) GINOP 2.3.2-15-2016-00014 Evomer, GINOP 2.3.2-15-2016-00015 I-KOM and the Frontline Research project KKP129924 and the Balzan research grant to ÉK.

REFERENCES

Alloing, G., Mandon, K., Boncompagni, E., Montrichard, F., and Frendo, P. (2018). Involvement of glutaredoxin and thioredoxin systems in the nitrogen-fixing symbiosis between legumes and rhizobia. *Antioxidants* 7:182. doi: 10.3390/antiox7120182

Alunni, B., Kevei, Z., Redondo-Nieto, M., Kondorosi, A., Mergaert, P., and Kondorosi, E. (2007). Genomic organization and evolutionary insights on GRP and NCR genes, two large nodule-specific gene families in *Medicago truncatula*. *Mol. Plant. Microbe Interact.* 20, 1138–1148. doi: 10.1094/MPMI-20-9-1138

Arnold, M. F. F., Penterman, J., Shabab, M., Chen, E. J., and Walker, G. C. (2018). Important late-stage symbiotic role of the *Sinorhizobium meliloti*

exopolysaccharide succinoglycan. *J. Bacteriol.* 200:e00665-17. doi: 10.1128/JB.00665-17

Arnold, M. F. F., Shabab, M., Penterman, J., Boehme, K. L., Griffitts, J. S., and Walker, G. C. (2017). Genome-wide sensitivity analysis of the microsymbiont Sinorhizobium meliloti to symbiotically important, defensin-like host peptides. *mBio* 8:e01060-17. doi: 10.1128/mBio.01060-17

Balogh, E., Mosolygó, T., Tiricz, H., Szabó, Á, Karai, A., Kerekes, F., et al. (2014). Anti-chlamydial effect of plant peptides. *Acta Microbiol. Immunol. Hung.* 61, 229–239. doi: 10.1556/AMicr.61.2014.2.12

Barrière, Q., Guefrachi, I., Gully, D., Lamouche, F., Pierre, O., Fardoux, J., et al. (2017). Integrated roles of BclA and DD-carboxypeptidase 1 in *Bradyrhizobium* differentiation within NCR-producing and NCR-lacking Root Nodules. *Sci. Rep.* 7:9063. doi: 10.1038/s41598-017-08830-0

Crooks, G. E., Hon, G., Chandonia, J.-M., and Brenner, S. E. (2004). WebLogo: a sequence logo generator. *Genome Res.* 14, 1188–1190. doi: 10.1101/gr.849004

Czernic, P., Gully, D., Cartieaux, F., Moulin, L., Guefrachi, I., Patrel, D., et al. (2015). Convergent evolution of endosymbiont differentiation in Dalbergioid and Inverted Repeat-Lacking Clade legumes mediated by nodule-specific cysteine-rich peptides. *Plant Physiol.* 169, 1254–1265. doi: 10.1104/pp.15.00584

Durgo, H., Klement, E., Hunyadi-Gulyas, E., Szucs, A., Kereszt, A., Medzihradszky, K. F., et al. (2015). Identification of nodule-specific cysteine-rich plant peptides in endosymbiotic bacteria. *Proteomics* 15, 2291–2295. doi: 10.1002/pmic.201400385

Farkas, A., Maróti, G., Dürgõ, H., Györgypál, Z., Lima, R. M., Medzihradszky, K. F., et al. (2014). *Medicago truncatula* symbiotic peptide NCR247 contributes to bacteroid differentiation through multiple mechanisms. *Proc. Natl. Acad. Sci. U.S.A.* 111, 5183–5188. doi: 10.1073/pnas.1404169111

Farkas, A., Maróti, G., Kereszt, A., and Kondorosi, É (2017). Comparative analysis of the bacterial membrane disruption effect of two natural plant antimicrobial peptides. *Front. Microbiol.* 8:51. doi: 10.3389/fmicb.2017.00051

Graham, P. H., and Vance, C. P. (2003). Legumes: importance and constraints to greater use. *Plant Physiol.* 131, 872–877. doi: 10.1104/pp.017004

Guefrachi, I., Nagymihaly, M., Pislariu, C. I., Van de Velde, W., Ratet, P., Mars, M., et al. (2014). Extreme specificity of NCR gene expression in *Medicago truncatula*. *BMC Genomics* 15:712. doi: 10.1186/1471-2164-15-712

Guefrachi, J., Pierre, O., Timchenko, T., Alunni, B., Barrière, Q., Czernic, P., et al. (2015). *Bradyrhizobium* BclA is a peptide transporter required for bacterial differentiation in symbiosis with *Aeschynomene* Legumes. *Mol. Plant Microbe. Interact.* 28, 1155–1166. doi: 10.1094/MPMI-04-15-0094-R

Haag, A. F., Baloban, M., Sani, M., Kerscher, B., Pierre, O., Farkas, A., et al. (2011). Protection of *Sinorhizobium* against host cysteine-rich antimicrobial peptides is critical for symbiosis. *PLoS Biol.* 9:e1001169. doi: 10.1371/journal.pbio.1001169

Haag, A. F., Kerscher, B., Dall'Angelo, S., Sani, M., Longhi, R., Baloban, M., et al. (2012). Role of cysteine residues and disulfide bonds in the activity of a legume root nodule-specific, cysteine-rich peptide. *J. Biol. Chem.* 287, 10791–10798. doi: 10.1074/jbc.M111.311316

Hancock, R. E. W., and Sahl, H.-G. (2006). Antimicrobial and host-defense peptides as new anti-infective therapeutic strategies. *Nat. Biotechnol.* 24, 1551–1557. doi: 10.1038/nbt1267

Horváth, B., Domonkos, Á, Kereszt, A., Szûcs, A., Ábrahám, E., Ayaydin, F., et al. (2015). Loss of the nodule-specific cysteine rich peptide, NCR169, abolishes symbiotic nitrogen fixation in the *Medicago truncatula* dnf7 mutant. *Proc. Natl. Acad. Sci. U.S.A.* 112, 15232–15237. doi: 10.1073/pnas.1500777112

Jenei, S., Tiricz, H., Szolomájer, J., Tímár, E., Klement, É, Al Bouni, M. A., et al. (2020). Potent chimeric antimicrobial derivatives of the *Medicago truncatula* NCR247 symbiotic peptide. *Front. Microbiol.* 11:270. doi: 10.3389/fmicb.2020.00270

Kim, M., Chen, Y., Xi, J., Waters, C., Chen, R., and Wang, D. (2015). An antimicrobial peptide essential for bacterial survival in the nitrogen-fixing symbiosis. *Proc. Natl. Acad. Sci. U.S.A.* 112, 15238–15243. doi: 10.1073/pnas.1500123112

Kondorosi, E., Mergaert, P., and Kereszt, A. (2013). A paradigm for endosymbiotic life: cell differentiation of *Rhizobium* bacteria provoked by host plant factors. *Annu. Rev. Microbiol.* 67, 611–628. doi: 10.1146/annurev-micro-092412-155630

Kondorosi-Kuzsel, E., Mergaert, P., Van de Velde, W., Maroti, G., Farkas, A., and Kereszt, A. (2010). *Nodule specific medicago peptides having antimicrobial activity and pharmaceutical compositions containing the same. International Patent EP2442823B1, WO2010146067Al.*

Larkin, M. A., Blackshields, G., Brown, N. P., Chenna, R., McGettigan, P. A., McWilliam, H., et al. (2007). Clustal W and Clustal X version 2.0. *Bioinformatics* 23, 2947–2948. doi: 10.1093/bioinformatics/btm404

Maunoury, N., Redondo-Nieto, M., Bourcy, M., Van de Velde, W., Alunni, B., Laporte, P., et al. (2010). Differentiation of symbiotic cells and endosymbionts in *Medicago truncatula* nodulation are coupled to two transcriptome-switches. *PLoS One* 5:e9519. doi: 10.1371/journal.pone.0009519

Mergaert, P. (2018). Role of antimicrobial peptides in controlling symbiotic bacterial populations. *Nat. Prod. Rep.* 35, 336–356. doi: 10.1039/C7NP00056A

Mergaert, P., Nikovics, K., Kelemen, Z., Maunoury, N., Vaubert, D., Kondorosi, A., et al. (2003). A novel family in *Medicago truncatula* consisting of more than 300 nodule-specific genes coding for small, secreted polypeptides with conserved cysteine motifs. *Plant Physiol.* 132, 161–173. doi: 10.1104/pp.102.018192

Mergaert, P., Uchiumi, T., Alunni, B., Evanno, G., Cheron, A., Catrice, O., et al. (2006). Eukaryotic control on bacterial cell cycle and differentiation in the Rhizobium–legume symbiosis. *Proc. Natl. Acad. Sci. U.S.A.* 103, 5230–5235. doi: 10.1073/pnas.0600912103

Mikuláss, K. R., Nagy, K., Bogos, B., Szegletes, Z., Kovács, E., Farkas, A., et al. (2016). Antimicrobial nodule-specific cysteine-rich peptides disturb the integrity of bacterial outer and inner membranes and cause loss of membrane potential. *Ann. Clin. Microbiol. Antimicrob.* 15:43. doi: 10.1186/s12941-016-0159-8

Montiel, J., Downie, J. A., Farkas, A., Bihari, P., Herczeg, R., Bálint, B., et al. (2017). Morphotype of bacteroids in different legumes correlates with the number and type of symbiotic NCR peptides. *Proc. Natl. Acad. Sci. U.S.A.* 114, 5041–5046. doi: 10.1073/pnas.1704217114

Mwangi, J., Hao, X., Lai, R., and Zhang, Z.-Y. (2019). Antimicrobial peptides: new hope in the war against multidrug resistance. *Zool. Res.* 40, 488–505. doi: 10.24272/j.issn.2095-8137.2019.062

Oono, R., and Denison, R. F. (2010). Comparing symbiotic efficiency between swollenversus nonswollen rhizobial bacteroids. *Plant Physiol.* 154, 1541–1548. doi: 10.1104/pp.110.163436

Ördögh, L., Vörös, A., Nagy, I., Kondorosi, É, and Kereszt, A. (2014). Symbiotic plant peptides eliminate Candida albicans both in vitro and in an epithelial infection model and inhibit the proliferation of immortalized human cells. *BioMed Res. Int.* 2014:320796. doi: 10.1155/2014/320796

Parisi, K., Shafee, T. M. A., Quimbar, P., van der Weerden, N. L., Bleackley, M. R., and Anderson, M. A. (2019). The evolution, function and mechanisms of action for plant defensins. *Semin. Cell Dev. Biol.* 88, 107–118. doi: 10.1016/j.semcdb.2018.02.004

Penterman, J., Abo, R. P., De Nisco, N. J., Arnold, M. F. F., Longhi, R., Zanda, M., et al. (2014). Host plant peptides elicit a transcriptional response to control the *Sinorhizobium meliloti* cell cycle during symbiosis. *Proc. Natl. Acad. Sci. U.S.A.* 111, 3561–3566. doi: 10.1073/pnas.1400450111

Pfalzgraff, A., Brandenburg, K., and Weindl, G. (2018). Antimicrobial peptides and their therapeutic potential for bacterial skin infections and wounds. *Front. Pharmacol.* 9:281. doi: 10.3389/fphar.2018.00281

Price, P. A., Tanner, H. R., Dillon, B. A., Shabab, M., Walker, G. C., and Griffitts, J. S. (2015). Rhizobial peptidase HrrP cleaves host-encoded signaling peptides and mediates symbiotic compatibility. *Proc. Natl. Acad. Sci. U.S.A.* 112, 15244–15249. doi: 10.1073/pnas.1417797112

Ribeiro, C. W., Baldacci-Cresp, F., Pierre, O., Larousse, M., Benyamina, S., Lambert, A., et al. (2017). Regulation of differentiation of nitrogen-fixing bacteria by microsymbiont targeting of plant thioredoxin s1. *Curr. Biol.* 27, 250–256. doi: 10.1016/j.cub.2016.11.013

Roux, B., Rodde, N., Jardinaud, M.-F., Timmers, T., Sauviac, L., Cottret, L., et al. (2014). An integrated analysis of plant and bacterial gene expression in symbiotic root nodules using laser-capture microdissection coupled to RNA sequencing. *Plant J.* 77, 817–837. doi: 10.1111/tpj.12442

Roy, P., Achom, M., Wilkinson, H., Lagunas, B., and Gifford, M. L. (2020). Symbiotic outcome modified by the diversification from 7 to over 700 nodule-specific cysteine-rich peptides. *Genes* 11:348. doi: 10.3390/genes11040348

Satgé, C., Moreau, S., Sallet, E., Lefort, G., Auriac, M.-C., Remblière, C., et al. (2016). Reprogramming of DNA methylation is critical for nodule

development in *Medicago truncatula*. *Nat. Plants* 2, 1–10. doi: 10.1038/nplants.2016.166

Sathoff, A. E., and Samac, D. A. (2018). Antibacterial activity of plant defensins. *Mol. Plant. Microbe. Interact.* 32, 507–514. doi: 10.1094/MPMI-08-18-0229-CR

Shabab, M., Arnold, M. F. F., Penterman, J., Wommack, A. J., Bocker, H. T., Price, P. A., et al. (2016). Disulfide cross-linking influences symbiotic activities of nodule peptide NCR247. *Proc. Natl. Acad. Sci. U.S.A.* 113, 10157–10162. doi: 10.1073/pnas.1610724113

Tiricz, H., Szûcs, A., Farkas, A., Pap, B., Lima, R. M., Maróti, G., et al. (2013). Antimicrobial nodule-specific cysteine-rich peptides induce membrane depolarization-associated changes in the transcriptome of *Sinorhizobium meliloti*. *Appl. Environ. Microbiol.* 79, 6737–6746. doi: 10.1128/AEM.01791-13

Trujillo, D. I., Silverstein, K. A. T., and Young, N. D. (2019). Nodule-specific PLAT domain proteins are expanded in the *Medicago* lineage and required for nodulation. *New Phytol.* 222, 1538–1550. doi: 10.1111/nph.15697

Van de Velde, W., Zehirov, G., Szatmari, A., Debreczeny, M., Ishihara, H., Kevei, Z., et al. (2010). Plant peptides govern terminal differentiation of bacteria in symbiosis. *Science* 327, 1122–1126. doi: 10.1126/science.1184057

Velivelli, S. L. S., Czymmek, K. J., Li, H., Shaw, J. B., Buchko, G. W., and Shah, D. M. (2020). Antifungal symbiotic peptide NCR044.1 exhibits unique structure and multi-faceted mechanisms of action that confer plant protection. *bioRxiv [Preprint]* doi: 10.1101/2020.02.19.956318

Wang, G. (2020). The antimicrobial peptide database provides a platform for decoding the design principles of naturally occurring antimicrobial peptides. *Protein Sci.* 29, 8–18. doi: 10.1002/pro.3702

Waterhouse, A. M., Procter, J. B., Martin, D. M. A., Clamp, M., and Barton, G. J. (2009). Jalview version 2: a multiple sequence alignment editor and analysis workbench. *Bioinformatics* 25, 1189–1191. doi: 10.1093/bioinformatics/btp033

Yount, N. Y., and Yeaman, M. R. (2004). Multidimensional signatures in antimicrobial peptides. *Proc. Natl. Acad. Sci. U.S.A.* 101, 7363–7368. doi: 10.1073/pnas.0401567101

Conflict of Interest: The authors declare that the research was conducted in the absence of any commercial or financial relationships that could be construed as a potential conflict of interest.

frontiers in Microbiology

REVIEW
published: 15 April 2021
doi: 10.3389/fmicb.2021.630695

Bacteriocins: An Overview of Antimicrobial, Toxicity, and Biosafety Assessment by *in vivo* Models

Diego Francisco Benítez-Chao[1,2†], Angel León-Buitimea[1,2†], Jordy Alexis Lerma-Escalera[1,2] and José Rubén Morones-Ramírez[1,2]*

[1] *Facultad de Ciencias Químicas, Universidad Autónoma de Nuevo León, San Nicolás de los Garza, Mexico,* [2] *Centro de Investigación en Biotecnología y Nanotecnología, Facultad de Ciencias Químicas, Parque de Investigación e Innovación Tecnológica, Universidad Autónoma de Nuevo León, Apodaca, Mexico*

OPEN ACCESS

Edited by:
Adler Ray Dillman, University of California, Riverside, United States

Reviewed by:
Piyush Baindara, University of Missouri, United States
Fliss Ismail, Laval University, Canada
Takeshi Zendo, Kyushu University, Japan

***Correspondence:**
José Rubén Morones-Ramírez
jose.moronesrmr@uanl.edu.mx

[†] *These authors have contributed equally to this work*

Specialty section:
This article was submitted to Antimicrobials, Resistance and Chemotherapy, a section of the journal Frontiers in Microbiology

Received: *18 November 2020*
Accepted: *08 March 2021*
Published: *15 April 2021*

Citation:
Benítez-Chao DF, León-Buitimea A, Lerma-Escalera JA and Morones-Ramírez JR (2021) Bacteriocins: An Overview of Antimicrobial, Toxicity, and Biosafety Assessment by in vivo Models. Front. Microbiol. 12:630695. doi: 10.3389/fmicb.2021.630695

The world is facing a significant increase in infections caused by drug-resistant infectious agents. In response, various strategies have been recently explored to treat them, including the development of bacteriocins. Bacteriocins are a group of antimicrobial peptides produced by bacteria, capable of controlling clinically relevant susceptible and drug-resistant bacteria. Bacteriocins have been studied to be able to modify and improve their physicochemical properties, pharmacological effects, and biosafety. This manuscript focuses on the research being developed on the biosafety of bacteriocins, which is a topic that has not been addressed extensively in previous reviews. This work discusses the studies that have tested the effect of bacteriocins against pathogens and assess their toxicity using *in vivo* models, including murine and other alternative animal models. Thus, this work concludes the urgency to increase and advance the *in vivo* models that both assess the efficacy of bacteriocins as antimicrobial agents and evaluate possible toxicity and side effects, which are key factors to determine their success as potential therapeutic agents in the fight against infections caused by multidrug-resistant microorganisms.

Keywords: bacteriocins, antibiotics, antimicrobial resistance, antibacterial peptide, toxicity, biosafety, *in vivo* model

INTRODUCTION

According to the WHO, diseases caused by multidrug-resistant (MDR) pathogens are a serious worldwide public health problem (World Health Organization, 2019c). The rapid spread of MDR pathogens have reduced the effectiveness of common antibiotics (Gupta and Datta, 2019). Therefore, there is a particular need for the development of new antimicrobial agents, specifically those directed against MDR bacteria (Fair and Tor, 2014). Bacteriocins represent the most important group of antimicrobial peptides with applications in human health (Marshall and Arenas, 2003). The ability of bacteriocins to kill or inhibit relevant pathogenic bacteria (including MDR pathogens) *in vitro* has been well documented (Cui et al., 2012; Gabrielsen et al., 2014; Perez et al., 2014; Newstead et al., 2020). However, the use of animal models is an important part in the

research toward the development of new therapeutic agents. There are many animal models used for screening drugs or chemical compounds in preclinical studies (Zwierzyna and Overington, 2017). Mice are the best-known animal models for *in vivo* bacteriocin efficacy studies. Other animal species, less frequently used, are guinea pigs, rabbits, and hamsters (Badyal and Desai, 2014). Therefore, the present review addresses the antimicrobial effects, toxicity, and biosafety of bacteriocins in *in vivo* systems. The bacteriocins here included are those naturally synthesized by native or recombinant producers, those chemically synthetized or bioengineered bacteriocins, those obtained from direct application of cultures with bacteriocin-producers, and those bacteriocins produced in cell-free supernatants (CFSs). Moreover, we here discuss the toxicity and biosafety *in vivo* assays, in different animal models, that have been reported during the exploration of antimicrobial effects.

ANTIMICROBIAL RESISTANCE: GLOBAL EMERGENCY

The death toll caused by drug-resistant infections has been dangerously rising every year within the last two decades. According to World Health Organization (2019c), at least 700,000 people died annually around the world because of this. In Europe, deaths raised from 25,000 in 2007 (European Centre for Disease Prevention and Control, 2009) to 33,110 in 2015 (Cassini et al., 2019). Moreover, according to WHO Africa, 54,000 cases of MDR tuberculosis were detected in 42 countries, and approximately 3200 cases of extensively drug-resistant (XDR) tuberculosis were notified in eight countries from the African region from 2004 to 2011 (Ndihokubwayo et al., 2013). China, one of the most populated countries, reported that between 2005 and 2017, the range of isolated drug-resistant bacteria varied from 22,774 to 190,610 (Qu et al., 2019). During 2017 in India, a study reported that 70% of drug-resistant Gram-negative isolates corresponded to *Escherichia coli, Klebsiella pneumoniae, Acinetobacter baumannii*, and *Pseudomonas aeruginosa* (Taneja and Sharma, 2019). Regarding the United States, 23,000 deaths were counted in 2013; 6 years later, in 2019, numbers increased to 35,000 deaths associated with antibiotic-resistant infections (Frieden, 2013). In particular, Mexico has a dramatic lack of information and epidemiological surveillance for antibiotic resistance (Amabile-Cuevas, 2010). Recently, a 6-month study assessed the resistance rates of several bacterial pathogens in 47 Mexican centers. They included almost 23,000 strains, and their results showed that the most common drug-resistant strains were *E. coli*, *Klebsiella* sp., *Enterobacter* sp., *P. aeruginosa*, *Acinetobacter* sp., vancomycin-resistant *Enterococcus faecium*, and methicillin-resistant *Staphylococcus aureus* (MRSA) (Garza-González et al., 2019). According to the WHO, if severe actions are not taken by 2050, it is estimated that 10 million people will die annually around the world due to diseases caused by MDR pathogens. This situation may cause a severe economic impact with consequences similar to the 2009 Global Financial Crisis (World Health Organization, 2019c).

CURRENT TREATMENTS FOR BACTERIAL INFECTIONS

Since their discovery in 1928, antibiotics have effectively controlled bacterial infections (Podolsky, 2018). The current treatments for bacterial infections include bactericidal or bacteriostatic agents from different classes of antibiotics. The most common classes of drugs are penicillins, cephalosporins, quinolones, macrolides, tetracyclines, glycopeptides, and monobactams, among others (Taylor et al., 2002).

Within the last two decades, a variety of antibiotics have been approved to treat infections caused by Gram-positive and Gram-negative bacteria. Novel antibiotics against Gram-positive bacteria include β-lactams (ceftaroline and ceftobiprole), glycopeptides (dalbavancin, oritavancin, and telavancin), oxazolidinones (tedizolid phosphate), quinolones (besifloxacin, delafloxacin, and ozenoxacin), and tetracyclines (omadacycline). The main advantage of the previously mentioned antibiotics is their efficiency in the treatment of bacterial infections caused by MDR strains (Koulenti et al., 2019b). Recently approved treatments to combat MDR Gram-negative bacteria include antibiotic combinations of β-lactam/β-lactamase inhibitors (ceftolozane/tazobactam, ceftazidime/avibactam, and meropenem/vaborbactam), and aminoglycosides (plazomicin) combined with tetracyclines (eravacycline) (Koulenti et al., 2019a). Nonetheless, misuse and overuse of these combinatorial treatments have contributed to further development of antibiotic resistance (Malik and Bhattacharyya, 2019).

The rapid spread of MDR and XDR bacteria in both hospitals and community settings has reduced the effectiveness of antibiotics (Gupta and Datta, 2019). One of the main concerns regarding antibiotic resistance is that some bacteria have become resistant to almost all currently available antibiotics. Therefore, these bacteria represent a severe public health problem worldwide. Of particular interest are the following strains: MRSA, vancomycin-intermediate and -resistant; *E. faecium,* vancomycin-resistant; *Enterobacteriaceae,* carbapenem-resistant, extended-spectrum beta-lactamase (ESBL)-producing; *A. baumannii*, carbapenem-resistant; and *P. aeruginosa*, carbapenem-resistant (World Health Organization, 2017).

Preventing and controlling the spread of antibiotic resistance is necessary to invest in research and development of new agents with therapeutic potential to treat bacterial infections. According to data from the WHO, there is an arsenal of 50 antimicrobial agents and their combinations in clinical development. Thirty-two are antibiotics active against the WHO priority pathogens, ten are biological agents, two are classified as innovative agents, and two are active against MDR Gram-negative bacteria (World Health Organization, 2019a).

BACTERIOCINS AS ALTERNATIVE ANTIMICROBIAL AGENTS

There is a particular need for new antimicrobial agents, specifically those directed against antibiotic-resistant bacteria (Fair and Tor, 2014). Defensins and bacteriocins represent

the most important groups of antimicrobial peptides with applications in human health (Marshall and Arenas, 2003). Defensins are small cysteine-rich (forming three to six disulfide bonds) cationic antimicrobial peptides ubiquitous among eukaryotes that form an essential element of innate immunity. They consist of two analogous superfamilies and an extensive convergent evolution is the source of their similarities (Shafee et al., 2016). Bacteriocins are ribosomally synthesized peptides secreted by a variety of bacteria for the purpose of killing other bacteria. Thereby, whereas defensins are important components of the host immune response against infection in eukaryotes (Arnett and Seveau, 2011), bacteriocins participate in removing microbial competition in prokaryotes (Cotter et al., 2013).

The way to classify defensins and bacteriocins has been based on their biochemical (net charge) and/or structural features (linear/circular/amino acid composition) and there is a current search for common patterns that might help to distinguish them (Tossi and Sandri, 2002; Zasloff, 2002). To determine whether all molecules are homologous or have independently evolved similar features, the best evidence lies in the structure. The antimicrobial peptides can be differentiated from their overall three-dimensional structure and the spacing of half-cystine residues involved in intrachain disulfide bonds (Marshall and Arenas, 2003). To date, only two bacteriocins (bactofencin and laterosporulin) have been expressed as defensin-like bacteriocins. Bactofencin is a disulfide bond-containing bacteriocin with highly conserved cysteine residues and structurally related to eukaryotic defensins due to their highly cationic nature (O'Shea et al., 2013; O'Connor et al., 2018). The laterosporulin has been previously identified from a *Brevibacillus laterosporus* strain GI-9 and contain disulfide bonds in positions homologous to eukaryotic defensins (Singh et al., 2012). The presence of disulfide connectivity suggests its similarity to β-defensins while its architectural similarity is related to α-defensins (Singh et al., 2015). Recently, laterosporuli10, a novel defensin-like bacteriocin (class II bacteriocin) from the *Brevibacillus* sp. strain SKDU10, was characterized. This bacteriocin showed 57.6% homology with laterosporulin and differences in the molecular weight and the number of cationic amino acids. It was highly efficient in killing *S. aureus* (Gram-positive bacteria) and the *Mycobacterium tuberculosis* H37Rv strain when compared to laterosporulin (Baindara et al., 2017). Interestingly, Class II bacteriocins are easily manipulated by genetic engineering techniques because they do not have large post-translational modifications and it is possible to obtain variants according to the technological requirements and needs (Zheng and Sonomoto, 2018; Kumariya et al., 2019). Therefore, this technique could be useful to develop new antimicrobial peptides to be used as an alternative to common antibiotics.

As stated above, bacteriocins represent an interesting solution to reduce the development of resistance. Besides, bacteriocins are continuously evolving with high potential against clinically relevant pathogens (Piper et al., 2009; Bonhi and Imran, 2019). Bacteriocins can be easily manipulated by bioengineering techniques (Field et al., 2010). Unlikely to antibiotics, bacteriocins can be engineered to attach anywhere on the cellular outer membrane because they do not have a specific receptor (Bonhi and Imran, 2019) and they can be produced *in situ* by probiotics (Dobson et al., 2012; O'Shea et al., 2012). Consequently, this represents a new path in bacteriocin research that will undoubtedly lead to the development of new therapeutic strategies with highly relevant clinical applications (Chikindas et al., 2018).

ANTIBACTERIAL ACTIVITY OF BACTERIOCINS IN *IN VITRO* STUDIES

In vitro antimicrobial activity assays are the first step to evaluate the biological capacity of bacteriocins against clinically relevant bacterial pathogens (Ansari et al., 2018; Peng et al., 2019). However, if the conditions used in the *in vitro* models are not adequate to assess a specific effect, then the probabilities of success in the *in vivo* models will be very low (Blay et al., 2007; Umu et al., 2016). Fortunately, many bacteriocins have been successfully tested using *in vitro* assays against relevant bacterial pathogens (including MDR pathogens) (Cui et al., 2012; Gabrielsen et al., 2014; Perez et al., 2014; Newstead et al., 2020). Some examples include bacteriocin AS-48, which is active against reference and clinical strains of *M. tuberculosis* (Aguilar-Pérez et al., 2018). Pentocin JL-1 has also been demonstrated to have antibacterial activity against Gram-positive and Gram-negative bacteria, particularly MDR *S. aureus* (Jiang et al., 2017). Other examples, such as the novel entianin, which has activity against MRSA (ATCC 43300) and vancomycin-resistant *Enterococcus faecalis* (ATCC 51299) strains (Fuchs et al., 2011), and bacteriocins klebicins have been demonstrated to be active against MDR and carbapenem-resistant *Klebsiella* species (Denkovskienė et al., 2019). Moreover, novel enterocins DD28 and DD93 showed anti-staphylococcal activity in MRSA (Al Atya et al., 2016). It is important to mention that many current reports on the study of bacteriocins are focused on pathogens considered by WHO as a priority (World Health Organization, 2017) such as carbapenem-resistant *E. coli* or *K. pneumoniae* (Chen et al., 2019), vancomycin-resistant, and MDR *E. faecium* (Phumisantiphong et al., 2017).

As expected, bacteriocins have an outstanding record to kill or reduce pathogens and drug-resistant pathogens during *in vitro* assessments (Fuchs et al., 2011; Cui et al., 2012; Gabrielsen et al., 2014; Ishibashi et al., 2014; Al Atya et al., 2016; Jiang et al., 2017; Aguilar-Pérez et al., 2018; Ansari et al., 2018; Denkovskienė et al., 2019; Peng et al., 2019; Newstead et al., 2020). Conventionally, bacteriocins display a non-toxic behavior at *in vitro* assays (Cebrián et al., 2019). Thus, the promising results obtained after *in vitro* assays must be extrapolated into *in vivo* assays (Kokai-Kun et al., 2003). Furthermore, at this stage, internal factors of the host (pharmacokinetic parameters) should be considered (Meade et al., 2020) as well as the potential bacteriocin-induced toxicity (Gupta et al., 2014). Therefore, the use of animal models is mandatory in the development of a new therapeutic agent and the successful results obtained from these experiments are essential to close the translational gap to the clinic (Denayer et al., 2014). The description of the preclinical drug discovery and development process is shown in **Figure 1**.

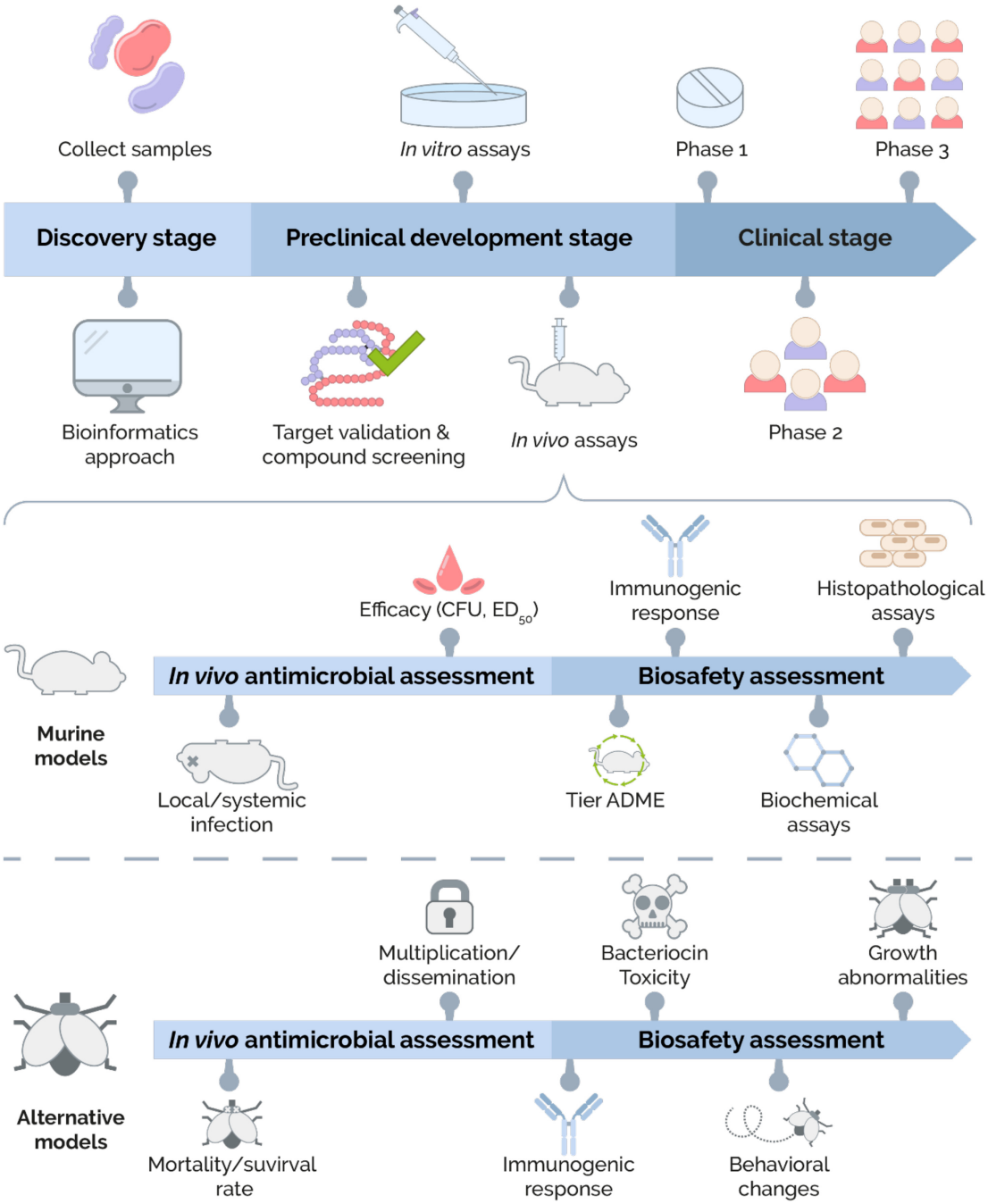

FIGURE 1 | Overview of the bacteriocin development process. The bacteriocin development process is divided into three big stages: **Discovery**, **Preclinical development,** and **Clinical development.** In the **Discovery stage**, two main approaches for bacteriocins are identified. The traditional approach consists of collecting environmental samples to isolate bacteriocin-producers. On the other hand, bacteriocins can be obtained by designing and analyzing databases using a bioinformatic approach. Next, the **Preclinical development stage** is divided into three subcategories: target validation and compound screening, *in vitro* assays, and *in vivo* assays. The first subcategory focuses on screening, structure–function analysis, and characterization of bacteriocins. The second subcategory's main goal is to demonstrate the antimicrobial activity and cytotoxicity effects by ***in vitro* assays**. The third subcategory includes the ***in vivo* assays**. The *in vivo* antimicrobial activity and biosafety assessment of bacteriocins can be carried out using murine and alternative models. The *in vivo* antimicrobial assessment in murine models includes the use of local and systemic infection models in rodents and the evaluation of efficacy. The biosafety assessment includes evaluating various parameters, such as pharmacokinetics profile (ADME), immunogenic response, and biochemical and histopathological analysis. On the other hand, the *in vivo* antimicrobial assessment in alternatives models (e.g., fruit fly, zebrafish, roundworm, greater wax moth, or brine shrimp) allows determining the mortality/survival rates and the ability of bacteriocin to block multiplication/dissemination of pathogenic agent. Biological parameters such as the immunogenic response, bacteriocin toxicity, behavioral changes, and growth abnormalities are evaluated during the biosafety evaluation. Once bacteriocin has shown to be effective and safe in *in vivo* models, it advances to the **Clinical development stage** where its dose, efficacy, and side effects are evaluated through different phases (Phases 1–3) until its approval and commercialization.

IN VIVO ASSESSMENT OF BACTERIOCINS

There are many animal models used for screening drugs or chemical compounds in preclinical testing (pharmacological bioassays) (Zwierzyna and Overington, 2017) and specific toxicity studies (toxicological bioassays) (Creton et al., 2010). Rodents (rats and mice) are the most frequently used animal species. Other animal species, less frequently used, are guinea pigs, rabbits, and hamsters (Badyal and Desai, 2014). Invertebrate models can be used to assess many biological activities, and these include *Drosophila melanogaster* (fruit fly) and *Caenorhabditis elegans* (a nematode worm) (Badyal and Desai, 2014). Finally, zebrafish is the most used rapidly developing vertebrate, and it has proven to be an excellent model for toxicity testing (Segner et al., 2003).

In vivo Assessment of Bacteriocins in Murine Models

In terms of genomics, the strategies for cloning, gene knockout, and gene or genome modifications are very well-described. Genes are very well-conserved between mice and humans since they share 90% of their total genes, and they are also available to develop spontaneous mutations. In terms of biology, mice are small and easy to handle; they can be easily transported and raised in a laboratory. Gestation times of mice are relatively short, and a large number of offspring can be obtained for *in vivo* purposes (Masopust et al., 2017). Therefore, mice are the best-known animal model for *in vivo* bacteriocin efficacy studies.

As mentioned earlier, the ability of bacteriocins to kill or inhibit pathogenic bacteria *in vitro* has been well documented. Bacteriocins represent one of the most studied microbial defense systems (Cavera et al., 2015). They may facilitate the introduction of a producer into an established niche, directly inhibit the invasion of competing strains or pathogens, or modulate the composition of the microbiota and influence the host immune system (Dobson et al., 2012). Therefore, understanding that bacteriocins may function in several ways, studies involving direct correlations between *in vitro* efficacy and *in vivo* protection are needed.

To date, bacteriocins have showed a promising efficacy as antibiotic alternatives in *in vivo* studies. Bacteriocin application focuses in the administration at the site of the infection or susceptible areas, evading an immune response and maintaining the stability of the bacteriocin (Arthur et al., 2014). Therefore, selection of optimal bacteriocin and delivery systems has been complicated. Two factors seem to play an important role in *in vivo* efficacy of bacteriocins: pharmacokinetic parameters and route of administration.

First, pharmacokinetic parameters (e.g., bioavailability, stability, solubility in physiological conditions, and susceptibility to enzymatic proteolysis in bloodstream) are important determinants of the efficacy of bacteriocins (Soltani et al., 2021). Bacteriocins administered orally are exposed to the hostile environment (enzymatic and pH degradation) in the gastrointestinal tract; they are highly susceptible to degradation once they reach the small intestine. On the other hand, parenteral administration may offer some means of avoiding proteolytic degradation of bacteriocins in the gastrointestinal tract. Nevertheless, the efficacy may be reduced since bacteriocins will be in contact with proteases involved in hemostasis and fibrinolysis in the bloodstream (Meade et al., 2020). To reduce or avoid these problems, bacteriocins can be engineered to be less susceptible to proteolytic degradation by changing D-amino acids (Soltani et al., 2021). Also, nanotechnology seems to be a valuable strategy to improve the physicochemical properties of the bacteriocins (Farokhzad and Langer, 2009). The nano-encapsulation [e.g., lipid-based nanoparticles (nanoliposomes and solid lipid nanoparticles), carbohydrate-based nanoparticles (chitosan/alginate and phytoglycogen nanoparticles), and conjugation with nanosized metal] of bacteriocins could protect them from enzymatic degradation, hence increasing their stability for longer periods (Fahim et al., 2016).

Second, the route of administration determines the onset and the duration of the pharmacological effect, the efficacy, and the adverse effects of drugs. The main routes of bacteriocin administration, such as intranasal (McCaughey et al., 2016a,b), intragastric (Wongsen et al., 2019), intraperitoneal (Piper et al., 2012; Sahoo et al., 2017), subcutaneous (Kers et al., 2018a,b; Pulse et al., 2019), and topical (Van Staden et al., 2016; Cebrián et al., 2019) have demonstrated excellent efficacy in murine models. However, the efficacy of the different routes of administration has not been directly compared and likely depends on the pathogen targeted (Lohans and Vederas, 2012). In the same way, *in vivo* toxicity testing has been conducted to identify possible adverse effects resulting from exposure to bacteriocins. As described below, many studies have been done to investigate toxicity and biosafety of bacteriocins using different type of applications, such as oral, intraperitoneal, nasal, and topical. In particular, topical application of bacteriocins has been reported to be successfully tested for skin infection with no toxicity effects. For example, the circular bacteriocin AS-48 was evaluated and the results indicated that this bacteriocin did not induce skin sensitization or cause allergic contact dermatitis (Cebrián et al., 2019). Topical formulation with two broad-spectrum bacteriocins: garvicin KS and micrococcin P1 was used in a murine skin infection model. The formulation had a significant antibacterial effect and animals showed no changes of behavior or obvious toxic effects (Ovchinnikov et al., 2020). Therefore, there is a growing interest for the study of the therapeutic properties and side effects of bacteriocins using *in vivo* systems (Abanoz and Kunduhoglu, 2018; Bagci et al., 2019; Iseppi et al., 2019; Lynch et al., 2019; Lajis, 2020; Meade et al., 2020).

Latest publications on *in vivo* assessment of bacteriocins using murine models contain as minimum parameters the measurement of the antimicrobial activity of bacteriocin on the animal model, the assessment of immunogenic response, biochemical analysis, and histopathological analysis. To support this paragraph, we have summarized some of the relevant bacteriocins with their *in vivo* antimicrobial (**Table 1**) and toxicity and biosafety (**Table 2**) activities in murine models over the last 20 years. In this context, we included bacteriocin studies that have

TABLE 1 | *In vivo* antimicrobial assessment of bacteriocins using murine models.

Bacteriocin	Producer	Target	Host	Administration route	Antimicrobial activity	References
***In vivo* assessment of purified or partially purified bacteriocins in murine models**						
Naturally synthetized bacteriocins by native producers						
Mersacidin	*Bacillus* sp. HIL Y-85 54728	MRSA strain 99308	Female BALB/cA mice	Nasal	MRSA was absent in nasal cavity after treatment. Serum levels of IL-1β (inflammatory cytokine for innate immunity) and TNFα (master regulator of inflammatory response) were decreased.	Kruszewska et al., 2004
Mutacin B-Ny266	*S. mutans* Ny266	MSSA Strain	Mice	Intraperitoneal	Survival rate of infected mice with low and high doses of MSSA was 30 and 0%, respectively. Survival rate in infected mice with low and high doses of MSSA treated with B-Ny266 at 1, 3, and 10 mg/kg was 100%	Mota-Meira et al., 2005
Nisin, clausin, AmyA	*B. amyloliquefaciens* (only AmyA)	*S. aureus* Xen 36	Adult female nude mice	Skin	All antimicrobial treatments (CPVA, mupirocin, nisin, clausin, and AmyA) gradually reduced the size of wound skin infections with *S. aureus* after 7 days, although clausin- and nisin-treated wounds were smaller than CPVA-treated wounds.	Van Staden et al., 2016
Penisin	*Paenibacillus* sp. Strain A3	MRSA Strain	Male BALB/c mice	Intraperitoneal	Penisin was significantly effective at 80 and 100 mg/kg, as MRSA load decreased to 91 from 96% in mice, respectively. Survival rate in penisin-treated infected and untreated mice was 88 and 0% after day 4, respectively.	Baindara et al., 2016
AS-48	*E. faecalis strain* UGRA10	*T. cruzi* Arequipa strain	Female BALB/c mice	Intraperitoneal	55% of organs/tissues were parasite-free in mice treated with AS-48 at 1 mg/kg in both acute and chronic infection. 33 and 55% or organs were free of parasites after treatment with benznidazole at 100 mg/kg, respectively.	Martín-Escolano et al., 2020
Naturally synthetized bacteriocins by heterologous producers						
Lacticin 3147	*L. lactis* subsp. *cremoris* MG1363	*S. aureus* Xen 29	Female BALB/c mice	Intraperitoneal	Prevented the systemic spread of *S. aureus.* Microbial levels were decreased in the thoracic, abdominal cavity, and spleen but increased in liver and remained the same in kidney.	Piper et al., 2012
Pyocins S2, S5, AP41, and L1	*E. coli BL21(DE3)* pLysS	*P. aeruginosa* P8	Female C57/BL6 mice	Intranasally	Mice were previously infected with P8 and treated later with S2, S5, AP41, or L1. All pyocin-treated mice survived to end point (24 h post infection). S5 had the highest efficacy because no P8 was recovered in any S5-treated infected mice. All the other pyocins reduce the bacterial load by 4-log units.	McCaughey et al., 2016b
Pyocin SD2	*E. coli BL21(DE3)* pLysS	*P. aeruginosa* PAO1	Female C57/BL6 mice	Intranasally	Pyocin SD2-treated mice previously infected with PAO1 had no signs of illness and survived to end point (24 h post infection) and low counts of PAO1 were recovered from lungs (5 CFU/lung). Untreated infected mice were culled at 6 h due to severity of illness and high counts of PAO1 (10^5 CFU/lung)	McCaughey et al., 2016a
Plantaricin E/F	*L. lactis* NZ3900	*E. coli* EPEC K1.1	ddY male mice	Oral	EPEC K1.1 was orally given to mice at 10^8 CFU/ml. Then, plantaricin E and F were given at different dosages for 7 days. Leukocyte, hematocrit (due to diarrhea), and hemoglobin levels (due to damage) were increased, and erythrocyte numbers lowered during infection. After treatment with plantaricins, mice improved their healthy. Plantaricin E at 250 and 500 mg/kg and Plantaricin F at 500 mg/kg reduced inflammatory in mice as indicator of infection.	Hanny et al., 2019
Chemically synthetized bacteriocins						
Lysostaphin	Chemical Synthetized	MRSA (MBT 5040 and 12/12 strains), MSSA (Newman, ATCC 49521, ATCC 12605) and mupirocin-resistant (SA 3865 MupR)	Female cotton rats and female ICR mice	Nasal	Nasal colonization by *S. aureus* was eradicated at 93% in cotton rats with a single dosage of lysostaphin cream. Also, two methicillin-susceptible strains (ATCC 49521 and ATCC 12605), MRSA strain 12/12, and mupirocin-resistant SA 3865 MupR were eradicated. No antibacterial effect was observed with nisin cream at 5% (positive control).	Kokai-Kun et al., 2003
Epidermicin NI01	Chemical Synthetized	MRSA ATCC 43300	Female Cotton rats	Nasal	Untreated infected rats had mean values 3.79 $\log_{10}$ CFU/nares. MRSA-infected rats treated with NI01 at 0.8% had mean values 0.78 $\log_{10}$ CFU/nares.	Halliwell et al., 2017
***In vivo* assessment of bioengineered bacteriocins in murine models**						
Nisin A and Nisin V	*L. lactis* NZ9700 and *L. lactis* NZ9800nisA:M21V	*L. monocytogenes* EGDe	Female BALB/c mice	Intraperitoneal	Bioimaging of mice was used to quantify the bioluminescent bacteria (NZ9800NISA:M21V) in organs. Nisin V exerted a better antibacterial activity in the liver and spleen than nisin A	Campion et al., 2013
OG253	*S. mutans* 152 producing OG253 (Phe1Ile)	*C. difficile* UNT103-1	Male Golden Syrian hamsters	Subcutaneous	Survival rate for OG253-treated challenged mice were 100% while vancomycin-treated mice were 33% after 21 days. All untreated challenged mice died by day 9.	Kers et al., 2018b

(Continued)

TABLE 1 | Continued

Bacteriocin	Producer	Target	Host	Administration route	Antimicrobial activity	References
OG716 and OG718	*S. mutans* 152 producing OG716 and *S. mutans* 152 producing OG718	*C. difficile* UNT103-1	Male Golden Syrian hamsters	Subcutaneous	Survival rate for OG716-treated challenged mice were 100% and vancomycin-treated mice were 83% after treatment. Control challenged mice were dead before day 5.	Kers et al., 2018a
OG716 and OG718	*S. mutans* 152 producing OG716 and *S. mutans* 152 producing OG718	*C. difficile* UNT103-1	Male Golden Syrian hamsters	Subcutaneous	*C. difficile* CFU levels in untreated challenged hamster cecum were 6.66 log_{10} CFU/ml. OG716-treated mice at 105 or 180 mg/kg body weight per day had values between <2.4 and 2.51 log_{10} CFU/ml, respectively. OG718-treated mice at 180 mg/kg BW per day had values of 3.18 log_{10} CFU/ml.	Pulse et al., 2019
***In vivo* assessment of bacteriocin-producer directly in murine models**						
Bacterial dose	*Lb. salivarius* UCC118	*L. monocytogenes* EGDe	A/J mice	Oral	*L. monocytogenes* log CFU/g levels in liver and spleen for untreated mice were 4 and 5, respectively. UCC118-treated mice had significantly lower listerial CFU levels.	Corr et al., 2007
Bacterial dose	*E. mundtii* ST4SA and *L. plantarum* 423	*S. enterica* serovar Typhimurium	Male Wistar rats	Oral	Rats were daily administered with *L. plantarum* 423 and *E. mundtii* ST4S for 7 days and then challenged with *S. enterica*. Rats gained weight (alone or combination), suggesting that bacteriocin-producers prevented the system spread of *S. enterica*.	Dicks and ten Doeschate, 2010
Bacterial dose	*E. faecium* KH24	*S. enteritidis*	Swiss Albino male mice	Oral	Mice previously fed with KH24 showed a rise in weight and 1 log CFU/g decrease in *S. enteritidis* in the small and large intestine. Neither salmonella nor enterococcal count was observed in liver and spleen.	Bhardwaj et al., 2010
Bacterial dose	*L. plantarum* B7	*S. typhimurium* ATCC 13311	Male albino mice	Oral	*S. typhimurium* levels in feces of untreated infected mice (7.42 ± 0.05 logCFU/g) were higher than B7-treated infected mice (8.86 ± 0.02 logCFU/g). Serum levels of TNF-a, IL-6, and CXCL1 were higher in untreated infected mice than in pretreated infected mice.	Wongsen et al., 2019

measured their effects in murine models using purified or partially purified bacteriocins (including naturally synthesized bacteriocins by native and heterologous producers and chemically synthetized bacteriocins), bioengineering bacteriocins, or the bacteriocin-producer microorganism directly in the host.

In vivo Assessment of Purified or Partially Purified Bacteriocins in Murine Models

For categorization purposes, in this section, we only include studies of bacteriocins that were applied purely or partially purified in murine models. We here consider bacteriocins that were chemically synthesized and those that were naturally synthesized from a native bacteriocin-producer or by a heterologous bacteriocin-producer.

Naturally synthetized bacteriocins by native producers

This group is characteristic since it is a straightforward system that produces bacteriocins. Native bacteriocin-producers usually excrete bacteriocins by dedicated membrane-associated ATP-binding cassette (ABC) transporters or by the general secretion (*sec*) pathway of the cell (Munoz et al., 2011).

Mersacidin is a lantibiotic-type bacteriocin that was isolated and purified from *Bacillus* spp. HIL Y-85 54728. It has been tested in female BALB/cA mice infected by *S. aureus* 99308. Results showed a decrease in the inflammatory response of the host (Kruszewska et al., 2004; Parameswaran and Patial, 2010; Kaneko et al., 2019). Mutacin B-Ny266 is naturally produced from *Streptococcus mutans* Ny266. Its antibacterial effect was proved in mice infected with methicillin-susceptible *S. aureus* (MSSA) strain. Moreover, no mortality was observed in mutacin B-Ny266-treated mice (Mota-Meira et al., 2005). Another bacteriocin is nisin; it has been tested along with clausin and the two components (α- and β-peptides) bacteriocin amyloliquecidin (AmyA) from *Bacillus amyloliquefaciens* against a bioluminescent strain of *S. aureus* Xen 36 in adult female nude mice in a wound skin infection model. Interestingly, all antimicrobial treatments reduced the bacterial load after 7 days of treatment (Van Staden et al., 2016). Penisin, from *Paenibacillus* sp. Strain A3, was used to effectively protect mice from a MRSA infection. Penisin-treated infected mice had a significant higher survival rate than untreated infected mice (Baindara et al., 2016). TSU4 is a bacteriocin recovered from *Lactobacillus animalis* TSU4. This bacteriocin was used in BALB/c mice to evaluate the acute and sub-chronic toxicity tests. Biochemical and histopathological analysis was performed. The bacteriocin demonstrated to be safe in a sub-chronic toxicity test. No antimicrobial *in vivo* test was performed (Sahoo et al., 2017). Finally, AS-48 bacteriocin is produced by *E. faecalis* strain UGRA10. The immunogenic response and biochemical and histopathological effects were analyzed in BALB/c mice (Cebrián et al., 2019). Later, its activity as antiprotozoal peptide was tested in BALB/c mice challenged with *Trypanosoma cruzi* strain Arequipa (Chaga's disease etiological agent). Results demonstrated that this bacteriocin reduced the acute infection in mice (Martín-Escolano et al., 2020).

TABLE 2 | *In vivo* toxicity and biosafety assessment of bacteriocins using murine models.

Bacteriocin	Producer	Host	Toxicity and biosafety assessment	References
***In vivo* assessment of purified or partially purified bacteriocins in murine models**				
Naturally synthetized bacteriocins by native producers				
Mutacin B-Ny266	*S. mutans* Ny266	Mice	No toxicity was recorded of B-Ny266 at 10 mg/kg	Mota-Meira et al., 2005
Nisin, clausin, AmyA	*B. amyloliquefaciens* (only AmyA)	Mice	CPVA, mupirocin, nisin, clausin, and AmyA gradually reduced the size of non-infected wounds after 7 days. No toxicity assessment was displayed.	Van Staden et al., 2016
TSU4	*L. animalis* TSU4	Male BALB/c mice	TSU4 over 200 mg/kg body weight was safe enough. No significant impact of bacteriocin on the kidney and liver after sub-chronic toxicity test.	Sahoo et al., 2017
AS-48	*E. faecalis* strain UGRA10	Female BALB/c mice	Serum biochemical measurements were performed to evaluate *in vivo* toxicity in mice (5 mg/kg). AS-48 made changes in biochemical measurements. No mice died or lost more than 5% body weight. After 7 days, mice returned to normal levels.	Cebrián et al., 2019
AS-48	*E. faecalis strain* UGRA10	Female BALB/c mice	None of the treated mice died and lost more than 10% body weight after treatment.	Martín-Escolano et al., 2020
Naturally synthetized bacteriocins by heterologous producers				
Pyocins S2, S5, AP41, and L1	*E. coli BL21(DE3)* pLysS	Female C57/BL6 mice	Pyocins S2, S5, and L1 except AP41 were stables in the lung and do not cause inflammation or tissue damage in murine lung. AP41 was presumably degraded in lungs.	McCaughey et al., 2016b
Plantaricin E/F	*L. lactis* NZ3900	Male ddY mice	Bacteriocin E or F at concentrations ranging from 50, 100, 1000, and 5000 mg/kg body weight had no mortality in mice. Hematological and biochemical parameters displayed normal levels and histopathology shows normal liver and kidney cells. The leukocyte, hematocrit, and hemoglobin levels in mice were improved after bacteriocin treatment; also, the malondialdehyde (MDA) indicator levels were reduced.	Hanny et al., 2019
Chemically synthetized bacteriocins				
Epidermicin NI01	Chemical synthetized	Female Cotton rats	Histology studies of the nasal cavities demonstrated mild to a marked epithelial abnormality with a decreasing gradient of severity from the anterior to posterior regions of the mice nasal cavities in epidermicin NI01 at 0.2%. No cytotoxic activity, necrosis, or presence of blood was noted.	Halliwell et al., 2017
***In vivo* assessment of bioengineered bacteriocins in murine models**				
OG716 and OG718	*S. mutans* 152 producing OG716 and *S. mutans* 152 producing OG718	Male Golden Syrian hamsters	OG716 and OG718 were administered at doses of 180 mg/kg body weight (mg/kg BW) of hamsters challenged with *C. difficile* protected to the rodent since survival rate was around 80% after 22 days of treatment	Pulse et al., 2019
***In vivo* assessment of bacteriocin-producer directly in murine models**				
Bacterial dose	*E. mundtii* ST4SA and *L. plantarum* 423	Male Wistar rats	Endotoxin levels were lowered in rats that received *L. plantarum* 423 and *E. mundtii* ST4SA. No signs of splenomegaly or hepatomegaly were observed in tissue samples taken from the liver and spleen, and no abnormal morphological changes were observed in the epithelium of the ileum and colon.	Dicks and ten Doeschate, 2010
Bacterial dose	*E. faecium* KH24	Swiss Albino male mice	Total fecal enterococcal, *Lactobacilli*, and coliform counts (log CFU/g fecal sample) were higher in mice fed with bacteriocin-producer strains than non-bacteriocin-producer strains.	Bhardwaj et al., 2010
Bacterial dose	*L. acidophilus* JCM1132 (bacteriocin-producer) and CCFM720 (non-bacteriocin-producer)	C57BL/6J male mice	JCM1132 strain (bacteriocin-producer) reduced the proinflammatory cytokine IL-6 in mice. CCFM720 strain (non-bacteriocin-producer) decreased concentration of anti-inflammatory factor IL-10. Both strains showed low immunogenicity. No significant immune response was recorded. CCFM720 favored the prevention of metabolic diseases. JCM1132 showed weak inflammatory response in comparison to CCFM720-treated mice.	Wang et al., 2020

Naturally synthetized bacteriocins by heterologous producers

Occasionally, the internal mechanisms of the native bacteriocin-producers to produce and excrete the bacteriocins are not enough. The objective to produce the bacteriocin in a heterologous expression system is to increase the bacteriocin production yield from native producers by facilitating the control of gene expression or increasing the production levels (Mesa-Pereira et al., 2018).

Lacticin 3147 is a two-peptide bacteriocin that is heterologous-produced in the recombinant strain *Lactococcus lactis* subsp. *cremoris* MG1363. This bacteriocin has been tested in an animal model, and the results have showed that it was able to reduce

in vivo infection with *S. aureus* Xen 29 in mice (Piper et al., 2012). A very well-known example of bacteriocins from Gram-negative bacteria are pyocins, which are believed to be produced in 90% of *P. aeruginosa* strains (Michel-Briand and Baysse, 2002). The heterologous-produced pyocins S2, S5, AP41, and L1 were used to study their protective function in an acute *P. aeruginosa* lung infection in C57/BL6 mice. Among all the pyocins, S5 was the best because no pathogenic bacteria were recovered from any of the S5 treated mice. The remaining pyocins were able to reduce the bacterial count in their respective treated mice (McCaughey et al., 2016b). Shortly after, from the heterologous-produced pyocins SD1, SD2, and SD3, pyocin SD2 exerted the best performance among the other pyocins when it was tested in previously challenged C57/BL6 mice with *P. aeruginosa* PAO1. Treated mice were able to survive, and no signs of illness were reported (McCaughey et al., 2016a). On the other hand, plantaricin E/F are two bacteriocins (plantaricin E and F) that have been heterologously produced in *L. lactis* NZ3900. The *in vivo* effects of both plantaricins were tested independently in a murine model infection. The favorable results obtained in antibacterial and toxicological tests suggest that plantaricin E or F are unharmful compounds that can be considered as a strong antibiotic candidate (Hanny et al., 2019).

Chemically synthetized bacteriocins

Chemically synthesized bacteriocins are bacteriocins that were previously reported on non-modified bacteriocin-producer strains, and their antimicrobial effect have been measured on *in vivo* assays, but they have been synthesized chemically; some examples are lysostaphin and epidermicin NI01. First, lysostaphin was formulated on a petroleum-based cream, and it was able to eradicate *S. aureus* strain MBT 5040 in cotton rats after one single application (Kokai-Kun et al., 2003). Second, the efficacy of epidermicin NI01, for eradicating the nasal burden of MRSA strain ATCC 43300 in a cotton rat model, was carried out. Results showed that a single dose of topical epidermicin NI01 was effective in eradication of MRSA from the nares of rats (Halliwell et al., 2017).

In vivo Assessment of Bioengineered Bacteriocins in Murine Models

Bioengineered bacteriocins are a group of bacteriocins whose characteristics have been modified to upgrade their properties. These modifications consist of the generation of novel bacteriocin variants that enhance the antimicrobial activity or expand the antibacterial spectrum and anti-biofilm efficacy or improve their physicochemical properties (Field et al., 2018). Some examples of this type of bacteriocins are described below.

In vivo activity of nisin A and nisin V against *Listeria monocytogenes* was evaluated in mice. Nisin V (a modified version of Nisin A) was more effective than Nisin A to controlling infection (Campion et al., 2013). *Mutacin* 1140 (MU1140) is a lantibiotic produced by *S. mutans*. A study to identify a lead compound for the treatment of *Clostridium difficile*-associated diarrhea was carried out. The variant OG253 emerged as the lead compound based on superior *in vivo* efficacy along with an apparent lack of relapse in a hamster model of infection (Kers et al., 2018b). *In vivo* testing of another MU1140-derived variant (OG716) conferred 100% survival and no relapse at 3 weeks post *C. difficile* infection (Kers et al., 2018a). Also, the effect of OG716 is determined using an *in vivo* hamster model of *C. difficile*-associated disease. Results demonstrated that OG716 was an excellent compound to treat *C. difficile* enteritis in hamsters (Kers et al., 2018a).

In vivo Assessment of Bacteriocin-Producer Directly in Murine Models

Bacteriocin-producers act similarly to probiotics because both can be consumed and exert a health benefit to the host. As long as they stay in the host, they may act as colonizing peptides, killing peptides, or serve as signaling peptides (signaling other bacteria or the immune system) (Dobson et al., 2012). It has been shown that bacteriocin production by bacteriocin-producers in the gut of the host can modulate the niche competition by preventing the intestinal colonization of MDR bacteria without disturbing the natural microbiota, therefore limiting the infection (Kommineni et al., 2015; Hegarty et al., 2016).

A study demonstrated that *Lactobacillus salivarius* UCC118 (a sequenced and genetically tractable probiotic strain of human origin) significantly protected mice against infection with the invasive foodborne pathogen *L. monocytogenes* (Corr et al., 2007). In other study, rats were administered daily with *Lactobacillus plantarum* 423 and *Enterococcus mundtii* ST4SA. Then, they were challenged by infection with *Salmonella enterica* serovar *Typhimurium*. Results showed that *L. plantarum* 423 was more effective than *E. mundtii* ST4SA (Dicks and ten Doeschate, 2010). Bhardwaj et al. (2010) performed the safety assessment and evaluation of probiotic potential of bacteriocinogenic *E. faecium* KH 24 strain using an *in vivo* model. Mice were challenged with *Salmonella enteritidis* MTCC 3291 and fed with *E. faecium* KH 24 strain. Results showed beneficial intestinal results (decreased counts of bacteria and coliform, and enhanced growth of lactobacilli) (Bhardwaj et al., 2010). The protective effects of *L. plantarum* B7 on diarrhea in mice induced by *Salmonella typhimurium* ATCC 13311 was evaluated. Results demonstrated that *L. plantarum* B7 could inhibit growth of *S. typhimurium*, decrease levels of proinflammatory cytokines, and attenuate symptoms of diarrhea induced in mice by *S. typhimurium* (Wongsen et al., 2019). Another study evaluated the effects of the bacteriocin-producing *Lactobacillus acidophilus* strain JCM1132 and its non-producing spontaneous mutant, *L. acidophilus* CCFM720, on the physiological statuses and gut microbiota of healthy mice. The results showed that both strains can have different effects on the host such as prevention of metabolic diseases and reduced inflammatory response (Wang et al., 2020).

In vivo Assessment of Bacteriocins in Alternative Models

The use of alternative models has gained great popularity among the scientific community since these models are simple, fast, and cheaper than current murine models (Apidianakis and Rahme, 2009; Jennings, 2011; OECD, 2013; Rajabi et al., 2015; Son et al., 2016; Herndon et al., 2017; Ignasiak and Maxwell, 2017; Jackson et al., 2017; Tseng et al., 2019). As we previously mentioned, some

of these alternative models include *D. melanogaster* (fruit fly), *Danio rerio* (zebrafish embryos), *C. elegans* (roundworm larvae), *Galleria mellonella* (greater wax moth larvae), and *Artemia salina* (brine shrimp larvae) (Freires et al., 2017). These alternative models allow evaluating bacteriocins and their potential effects on a living organism (such as antimicrobial activity, antibiofilm effect, immunogenic response, and toxicity) (Niu et al., 2014; Thomsen et al., 2016; Hunt, 2017; Cutuli et al., 2019; Yi et al., 2019). Also, murine models and alternative models do not share the same ethical considerations since the first ones have more restrictions when it comes to conducting experiments (Baertschi and Gyger, 2011; Desalermos et al., 2011; Jennings, 2011; Hamidi et al., 2014; Simonetti et al., 2016; Tsai et al., 2016; Ignasiak and Maxwell, 2017).

A compilation of bacteriocin studies with their *in vivo* antimicrobial activity (**Table 3**) and/or toxicity and biosafety (**Table 4**) activity using alternative models over the last 10 years is shown below. In this context, we included studies that have measured bacteriocin effects in alternative models using purified or partially purified bacteriocins (including naturally synthetized bacteriocins by native and heterologous producers and chemically synthesized bacteriocins) or CFS with bacteriocin-like substance or with a bacteriocin-producer directly in the host.

In vivo Assessment of Purified Bacteriocins in Alternative Models

Naturally synthetized bacteriocins by native producers

A fruit fly model (*D. melanogaster*) was used to evaluate the acute toxicity of antimicrobial peptide LR14. The results showed that the peptide had a dose-dependent toxicity property (Gupta et al., 2014). Another study used the same *in vivo* model to evaluate the efficacy of peptide NAI-107 as treatment in MRSA infections. The authors reported that this peptide was able to rescue adult flies from fatal infection with efficacy equivalent to that of reference antibiotic (vancomycin) (Thomsen et al., 2016). The antibacterial spectrum and cytotoxicity of a bacteriocin produced by *Lactobacillus lactis* strain in *A. salina* nauplii. The antibacterial activity of bacteriocin showed a broad range against foodborne pathogens. Also, the purified bacteriocin showed cytotoxicity in brine shrimps (Rajaram et al., 2010). Son et al. (2016) identified a novel bacteriocin produced by

TABLE 3 | *In vivo* antimicrobial assessment of bacteriocins using alternative models.

Bacteriocin	Producer	Target	Host (Linnaeus/ common name)	Antimicrobial activity	References
Naturally synthetized bacteriocins by native producers					
NAI-107	ND	*S. aureus* USA300 (MRSA)	*D. melanogaster* (fruit fly)	One dosage of NAI-107 (100 × MIC) rescued 50–60% of MRSA-infected adult flies after 96 h.	Thomsen et al., 2016
Lichenicin 146	*B. licheniformis* strain 146	*S. aureus* RF122	*C. elegans* (roundworm)	Survival rate of untreated infected nematodes was less than 10%, but treated nematodes had 74%.	Son et al., 2016
Naturally synthetized bacteriocins by heterologous producers					
Pyocin S2	*E. coli*	*P. aeruginosa* YHP14	*G. mellonella* (greater wax moth)	Untreated infected larvae died after 12–14 h. YHP14 level counts in subjects were 5×10^8 and 1×10^9 CFU at death time. Treated larvae had 100% survival rate after 72 h.	Smith et al., 2012
Peocin	*E. coli* BL21	*A. hydrophila*	*D. rerio* (zebrafish)	Survival rates of infected zebrafish embryos were 63.3 ± 7.63 and 71.67 ± 2.88% when 1 and 5 μg, respectively, were applied.	Tseng et al., 2019
Chemically synthetized bacteriocin					
Epidermicin NI01	Chemically synthetized	MRSA and MSSA ATCC 11195	*G. mellonella* (greater wax moth)	Epidermicin at 200 mg/kg effectively increased the survival of infected larvae after 2 h post infection with either MRSA or MSSA.	Gibreel and Upton, 2013
Bacteriocin-producers used directly					
Bacterial dose	*Bacillus* sp. LT3	*V. campbellii*	*A. franciscana* (brine shrimp)	Larvae pretreated with LT3 cultures at 10^7 cells/ml exerted a protective effect in larvae challenged with *V. campbellii*.	Niu et al., 2014
Bacterial dose	*L. fermentum* JDFM216	*S. aureus* and *E. coli* O157:H7	*C. elegans* (roundworm)	Previously colonized worms with bacteriocin-producer prolonged the lifespan of the nematodes infected against *S. aureus* and O157:H7. Uncolonized infected worms died after 10 days.	Park et al., 2018
AS-48	*E. faecalis* UGRA10	*L. garvieae*	*O. mykiss* (rainbow trout)	Trout challenged with *L. garvieae* and UGRA10 administered in diet 30 days before infection had a cumulative survival rate of 50% compared with 0% for control fish.	Baños et al., 2019
Bacterial dose	*P. pentosaceus* SL001	*A. hydrophila*	*C*tenopharyngodon *idella* (grass carp)	Cumulative mortality rates in untreated grass (only with *A. hydrophila*) was among 90%, but adapted grass was 51.7% (SL001 plus *A. hydrophila*).	Gong et al., 2019
Bacterial dose	*C. aquaticum*	*A. hydrophila* and *S. iniae*	*D. rerio* (zebrafish)	Fish previously fed with 10^6 CFU/g *C. aquaticum* had survival rates 49.9 ± 3.88% when infected with *A. hydrophila* or 53.3 ± 7.69% when infected with *S. iniae*. Unprotected fish and infected with *A. hydrophila* or *S. iniae* had survival rates among 28.8 ± 7.69 or 17.7 ± 3.85%, respectively	Yi et al., 2019

TABLE 4 | *In vivo* toxicity and biosafety assessment of bacteriocins using alternative models.

Bacteriocin	Producer	Host (Linnaeus/ common name)	Toxicity and biosafety	References
Naturally synthetized bacteriocins by native producers				
Unnamed bacteriocin	*L. lactis*	*A. salina* (brine shrimp)	LC_{50} value was 21.54 μg/ml. The immune response was not measured.	Rajaram et al., 2010
LR14	*L. plantarum* LR/14	*D. melanogaster* (fruit fly)	LC_{50} value was 10 mg/ml. 100% lethality was observed at 20 mg/ml. No significant mortality was reported at 1, 2, and 5 mg/ml.	Gupta et al., 2014
NAI-107 and nisin	ND	*D. melanogaster* (fruit fly)	Immunogenic response NAI-107 and nisin (both alone) were measured by quantifying expression of *drs*, *cecA1*, and *attB*. In general, NAI-107 (100 × MIC) has shown a significantly low immunogenic response than nisin (3 × MIC). Survival rate of NAI-107-treated (alone) flies was higher than nisin-treated (alone) flies. Thus, NAI-107-treated flies exerted lower toxicity.	Thomsen et al., 2016
AS-48	*E. faecalis* UGRA10	*D. rerio* (zebrafish)	Concentrations at 0.64 and 1.39 μM were unharmful for 24 to 48 h. No damage at 3 μM in the first 24 h, but 30% of embryos were dead after 48 h post-treatment. 100% lethality was observed at 6.4 and 14 μM after 24 to 48 h post-treatment.	Cebrián et al., 2019
Naturally synthetized bacteriocins by heterologous producers				
Pyocin S2	*E. coli*	*G. mellonella* (greater wax moth)	Uninfected pyocin-treated moth larvae (control) had a survival rate of 100% with pyocin at 27 mg/kg.	Smith et al., 2012
Peocin	*E. coli* BL21	*D. rerio* (zebrafish)	No toxicity was recorded when 5 μg of peocin was used. However, mortality increased when dosages were over 10 and 20 μg.	Tseng et al., 2019
Chemically synthetized bacteriocin				
Epidermicin NI01	Chemically synthetized	*G. mellonella* (greater wax moth)	Bacteriocin suspensions at 200 mg/kg were unharmful (neither dead nor injuries) to larvae. No significant differences were found in the hemocyte density (indicator larval immune system) between control and epidermicin-treated larvae.	Gibreel and Upton, 2013
Cell-free supernatant with bacteriocin-like substance				
Bacteriocin	*E. hirae*	*A. salina* (brine shrimp)	No toxicity was recorded with CFS/BLIS at 10 and 100 mg/ml.	Azab et al., 2016
Bacteriocin	*L. curvatus* P99	*D. melanogaster* (fruit fly)	Concentrations lower than or equal to 42,109.5 AU/ml were unharmful (survival rate 98.9%). Concentrations greater than 50,000 AU/ml were lethal (survival rate less than 50%)	Funck et al., 2019
Bacteriocin-producers used directly				
Bacterial dose	*Bacillus* sp. LT3	*A. franciscana* (brine shrimp)	Innate immune response genes for melanization and coagulation (*proPO* and *tgase*) were not stimulated by the presence of LT3 strain (alone)	Niu et al., 2014
Bacterial dose	*L. fermentum* JDFM216	*C. elegans* (roundworm)	Bacteriocin-producer enhances the expression of *pmk-1* pathway in *C. elegans* and, thus, stimulates the immune response and longevity of *C. elegans.*	Park et al., 2018
AS-48	*E. faecalis* UGRA10	*O. mykiss* (rainbow trout)	UGRA10 was administrated in tanks filled with the fish and water for 15 days. No deaths or visible signs and injuries were seen. No cytotoxicity was observed in R1 cell line and trout.	Baños et al., 2019
Bacterial dose	*P. pentosaceus* SL001	*C. idella* (grass carp)	No mortality neither adverse effects were reported at high population concentrations in fish diet	Gong et al., 2019
Bacterial dose	*C. aquaticum*	*D. rerio* (zebrafish)	Zebrafish injected with the bacteriocin-producer increased in the expression of carbohydrate metabolism-related genes in the liver and innate immune-related genes were induced.	Yi et al., 2019

Bacillus licheniformis strain 146 (lichenicin 146) with a high *in vivo* antimicrobial activity in liquid *C. elegans–S. aureus* assay (Son et al., 2016).

AS-48 is a bacteriocin produced by *Enterococcus* strains. The toxicity of this bacteriocin has been evaluated in *in vivo* models. In zebrafish embryos, the AS-48 was highly toxic; however, in a murine model, no toxicity was observed (Cebrián et al., 2019).

Naturally synthetized bacteriocins by heterologous producers

A nonvertebrate host, the *G. mellonella* caterpillar, was used to evaluate the activity of pyocin S2 against *P. aeruginosa* YHP14 biofilms. Results showed a potent antibiofilm activity *in vivo*, representing a potential therapeutic option (Smith et al., 2012). The antimicrobial activity of peocin, a bacteriocin produced by the probiotic *Paenibacillus ehimensis* NPUST1, was demonstrated in aquatic, food spoilage, clinical, and antibiotic-resistant pathogens. For example, a significant increase in survival rates was observed in peocin-treated zebrafish after *Aeromonas hydrophila* challenge (Tseng et al., 2019).

Chemically synthetized bacteriocin

A study reported that epidermicin NI01 had a protective effect of *G. mellonella* larvae from infection with clinically isolated MRSA. The authors reported that epidermicin NI01 did not induce toxicity and did not trigger the larvae immune system (Gibreel and Upton, 2013).

In vivo assessment of CFS with bacteriocin-like substance in alternative models

The *in vivo* assessment of bacteriocins in alternative models has been evaluated using a CFS that contains a bacteriocin like-substance (BLIS). For example, *A. salina* brine shrimp showed no toxicity of CFS with BLIS from *Enterococcus hirae* (Azab et al., 2016). Recently, CFS from *Lactobacillus curvatus* P99 cultures showed no toxic effect in *D. melanogaster* flies (Funck et al., 2019).

In vivo Assessment of Bacteriocin-Producer Directly in Alternative Models

The evaluation of the probiotic effect of *Bacillus* sp. LT3 was performed in brine shrimp *Artemia franciscana* larvae challenged with *Vibrio campbellii* LMG 21363. *Bacillus* sp. LT3 was able to colonize the brine shrimp gastrointestinal tract and therefore increased their survival (Niu et al., 2014). A *C. elegans* model was used to evaluate the functionality of *Lactobacillus fermentum* strain JDFM216 (a novel probiotic bacterium). Interestingly, the probiotic bacterium was found to be toxic to the *C. elegans* host. Therefore, it has beneficial effects on longevity and immunity of *C. elegans* (Park et al., 2018). The effect of *Pediococcus pentosaceus* strain (SL001) in growth-related and immune-related genes was evaluated in grass carps. Results showed that the strain was able to enhance immunity and promoter growth of grass carps (Gong et al., 2019). A recent study evaluated the effect of probiotic *Chromobacterium aquaticum* on zebrafish model. Fish was challenged with *A. hydrophila* and *Streptococcus iniae* and then treated with probiotic. The probiotic-treated fish had a higher survival rate than the non-treated fish (Yi et al., 2019). Finally, the effect of *E. faecalis* UGRA10 and its bacteriocin AS-48 (multiple baths and single dose) was tested against *Lactococcus garvieae* in an *Oncorhynchus mykiss* rainbow trout fish model. Neither the strain nor its bacteriocin showed toxic effects, displaying a protective effect against *L. garvieae* infection (Baños et al., 2019).

The *in vivo* assessment models are important to evaluate bacteriocins. This review included various bacteriocins that were assessed by different *in vivo* models. The animal model must be

TABLE 5 | Animal models as a tool to bacteriocins analysis: strengths and limitations.

Animal model	Strengths	Limitations	References
Mice	Physiology and genetics similarities to humans. Mouse genome is very similar to human. Therefore, it is a powerful tool for modeling specific genetic diseases. Extremely useful for studying complex biological systems (e.g., immune, endocrine nervous, cardiovascular, and skeletal systems). Useful for toxicity and safety assessments of new compounds. Cost-effective model because they are small, inexpensive, and easy to maintenance.	Legal and ethical considerations. Relatively large numbers of animals are needs for research. Mice models of human disease should not be utilized to supplant testing in conventional animal models.	Bryda, 2013; Morgan et al., 2013; Perlman, 2016; Andersen and Winter, 2019
Drosophila melanogaster (fruit fly)	Ideal for the study of genetics and development. Used to test the toxicity of chemical. 75% of the genes that cause disease in humans are also found in the fruit fly. It is relatively straightforward to mutate (disrupt or alter). Low cost to maintain in the laboratory. No ethical considerations.	Important vertebrate-specific pathogenetic factors may be ignored. Lack of an adaptive immune system and dramatically different drug effects when compared to human studies.	Jeibmann and Paulus, 2009; Pandey and Nichols, 2011; Rand et al., 2014; Mirzoyan et al., 2019
Caenorhabditis elegans (roundworm larvae)	Most widely used and versatile model for biological and genomic research. Used in longevity and senescence studies. Ideal for neural networks and behavior studies. Simple anatomy, optical transparency, short lifespan. Easy to work with; minimal nutritional and growth requirements.	Fewer gene homologs in mammals. Worm has two sexes (male and hermaphrodites). Down-regulation or desensitization of target genes or proteins.	Teschendorf and Link, 2009; Tissenbaum, 2015; Meneely et al., 2019
Danio rerio (zebrafish embryos)	70% of human genes have at least one obvious zebrafish ortholog. Used successfully to study human disease-related genes. Ideal model organism for studying early development. Drug safety testing and ecotoxicological screening. Its small size, accessibility, and transparency allow the analysis of thousands of live animals at single-cell resolution. This system is cheap and fast to develop, and it can be used by small laboratories.	Legal and ethical considerations (some countries). They require water system to maintain them. They are not as closely related to humans as mouse is (e.g., anatomy and physiology). Genes with similar sequences often have overlapping or partially redundant functions, resulting in no or subtle defects on disruption of a single gene.	Ali et al., 2011; Howe et al., 2013; Schier, 2013; Sloman et al., 2019
Galleria mellonella (greater wax moth larvae)	Used to study pathogenesis, virulence mechanisms, and immune response. Important tool for the preliminary screening of antimicrobial compounds. Rapid and reliable evaluation of the activity and toxicity of novel antimicrobial drugs. Larvae can survive at mammalian physiological temperature (37°C). Good correlation between toxicity in Galleria and that in rodents.	Lack of standardized procedures to use as a non-mammalian infection model. Toxicity experimental data (LD50) do not necessarily correlate to human values.	Ignasiak and Maxwell, 2017; Cutuli et al., 2019
Artemia salina (brine shrimp larvae)	It is a preliminary toxicity screen. Used in applied toxicology and ecotoxicity studies (high throughput cytotoxicity test of bioactive chemicals). Rapid hatching and easy accessibility of nauplii in a cost-efficient way. Easy handling under laboratory conditions.	Lack of standardized experimental conditions (temperature, salinity, aeration, light, and pH). Use the same age of *larvae* at the start of every test.	Nunes et al., 2006; Hamidi et al., 2014; Wu, 2014; Yu and Lu, 2018

chosen according on the expect effects for the bacteriocins. Below is summarized (**Table 5**) some advantages and disadvantages of murine, fruit flies, zebrafish, roundworm, greater wax moth, and brine shrimp for drug discovery trials. We included the limitations and strengths of each model as well as their scope of interest, time to reach the optimal developmental stage according to model, frequency of use in drug discovery studies, infrastructural and cost requirements for rearing, special qualifications, and ethical considerations, among others, which seem to be expected for the evaluation of new bacteriocins depending on the used model.

FUTURE TRENDS IN BACTERIOCIN DEVELOPMENT AND DESIGN

Bacteriocins represent a potential drug alternative for replacing current antibiotics to treat diseases caused by resistant bacteria. According to the body of knowledge that has been developed in the field, in general, bacteriocins can retain their *in vivo* antimicrobial properties in a challenged host, while at the same time, they showed a null or reduced toxic effect. According to 2019 WHO's Antibacterial Agent in Preclinical Development Book, 27 of 252 antimicrobial agents in preclinical revision status are considered as antimicrobial peptides. From the total antimicrobial peptides, 12 peptides are on lead optimization (LO) phase, 12 peptides are in Preclinical Candidate (PCC) phase and, three peptides are on CTA/IND-enabling studies (World Health Organization, 2019b). In an independent study, Theuretzbacher et al. (2020) identified the current global antibacterial pipeline and found that 135 of 407 preclinical projects from 314 private and public institutions were related to producing synthetic and natural antimicrobial peptides, natural products, and LpxC inhibitors, and most of these molecules are targeting Gram-negative bacteria. Therefore, bacteriocins may have a window of opportunity to face the drug-resistant bacteria crisis since the WHO is demanding research and development of new drugs to target the most wanted drug-resistant pathogens, many of them Gram-negative bacteria (World Health Organization, 2017).

Although it is a fact that the current literature for bacteriocins produced from Gram-negative bacteria is dominated by bacteriocins toward Gram-positive bacteria (Jamali et al., 2019), there is an acceptable amount of bacteriocins reported to have a strong activity against Gram-negative bacteria, including the pathogenic strains. For example, the S-type pyocin group from the *P. aeruginosa* (Ghequire and De Mot, 2014) or the microcin and colicin groups that are vastly reported for *E. coli*, and other examples in less quantity but not less relevant, are bacteriocins produced by *K. pneumoniae, Citrobacter freundii*, *Shigella boydii*, and *Serratia marcescens* (Yang et al., 2014).

The future of bacteriocins lies not only in their discovery but also in their testing for toxicity to prove their safe use in a preclinical phase as candidates for therapeutic processes. An increasing approach that can be exploited for bacteriocins is the use of alternative models to the murine model to evaluate their *in vivo* antimicrobial and/or toxicity effects. According to Freires et al. (2017), there is an increase in drug studies using alternative organisms to murine, since there was a rise of 909% in drug discovery from 1990 to 2015.

Finally, we have stated that bioengineering is an important tool along with the current technologies to discover new bacteriocins, since they can improve their antimicrobial activity or change their physicochemical properties. Moreover, new strategies are being introduced in the design of bacteriocins. Fields et al. (2020a) were the first to design the very first fully *de novo* bacteriocin by using a machine-learning approach. Fields et al. (2020b) also constructed a library of the linear peptides from the membrane-interacting region of circular bacteriocin with pore-formation dynamics by selective aminoacidic substitution. On the other hand, Acuña et al. (2012) were the first to design chimeric bacteriocins that retained the properties to kill both Gram-positive and Gram-negative bacteria. Moreover, other authors have preferred to repurpose the bacteriocins by exploiting their capability against tumor cells (Varas et al., 2020) or by exploring synergistic effects of bacteriocins while combining with renowned antibiotics (Mathur et al., 2017) or with other bacteriocins (Hanchi et al., 2017).

CONCLUSION

Bacteriocins are strong candidates to be used as future therapeutic agents. Recent studies have shown the antibacterial activity of bacteriocins using *in vitro* models. Nonetheless, the next step in the development of a new bacteriocin-based therapeutic agents involves the use of animal models. The antimicrobial and/or toxic effects of the bacteriocins have been studied in murine models and the most recent alternative animal models such as fruit flies, zebrafish embryos, roundworm, greater wax moth, or the brine shrimp. These results have demonstrated that bacteriocins can exert a variety of positive responses in the host such as modification of the immunogenic response, alteration of the inflammatory response, and the reduction of biochemical and histopathological parameters related with infection. However, approximately half of the bacteriocins tested in mice (47.4%) performed antimicrobial assay, but no toxicity assays were described. On the other hand, 20% of the studies carried out in alternative models evaluated antimicrobial activity, but no toxicity was reported. These data reveal the lack of toxicity and biosafety studies of bacteriocin *in vivo* models, which are crucial to advance into clinical trials. Therefore, it is imperative to use *in vivo* models to assess the therapeutic efficacy of bacteriocins as well as their toxic effects; both successful results will lead toward clinical research phases and the development of bacteriocin-based therapeutics to treat infections caused by antimicrobial-resistant Gram-positive and Gram-negative bacteria.

AUTHOR CONTRIBUTIONS

DB-C, AL-B, and JM-R: conceptualization. DB-C, AL-B, JL-E, and JM-R: writing—original draft preparation and writing—review and editing. AL-B and JM-R: supervision. All authors contributed to the article and approved the submitted version.

FUNDING

We would like to acknowledge Paicyt 2019–2020 and 2020–2021, Science Grants from the Universidad Autónoma de Nuevo León, and CONACyT Grants for the following: Basic science Grant 221332, Fronteras de la Ciencia Grant 1502, and Infraestructura Grant 279957. DB-C and JL-E acknowledge the support from Beca Nacional de Posgrado from CONACyT, and AL-B acknowledges the support from Beca de Posdoctorado Nacional.

REFERENCES

Abanoz, H. S., and Kunduhoglu, B. (2018). Antimicrobial activity of a bacteriocin produced by *Enterococcus faecalis* KT11 against some pathogens and antibiotic-resistant bacteria. *Korean J. Food Sci. Anim. Resour.* 38, 1064–1079. doi: 10.5851/kosfa.2018.e40

Acuña, L., Picariello, G., Sesma, F., Morero, R. D., and Bellomio, A. (2012). A new hybrid bacteriocin, Ent35-MccV, displays antimicrobial activity against pathogenic gram-positive and gram-negative bacteria. *FEBS Open Biol.* 2, 12–19. doi: 10.1016/j.fob.2012.01.002

Aguilar-Pérez, C., Gracia, B., Rodrigues, L., Vitoria, A., Cebrián, R., Deboosère, N., et al. (2018). Synergy between circular bacteriocin AS-48 and ethambutol against *Mycobacterium tuberculosis*. *Antimicrob. Agents Chemother.* 62:e0359-18. doi: 10.1128/AAC.00359-18

Al Atya, A. K., Belguesmia, Y., Chataigne, G., Ravallec, R., Vachée, A., Szunerits, S., et al. (2016). Anti-MRSA activities of enterocins DD28 and DD93 and evidences on their role in the inhibition of biofilm formation. *Front. Microbiol.* 7:817. doi: 10.3389/fmicb.2016.00817

Ali, S., Champagne, D. L., Spaink, H. P., and Richardson, M. K. (2011). Zebrafish embryos and larvae: a new generation of disease models and drug screens. *Birth. Defect. Res. Part C Embryo Today Rev.* 93, 115–133. doi: 10.1002/bdrc.20206

Amabile-Cuevas, C. F. (2010). Antibiotic resistance in Mexico: a brief overview of the current status and its causes. *J. Infect. Dev. Ctries.* 4, 126–131. doi: 10.3855/jidc.427

Andersen, M. L., and Winter, L. M. F. (2019). Animal models in biological and biomedical research - experimental and ethical concerns. *An. Acad. Bras. Cienc.* 91:e20170238. doi: 10.1590/0001-3765201720170238

Ansari, A., Zohra, R. R., Tarar, O. M., Qader, S. A. U., and Aman, A. (2018). Screening, purification and characterization of thermostable, protease resistant Bacteriocin active against methicillin resistant *Staphylococcus aureus* (MRSA). *BMC Microbiol.* 18:192. doi: 10.1186/s12866-018-1337-y

Apidianakis, Y., and Rahme, L. G. (2009). *Drosophila melanogaster* as a model host for studying *Pseudomonas aeruginosa* infection. *Nat. Protoc.* 4, 1285–1294. doi: 10.1038/nprot.2009.124

Arnett, E., and Seveau, S. (2011). The multifaceted activities of mammalian defensins. *Curr. Pharm. Des.* 17, 4254–4269. doi: 10.2174/138161211798999348

Arthur, T. D., Cavera, V. L., and Chikindas, M. L. (2014). On bacteriocin delivery systems and potential applications. *Future Microbiol.* 9, 235–248. doi: 10.2217/fmb.13.148

Azab, E. A., Elsilk, S. E., Abd El-Salam, I. S., and Tahwash, A. M. (2016). Determination of the Bacteriocin-like substances produced by *Enterococcus hirae* isolated from traditional Egyptian food (Koskos). *Biosci. Biotechnol. Res. Asia* 13, 803–813. doi: 10.13005/bbra/2100

Badyal, D. K., and Desai, C. (2014). Animal use in pharmacology education and research: the changing scenario. *Indian J. Pharmacol.* 46, 257–265. doi: 10.4103/0253-7613.132153

Baertschi, B., and Gyger, M. (2011). Ethical considerations in mouse experiments. *Curr. Protoc. Mouse Biol.* 1, 155–167. doi: 10.1002/9780470942390.mo100161

Bagci, U., Ozmen Togay, S., Temiz, A., and Ay, M. (2019). Probiotic characteristics of bacteriocin-producing *Enterococcus faecium* strains isolated from human milk and colostrum. *Folia Microbiol.* 64, 735–750. doi: 10.1007/s12223-019-00687-2

Baindara, P., Chaudhry, V., Mittal, G., Liao, L. M., Matos, C. O., Khatri, N., et al. (2016). Characterization of the antimicrobial peptide penisin, a class Ia novel lantibiotic from *Paenibacillus* sp, Strain A3. *Antimicrob. Agents Chemother.* 60, 580–591. doi: 10.1128/AAC.01813-15

Baindara, P., Kapoor, A., Korpole, S., and Grover, V. (2017). Cysteine-rich low molecular weight antimicrobial peptides from *Brevibacillus* and related genera for biotechnological applications. *World J. Microbiol. Biotechnol.* 33:124. doi: 10.1007/s11274-017-2291-9

Baños, A., Ariza, J. J., Nuñez, C., Gil-Martínez, L., García-López, J. D., Martínez-Bueno, M., et al. (2019). Effects of *Enterococcus faecalis* UGRA10 and the enterocin AS-48 against the fish pathogen *Lactococcus garvieae*, Studies in vitro and in vivo. *Food Microbiol.* 77, 69–77. doi: 10.1016/j.fm.2018.08.002

Bhardwaj, A., Gupta, H., Kapila, S., Kaur, G., Vij, S., and Malik, R. K. (2010). Safety assessment and evaluation of probiotic potential of bacteriocinogenic *Enterococcus faecium* KH 24 strain under *in vitro* and *in vivo* conditions. *Int. J. Food Microbiol.* 141, 156–164. doi: 10.1016/j.ijfoodmicro.2010.05.001

Blay, G., Le Lacroix, C., Zihler, A., and Fliss, I. (2007). *In vitro* inhibition activity of nisin A, nisin Z, pediocin PA-1 and antibiotics against common intestinal bacteria. *Lett. Appl. Microbiol.* 45, 252–257. doi: 10.1111/j.1472-765X.2007.02178.x

Bonhi, K. L. R., and Imran, S. (2019). Role of bacteriocin in tackling the global problem of multi-drug resistance: an updated review. *Biosci. Biotechnol. Res. Commun.* 12, 601–608. doi: 10.21786/bbrc/12.3/8

Bryda, E. C. (2013). The mighty mouse: the impact of rodents on advances in biomedical research. *Mo. Med.* 110, 207–211.

Campion, A., Casey, P. G., Field, D., Cotter, P. D., Hill, C., and Ross, R. P. (2013). *In vivo* activity of Nisin A and Nisin V against *Listeria monocytogenes* in mice. *BMC Microbiol.* 13:23. doi: 10.1186/1471-2180-13-23

Cassini, A., Högberg, L. D., Plachouras, D., Quattrocchi, A., Hoxha, A., Simonsen, G. S., et al. (2019). Attributable deaths and disability-adjusted life-years caused by infections with antibiotic-resistant bacteria in the EU and the European economic Area in 2015: a population-level modelling analysis. *Lancet Infect. Dis.* 19, 56–66. doi: 10.1016/S1473-3099(18)30605-4

Cavera, V. L., Arthur, T. D., Kashtanov, D., and Chikindas, M. L. (2015). Bacteriocins and their position in the next wave of conventional antibiotics. *Int. J. Antimicrob. Agents* 46, 494–501. doi: 10.1016/j.ijantimicag.2015.07.011

Cebrián, R., Rodríguez-Cabezas, M. E., Martín-Escolano, R., Rubiño, S., Garrido-Barros, M., Montalbán-López, M., et al. (2019). Preclinical studies of toxicity and safety of the AS-48 bacteriocin. *J. Adv. Res.* 20, 129–139. doi: 10.1016/j.jare.2019.06.003

Chen, C. C., Lai, C. C., Huang, H. L., Huang, W. Y., Toh, H. S., Weng, T. C., et al. (2019). Antimicrobial activity of *Lactobacillus* species against carbapenem-resistant *Enterobacteriaceae*. *Front. Microbiol.* 10:789. doi: 10.3389/fmicb.2019.00789

Chikindas, M. L., Weeks, R., Drider, D., Chistyakov, V. A., and Dicks, L. M. (2018). Functions and emerging applications of bacteriocins. *Curr. Opin. Biotechnol.* 49, 23–28. doi: 10.1016/j.copbio.2017.07.011

Corr, S. C., Li, Y., Riedel, C. U., O'Toole, P. W., Hill, C., and Gahan, C. G. M. (2007). Bacteriocin production as a mechanism for the antiinfective activity of *Lactobacillus salivarius* UCC118. *Proc. Natl. Acad. Sci. U.S.A.* 104, 7617–7621. doi: 10.1073/pnas.0700440104

Cotter, P. D., Ross, R. P., and Hill, C. (2013). Bacteriocins — a viable alternative to antibiotics? *Nat. Rev. Microbiol.* 11, 95–105. doi: 10.1038/nrmicro2937

Creton, S., Dewhurst, I. C., Earl, L. K., Gehen, S. C., Guest, R. L., Hotchkiss, J. A., et al. (2010). Acute toxicity testing of chemicals—Opportunities to avoid redundant testing and use alternative approaches. *Crit. Rev. Toxicol.* 40, 50–83. doi: 10.3109/10408440903401511

Cui, Y., Zhang, C., Wang, Y., Shi, J., Zhang, L., Ding, Z., et al. (2012). Class IIa bacteriocins: diversity and new developments. *Int. J. Mol. Sci.* 13, 16668–16707. doi: 10.3390/ijms131216668

Cutuli, M. A., Petronio Petronio, G., Vergalito, F., Magnifico, I., Pietrangelo, L., Venditti, N., et al. (2019). *Galleria mellonella* as a consolidated *in vivo* model hosts: new developments in antibacterial strategies and novel drug testing. *Virulence* 10, 527–541. doi: 10.1080/21505594.2019.1621649

Denayer, T., Stöhrn, T., and Van Roy, M. (2014). Animal models in translational medicine: validation and prediction. *New Horizons Transl. Med.* 2, 5–11. doi: 10.1016/j.nhtm.2014.08.001

Denkovskienė, E., Paškevičius, Š, Misiūnas, A., Stočkūnaitė, B., Starkevič, U., Vitkauskienė, A., et al. (2019). Broad and efficient control of *Klebsiella* pathogens by peptidoglycan-degrading and pore-forming Bacteriocins klebicins. *Sci. Rep.* 9:15422. doi: 10.1038/s41598-019-51969-1

Desalermos, A., Muhammed, M., Glavis-Bloom, J., and Mylonakis, E. (2011). Using *Caenorhabditis elegans* for antimicrobial drug discovery. *Expert Opin. Drug Discov.* 6, 645–652. doi: 10.1517/17460441.2011.573781

Dicks, L. M. T., and ten Doeschate, K. (2010). *Enterococcus mundtii* ST4SA and *Lactobacillus plantarum* 423 alleviated symptoms of *Salmonella* infection, as determined in wistar rats challenged with *Salmonella enterica* serovar *Typhimurium*. Curr. Microbiol. 61, 184–189. doi: 10.1007/s00284-010-9594-5

Dobson, A., Cotter, P. D., Ross, R. P., and Hill, C. (2012). Bacteriocin production: a probiotic trait? *Appl. Environ. Microbiol.* 78, 1–6. doi: 10.1128/AEM.05576-11

European Centre for Disease Prevention and Control (2009). *ECDC/EMEA Joint Technical Report: The Bacterial Challenge: Time to React. ECDC/EMEA*. Available online at: https://www.ecdc.europa.eu/en/publications-data/ecdcemea-joint-technical-report-bacterial-challenge-time-react (accessed October 8, 2020).

Fahim, H. A., Khairalla, A. S., and El-Gendy, A. O. (2016). Nanotechnology: a valuable strategy to improve bacteriocin formulations. *Front. Microbiol.* 7:1385. doi: 10.3389/fmicb.2016.01385

Fair, R. J., and Tor, Y. (2014). Antibiotics and bacterial resistance in the 21st century. *Perspect. Medicin. Chem.* 6, 25–64. doi: 10.4137/PMC.S14459

Farokhzad, O. C., and Langer, R. (2009). Impact of nanotechnology on drug delivery. *ACS Nano* 3, 16–20. doi: 10.1021/nn900002m

Field, D., Hill, C., Cotter, P. D., and Ross, R. P. (2010). The dawning of a "Golden era" in lantibiotic bioengineering. *Mol. Microbiol.* 78, 1077–1087. doi: 10.1111/j.1365-2958.2010.07406.x

Field, D., Ross, R. P., and Hill, C. (2018). Developing bacteriocins of lactic acid bacteria into next generation biopreservatives. *Curr. Opin. Food Sci.* 20, 1–6. doi: 10.1016/j.cofs.2018.02.004

Fields, F. R., Freed, S. D., Carothers, K. E., Hamid, M. N., Hammers, D. E., Ross, J. N., et al. (2020a). Novel antimicrobial peptide discovery using machine learning and biophysical selection of minimal bacteriocin domains. *Drug Dev. Res.* 81, 43–51. doi: 10.1002/ddr.21601

Fields, F. R., Manzo, G., Hind, C., Janardhanan, J., Foik, I. P., Do Carmo Silva, P., et al. (2020b). Synthetic antimicrobial peptide tuning permits membrane disruption and interpeptide synergy. *ACS Pharmacol. Transl. Sci.* 3, 418–424. doi: 10.1021/acsptsci.0c00001

Freires, I. A., Sardi, J., de, C. O., de Castro, R. D., and Rosalen, P. L. (2017). Alternative Animal and non-animal models for drug discovery and development: bonus or burden? *Pharm. Res.* 34, 681–686. doi: 10.1007/s11095-016-2069-z

Frieden, T. (2013). *Antibiotic resistance threats in the United States, 2013. Centers Dis. Control Prev. CS239559-B*. Available online at: https://www.cdc.gov/drugresistance/pdf/ar-threats-2013-508.pdf (accessed March 22, 2021).

Fuchs, S. W., Jaskolla, T. W., Bochmann, S., Kötter, P., Wichelhaus, T., Karas, M., et al. (2011). Entianin, a novel subtilin-like lantibiotic from *Bacillus subtilis* subsp. *spizizenii* DSM 15029^{T} with high antimicrobial activity. *Appl. Environ. Microbiol.* 77, 1698–1707. doi: 10.1128/AEM.01962-10

Funck, G. D., de Lima Marques, J., da Silva Dannenberg, G., dos Santos Cruxen, C. E., Sehn, C. P., Prigol, L., et al. (2019). Characterization, toxicity, and optimization for the growth and production of bacteriocin-like substances by *Lactobacillus curvatus*. *Probiotics Antimicrob. Proteins*. 12, 91–101. doi: 10.1007/s12602-019-09531-y

Gabrielsen, C., Brede, D. A., Nes, I. F., and Diep, D. B. (2014). Circular bacteriocins: biosynthesis and mode of action. *Appl. Environ. Microbiol.* 80, 6854–6862. doi: 10.1128/AEM.02284-14

Garza-González, E., Morfín-Otero, R., Mendoza-Olazarán, S., Bocanegra-Ibarias, P., Flores-Treviño, S., Rodríguez-Noriega, O., et al. (2019). A snapshot of antimicrobial resistance in Mexico. Results from 47 centers from 20 states during a six-month period. *PLoS One* 14:e0209865. doi: 10.1371/journal.pone.0209865

Ghequire, M. G. K., and De Mot, R. (2014). Ribosomally encoded antibacterial proteins and peptides from *Pseudomonas*. *FEMS Microbiol. Rev.* 38, 523–568. doi: 10.1111/1574-6976.12079

Gibreel, T. M., and Upton, M. (2013). Synthetic epidermicin NI01 can protect *Galleria mellonella* larvae from infection with *Staphylococcus aureus*. *J. Antimicrob. Chemother.* 68, 2269–2273. doi: 10.1093/jac/dkt195

Gong, L., He, H., Li, D., Cao, L., Khan, T. A., Li, Y., et al. (2019). A new isolate of *Pediococcus pentosaceus* (SL001) with antibacterial activity against fish pathogens and potency in facilitating the immunity and growth performance of grass carps. *Front. Microbiol.* 10:1384. doi: 10.3389/fmicb.2019.01384

Gupta, R., Sarkar, S., and Srivastava, S. (2014). In vivo toxicity assessment of antimicrobial peptides (AMPs LR14) Derived from *Lactobacillus plantarum* Strain LR/14 in *Drosophila melanogaster*. *Probiotics Antimicrob. Proteins* 6, 59–67. doi: 10.1007/s12602-013-9154-y

Gupta, V., and Datta, P. (2019). Next-generation strategy for treating drug resistant bacteria: antibiotic hybrids. *Indian J. Med. Res.* 149, 97–106. doi: 10.4103/ijmr.IJMR_755_18

Halliwell, S., Warn, P., Sattar, A., Derrick, J. P., and Upton, M. (2017). A single dose of epidermicin NI01 is sufficient to eradicate MRSA from the nares of cotton rats. *J. Antimicrob. Chemother.* 72, 778–781. doi: 10.1093/jac/dkw457

Hamidi, İR., Jovanova, B., and Panovska, K. (2014). Toxicîlogical evaluation of the plant products using Brine Shrimp (*Artemia salina* L.) model. *Maced. Pharm. Bull.* 60, 9–18.

Hanchi, H., Hammami, R., Gingras, H., Kourda, R., Bergeron, M. G., Ben Hamida, J., et al. (2017). Inhibition of MRSA and of *Clostridium difficile* by durancin 61A: synergy with bacteriocins and antibiotics. *Future Microbiol.* 12, 205–212. doi: 10.2217/fmb-2016-0113

Hanny, E. L. L., Mustopa, A. Z., Budiarti, S., Darusman, H. S., Ningrum, R. A., and Fatimah (2019). Efficacy, toxicity study and antioxidant properties of plantaricin E and F recombinants against enteropathogenic *Escherichia coli* K1.1 (EPEC K1.1). *Mol. Biol. Rep.* 46, 6501–6512. doi: 10.1007/s11033-019-05096-9

Hegarty, J. W., Guinane, C. M., Ross, R. P., Hill, C., and Cotter, P. D. (2016). Bacteriocin production: a relatively unharnessed probiotic trait? *F1000Research* 5:2587. doi: 10.12688/f1000research.9615.1

Herndon, L. A., Wolkow, C. A., Driscoll, M., and Hall, D. H. (2017). Effects of ageing on the basic biology and anatomy of *C. elegans*. *Healthy Age. Longev.* 5, 9–39. doi: 10.1007/978-3-319-44703-2_2

Howe, K., Clark, M. D., Torroja, C. F., Torrance, J., Berthelot, C., Muffato, M., et al. (2013). The zebrafish reference genome sequence and its relationship to the human genome. *Nature* 496, 498–503. doi: 10.1038/nature12111

Hunt, P. R. (2017). The *C. elegans* model in toxicity testing. *J. Appl. Toxicol.* 37, 50–59. doi: 10.1002/jat.3357

Ignasiak, K., and Maxwell, A. (2017). *Galleria mellonella* (greater wax moth) larvae as a model for antibiotic susceptibility testing and acute toxicity trials. *BMC Res. Notes* 10:428. doi: 10.1186/s13104-017-2757-8

Iseppi, R., Messi, P., Camellini, S., and Sabia, C. (2019). Bacteriocin activity of *Lactobacillus brevis* and *Lactobacillus paracasei* ssp. *paracasei*. *J. Med. Microbiol.* 68, 1359–1366. doi: 10.1099/jmm.0.001045

Ishibashi, N., Himeno, K., Masuda, Y., Perez, R. H., Iwatani, S., Zendo, T., et al. (2014). Gene cluster responsible for secretion of and immunity to multiple bacteriocins, the NKR-5-3 enterocins. *Appl. Environ. Microbiol.* 80, 6647–6655. doi: 10.1128/AEM.02312-14

Jackson, S. J., Andrews, N., Ball, D., Bellantuono, I., Gray, J., Hachoumi, L., et al. (2017). Does age matter? The impact of rodent age on study outcomes. *Lab. Anim.* 51, 160–169. doi: 10.1177/0023677216653984

Jamali, H., Krylova, K., and Dozois, C. M. (2019). The 100 Top-cited scientific papers focused on the topic of bacteriocins. *Int. J. Pept. Res. Ther.* 25, 933–939. doi: 10.1007/s10989-018-9741-6

Jeibmann, A., and Paulus, W. (2009). *Drosophila melanogaster* as a model organism of brain diseases. *Int. J. Mol. Sci.* 10, 407–440. doi: 10.3390/ijms10020407

Jennings, B. H. (2011). *Drosophila* -a versatile model in biology & medicine. *Mater. Today*. 14, 190–195. doi: 10.1016/S1369-7021(11)70113-4

Jiang, H., Zou, J., Cheng, H., Fang, J., and Huang, G. (2017). Purification, characterization, and mode of action of Pentocin JL-1, a novel bacteriocin isolated from *Lactobacillus pentosus*, against drug-resistant *Staphylococcus aureus*. *Biomed Res. Int.* 2017:7657190. doi: 10.1155/2017/7657190

Kaneko, N., Kurata, M., Yamamoto, T., Morikawa, S., and Masumoto, J. (2019). The role of interleukin-1 in general pathology. *Inflamm. Regen.* 39:12. doi: 10.1186/s41232-019-0101-5

Kers, J. A., DeFusco, A. W., Park, J. H., Xu, J., Pulse, M. E., Weiss, W. J., et al. (2018a). OG716: designing a fit-for-purpose lantibiotic for the treatment of *Clostridium difficile* infections. *PLoS One* 13:e0197467. doi: 10.1371/journal.pone.0197467

Kers, J. A., Sharp, R. E., Defusco, A. W., Park, J. H., Xu, J., Pulse, M. E., et al. (2018b). Mutacin 1140 lantibiotic variants are efficacious against *Clostridium difficile* infection. *Front. Microbiol.* 9:415. doi: 10.3389/fmicb.2018.00415

Kokai-Kun, J. F., Walsh, S. M., Chanturiya, T., and Mond, J. J. (2003). Lysostaphin cream eradicates *Staphylococcus aureus* nasal colonization in a cotton rat model. *Antimicrob. Agents Chemother.* 47, 1589–1597. doi: 10.1128/AAC.47.5.1589-1597.2003

Kommineni, S., Bretl, D. J., Lam, V., Chakraborty, R., Hayward, M., Simpson, P., et al. (2015). Bacteriocin production augments niche competition by enterococci in the mammalian gastrointestinal tract. *Nature* 526, 719–735. doi: 10.1038/nature15524

Koulenti, D., Song, A., Ellingboe, A., Abdul-Aziz, M. H., Harris, P., Gavey, E., et al. (2019a). Infections by multidrug-resistant Gram-negative Bacteria: what's new in our arsenal and what's in the pipeline? *Int. J. Antimicrob. Agents* 53, 211–224. doi: 10.1016/j.ijantimicag.2018.10.011

Koulenti, D., Xu, E., Mok, I. Y. S., Song, A., Karageorgopoulos, D. E., Armaganidis, A., et al. (2019b). Novel antibiotics for multidrug-resistant gram-positive microorganisms. *Microorganisms* 7:270. doi: 10.3390/microorganisms7080270

Kruszewska, D., Sahl, H. G., Bierbaum, G., Pag, U., Hynes, S. O., and Ljungh, Å (2004). Mersacidin eradicates methicillin-resistant *Staphylococcus aureus* (MRSA) in a mouse rhinitis model. *J. Antimicrob. Chemother.* 54, 648–653. doi: 10.1093/jac/dkh387

Kumariya, R., Garsa, A. K., Rajput, Y. S., Sood, S. K., Akhtar, N., and Patel, S. (2019). Bacteriocins: classification, synthesis, mechanism of action and resistance development in food spoilage causing bacteria. *Microb. Pathog.* 128, 171–177. doi: 10.1016/j.micpath.2019.01.002

Lajis, A. F. B. (2020). Biomanufacturing process for the production of bacteriocins from Bacillaceae family. *Bioresour. Bioprocess* 7:8. doi: 10.1186/s40643-020-0295-z

Lohans, C. T., and Vederas, J. C. (2012). Development of Class IIa Bacteriocins as therapeutic agents. *Int. J. Microbiol.* 2012:386410. doi: 10.1155/2012/386410

Lynch, D., O'Connor, P. M., Cotter, P. D., Hill, C., Field, D., and Begley, M. (2019). Identification and characterisation of capidermicin, a novel bacteriocin produced by *Staphylococcus capitis*. *PLoS One* 14:e0223541. doi: 10.1371/journal.pone.0223541

Malik, B., and Bhattacharyya, S. (2019). Antibiotic drug-resistance as a complex system driven by socio-economic growth and antibiotic misuse. *Sci. Rep.* 9:9788. doi: 10.1038/s41598-019-46078-y

Marshall, S. H., and Arenas, G. (2003). Antimicrobial peptides: a natural alternative to chemical antibiotics and a potential for applied biotechnology. *Electron. J. Biotechnol.* 6, 96–109.

Martín-Escolano, R., Cebrián, R., Maqueda, M., Romero, D., Rosales, M. J., Sánchez-Moreno, M., et al. (2020). Assessing the effectiveness of AS-48 in experimental mice models of Chagas' disease. *J. Antimicrob. Chemother.* 75, 1537–1545. doi: 10.1093/jac/dkaa030

Masopust, D., Sivula, C. P., and Jameson, S. C. (2017). Of mice, dirty mice, and men: using mice to understand human immunology. *J. Immunol.* 199, 383–388. doi: 10.4049/jimmunol.1700453

Mathur, H., Field, D., Rea, M. C., Cotter, P. D., Hill, C., and Ross, R. P. (2017). Bacteriocin-antimicrobial synergy: a medical and food perspective. *Front. Microbiol.* 8:1205. doi: 10.3389/fmicb.2017.01205

McCaughey, L. C., Josts, I., Grinter, R., White, P., Byron, O., Tucker, N. P., et al. (2016a). Discovery, characterization and in vivo activity of pyocin SD2, a protein antibiotic from *Pseudomonas aeruginosa*. *Biochem. J.* 473, 2345–2358. doi: 10.1042/BCJ20160470

McCaughey, L. C., Ritchie, N. D., Douce, G. R., Evans, T. J., and Walker, D. (2016b). Efficacy of species-specific protein antibiotics in a murine model of acute *Pseudomonas aeruginosa* lung infection. *Sci. Rep.* 6:30201. doi: 10.1038/srep30201

Meade, E., Slattery, M. A., and Garvey, M. (2020). Bacteriocins, potent antimicrobial peptides and the fight against multi drug resistant species: resistance is futile? *Antibiotics* 9:32. doi: 10.3390/antibiotics9010032

Meneely, P. M., Dahlberg, C. L., and Rose, J. K. (2019). Working with worms: *Caenorhabditis elegans* as a model organism. *Curr. Protoc. Essent. Lab. Tech.* 19:e35. doi: 10.1002/cpet.35

Mesa-Pereira, B., Rea, M. C., Cotter, P. D., Hill, C., and Ross, R. P. (2018). Heterologous expression of biopreservative bacteriocins with a view to low cost production. *Front. Microbiol.* 9:1654. doi: 10.3389/fmicb.2018.01654

Michel-Briand, Y., and Baysse, C. (2002). The pyocins of *Pseudomonas aeruginosa*. *Biochimie* 84, 499–510. doi: 10.1016/S0300-9084(02)01422-0

Mirzoyan, Z., Sollazzo, M., Allocca, M., Valenza, A. M., Grifoni, D., and Bellosta, P. (2019). *Drosophila melanogaster*: a model organism to study cancer. *Front. Genet.* 10:51. doi: 10.3389/fgene.2019.00051

Morgan, S. J., Elangbam, C. S., Berens, S., Janovitz, E., Vitsky, A., Zabka, T., et al. (2013). Use of animal models of human disease for nonclinical safety assessment of novel pharmaceuticals. *Toxicol. Pathol.* 41, 508–518. doi: 10.1177/0192623312457273

Mota-Meira, M., Morency, H., and Lavoie, M. C. (2005). *In vivo* activity of mutacin B-Ny266. *J. Antimicrob. Chemother.* 56, 869–871. doi: 10.1093/jac/dki295

Munoz, M., Jaramillo, D., del Pilar Melendez, A. J., Almeciga-Diaz, C., and Sanchez, F. O. (2011). Native and heterologous production of bacteriocins from gram-positive microorganisms. *Recent Pat. Biotechnol.* 5, 199–211. doi: 10.2174/187220811797579088

Ndihokubwayo, J. B., Yahaya, A. A., Desta, A. T., Ki-Zerbo, G., Odei, E. A., Keita, B., et al. (2013). *Antimicrobial Resistance in the African Region: Issues, Challenges and Actions Proposed*. Available online at: https://www.afro.who.int/sites/default/files/2017-06/amr-paper-march-2013-jbn-and-all.pdf (accessed January 29, 2021).

Newstead, L. L., Varjonen, K., Nuttall, T., and Paterson, G. K. (2020). Staphylococcal-produced bacteriocins and antimicrobial peptides: their potential as alternative treatments for *Staphylococcus aureus* infections. *Antibiotics* 9:40. doi: 10.3390/antibiotics9020040

Niu, Y., Defoirdt, T., Baruah, K., Van de Wiele, T., Dong, S., and Bossier, P. (2014). *Bacillus* sp. LT3 improves the survival of gnotobiotic brine shrimp (*Artemia franciscana*) larvae challenged with *Vibrio campbellii* by enhancing the innate immune response and by decreasing the activity of shrimp-associated vibrios. *Vet. Microbiol.* 173, 279–288. doi: 10.1016/j.vetmic.2014.08.007

Nunes, B. S., Carvalho, F. D., Guilhermino, L. M., and Van Stappen, G. (2006). Use of the genus *Artemia* in ecotoxicity testing. *Environ. Pollut.* 144, 453–462. doi: 10.1016/j.envpol.2005.12.037

O'Connor, P. M., O' Shea, E. F., Cotter, P. D., Hill, C., and Ross, R. P. (2018). The potency of the broad spectrum bacteriocin, bactofencin A, against staphylococci is highly dependent on primary structure, N-terminal charge and disulphide formation. *Sci. Rep.* 8:11833. doi: 10.1038/s41598-018-30271-6

OECD (2013). "Test No. 236: Fish Embryo Acute Toxicity (FET) test," in *OECD Guidelines for the Testing of Chemicals, Section 2*, ed. OECD Library (Paris: OECD), 1–22. doi: 10.1787/9789264203709-en

O'Shea, E. F., Cotter, P. D., Stanton, C., Ross, R. P., and Hill, C. (2012). Production of bioactive substances by intestinal bacteria as a basis for explaining probiotic mechanisms: bacteriocins and conjugated linoleic acid. *Int. J. Food Microbiol.* 152, 189–205. doi: 10.1016/j.ijfoodmicro.2011.05.025

O'Shea, E. F., O'Connor, P. M., O'Sullivan, O., Cotter, P. D., Ross, R. P., and Hill, C. (2013). Bactofencin A, a New Type of Cationic Bacteriocin with Unusual Immunity. *mBio* 4:e0498-13. doi: 10.1128/mBio.00498-13

Ovchinnikov, K. V., Kranjec, C., Thorstensen, T., Carlsen, H., and Diep, D. B. (2020). Successful Development of Bacteriocins into Therapeutic Formulation for Treatment of MRSA Skin Infection in a Murine Model. *Antimicrob. Agents Chemother.* 64:e00829-20. doi: 10.1128/AAC.00829-20

Pandey, U. B., and Nichols, C. D. (2011). Human disease models in *Drosophila melanogaster* and the role of the fly in therapeutic drug discovery. *Pharmacol. Rev.* 63, 411–436. doi: 10.1124/pr.110.003293

Parameswaran, N., and Patial, S. (2010). Tumor necrosis factor-a signaling in macrophages. *Crit. Rev. Eukaryot. Gene Expr.* 20, 87–103. doi: 10.1615/CritRevEukarGeneExpr.v20.i2.10

Park, M. R., Ryu, S., Maburutse, B. E., Oh, N. S., Kim, S. H., Oh, S. et al. (2018). Probiotic *Lactobacillus fermentum* strain JDFM216 stimulates the longevity and immune response of *Caenorhabditis elegans* through a nuclear hormone receptor. *Sci. Rep.* 8:7441. doi: 10.1038/s41598-018-25333-8

Peng, J., Long, H., Liu, W., Wu, Z., Wang, T., Zeng, Z., et al. (2019). Antibacterial mechanism of peptide Cec4 against *Acinetobacter baumannii*. *Infect. Drug Resist.* 12, 2417–2428. doi: 10.2147/IDR.S214057

Perez, R. H., Zendo, T., and Sonomoto, K. (2014). Novel bacteriocins from lactic acid bacteria (LAB): various structures and applications. *Microb. Cell Fact.* 13:S3. doi: 10.1186/1475-2859-13-S1-S3

Perlman, R. L. (2016). Mouse models of human disease: an evolutionary perspective. *Evol. Med. Public Heal.* 2016, 170–176. doi: 10.1093/emph/eow014

Phumisantiphong, U., Siripanichgon, K., Reamtong, O., and Diraphat, P. (2017). A novel bacteriocin from *Enterococcus faecalis* 478 exhibits a potent activity against vancomycin-resistant *Enterococci*. *PLoS One* 12:e0186415. doi: 10.1371/journal.pone.0186415

Piper, C., Casey, P. G., Hill, C., Cotter, P. D., and Ross, R. P. (2012). The lantibiotic lacticin 3147 prevents systemic spread of *Staphylococcus aureus* in a murine infection model. *Int. J. Microbiol.* 2012:806230. doi: 10.1155/2012/806230

Piper, C., Cotter, P., Ross, R., and Hill, C. (2009). Discovery of medically significant *Lantibiotics*. *Curr. Drug Discov. Technol.* 6, 1–18. doi: 10.2174/157016309787581075

Podolsky, S. H. (2018). The evolving response to antibiotic resistance (1945-2018). *Palgrave Commun.* 4:124. doi: 10.1057/s41599-018-0181-x

Pulse, M. E., Weiss, W. J., Kers, J. A., DeFusco, A. W., Park, J. H., and Handfield, M. (2019). Pharmacological, toxicological, and dose range assessment of OG716, a novel lantibiotic for the treatment of *Clostridium difficile*-associated infection. *Antimicrob. Agents Chemother.* 63:e01904-18. doi: 10.1128/AAC.01904-18

Qu, J., Huang, Y., and Lv, X. (2019). Crisis of antimicrobial resistance in china: now and the future. *Front. Microbiol.* 10:2240. doi: 10.3389/fmicb.2019.02240

Rajabi, S., Ramazani, A., Hamidi, M., and Naji, T. (2015). *Artemia salina* as a model organism in toxicity assessment of nanoparticles. *DARU J. Pharm. Sci.* 23:20. doi: 10.1186/s40199-015-0105-x

Rajaram, G., Manivasagan, P., Gunasekaran, U., Ramesh, S., Ashokkumar, S., Thilagavathi, B., et al. (2010). Isolation, identification and characterization of bacteriocin from *Lactobacillus lactis* and its antimicrobial and cytotoxic properties. *African J. Pharm. Pharmacol.* 4, 895–902. doi: 10.5897/AJPP.9000197

Rand, M. D., Montgomery, S. L., Prince, L., and Vorojeikina, D. (2014). Developmental toxicity assays using the *Drosophila* model. *Curr. Protoc. Toxicol.* 59, 1.12.1–1.12.20. doi: 10.1002/0471140856.tx0112s59

Sahoo, T. K., Jena, P. K., Prajapati, B., Gehlot, L., Patel, A. K., and Seshadri, S. (2017). *In vivo* assessment of immunogenicity and toxicity of the bacteriocin TSU4 in BALB/c mice. *Probiotics Antimicrob. Proteins* 9, 345–354. doi: 10.1007/s12602-016-9249-3

Schier, A. F. (2013). Zebrafish earns its stripes. *Nature* 496, 443–444. doi: 10.1038/nature12094

Segner, H., Caroll, K., Fenske, M., Janssen, C. R., Maack, G., Pascoe, D., et al. (2003). Identification of endocrine-disrupting effects in aquatic vertebrates and invertebrates: report from the European IDEA project. *Ecotoxicol. Environ. Saf.* 54, 302–314. doi: 10.1016/S0147-6513(02)00039-8

Shafee, T. M. A., Lay, F. T., Hulett, M. D., and Anderson, M. A. (2016). The defensins consist of two independent, convergent protein superfamilies. *Mol. Biol. Evol.* 33, 2345–2356. doi: 10.1093/molbev/msw106

Simonetti, R. B., Santos Marques, L., Streit, D. P. Jr., and Oberst, R. (2016). *Zebrafish* (*Danio rerio*): ethics in animal experimentation. *IOSR J. Agric. Vet. Sci. Ver.* 9, 2319–2372. doi: 10.9790/2380-090701106110

Singh, P. K., Chittpurna, Ashish, Sharma, V., Patil, P. B., and Korpole, S. (2012). Identification, purification and characterization of *Laterosporulin*, a Novel bacteriocin produced by *Brevibacillus* sp. Strain GI-9. *PLoS One* 7:e31498. doi: 10.1371/journal.pone.0031498

Singh, P. K., Solanki, V., Sharma, S., Thakur, K. G., Krishnan, B., and Korpole, S. (2015). The intramolecular disulfide-stapled structure of laterosporulin, a class IId bacteriocin, conceals a human defensin-like structural module. *FEBS J.* 282, 203–214. doi: 10.1111/febs.13129

Sloman, K. A., Bouyoucos, I. A., Brooks, E. J., and Sneddon, L. U. (2019). Ethical considerations in fish research. *J. Fish Biol.* 94, 556–577. doi: 10.1111/jfb.13946

Smith, K., Martin, L., Rinaldi, A., Rajendran, R., Ramage, G., and Walker, D. (2012). Activity of pyocin S2 against *Pseudomonas aeruginosa* biofilms. *Antimicrob. Agents Chemother.* 56, 1599–1601. doi: 10.1128/AAC.05714-11

Soltani, S., Hammami, R., Cotter, P. D., Rebuffat, S., Said, L., Ben, E., et al. (2021). Bacteriocins as a new generation of antimicrobials: toxicity aspects and regulations. *FEMS Microbiol. Rev.* 45, 1–24. doi: 10.1093/femsre/fuaa039

Son, S. J., Park, M. R., Ryu, S. D., Maburutse, B. E., Oh, N. S., Park, J., et al. (2016). Short communication: *In vivo* screening platform for bacteriocins using *Caenorhabditis elegans* to control mastitis-causing pathogens. *J. Dairy Sci.* 99, 8614–8621. doi: 10.3168/jds.2016-11330

Taneja, N., and Sharma, M. (2019). Antimicrobial resistance in the environment: the Indian scenario. *Indian J. Med. Res.* 149, 119–128. doi: 10.4103/ijmr.IJMR_331_18

Taylor, P. W., Stapleton, P. D., and Paul Luzio, J. (2002). New ways to treat bacterial infections. *Drug Discov. Today* 7, 1086–1091. doi: 10.1016/S1359-6446(02)02498-4

Teschendorf, D., and Link, C. D. (2009). What have worm models told us about the mechanisms of neuronal dysfunction in human neurodegenerative diseases? *Mol. Neurodegener.* 4:38. doi: 10.1186/1750-1326-4-38

Theuretzbacher, U., Outterson, K., Engel, A., and Karlén, A. (2020). The global preclinical antibacterial pipeline. *Nat. Rev. Microbiol.* 18, 275–285. doi: 10.1038/s41579-019-0288-0

Thomsen, T. T., Mojsoska, B., Cruz, J. C. S., Donadio, S., Jenssen, H., Løbner-Olesen, A., et al. (2016). The lantibiotic NAI-107 efficiently rescues *Drosophila melanogaster* from infection with methicillin-resistant *Staphylococcus aureus* USA300. *Antimicrob. Agents Chemother.* 60, 5427–5436. doi: 10.1128/AAC.02965-15

Tissenbaum, H. A. (2015). Using *C. elegans* for aging research. *Invertebr. Reprod. Dev.* 59, 59–63. doi: 10.1080/07924259.2014.940470

Tossi, A., and Sandri, L. (2002). Molecular diversity in gene-encoded, cationic antimicrobial polypeptides. *Curr. Pharm. Des.* 8, 743–761. doi: 10.2174/1381612023395475

Tsai, C. J. Y., Loh, J. M. S., and Proft, T. (2016). *Galleria mellonella* infection models for the study of bacterial diseases and for antimicrobial drug testing. *Virulence* 7, 214–229. doi: 10.1080/21505594.2015.1135289

Tseng, C. C., Murni, L., Han, T. W., Arfiati, D., Shih, H. T., and Hu, S. Y. (2019). Molecular characterization and heterologous production of the Bacteriocin Peocin, a DNA Starvation/stationary phase protection protein, from *Paenibacillus ehimensis* NPUST1. *Molecules* 24:2516. doi: 10.3390/molecules24132516

Umu, ÖC. O., Bäuerl, C., Oostindjer, M., Pope, P. B., Hernández, P. E., Pérez-Martínez, G., et al. (2016). The potential of class II bacteriocins to modify gut microbiota to improve host health. *PLoS One* 11:e0164036. doi: 10.1371/journal.pone.0164036

Van Staden, A. D. P., Heunis, T., Smith, C., Deane, S., and Dicks, L. M. T. (2016). Efficacy of lantibiotic treatment of *Staphylococcus aureus*-induced skin infections, monitored by *in vivo* bioluminescent imaging. *Antimicrob. Agents Chemother.* 60, 3948–3955. doi: 10.1128/AAC.02938-15

Varas, M. A., Muñoz-Montecinos, C., Kallens, V., Simon, V., Allende, M. L., Marcoleta, A. E., et al. (2020). Exploiting Zebrafish Xenografts for Testing the in vivo antitumorigenic activity of Microcin E492 against human colorectal cancer cells. *Front. Microbiol.* 11:405. doi: 10.3389/fmicb.2020.00405

Wang, G., Yu, Y., Garcia-gutierrez, E., Jin, X., He, Y., Wang, L., et al. (2020). *Lactobacillus acidophilus* JCM 1132 strain and its mutant with different bacteriocin-producing behaviour have various in situ effects on the gut microbiota of healthy mice. *Microorganisms* 8:49. doi: 10.3390/microorganisms8010049

Wongsen, S., Werawatganon, D., and Tumwasorn, S. (2019). Lactobacillus plantarum B7 attenuates *Salmonella typhimurium* infection in mice: preclinical study *in vitro* and *in vivo*. *Asian Biomed.* 12, 211–218. doi: 10.1515/abm-2019-0022

World Health Organization (2017). *WHO Publishes List of Bacteria for Which New Antibiotics are Urgently Needed. WHO Jt. News Release*. Available online at: https://www.who.int/news/item/27-02-2017-who-publishes-list-of-bacteria-for-which-new-antibiotics-are-urgently-needed (accessed January 17, 2020).

World Health Organization (2019a). *2019 Antibacterial Agents in Clinical Development: an Analysis of the Antibacterial Clinical Development Pipeline. WHO*. Available online at: https://www.who.int/publications/i/item/9789240000193 (accessed October 8, 2020).

World Health Organization (2019b). *Antibacterial Agents in Preclinical Development: an Open Access Database. WHO. WHO/EMP/IAU/2019.12*. Available online at: https://apps.who.int/iris/handle/10665/330290 (accessed March 22, 2021).

World Health Organization (2019c). *New Report Calls for Urgent Action to Avert Antimicrobial Resistance Crisis. WHO Jt. News Release*. Available online

at: https://www.who.int/news/item/29-04-2019-new-report-calls-for-urgent-action-to-avert-antimicrobial-resistance-crisis (accessed January 14, 2020).

Wu, C. (2014). An important player in brine shrimp lethality bioassay: the solvent. *J. Adv. Pharm. Technol. Res.* 5, 57–58.

Yang, S.-C., Lin, C.-H., Sung, C. T., and Fang, J.-Y. (2014). Antibacterial activities of bacteriocins: application in foods and pharmaceuticals. *Front. Microbiol.* 5:241. doi: 10.3389/fmicb.2014.00241

Yi, C. C., Liu, C. H., Chuang, K. P., Chang, Y. T., and Hu, S. Y. (2019). A potential probiotic *Chromobacterium aquaticum* with bacteriocin-like activity enhances the expression of indicator genes associated with nutrient metabolism, growth performance and innate immunity against pathogen infections in zebrafish (Danio rerio). *Fish Shellfish Immunol.* 93, 124–134. doi: 10.1016/j.fsi.2019.07.042

Yu, J., and Lu, Y. (2018). *Artemia* spp. Model-A well-established method for rapidly assessing the toxicity on an environmental perspective. *Medical Research Archives* 6, 1–15. doi: 10.18103/mra.v6i2.1700

Zasloff, M. (2002). Antimicrobial peptides of multicellular organisms. *Nature* 415, 389–395. doi: 10.1038/415389a

Zheng, S., and Sonomoto, K. (2018). Diversified transporters and pathways for bacteriocin secretion in gram-positive bacteria. *Appl. Microbiol. Biotechnol.* 102, 4243–4253. doi: 10.1007/s00253-018-8917-5

Zwierzyna, M., and Overington, J. P. (2017). Classification and analysis of a large collection of in vivo bioassay descriptions. *PLoS Comput. Biol.* 13:e1005641. doi: 10.1371/journal.pcbi.1005641

Conflict of Interest: The authors declare that the research was conducted in the absence of any commercial or financial relationships that could be construed as a potential conflict of interest.

frontiers in Microbiology

REVIEW
published: 14 July 2021
doi: 10.3389/fmicb.2021.555022

Antimicrobial Peptides: Novel Source and Biological Function With a Special Focus on Entomopathogenic Nematode/Bacterium Symbiotic Complex

Surajit De Mandal[1], Amrita Kumari Panda[2], Chandran Murugan[3], Xiaoxia Xu[1]*, Nachimuthu Senthil Kumar[4] and Fengliang Jin[1]**

[1] Laboratory of Bio-Pesticide Creation and Application of Guangdong Province, College of Agriculture, South China Agricultural University, Guangzhou, China, [2] Department of Biotechnology, Sarguja University, Ambikapur, India, [3] SRM Research Institute, SRM Institute of Science and Technology, Kattankulathur, India, [4] Department of Biotechnology, Mizoram University, Aizawl, India

OPEN ACCESS

Edited by:
András Fodor, University of Szeged, Hungary

Reviewed by:
Maurizio Francesco Brivio, University of Insubria, Italy
Sinosh Skariyachan, St. Pius X College, India

***Correspondence:**
Surajit De Mandal
surajit_micro@yahoo.co.in
Fengliang Jin
jingjin@scau.edu.cn
Xiaoxia Xu
xuxiaoxia111@scau.edu.cn

Specialty section:
This article was submitted to Microbial Symbioses, a section of the journal Frontiers in Microbiology

Received: *23 April 2020*
Accepted: *14 June 2021*
Published: *14 July 2021*

Citation:
De Mandal S, Panda AK, Murugan C, Xu X, Senthil Kumar N and Jin F (2021) Antimicrobial Peptides: Novel Source and Biological Function With a Special Focus on Entomopathogenic Nematode/Bacterium Symbiotic Complex. Front. Microbiol. 12:555022. doi: 10.3389/fmicb.2021.555022

The rapid emergence of multidrug resistant microorganisms has become one of the most critical threats to public health. A decrease in the effectiveness of available antibiotics has led to the failure of infection control, resulting in a high risk of death. Among several alternatives, antimicrobial peptides (AMPs) serve as potential alternatives to antibiotics to resolve the emergence and spread of multidrug-resistant pathogens. These small proteins exhibit potent antimicrobial activity and are also an essential component of the immune system. Although several AMPs have been reported and characterized, studies associated with their potential medical applications are limited. This review highlights the novel sources of AMPs with high antimicrobial activities, including the entomopathogenic nematode/bacterium (EPN/EPB) symbiotic complex. Additionally, the AMPs derived from insects, nematodes, and marine organisms and the design of peptidomimetic antimicrobial agents that can complement the defects of therapeutic peptides have been used as a template.

Keywords: antimicrobial peptides, multidrug-resistant pathogens, insects, nematodes, marine

INTRODUCTION

Antimicrobial peptides (AMPs) are small molecules that generally consist of 10–50 amino acids and are highly conserved in a wide range of species, including insects, nematodes, microbes, and mammals. AMPs serve as an essential component of the body's immune system and defend against exogenous pathogens. They possess significant structural variations in the α-helices, β-strands with one or more disulfide bridges, loop, and extended structures associated with their broad-spectrum activities (Hancock, 2001; Pushpanathan et al., 2013). Other important factors associated with the functional activities of AMPs are size, hydrophobicity, charge, amphipathic stereo-geometry, and

peptide self-association to the biological membrane (Nissen-Meyer and Nes, 1997; Marcos and Gandía, 2009; Pushpanathan et al., 2013). AMPs can be considered potential drug candidates to treat pathogenic microorganisms due to their broad-spectrum activity, lesser toxicity, decreased resistance development by the target cells, and capability to modulate the host immune response (Hancock and Patrzykat, 2002; Xu et al., 2019). AMPs can ameliorate the drug-resistant crisis and associated toxicity with conventional AMP drugs and also can be employed as an alternative to antibiotics (Lewies et al., 2019). They exhibit several similarities to antibiotics, such as killing microbial cells and targeting a broad spectrum of pathogens, including antibiotic resistance.

Moreover, compared to antibiotics, AMPs have unique epitopes that serve as protease recognition sites, thereby less likely to be targeted by the protease (Zasloff, 2002; Lai and Gallo, 2009). Different mechanisms, such as inhibition of gene expression or protein synthesis, inhibition of cell wall synthesis, or delocalization of bacterial cell surface proteins are commonly employed by the AMPs (Baltzer and Brown, 2011). Most of the AMPs are cationic and capable of adapting to amphipathic conformations. This helps them interact with the negatively charged bacterial cell wall and integrate it into the lipid bilayers (Haney et al., 2017; Zharkova et al., 2019). The success of AMPs against multidrug-resistant pathogens is due to the widescale multitargeted action (Zharkova et al., 2019). They are also active at lower minimum inhibitory concentrations (MICs) as compared to antibiotics. AMPs demonstrate higher killing effects and show a narrower mutation-selection window, accounting for the less likely development of resistance to AMP (Fantner et al., 2010; Yu et al., 2018). They are also active against biofilm-producing antibiotic-resistant microbes and induce non-opsonic phagocytosis. However, the combined use of AMPs with other antimicrobial compounds such as specific antibiotics may play a vital role against multidrug-resistant pathogens and associated adverse health conditions. In addition, some AMPs have been identified to exhibit antiviral activities (Chia et al., 2010; Van Der Does et al., 2010; Chung and Kocks, 2011; Steckbeck et al., 2014; Elnagdy and AlKhazindar, 2020). The AMPs play an essential role in modulating immunogenic activities, improving wound healing, enhancing chemokine production, exhibiting anti-inflammatory properties, regulating epithelial cell differentiation, and modulating angiogenesis (Koczulla and Bals, 2007; Mahlapuu et al., 2016; Otvos, 2016; Patrulea et al., 2020; **Figure 1**). Nowadays, scientists are participating in developing enhanced AMPs with novel modes of actions to replace or complement traditional antibiotics to treat various diseases (Morikawa et al., 1992; Wang et al., 2016). So far, 3257 AMPs have been reported from six kingdoms (bacteria, archaea, fungi, protists, plants, and animals) in the Antimicrobial Peptide Database[1] (Wang et al., 2016). This review provides insights into developing different AMPs from novel sources and their multifunctional properties and elaborates their future prospects (**Figure 2**). Particular focus has been given to the AMPs in bacteria that form a symbiotic relationship with the entomopathogenic nematodes (EPNs), displaying varied modes of actions.

AMPS IN INSECTS

Insects represent the largest class in the animal kingdom and are found in most of the biological niches. One of the critical features of their successful adaptation is their resistance to various pathogens. The AMPs play a critical role in innate immunity against insect pathogens (Bulet et al., 1999). They produce a large number of AMPs that varies between species, ranging from 50 (*Harmonia axyridis*) to 0 (*Hermetia illucens*) (Gerardo et al., 2010; Vilcinskas, 2013; Vogel et al., 2018). Cecropin, the first insect AMP, was isolated and characterized from *Hyalophora cecropia* (Steiner et al., 1981). Since then, many insect AMPs have been reported, which are mainly classified into three groups based on the sequence and structural features, i.e., linear peptides with α-helices that lack cysteine residues and cyclic peptides containing cysteine residues and peptides with an overexpression of proline and glycine residues (Hetru, 1998; Bulet et al., 1999). The most explored insect AMPs are defensin, cecropin, drosocin, attacin, diptericin, ponericin, drosomycin, and metchnikowin. However, it is expected that insects may have more AMPs with novel modes of action (Mylonakis et al., 2016).

Cecropins are small peptides that destroy bacterial cell membranes, inhibit proline uptake, and cause leaky membranes (Moore et al., 1996). It has also been reported that cecropin A (CecA) destroys uropathogenic *Escherichia coli* (UPEC) cells, alone or in combination with nalidixic acid (NAL), and could be a practical approach to treat antibiotic-resistant UPEC infections (Kalsy et al., 2020). CecA from *H. cecropia* exhibits only antibacterial activity, whereas CecA from *Anopheles gambiae* exhibits antibacterial and antifungal activities (Bulet et al., 2004). BR003-CecA from *Aedes aegypti* actively inhibits multiple species of Gram-negative bacteria (GNB), including *A. baumannii* (Jayamani et al., 2015). Cec D from *Galleria mellonella* exhibits vigorous activity against Gram-positive bacterium (GPB) *Listeria monocytogenes* (Mukherjee et al., 2011). Defensins are the second primary class of inducible insect AMPs active against GPB, including *Staphylococcus aureus*, but are less active against GNB (Hetru et al., 2003; Gomes and Fernandes, 2010). Few defensins also possess antifungal activities against filamentous fungi, e.g., gallerimycin from the greater wax moth *G. mellonella* (Langen et al., 2006). Insect defensin-like peptides are found in *Leiurus quinquestriatus* and *Androctonus australis* (Cociancich et al., 1993; Ehret-Sabatier et al., 1996). Defensin-like peptide 4 (DLP4) reported from the black soldier fly is active against GPB (Park et al., 2015).

The AMP drosocin, isolated from *Drosophila melanogaster*, is a 19-residue peptide containing six proline and four arginine residues (McManus et al., 1999). Glycosylated drosocin is active against *E. coli* and fungi (Imler and Bulet, 2005). These O-glycosylated AMPs are also found in other insects such as *Pyrrhocoris apterus* (pyrrhocoricin), *Bombyx mori* (lebocins), and *Myrmecia gulosa* (formations) (Cociancich et al., 1994; Hara and Yamakawa, 1995; Mackintosh et al., 1998; Wu et al., 2018).

[1] http://aps.unmc.edu/AP/main.php/

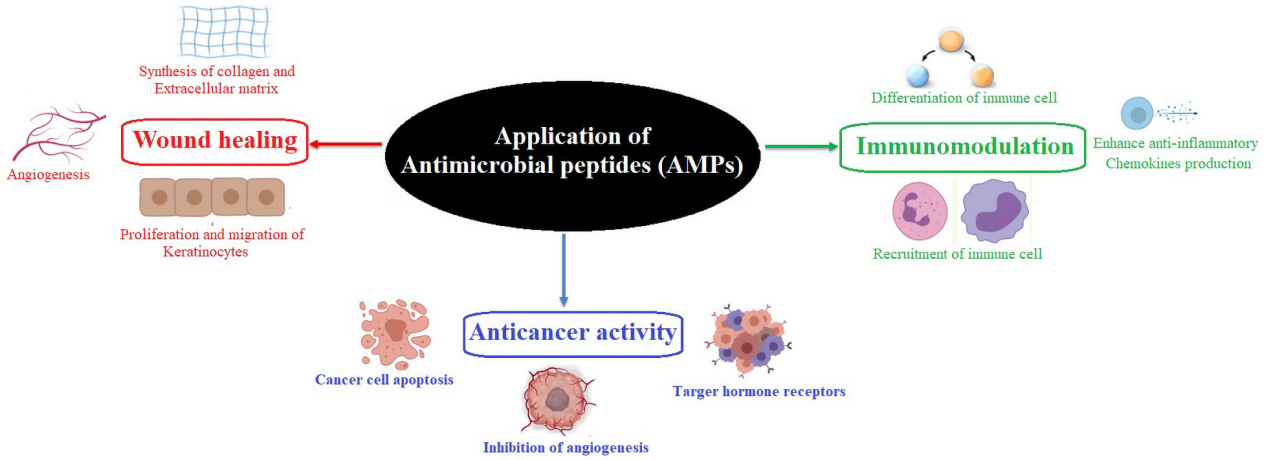

FIGURE 1 | Role of an antimicrobial peptide in immunomodulation, wound healing, and anticancer activity.

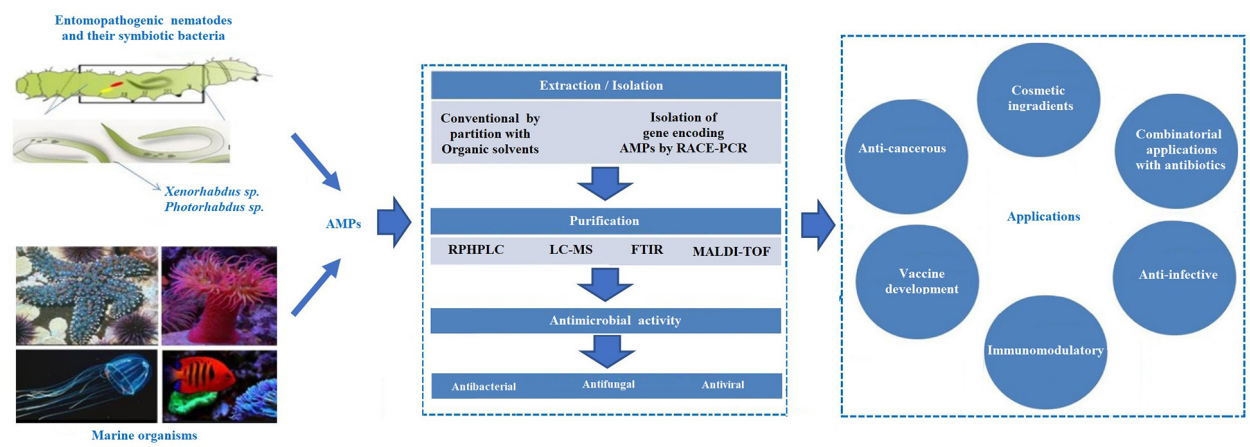

FIGURE 2 | Schematic representation of the antimicrobial peptides (AMPs) extracted from the different source and their applications.

Attacins, glycine-rich AMP, were first discovered in *H. cecropia* and is active against GNB (Hultmark et al., 1983; Carlsson et al., 1991). Attacins from *Spodoptera exigua* exhibit activity against *E. coli*, *Pseudomonas cichorii*, *Bacillus subtilis*, *L. monocytogenes*, *Trypanosoma brucei*, *Citrobacter freundii*, and *Candida albicans* (Hu and Aksoy, 2005; Kwon et al., 2008; Bang et al., 2012). Attacins and attacin-related proteins are also isolated from *B. mori*, *Heliothis virescens*, *Trichoplusia ni*, *Samia cynthia ricini*, and *Musca domestica* (Dushay et al., 2000; Geng et al., 2004).

Diptericin (9 kDa), found in *D. melanogaster*, *Sarcophaga peregrina*, and *Mayetiola destructor*, is active against GNB such as *E. coli*, *Erwinia herbicola* T, and *E. carotovora* (Keppi et al., 1989; Ishikawa et al., 1992; Reichhart et al., 1992).

However, limited reports are available on antifungal peptides in insects such as drosomycin from *D. melanogaster*, termicin from termites, heliomicin from *H. virescens*, and gallerimycin peptide from *G. mellonella* (Fehlbaum et al., 1994; Da Silva et al., 2003; Schuhmann et al., 2003). The antifungal peptide drosomycin is active against fungal pathogens, whereas thanatin is effective against a broad range of β-lactamase-producing *E. coli* (Bulet et al., 1999; Hou et al., 2011).

Xu et al. (2019) reported a novel Moricin (Px-Mor) from the diamondback moth that showed a broad-spectrum activity against GPB, GNB, and fungi, including the opportunistic human pathogen *Aureobasidium pullulans*. They suggested that Px-Mor can be used as a potential topical antimicrobial agent (Xu et al., 2019). These results indicate the importance of insect-derived AMPs against pathogens and could be further employed against multidrug-resistant pathogens or in combination with existing antibiotics (**Table 1**).

AMPS IN NEMATODE

Antimicrobial peptides are produced by microorganisms associated with insect symbioses and play a significant role in maintaining the symbiotic microbe in specific anatomical

TABLE 1 | Recently identified insect AMPs with their mechanism of action.

Name of AMP	Type of AMP	Source	3D structure	Pathogenic species	Molecular mechanism	Inhibitory concentration	References
ETD151 (Heliomicin)	Defensin	*Heliothis virescens*	Combine helix and beta structure	*Botrytis cinerea*	Interact with glucosylceramides of the fungal membrane	IC_{50} = 0.59 μM	Aumer et al., 2020
Holosins		*Ixodes holocyclus*	Cys-stabilized α/β-fold	*Staphylococcus aureus*, *Listeria grayi*, *F. graminearum*, and *C. albicans*	Peptide–lipid interactions result in the formation of membrane penetrating pores	MIC = 8 μM MIC = 5 μM	Cabezas-Cruz et al., 2019
Oxysterlins	Cecropin	*Oxysternon conspicillatum*	Linear α-helix	*Staphylococcus saprophyticus*, *Klebsiella pneumoniae*, and *Pseudomonas aeruginosa*	Membrane lysis due to formation of pores	MIC = 12.5 μg/ml MIC = 3.12 μg/ml MIC = 12.5 μg/ml	Toro Segovia et al., 2017
Cecropin D		*Galleria mellonella*	α-Helix	*K. pneumoniae* (MDR), *P. aeruginosa* (MDR)		MIC = 256 μg/ml MIC = 32 μg/ml	Ocampo-Ibáñez et al., 2020
Cecropin B		*Antheraea pernyi*		*P. aeruginosa*		MIC = 0.4 μg/ML	Wu et al., 2012; Yang et al., 2018; Gholizadeh and Moradi, 2020
Cecropin AD		*Hyalophora cecropia*		*Staphylococcus aureus*		MIC = 0.2 μg/ml	
Hl-attacin	Attacin	*Hermetia illucens*	Unknown	*E. coli* and methicillin-resistant *Staphylococcus aureus*	Blocking the synthesis of the major outer membrane proteins, thus disturbing the integrity of the cell wall	NS	Shin and Park, 2019
Prolixicin		*Rhodnius prolixus*		*E. coli*, *Citrobacter freundii*, *Enterobacter aerogenes*, and *Bacillus coagulans*		MIC = 1.6 μM MIC = 12.5 μM	Ursic-Bedoya et al., 2011
SILeb-1	Lebocin	*Spodoptera litura*	Rich	*E. coli* and *B. subtilis*	Disrupt cell membrane and cause cell elongation	MIC = 50 μM	Yang et al., 2018; Yang et al., 2020
Apidaecin IB	Drosocin	*Apis cerana*	Rich	*Escherichia coli* and *Klebsiella pneumoniae*	Binds to the substrate binding site of *E. coli* DnaK to compete with natural substrates	NS	Berthold and Hoffmann, 2014; Feng et al., 2020
Api795	Apidaecin			*P. aeruginosa*	Insert into bacterial mimic membranes and initiates a structural change leading to a thicker and more rigid membrane layer	MIC = 8 μg/ml	Bluhm et al., 2016
EtDip	Diptericin	*Eristalis tenax*	Unknown	*Candida albicans* FH2173 and *Mycobacterium smegmatis* ATCC 607		MIC > 1024 μg/ml MIC = 64 μg/ml	Hirsch et al., 2020
Mtk	Metchnikowin	*Drosophila melanogaster*	Rich	*Fusarium graminearum*	Interacts with the fungal enzyme β(1,3)-glucanosyltransferase Gel1 (*Fg*BGT), which is one of the enzymes responsible for fungal cell wall synthesis	NS	Moghaddam et al., 2017

(Continued)

TABLE 1 | Continued

Name of AMP	Type of AMP	Source	3D structure	Pathogenic species	Molecular mechanism	Inhibitory concentration	References
Ponericin-Q42	Ponericins	*Ectatomma quadridens*	α-Helical folds	*Arthrobacter globiformis*, *B. subtilis*, *E. coli* MH1, and *P. aeruginosa* PAO1	Membrane blebbing, formation of swollen cells and finally membrane destruction and cell death	MIC = 0.2 μM MIC = 0.6 μM MIC = 10 μM	Pluzhnikov et al., 2014
Jelleine-I	Jelleines	*Apis mellifera*	Unknown	*Candida glabrata* and *C. albicans*	Increase the production of cellular ROS and bind with genome DNA	MIC and MFC = 30 μg/ml MIC and MFC = 61 μg/ml	Jia et al., 2018
Pyrrhocoricin	Pyrrhocoricin	*Pyrrhocoris apterus*	Non-helix beta	Cell-free *E. coli* system and *Cryptosporidium parvum*	Inhibit the protein folding activity of the ATP-dependent DnaK/DnaJ molecular chaperone system	IC for transcription = 427 μM	Boxell et al., 2008; Taniguchi et al., 2016
Melittin	Melittin	*Apis mellifera*	Helix	*Lactobacillus casei* and *Streptococcus mutans*	Interact with bacterial membrane	MIC = 4 μg/ml MIC = 40 μg/ml	Leandro et al., 2015

compartments (Ovchinnikova et al., 2004; Tasiemski et al., 2015). A lot of the literature have highlighted the EPN/entomopathogenic bacterium (EPB) symbioses. Nematodes are specialized organisms with the ability to adapt both free-living and parasitic lifestyle in different environments. Nematodes also serve as a novel invertebrate model to study innate immunity and host–pathogen interactions (Kurz and Tan, 2004; Nicholas and Hodgkin, 2004). EPNs and their associated bacteria have evolved with several defense mechanisms to elude and counteract the host (insect) immune responses (Brivio et al., 2018; Brivio and Mastore, 2020). The nematode *Steinernema carpocapsae* can produce proteolytic secretions that can interfere with the host immune system in *S. feltiae*, *S. glaseri*, and *G. mellonella* (Balasubramanian et al., 2010; Chaubey and Garg, 2019). Similarly, the surface proteins of *S. glaseri* protect from encapsulation by the host immune system of *Popillia japonica* (Wang and Gaugler, 1999; Chaubey and Garg, 2019). It has also been reported that symbiotic bacteria and nematode cooperate to overcome the host immune response. Many defense molecules are produced as immune effectors against various microbial infections (Bulet et al., 2004). The AMP cecropins are found in the worm *Ascaris suum* (cecropin-P1, cecropin-P2, cecropin-P3, and cecropin-P4), a parasite inhabiting the intestine of pigs. These short AMPs, rich in serine residues, are stabilized by the disulfide bonds and contain potential antimicrobial activities against BPB (*S. aureus*, *B. subtilis*, *Micrococcus luteus*) and GNB (*Pseudomonas aeruginosa*, *Salmonella typhimurium*, *Serratia marcescens*, and *E. coli*) and are less effective against fungi (*Saccharomyces cerevisiae*, *C. albicans*) (Andrä et al., 2001; Andersson et al., 2003; Pillai et al., 2005; Bruno et al., 2019). Cecropin P1-like sequences were also identified in two other species, i.e., *Ascaris lumbricoides* and *Toxocara canis* (Pillai et al., 2005).

Another group of AMPs called the caenopores belong to the saposin-like protein (SAPLIP) superfamily detected in *Caenorhabditis elegans*. It contains conserved positions of six cysteine residues. Caenopore-1 (SPP-1), caenopore-5 (SPP-5), and caenopore-12 (SPP-12) exhibit antimicrobial activity against *B. megaterium*, *E. coli*, and SPP-12 *Bacillus thuringiensis* (Roeder et al., 2010; Hoeckendorf et al., 2012).

Defensins are the most studied AMPs in nematodes. *Ascaris suum* antibacterial factors (ASABFs) was the first nematode defensin identified in *C. elegans*. They are short AMPs with eight cysteine residues that form four disulfide bonds except for ASABF-6Cys-α (Minaba et al., 2009; Tarr, 2012). These peptides are primarily active against GPB, especially the common pathogen *S. aureus*. However, it is less effective against GNB and yeast (Tarr, 2012). A recent study by Lim et al. (2016) reported two novel *C. elegans* AMPs (NLP-31 and Y43C5A.3) that exhibit antimicrobial activity against *Burkholderia pseudomallei*, the causative agent of melioidosis, by interfering with DNA synthesis. They also revealed that these AMPs might act by modulating host cytokine production to interfere with the inflammatory response, and modifications could enhance anti-*B. pseudomallei* activities (Lim et al., 2016).

AMPS LINKED WITH EPN/EPB SYMBIOTIC COMPLEX

Several bacterial genera belonging to the Enterobacteriaceae family are mutualistically associated with the EPNs (Boemare, 2002). These EPNs, with their symbiotic bacteria, are lethal to many soil insects, as they synthesize diverse secondary metabolites, including small AMPs. These nematode-associated microbes exist in two distinct phases: phase 1, where they are generally associated with the nematodes, and phase 2, where they may also colonize with the nematode. However, they have never been reported to be associated with the naturally occurring nematodes. Both the phases have distinguished physiological, biochemical, and behavioral features; also phase 1 is considered more virulent than phase 2 (Akhurst et al., 1990; Volgyi et al., 1998; Abdel-Razek, 2002; Sugar et al., 2012). During the infective juvenile (IJ) stage, the nematodes enter inside the insects by piercing the body wall or via natural openings and releasing these bacteria inside the hemocoel. They reproduce exponentially, producing bioactive compounds with broad-spectrum antimicrobial activities (Sanda et al., 2018). They provide nutrients to the nematodes and protect them from environmental predators such as bacteria and fungi. They also compete for nutrition with other microbes, including the saprophytic soil microbes and the bacteria present in the insect gut or cuticle of the nematode. The elimination of the competitors is facilitated by the production of colicin E3-type killer proteins, insect toxin complexes, phage-derived bacteriocins, and several secondary metabolites (Thaler et al., 1995; Ffrench-Constant and Waterfield, 2006; Singh and Banerjee, 2008; Bode, 2009; Piel, 2009). The presence of high content of non-ribosomal peptide synthetase (NRPS) and polyketide synthase (PKS) genes facilitates them to produce novel and new bioactive molecules (Tobias et al., 2017). These bioactive molecules disrupt the insect's metabolic and functional properties, leading to septicemia (Khandelwal and Banerjee-Bhatnagar, 2003; Tran and Goodrich-Blair, 2009; Ellis and Kuehn, 2010; Brivio et al., 2018). Nematodes also play a significant role in the pathogenicity of the nemato-bacterial complex (Han and Ehlers, 2000; Chang et al., 2019). The EPNs, along with the mutualistic bacteria, kill their host within 48−72 h (Forst and Nealson, 1996). These features are now being exploited for the biological control of pests (Brivio and Mastore, 2018).

The bacterial genus *Xenorhabdus* is often found in close association with EPNs of the family Steinernematidae (Webster et al., 2002). *Xenorhabdus* synthesizes and releases antibiotic compounds in the host hemocoel that suppresses the microbial competitors, thereby manipulating the environment to promote growth, proliferation, and nematode development (Vallet-Gely et al., 2008; Richards and Goodrich-Blair, 2009; Gaugler, 2018). The antimicrobial compounds produced by these bacterial genera are highly toxic to the insect but not toxic to the nematodes. Various surface structures such as pili/fimbriae, flagella, and the outer membrane vesicles (OMVs) present in the *Xenorhabdus* interact with the host and promote adhesion and invasion of the host tissues. They also promote larvicidal activity by releasing proteases, lytic factors, and phospholipase C (Brivio et al., 2018). Ribosomal-encoded bacteriocins (xenorhabdicins) are found in *Xenorhabdus nematophilus*. These AMPs compete against more closely related bacteria, such as other *Xenorhabdus* and *Photorhabdus* strains (Thaler et al., 1995). The indole-containing Xenematide from *Xenorhabdus nematophila* exhibits moderate antibacterial and insecticidal activities (Lang et al., 2008). Two novel depsipeptides, xenematides F and G, were isolated from *Xenorhabdus budapestensis* SN84 with high antibacterial activity (Xi et al., 2019).

The cyclic peptide-antimicrobial-*Xenorhabdus* (PAX) lipopeptides, obtained by the fermentation of the *X. nematophila* F1 strain, exhibit significant activity against plants and human fungal pathogens and moderately effective against a few bacteria and yeast (Gualtieri et al., 2009). Two novel AMPs GP-19 and EP-20 from the bacterial strain *X. budapestensis* NMC-10. GP-19 exhibited inhibitory activity mainly against bacteria, while EP-20 was highly effective against plant pathogens. The synthetic GP-19 and EP-20 peptide exhibited inhibitory activities against the fungal pathogen *Verticillium dahlia* and *Phytophthora capsici* with EC_{50} values of 17.54 and 3.14 μg/ml, respectively (Xiao et al., 2012).

The AMPs xenocoumacin 1 (XCN 1) and 2 (XCN 2), from the bacterium *X. nematophila*, is effective against GPB and fungi. This peptide is synthesized by the PKS/NRPS multienzyme (xcnA-N) (McInerney et al., 1991; Reimer, 2013). Six novel linear peptides (rhabdopeptides) in *X. nematophila* and two other rhabdopeptide derivatives by *X. cabanillasii* were also identified (Reimer et al., 2013).

Nematophins, from *X. nematophila* YL001, inhibit mycelial growth of *Rhizoctonia solani* and *Phytophthora infestans* with an EC_{50} value of 40.00 and 51.25 μg/ml, respectively, and can be employed as a potential biopesticide in the agriculture sector (Zhang et al., 2019). Similarly, the novel peptide, xenoamicin, tridecadepsipeptides with hydrophobic amino acids, from the entomopathogenic *X. doucetiae* DSM 17909 and *X. mauleonii* DSM 17908 was effective against *Plasmodium falciparum* (Zhou et al., 2013).

Another dipeptide xenobactin was isolated from *Xenorhabdus* sp., strain PB30.3, and szentiamide from *X. szentirmaii*. Both AMPs are active against *P. falciparum* and have moderately effective against *T. brucei rhodesiense* and *Trypanosoma cruzi* (Nollmann et al., 2012; Grundmann et al., 2013). Similarly, the depsipentapeptide chaiyaphumine A from *Xenorhabdus* sp. PB61.4 was effective against *P. falciparum* (IC_{50} of 0.61 μM) and other protozoal tropical disease-causing agents (Grundmann et al., 2014). *Xenorhabdus indica* can produce depsipeptides and lipodepsipeptides with an additional fatty acid chain linked to one of the amino acids, also called taxlllaids (A–G), and exhibits antiprotozoal activity (Kronenwerth et al., 2014). Taken together, these reports suggest that the mutualistic association between *Xenorhabdus* and Steinernematidae could serve as a potential source for novel AMPs against bacteria, fungi, and protozoal disease-causing agents.

The bacterium *Photorhabdus* spp. forms a symbiotic relationship with the EPNs of the genus *Heterorhabditis* (Gerrard et al., 2006). They cause pathogenicity in most insects post invading the hemolymph (Boemare et al., 1997). Genomic

analysis of Photorhabdus can interpret the relation between pathogenesis and symbiosis, thereby providing vital information for the development of biocontrol agents. The genomic sequence of *P. luminescens* subsp. *laumondii* strain TT01 revealed several genes that encode toxins, hemolysins, adhesins, hemolysins, proteases, lipases, and a wide array of antibiotics. Two identified protein, PirA and PirB, exhibit similarity to both δ-endotoxins (*B. thuringiensis*) and a developmentally regulated protein from a beetle (Leptinotarsa decemlineata) (Duchaud et al., 2003; Waterfield et al., 2005). Research on the larvicidal activity of *Photorhabdus* sp. showed that *Photorhabdus* insect-related (Pir) protein is associated with high toxicity against the primary vector of dengue virus *A. aegypti* and *Aedes albopictus* (Ahantarig et al., 2009). These novel insecticidal proteins could further be exploited to develop alternative agents to control insect pests. Genomic analysis of *P. luminescens* subsp. *laumondii* strain TT01 indicates the presence of several enzymes associated with the secondary metabolite biosynthesis. The genomic sequence analysis identifies biosynthetic gene clusters associated with the synthesis of linear or cyclized peptides, lipopeptides, or depsipeptides; NRPS; unusual fatty acid synthase or a FAS/PKS hybrid; and siderophore biosynthesis (Bode, 2009). *Photorhabdus* sp. also produces numerous antimicrobials such as isopropyl stilbene, ethylstilbenes, anthraquinones (AQs) photobactin, ethyl stilbene, epoxystilbene, and ulbactin E (Li et al., 1995; Webster et al., 2002; Bode, 2009). The bioactive compounds exhibit a broad range of antimicrobial activities. *Photorhabdus* antibacterial compounds include trans-stilbenes and anthraquinone pigments (Boemare and Akhurst, 2002) that have enthralled substantial interest in the agronomic and pharmaceutical sectors (Webster et al., 2002; Hazir et al., 2016). Phthalic acid or 1,2-benzene dicarboxylic acid purified from *Photorhabdus temperata* M1021 exhibits an antibacterial activity with MIC values of 0.1 and 0.5 M (Ullah et al., 2014), benzaldehyde exhibits an antibacterial activity with MIC values of 6 and 10 mM, and antifungal activity with MIC values between 8 and 10 mM (Ullah et al., 2015). *P. temperata* subsp. *temperata* inhibits the growth of 10 strains of drug-resistant bacteria (Muangpat et al., 2017), including *S. typhimurium* KCTC 1926 and *M. luteus* KACC 10488 (Jang et al., 2012). Therefore, *Photorhabdus* spp. can be a suitable biocontrol agent in drug industries. AMPs from nemato-bacterial complexes with their inhibitory concentrations are shown in **Table 2**.

THE TARGETS AND MECHANISM OF ACTION OF AMPS DERIVED FROM NEMATOBACTERIAL COMPLEXES

The AMPs from *Xenorhabdus* spp. and *Photorhabdus* spp. are non-lethal to nematode but toxic to insect pathogens and other opportunistic microorganisms with unique targets and modes of action. This section highlights some of the recently identified AMPs from EPB with novel modes of action, namely, nematophin, odilorhabdin, darobactin, and photoditritide (**Figure 3**).

Nematophin

First isolated from *X. nematophilus* strain BC1 (Li et al., 1997), it contains 3-indoleethyl (3′-methyl-2′-oxo) pentanamide with an N-terminal α-keto group and a C-terminal tryptamine residue. Recently, few novel nematophin analogs were identified from *Xenorhabdus* strains (Cai et al., 2017). Nematophin is effective against *S. aureus* (MIC = 0.125 μg/ml) (Li et al., 1997), methicillin-resistant *S. aureus* (MRSA) (MIC = 1.5 μg/ml), and fungal pathogens, *Botrytis cinerea* (MIC = 12 μg/ml) (Li et al., 1997) and *R. solani* (MIC = 40 μg/ml) (Zhang et al., 2019). The synthetic nematophin analog with *N*-methyl substitution exhibits nanomolar activity toward *S. aureus* (15 ng/ml), *S. intermedius* 9503 (50 ng/ml) (Himmler et al., 1998), *S. hyicus* (60 ng/ml), MRSA ATCC 43300 (31 ng/ml), and methicillin-susceptible *S. aureus* ATCC 29213 (125 ng/ml) (Wesche et al., 2019). Recent studies indicate that nematophin is a potent biopesticide against a necrotrophic fungal pathogen *R. solani*. It interferes with the sclerotial development and hyphal morphology of *R. solani* at 40.00 μg/ml and germination at 15.00 μg/ml. The ultrastructure shows that the hyphae becomes twisted, shriveled, and deformed at the growing points after the exposure to nematophin at 40.00 μg/ml, and the mitochondrial structural abnormalities such as reduction in number, vacuolar degeneration, and fuzzy cristae are also observed (**Figure 3A**).

Odilorhabdin

This is a new class of AMP with broad-spectrum activity encoded by the enzymes (of NRPS gene cluster) of *X. nematophila*. This peptide binds to the decoding center of the small ribosomal subunit, leading to faulty coding procedure and prohibits non-cognate aminoacyl-tRNAs binding (Pantel et al., 2018). Odilorhabdin can directly bind with the new site on 16S rRNA (**Figure 3B**) and with the anticodon loop of the A-site aminoacyl-tRNA concurrently, resulting in the precision of translation decreased. At very high concentrations, odilorhabdin hinders the ribosome movement on mRNA (Pantel et al., 2018). Studies reported that odilorhabdin acts against Gram-negative and Gram-positive bacterial pathogens, including carbapenem-resistant Enterobacteriaceae, which strain especially shows resistance toward many classes of available antibiotics and causes severe infections with a 50% mortality rate (van Duin et al., 2013).

Darobactin

It is a novel peptide antibiotic produced by *Photorhabdus khanii* HGB1456 (Imai et al., 2019) that is effective against several Gram-negative drug-resistant pathogens. Instead of targeting the enzymes, darobactin targets outer membrane chaperone BamA (**Figure 3C**), catalyzing the insertion and folding of β-barrel outer membrane proteins in many Gram-negative pathogens. As the target of darobactin is a cell surface protein, there is no permeability obstacle encountered (Imai et al., 2019). No antibiotics were reported to act on the two surface proteins, namely, BamA and LptD, present on the GNB; therefore, darobactin could act as a potential drug candidate due to its

TABLE 2 | Antimicrobial peptides from nematobacterial complexes with their inhibitory concentrations.

Name of AMP	Source	Pathogenic species	Inhibitory concentration	References
Xenematide C	*Xenorhabdus budapestensis* SN19	*Botrytis cinerea*	EC_{50} = 22.71 μg/ml	Xing-zhong et al., 2016
Xenematides F	*Xenorhabdus budapestensis* SN84	*P. aeruginosa*	MIC = 32 μg/ml	Xi et al., 2019
Xenematides G		*B. subtilis*	MIC = 16 μg/ml	
PAX lipopeptides Xenocoumacin 2	*Xenorhabdus khoisanae* SB10	*B. subtilis* subsp. *subtilis Escherichia coli Candida albicans*	NS	Dreyer et al., 2019
Diketopiperazines	EPN *Rhabditis* sp.	*Penicillium expansum*	MIC = 2 μg/ml	Kumar et al., 2013
Nematophin	*Xenorhabdus nematophila* YL001	*Rhizoctonia solani Phytophthora infestans*	EC_{50} = 40.00 μg/ml EC_{50} = 51.25 μg/ml	Zhang et al., 2019
Nematophin	*Xenorhabdus* PB62.4	*Staphylococcus aureus*	MIC = 0.7 μg/ml	Cai et al., 2017
GP-19 EP-20	*Xenorhabdus budapestensis* NMC-10	*Verticillium dahlia Phytophthora capsici*	EC_{50} = 17.54 μg/ml EC_{50} = 3.14 μg/ml	Xiao et al., 2012
Threonine–glutamine dipeptide) domain containing protein	*Bacillus cereus*	*E. coli*, *S. aureus*, and *B. subtilis*	MIC = 62.55 μg/ml MIC = 125 μg/ml MIC = 250 μg/ml	Anju et al., 2015
Xenocoumacin 1 Xenocoumacin 2	*Xenorhabdus nematophila*	*Botrytis cinerea*	Inhibition rate of 100 ml/L cell-free filtrate on the mycelial growth of the pathogens is 100%	Guo et al., 2017
Nematophins, Xenocoumacins and Xenorhabdins	*Xenorhabdus* assam-isolate (SG as1)	*Macrophomina phaseolina*	EC_{50} = 55.98 μg/ml	Sharma et al., 2016
Cabanillasin	*Xenorhabdus cabanillasii*	*Fusarium oxysporum*	IC_{50} = 6.25 μg/ml	Houard et al., 2013
Xenobactin	*Xenorhabdus* sp. PB30.3	*Micrococcus luteus Plasmodium falciparum* NF 54 *Trypanosoma brucei rhodesiense* STIB900 *Trypanosoma cruzi* Tulahuen C4	MIC = 64 μg/ml IC_{50} = 12.45 μg/ml IC_{50} = 12.45 μg/ml IC_{50} = 67.03 μg/ml	Grundmann et al., 2013
Xenortide D	*Xenorhabdus nematophila*	*Plasmodium falciparum Trypanosoma brucei*	NS	Reimer et al., 2014
Taxlllaids	*Xenorhabdus indica* (DSM 17382)	*Plasmodium falciparum*	NS	Kronenwerth et al., 2014
Phototemtide A	*Photorhabdus temperata* Meg1	*Plasmodium falciparum Trypanosoma brucei rhodesiense*	IC_{50} = 9.8 μM IC_{50} = 62 μM	Zhao L. et al., 2020

distinctive sizeable molecular structure fused rings and unusual cell surface target (Konovalova et al., 2017).

Photoditritide

Photoditritide is the first non-proteinogenic peptide reported from *P. temperata* Meg1 through promoter exchange (Maglangit et al., 2021). Photoditritide 19 consists of two tyrosines, two homo-arginines, and two tryptophans (Bode et al., 2015). It is effective against *E. coli* (MIC = 24 μM), *M. luteus* (MIC = 3.0 μM), and antiprotozoal activity against *P. falciparum* (IC_{50} = 27 μM), *T. cruzi* (IC_{50} = 71 μM), and *T. brucei rhodesiense* (IC_{50} = 13 μM) (Bode et al., 2015).

The increasing evidence of antibiotic resistance is a serious issue. Drug-resistant pathogens develop new resistance mechanisms and interfere in the treatment of common infections. Moreover, multidrug resistance pathogenic strains have developed tolerance against most of the available antibiotics. Researchers searching for novel sources of antimicrobial agents through synthetic compound library screening have mostly failed to get efficient antimicrobial agents (Payne et al., 2007). Therefore, exploiting new natural antimicrobial sources to fill the research gap in antimicrobial drug discovery is a promising approach. Most of the antibiotics used to date belong to soil actinomycetes. The present review aims to compile novel natural sources, highlighting the unnoticed and ignored sources to identify new AMPs with a unique mode of action. The marine ecosystem presents a vast repository of microorganisms, invertebrates, and vertebrates that produce various natural products and AMPs with the perspective of treating several infectious diseases (Bertrand and Munoz-Garay, 2019).

MARINE-DERIVED ANTIMICROBIAL PEPTIDES

The marine ecosystem encompasses an unprecedented variety of organisms that have shown remarkable contribution in discovering and developing novel biomolecules, nutraceuticals, and secondary metabolites that pave the way to produce antimicrobial agents (Malve, 2016; Sekurova et al., 2019; **Figure 1**). AMPs derived from marine sources

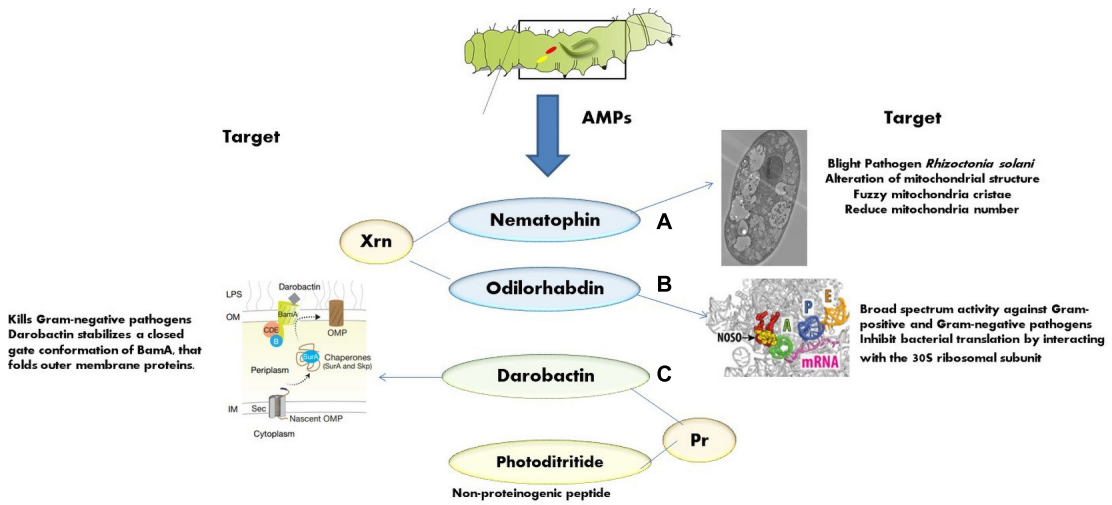

FIGURE 3 | Mode of action of various AMPs: **(A)** nematophins act on mitochondrial structure of *Rhizoctonia solani* [adapted from Zhang et al. (2019)]; **(B)** odilorhabdins act on the ribosome and inhibit protein synthesis in Gram-negative bacteria [adapted from Pantel et al. (2018)]; **(C)** darobactins act on outer membrane chaperone [adapted from Imai et al. (2019)].

are novel and revolutionary therapeutic agents with distinctive pharmacological properties such as antimicrobial, antiproliferative, antioxidant, anticoagulant, antihypertensive, antidiabetic, and antiobesity properties (Jo et al., 2017).

Antimicrobial Peptides Derived From Marine Invertebrates

Marine invertebrates produce AMPs to activate innate immune machinery to recognize, neutralize, and eliminate invading pathogens (Loker et al., 2004). A wide variety of corals produce structurally unique bioactive metabolites that can serve as significant novel compounds in drug development against various human diseases. For example, the marine fungus *Simplicillium* sp. associated with soft coral *Sinularia* sp. synthesizes five new peptides, including *Sinularia* peptides A–E. These bioactive AMPs exhibit significant antimicrobial activity against *Mycobacterium tuberculosis*, *Colletotrichum asianum*, and *Pyricularia oryzae* Cav. Mollusks such as *Mytilus edulis*, *Ruditapes decussatus*, and oyster *Mytilus galloprovincialis* produce AMPs such as myticins and mytilin. A cyclic hexapeptide, cyclo-(Gly-Leu-Val-IIe-Ala-Phe), bacicyclin isolated from *Bacillus* sp. associated with *M. edulis*, exhibits antibacterial activities against clinically relevant bacterial strains such as *S. aureus* and *Enterococcus faecalis* (Wiese et al., 2018; Zanjani et al., 2018). AMPs derived from marine invertebrates can modulate the lifecycle of bacterial biofilm and also inhibit biofilm formation. Crustin, an antibacterial protein, consists of alanine or threonine, glycine, and glutamine residues at their cleavage site and is derived from the hemolymph of crustaceans (Destoumieux-Garzón et al., 2016). It effectively inhibits biofilm formation of various antibiotic-resistant bacterial strains, including *B. pumilis* and *B. thuringiensis* and also is effective against *Aeromonas hydrophila* and *E. coli* (Rekha et al., 2018; Sivakamavalli et al., 2020). A novel antibacterial peptide named PcnAMP, extracted from *Procambarus clarkia* (Pcn) (a red swamp crayfish), exhibits a significant inhibitory effect against Gram-positive and GNB strains such as *S. aureus* and *M. luteus* (Zhao B. R. et al., 2020). AMPs from ascidian *Didemnum* sp. exhibit an antibacterial effect against human pathogens *E. faecalis*, *S. marcescens*, *S. typhimurium*, and *S. aureus* at MICs of 2.30, 2.17, 2.05, and 1.95 μg/ml, respectively (Arumugam et al., 2020). The AMPs halocyntin and papillosin from tunicate *H. papillosa* exhibit antibacterial activity against *M. luteus* and *E. coli* (Palanisamy et al., 2017). A novel AMP myticusin-beta isolated from the mantle of *Mytilus coruscus* exhibits a broad range of antibacterial activity and acts as a substitute to antibiotics (Oh et al., 2020). Therefore, the diverse forms of marine invertebrates act as natural reservoirs for novel AMPs, which can be exploited for the treatment of various microbial infections (Thoms et al., 2007; Destoumieux-Garzón et al., 2016; **Table 3**).

Antimicrobial Peptides From Marine Microorganisms

Marine microbial systems are the significant resources of AMPs with unique pharmacological features, including antimicrobial, cytostatic, animal growth, immunosuppressant, antiviral, antimalarial, antiparasitic, promoters, and insecticides activities (Semreen et al., 2018). AMPs extracted from symbiotic marine microorganisms exhibit enhanced broad-spectrum antimicrobial activity. These natural compounds are now being exploited to resolve the microbial drug-resistance problem. Hyporientalin A, an anti-*Candida* peptaibol, a moronecidin-like peptide from *Trichoderma orientale* strains, symbiotic fungi of Mediterranean marine sponge *Cymbaxinella damicornis*, inhibits the growth of clinical isolates of *C. albicans*, Gram-positive and Gram-negative bacteria (Touati et al., 2018). Cyclic lipopeptide Fengycins from marine bacterium

TABLE 3 | Antimicrobial peptides from marine organisms.

Name of the peptide	Source of peptide	Mode of action	Inhibitory concentration	References
An antimicrobial peptide from marine invertebrates				
Sinulariapeptides A–E	*Coral Sinularia* sp.	Inhibitory effects against protein tyrosine phosphatases of *Mycobacterium tuberculosis* (MptpA and MptpB)	IC_{50} values of 35.0 and 25.9 μM against MptpA and MptpB	Dai et al., 2018
Bacicyclin	*Mytilus edulis*	Cell membrane damage of *Enterococcus faecalis* and *Staphylococcus aureus*	MIC values of *Enterococcus faecalis* and *Staphylococcus aureus* was noted to be 8 and 12 mM, respectively	Wiese et al., 2018
Crustin	*Portunus pelagicus*	The growth reduction and biofilm inhibition potential of on Gram-positive bacteria and Gram-negative bacteria	MIC of both Gram-positive and Gram-negative bacteria was noted to be 30 and 20 μg/ml, respectively	Rekha et al., 2018
An antimicrobial peptide from marine microorganisms				
Hyporientalin A	*Trichoderma orientale*	Growth inhibitory effects toward clinical isolates like *Candida albicans*	MICs of *Candida albicans* species (247FN and 098 VC) was noted to be 2.55–4.92 μM, respectively	Touati et al., 2018
Fengycins	*Bacillus subtilis*	Inducing the mitochondrial membrane potential (MMP), reactive oxygen species (ROS), downregulate the ROS-scavenging enzymes and chromatin condensation in plant-pathogenic fungus *Magnaporthe grisea*		Zhang and Sun, 2018
EeCentrocin 1	*Echinus esculentus*	Cell membrane damage	MIC of *Corynebacterium glutamicum* and *S. aureus* (MIC = 0.78 μM)	Solstad et al., 2019
Tetrapeptides 1	*Streptomyces* sp.	Growth inhibition of *Burkholderia gladioli* and *Burkholderia glumae*	MIC was noted to be 0.068 and 1.1 mM in *Burkholderia gladioli* and *Burkholderia glumae*	Betancur et al., 2019
Thr-Pro-Asp-Ser -Glu-Ala-Leu (TPDSEAL)	*Porphyra yezoensis*	The surface of *S. aureus* became blurred, loose, irregular, and cell wall damage		Jiao et al., 2019
An antimicrobial peptide from marine vertebrates				
Epinecidin-1	*Epinephelus coioides*	Disrupted the membrane of metronidazole-resistant *Trichomonas vaginalis* and completely killed the pathogen	Minimal Epi-1 concentration was noted to be 62.5 μg/ml to produce 100% growth inhibition of *Trichomonas vaginalis*	Huang et al., 2019
Tissue factor pathway inhibitor 1 (TFPI-2)	*Sciaenops ocellatus*	TFPI-2 destroying cell membrane integrity, penetrating the cytoplasm and inducing degradation of genomic DNA and total RNA	MICs of TFPI-2 against *M. luteus*, *S. aureus*, *V. litoralis*, *V. ichthyoenteri*, *V. vulnificus*, and *V. scophthalmi* were 3, 6, 11, 85, 170, and 340 μM, respectively	He et al., 2018
Caspian trout (CtHep)	*Salmo caspius*	The growth inhibition of infectious bacteria	MICs concentration was noted to be 50 and 12.5 μM for *Aeromonas hydrophila* and *Bacillus subtilis*	Shirdel et al., 2019

B. subtilis (BS155) is effective against the plant-pathogenic fungus *Magnaporthe grisea*. Host-dependent marine microbes are excellent sources of many active antimicrobial cyclic peptides (e.g., the cyclolipopeptides cyclodysidins A–D). These peptides, secondary metabolites of *Streptomyces* sp. associated with sponge *Dysidea tupha*, exhibit broad-spectrum antimicrobial activities (Indraningrat et al., 2016). Different marine gamma-proteobacteria associated with seaweeds, particularly, *Pseudomonas* sp., are the primary sources in cyclotetrapeptide cyclo-(isoleucyl-prolyl-leucyl-alanyl), cyclic heptapeptide, scopularides A and B, and ogipeptin A–C. These peptides exhibit intense antimicrobial and anthelmintic activities. Ogipeptin is a powerful agent suppressing the immunostimulatory role of lipopolysaccharides present in the cell wall of GNB (Betancur et al., 2019). Similarly, the marine sponge *Tethya aurantium* associated with fungus *Scopulariopsis brevicaulis* synthesizes cyclodepsipeptides scopularides A and B that exhibit effective cytotoxic activity against pathogens (Agrawal et al., 2017). New cyclic lipopeptides maribasins A and B from the broth culture of marine microorganism *B. marinus* exhibit broad-spectrum activities against phytopathogens such as *Fusarium oxysporum*, *Fusarium graminearum*, *Verticillium alboatrum*, *Alternaria solani*, and *R. solani* with the MICs of 25–200 mg/ml (Zhang et al., 2010). Additionally, the two new cyclic tetrapeptides, from the marine strain *Streptomyces* sp., are effective against *Burkholderia gladioli* and *Burkholderia glumae* at MIC of 0.068 and 1.1 mM, respectively. Furthermore, tetrapeptide-2 is effective against *B. glumae* (MIC = 1.1 mM) and fungal phytopathogens (Betancur et al., 2019). Hence, the diversified marine microorganisms prove to be an effective substitute to the existing antibiotics, thereby reducing the probability of antibiotic-resistant pathogens (**Table 3**).

Antimicrobial Peptides From Marine Vertebrates

Antimicrobial peptides in marine vertebrates are mainly localized in body fluids, mucous layers, and epithelial surfaces (Edilia Avila, 2017). AMPs participate in body defense mechanisms to eliminate the invading pathogens and enhance physiological and metabolic processes such as toxin neutralization, wound healing, angiogenesis, and iron metabolism. For instance, epinecidin-1 (Epi-1) disrupts the cell membrane of metronidazole-resistant *Trichomonas vaginalis* and terminates the pathogen with a minimal dose of 62.5 μg/ml. *T. vaginalis* treated with different concentrations of Epi-1 (62.5, 125, 250, or 500 μg/ml) exhibits 100% growth inhibition (Huang et al., 2019). 3C-terminal peptide tissue factor pathway inhibitor 1 (TFPI-1) from *Cyprinus carpio* (common carp) exhibits bactericidal effects against *M. luteus*, *S. aureus*, and *Vibrio vulnificus* (Su et al., 2020). Orange-spotted grouper (*Epinephelus coioides*) derived from AMP EPI is effective against GPB (Su and Chen, 2020). Cysteine-rich Hepcidins (CtHep) from vertebrates such as fish, reptiles, and amphibians can significantly inhibit *Streptococcus iniae* and *A. hydrophila* (Shirdel et al., 2019). Marine betta fish *Betta splendens* produce four families of AMPs, including defensins, piscidins, hepcidins, and LEAP-2, which vigorously suppress the growth of fungi, bacteria, virus, and parasites (Amparyup et al., 2020). A short novel peptide synthesized from the core region of the LCNKL2 of a marine fish *Larimichthys crocea* inhibits *S. aureus* and *Vibrio harveyi* (Zhou et al., 2019). Antibacterial activity of piscidin-5 like AMP has been reported from *L. crocea* (Pan et al., 2019). Therefore, AMPs are essential to induce adaptive response and participate in a vertebrate's metabolic and reproductive processes (**Table 3**).

CONCLUSION

The exponentially increasing cases of antibiotic resistance requires the introduction of novel and alternative drug molecules. Insects, nematodes, insect–nematode–bacterial associations and marine organisms could be promising sources for natural AMPs to address the challenges of multidrug-resistant infections. The conventional method of overmining natural antibiotic sources has failed to develop new drugs to overcome drug resistance. Genomic analysis indicates the presence of several gene clusters for the novel secondary metabolite biosynthesis. The exploitation of these secondary metabolites might lead to the discovery of potential antimicrobial compounds. This review thereby highlights the symbiotic bacteria–EPN complexes as prospective antimicrobial peptide sources and opens the window to new sources of intervention and invention of natural bioactive compounds to combat antimicrobial resistance. Further research is required to understand the metabolic pathways to optimize the conditions for large-scale production and commercialization of these drug molecules as adequate substitutes.

AUTHOR CONTRIBUTIONS

SD, FJ, and XX conceptualized the manuscript. SD, AP, and CM drafted the manuscript. AP was responsible for preparing the figures in the manuscript. FJ, NS, SD, AP, and CM assisted in revising the manuscript. All authors contributed to the article and approved the submitted version.

FUNDING

This work was supported by a grant from the National Natural Science Foundation of China (31972345) and Natural Science Foundation of Guangdong Province of China (2019A151501122).

ACKNOWLEDGMENTS

We would like to thank the reviewers for their invaluable comments and suggestions.

REFERENCES

Abdel-Razek, A. (2002). Pathogenicity of bacteria symbiotically associated with insect pathogenic nematodes against the greater wax moth, *Galleria mellonella* (L.). *Arch. Phytopathol. Plant Protection* 35, 53–60. doi: 10.1080/03235400210000095 79

Agrawal, S., Acharya, D., Adholeya, A., Barrow, C. J., and Deshmukh, S. K. (2017). Nonribosomal peptides from marine microbes and their antimicrobial and anticancer potential. *Front. Pharmacol.* 8:828.

Ahantarig, A., Chantawat, N., Waterfield, N. R., Kittayapong, P. J. A., and Microbiology, E. (2009). PirAB toxin from Photorhabdus asymbiotica as a larvicide against dengue vectors. *Appl. Environ. Microbiol.* 75, 4627–4629. doi: 10.1128/aem.00221-09

Akhurst, R., Boemare, N., Gaugler, R., and Kaya, H. (1990). *Entomopathogenic Nematodes in Biological Control*. Boca Raton, Fla: CRC Press.

Amparyup, P., Charoensapsri, W., Samaluka, N., Chumtong, P., Yocawibun, P., and Imjongjirak, C. (2020). Transcriptome analysis identifies immune-related genes and antimicrobial peptides in Siamese fighting fish (*Betta splendens*). *Fish Shellfish Immunol.* 99, 403–413. doi: 10.1016/j.fsi.2020.02.030

Andersson, M., Boman, A., and Boman, H. (2003). Ascaris nematodes from pig and human make three anti-bacterial peptides: isolation of cecropin P1 and two ASABF peptides. *Cell. Mol. Life Sci.* 60, 599–606. doi: 10.1007/s000180300051

Andrä, J., Berninghausen, O., and Leippe, M. (2001). Cecropins, antibacterial peptides from insects and mammals, are potently fungicidal against *Candida albicans*. *Med. Microbiol. Immunol.* 189, 169–173. doi: 10.1007/s430-001-8025-x

Anju, K., Archana, M., Mohandas, C., and Nambisan, B. J. (2015). Purification and identification of an antibacterial protein from the symbiotic bacteria associated with novel entomopathogenic nematode, Rhabditis (Oscheius) sp. *World J. Microbiol. Biotechnol.* 31, 621–632. doi: 10.1007/s11274-015-1816-3

Arumugam, V., Venkatesan, M., Ramachandran, K., Ramachandran, S., Palanisamy, S. K., and Sundaresan, U. (2020). Purification, characterization and antibacterial properties of peptide from marine ascidian *Didemnum* sp. *Int. J. Pept. Res. Ther.* 26, 201–208. doi: 10.1007/s10989-019-09829-z

Aumer, T., Voisin, S. B. N., Knobloch, T., Landon, C. L., and Bulet, P. J. (2020). Impact of an antifungal insect defensin on the proteome of the phytopathogenic fungus *Botrytis cinerea*. *ACS Publications* 19, 1131–1146. doi: 10.1021/acs.jproteome.9b00638

Balasubramanian, N., Toubarro, D., and Simoes, N. (2010). Biochemical study and in vitro insect immune suppression by a trypsin-like secreted protease from the nematode *Steinernema carpocapsae*. *Parasite Immunol.* 32, 165–175. doi: 10.1111/j.1365-3024.2009.01172.x

Baltzer, S. A., and Brown, M. H. (2011). Antimicrobial peptides–promising alternatives to conventional antibiotics. *J. Mol. Microbiol. Biotechnol.* 20, 228–235. doi: 10.1159/000331009

Bang, K., Park, S., Yoo, J. Y., and Cho, S. (2012). Characterization and expression of attacin, an antibacterial protein-encoding gene, from the beet armyworm, *Spodoptera exigua* (Hübner)(Insecta: Lepidoptera: Noctuidae). *Mol. Biol. Rep.* 39, 5151–5159. doi: 10.1007/s11033-011-1311-3

Berthold, N., and Hoffmann, R. J. P. (2014). Cellular uptake of apidaecin 1b and related analogs in Gram-negative bacteria reveals novel antibacterial mechanism for proline-rich antimicrobial peptides. *Protein Pept. Lett.* 21, 391–398. doi: 10.2174/0929866513206660104

Bertrand, B., and Munoz-Garay, C. (2019). Marine antimicrobial peptides: a promising source of new generation antibiotics and other bio-active molecules. *J. Int. J. Peptide Res. Therapeutics* 25, 1441–1450. doi: 10.1007/s10989-018-9789-3

Betancur, L. A., Forero, A. M., Romero-Otero, A., Sepúlveda, L. Y., Moreno-Sarmiento, N. C., Castellanos, L., et al. (2019). Cyclic tetrapeptides from the marine strain Streptomyces sp. PNM-161a with activity against rice and yam phytopathogens. *J. Antibiotics* 72, 744–751. doi: 10.1038/s41429-019-0201-0

Bluhm, M. E., Schneider, V. A., Schäfer, I., Piantavigna, S., Goldbach, T., Knappe, D., et al. (2016). N-terminal Ile-Orn-and Trp-Orn-motif repeats enhance membrane interaction and increase the antimicrobial activity of apidaecins against *Pseudomonas aeruginosa*. *Front. Cell Dev. Biol.* 4:39.

Bode, E., Brachmann, A. O., Kegler, C., Simsek, R., Dauth, C., Zhou, Q., et al. (2015). Simple "on-demand" production of bioactive natural products. *J. Chem. Bio Chem.* 16, 1115–1119. doi: 10.1002/cbic.201500094

Bode, H. B. (2009). Entomopathogenic bacteria as a source of secondary metabolites. *Curr. Opin. Chem. Biol.* 13, 224–230. doi: 10.1016/j.cbpa.2009.02.037

Boemare, N. (2002). Systematics of Photorhabdus and Xenorhabdus. *Entomopathogenic Nematol.* 60(Pt 8), 1921–1937.

Boemare, N., and Akhurst, R. (2002). *Genera Photorhabdus and Xenorhabdus*. Berlin: Springer.

Boemare, N., Givaudan, A., Brehélin, M., and Laumond, C. J. S. (1997). Symbiosis and pathogenicty of nematode-bacterium complexes. *Biol. Bull.* 223, 85–102.

Boxell, A., Lee, S. H. C., Jefferies, R., Watt, P., Hopkins, R., Reid, S., et al. (2008). Pyrrhocoricin as a potential drug delivery vehicle for *Cryptosporidium parvum*. *Exp. Parasitol.* 119, 301–303. doi: 10.1016/j.exppara.2008.02.005

Brivio, M. F., and Mastore, M. (2018). Nematobacterial complexes and insect hosts: different weapons for the same war. *Insects* 9:117. doi: 10.3390/insects9030117

Brivio, M. F., and Mastore, M. J. I. (2020). When appearance misleads: the role of the entomopathogen surface in the relationship with its host. *Insects* 11:387. doi: 10.3390/insects11060387

Brivio, M. F., Toscano, A., De Pasquale, S. M., De Lerma Barbaro, A., Giovannardi, S., Finzi, G., et al. (2018). Surface protein components from entomopathogenic nematodes and their symbiotic bacteria: effects on immune responses of the greater wax moth, *Galleria mellonella* (Lepidoptera: Pyralidae). *Pest. Manag. Sci.* 74, 2089–2099. doi: 10.1002/ps.4905

Bruno, R., Maresca, M., Canaan, S., Cavalier, J.-F., Mabrouk, K., Boidin-Wichlacz, C., et al. (2019). Worms' antimicrobial peptides. *Mar. Drugs* 17:512. doi: 10.3390/md17090512

Bulet, P., Hetru, C., Dimarcq, J.-L., and Hoffmann, D. (1999). Antimicrobial peptides in insects; structure and function. *Dev. Compar. Immunol.* 23, 329–344.

Bulet, P., Stöcklin, R., and Menin, L. (2004). Anti-microbial peptides: from invertebrates to vertebrates. *Immunol. Rev.* 198, 169–184. doi: 10.1111/j.0105-2896.2004.0124.x

Cabezas-Cruz, A., Tonk, M., Bleackley, M. R., Valdés, J. J., Barrero, R. A., Hernández-Jarguín, A., et al. (2019). Antibacterial and antifungal activity of defensins from the Australian paralysis tick, *Ixodes holocyclus*. *Ticks Tick Borne Dis.* 10:101269. doi: 10.1016/j.ttbdis.2019.101269

Cai, X., Challinor, V. L., Zhao, L., Reimer, D., Adihou, H. L. N., Grün, P., et al. (2017). Biosynthesis of the antibiotic nematophin and its elongated derivatives in entomopathogenic bacteria. *J. Org. Lett.* 19, 806–809. doi: 10.1021/acs.orglett.6b03796

Carlsson, A., Engström, P., Palva, E. T., and Bennich, H. (1991). Attacin, an antibacterial protein from *Hyalophora cecropia*, inhibits synthesis of outer membrane proteins in *Escherichia coli* by interfering with omp gene transcription. *Infect. Immun.* 59, 3040–3045. doi: 10.1128/iai.59.9.3040-3045.1991

Chang, D. Z., Serra, L., Lu, D., Mortazavi, A., and Dillman, A. R. (2019). A core set of venom proteins is released by entomopathogenic nematodes in the genus Steinernema. *PLoS Pathog.* 15:e1007626. doi: 10.1371/journal.ppat.1007626

Chaubey, A. K., and Garg, A. P. (2019). "Entomopathogenic nematodes in the biological control of insect pests with reference to insect immunity," in *Plant Biotic Interactions*, eds A. Varma, S. Tripathi, and R. Prasad (Berlin: Springer).

Chia, T.-J., Wu, Y.-C., Chen, J.-Y., and Chi, S.-C. (2010). Antimicrobial peptides (AMP) with antiviral activity against fish nodavirus. *J. Fish Shellfish Immunol.* 28, 434–439. doi: 10.1016/j.fsi.2009.11.020

Chung, Y.-S. A., and Kocks, C. J. (2011). Recognition of pathogenic microbes by the Drosophila phagocytic pattern recognition receptor eater. *J. Biol. Chem.* 286, 26524–26532. doi: 10.1074/jbc.m110.214007

Cociancich, S., Dupont, A., Hegy, G., Lanot, R., Holder, F., Hetru, C., et al. (1994). Novel inducible antibacterial peptides from a hemipteran insect, the sap-sucking bug *Pyrrhocoris apterus*. *Biochem. J.* 300, 567–575. doi: 10.1042/bj3000567

Cociancich, S., Goyffon, M., Bontems, F., Bulet, P., Bouet, F., Menez, A., et al. (1993). Purification and characterization of a scorpion defensin, a 4kDa antibacterial peptide presenting structural similarities with insect defensins and scorpion toxins. *Biochem. Biophys. Res. Commun.* 194, 17–22. doi: 10.1006/bbrc.1993.1778

Da Silva, P., Jouvensal, L., Lamberty, M., Bulet, P., Caille, A., and Vovelle, F. (2003). Solution structure of termicin, an antimicrobial peptide from the termite Pseudacanthotermes spiniger. *Protein Sci.* 12, 438–446. doi: 10.1110/ps.0228303

Dai, Y., Lin, Y., Pang, X., Luo, X., Wang, J., Zhou, X., et al. (2018). Peptides from the soft coral-associated fungus Simplicillium sp. SCSIO41209. *J Phytochem.* 154, 56–62. doi: 10.1016/j.phytochem.2018.06.014

Destoumieux-Garzón, D., Rosa, R. D., Schmitt, P., Barreto, C., Vidal-Dupiol, J., Mitta, G., et al. (2016). Antimicrobial peptides in marine invertebrate health and disease. *Philos. Trans. R. Soc. B Biol. Sci.* 371:20150300. doi: 10.1098/rstb.2015.0300

Dreyer, J., Rautenbach, M., Booysen, E., van Staden, A., Deane, S., and Dicks, L. J. (2019). Xenorhabdus khoisanae SB10 produces Lys-rich PAX lipopeptides and a Xenocoumacin in its antimicrobial complex. *BMC Microbiol.* 19:132.

Duchaud, E., Rusniok, C., Frangeul, L., Buchrieser, C., Givaudan, A., Taourit, S., et al. (2003). The genome sequence of the entomopathogenic bacterium *Photorhabdus luminescens*. *Nat. Biotechnol.* 21, 1307–1313.

Dushay, M. S., Roethele, J. B., Chaverri, J. M., Dulek, D. E., Syed, S. K., Kitami, T., et al. (2000). Two attacin antibacterial genes of *Drosophila melanogaster*. *Gene* 246, 49–57. doi: 10.1016/s0378-1119(00)00041-x

Edilia Avila, E. (2017). Functions of antimicrobial peptides in vertebrates. *Curr. Protein Pept. Sci.* 18, 1098–1119.

Ehret-Sabatier, L., Loew, D., Goyffon, M., Fehlbaum, P., Hoffmann, J. A., van Dorsselaer, A., et al. (1996). Characterization of novel cysteine-rich antimicrobial peptides from scorpion blood. *J. Biol. Chem.* 271, 29537–29544. doi: 10.1074/jbc.271.47.29537

Ellis, T. N., and Kuehn, M. J. (2010). Virulence and immunomodulatory roles of bacterial outer membrane vesicles. *Microbiol. Mol. Biol. Rev.* 74, 81–94. doi: 10.1128/mmbr.00031-09

Elnagdy, S., and AlKhazindar, M. J. (2020). The potential of antimicrobial peptides as an antiviral therapy against COVID-19. *ACS Pharmacol. Transl. Sci.* 3, 780–782. doi: 10.1021/acsptsci.0c00059

Fantner, G. E., Barbero, R. J., Gray, D. S., and Belcher, A. M. (2010). Kinetics of antimicrobial peptide activity measured on individual bacterial cells using high-speed atomic force microscopy. *Nat. Nanotechnol.* 5, 280–285. doi: 10.1038/nnano.2010.29

Fehlbaum, P., Bulet, P., Michaut, L., Lagueux, M., Broekaert, W. F., Hetru, C., et al. (1994). Insect immunity. septic injury of Drosophila induces the synthesis of a potent antifungal peptide with sequence homology to plant antifungal

peptides. *J. Biol. Chem.* 269, 33159–33163. doi: 10.1016/s0021-9258(20)30111-3

Feng, M., Fei, S., Xia, J., Labropoulou, V., Swevers, L., and Sun, J. J. (2020). Antimicrobial peptides as potential antiviral factors in insect antiviral immune response. *Front. Immunol.* 11:2030.

Ffrench-Constant, R., and Waterfield, N. J. (2006). An ABC guide to the bacterial toxin, complexes. *Adv. Appl. Microbiol.* 58, 169–183. doi: 10.1016/s0065-2164(05)58005-5

Forst, S., and Nealson, K. J. (1996). Molecular biology of the symbiotic-pathogenic bacteria Xenorhabdus spp. and Photorhabdus spp. *Microbiol. Rev.* 60:21. doi: 10.1128/mr.60.1.21-43.1996

Gaugler, R. (2018). *Entomopathogenic Nematodes in Biological Control*. Boca Raton: CRC press.

Geng, H., An, C.-J., Hao, Y.-J., Li, D.-S., and Du, R.-Q. (2004). Molecular cloning and expression of attacin from housefly (*Musca domestica*). *Acta Genet. Sin.* 31, 1344–1350.

Gerardo, N. M., Altincicek, B., Anselme, C., Atamian, H., Barribeau, S. M., De Vos, M., et al. (2010). Immunity and other defenses in pea aphids, *Acyrthosiphon pisum*. *Genome Biol.* 11:R21.

Gerrard, J. G., Joyce, S. A., and Clarke, D. J. (2006). Nematode symbiont for *Photorhabdus asymbiotica*. *Emerg. Infect. Dis.* 12:1562.

Gholizadeh, A., and Moradi, B. J. (2020). Cecropins activity against bacterial pathogens. *Infect. Dis. Clin. Pract.* 29, e6–e12.

Gomes, P. D. S., and Fernandes, M. H. (2010). Defensins in the oral cavity: distribution and biological role. *J. Oral Pathol. Med.* 39, 1–9. doi: 10.1111/j.1600-0714.2009.00832.x

Grundmann, F., Kaiser, M., Kurz, M., Schiell, M., Batzer, A., and Bode, H. B. (2013). Structure determination of the bioactive depsipeptide xenobactin from Xenorhabdus sp. PB30. 3. *RSC Adv.* 3, 22072–22077. doi: 10.1039/c3ra44721a

Grundmann, F., Kaiser, M., Schiell, M., Batzer, A., Kurz, M., Thanwisai, A., et al. (2014). Antiparasitic Chaiyaphumines from entomopathogenic Xenorhabdus sp. PB61. 4. *J. Nat. Prod.* 77, 779–783. doi: 10.1021/np4007525

Gualtieri, M., Aumelas, A., and Thaler, J.-O. (2009). Identification of a new antimicrobial lysine-rich cyclolipopeptide family from *Xenorhabdus nematophila*. *J. Antibiot.* 62, 295–302. doi: 10.1038/ja.2009.31

Guo, S., Zhang, S., Fang, X., Liu, Q., Gao, J., Bilal, M., et al. (2017). Regulation of antimicrobial activity and xenocoumacins biosynthesis by pH in Xenorhabdus nematophila. *Microbiol. Cell Factories* 16:203.

Han, R., and Ehlers, R.-U. (2000). Pathogenicity, development, and reproduction of Heterorhabditis bacteriophora and *Steinernema carpocapsae* under axenic in vivo conditions. *J. Invertebr. Pathol.* 75, 55–58. doi: 10.1006/jipa.1999.4900

Hancock, R. E. (2001). Cationic peptides: effectors in innate immunity and novel antimicrobials. *Lancet Infect. Dis.* 1, 156–164. doi: 10.1016/s1473-3099(01)00092-5

Hancock, R., and Patrzykat, A. (2002). Clinical development of cationic antimicrobial peptides: from natural to novel antibiotics. *Curr. Drug Targets Infect. Disord.* 2, 79–83. doi: 10.2174/1568005024605855

Haney, E. F., Mansour, S. C., and Hancock, R. E. (2017). Antimicrobial peptides: an introduction. *J. Antimicrobial Peptides* 1548, 3–22. doi: 10.1007/978-1-4939-6737-7_1

Hara, S., and Yamakawa, M. (1995). A novel antibacterial peptide family isolated from the silkworm, *Bombyx mori*. *Biochem. J.* 310, 651–656. doi: 10.1042/bj3100651

Hazir, S., Shapiro-Ilan, D. I., Bock, C. H., Hazir, C., Leite, L. G., and Hotchkiss, M. W. (2016). Relative potency of culture supernatants of Xenorhabdus and Photorhabdus spp. on growth of some fungal phytopathogens. *Eur. J. Plant Pathol.* 146, 369–381. doi: 10.1007/s10658-016-0923-9

He, S.-W., Wang, J.-J., Du, X., Yue, B., Wang, G.-H., Zhou, S., et al. (2018). A teleost TFPI-2 peptide that possesses a broad antibacterial spectrum and immune-stimulatory properties. *Fish Shellfish Immunol.* 82, 469–475. doi: 10.1016/j.fsi.2018.08.051

Hetru, C. (1998). Antimicrobial peptides from insects. Molecular mechanisms of immune responses in insects. *Dev. Comp. Immunol.* 23, 329–344.

Hetru, C., Troxler, L., and Hoffmann, J. A. (2003). Drosophila melanogaster antimicrobial defense. *J. Infect. Dis.* 187, S327–S334.

Himmler, T., Pirro, F., and Schmeer, N. (1998). Synthesis and antibacterial in vitro activity of novel analogues of nematophin. *J. Bioorganic Med. Chem. Lett.* 8, 2045–2050. doi: 10.1016/s0960-894x(98)00358-8

Hirsch, R., Wiesner, J., Bauer, A., Marker, A., Vogel, H., Hammann, P. E., et al. (2020). Antimicrobial peptides from rat-tailed maggots of the drone fly eristalis tenax show potent activity against multidrug-resistant gram-negative bacteria. *Microorganisms* 8:626. doi: 10.3390/microorganisms8050626

Hoeckendorf, A., Stanisak, M., and Leippe, M. (2012). The saposin-like protein SPP-12 is an antimicrobial polypeptide in the pharyngeal neurons of *Caenorhabditis elegans* and participates in defence against a natural bacterial pathogen. *Biochem. J.* 445, 205–212. doi: 10.1042/bj20112102

Hou, Z., Lu, J., Fang, C., Zhou, Y., Bai, H., Zhang, X., et al. (2011). Underlying mechanism of in vivo and in vitro activity of C-terminal–amidated thanatin against clinical isolates of extended-spectrum β-lactamase–producing *Escherichia coli*. *J. Infect. Dis.* 203, 273–282. doi: 10.1093/infdis/jiq029

Houard, J., Aumelas, A., Noël, T., Pages, S., Givaudan, A., Fitton-Ouhabi, V., et al. (2013). Cabanillasin, a new antifungal metabolite, produced by entomopathogenic *Xenorhabdus cabanillasii* JM26. *J. Antibiotics* 66, 617–620. doi: 10.1038/ja.2013.58

Hu, Y., and Aksoy, S. (2005). An antimicrobial peptide with trypanocidal activity characterized from Glossina morsitans morsitans. *Insect Biochem. Mol. Biol.* 35, 105–115. doi: 10.1016/j.ibmb.2004.10.007

Huang, H.-N., Chuang, C.-M., Chen, J.-Y., and Chieh-Yu, P. (2019). Epinecidin-1: a marine fish antimicrobial peptide with therapeutic potential against trichomonas vaginalis infection in mice. *Peptides* 112, 139–148. doi: 10.1016/j.peptides.2018.12.004

Hultmark, D., Engström, A., Andersson, K., Steiner, H., Bennich, H., and Boman, H. (1983). Insect immunity. Attacins, a family of antibacterial proteins from *Hyalophora cecropia*. *EMBO J.* 2, 571–576. doi: 10.1002/j.1460-2075.1983.tb01465.x

Imai, Y., Meyer, K. J., Iinishi, A., Favre-Godal, Q., Green, R., Manuse, S., et al. (2019). A new antibiotic selectively kills Gram-negative pathogens. *Nature* 576, 459–464.

Imler, J.-L., and Bulet, P. (2005). "Antimicrobial peptides in Drosophila: structures, activities and gene regulation," in *Mechanisms of Epithelial Defense*, eds D. Kabelit and J. M. Schroder (Switzerland: Karger Publishers).

Indraningrat, A. A. G., Smidt, H., and Sipkema, D. (2016). Bioprospecting sponge-associated microbes for antimicrobial compounds. *Mar. Drugs* 14:87. doi: 10.3390/md14050087

Ishikawa, M., Kubo, T., and Natori, S. (1992). Purification and characterization of a diptericin homologue from *Sarcophaga peregrina* (flesh fly). *Biochem. J.* 287, 573–578. doi: 10.1042/bj2870573

Jang, E.-K., Ullah, I., Lim, J.-H., Lee, I.-J., Kim, J.-G., and Shin, J.-H. (2012). Physiological and molecular characterization of a newly identified entomopathogenic bacteria, Photorhabdus temperata M1021. *J. Microbiol. Biotechnol.* 22, 1605–1612. doi: 10.4014/jmb.1203.03068

Jayamani, E., Rajamuthiah, R., Larkins-Ford, J., Fuchs, B. B., Conery, A. L., Vilcinskas, A., et al. (2015). Insect-derived cecropins display activity against *Acinetobacter baumannii* in a whole-animal high-throughput *Caenorhabditis elegans* model. *Antimicrob. Agents Chemother.* 59, 1728–1737. doi: 10.1128/aac.04198-14

Jia, F., Wang, J., Peng, J., Zhao, P., Kong, Z., Wang, K., et al. (2018). The in vitro, in vivo antifungal activity and the action mode of Jelleine-I against Candida species. *Amino Acids* 50, 229–239. doi: 10.1007/s00726-017-2507-1

Jiao, K., Gao, J., Zhou, T., Yu, J., Song, H., Wei, Y., et al. (2019). Isolation and purification of a novel antimicrobial peptide from *Porphyra yezoensis*. *J. Food Biochem.* 43:e12864.

Jo, C., Khan, F. F., Khan, M. I., and Iqbal, J. (2017). Marine bioactive peptides: types, structures, and physiological functions. *Food Rev. Intl.* 33, 44–61. doi: 10.1080/87559129.2015.1137311

Kalsy, M., Tonk, M., Hardt, M., Dobrindt, U., Zdybicka-Barabas, A., Cytrynska, M., et al. (2020). The insect antimicrobial peptide cecropin a disrupts uropathogenic *Escherichia coli* biofilms. *npj Biofilms Microbiomes* 6:6.

Keppi, E., Pugsley, A. P., Lambert, J., Wicker, C., Dimarcq, J. L., Hoffmann, J. A., et al. (1989). Mode of action of diptericin A, a bactericidal peptide induced in the hemolymph of *Phormia terranovae* larvae. *Arch. Insect. Biochem. Physiol.* 10, 229–239. doi: 10.1002/arch.940100306

Khandelwal, P., and Banerjee-Bhatnagar, N. (2003). Insecticidal activity associated with the outer membrane vesicles of *Xenorhabdus nematophilus*. *Appl. Environ. Microbiol.* 69, 2032–2037. doi: 10.1128/aem.69.4.2032-2037.2003

Koczulla, R., and Bals, R. (2007). "Cathelicidin antimicrobial peptides modulate angiogenesis," in *Therapeutic Neovascularization-Quo Vadis?*, eds E. Deindl and C. Kupatt (Netherlands: Springer), 191–196. doi: 10.1007/1-4020-5955-8_10

Konovalova, A., Kahne, D. E., and Silhavy, T. J. (2017). Outer membrane biogenesis. *J. Annu. Rev. Microbiol.* 71, 539–556.

Kronenwerth, M., Bozhüyük, K. A., Kahnt, A. S., Steinhilber, D., Gaudriault, S., Kaiser, M., et al. (2014). Characterisation of Taxlllaids A–G; natural products from Xenorhabdus indica. *Chem. A Eur. J.* 20, 17478–17487. doi: 10.1002/chem.201403979

Kumar, N., Mohandas, C., Nambisan, B., Kumar, D. S., and Lankalapalli, R. S. J. (2013). Isolation of proline-based cyclic dipeptides from Bacillus sp. N strain associated with rhabitid entomopathogenic nematode and its antimicrobial properties. *Biotechnology* 29, 355–364. doi: 10.1007/s11274-012-1189-9

Kurz, C. L., and Tan, M. W. (2004). Regulation of aging and innate immunity in C. elegans. *Aging Cell* 3, 185–193. doi: 10.1111/j.1474-9728.2004.00108.x

Kwon, Y., Kim, H., Kim, Y., Kang, Y., Lee, I., Jin, B., et al. (2008). Comparative analysis of two attacin genes from *Hyphantria cunea*. *Comp. Biochem. Physiol. Part B Biochem. Mol. Biol.* 151, 213–220. doi: 10.1016/j.cbpb.2008.07.002

Lai, Y., and Gallo, R. L. (2009). AMPed up immunity: how antimicrobial peptides have multiple roles in immune defense. *J. Trends Immunol.* 30, 131–141. doi: 10.1016/j.it.2008.12.003

Lang, G., Kalvelage, T., Peters, A., Wiese, J., and Imhoff, J. F. (2008). Linear and cyclic peptides from the entomopathogenic bacterium *Xenorhabdus nematophilus*. *J. Nat. Prod.* 71, 1074–1077. doi: 10.1021/np800053n

Langen, G., Imani, J., Altincicek, B., Kieseritzky, G., Kogel, K.-H., and Vilcinskas, A. (2006). Transgenic expression of gallerimycin, a novel antifungal insect defensin from the greater wax moth Galleria mellonella, confers resistance to pathogenic fungi in tobacco. *Biol. Chem.* 387, 549–557. doi: 10.1515/bc.2006.071

Leandro, L. F., Mendes, C. A., Casemiro, L. A., Vinholis, A. H., Cunha, W. R., Almeida, R. D., et al. (2015). Antimicrobial activity of apitoxin, melittin and phospholipase A2 of honey bee (*Apis mellifera*) venom against oral pathogens. *An. Acad. Bras. Cienc.* 87, 147–155. doi: 10.1590/0001-3765201520130511

Lewies, A., Du Plessis, L. H., and Wentzel, J. F. (2019). Antimicrobial peptides: the Achilles' heel of antibiotic resistance? *J. Probiotics Antimicrob. Proteins* 11, 370–381. doi: 10.1007/s12602-018-9465-0

Li, J., Chen, G., and Webster, J. M. (1997). Nematophin, a novel antimicrobial substance produced by *Xenorhabdus nematophilus* (Enterobactereaceae). *Can. J. Microbiol.* 43, 770–773. doi: 10.1139/m97-110

Li, J., Chen, G., Wu, H., and Webster, J. M. (1995). Identification of two pigments and a hydroxystilbene antibiotic from *Photorhabdus luminescens*. *Appl. Environ. Microbiol.* 61, 4329–4333. doi: 10.1128/aem.61.12.4329-4333.1995

Lim, M.-P., Firdaus-Raih, M., and Nathan, S. (2016). Nematode peptides with host-directed anti-inflammatory activity rescue *Caenorhabditis elegans* from a *Burkholderia pseudomallei* infection. *Front. Microbiol.* 7:1436.

Loker, E. S., Adema, C. M., Zhang, S. M., and Kepler, T. B. (2004). Invertebrate immune systems–not homogeneous, not simple, not well understood. *Immunol. Rev.* 198, 10–24. doi: 10.1111/j.0105-2896.2004.0117.x

Mackintosh, J. A., Veal, D. A., Beattie, A. J., and Gooley, A. A. (1998). Isolation from an ant *Myrmecia gulosa* of two inducible O-glycosylated proline-rich antibacterial peptides. *J. Biol. Chem.* 273, 6139–6143. doi: 10.1074/jbc.273.11.6139

Maglangit, F., Yu, Y., and Deng, H. (2021). Bacterial pathogens: threat or treat (a review on bioactive natural products from bacterial pathogens). *J. Nat. Product Rep.* 38, 782–821. doi: 10.1039/d0np00061b

Mahlapuu, M., Håkansson, J., Ringstad, L., and Björn, C. (2016). Antimicrobial peptides: an emerging category of therapeutic agents. *J. Front. Cell. Infect. Microbiol.* 6:194.

Malve, H. (2016). Exploring the ocean for new drug developments: marine pharmacology. *J. Pharm. Bioallied Sci.* 8, 83–91. doi: 10.4103/0975-7406.171700

Marcos, J. F., and Gandía, M. (2009). Antimicrobial peptides: to membranes and beyond. *J. Expert Opin. Drug Discov.* 4, 659–671. doi: 10.1517/17460440902992888

McInerney, B. V., Taylor, W. C., Lacey, M. J., Akhurst, R. J., and Gregson, R. P. (1991). Biologically active metabolites from Xenorhabdus spp., Part 2. Benzopyran-1-one derivatives with gastroprotective activity. *J. Nat. Prod.* 54, 785–795. doi: 10.1021/np50075a006

McManus, A. M., Otvos, L., Hoffmann, R., and Craik, D. J. (1999). Conformational studies by NMR of the antimicrobial peptide, drosocin, and its non-glycosylated derivative: effects of glycosylation on solution conformation. *Biochemistry* 38, 705–714. doi: 10.1021/bi981956d

Minaba, M., Ueno, S., Pillai, A., and Kato, Y. (2009). Evolution of ASABF (Ascaris suum antibacterial factor)-type antimicrobial peptides in nematodes: Putative rearrangement of disulfide bonding patterns. *Dev. Comp. Immunol.* 33, 1147–1150. doi: 10.1016/j.dci.2009.06.011

Moghaddam, M.-R. B., Vilcinskas, A., and Rahnamaeian, M. J. (2017). The insect-derived antimicrobial peptide metchnikowin targets *Fusarium graminearum* β (1, 3) glucanosyltransferase Gel1, which is required for the maintenance of cell wall integrity. *Biol. Chem.* 398, 491–498. doi: 10.1515/hsz-2016-0295

Moore, A. J., Beazley, W. D., Bibby, M. C., and Devine, D. A. (1996). Antimicrobial activity of cecropins. *J. Antimicrob. Chemother.* 37, 1077–1089. doi: 10.1093/jac/37.6.1077

Morikawa, N., Hagiwara, K. I., and Nakajima, T. (1992). Brevinin-1 and-2, unique antimicrobial peptides from the skin of the frog, Rana brevipoda porsa. *Biochem. Biophys. Res. Commun.* 189, 184–190. doi: 10.1016/0006-291x(92)91542-x

Muangpat, P., Yooyangket, T., Fukruksa, C., Suwannaroj, M., Yimthin, T., Sitthisak, S., et al. (2017). Screening of the antimicrobial activity against drug resistant bacteria of Photorhabdus and Xenorhabdus associated with entomopathogenic nematodes from Mae Wong National Park, Thailand. *Front. Microbiol.* 8:1142.

Mukherjee, K., Mraheil, M. A., Silva, S., Müller, D., Cemic, F., Hemberger, J., et al. (2011). Anti-Listeria activities of *Galleria mellonella* hemolymph proteins. *Appl. Environ. Microbiol.* 77, 4237–4240. doi: 10.1128/aem.02435-10

Mylonakis, E., Podsiadlowski, L., Muhammed, M., and Vilcinskas, A. (2016). Diversity, evolution and medical applications of insect antimicrobial peptides. *Philos. Trans. R. Soc. B Biol. Sci.* 371:20150290. doi: 10.1098/rstb.2015.0290

Nicholas, H. R., and Hodgkin, J. (2004). Responses to infection and possible recognition strategies in the innate immune system of *Caenorhabditis elegans*. *Mol. Immunol.* 41, 479–493. doi: 10.1016/j.molimm.2004.03.037

Nissen-Meyer, J., and Nes, I. F. (1997). Ribosomally synthesized antimicrobial peptides: their function, structure, biogenesis, and mechanism of action. *Arch. Microbiol.* 167, 67–77. doi: 10.1007/s002030050418

Nollmann, F. I., Dowling, A., Kaiser, M., Deckmann, K., Grösch, S., and Bode, H. B. (2012). Synthesis of szentiamide, a depsipeptide from entomopathogenic *Xenorhabdus szentirmaii* with activity against *Plasmodium falciparum*. *Beilstein J. Org. Chem.* 8, 528–533. doi: 10.3762/bjoc.8.60

Ocampo-Ibáñez, I. D., Liscano, Y., Rivera-Sánchez, S. P., Oñate-Garzón, J., Lugo-Guevara, A. D., Flórez-Elvira, L. J., et al. (2020). A novel cecropin D-Derived short cationic antimicrobial peptide exhibits antibacterial activity against wild-type and multidrug-resistant strains of *Klebsiella pneumoniae* and *Pseudomonas aeruginosa*. *Evol. Bioinform Online* 16:1176934320936266.

Oh, R., Lee, M. J., Kim, Y.-O., Nam, B.-H., Kong, H. J., Kim, J.-W., et al. (2020). Myticusin-beta, antimicrobial peptide from the marine bivalve, *Mytilus coruscus*. *Fish Shellfish Immunol.* 99, 342–352. doi: 10.1016/j.fsi.2020.02.020

Otvos, L. (2016). Immunomodulatory effects of anti-microbial peptides. *J. Acta Microbiol. Immunol. Hungarica* 63, 257–277. doi: 10.1556/030.63.2016.005

Ovchinnikova, T. V., Aleshina, G. M., Balandin, S. V., Krasnosdembskaya, A. D., Markelov, M. L., Frolova, E. I., et al. (2004). Purification and primary structure of two isoforms of arenicin, a novel antimicrobial peptide from marine polychaeta *Arenicola marina*. *FEBS Lett.* 577, 209–214. doi: 10.1016/j.febslet.2004.10.012

Palanisamy, S. K., Rajendran, N., and Marino, A. (2017). Natural products diversity of marine ascidians (tunicates; ascidiacea) and successful drugs in clinical development. *Nat. Products Bioprospecting* 7, 1–111. doi: 10.1007/s13659-016-0115-5

Pan, Y., Zheng, L.-B., Mao, Y., Wang, J., Lin, L.-S., Su, Y.-Q., et al. (2019). The antibacterial activity and mechanism analysis of piscidin 5 like from *Larimichthys crocea*. *Dev. Comp. Immunol.* 92, 43–49. doi: 10.1016/j.dci.2018.10.008

Pantel, L., Florin, T., Dobosz-Bartoszek, M., Racine, E., Sarciaux, M., Serri, M., et al. (2018). Odilorhabdins, antibacterial agents that cause miscoding by binding at a new ribosomal site. *J. Mol. Cell* 70, 83–94.e87.

Park, S.-I., Kim, J.-W., and Yoe, S. M. (2015). Purification and characterization of a novel antibacterial peptide from black soldier fly (*Hermetia illucens*) larvae. *Dev. Comp. Immunol.* 52, 98–106. doi: 10.1016/j.dci.2015.04.018

Patrulea, V., Borchard, G., and Jordan, O. (2020). An update on antimicrobial peptides (AMPs) and their delivery strategies for wound infections. *J Pharmaceutics* 12:840. doi: 10.3390/pharmaceutics12090840

Payne, D. J., Gwynn, M. N., Holmes, D. J., and Pompliano, D. L. (2007). Drugs for bad bugs: confronting the challenges of antibacterial discovery. *J Nat. Rev. Drug Discov.* 6, 29–40. doi: 10.1038/nrd2201

Piel, J. (2009). Metabolites from symbiotic bacteria. *Nat. Prod. Rep.* 26, 338–362. doi: 10.1039/b703499g

Pillai, A., Ueno, S., Zhang, H., Lee, J. M., and Kato, Y. (2005). Cecropin P1 and novel nematode cecropins: a bacteria-inducible antimicrobial peptide family in the nematode *Ascaris suum*. *Biochem. J.* 390, 207–214. doi: 10.1042/bj20050218

Pluzhnikov, K. A., Kozlov, S. A., Vassilevski, A. A., Vorontsova, O. V., Feofanov, A. V., and Grishin, E. (2014). Linear antimicrobial peptides from Ectatomma quadridens ant venom. *Biochimie* 107, 211–215. doi: 10.1016/j.biochi.2014.09.012

Pushpanathan, M., Gunasekaran, P., and Rajendhran, J. (2013). Antimicrobial peptides: versatile biological properties. *J. Int. J. Peptides* 2013:675391.

Reichhart, J.-M., Meister, M., Dimarcq, J.-L., Zachary, D., Hoffmann, D., Ruiz, C., et al. (1992). Insect immunity: developmental and inducible activity of the Drosophila diptericin promoter. *EMBO J.* 11, 1469–1477. doi: 10.1002/j.1460-2075.1992.tb05191.x

Reimer, D. (2013). *Identification and Characterization of Selected Secondary Metabolite Biosynthetic Pathways from XENORHABDUS Nematophila*. Ph. D. thesis. Frankfurt: Johann Wolfgang Groethe-Universität.

Reimer, D., Cowles, K. N., Proschak, A., Nollmann, F. I., Dowling, A. J., Kaiser, M., et al. (2013). Rhabdopeptides as insect-specific virulence factors from entomopathogenic bacteria. *Chembiochem* 14, 1991–1997. doi: 10.1002/cbic.201300205

Reimer, D., Nollmann, F. I., Schultz, K., Kaiser, M., and Bode, H. (2014). Xenortide biosynthesis by entomopathogenic *Xenorhabdus nematophila*. *J. Nat. Prod.* 77, 1976–1980. doi: 10.1021/np500390b

Rekha, R., Vaseeharan, B., Ishwarya, R., Anjugam, M., Alharbi, N. S., Kadaikunnan, S., et al. (2018). Searching for crab-borne antimicrobial peptides: crustin from *Portunus pelagicus* triggers biofilm inhibition and immune responses of *Artemia salina* against GFP tagged Vibrio parahaemolyticus Dahv2. *Mol. Immunol.* 101, 396–408. doi: 10.1016/j.molimm.2018.07.024

Richards, G. R., and Goodrich-Blair, H. (2009). Masters of conquest and pillage: *Xenorhabdus nematophila* global regulators control transitions from virulence to nutrient acquisition. *Cell Microbiol.* 11, 1025–1033. doi: 10.1111/j.1462-5822.2009.01322.x

Roeder, T., Stanisak, M., Gelhaus, C., Bruchhaus, I., Grötzinger, J., and Leippe, M. (2010). Caenopores are antimicrobial peptides in the nematode *Caenorhabditis elegans* instrumental in nutrition and immunity. *Dev. Comp. Immunol.* 34, 203–209. doi: 10.1016/j.dci.2009.09.010

Sanda, N. B., Muhammad, A., Ali, H., and Hou, Y. (2018). Entomopathogenic nematode *Steinernema carpocapsae* surpasses the cellular immune responses of the hispid beetle, *Octodonta nipae* (Coleoptera: Chrysomelidae). *Microb. Pathog.* 124, 337–345. doi: 10.1016/j.micpath.2018.08.063

Schuhmann, B., Seitz, V., Vilcinskas, A., and Podsiadlowski, L. (2003). Cloning and expression of gallerimycin, an antifungal peptide expressed in immune response of greater wax moth larvae, *Galleria mellonella*. *Arch. Insect Biochem. Physiol.* 53, 125–133.

Sekurova, O. N., Schneider, O., and Zotchev, S. B. (2019). Novel bioactive natural products from bacteria via bioprospecting, genome mining and metabolic engineering. *Microbial Biotechnol.* 12, 828–844. doi: 10.1111/1751-7915.13398

Semreen, M. H., El-Gamal, M. I., Abdin, S., Alkhazraji, H., Kamal, L., Hammad, S., et al. (2018). Recent updates of marine antimicrobial peptides. *Saudi Pharmaceutical J.* 26, 396–409. doi: 10.1016/j.jsps.2018.01.001

Sharma, K., Walia, S., Ganguli, S., and Kundu, A. (2016). Analytical characterization of secondary metabolites from Indian Xenorhabdus species the symbiotic bacteria of entomopatathogenic nematode (Steinernema spp.) as Antifungal Agent. *Natl. Acad. Sci. Lett.* 39, 175–180. doi: 10.1007/s40009-016-0453-1

Shin, H. S., and Park, S. I. (2019). Novel attacin from *Hermetia illucens*: cDNA cloning, characterization, and antibacterial properties. *Prep. Biochem. Biotechnol.* 49, 279–285. doi: 10.1080/10826068.2018.1541807

Shirdel, I., Kalbassi, M. R., Hosseinkhani, S., Paknejad, H., and Wink, M. (2019). Cloning, characterization and tissue-specific expression of the antimicrobial peptide hepcidin from caspian trout (*Salmo caspius*) and the antibacterial activity of the synthetic peptide. *Fish Shellfish Immunol.* 90, 288–296. doi: 10.1016/j.fsi.2019.05.010

Singh, J., and Banerjee, N. (2008). Transcriptional analysis and functional characterization of a gene pair encoding iron-regulated xenocin and immunity proteins of *Xenorhabdus nematophila*. *J. Bacteriol.* 190, 3877–3885. doi: 10.1128/jb.00209-08

Sivakamavalli, J., James, R. A., Park, K., Kwak, I.-S., and Vaseeharan, B. (2020). Purification of WAP domain-containing antimicrobial peptides from green tiger shrimp *Peaneaus semisulcatus*. *Microb. Pathog.* 140:103920. doi: 10.1016/j.micpath.2019.103920

Solstad, R. G., Johansen, C., Stensvåg, K., Strøm, M. B., and Haug, T. (2019). Structure-activity relationship studies of shortened analogues of the antimicrobial peptide EeCentrocin 1 from the sea urchin Echinus esculentus. *J. Pept. Sci.* 26:e3233.

Steckbeck, J. D., Deslouches, B., and Montelaro, R. C. (2014). Antimicrobial peptides: new drugs for bad bugs? *Expert Opin. Biol. Ther.* 14, 11–14. doi: 10.1517/14712598.2013.844227

Steiner, H., Hultmark, D., Engström, Å, Bennich, H., and Boman, H. G. (1981). Sequence and specificity of two antibacterial proteins involved in insect immunity. *Nature* 292, 246–248. doi: 10.1038/292246a0

Su, B.-C., and Chen, J.-Y. (2020). Epinecidin-1: an orange-spotted grouper antimicrobial peptide that modulates *Staphylococcus aureus* lipoteichoic acid-induced inflammation in macrophage cells. *Fish Shellfish Immunol.* 99, 362–367. doi: 10.1016/j.fsi.2020.02.036

Su, Y.-L., Wang, G.-H., Wang, J.-J., Xie, B., Gu, Q.-Q., Hao, D.-F., et al. (2020). TC26, a teleost TFPI-1 derived antibacterial peptide that induces degradation of bacterial nucleic acids and inhibits bacterial infection in vivo. *Fish Shellfish Immunol.* 98, 508–514. doi: 10.1016/j.fsi.2020.01.057

Sugar, D. R., Murfin, K. E., Chaston, J. M., Andersen, A. W., Richards, G. R., deLéon, L., et al. (2012). Phenotypic variation and host interactions of *Xenorhabdus bovienii* SS-2004, the entomopathogenic symbiont of Steinernema jollieti nematodes. *Environ. Microbiol.* 14, 924–939. doi: 10.1111/j.1462-2920.2011.02663.x

Taniguchi, M., Ochiai, A., Kondo, H., Fukuda, S., Ishiyama, Y., Saitoh, E., et al. (2016). Pyrrhocoricin, a proline-rich antimicrobial peptide derived from insect, inhibits the translation process in the cell-free *Escherichia coli* protein synthesis system. *J. Biosci. Bioeng.* 121, 591–598. doi: 10.1016/j.jbiosc.2015.09.002

Tarr, D. (2012). Nematode antimicrobial peptides. *Invertebrate Survival J.* 9, 122–133.

Tasiemski, A., Massol, F., Cuvillier-Hot, V., Boidin-Wichlacz, C., Roger, E., Rodet, F., et al. (2015). Reciprocal immune benefit based on complementary production of antibiotics by the leech *Hirudo verbana* and its gut symbiont *Aeromonas veronii*. *Sci. Rep.* 5:17498.

Thaler, J.-O., Baghdiguian, S., and Boemare, N. (1995). Purification and characterization of xenorhabdicin, a phage tail-like bacteriocin, from the lysogenic strain F1 of Xenorhabdus nematophilus. *Appl. Environ. Microbiol.* 61, 2049–2052. doi: 10.1128/aem.61.5.2049-2052.1995

Thoms, C., Schupp, P. J., Custódio, M., Lôbo-Hajdu, G., Hajdu, E., and Muricy, G. (2007). Chemical defense strategies in sponges: a review. *Porifera Res. Biodivers. Innov. Sustainabil.* 28, 627–637.

Tobias, N. J., Wolff, H., Djahanschiri, B., Grundmann, F., Kronenwerth, M., Shi, Y.-M., et al. (2017). Natural product diversity associated with the nematode symbionts Photorhabdus and Xenorhabdus. *Nat. Microbiol.* 2, 1676–1685. doi: 10.1038/s41564-017-0039-9

Toro Segovia, L. J., Téllez Ramírez, G. A., Henao Arias, D. C., Rivera Duran, J. D., Bedoya, J. P., and Castaño Osorio, J. C. (2017). Identification and characterization of novel cecropins from the *Oxysternon conspicillatum* neotropic dung beetle. *PLoS One* 12:e0187914. doi: 10.1371/journal.pone.0187914

Touati, I., Ruiz, N., Thomas, O., Druzhinina, I. S., Atanasova, L., Tabbene, O., et al. (2018). Hyporientalin A, an anti-Candida peptaibol from a marine Trichoderma orientale. *World J. Microbiol. Biotechnol.* 34:98.

Tran, E. E. H., and Goodrich-Blair, H. (2009). CpxRA contributes to *Xenorhabdus nematophila* virulence through regulation of lrhA and modulation of insect immunity. *Appl. Environ. Microbiol.* 75, 3998–4006. doi: 10.1128/aem.02657-08

Ullah, I., Khan, A. L., Ali, L., Khan, A. R., Waqas, M., Hussain, J., et al. (2015). Benzaldehyde as an insecticidal, antimicrobial, and antioxidant compound produced by Photorhabdus temperata M1021. *J. Microbiol.* 53, 127–133. doi: 10.1007/s12275-015-4632-4

Ullah, I., Khan, A. L., Ali, L., Khan, A. R., Waqas, M., Lee, I.-J., et al. (2014). An insecticidal compound produced by an insect-pathogenic bacterium suppresses host defenses through phenoloxidase inhibition. *Molecules* 19, 20913–20928. doi: 10.3390/molecules191220913

Ursic-Bedoya, R., Buchhop, J., Joy, J., Durvasula, R., and Lowenberger, C. (2011). Prolixicin: a novel antimicrobial peptide isolated from *Rhodnius prolixus* with differential activity against bacteria and *Trypanosoma cruzi*. *Insect Mol. Biol.* 20, 775–786. doi: 10.1111/j.1365-2583.2011.01107.x

Vallet-Gely, I., Lemaitre, B., and Boccard, F. (2008). Bacterial strategies to overcome insect defences. *Nat. Rev. Microbiol.* 6, 302–313. doi: 10.1038/nrmicro1870

Van Der Does, A. M., Bogaards, S. J., Ravensbergen, B., Beekhuizen, H., Van Dissel, J. T., and Nibbering, P. H. (2010). Antimicrobial peptide hLF1-11 directs granulocyte-macrophage colony-stimulating factor-driven monocyte differentiation toward macrophages with enhanced recognition and clearance of pathogens. *J. Antimicrobial Agents* 54, 811–816. doi: 10.1128/aac.00652-09

van Duin, D., Kaye, K. S., Neuner, E. A., and Bonomo, R. A. (2013). Carbapenem-resistant Enterobacteriaceae: a review of treatment and outcomes. *J. Diagn. Microbiol. Infect. Dis.* 75, 115–120. doi: 10.1016/j.diagmicrobio.2012.11.009

Vilcinskas, A. (2013). Evolutionary plasticity of insect immunity. *J. Insect Physiol.* 59, 123–129. doi: 10.1016/j.jinsphys.2012.08.018

Vogel, H., Müller, A., Heckel, D. G., Gutzeit, H., and Vilcinskas, A. (2018). Nutritional immunology: diversification and diet-dependent expression of antimicrobial peptides in the black soldier fly *Hermetia illucens*. *Dev. Comp. Immunol.* 78, 141–148. doi: 10.1016/j.dci.2017.09.008

Volgyi, A., Fodor, A., Szentirmai, A., and Forst, S. (1998). Phase variation in *Xenorhabdus nematophilus*. *Appl. Environ. Microbiol.* 64, 1188–1193. doi: 10.1128/aem.64.4.1188-1193.1998

Wang, G., Li, X., and Wang, Z. (2016). APD3: the antimicrobial peptide database as a tool for research and education. *Nucleic Acids Res.* 44, D1087–D1093.

Wang, Y., and Gaugler, R. (1999). Steinernema glaseriSurface Coat protein suppresses the immune response of popillia japonica (Coleoptera: Scarabaeidae) Larvae. *Biol. Control* 14, 45–50. doi: 10.1006/bcon.1998.0672

Waterfield, N., George Kamita, S., Hammock, B. D., and Ffrench-Constant, R. (2005). The Photorhabdus Pir toxins are similar to a developmentally regulated insect protein but show no juvenile hormone esterase activity. *FEMS Microbiol. Lett.* 245, 47–52. doi: 10.1016/j.femsle.2005.02.018

Webster, J., Chen, G., Hu, K., and Li, J. (2002). *Entomopathogenic Nematology*. Wallingfort: CABI.

Wesche, F., Adihou, H., Wichelhaus, T. A., and Bode, H. B. (2019). Synthesis and SAR of the antistaphylococcal natural product nematophin from *Xenorhabdus nematophila*. *Beilstein J. Org. Chem.* 15, 535–541. doi: 10.3762/bjoc.15.47

Wiese, J., Abdelmohsen, U. R., Motiei, A., Humeida, U. H., and Imhoff, J. F. (2018). Bacicyclin, a new antibacterial cyclic hexapeptide from Bacillus sp. strain BC028 isolated from *Mytilus edulis*. *Bioorg. Med. Chem. Lett.* 28, 558–561. doi: 10.1016/j.bmcl.2018.01.062

Wu, Q., Patočka, J., and Kuča, K. (2018). Insect antimicrobial peptides, a mini review. *Toxins* 10:461. doi: 10.3390/toxins10110461

Wu, S., Zhang, F., Huang, Z., Liu, H., Xie, C., Zhang, J., et al. (2012). Effects of the antimicrobial peptide cecropin AD on performance and intestinal health in weaned piglets challenged with *Escherichia coli*. *Peptides* 35, 225–230. doi: 10.1016/j.peptides.2012.03.030

Xi, X., Lu, X., Zhang, X., Bi, Y., Li, X., and Yu, Z. (2019). Two novel cyclic depsipeptides Xenematides F and G from the entomopathogenic bacterium *Xenorhabdus budapestensis*. *J. Antibiot.* 72, 736–743. doi: 10.1038/s41429-019-0203-y

Xiao, Y., Meng, F., Qiu, D., and Yang, X. (2012). Two novel antimicrobial peptides purified from the symbiotic bacteria *Xenorhabdus budapestensis* NMC-10. *Peptides* 35, 253–260. doi: 10.1016/j.peptides.2012.03.027

Xing-zhong, L. U., Dan-shu, S., Chun-zhi, G., Xiao-mei, T., and Yu-hui, B. (2016). Isolation and identification of secondary metabolites from *Xenorhabdus budapestensis*. *Nat. Prod. Res. Dev.* 28, 828–832.

Xu, X., Zhong, A., Wang, Y., Lin, B., Li, P., Ju, W., et al. (2019). Molecular identification of a moricin family antimicrobial Peptide (Px-Mor) from Plutella xylostella with activities against the opportunistic human pathogen *Aureobasidium pullulans*. *Front. Microbiol.* 10:2211.

Yang, L. L., Zhan, M. Y., Zhuo, Y. L., Dang, X. L., Li, M. Y., Xu, Y., et al. (2020). Characterization of the active fragments of *Spodoptera litura* Lebocin-1. *Insect Biochem. Physiol.* 103:e21626.

Yang, L.-L., Zhan, M.-Y., Zhuo, Y.-L., Pan, Y.-M., Xu, Y., Zhou, X.-H., et al. (2018). Antimicrobial activities of a proline-rich proprotein from *Spodoptera litura*. *Dev. Comp. Immunol.* 87, 137–146.

Yu, G., Baeder, D. Y., Regoes, R. R., and Rolff, J. (2018). Predicting drug resistance evolution: insights from antimicrobial peptides and antibiotics. *J. Proc. R. Soc. B Biol. Sci.* 285:20172687.

Zanjani, N. T., Miranda-Saksena, M., Cunningham, A. L., and Dehghani, F. (2018). Antimicrobial peptides of marine crustaceans: the potential and challenges of developing therapeutic agents. *Curr. Med. Chem.* 25, 2245–2259.

Zasloff, M. (2002). Antimicrobial peptides of multicellular organisms. *Nature* 415, 389–395.

Zhang, D.-J., Liu, R.-F., Li, Y.-G., Tao, L.-M., and Tian, L. (2010). Two new antifungal cyclic lipopeptides from *Bacillus marinus* B-9987. *Chem. Pharm. Bull.* 58, 1630–1634.

Zhang, L., and Sun, C. (2018). Fengycins, cyclic lipopeptides from marine Bacillus subtilis strains, kill the plant-pathogenic fungus *Magnaporthe grisea* by inducing reactive oxygen species production and chromatin condensation. *Appl. Environ. Microbiol.* 84:e0445-18.

Zhang, S., Liu, Q., Han, Y., Han, J., Yan, Z., Wang, Y., et al. (2019). Nematophin, an antimicrobial dipeptide compound from *Xenorhabdus nematophila* YL001 as a potent biopesticide for Rhizoctonia solani control. *Front. Microbiol.* 10:1765.

Zhao, B.-R., Zheng, Y., Gao, J., and Wang, X.-W. (2020). Maturation of an antimicrobial peptide inhibits aeromonas hydrophila infection in crayfish. *J. Immunol.* 204, 487–497.

Zhao, L., Vo, T. D., Kaiser, M., and Bode, H. (2020). Phototemtide A, a cyclic lipopeptide heterologously expressed from photorhabdus temperata Meg1, shows selective antiprotozoal activity. *Chembiochem* 21, 1288–1292.

Zharkova, M. S., Orlov, D. S., Golubeva, O. Y., Chakchir, O. B., Eliseev, I. E., Grinchuk, T. M., et al. (2019). Application of antimicrobial peptides of the innate immune system in combination with conventional antibiotics—a novel way to combat antibiotic resistance? *J. Front. Cell. Infect. Microbiol.* 9:128.

Zhou, Q., Grundmann, F., Kaiser, M., Schiell, M., Gaudriault, S., and Batzer, A. (2013). Structure and biosynthesis of xenoamicins from entomopathogenic Xenorhabdus. *Chem. A Eur. J.* 19, 16772–16779.

Zhou, Q.-J., Wang, J., Mao, Y., Liu, M., Su, Y.-Q., Ke, Q.-Z., et al. (2019). Molecular structure, expression and antibacterial characterization of a novel antimicrobial peptide NK-lysin from the large yellow croaker *Larimichthys crocea*. *Aquaculture* 500, 315–321.

Conflict of Interest: The authors declare that the research was conducted in the absence of any commercial or financial relationships that could be construed as a potential conflict of interest.

frontiers in Microbiology

ORIGINAL RESEARCH
published: 08 October 2021
doi: 10.3389/fmicb.2021.746006

A Novel Antimicrobial Peptide Sparamosin$_{26-54}$ From the Mud Crab *Scylla paramamosain* Showing Potent Antifungal Activity Against *Cryptococcus neoformans*

Yan-Chao Chen[1], Ying Yang[1], Chang Zhang[1], Hui-Yun Chen[1,2,3], Fangyi Chen[1,2,3] and Ke-Jian Wang[1,2,3]**

[1] State Key Laboratory of Marine Environmental Science, College of Ocean and Earth Sciences, Xiamen University, Xiamen, China, [2] State-Province Joint Engineering Laboratory of Marine Bioproducts and Technology, College of Ocean and Earth Sciences, Xiamen University, Xiamen, China, [3] Fujian Innovation Research Institute for Marine Biological Antimicrobial Peptide Industrial Technology, College of Ocean and Earth Sciences, Xiamen University, Xiamen, China

OPEN ACCESS

Edited by:
András Fodor, University of Szeged, Hungary

Reviewed by:
Jesu Arockiaraj, SRM Institute of Science and Technology, India
Carlos Muñoz-Garay, Universidad Nacional Autónoma de México, Mexico

***Correspondence:**
Fangyi Chen
chenfangyi@xmu.edu.cn
Ke-Jian Wang
wkjian@xmu.edu.cn

Specialty section:
This article was submitted to Antimicrobials, Resistance and Chemotherapy, a section of the journal Frontiers in Microbiology

Received: *23 July 2021*
Accepted: *17 September 2021*
Published: *08 October 2021*

Citation:
Chen Y-C, Yang Y, Zhang C, Chen H-Y, Chen F and Wang K-J (2021) A Novel Antimicrobial Peptide Sparamosin$_{26-54}$ From the Mud Crab Scylla paramamosain Showing Potent Antifungal Activity Against Cryptococcus neoformans. Front. Microbiol. 12:746006. doi: 10.3389/fmicb.2021.746006

Due to the increasing prevalence of drug-resistant fungi and the limitations of current treatment strategies to fungal infections, exploration and development of new antifungal drugs or substituents are necessary. In the study, a novel antimicrobial peptide, named Sparamosin, was identified in the mud crab *Scylla paramamosain*, which contains a signal peptide of 22 amino acids and a mature peptide of 54 amino acids. The antimicrobial activity of its synthetic mature peptide and two truncated peptides (Sparamosin$_{1-25}$ and Sparamosin$_{26-54}$) were determined. The results showed that Sparamosin$_{26-54}$ had the strongest activity against a variety of Gram-negative bacteria, Gram-positive bacteria and fungi, in particular had rapid fungicidal kinetics (killed 99% *Cryptococcus neoformans* within 10 min) and had potent anti-biofilm activity against *C. neoformans*, but had no cytotoxic effect on mammalian cells. The RNA-seq results showed that after Sparamosin$_{26-54}$ treatment, the expression of genes involved in cell wall component biosynthesis, cell wall integrity signaling pathway, anti-oxidative stress, apoptosis and DNA repair were significantly up-regulated, indicating that Sparamosin$_{26-54}$ might disrupt the cell wall of *C. neoformans*, causing oxidative stress, DNA damage and cell apoptosis. The underlying mechanism was further confirmed. Sparamosin$_{26-54}$ could bind to several phospholipids in the cell membrane and effectively killed *C. neoformans* through disrupting the integrity of the cell wall and cell membrane observed by electron microscope and staining assay. In addition, it was found that the accumulation of reactive oxygen species (ROS) increased, the mitochondrial membrane potential (MMP) was disrupted, and DNA fragmentation was induced after Sparamosin$_{26-54}$ treatment, which are all hallmarks of apoptosis. Taken together, Sparamosin$_{26-54}$ has a good application prospect as an effective antimicrobial agent, especially for *C. neoformans* infections.

Keywords: antimicrobial peptide, Sparamosin$_{26-54}$, fungicidal effect, membrane permeability, apoptosis

INTRODUCTION

In addition to the serious threats caused by various virus outbreaks and drug-resistant bacterial infections, fungal infections are also similar headlines today. It is estimated that more than 1 billion people worldwide suffer from fungal diseases (Felix et al., 2017). Most fungal diseases are superficial infections of the skin and nails and mucosal infections of the oral cavity and genital tract, which are readily to diagnose and treat (Brown et al., 2012; Denning and Bromley, 2015). Invasive fungal infections mainly occur in immunocompromised patients, such as those infected with HIV or undergoing chemotherapy, which is associated with unacceptably high mortality (Miceli et al., 2011). It is estimated that nearly 2 million people die from fungal infections each year, and the death toll continues to rise (Pappas et al., 2010; Brown et al., 2012). About 90% of these deaths are caused by species belonging to one of the following four genera: *Cryptococcus*, *Candida*, *Aspergillus*, and *Pneumocystis*. *C. neoformans* is an opportunistic pathogen that exists widely in the environment and is one of the main species causing life-threatening cryptococcal meningitis. Globally, an estimated 223,100 cases of cryptococcal meningitis occur each year, resulting in 181,100 deaths (Rajasingham et al., 2017). Most deaths are reported to occur in low- and middle-income countries due to the lack of essential medicines and the high cost of effective treatment (Loyse et al., 2019).

In the past decades, a series of topical drugs have been used and moderate success has been achieved in the control of many superficial and mucosal infections. However, few drugs are available for invasive fungal infections (Perfect, 2017). Antifungal drugs are more difficult to develop than antibacterial drugs, because fungi are eukaryotes and have a high degree of similarity with mammalian cells, which means that there are relatively few differential targets to be exploited for antifungal drug development (Denning and Bromley, 2015). Currently, only four types of antifungal drugs (polyenes, flucytosine, azoles, and echinocandins) are used orally or intravenously for the treatment of invasive fungal infections in humans (Perfect, 2017). Although existing antifungal drugs are clinically useful, they do have some limitations, such as the development of drug resistance, undesirable side effects and host toxicity. The best example is the polyene antibiotic, amphotericin B, which was first isolated from the fermenter cultures of *Streptomyces nodosus* in 1959 (Dutcher et al., 1959). Amphotericin B has a relatively broad spectrum of action, and is still the drug of choice against serious infections with fungi such as *C. neoformans*, *Candida albicans,* or *Aspergillus fumigatus* (Lemke et al., 2005; Iyer et al., 2021). Like other polyene antibiotics, amphotericin B preferentially binds to ergosterol, which is the main sterol in fungal cell membranes, resulting in the disruption of cell membrane integrity (Campoy and Adrio, 2017). However, fungi can develop resistance to amphotericin B by reducing the content of ergosterol in the cell membrane. In recent years, some amphotericin B-resistant strains have been reported, including *C. neoformans*, *C. albicans,* and *A. fumigatus* (Ellis, 2002; Perlin et al., 2017). In addition, the adverse effects of amphotericin B are common, with nephrotoxicity being the most serious side effect (Fanos and Cataldi, 2000). Therefore, new antifungal agents are urgently needed to address the global threats of fungal pathogens and the limitations of existing antifungal drugs.

Antimicrobial peptides (AMPs) are considered to be natural antibiotics, which can be found in animals, plants and microorganisms, and function as the first line of host defense against the invasion of exogenous pathogen (Zasloff, 2002; Peschel and Sahl, 2006). They exert broad spectrum of activity against Gram-negative and Gram-positive bacteria, fungi, parasites, viruses and even antibiotic-resistant strains. The typical mechanism of AMPs action is to interact with cell membrane of microorganism through electrostatic interactions, causing membrane disruption, cytoplasmic leakage, and ultimately cell death. The proposed membrane disruption models include barrel-stave model, carpet model and toroidal-pore model (Brogden, 2005). Some AMPs also interfere with many important cellular functions, such as inhibition of cell wall synthesis, inhibition of nucleic-acid synthesis, inhibition of protein synthesis, inhibition of septum formation and inhibition of enzymatic activity (Brogden, 2005). Interestingly, the antimicrobial mechanism of AMPs is different from most clinically antibiotics that only target cell membrane/wall components (Rautenbach et al., 2016). This interactions with the fundamental physiological structure and multi-target modes make it difficult for microorganisms to develop resistance (Yeung et al., 2011), making AMPs the most promising potential alternative for conventional antibiotics.

Crustaceans are a group of invertebrates that only rely on the innate immune system to defend them against invading pathogenic microorganisms. The innate immune system of crustaceans is comprised of cellular and humoral responses. In terms of humoral responses, AMPs are one of the main effectors to eliminate pathogenic microorganisms (Rowley and Powell, 2007). There is clear evidence that many AMPs with potent antibacterial activity have been isolated from crustaceans, such as anti-lipopolysaccharide factors (ALFs), Hyastatin, scygonadin, Sphistin, etc. (Wang et al., 2007; Sperstad et al., 2009b; Liu et al., 2012; Chen et al., 2015). However, the number of AMPs with effective activity against fungi is reported to be very limited. Penaeidins, a family of cationic AMPs were isolated from shrimps, such as *Litopenaeus vannamei* (Destoumieux et al., 1997; Gueguen et al., 2006). The recombinant penaeidins (Pen-2 and Pen-3a) exhibit not only antibacterial activity against Gram-positive bacteria, but also antifungal activity against several filamentous fungi (including *Fusarium oxysporum*, which caused infections in penaeid shrimps) (Destoumieux et al., 1999; Shockey et al., 2009). Crustins are another well-studied AMPs with antifungal activity in crustaceans, which are cationic and cysteine-rich AMPs containing a whey acidic protein (WAP) domain in the C-terminus (Smith et al., 2008). A crustin gene, Cru*Ha*1 from the spider crab *Hyas araneus*, had moderate activity against *S. cerevisiae* and weak activity against *C. albicans* (Sperstad et al., 2009a). Several AMPs currently identified from crustaceans have antibacterial activity as well as antifungal activity, however, their antifungal mechanism has not yet been revealed. In addition, there are

more new antifungal peptides from crustaceans waiting to be discovered and studied.

In this study, we screened a new antimicrobial peptide based on the transcriptome database of the mud crab *S. paramamosain* established in our laboratory, and named it Sparamosin. The full-length cDNA sequence of Sparamosin gene was obtained. Sparamosin mature peptide and its two truncated peptides (Sparamosin$_{1-25}$ and Sparamosin$_{26-54}$) were chemically synthesized, and their *in vitro* antimicrobial activity were determined. Among these three peptides, Sparamosin$_{26-54}$ showed the strongest antimicrobial activity, which was used to carry out a series of follow-up studies, such as evaluating its anti-biofilm activity. To investigate the antifungal mechanism of Sparamosin$_{26-54}$ against *C. neoformans*, RNA-seq was used to identify the differentially expressed genes and the pathways involved. Confocal laser scanning microscopy, scanning electron microscope and transmission electron microscope were used to provide further evidence on the antifungal mechanism of Sparamosin$_{26-54}$ against *C. neoformans*. This study will provide basic information for the development of new antifungal drugs.

MATERIALS AND METHODS

Animals and Microorganisms

Mud crabs (*S. paramamosain*) were obtained from Zhangpu Fish Farm (Fujian, China), and testes from male crabs (body weight 300 ± 10 g) were used for RNA extraction. All commercially available strains used in this study were purchased from China General Microbiological Culture Collection Center (CGMCC), including *Pseudomonas fluorescens* (CGMCC NO. 1.3202), *Pseudomonas stutzeri* (CGMCC NO. 1.1803), *Pseudomonas aeruginosa* (CGMCC NO. 1.2421), *Acinetobacter baumannii* (CGMCC NO. 1.6769), *Escherichia coli* (CGMCC NO. 1.2385), *Staphylococcus aureus* (CGMCC NO. 1.2465), *Staphylococcus epidermidis* (CGMCC NO. 1.4260), *Bacillus cereus* (CGMCC NO. 1.3760), *Enterococcus faecium* (CGMCC NO. 1.131), *Enterococcus faecalis* (CGMCC NO. 1.2135), *C. neoformans* (CGMCC NO. 2.1563), *Aspergillus niger* (CGMCC NO. 3.316), *A. fumigatus* (CGMCC NO. 3.5835), *Fusarium graminearum* (CGMCC NO. 3.4521), and *F. oxysporum* (CGMCC NO. 3.6785). The bacterial strains were cultured in nutrient broth at 37°C, and the fungal strains were grown in potato dextrose agar (PDA) at 28°C. All experiments were carried out in strict accordance with the guidelines of the standard biosecurity and institutional safety procedures established by Xiamen University.

Cloning the Full-Length cDNA of Sparamosin

Rapid amplification of cDNA ends (RACE) PCR was performed to obtain the full-length cDNA of Sparamosin. Total RNA from the testes of normal mature crabs was extracted using TRIzol™ reagent (Invitrogen, United States) and cDNA was synthesized using PrimeScript™ RT reagent Kit with a gDNA Eraser Kit (Takara, China). In addition, RACE cDNA was prepared using SMARTer® RACE 5′/3′ Kit (Takara, China) and was used as a template for PCR. Gene-specific primers (**Supplementary Table 1**) were designed based on the obtained partial cDNA sequence from transcriptome database established by our laboratory to amplify the target gene, and the fragment was recombined into pMD18-T Vector (Takara, China) and sequenced by Bioray biotechnology (Xiamen, China).

Sequence Analysis, Peptides Design, and Synthesis

The signal peptide of Sparamosin was predicted by SignalP-4.1 Server[1] and the second structure of the mature peptide was predicted by PSIPRED 4.0.[2] The mature peptide was truncated between residue Ser^{25} and residue Gly^{26} to evaluate the antimicrobial activity of different helical regions. The physicochemical parameters of the peptides, such as molecular weight, theoretical isoelectric point, net positive charge and hydropathicity were predicted by ProtParam.[3] The total hydrophobicity was calculated through the Antimicrobial Peptide Database.[4] The peptides used in this study were chemically synthesized by Genscript (Nanjing, China). The purity and molecular weight of the peptides were further confirmed by high performance liquid chromatography and mass spectrometry, respectively. The powdered peptide could be stored for a long time at −80°C. The stock solutions were kept at −20°C for storage.

Antimicrobial Activity Assay

The antimicrobial activity was determined three times, each time in triplicate, in 96-well microplates according to previous reports with some modifications (Vitale et al., 2002; Wiegand et al., 2008; Castro et al., 2018). Briefly, microorganisms were harvested during their logarithmic growth phase and diluted in Mueller-Hinton broth to approximately 1×10^6 CFU/mL (bacteria) or diluted in RPMI 1640 medium buffered with 0.165 mol/L 3-morpholinopropane-1-sulfonic acid (pH 7.0, referred to as RPMI-MOPS) to approximately 2×10^4 cells/mL (yeasts or conidia of filamentous fungi). Then, the microbial suspension was added to each well and incubated with serial diluted peptides. The microplates were incubated in the dark at 37°C for 24 h (bacteria) or at 28°C for 48 h (yeasts or conidia of filamentous fungi). The minimum inhibitory concentration (MIC), minimum bactericidal concentration (MBC), and minimum fungicidal concentration (MFC) values were determined as previously described (Shan et al., 2016).

Cytotoxicity Assay

The cytotoxicity of Sparamosin$_{26-54}$ was determined on mouse hepatocytes (AML 12 cells) and human hepatocytes (L02 cells). CellTiter 96® AQ$_{ueous}$ one solution Cell Proliferation assay (Promega, United States) was used to assess cell viability. Briefly, 100 μL of AML 12 or L02 cells were seeded in 96-well microplates at 10^4 cells/well and incubated at 37°C overnight under 5%

[1]http://www.cbs.dtu.dk/services/SignalP/

[2]http://bioinf.cs.ucl.ac.uk/psipred/

[3]https://web.expasy.org/protparam/

[4]https://aps.unmc.edu/

CO_2. Then, the cells were incubated at 37°C for 24 h in a culture medium supplemented with various concentrations of Sparamosin$_{26-54}$ (0, 0.1, 1, 10, 100 μg/mL). After incubation, the cells were treated with 20 μL of MTS-PMS reagent for another 2 h, and then the absorbance value of each well was measured at 492 nm (Tecan, Switzerland).

Biofilm Inhibition Assays

The biofilm inhibition assays were performed in 96-well microplates according to previous reports with some modifications (Berditsch et al., 2015; Poonam et al., 2017). For the biofilm formation assay, *C. neoformans* cells were harvested in the logarithmic phase, diluted in RPMI-MOPS medium to a final cell density of approximately 1×10^6 cells/mL, and then aliquoted into microplates. Serially diluted concentrations of Sparamosin$_{26-54}$ were added to the wells, and the microplates were incubated at 35°C for 72 h without shaking to allow biofilm formation. The biofilm mass was evaluated by crystal violet (CV) staining as previously described (Berditsch et al., 2015). In experiments with preformed biofilms, *C. neoformans* cells were incubated at 35°C for 72 h without shaking to allow biofilm formation. Thereafter, RPMI-MOPS medium containing Sparamosin$_{26-54}$ and resazurin (final concentration 0.1 mM) was added to the wells, and the microplates were incubated at 35°C for another 24 h. The respiratory activity of cells in biofilm was evaluated by a modified resazurin assay as previously described (Berditsch et al., 2015).

Transcriptome Analysis of *C. neoformans* After Sparamosin$_{26-54}$ Treatment

C. neoformans suspensions at approximately 1×10^7 cells/mL in RPMI-MOPS were incubated with different concentrations of Sparamosin$_{26-54}$ (6, 12 μM) at 28°C for 1 h. Then, the cells were harvested for RNA extraction. Approximately 200 μL of freeze-dried cells were grinded in liquid nitrogen and the total RNA was isolated using TRIzol reagent. RNA-Seq was performed by Novogene Corporation (Beijing, China) using the Illumina NovaSeq platform, which could generate 150 bp paired-end reads. Reference genome and gene model annotation files of *C. neoformans* var. *neoformans* JEC21 were downloaded from GenBank (GCA_000091045.1). An index of the reference genome was constructed using Hisat2 (version 2.0.5), and paired-end clean reads were aligned with the reference genome using Hisat2 (version 2.0.5). FeatureCounts (version 1.5.0-p3) was used to calculate the number of reads mapped to each gene. The expected number of fragments per kilobase of transcript sequence per million base pairs sequenced (FPKM) for each gene was calculated based on the length of the gene and the count of reads mapped to that gene. Differential expression analysis of the two groups was performed using the DEGSeq2 R package (version 1.16.1). The *p*-value was adjusted using the Benjamini and Hochberg's method. The corrected *p*-value < 0.05 and $|\log_2(\text{Fold change})| > 1$ were set as thresholds for significant differential expression. The gene ontology (GO) enrichment analysis of differentially expressed genes (DEGs) was implemented by the clusterProfiler R package (version 3.4.4). GO terms with a corrected *p*-value < 0.05 were considered significantly enriched by DEGs.

To verify the results of RNA-Seq, five up-regulated genes encoding chitin synthase (CNA05300), Rho1 GTPase (CNG02630), catalase (CNL06020), DNA supercoiling (CND02890) and caspase (CNB00130) and six down-regulated genes encoding C-22 sterol desaturase (CNF03720), NADH dehydrogenase (CND01070), succinate dehydrogenase (CNA03530), ubiquinol-cytochrome *c* reductase complex core protein 2 (CNL04470), cytochrome *c* oxidase subunit V (CNK03240) and ATP synthase subunit alpha (CNF02280) were selected for quantitative real-time PCR (qRT-PCR). The qRT-PCR reactions were performed on qTOWER 2.2 real time PCR system (Analytik Jena AG, Germany) according to the FastStart Universal SYBR Green Master (ROX) kit (Roche, Switzerland) protocol. The cycling conditions were 50°C for 2 min, 95°C for 10 min, followed by 40 cycles of 95°C for 15 s, 60°C for 1 min. Gene expression levels were calculated using the $2\text{-}\Delta\Delta^{Ct}$ method (Livak and Schmittgen, 2001) and normalized to the abundance of the house-keeping gene *actin*. The primers of target genes were listed in **Supplementary Table 2**.

Localization of Sparamosin$_{26-54}$ in *C. neoformans*

The analysis of the localization of Sparamosin$_{26-54}$ in *C. neoformans* was carried out based on the previous report with slight modifications (Zhang et al., 2019). Briefly, *C. neoformans* cells were harvested in the logarithmic phase and washed with 10 mM sodium phosphate buffer (NaPB, pH 7.4). The cells were diluted in the same buffer to a final cell density of approximately 1×10^7 cells/mL, and incubated with 24 μM FITC-labeled Sparamosin$_{26-54}$ [synthesized by GL Biochem (Shanghai, China)] at room temperature for 30 min. After incubation, the cells were washed twice with 10 mM NaPB to remove unbound peptide. A confocal laser scanning microscopy (Zeiss, Germany) were used for imaging.

Protein-Phospholipid Interaction Assay

The polyclonal antibody of Sparamosin was prepared by GenScript (Nanjing, China) using the antigen site KVQHSIFSGLGPNPC, which was designed and optimized by OptimumAntigen Design Tool. The Sparamosin$_{26-54}$-phospholipid interactions were determined using PIP Strips™ (Echelon Biosciences, United States) according to the protocol. Briefly, the membrane was blocked with 3% (wt/vol) BSA at room temperature for 1 h, and then incubated with 2 μg/mL Sparamosin$_{26-54}$ at room temperature for 1 h. Then, the membrane was incubated with Sparamosin antibody (1:1,000, diluted in 1% [wt/vol] BSA) at room temperature for 2 h. After washing with PBST several times, the membrane was then incubated with HRP conjugated goat anti-rabbit IgG (1:5,000, diluted in 1% [wt/vol] BSA) at room temperature for 40 min. The peptides were visualized on a chemiluminescent imaging system (Tanon Science and Technology, United States) using immobilon™ western chemiluminescent HRP substrate (Millipore, United States).

Time-Killing Kinetics

The time-killing kinetics assay was carried out as previous described (Shan et al., 2016). Briefly, *C. neoformans* cells were diluted in RPMI-MOPS medium to a final cell density of approximately 1×10^6 cells/mL. Sparamosin$_{26-54}$ was incubated with *C. neoformans* at a concentration of 1 × or 2 × MIC. The culture was sampled diluted and plated on PDA plates at different time points. After 48 h of incubation, the surviving colonies were counted, and the untreated group was used as a control. The experiments were conducted three times independently.

Scanning Electron Microscope Analysis

The effect of Sparamosin$_{26-54}$ on *C. neoformans* was observed using SEM as described earlier (Datta et al., 2016). Briefly, *C. neoformans* cells were harvested in the logarithmic phase and resuspended at approximately 1×10^7 cells/mL in NaPB, and incubated with 24 μM Sparamosin$_{26-54}$ at room temperature for 1 h. After incubation, the cells were fixed with 2.5% (vol/vol) glutaraldehyde at 4°C for 2 h and washed three times before being placed on poly-L-lysine coated glass slides at 4°C for 30 min. The cells were subsequently dehydrated in a graded series of ethanol (30, 50, 70, 90, 95, and 100%), for 15 min each. Thereafter, the samples were dehydrated with tertiary butanol followed by freezing at 4°C and lyophilized using the critical point dryer. Finally, the specimens were coated with gold and observed under a field emission scanning electron microscope (Zeiss SUPRA 55, Germany).

Transmission Electron Microscope Analysis

The TEM analysis was carried out based on the previous report with slight modifications (Chen et al., 2003). Briefly, *C. neoformans* cells were prepared and incubated with Sparamosin$_{26-54}$ as described above for SEM analysis. After pre-fixation with 2.5% glutaraldehyde at 4°C overnight, the *C. neoformans* cells were washed three times with NaPB and then post-fixed with 1% osmium tetroxide at 4°C for 2.5 h. The fixed samples were washed three times with NaPB, dehydrated in a graded ethanol series (30, 50, 70, 90, and 100%), transferred to a graded mixture of absolute acetone and epoxy resin, and finally immersed in pure epoxy resin in a constant-temperature incubator overnight. Finally, the samples were sectioned using an ultramicrotome, stained with uranyl acetate and lead citrate, and observed using a transmission electron microscope (FEI, United States).

Live-Dead Staining Assay

The integrity of the cell membrane after Sparamosin$_{26-54}$ treatment was determined by live-dead staining according to the protocol of a LIVE/DEAD® FungaLight™ Yeast Viability Kit (Invitrogen, United States). Briefly, *C. neoformans* cells were prepared and incubated with Sparamosin$_{26-54}$ as described above for SEM analysis. After incubation, the cells were washed twice with PBS and placed on poly-L-lysine slides at room temperature for 15 min. The cells were washed twice and then stained with SYTO® 9 and PI for 15 min in the dark. Fluorescent images were obtained with a confocal laser scanning microscopy (Zeiss, Germany).

Calcein Leakage Assay

The calcein leakage assay was carried out according to a previous report with the following modifications (Vylkova et al., 2007). Briefly, *C. neoformans* cells were harvested in the logarithmic phase and washed with 10 mM NaPB. The cells were diluted in 10 mM NaPB to a final cell density of approximately 1×10^7 cells/mL and loaded with Calcein-AM (Thermo Fisher Scientific, United States) at a final concentration of 5 μM at room temperature for 2 h. Then, the cells were washed three times with 10 mM NaPB to remove unincorporated dye. Different concentrations of Sparamosin$_{26-54}$ (from 6 to 48 μM) were incubated with calcein-loaded cells in a 96-well microplate for analysis. In a microplate reader (Tecan, Switzerland), the fluorescence intensity of the induced calcein release was recorded every 15 min at the excitation and emission wavelengths of 485 nm and 530 nm, respectively. Percent leakage was calculated using the formula: percentage leakage (%) = $(F_{sample} - F_0)/(F_T - F_0) \times 100$. Where F_{sample} is the fluorescence intensity after adding Sparamosin$_{26-54}$, and F_0 is the fluorescence intensity determined by measuring the amount of calcein released from loaded cells without peptide treatment in 240 min, and F_T is the maximum fluorescence intensity measured after the cells were boiled for 10 min. After boiling, the fluorescence intensity of calcein-loaded *C. neoformans* was assumed to be equal to the total potentially available intracellular calcein.

DNA and ATP Release Assay

C. neoformans suspensions at 1×10^7 cells/mL in RPMI-MOPS were incubated with different concentrations of Sparamosin$_{26-54}$ (6, 12, and 24 μM) at 28°C for 0.5, 1, and 2 h. Then, the yeasts were collected by centrifugation, and the supernatant was subjected to DNA quantitative analysis in a NanoDrop 2000 spectrophotometer (Thermo Fisher Scientific, United States), or an ATP determination kit (Invitrogen, United States) for quantitative analysis of ATP, as described previously (Castro et al., 2018; Liu et al., 2020).

Apoptosis Analysis

The production of intracellular reactive oxygen species (ROS) was measured by fluorometric assay using 2,7-dichlorofuorescin diacetate (DCFH-DA), as described previously (Hwang et al., 2011b). Briefly, *C. neoformans* suspensions at 1×10^7 cells/mL in RPMI-MOPS were incubated with Sparamosin$_{26-54}$ (6, 12 μM) or 20 mM H_2O_2 at 28°C for 1 h. After incubation, the cells were washed with PBS and then stained with 10 μM of DCFH-DA (Nanjing Jiancheng Bioengineering Institute, China). The cells were then harvested and observed under fluorescence microscopy (Zeiss, Germany).

The mitochondrial membrane potential (MMP) was determined by fluorometric assay using 3,3′-dihexyloxacarbocyanine iodide $DiOC_6(3)$, as mentioned earlier (Hwang et al., 2011b). Briefly, *C. neoformans* suspensions at 1×10^7 cells/mL in RPMI-MOPS were incubated with Sparamosin$_{26-54}$ (6, 12 μM) or 20 mM H_2O_2 at 28°C for 3 h.

After incubation, the cells were washed with PBS, and incubated with 2 ng of $DiOC_6(3)$ (Sigma, United States) at 28°C for 30 min. The cells were then harvested and analyzed by flow cytometer (Becton Dickinson, United States).

Terminal deoxynucleotidyl transferase-mediated dUTP-nick end labeling (TUNEL) assay was carried out as described previously (Castro et al., 2018). Briefly, *C. neoformans* suspensions at 1×10^7 cells/mL in RPMI-MOPS were incubated with Sparamosin$_{26-54}$ (6, 12 μM) or amphotericin B (4 μg/mL) at 28°C for 24 h. After incubation, the cells were washed with PBS and fixed with 2% formaldehyde in PBS at room temperature for 30 min. Then, the cells were permeabilized with 0.1% Triton X-100 for 30 min and subjected to TUNEL reaction using one step TUNEL apoptosis assay kit (Beyotime, China), according to the manufacturer's instructions. Finally, all samples were examined by fluorescence microscopy (Zeiss, Germany).

Statistical Analysis

All data were represented as mean ± standard error of mean. Statistical analysis was performed with Student's *t*-test using GraphPad Prism 6 (GraphPad Software Inc., United States) and SPSS 25 (IBM Corp., United States). Two-tailed *p*-values were used for all analyses, and a p-value < 0.05 was considered statistically significant. Transcriptome analysis was performed using Novomagic (Novogene, China). Pearson analysis was used to correlate gene expression determined by RNA-seq and qRT-PCR.

RESULTS

Sequence Analysis and Truncated Peptides Design

The full-length cDNA sequence of Sparamosin was obtained (Genbank accession number MH423837). This gene consists of a 5′ untranslated region (UTR) of 181 bp, an open reading frame (ORF) of 231 bp and a 3′ UTR of 161 bp. The ORF of Sparamosin encodes a 76-amino acid protein, which contains a putative 22-amino acid signal peptide and a 54-amino acid mature peptide (**Figure 1A**). No similar nucleotide or amino acid sequence was found to match this sequence in the existing online databases, indicating that it is an uncharacterized protein. Two truncated peptides, Sparamosin$_{1-25}$ and Sparamosin$_{26-54}$ (which located in the 1st to 25th and 26th to 54th amino acid of the mature peptide, respectively), were designed and synthesized based on the secondary structure of Sparamosin mature peptide, which has two predicted α-helices located at residues Ile^{13}-Phe^{24} and residues Pro^{31}-Arg^{39}, respectively (**Figures 1B,C**). The key physicochemical parameters of Sparamosin and its truncated peptides were shown in **Figure 1D**. In addition, the peptide sequences of Cecropin A (Steiner et al., 1981), Magainin II (Zasloff, 1987), and LL-37 (Gudmundsson et al., 1996) were also analyzed as comparative controls. The measured molecular weights of Sparamosin and its truncated peptides were consistent with their theoretical values, indicating that these peptides were successfully synthesized. The hydrophobic residue ratio of six peptides ranged from 32 to 45%, the net charge ranged from −3 to + 6, and the hydrophobic moment ranged from 0.105 to 0.521. The results showed that unlike the other two synthetic peptides (Sparamosin and Sparamosin$_{1-25}$), the physicochemical parameters of Sparamosin$_{26-54}$ have values closer to those defined for AMP.

The Truncated Peptide Sparamosin$_{26-54}$ Has Potent and Broad-Spectrum Antimicrobial Activity Without Cytotoxicity

Our preliminary study on six commercially available CGMCC strains showed that Sparamosin$_{26-54}$ displayed stronger antimicrobial activity than Sparamosin, while no antimicrobial activity of Sparamosin$_{1-25}$ was observed in the tested strains (**Supplementary Table 3**). Then, we further evaluated the antimicrobial efficacy of Sparamosin$_{26-54}$ by determining its MIC, MBC and MFC against a series of strains. As shown in **Table 1**, Sparamosin$_{26-54}$ displayed a broad-spectrum antibacterial activity against several Gram-negative (*P. fluorescens*, *P. stutzeri*, *P. fluorescens*, *A. baumannii*, *E. coli*) and Gram-positive (*S. aureus*, *S. epidermidis*, *B. cereus*, *E. faecium*, *E. faecalis*) bacteria with MIC values in the range of 6–48 μM, as well as the MBC values lower than 48 μM. In addition, Sparamosin$_{26-54}$ showed a profound inhibitory effect against a pathogenic fungus *C. neoformans*, and could inhibit the conidial germination of several filamentous fungi, such as *A. niger*, *A. fumigatus*, *F. graminearum,* and *F. oxysporum* with MIC values in the range of 6–24 μM. However, it was not cytotoxic to mammalian cells tested (AML12 and L02 cells) (**Supplementary Figures 1A,B**), indicating that Sparamosin$_{26-54}$ had good biocompatibility.

Sparamosin$_{26-54}$ Has Anti-biofilm Activity Against *C. neoformans*

Since Sparamosin$_{26-54}$ showed good activity against planktonic *C. neoformans* cells, we further evaluated whether Sparamosin$_{26-54}$ could inhibit *C. neoformans* biofilm formation. The biofilm mass of *C. neoformans* was quantified by CV staining, and the results were shown in **Figures 2A,B**. The concentration of Sparamosin$_{26-54}$ required to inhibit *C. neoformans* biofilm formation was 12 μM. At a concentration of 48 μM, the inhibition rate of biofilm formation was more than 90%. In addition, we used the redox indicator resazurin to monitor the respiratory activity of the preformed *C. neoformans* biofilms treated with Sparamosin$_{26-54}$. The results showed that Sparamosin$_{26-54}$ could inhibit the respiration of *C. neoformans* in preformed biofilms. At a concentration of 48 μM, the inhibition rate of respiratory activity exceeded 50% (**Figures 2C,D**). These results suggested that Sparamosin$_{26-54}$ exhibited potent anti-biofilm activity against *C. neoformans*.

The Molecular Response of *C. neoformans* to Sparamosin$_{26-54}$

To build a comprehensive model of *C. neoformans* response to Sparamosin$_{26-54}$, RNA sequencing was used to determine DEGs in response to treatment with a low dose of Sparamosin$_{26-54}$.

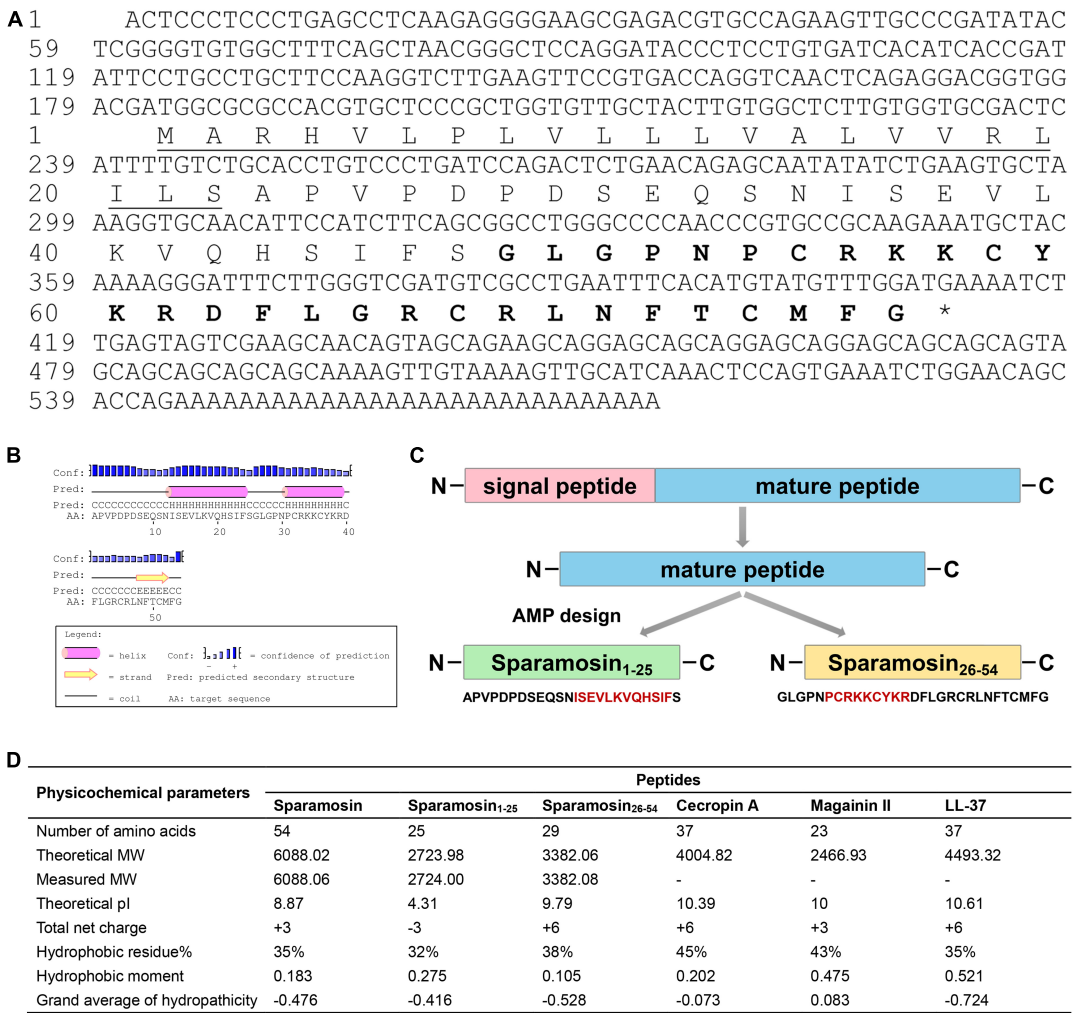

D

Physicochemical parameters	Peptides					
	Sparamosin	Sparamosin$_{1-25}$	Sparamosin$_{26-54}$	Cecropin A	Magainin II	LL-37
Number of amino acids	54	25	29	37	23	37
Theoretical MW	6088.02	2723.98	3382.06	4004.82	2466.93	4493.32
Measured MW	6088.06	2724.00	3382.08	-	-	-
Theoretical pI	8.87	4.31	9.79	10.39	10	10.61
Total net charge	+3	-3	+6	+6	+3	+6
Hydrophobic residue%	35%	32%	38%	45%	43%	35%
Hydrophobic moment	0.183	0.275	0.105	0.202	0.475	0.521
Grand average of hydropathicity	-0.476	-0.416	-0.528	-0.073	0.083	-0.724

FIGURE 1 | Sequence analysis and peptide design process. **(A)** Full-length cDNA and deduced amino acid sequence of Sparamosin. The underline indicates the putative signal peptide. The amino acid sequence of Sparamosin$_{26-54}$ is shown in bold. The cDNA sequence has been deposited in GenBank and the accession number is MH423837. **(B)** The predicted secondary structure of Sparamosin mature peptide. There are two predicted α-helices located at residues Ile^{13}-Phe^{24} and residues Pro^{31}-Arg^{39}, respectively. **(C)** The design process of truncated peptide. The red amino acid sequence represents the predicted α-helix structure. **(D)** The key physicochemical parameters of Sparamosin mature peptide and its truncated peptides, Cecropin A, Magainin II, and LL-37 were calculated by using online tools. Their molecular weight (MW) were measured by electrospray ionization mass spectrometry (ESI-MS).

We obtained 2,573 genes (up-regulated, 1,474; down-regulated, 1,099) and 3,157 genes (up-regulated, 1,602; down-regulated, 1,555) that were differentially expressed after 0.25 × and 0.5 × MIC Sparamosin$_{26-54}$ treatment, respectively (**Supplementary Tables 4**, **5**). Overlapping analysis showed that 1,330 genes were commonly up-regulated under both Sparamosin$_{26-54}$ concentrations tested, while 1,023 genes were commonly down-regulated under the same conditions (**Figure 3A** and **Supplementary Tables 6**, **7**). To further investigate the biological processes involving these up-regulated or down-regulated genes, two DEG lists were separately analyzed for enrichment of GO terms. Genes up-regulated after Sparamosin$_{26-54}$ treatment were associated with several significantly enriched biological processes, including cell wall organization or biogenesis, transmembrane transport, lipid oxidation, DNA repair, etc. (**Supplementary Table 8**). In the biological process category of the down-regulated genes, translation and metabolic processes were significantly enriched (**Supplementary Table 8**). **Figure 3B** is a heatmap showing the up-regulated genes involved in the biosynthesis of cell wall component, CWI signaling pathway, anti-oxidative stress, apoptosis and DNA repair, as well as the downregulated genes involved in the ergosterol biosynthesis pathway and mitochondrial oxidative phosphorylation in *C. neoformans* cells after Sparamosin$_{26-54}$ treatment. To verify the RNA-Seq results, a total of 11 genes were selected including 5 up-regulated and 6 down-regulated from DGEs for qRT-PCR analysis. As shown in **Figures 3C,D**, the qRT-PCR results showed that the expression patterns of selected genes were consistent to those obtained by RNA-seq and the Pearson correlation analysis revealed that these

TABLE 1 | Antimicrobial activity of synthetic Sparamosin$_{26-54}$.

Microbial strains	CGMCC No.[a]	MIC[b] (μM)	MBC[c]/MFC[d] (μM)	MIC (μM)
Gram-negative bacteria		**Sparamosin$_{26-54}$**		**LL-37**
Pseudomonas fluorescens	1.3202	6–12	12–24	3–6
Pseudomonas stutzeri	1.1803	6–12	12–24	3–6
Pseudomonas aeruginosa	1.2421	12–24	24–48	12–24
Acinetobacter baumannii	1.6769	12–24	12–24	3–6
Escherichia coli	1.2385	24–48	24–48	6–12
Gram-positive bacteria		**Sparamosin$_{26-54}$**		**LL-37**
Staphylococcus aureus	1.2465	12–24	24–48	6–12
Staphylococcus epidermidis	1.4260	6–12	12–24	6–12
Bacillus cereus	1.3760	24–48	>48	12–24
Enterococcus faecium	1.131	6–12	6–12	3–6
Enterococcus faecalis	1.2135	12–24	12–24	3–6
Fungi		**Sparamosin$_{26-54}$**		**Amphotericin B**
Cryptococcus neoformans	2.1563	6–12	12–24	0.12–0.24
Aspergillus niger	3.316	6–12	>48	0.12–0.24
Aspergillus fumigatus	3.5835	12–24	>48	0.24–0.48
Fusarium graminearum	3.4521	6–12	>48	0.12–0.24
Fusarium oxysporum	3.6785	6–12	>48	0.12–0.24

[a]*CGMCC NO., China General Microbiological Culture Collection Center Number.* [bcd]*The values of MIC and MBC/MFC are expressed as the interval [a]-[b]. [a] is the highest concentration with visible microbial growth in the tested, and [b] is the lowest concentration with no visible microbial growth.*

genes were significantly correlated between the RT-qPCR and RNA-seq (Pearson correlation coefficient > 0.98). Thus, the qRT-PCR results confirmed the reliability of the RNA-Seq data.

Sparamosin$_{26-54}$ Exerts Its Antifungal Activity Through Targeting Fungal Membrane

In many cases, binding to the surface of fungal cell is the first step for AMPs to kill fungi. Therefore, we hypothesized that Sparamosin$_{26-54}$ might directly bind to the cell surface of *C. neoformans*. To test this hypothesis, the distribution of Sparamosin$_{26-54}$ in *C. neoformans* was investigated by FITC-labeled Sparamosin$_{26-54}$. As shown in **Figure 4A**, the fluorescence of FITC-labeled Sparamosin$_{26-54}$ was mainly located on the cell surface, indicating that Sparamosin$_{26-54}$ might interact with the cell walls/membranes. To further determine the binding properties of Sparamosin$_{26-54}$ to cell wall or cell membrane components, a modified ELISA assay and chitin-binding assay were performed. The results showed that Sparamosin$_{26-54}$ could not bind glucan or chitin (data not shown). Next, we assessed the ability of Sparamosin$_{26-54}$ to bind different bioactive membrane phospholipids using the protein-phospholipid interaction assay. As shown in **Figures 4B,C**, Sparamosin$_{26-54}$ strongly bound to phosphoinositides (PIPs) and phosphatidic acid (PA), but weakly bound to a variety of other phospholipids, including lysophosphatidic acid (LPA), lysophosphocholine (LPC), phosphatidylinositol (PI), phosphatidylethanolamine (PE), phosphatidylcholine (PC), sphingosine 1-phosphate (S1P), and phosphatidylserine (PS). These results suggest that Sparamosin$_{26-54}$ might bind to fungal cell membrane rather than cell wall.

The time-killing curves for Sparamosin$_{26-54}$ on *C. neoformans* was determined at the concentrations of 1 × and 2 × MIC. As shown in **Figure 5A**, Sparamosin$_{26-54}$ showed rapid killing activity against *C. neoformans* and completely killed the fungus within 10 min. This rapid fungicidal rate indicated that Sparamosin$_{26-54}$ might kill *C. neoformans* by disrupting the integrity of cell membrane. To further evaluate the effect of Sparamosin$_{26-54}$ on the permeability of the *C. neoformans* cell membrane, the release of calcein, DNA and ATP were measured. As shown in **Figure 5B**, when exposed to Sparamosin$_{26-54}$, calcein leaked from calcein-loaded *C. neoformans* in a time- and concentration-dependent manner. In addition, Sparamosin$_{26-54}$ increased the amount of DNA and ATP detected in the supernatant of the *C. neoformans* suspensions (**Figures 5C,D**). Then, we employed SEM and TEM to observe the changes in the morphology and ultrastructure of *C. neoformans* cells after Sparamosin$_{26-54}$ treatment (**Figures 6A,B**). The SEM images of the peptide-treated cells showed that Sparamosin$_{26-54}$ had a morbid effect on *C. neoformans* cells surface. After treatment with 24 μM Sparamosin$_{26-54}$ for 1 h, the surface of the fungal cells became rough and corrugated. In contrast, the control cells that were not treated with Sparamosin$_{26-54}$ exhibited a bright and smooth surface. The TEM image of the peptide-treated cells clearly showed the disruption of cell wall and cell membrane and the leakage of intracellular contents, while the fungal cells in the control group showed an intact cell wall and cell membrane and a homogeneous cytoplasm. SYTO 9 can enter all yeasts regardless of their membrane integrity, while PI can only enter yeasts with damaged membranes. Therefore, the integrity of the *C. neoformans* cell membrane was observed by staining with SYTO 9/PI. As shown in **Figure 6C**, the untreated cells were stained only with SYTO 9 instead of PI, while cells treated with Sparamosin$_{26-54}$ were stained with SYTO 9 and PI. Taken together, these results suggested that Sparamosin$_{26-54}$ disrupts the integrity of the cell wall and cell membrane of *C. neoformans*.

Sparamosin$_{26-54}$ Induces Apoptosis in *C. neoformans*

Among the DEGs identified, a gene coding for a metacaspase was found to be up-regulated under Sparamosin$_{26-54}$ treatment, indicating that Sparamosin$_{26-54}$ may induce apoptosis in *C. neoformans*. Thus, we first used DCFH-DA probe to measure intracellular ROS in *C. neoformans* during exposure to Sparamosin$_{26-54}$. As shown in **Figure 7A**, cells treated with 20 mM H_2O_2 as a positive control showed increased DCH staining compared to untreated cells. In accordance with this, cells exposed to Sparamosin$_{26-54}$ (6 and 12 μM) displayed a significant increase in intracellular ROS levels compared to untreated cells. These data indicated that Sparamosin$_{26-54}$ treatment resulted in the accumulation of ROS in *C. neoformans*. The dissipation of MMP is considered to be an early and key cellular event in the occurrence of

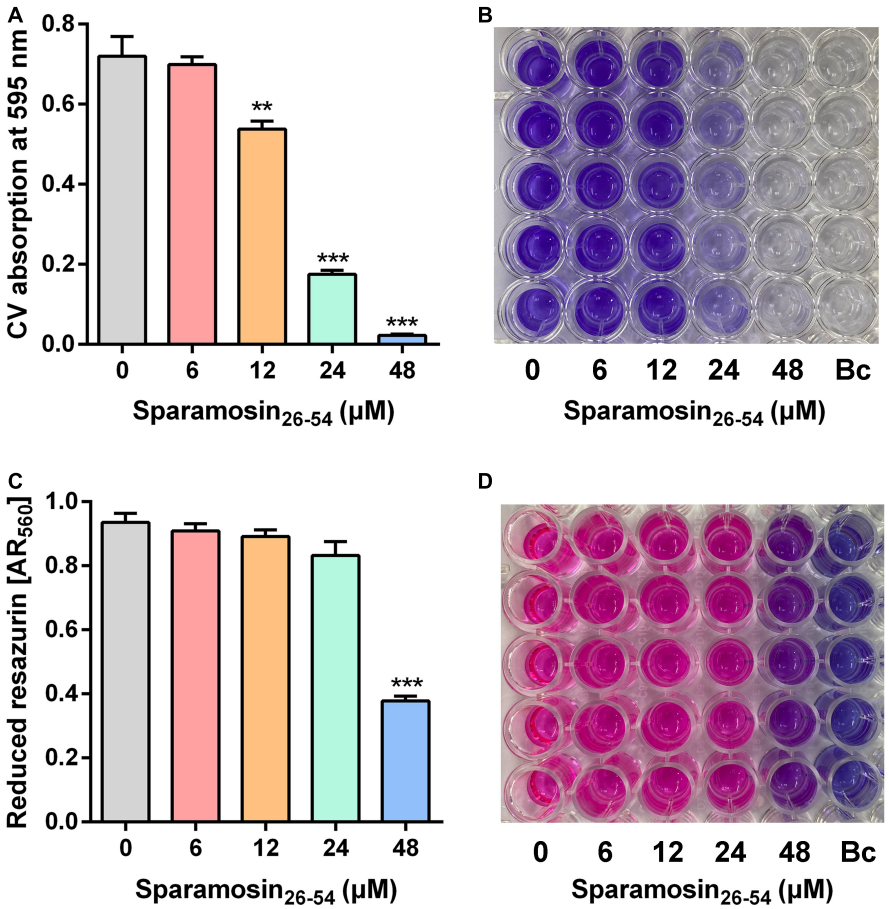

FIGURE 2 | The inhibitory effect of Sparamosin$_{26-54}$ against *C. neoformans* biofilm. **(A,B)** The inhibitory effect of Sparamosin$_{26-54}$ on the formation of *C. neoformans* biofilm. The biofilm mass was quantified by CV staining, and the absorbance at 595 nm was measured. Bc, blank control. **(C,D)** The inhibitory effect of Sparamosin$_{26-54}$ against the preformed biofilm of *C. neoformans*. The amount of reduced resazurin (resorufin) was determined by measuring the absorbance at 560 nm, and the residual amount of oxidized resazurin was quantified by measuring the absorbance at 620 nm. The corrected A_{560} value (AR_{560}) was calculated using the following formula: $AR_{560} = A_{560} - (A_{620} \times R_O)$ and $R_O = AO_{560}/AO_{620}$, where A_{560} and A_{620} are sample absorbance and AO_{560} and AO_{620} are the absorbance of RPMI-MOPS medium containing 0.1 mM resazurin. Bc, blank control. Data represent mean ± standard error of mean from three independent biological replicates. Significant difference between control group and Sparamosin$_{26-54}$ treatment group was indicated by asterisks as $^{**}p < 0.01$; $^{***}p < 0.001$.

apoptosis (Barroso et al., 2006). To investigate mitochondria-mediated pathway during apoptosis in *C. neoformans* induced by Sparamosin$_{26-54}$, we next examined MMP of *C. neoformans* by using $DiOC_6(3)$ which is a membrane potential-sensitive dye that aggregating in healthy mitochondria. After treatment with 6 and 12 μM Sparamosin$_{26-54}$ for 3 h, MMP was observed by the decrease of the fluorescence intensity of $DiOC_6(3)$, indicating that Sparamosin$_{26-54}$ disrupted the MMP of *C. neoformans* (**Figure 7B**). To obtain more evidence of apoptosis in *C. neoformans* induced by Sparamosin$_{26-54}$, the TUNEL assay was conducted, which is one of the most reliable methods for identifying the late stage of yeast cell apoptosis, and is used to visualize the amount of DNA fragmentation in individual cells. We used amphotericin B as a positive control because it has been proven to induce apoptosis in *C. neoformans* cells (Castro et al., 2018). The microscopic images showed the presence of green fluorescence in the cells treated with 6 and 12 μM Sparamosin$_{26-54}$, which was consistent with the positive control cells treated with 4 μg/mL amphotericin B (**Figure 7C**). Since accumulation, MMP dissipation and DNA fragmentation are all hallmarks of apoptosis (Munoz et al., 2012), our data collectively confirmed that *C. neoformans* treated with Sparamosin$_{26-54}$ exhibited apoptosis mechanism.

DISCUSSION

C. neoformans is an important fungal pathogen, causing life-threatening pneumonia and meningitis in immunocompromised patients. However, the existing treatment options for cryptococcosis have been hampered by their inherent toxicity to humans and the increase in their drug-resistance. This situation urgently requires the development of novel antifungal agents. Due to the broad-spectrum antimicrobial activities and unique mode of action against human pathogens, natural AMPs have attracted more and more attention as potential alternatives for

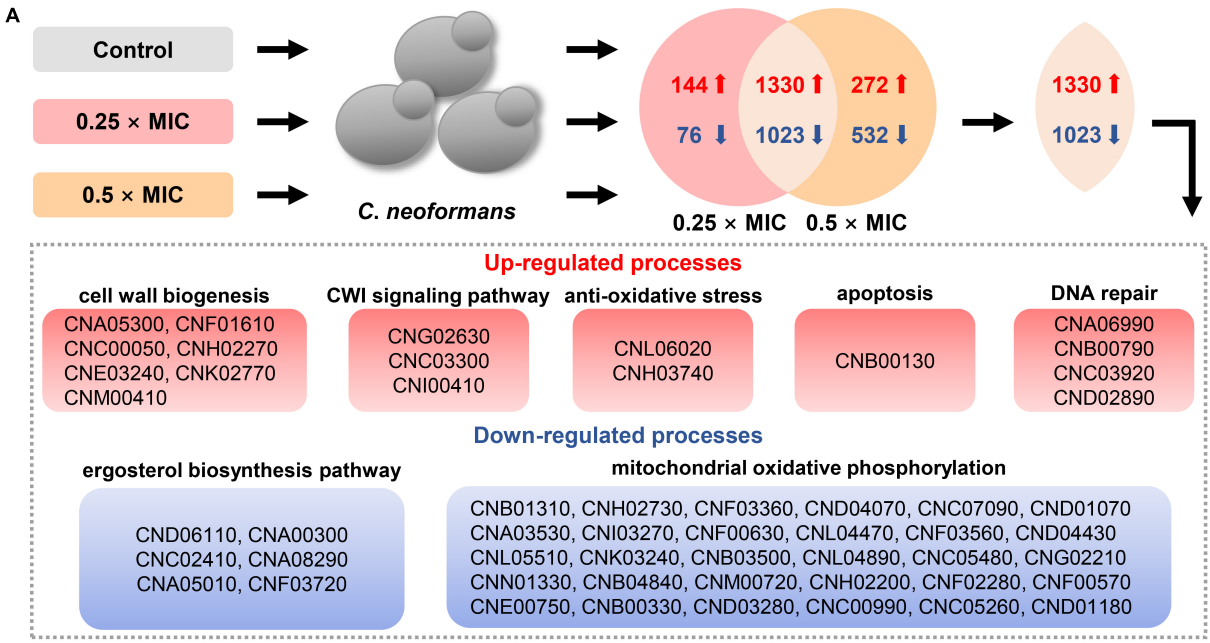

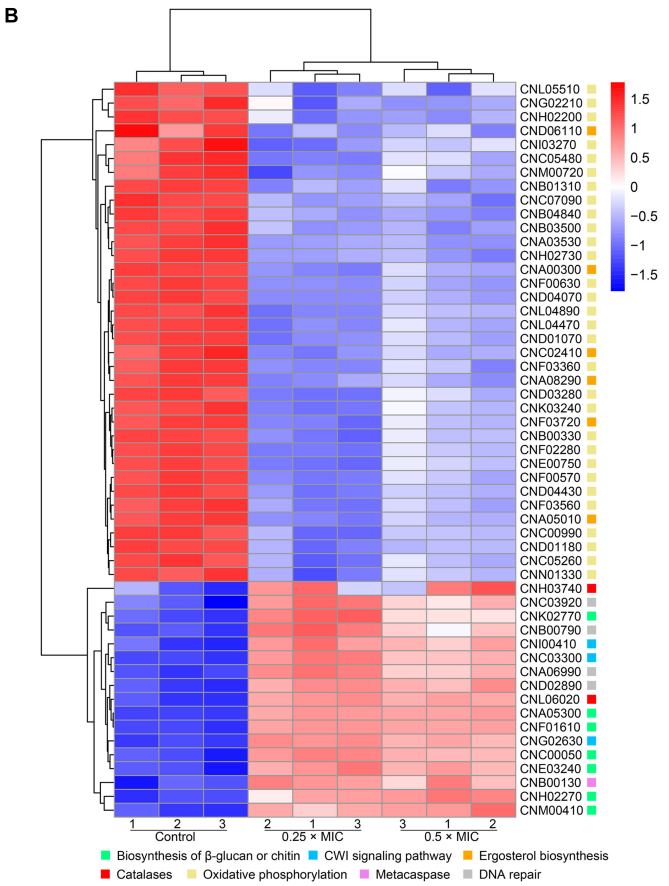

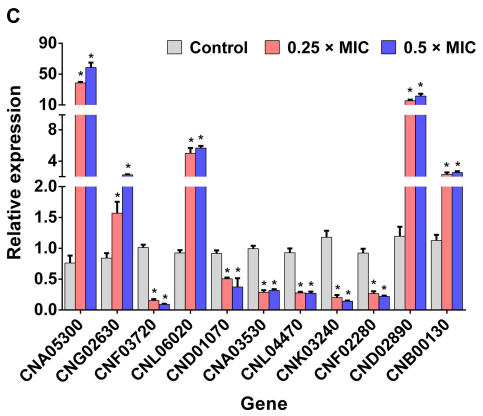

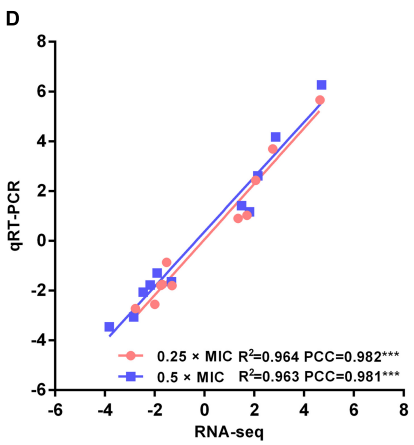

FIGURE 3 | Transcriptomic analysis of Sparamosin$_{26-54}$-treated *C. neoformans*. **(A)** A common transcriptional response to different concentrations of Sparamosin$_{26-54}$ was identified by RNA-seq. **(B)** Heatmap of partial up-regulated and down-regulated genes. **(C)** Gene expression profiles of 11 DEGs in Sparamosin$_{26-54}$-treated *C. neoformans*. Significant difference between control group and Sparamosin$_{26-54}$ treatment group was indicated by asterisks as $^{*}p < 0.05$. **(D)** Correlation analysis between qRT-PCR and RNA-Seq results. PCC, Pearson correlation coefficients. $^{***}p < 0.001$.

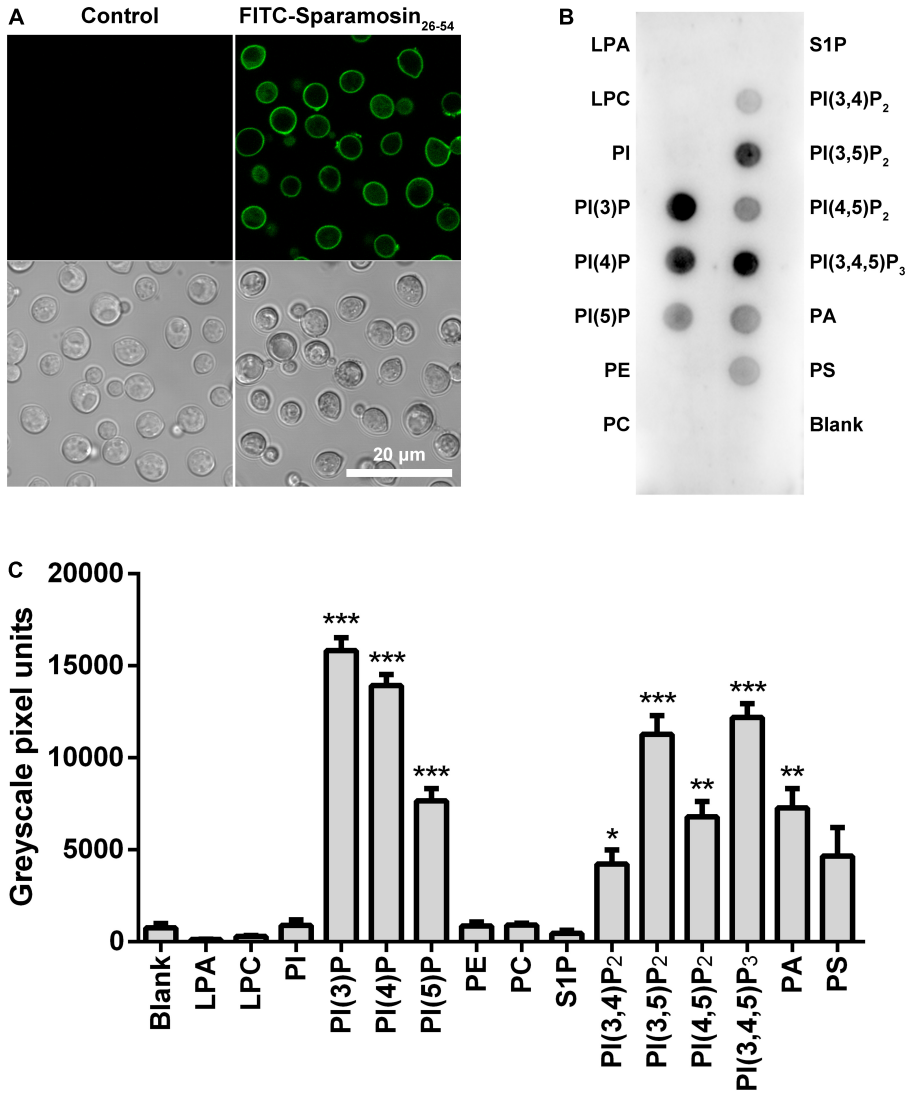

FIGURE 4 | Localization of Sparamosin$_{26-54}$ in *C. neoformans*. **(A)** The fungal cells were incubated with FITC-labeled Sparamosin$_{26-54}$, and images were acquired using a confocal laser scanning microscopy. **(B)** Detection of Sparamosin$_{26-54}$ binding to cellular lipids by protein-phospholipid interaction assay. **(C)** The densitometry analysis of PIP Strips™ probed with Sparamosin$_{26-54}$ by Image J software. Data represent mean ± standard error of mean from three independent biological replicates. Significant difference between blank group and cellular lipids group was indicated by asterisks as $^{*}p < 0.05$; $^{**}p < 0.01$; $^{***}p < 0.001$. LPA, lysophosphatidic acid; LPC, lysophosphocholine; PI, phosphatidylinositol; PI(3)P, phosphatidylinositol (3)-phosphate; PI(4)P, phosphatidylinositol (4)-phosphate; PI(5)P, phosphatidylinositol (5)-phosphate; PE, phosphatidylethanolamine; PC, phosphatidylcholine; S1P, sphingosine 1-phosphate; PI(3,4)P_2, phosphatidylinositol (3,4)-bisphosphate; PI(3,5)P_2, phosphatidylinositol (3,5)-bisphosphate; PI(4,5)P_2, phosphatidylinositol (4,5)-bisphosphate; PI(3,4,5)P_3, phosphatidylinositol (3,4,5)-trisphosphate; PA, phosphatidic acid; PS, phosphatidylserine.

conventional antibiotics. To date, over 3,000 natural AMPs have been found (antimicrobial peptide database 3, APD3) (Wang et al., 2016). In the past few decades, dozens of AMPs have been identified from the mud crab *S. paramamosain*, such as crustins, anti-lipopolysaccharide factors, and several gonadal-specific AMPs including scygonadin, SCY2 and scyreprocin (Huang et al., 2006; Wang et al., 2007; Qiao et al., 2016; Wang et al., 2018; Yang et al., 2020; Long et al., 2021). In the study, we identified a novel AMP named Sparamosin from *S. paramamosain*, and found that its truncated peptide Sparamosin$_{26-54}$ showed broad-spectrum antimicrobial activity. Furthermore, Sparamosin$_{26-54}$ exerts potent inhibitory effect against the three infection forms of *C. neoformans* (that is, planktonic cells, biofilm formation and preformed biofilm). It has multiple antifungal mechanisms against *C. neoformans*, including disruption of the cell wall and cell membrane integrity and induction of apoptosis. Transcriptome analysis showed that after Sparamosin$_{26-54}$ treatment, the expression of genes related to cell wall component biosynthesis, CWI signaling pathway, anti-oxidative stress, apoptosis, DNA repair, ergosterol biosynthesis pathway and mitochondrial oxidative phosphorylation were significantly modulated in

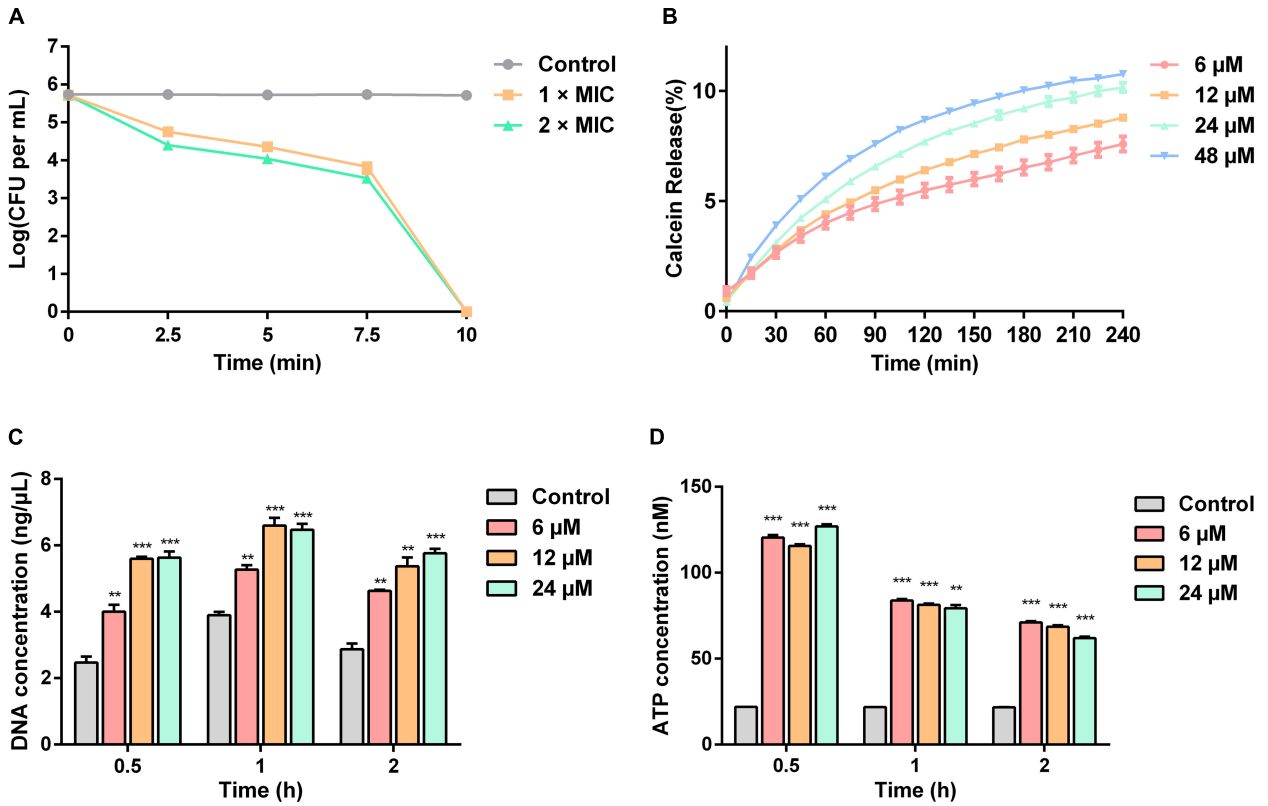

FIGURE 5 | Sparamosin$_{26-54}$ kills *C. neoformans* via disrupting the integrity of cell membranes. **(A)** The time-killing curves of Sparamosin$_{26-54}$ against *C. neoformans*. **(B)** The time course of calcein release from *C. neoformans* induced by Sparamosin$_{26-54}$. **(C)** The concentration of extracellular DNA in *C. neoformans* after Sparamosin$_{26-54}$ treatment. The amount of extracellular DNA in the supernatants was quantified by spectrophotometry at 260 nm. **(D)** The concentration of extracellular ATP in *C. neoformans* after Sparamosin$_{26-54}$ treatment. The amount of extracellular ATP was detected using the ATP determination kit. Data represent mean ± standard error of mean from three independent biological replicates. Significant difference between control group and Sparamosin$_{26-54}$ treatment group was indicated by asterisks as $^{**}p < 0.01$; $^{***}p < 0.001$.

C. neoformans. These obtained results provide important reference for the further development of Sparamosin$_{26-54}$ as a new antifungal drug.

Sequence modification is an effective strategy to improve the performance of natural AMPs. Various sequence modification methods attempted to modify natural AMPs by deleting, adding, or replacing one or more amino acid residues, truncating peptides, or assembling chimeric peptides from fragments of different natural AMPs. Many AMPs, such as cecropins, LL-37, magainins, and melittins, are finally obtained through sequence modification (Oh et al., 2000; Wu et al., 2014; Wang et al., 2019). Due to the synthetic mature peptide of Sparamosin exerts moderate inhibitory effect against bacteria and fungi, two truncated peptides, Sparamosin$_{1-25}$ and Sparamosin$_{26-54}$, were designed and synthesized based on the secondary structure and physicochemical parameters of Sparamosin. Through predicting the secondary structure of Sparamosin, we found that there were two α-helices located at residues Ile^{13}-Phe^{24} and residues Pro^{31}-Arg^{39}, respectively. The α-helical AMPs, such as cecropin, magainin and LL-37, are one of the most widely studied AMPs (Beevers and Dixon, 2010; Nguyen et al., 2011). Many of these α-helical AMPs are usually cationic and amphipathic with potent antimicrobial activities against bacteria and fungi (Hancock and Sahl, 2006). The mechanism of action of α-helical AMPs is mainly composed of two steps, that is, the initial binding of cationic AMPs with the negatively charged components on the microbial cell surface and the subsequent membrane disruption (Huang, 2000; Beevers and Dixon, 2010). The crucial physicochemical parameters of peptides were calculated by using online tools. In this study, the hydrophobic residue ratio of Sparamosin and its truncated peptides ranged from 32 to 38%, and the net charge varied from −3 to + 6. Hydrophobicity is defined as the percentage of hydrophobic residues in the peptide and is an important parameter to determine the activity of AMPs. The hydrophobicity exceeds a threshold to confer antimicrobial activity, and there is an upper limit, beyond which the host cells will rupture and cell selectivity will be lost (Frederiksen et al., 2020). Therefore, the percentage of hydrophobic residues in AMPs characterized to date is approximately 40–60% (Tossi et al., 2000). Cationicity is another important parameter that affects the antimicrobial activity of AMPs. Most AMPs are positively charged, and charges from + 4 to + 6 seem to be the most common (Tossi et al., 2000). Within a certain range, an increase in the total charge of cationic peptides will often lead to an

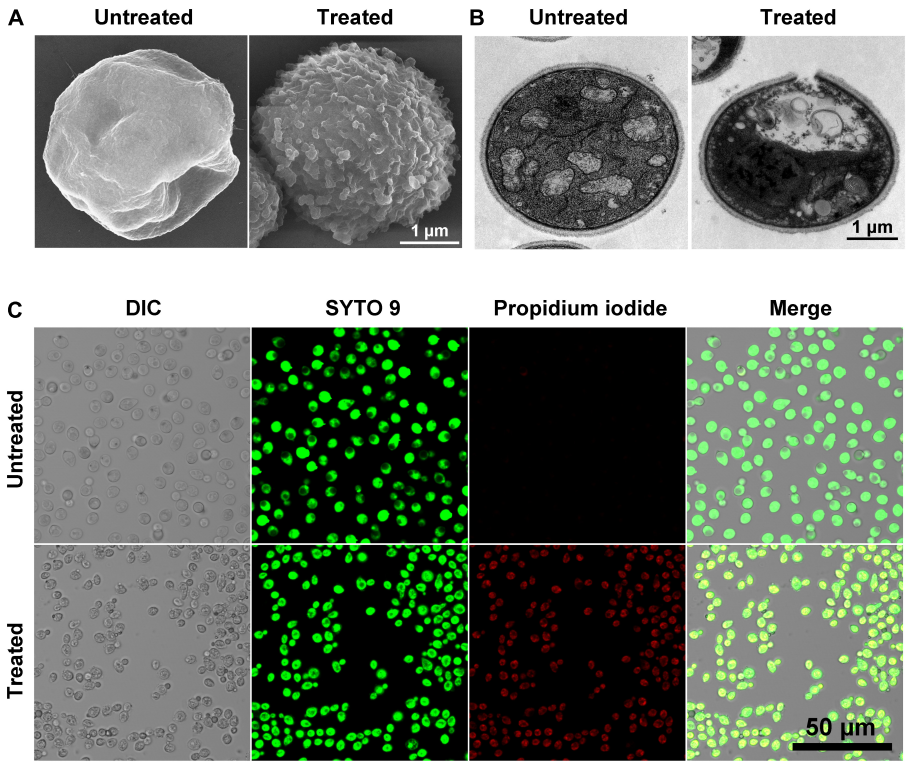

FIGURE 6 | Scanning electron microscope (SEM), transmission electron microscope (TEM) and confocal laser scanning microscopy (CLSM) images show the effect of Sparamosin$_{26\text{-}54}$ on *C. neoformans*. **(A,B)** The morphology of *C. neoformans* treated with Sparamosin$_{26\text{-}54}$ observed by SEM and TEM. **(C)** Live-dead staining assay shows the differentially stained cells after Sparamosin$_{26\text{-}54}$ treatment.

increase in affinity for microbial membranes, thereby enhancing their antimicrobial activity (Dathe et al., 2001). It should be noted that hydrophobicity and cationicity are not independent, they complement each other and together determine the antimicrobial activity of AMPs. Among Sparamosin and its truncated peptides, Sparamosin$_{1-25}$ has no antimicrobial activities against the tested strains, and Sparamosin$_{26-54}$ displayed stronger antimicrobial activity than Sparamosin. Compared with Sparamosin, the hydrophobic residue ratio of the Sparamosin$_{26-54}$ increased from 35 to 38%, and the net charge increased from + 3 to + 6, which might the main reason why its activity is stronger than Sparamosin. The underlying mechanism still need further evidence.

It is noteworthy that Sparamosin$_{26-54}$ also showed excellent anti-biofilm activity against *C. neoformans*. In the present study, we found that Sparamosin$_{26-54}$ could effectively prevent the formation of biofilm, presumably due to the reduction of the planktonic population, and cause the damage to the growth of preformed biofilms through a strong inhibition of respiration. A biofilm is an organized aggregate of microbial cells that attached to a solid surface and enclosed in an extracellular polymeric substance matrix (Donlan, 2002). *C. neoformans* is a yeast-like fungus with polysaccharide capsules that can form biofilms on polystyrene plates and medical devices (Martinez and Casadevall, 2005). The biofilm formation of *C. neoformans* includes fungal surface adhesion, microcolony formation, and matrix production (Martinez and Casadevall, 2005). Fungal cells within biofilms display unique phenotypic characteristics that can increase the resistance to the host's immune system and antifungal agents (Lilit et al., 2017; Kean and Ramage, 2019). Azole drugs such as voriconazole and fluconazole can only effectively inhibit planktonic fungal cells, but have little effect on fungal biofilms (Martinez and Casadevall, 2006). Amphotericin B and caspofungin are the two most effective drugs for preventing the formation of *C. neoformans* biofilm and against mature biofilms (Martinez and Casadevall, 2006). However, the effective concentration of amphotericin B and caspofungin against *C. neoformans* biofilm is higher than the therapeutic range, thus causing serious toxicity (Martinez and Casadevall, 2006; Delattin et al., 2014). In fact, most of the currently available antibiotics are unable to address chronic infections caused by biofilm effectively (Roy et al., 2018; Vuotto and Donelli, 2019). In addition to broad-spectrum bactericidal and fungicidal activities, more and more evidences showed that AMPs can also exhibit anti-biofilm activity against both bacterial and fungal biofilm in three different ways by reducing planktonic population, preventing cells from initially adhering to the surface, and eradicating established biofilms. For example, a shortened variant of mouse cathelicidin-related AMP, termed AS10, inhibits the formation of *C. albicans* biofilms, and acts synergistically with common antifungal drugs (such as amphotericin B and caspofungin) against mature biofilms

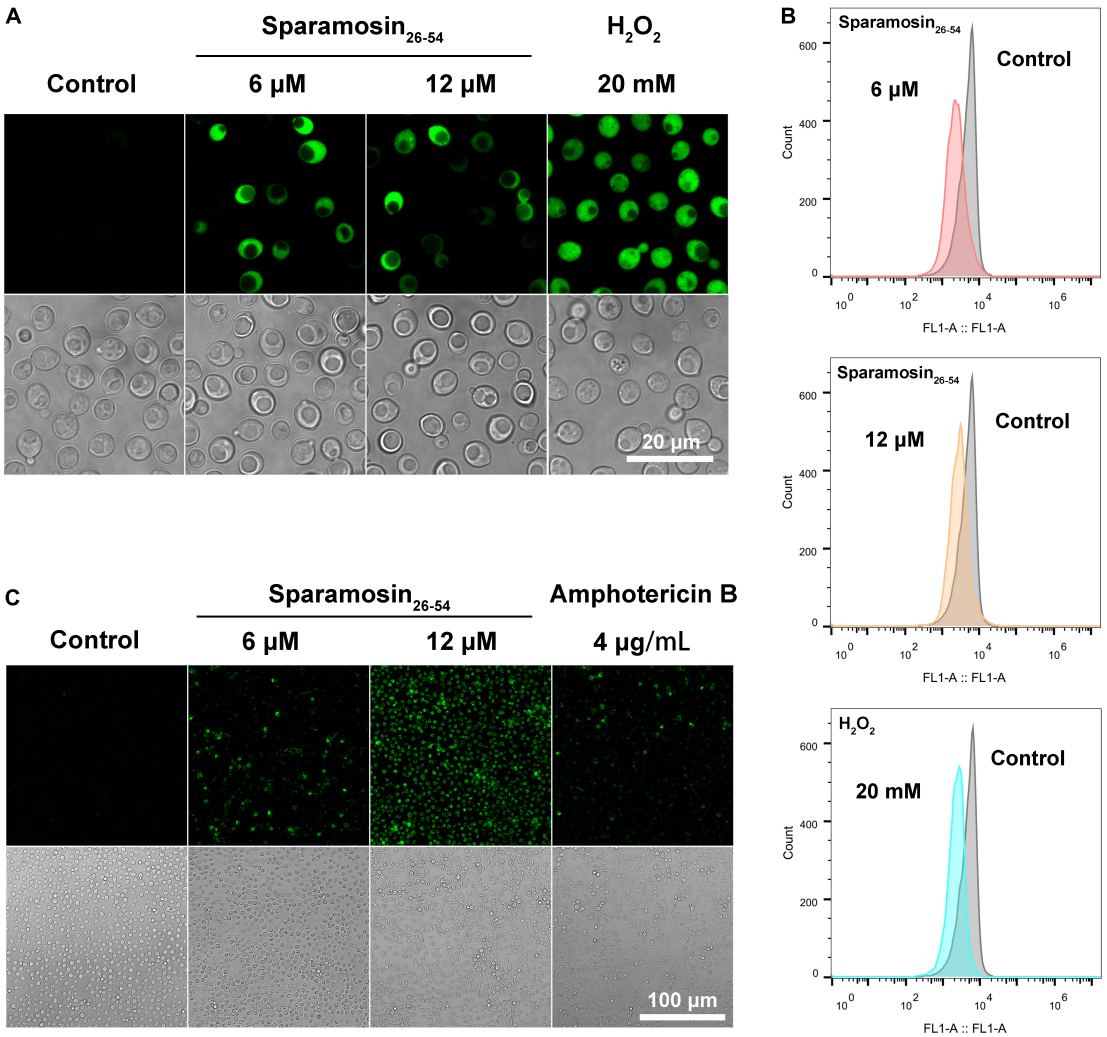

FIGURE 7 | Sparamosin$_{26\text{-}54}$ induces apoptosis in *C. neoformans*. **(A)** Detection of intracellular ROS accumulation in Sparamosin$_{26\text{-}54}$-treated *C. neoformans* using DCFH-DA. **(B)** Analysis of mitochondrial membrane depolarization in *C. neoformans* after Sparamosin$_{26\text{-}54}$ treatment. **(C)** Analysis of DNA damage in Sparamosin$_{26\text{-}54}$-treated *C. neoformans* by the TUNEL assay.

(De Brucker et al., 2014). The mud crab AMP Scyreprocin could not only inhibit the biofilm formation, but also eradicate mature biofilms of *C. albicans* and *C. neoformans* (Yang et al., 2020). Therefore, the research and development of AMPs with anti-biofilm activity has more clinical significance. The anti-biofilm mechanism of Sparamosin$_{26-54}$ and the efficacy of Sparamosin$_{26-54}$ combined with standard antifungal drugs is worthy of further study.

The proposed antifungal mechanisms of AMPs are diverse, including cell wall integrity disruption, cell membrane permeabilization as well as apoptosis induction (Hwang et al., 2011b; Cho et al., 2012; Ma et al., 2020). Many studies have also shown that AMPs and pore-forming toxins have a similar mechanism of action, that is, the formation of holes in the cell membrane (Gilbert et al., 2014; Etxaniz et al., 2018). It has been reported that pore-forming toxins could trigger very diverse response pathways in eukaryotic cells (Gonzalez et al., 2011; Kao et al., 2011). When the plasma membrane is damaged by pore-forming toxins, cells activate signaling pathways to restore plasma membrane integrity and ion homeostasis (Gonzalez et al., 2011). In addition, pore-forming toxins can induce cell death by inducing apoptosis and pyrophosis (Genestier et al., 2005; Shoma et al., 2008). To investigate the antifungal mechanism of Sparamosin$_{26-54}$, we used RNA-Seq to study the transcriptomic profile of *C. neoformans* treated with sublethal concentrations of Sparamosin$_{26-54}$. As reported previously, sublethal concentrations of AMPs can lead to fungal cell dysfunction. For example, the plant defensin HsAFP1 at 2 × FC50 (FC50, fungicidal concentration resulting in 50% killing) induces autophagy, vacuolar dysfunction and cell cycle impairment in *C. albican* (Struyfs et al., 2020). The *Musca domestica* antifungal peptide-1 (MAF-1) at 1 × MIC induces the expression of genes related to oxidative stress response and cell wall synthesis and inhibits the expression of genes related

to metabolism and fatty acid biosynthesis in *C. albican* (Wang et al., 2017). In the study, *C. neoformans* cells were incubated with different concentrations of Sparamosin$_{26-54}$ (0.25 × MIC, 0.5 × MIC) for 1 h before RNA sequencing. We compared the differential gene-expression profile of Sparamosin$_{26-54}$ treatment at 0.25 × MIC and 0.5 × MIC to the untreated control to identify a set of genes commonly perturbed by Sparamosin$_{26-54}$ treatment. This analysis revealed that genes involved in the biosynthesis of cell wall component, CWI signaling pathway, anti-oxidative stress, apoptosis and DNA repair were upregulated under Sparamosin$_{26-54}$ treatment, while genes associated with the ergosterol biosynthesis pathway and mitochondrial oxidative phosphorylation were down-regulated under the same condition. It is not clear which genes or signaling pathways are specifically involved in the cellular response to Sparamosin$_{26-54}$. The use of inhibitors or regulators of specific signaling pathways to demonstrate the involvement of pathways in the cell death process deserves further investigation.

We propose that cellular changes and damage initiated through interaction with primary targets of Sparamosin$_{26-54}$ result in activation of intracellular signaling pathways. Fungal cell membrane is potential target for AMPs and is rich in a variety of lipids such as glycerophospholipids, sphingolipids and sterols. In this study, we identified the glycerophospholipid targets of Sparamosin$_{26-54}$ as PIPs and PA. In addition, the rapid fungicidal effect of Sparamosin$_{26-54}$ against *C. neoformans* was associated with increased plasma membrane permeability, which can be detected by releasing calcein from fungal cells, leaking DNA and ATP to the supernatant, and positively staining yeasts with PI, and observed by SEM and TEM. Thus, it could be speculated that the binding of Sparamosin$_{26-54}$ to PIPs and PA induces the membrane permeability of *C. neoformans*. PIPs are usually found on the inner leaflet of eukaryotic cells and play a major role in many important membrane-related processes, such as signal transduction, ion channel function, endocytosis, exocytosis, etc. (McLaughlin and Murray, 2005). Although PIPs commonly exist in eukaryotic cells, the relative contributions of negative and neutral glycerophospholipids in cell membrane of fungi and mammal are different (Rautenbach et al., 2016). Generally, fungal cell membranes are mainly composed of PI and PS, which tend to be high electronegative, while mammalian cell membranes rich in zwitterionic phospholipids PC are usually neutral in net charge (Rautenbach et al., 2016). These electrostatic differences between fungi and mammalian cells may allow a stronger initial electrostatic interaction between the cationic AMPs and the fungal cell surface. Certain plant defensins have been observed to bind PIPs preferentially. For example, the *Nicotiana alata* defensin NaD1 could bind to a wide range of PIPs, while the tomato defensin TPP3 specifically bound to PI(4,5)P_2 (Baxter et al., 2015; Payne et al., 2016). The binding of NaD1 to PI(4,5)P_2 leads to the formation of an oligomeric complex, that is critical for cytolytic activity (Poon et al., 2014). This unique peptide-lipid interaction was common in plant defensins, which may be one of the important mechanisms of plants against fungal infection. Interestingly, we found that AMPs from marine animal and plant have the similar binding properties to membrane phospholipid, suggesting that Sparamosin$_{26-54}$ and plant defensins have similar mechanisms of action. Further studies are needed to understand the role of phospholipids binding in Sparamosin$_{26-54}$-induced membrane permeabilization of *C. neoformans*.

In addition to the membrane disruption, some AMPs can also induce oxidative stress, DNA damage and apoptosis in yeasts (Cho and Lee, 2011; Hwang et al., 2011a,b). ROS, such as hydrogen peroxide (H_2O_2), hydroxyl radicals (OH·) and superoxide anions (O_2^-), are considered to be early signal mediators of apoptosis (Fleury et al., 2002). The ROS produced by aerobic metabolism usually exist in cells in balance with antioxidant enzymes (such as catalase, superoxide dismutase, and glutathione peroxidase) (Dantas et al., 2015). Previous studies have shown that the increase in ROS upon AMPs treatment also occurs in fungi, which supports our findings (Hwang et al., 2011a; Wang et al., 2015). Excessive ROS has multiple deleterious effects on the essential structures of fungi (such as nucleic acid, DNA, amino acid residues, and cell membrane) resulting in cell death (Perrone et al., 2008). Mitochondria play an important role in energy conversion, cell signaling and apoptosis pathway (Turrens, 2003). The cell permeability and lipophilic dye, $DiOC_6(3)$, which accumulates in healthy mitochondria and is widely used to investigate the mitochondria-mediated pathways during apoptosis (Zamzami et al., 1996; Kataoka et al., 2005). Our present study demonstrated that after treatment with Sparamosin$_{26-54}$, $DiOC_6(3)$ dye no longer accumulated in mitochondria, resulting in a decrease in green fluorescence, suggesting that Sparamosin$_{26-54}$ might lead to the opening of mitochondrial membrane transition pores and induce the dissipation of the MMP. The dysfunction of mitochondria leads to an energy crisis and promotes the release of proapoptotic factors from mitochondria into the cytosol, which then activates caspase (Heiskanen et al., 1999; Pereira et al., 2007). During apoptosis, chromatin DNA is cut into small fragments by the activation of endonucleases, which is an irreversible step of apoptosis. The labeling and observation of DNA fragmentation by TUNEL assay is one of the most reliable methods to identify the phenotype of late apoptosis in yeasts (Ribeiro et al., 2006). Taken together, our comprehensive physiological effect data (including ROS accumulation, MMP dissipation and DNA fragmentation) indicated that Sparamosin$_{26-54}$ induced apoptosis in *C. neoformans*.

In summary, the present study demonstrated the antifungal activity and related mechanism of Sparamosin$_{26-54}$, which is a novel AMP found in mud crab *S. paramamosain*. The synthetic Sparamosin$_{26-54}$ showed potent activity against three infection forms of *C. neoformans* (planktonic, biofilm formation and preformed biofilm). It was confirmed that this peptide can effectively kill *C. neoformans* via multiple modes of action, including disrupting the integrity of the cell wall and cell membrane and inducing apoptosis. These results indicated that the novel AMP Sparamosin$_{26-54}$ is expect to be a promising antifungal drug that could be used to control *C. neoformans* infection in the future.

DATA AVAILABILITY STATEMENT

The datasets presented in this study can be found in online repositories. The names of the repository/repositories and accession number(s) can be found below: https://www.ncbi.nlm.nih.gov/, PRJNA751241. The GenBank accession number is MH423837.

AUTHOR CONTRIBUTIONS

K-JW and FC: conceptualization, funding acquisition, project administration, supervision, and writing—review and editing. Y-CC: data curation, formal analysis, investigation, methodology, and writing—original draft. YY, CZ, and H-YC: investigation and methodology. All authors contributed to the article and approved the submitted version.

FUNDING

This study was supported by a grant (grant No. 41806162) from the National Natural Science Foundation of China (NSFC), the Fujian Marine Economic Development Subsidy Fund Project (grant No. FJHJF-L-2019-1) from the Fujian Ocean and Fisheries Department, the Xiamen Ocean and Fishery Development Special Fund Project (grant No. 20CZP011HJ06) from the Xiamen Municipal Bureau of Ocean Development, a grant (grant No. 3502Z20203012) from the Xiamen Science and Technology Planning Project, and the Fundamental Research Funds from Central Universities (grant No. 20720190109).

ACKNOWLEDGMENTS

We thank laboratory engineers Hui Peng and Zhiyong Lin for providing technical assistance.

SUPPLEMENTARY MATERIAL

The Supplementary Material for this article can be found online at: https://www.frontiersin.org/articles/10.3389/fmicb.2021.746006/full#supplementary-material

REFERENCES

Barroso, G., Taylor, S., Morshedi, M., Manzur, F., and Oehninger, S. (2006). Mitochondrial membrane potential integrity and plasma membrane translocation of phosphatidylserine as early apoptotic markers: a comparison of two different sperm subpopulations. *Fertil. Steril.* 85, 149–154. doi: 10.1016/j.fertnstert.2005.06.046

Baxter, A. A., Richter, V., Lay, F. T., Poon, I. K., Adda, C. G., Veneer, P. K., et al. (2015). The tomato defensin TPP3 binds phosphatidylinositol (4, 5)-bisphosphate via a conserved dimeric cationic grip conformation to mediate cell lysis. *Mol. Cell. Biol.* 35, 1964–1978. doi: 10.1128/MCB.00282-15

Beevers, A. J., and Dixon, A. M. (2010). Helical membrane peptides to modulate cell function. *Chem. Soc. Rev.* 39, 2146–2157. doi: 10.1039/b912944h

Berditsch, M., Jger, T., Strempel, N., Schwartz, T., and Ulrich, A. S. (2015). Synergistic effect of membrane-active peptides polymyxin B and gramicidin S on multidrug-resistant strains and biofilms of *Pseudomonas aeruginosa*. *Antimicrob. Agents Chemother.* 59:5288. doi: 10.1128/AAC.00682-15

Brogden, K. A. (2005). Antimicrobial peptides: pore formers or metabolic inhibitors in bacteria? *Nat. Rev. Microbiol.* 3, 238–250. doi: 10.1038/nrmicro1098

Brown, G. D., Denning, D. W., Gow, N. A., Levitz, S. M., Netea, M. G., and White, T. C. (2012). Hidden killers: human fungal infections. *Sci. Transl. Med.* 4:165rv113. doi: 10.1126/scitranslmed.3004404

Campoy, S., and Adrio, J. L. (2017). Antifungals. *Biochem. Pharmacol.* 133, 86–96. doi: 10.1016/j.bcp.2016.11.019

Castro, S. C. D., Taissa, V., Sonia, R., and Kelly, I. (2018). Miltefosine has a postantifungal effect and induces apoptosis in *Cryptococcus yeasts*. *Antimicrob. Agents Chemother.* 62:e00312-18. doi: 10.1128/AAC.00312-18

Chen, B., Fan, D.-Q., Zhu, K.-X., Shan, Z.-G., Chen, F.-Y., Hou, L., et al. (2015). Mechanism study on a new antimicrobial peptide Sphistin derived from the N-terminus of crab histone H2A identified in haemolymphs of *Scylla paramamosain*. *Fish Shellfish Immunol.* 47, 833–846. doi: 10.1016/j.fsi.2015.10.010

Chen, H. M., Chan, S. C., Lee, J. C., Chang, C. C., Murugan, M., and Jack, R. W. (2003). Transmission electron microscopic observations of membrane effects of antibiotic cecropin B on *Escherichia coli*. *Microsc. Res. Tech.* 62, 423–430. doi: 10.1002/jemt.10406

Cho, J., Hwang, I.-S., Choi, H., Hwang, J. H., Hwang, J.-S., and Lee, D. G. (2012). The novel biological action of antimicrobial peptides via apoptosis induction. *J. Microbiol. Biotechnol.* 22, 1457–1466. doi: 10.4014/jmb.1205.05041

Cho, J., and Lee, D. G. (2011). Oxidative stress by antimicrobial peptide pleurocidin triggers apoptosis in *Candida albicans*. *Biochimie* 93, 1873–1879.

Dantas, A. D. S., Day, A., Ikeh, M., Kos, I., Achan, B., and Quinn, J. (2015). Oxidative stress responses in the human fungal pathogen, *Candida albicans*. *Biomolecules* 5, 142–165. doi: 10.3390/biom5010142

Dathe, M., Nikolenko, H., Meyer, J., Beyermann, M., and Bienert, M. (2001). Optimization of the antimicrobial activity of magainin peptides by modification of charge. *FEBS Lett.* 501, 146–150. doi: 10.1016/s0014-5793(01)02648-5

Datta, A., Yadav, V., Ghosh, A., Choi, J., Bhattacharyya, D., Kar, R. K., et al. (2016). Mode of action of a designed antimicrobial peptide: high potency against *Cryptococcus neoformans*. *Biophys. J.* 111, 1724–1737. doi: 10.1016/j.bpj.2016.08.032

De Brucker, K., Delattin, N., Robijns, S., Steenackers, H., Verstraeten, N., Landuyt, B., et al. (2014). Derivatives of the mouse cathelicidin-related antimicrobial peptide (CRAMP) inhibit fungal and bacterial biofilm formation. *Antimicrob. Agents Chemother.* 58, 5395–5404. doi: 10.1128/AAC.03045-14

Delattin, N., Cammue, B. P., and Thevissen, K. (2014). Reactive oxygen species-inducing antifungal agents and their activity against fungal biofilms. *Future Med. Chem.* 6, 77–90. doi: 10.4155/fmc.13.189

Denning, D. W., and Bromley, M. J. (2015). Infectious Disease. How to bolster the antifungal pipeline. *Science* 347, 1414–1416. doi: 10.1126/science.aaa6097

Destoumieux, D., Bulet, P., Loew, D., Van Dorsselaer, A., Rodriguez, J., and Bachere, E. (1997). Penaeidins, a new family of antimicrobial peptides isolated from the shrimp *Penaeus vannamei* (Decapoda). *J. Biol. Chem.* 272, 28398–28406. doi: 10.1074/jbc.272.45.28398

Destoumieux, D., Bulet, P., Strub, J. M., van Dorsselaer, A., and Bachère, E. (1999). Recombinant expression and range of activity of penaeidins, antimicrobial peptides from penaeid shrimp. *Eur. J. Biochem.* 266, 335–346. doi: 10.1046/j.1432-1327.1999.00855.x

Donlan, R. M. (2002). Biofilms: microbial life on surfaces. *Emerg. Infect. Dis.* 8:881. doi: 10.3201/eid0809.020063

Dutcher, J. D., William, G., Pagano, J. F., and John, V. (1959). *Amphotericin b, Its Production, and Its Salts*. US patent application 2,908,611. Washington, DC: US Environmental Protection Agency.

Ellis, D. (2002). Amphotericin B: spectrum and resistance. *J. Antimicrob. Chemother.* 49(Suppl._1), 7–10. doi: 10.1093/jac/49.suppl_1.7

Etxaniz, A., González-Bullón, D., Martín, C., and Ostolaza, H. (2018). Membrane repair mechanisms against permeabilization by pore-forming toxins. *Toxins* 10:234. doi: 10.3390/toxins10060234

Fanos, V., and Cataldi, L. (2000). Amphotericin B-induced nephrotoxicity: a review. *J. Chemother.* 12, 463–470. doi: 10.1179/joc.2000.12.6.463

Felix, B., Sara, G., Rita, O., and David, D. (2017). Global and multi-national prevalence of fungal diseases-estimate precision. *J. Fungi* 3:57. doi: 10.3390/jof3040057

Fleury, C., Mignotte, B., and Vayssière, J. (2002). Mitochondrial reactive oxygen species in cell death signaling. *Biochimie* 84, 131–141. doi: 10.1016/s0300-9084(02)01369-x

Frederiksen, N., Hansen, P. R., Zabicka, D., Tomczak, M., Urbas, M., Domraceva, I., et al. (2020). Alternating cationic-hydrophobic peptide/peptoid hybrids: influence of hydrophobicity on antibacterial activity and cell selectivity. *ChemMedChem* 15, 2544–2561. doi: 10.1002/cmdc.202000526

Genestier, A. L., Michallet, M. C., Prévost, G., Bellot, G., Chalabreysse, L., Peyrol, S., et al. (2005). Staphylococcus aureus panton-valentine leukocidin directly targets mitochondria and induces Bax-independent apoptosis of human neutrophils. *J. Clin. Invest.* 115, 3117–3127. doi: 10.1172/jci22684

Gilbert, R. J., Dalla Serra, M., Froelich, C. J., Wallace, M. I., and Anderluh, G. (2014). Membrane pore formation at protein-lipid interfaces. *Trends Biochem. Sci.* 39, 510–516. doi: 10.1016/j.tibs.2014.09.002

Gonzalez, M. R., Bischofberger, M., Frêche, B., Ho, S., Parton, R. G., and van der Goot, F. G. (2011). Pore-forming toxins induce multiple cellular responses promoting survival. *Cell Microbiol.* 13, 1026–1043. doi: 10.1111/j.1462-5822.2011.01600.x

Gudmundsson, G. H., Agerberth, B., Odeberg, J., Bergman, T., Olsson, B., and Salcedo, R. (1996). The human gene FALL39 and processing of the cathelin precursor to the antibacterial peptide LL-37 in granulocytes. *Eur. J. Biochem.* 238, 325–332. doi: 10.1111/j.1432-1033.1996.0325z.x

Gueguen, Y., Garnier, J., Robert, L., Lefranc, M.-P., Mougenot, I., De Lorgeril, J., et al. (2006). PenBase, the shrimp antimicrobial peptide penaeidin database: sequence-based classification and recommended nomenclature. *Dev. Comp. Immunol.* 30, 283–288. doi: 10.1016/j.dci.2005.04.003

Hancock, R. E., and Sahl, H.-G. (2006). Antimicrobial and host-defense peptides as new anti-infective therapeutic strategies. *Nat. Biotechnol.* 24, 1551–1557. doi: 10.1038/nbt1267

Heiskanen, K. M., Bhat, M. B., Wang, H.-W., Ma, J., and Nieminen, A.-L. (1999). Mitochondrial depolarization accompanies cytochrome c release during apoptosis in PC6 cells. *J. Biol. Chem.* 274, 5654–5658. doi: 10.1074/jbc.274.9.5654

Huang, H. W. (2000). Action of antimicrobial peptides: two-state model. *Biochemistry* 39, 8347–8352. doi: 10.1021/bi000946l

Huang, W. S., Wang, K. J., Yang, M., Cai, J. J., Li, S. J., and Wang, G. Z. (2006). Purification and part characterization of a novel antibacterial protein Scygonadin, isolated from the seminal plasma of mud crab, *Scylla serrata* (Forskål, 1775). *J. Exp. Mar. Biol. Ecol.* 339, 37–42. doi: 10.1016/j.jembe.2006.06.029

Hwang, B., Hwang, J.-S., Lee, J., and Lee, D. G. (2011b). The antimicrobial peptide, psacotheasin induces reactive oxygen species and triggers apoptosis in *Candida albicans*. *Biochem. Biophys. Res. Commun.* 405, 267–271. doi: 10.1016/j.bbrc.2011.01.026

Hwang, B., Hwang, J.-S., Lee, J., Kim, J.-K., Kim, S. R., Kim, Y., et al. (2011a). Induction of yeast apoptosis by an antimicrobial peptide, Papiliocin. *Biochem. Biophys. Res. Commun.* 408, 89–93. doi: 10.1016/j.bbrc.2011.03.125

Iyer, K. R., Revie, N. M., Fu, C., Robbins, N., and Cowen, L. E. (2021). Treatment strategies for cryptococcal infection: challenges, advances and future outlook. *Nat. Rev. Microbiol.* 19, 454–466. doi: 10.1038/s41579-021-00511-0

Kao, C. Y., Los, F. C., Huffman, D. L., Wachi, S., Kloft, N., Husmann, M., et al. (2011). Global functional analyses of cellular responses to pore-forming toxins. *PLoS Pathog.* 7:e1001314. doi: 10.1371/journal.ppat.1001314

Kataoka, M., Fukura, Y., Shinohara, Y., and Baba, Y. (2005). Analysis of mitochondrial membrane potential in the cells by microchip flow cytometry. *Electrophoresis* 26, 3025–3031. doi: 10.1002/elps.200410402

Kean, R., and Ramage, G. (2019). Combined antifungal resistance and biofilm tolerance: the global threat of *Candida auris*. *mSphere* 4:e00458-19. doi: 10.1128/mSphere.00458-19

Lemke, A., Kiderlen, A., and Kayser, O. (2005). Amphotericin b. *Appl. Microbiol. Biotechnol.* 68, 151–162. doi: 10.1007/s00253-005-1955-9

Lilit, A., David, S., Silvana, V., Eliseo, E., Raddy, R., and Luis, M. (2017). The crucial role of biofilms in Cryptococcus neoformans survival within macrophages and colonization of the central nervoussystem. *J. Fungi Open Access Mycol. J.* 3:10. doi: 10.3390/jof3010010

Liu, H.-P., Chen, R.-Y., Zhang, Q.-X., Wang, Q.-Y., Li, C.-R., Peng, H., et al. (2012). Characterization of two isoforms of antiliopolysacchride factors (Sp-ALFs) from the mud crab *Scylla paramamosain*. *Fish Shellfish Immunol.* 33, 1–10. doi: 10.1016/j.fsi.2012.03.014

Liu, J., Chen, F., Wang, X., Peng, H., Zhang, H., and Wang, K.-J. (2020). The synergistic effect of mud crab antimicrobial peptides Sphistin and Sph12-38 with antibiotics azithromycin and rifampicin enhances bactericidal activity against *Pseudomonas aeruginosa*. *Front. Cell. Infect. Microbiol.* 10:e572849. doi: 10.3389/fcimb.2020.572849

Livak, K. J., and Schmittgen, T. D. (2001). Analysis of relative gene expression data using real-time quantitative PCR and the 2-ΔΔCT method. *Methods* 25, 402–408. doi: 10.1006/meth.2001.1262

Long, S., Chen, F., and Wang, K.-J. (2021). Characterization of a new homologous anti-lipopolysaccharide factor SpALF7 in mud crab *Scylla paramamosain*. *Aquaculture* 534:736333. doi: 10.1016/j.aquaculture.2020.736333

Loyse, A., Burry, J., Cohn, J., Ford, N., Chiller, T., Ribeiro, I., et al. (2019). Leave no one behind: response to new evidence and guidelines for the management of cryptococcal meningitis in low-income and middle-income countries. *Lancet Infect. Dis.* 19, e143–e147. doi: 10.1016/S1473-3099(18)30493-6

Ma, H., Zhao, X., Yang, L., Su, P., Fu, P., Peng, J., et al. (2020). Antimicrobial peptide AMP-17 affects *Candida albicans* by disrupting its cell wall and cell membrane integrity. *Infect. Drug Resist.* 13:2509. doi: 10.2147/IDR.S250278

Martinez, L. R., and Casadevall, A. (2005). Specific antibody can prevent fungal biofilm formation and this effect correlates with protective efficacy. *Infect. Immun.* 73, 6350–6362. doi: 10.1128/IAI.73.10.6350-6362.2005

Martinez, L. R., and Casadevall, A. (2006). Susceptibility of Cryptococcus neoformans biofilms to antifungal agents in vitro. *Antimicrob. Agents Chemother.* 50, 1021–1033. doi: 10.1128/AAC.50.3.1021-1033.2006

McLaughlin, S., and Murray, D. (2005). Plasma membrane phosphoinositide organization by protein electrostatics. *Nature* 438, 605–611. doi: 10.1038/nature04398

Miceli, M. H., Díaz, J. A., and Lee, S. A. (2011). Emerging opportunistic yeast infections. *Lancet Infect. Dis.* 11, 142–151. doi: 10.1016/S1473-3099(10)70218-8

Munoz, A. J., Wanichthanarak, K., Meza, E., and Petranovic, D. (2012). Systems biology of yeast cell death. *FEMS Yeast Res.* 12, 249–265. doi: 10.1111/j.1567-1364.2011.00781.x

Nguyen, L. T., Haney, E. F., and Vogel, H. J. (2011). The expanding scope of antimicrobial peptide structures and their modes of action. *Trends Biotechnol.* 29, 464–472. doi: 10.1016/j.tibtech.2011.05.001

Oh, D., Shin, S. Y., Lee, S., Kang, J. H., Kim, S. D., Ryu, P. D., et al. (2000). Role of the hinge region and the tryptophan residue in the synthetic antimicrobial peptides, cecropin A(1-8)-magainin 2(1-12) and its analogues, on their antibiotic activities and structures. *Biochemistry* 39, 11855–11864. doi: 10.1021/bi000453g

Pappas, P. G., Alexander, B. D., Andes, D. R., Hadley, S., Kauffman, C. A., Freifeld, A., et al. (2010). Invasive fungal infections among organ transplant recipients: results of the transplant-associated infection surveillance network (TRANSNET). *Clin. Infect. Dis.* 50, 1101–1111. doi: 10.1086/651262

Payne, J. A., Bleackley, M. R., Lee, T.-H., Shafee, T. M., Poon, I. K., Hulett, M. D., et al. (2016). The plant defensin NaD1 introduces membrane disorder through a specific interaction with the lipid, phosphatidylinositol 4, 5 bisphosphate. *Biochim. Biophys. Acta Biomembr.* 1858, 1099–1109. doi: 10.1016/j.bbamem.2016.02.016

Pereira, C., Camougrand, N., Manon, S., Sousa, M. J., and Côrte-Real, M. (2007). ADP/ATP carrier is required for mitochondrial outer membrane permeabilization and cytochrome c release in yeast apoptosis. *Mol. Microbiol.* 66, 571–582. doi: 10.1111/j.1365-2958.2007.05926.x

Perfect, J. R. (2017). The antifungal pipeline: a reality check. *Nat. Rev. Drug Discov.* 16, 603–616. doi: 10.1038/nrd.2017.46

Perlin, D. S., Rautemaa-Richardson, R., and Alastruey-Izquierdo, A. (2017). The global problem of antifungal resistance: prevalence, mechanisms, and management. *Lancet Infect. Dis.* 17, e383–e392. doi: 10.1016/S1473-3099(17)30316-X

Perrone, G. G., Tan, S.-X., and Dawes, I. W. (2008). Reactive oxygen species and yeast apoptosis. *Biochim. Biophys. Acta Mol. Cell Res.* 1783, 1354–1368.

Peschel, A., and Sahl, H.-G. (2006). The co-evolution of host cationic antimicrobial peptides and microbial resistance. *Nat. Rev. Microbiol.* 4, 529–536. doi: 10.1038/nrmicro1441

Poon, I. K., Baxter, A. A., Lay, F. T., Mills, G. D., Adda, C. G., Payne, J. A., et al. (2014). Phosphoinositide-mediated oligomerization of a defensin induces cell lysis. *eLife* 3:e01808. doi: 10.7554/eLife.01808

Poonam, K., Rutusmita, M., Neha, A., Apurva, C., Rashmi, G., Partha, R., et al. (2017). Antifungal and anti-biofilm activity of essential oil active components against Cryptococcus neoformans and *Cryptococcus laurentii*. *Front. Microbiol.* 8:2161. doi: 10.3389/fmicb.2017.02161

Qiao, K., Xu, W.-F., Chen, H.-Y., Peng, H., Zhang, Y.-Q., Huang, W.-S., et al. (2016). A new antimicrobial peptide SCY2 identified in *Scylla paramamosain* exerting a potential role of reproductive immunity. *Fish Shellfish Immunol.* 51, 251–262. doi: 10.1016/j.fsi.2016.02.022

Rajasingham, R., Smith, R. M., Park, B. J., Jarvis, J. N., Govender, N. P., Chiller, T. M., et al. (2017). Global burden of disease of HIV-associated cryptococcal meningitis: an updated analysis. *Lancet Infect. Dis.* 17, 873–881. doi: 10.1016/S1473-3099(17)30243-8

Rautenbach, M., Troskie, A. M., and Vosloo, J. A. (2016). Antifungal peptides: to be or not to be membrane active. *Biochimie* 130, 132–145. doi: 10.1016/j.biochi.2016.05.013

Ribeiro, G. F., Côrte-Real, M., and Johansson, B. (2006). Characterization of DNA damage in yeast apoptosis induced by hydrogen peroxide, acetic acid, and hyperosmotic shock. *Mol. Biol. Cell* 17, 4584–4591. doi: 10.1091/mbc.e06-05-0475

Rowley, A. F., and Powell, A. (2007). Invertebrate immune systems-specific, quasi-specific, or nonspecific? *J. Immunol.* 179, 7209–7214. doi: 10.4049/jimmunol.179.11.7209

Roy, R., Tiwari, M., Donelli, G., and Tiwari, V. (2018). Strategies for combating bacterial biofilms: a focus on anti-biofilm agents and their mechanisms of action. *Virulence* 9, 522–554. doi: 10.1080/21505594.2017.1313372

Shan, Z., Zhu, K., Peng, H., Chen, B., Liu, J., Chen, F., et al. (2016). The new antimicrobial peptide SpHyastatin from the mud crab *Scylla paramamosain* with multiple antimicrobial mechanisms and high effect on bacterial infection. *Front. Microbiol.* 7:1140. doi: 10.3389/fmicb.2016.01140

Shockey, J. E., O'Leary, N. A., de la Vega, E., Browdy, C. L., Baatz, J. E., and Gross, P. S. (2009). The role of crustins in *Litopenaeus vannamei* in response to infection with shrimp pathogens: an in vivo approach. *Dev. Comp. Immunol.* 33, 668–673. doi: 10.1016/j.dci.2008.11.010

Shoma, S., Tsuchiya, K., Kawamura, I., Nomura, T., Hara, H., Uchiyama, R., et al. (2008). Critical involvement of pneumolysin in production of interleukin-1alpha and caspase-1-dependent cytokines in infection with Streptococcus pneumoniae in vitro: a novel function of pneumolysin in caspase-1 activation. *Infect. Immun.* 76, 1547–1557. doi: 10.1128/iai.01269-07

Smith, V. J., Fernandes, J. M., Kemp, G. D., and Hauton, C. (2008). Crustins: enigmatic WAP domain-containing antibacterial proteins from crustaceans. *Dev. Comp. Immunol.* 32, 758–772. doi: 10.1016/j.dci.2007.12.002

Sperstad, S. V., Haug, T., Vasskog, T., and Stensvåg, K. (2009b). Hyastatin, a glycine-rich multi-domain antimicrobial peptide isolated from the spider crab (*Hyas araneus*) hemocytes. *Mol. Immunol.* 46, 2604–2612. doi: 10.1016/j.molimm.2009.05.002

Sperstad, S. V., Haug, T., Paulsen, V., Rode, T. M., Strandskog, G., Solem, S. T., et al. (2009a). Characterization of crustins from the hemocytes of the spider crab, *Hyas araneus*, and the red king crab, *Paralithodes camtschaticus*. *Dev. Comp. Immunol.* 33, 583–591. doi: 10.1016/j.dci.2008.10.010

Steiner, H., Hultmark, D., Engstrm, H. H. B., and Boman, H. G. (1981). Sequence and specificity of two antibacterial proteins involved in insect immunity. *Nature* 292, 246–248. doi: 10.1038/292246a0

Struyfs, C., Cools, T. L., De Cremer, K., Sampaio-Marques, B., Ludovico, P., Wasko, B. M., et al. (2020). The antifungal plant defensin HsAFP1 induces autophagy, vacuolar dysfunction and cell cycle impairment in yeast. *Biochim. Biophys. Acta Biomembr.* 1862:183255. doi: 10.1016/j.bbamem.2020.183255

Tossi, A., Sandri, L., and Giangaspero, A. (2000). Amphipathic, alpha-helical antimicrobial peptides. *Biopolymers* 55, 4–30.

Turrens, J. F. (2003). Mitochondrial formation of reactive oxygen species. *J. Physiol.* 552, 335–344.

Vitale, R. G., Mouton, J. W., Afeltra, J., Meis, J. F., and Verweij, P. E. (2002). Method for measuring postantifungal effect in *Aspergillus species*. *Antimicrob. Agents Chemother.* 46, 1960–1965. doi: 10.1128/AAC.46.6.1960-1965.2002

Vuotto, C., and Donelli, G. (2019). Novel treatment strategies for biofilm-based infections. *Drugs* 79, 1635–1655. doi: 10.1007/s40265-019-01184-z

Vylkova, S., Nayyar, N., Li, W., and Edgerton, M. (2007). Human β-defensins kill *Candida albicans* in an energy-dependent and salt-sensitive manner without causing membrane disruption. *Antimicrob. Agents Chemother.* 51, 154–161. doi: 10.1128/AAC.00478-06

Wang, G., Li, X., and Wang, Z. (2016). APD3: the antimicrobial peptide database as a tool for research and education. *Nucleic Acids Res.* 44, 1087–1093. doi: 10.1093/nar/gkv1278

Wang, G., Narayana, J. L., Mishra, B., Zhang, Y., Wang, F., Wang, C., et al. (2019). Design of antimicrobial peptides: progress made with human cathelicidin LL-37. *Adv. Exp. Med. Biol.* 1117, 215–240. doi: 10.1007/978-981-13-3588-4_12

Wang, H., Zhang, J.-X., Wang, Y., Fang, W.-H., Wang, Y., Zhou, J.-F., et al. (2018). Newly identified type II crustin (SpCrus2) in *Scylla paramamosain* contains a distinct cysteine distribution pattern exhibiting broad antimicrobial activity. *Dev. Comp. Immunol.* 84, 1–13. doi: 10.1016/j.dci.2018.01.021

Wang, K., Dang, W., Xie, J., Zhu, R., Sun, M., Jia, F., et al. (2015). Antimicrobial peptide protonectin disturbs the membrane integrity and induces ROS production in yeast cells. *Biochim. Biophys. Acta Biomembr.* 1848, 2365–2373. doi: 10.1016/j.bbamem.2015.07.008

Wang, K.-J., Huang, W.-S., Yang, M., Chen, H.-Y., Bo, J., Li, S.-J., et al. (2007). A male-specific expression gene, encodes a novel anionic antimicrobial peptide, scygonadin, in *Scylla serrata*. *Mol. Immunol.* 44, 1961–1968. doi: 10.1016/j.molimm.2006.09.036

Wang, T., Xiu, J., Zhang, Y., Wu, J., Ma, X., Wang, Y., et al. (2017). Transcriptional responses of *Candida albicans* to antimicrobial peptide MAF-1A. *Front. Microbiol.* 8:894. doi: 10.3389/fmicb.2017.00894

Wiegand, I., Hilpert, K., and Hancock, R. E. (2008). Agar and broth dilution methods to determine the minimal inhibitory concentration (MIC) of antimicrobial substances. *Nat. Protoc.* 3:163. doi: 10.1038/nprot.2007.521

Wu, R., Wang, Q., Zheng, Z., Zhao, L., Shang, Y., Wei, X., et al. (2014). Design, characterization and expression of a novel hybrid peptides melittin (1-13)-LL37 (17-30). *Mol. Biol. Rep.* 41, 4163–4169. doi: 10.1007/s11033-013-2900-0

Yang, Y., Chen, F., Chen, H.-Y., Peng, H., Hao, H., and Wang, K.-J. (2020). A novel antimicrobial peptide scyreprocin from mud crab *Scylla paramamosain* showing potent antifungal and anti-biofilm activity. *Front. Microbiol.* 11:1589. doi: 10.3389/fmicb.2020.01589

Yeung, A. T., Gellatly, S. L., and Hancock, R. E. (2011). Multifunctional cationic host defence peptides and their clinical applications. *Cell. Mol. Life Sci.* 68:2161. doi: 10.1007/s00018-011-0710-x

Zamzami, N., Marchetti, P., Castedo, M., Hirsch, T., Susin, S. A., Masse, B., et al. (1996). Inhibitors of permeability transition interfere with the disruption of the mitochondrial transmembrane potential during apoptosis. *FEBS Lett.* 384, 53–57. doi: 10.1016/0014-5793(96)00280-3

Zasloff, M. (1987). Magainins, a class of antimicrobial peptides from *Xenopus* skin: isolation, characterization of two active forms, and partial cDNA sequence of a precursor. *Proc. Natl. Acad. Sci. U.S.A.* 84, 5449–5453. doi: 10.1073/pnas.84.15.5449

Zasloff, M. (2002). Antimicrobial peptides of multicellular organisms. *Nature* 415, 389–395. doi: 10.1038/415389a

Zhang, R., Wang, Z., Tian, Y., Yin, Q., Cheng, X., Lian, M., et al. (2019). Efficacy of antimicrobial peptide DP7, designed by machine-learning method, against

methicillin-resistant *Staphylococcus aureus*. *Front. Microbiol.* 10:1175. doi: 10.3389/fmicb.2019.01175

Conflict of Interest: The authors declare that the research was conducted in the absence of any commercial or financial relationships that could be construed as a potential conflict of interest.

Publisher's Note: All claims expressed in this article are solely those of the authors and do not necessarily represent those of their affiliated organizations, or those of the publisher, the editors and the reviewers. Any product that may be evaluated in this article, or claim that may be made by its manufacturer, is not guaranteed or endorsed by the publisher.

frontiers in Microbiology

ORIGINAL RESEARCH
published: 04 November 2021
doi: 10.3389/fmicb.2021.722661

Identification and Antifungal Mechanism of a Novel Actinobacterium *Streptomyces huiliensis* sp. nov. Against *Fusarium oxysporum* f. sp. *cubense* Tropical Race 4 of Banana

Dengfeng Qi[1], Liangping Zou[1], Dengbo Zhou[1], Miaoyi Zhang[1], Yongzan Wei[1], Lu Zhang[2], Jianghui Xie[1]* and Wei Wang[1]**

[1] *Key Laboratory of Biology and Genetic Resources of Tropical Crops, Ministry of Agriculture, Institute of Tropical Bioscience and Biotechnology, Chinese Academy of Tropical Agricultural Sciences, Haikou, China,* [2] *College of Life Science, Hainan Normal University, Haikou, China*

OPEN ACCESS

Edited by:
Eustachio Tarasco, University of Bari Aldo Moro, Italy

Reviewed by:
Sukhendu Mandal, University of Calcutta, India
Natsuko Ichikawa, National Institute for Testing and Evaluation (NITE), Israel

***Correspondence:**
Lu Zhang
luzhangtest@163.com; zhanglutest@163.com
Jianghui Xie
2453880045@qq.com; xiejianghui@itbb.org.cn
Wei Wang
wangweisys@ahau.edu.cn

Specialty section:
This article was submitted to Antimicrobials, Resistance and Chemotherapy, a section of the journal Frontiers in Microbiology

Received: *10 June 2021*
Accepted: *14 October 2021*
Published: *04 November 2021*

Citation:
Qi D, Zou L, Zhou D, Zhang M, Wei Y, Zhang L, Xie J and Wang W (2021) Identification and Antifungal Mechanism of a Novel Actinobacterium Streptomyces huiliensis sp. nov. Against Fusarium oxysporum f. sp. cubense Tropical Race 4 of Banana. Front. Microbiol. 12:722661. doi: 10.3389/fmicb.2021.722661

Banana is an important fruit crop. *Fusarium* wilt caused by *Fusarium oxysporum* f. sp. *cubense* tropical race 4 (Foc TR4) seriously threatens the global banana industry. It is difficult to control the disease spread using chemical measures. In addition, commercial resistant cultivars are also lacking. Biological control is considered as a promising strategy using antagonistic microbes. Actinomycetes, especially *Streptomyces*, are potential sources of producing novel bioactive secondary metabolites. Here, strain SCA2-4^T with strong antifungal activity against Foc TR4 was isolated from the rhizospheric soil of *Opuntia stricta* in a dry hot valley. The morphological, physiological and chemotaxonomic characteristics of the strain were consistent with the genus *Streptomyces*. Based on the homology alignment and phylogenetic trees of 16S *rRNA* gene, the taxonomic status of strain SCA2-4^T exhibited a paradoxical result and low bootstrap value using different algorithms in the MEGA software. It prompted us to further discriminate this strain from the closely related species by the multilocus sequence analysis (MLSA) using five house-keeping gene alleles (*atpD*, *gyrB*, *recA*, *rpoB,* and *trpB*). The MLSA trees calculated by three algorithms demonstrated that strain SCA2-4^T formed a distinct clade with *Streptomyces mobaraensis* NBRC 13819^T. The MLSA distance was above 0.007 of the species cut-off. Average nucleotide identity (ANI) values between strain SCA2-4^T genome and two standard strain genomes were below 95-96% of the novel species threshold. Strain SCA2-4^T was assigned to a novel species of the genus *Streptomyces* and named as *Streptomyces huiliensis* sp. nov. The sequenced complete genome of SCA2-4^T encoded 51 putative biosynthetic gene clusters of secondary metabolites. Genome alignment revealed that ten gene clusters were involved in the biosynthesis of antimicrobial metabolites. It was supported that strain SCA2-4^T showed strong antifungal activities against the pathogens of banana

fungal diseases. Extracts abstracted from the culture filtrate of strain SCA2-4^T seriously destroyed cell structure of Foc TR4 and inhibited mycelial growth and spore germination. These results implied that strain SCA2-4^T could be a promising candidate for biological control of banana *Fusarium* wilt.

Keywords: *Streptomyces*, novel species, identification, banana Fusarium wilt, antifungal activities, genome sequencing

INTRODUCTION

Banana (*Musa* spp.) is one of the most popular fruits in the tropical and sub-tropical regions of the world. It is considered to be the fourth most important crop following rice, wheat and corn in the developing countries (Mohandas and Ravishankar, 2016). Banana *Fusarium* wilt seriously threatened the global banana industry. The disease was caused by the soil-borne fungi, containing four physiological races (abbreviated as Foc 1–Foc 4) based on their host specificity. Especially, tropical race 4 (Foc TR4) can infect almost all banana cultivars (Ploetz, 2015). They can survive in the soil as chlamydospores for more than 20 years (Ploetz, 2015). It is difficult to control the disease spread using chemical measures. In addition, commercial resistant cultivars are also lacking. Biological control is considered as a promising strategy using antagonistic microbes.

Actinobacteria are rich in bioactive secondary metabolites exhibiting antimicrobial, antitumor and/or antiviral activities (Watve et al., 2001; Guo et al., 2008). These microbes are widely distributed in diverse ecosystems such as soil, air and salt water. More than 50% of the known antibiotics come from Actinobacteria. The genus *Streptomyces* is the largest genus of Actinobacteria. Over 1000 species of *Streptomyces* are identified[1]. Notably, 75% of antibiotics are produced by *Streptomyces* species (Bérdy, 2005). *Streptomyces* have been used as biocontrol agents against soil-borne diseases such as Foc TR4. *Streptomyces* g10 isolated from a coastal mangrove exhibited a strong antagonistic activity against banana *Fusarium* wilt (Getha et al., 2005). Endophytic *Streptomyces* sp. S76 and *Streptomyces* sp. S96 showed antifungal activity against Foc TR4 (Cao et al., 2004, 2005). We previously reported *Streptomyces* sp. CB-75, SCA3-4, and JBS5-6 isolated from rhizosphere soil strongly inhibited mycelial growth of Foc TR4 and spore germination (Chen et al., 2018; Qi et al., 2019; Jing et al., 2020). However, *Streptomyces* species are still the most potential candidates to produce novel types of secondary metabolites (Bérdy, 2005). Based on their genome information, more than 90% of *Streptomyces* bioactive metabolites are waiting to be discovered (Watve et al., 2001; Guo et al., 2008). Therefore, the isolation and identification of *Streptomyces* remains a perennial attention.

In our present study, strain SCA2-4^T was isolated from a rhizosphere soil sample of *Opuntia stricta* in a dry hot valley. The alignment of 16S *rRNA* gene and multilocus sequence analysis (MLSA) indicated that the strain had the closest taxonomic relationship with *Streptomyces orinoci* NBRC 13466^T and *Streptomyces mobaraensis* NBRC 13819^T. The MLSA distance and average nucleotide identity (ANI) demonstrated that the strain belonged to a novel *Streptomyces* species, named with *Streptomyces huiliensis* sp. nov. Extracts of strain SCA2-4^T exhibited a strong antifungal activity against Foc TR4. Bioinformatics analysis showed that the strain genome contained a number of genes coding antifungal secondary metabolites, suggesting that it will have an application potential in biocontrol for phytopathogenic fungi.

MATERIALS AND METHODS

Isolation of Actinobacteria

Soil sample was collected from rhizosphere of *Opuntia stricta* in a dry hot valley of the Huili County, Sichuan Province, China in 2014. One gram of soil sample was homogenized in 9 mL of sterile water and heated at 55°C for 20 min. The homogenate was diluted by a serial dilution method and spread on a starch casein agar (SCA) medium (Kuster and Williams, 1964) (10 g of soluble starch, 0.3 g of casein, 2.0 g of KNO_3, 2.0 g of NaCl, 2.0 g of K_2HPO_4, 0.05 g of $MgSO_4{\cdot}7H_2O$, 0.02 g of $CaCO_3$, 0.01 g of $FeSO_4{\cdot}H_2O$, and 18 g of agar in 1 L of sterile water, pH 7.0–7.4) supplemented with 50 mg/L of $K_2Cr_2O_7$ and 50 mg/L of nystatin. The plates were incubated at 28°C for 7 days. Colonies with different morphological characteristics were selected and purified on the YE agar medium (4 g of yeast extract, 10 g of malt extract, 4 g of glucose and 20 g of agar in 1 L of distilled water, pH 7.3). The purified isolate was stocked in 20% (v/v) of glycerol at −80°C.

Antifungal Activity of Actinobacteria

Antagonistic activities of the purified actinobacteria against Foc TR4 (ATCC 76255) were screened on potato dextrose agar (PDA) plates using a conventional spot inoculation method (Qi et al., 2019). A hyphal block (5-mm diameter) of Foc TR4 was inoculated on the center of PDA plate. Four blocks (5-mm diameter) of the isolates were placed on four symmetrical points of PDA plate. Three replicates were set for each experiment. The plate inoculated only with pathogen was used as a control. Antifungal activity was detected until pathogenic mycelium covered the whole plate in control group at 28°C. The growth diameters of Foc TR4 were measured using a cross method (Qi et al., 2019). The inhibitory zone and the percentage of fungal growth inhibition were calculated using the following formula:

The inhibitory percentage of growth = $[(C - T)/C] \times 100\%$

where C and T represented average growth diameters of tested pathogen in the control and treated plates, respectively (Aghighi et al., 2004).

[1]http://www.bacterio.net/

Based on its strong antifungal activity against Foc TR4, strain SCA2-4^T was selected as a target strain to determine antifungal activity against other fungi including *F. oxysporum* f. sp. *cubense* Race 1 (Foc 1; ACCC 31271), *Curvularia fallax* (ATCC 38579), and *Curvularia lunata* (ACCC 36365). These fungi were kindly provided by the Institute of Environment and Plant Protection, China Academy of Tropical Agricultural Sciences, Haikou, China.

Phylogenetic and Genomic Analyses of Strain SCA2-4^T

Extraction of genomic DNA was performed as described by Ahmad et al. (2017). The whole genome of strain SCA2-4^T was sequenced and assembled by the Shanghai Majorbio Bio-pharm Technology Co., Ltd., The complete 16S *rRNA* gene selected from its genome sequence was aligned with the EzTaxon server (Yoon et al., 2017a) and the NCBI database (Altschul et al., 1990). The phylogenetic trees were generated by the three algorithms including the Neighbor-Joining method, the Maximum-Likelihood method and the Maximum-Parsimony method in MEGA 7.0 (Kumar et al., 2016). The evolutionary distance was calculated by the Kimura's two-parameter model (Kimura, 1980). The confidence level of phylogenetic tree was investigated using the bootstrap analysis on 1000 replicates (Felsenstein, 1985). In addition, five standard housekeeping genes including *atpD* (ATP synthase, beta subunit), *gyrB* (DNA gyrase B subunit), *recA* (recombinase A), *rpoB* (RNA polymerase, beta subunit), and *trpB* (tryptophan synthetase, beta subunit) were chosen from strain SCA2-4 ^{T} genome to perform a multilocus sequence analysis (MLSA) (Brady et al., 2008). The length of 9399 bp gene sequences including concatenated *atpD*, *gyrB*, *recA*, *rpoB* and *trpB* were compared with the five housekeeping genes of 16 related standard strains from GenBank (**Supplementary Table 1**). The MLSA phylogenetic trees were constructed using the Neighbor-Joining method (Saitou and Nei, 1987) the Maximum-Likelihood (Felsenstein, 1981) and the Maximum-Parsimony (Fitch, 1971). Average nucleotide identity (ANI) between genomes was calculated using the online OrthoANI (Yoon et al., 2017b). The G + C content of strain SCA2-4^T was estimated in the light of sequenced complete genome. The genome sequences of standard strains were downloaded from the public genome database of EzBioCloud[2].

Morphological Characteristics

The morphological profiles of strain SCA2-4^T were observed using a scanning electron microscopy (ZEISS, Germany) after inoculation on YE agar medium at 28℃ for 21 days. The sample was prepared as described by Kumar et al. (2014). The growth characteristics of strain SCA2-4^T were detected on six standard ISP media, containing yeast extract-malt extract agar (ISP2 or YE), oatmeal agar (ISP3), inorganic salts-starch agar (ISP4), glycerol-asparagine agar (ISP5), peptone yeast-iron agar (ISP6), and tyrosine agar (ISP7) (Shirling and Gottlieb, 1966). The formation of melanoid pigments was observed on ISP6 and ISP7 at 28℃ for 14 days. Colors of substrate and aerial mycelia as well as diffusible pigments were judged by comparing with the ISCC-NBS color charts (Kelly, 1958). The tolerance of NaCl (0–9%, at intervals of 1%, w/v) and temperature (16–46℃, at intervals of 1℃) for growth was examined on the YE plates. The effect of pH on growth was evaluated in the NB broth (1.0 g of yeast powder, 0.8 g of beef extract, 2.0 g of casein, and 10.0 g of glycerol) with pH 4–10 (at intervals of 1) at 28℃ for 14 days. Physiological and biochemical characteristics were determined according to the methods of Williams et al. (1983).

Chemotaxonomic Characteristics

The biomass of strain SCA2-4^T was collected by centrifugation at 8000 rpm for 20 min after growing in a shaken flask of the TSB broth (15.0 g of tryptone, 5.0 g of soytone, 30.0 g of sodium chloride, 1 L of sterile water, pH 7.1–7.5) at 25℃ for 5 d. Respiration quinone was extracted from the lyophilized mycelia (0.5 g) by a reverse-phase partition high-performance liquid chromatography (HPLC) (Sasser, 1990). The cellular fatty acids were analyzed according to the standard Microbial Identification System (Sherlock Version 6.1, MIDI database) by a gas chromatography (56890N, Agilent Technologies) (Komagata and Suzuki, 1987). The polar lipids were extracted from dry mycelia and individually separated by a two-dimensional thin-layer chromatography (TLC) on silica gel plates (Art 5554, DC-Alufolien Kieselgel 60F 254, Merck, Germany) (Minnikin et al., 1979).

Bioinformatic Analysis of Strain SCA2-4^T

The complete genome of strain SCA2-4^T was sequenced using a paired-end sequencing method in the Illumina Hiseq × Ten platform (Illumina, San Diego, CA, United States) by the Shanghai Majorbio Bio-pharm Technology Co., Ltd., (Shanghai, China). Data were analyzed on the free online platform of the Majorbio Cloud Platform[3]. Clean sequencing data were optimized using the GapCloser v1.12 (Luo et al., 2012) and were subsequently assembled using the SOAPdenovo v2.04. The protein-coding genes were predicted by the Glimmer v3.02 (Delcher et al., 2007[4]). Gene functions were annotated using six databases (NR, Swiss-Prot, Pfam, EggNOG, GO, and KEGG). The biosynthetic gene clusters of secondary metabolites were predicted using the online antiSMASH v 6.0.1 software (Kai et al., 2017[5]).

Recovering Extracts From the Culture Filtrate of Strain SCA2-4^T

In order to determine whether secondary metabolites of strain SCA2-4^T can inhibit growth of Foc TR4 or not, it was first fermented in the broth medium (15 g of corn flour, 10 g of glucose, 0.5 g of K_2HPO_4, 0.5 g of NaCl, 0.5 g of $MgSO_4$, 3 g of beef extract, 10 g of yeast extract, 10 g of soluble starch, 2 g of $CaCO_3$, pH 7.2–7.4) at 150 rpm and 28℃ for 7 days. The secondary metabolites in fermentation broth were extracted with ethyl acetate (v/v = 1:1). After

[2]https://www.ezbiocloud.net/search?tn=Nocardioides

[3]http://www.majorbio.com/

[4]http://ccb.jhu.edu/software/glimmer/index.shtml

[5]http://antismash.secondarymetabolites.org/#!/start

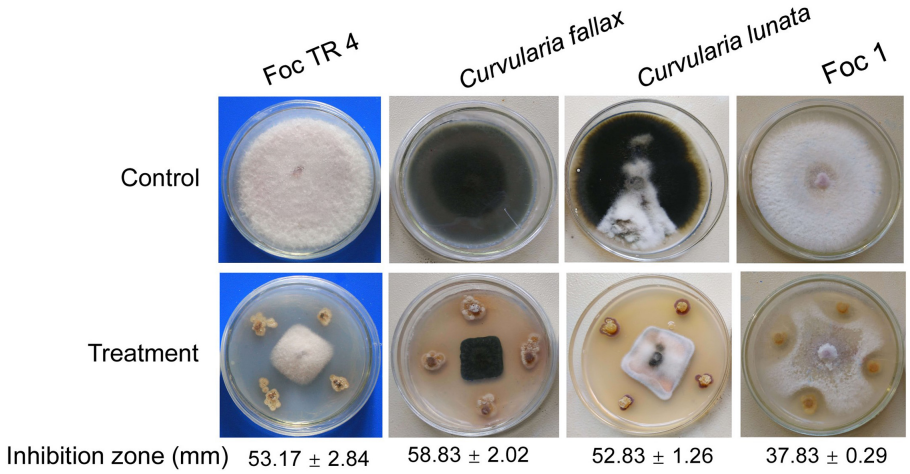

FIGURE 1 | Antifungal activity of strain SCA2-4^T against four banana fungal pathogens. Foc TR4: *Fusarium oxysporum* f. sp. *cubense* tropical race 4; Foc 1: *Fusarium oxysporum* f. sp. *cubense* 1.

mycelia were removed with the Whatman No.1 filter, secondary metabolites in organic solvent were collected using a separating funnel and evaporated using a rotary vacuum evaporator (EYELA, N-1300, Japan). The extracts were dissolved in 10% of dimethyl sulfoxide (DMSO) with 20 mg/mL of a final concentration.

Analysis of Minimum Inhibitory Concentration and Antifungal Activity of Extracts

Minimum inhibitory concentration (MIC) of extracts against Foc TR4 was analyzed using a 96-well plate (Nunc MicroWell, Roskilde, Denmark) (Wang et al., 2013). The stock solution was sterilized through a 0.22-μm sterile filter (Millipore, Bedford, MA, United States) and diluted to a concentration range of 100–0.781 μg/mL by a two-fold serial dilution method (Qi et al., 2019). Each well contained 80 μL of the Roswell Park Memorial Institute (RPMI) mycological media, one hundred microliters of fungal suspension at 1.0 × 10 ^{5} CFU (colony-forming units)/mL and 20 μL of extract solution. Twenty microliters of 10% DMSO replacing extract solution was used as a negative control. The same volume of cycloheximide (50–0.391 μg/mL) or nystatin (50–0.391 μg/mL) replacing extract solution was used as a positive control. The 96-well plate was covered with a plastic membrane and cultured at 150 rpm for 24 h at 28℃. MIC value was determined as our description (Qi et al., 2019). Antifungal activity of extracts against Foc TR4 was assessed using an agar-well diffusion method (Tepe et al., 2005). 100 μL of extracts (16 × MIC) was added to each well. An equal amount of DMSO (10%, v/v) was used as a control. A 5 mm-diameter hyphal disk was placed on the plate center. The growth diameter of fungi was measured after cultured 28℃ for 7 days. All experiments were repeated in triplicate. The growth inhibition percentage was calculated according to the above method.

Effect of Extracts on Cell Structure of Foc TR4

Effect of strain SCA2-4^T extracts on cell structure of Foc TR4 was observed by a transmission electron microscope (TEM, HT7700, Hitachi, Japan) (Nogueira et al., 2010). Foc TR4 mycelia exposed to extracts were fixed with glutaraldehyde (2.5%, v/v) for 3 h and washed three times with PBS (0.1 mol/L, pH 7.0). Foc TR4 mycelia treated with 10% (v/v) of DMSO were used as a control. Mycelial samples were postfixed with 1% (w/v) of osmium tetroxide in PBS (0.1 mol/L, pH 7.3) for 3 h at room temperature and rinsed three times with same buffer. Thereafter, samples were dehydrated in a graded ethanol solution (70, 80, 90, 95, and 100%) for 20 min, respectively. Dehydrated specimens were then embedded in the Epon 812 resin at 37°C for 12 h, 45°C for 12 h, and 60°C for 24 h, respectively. The samples were cut into ultrathin sections (approximately 50 nm in thickness) using an ultramicrotome (EM UC6, Leica, Germany). After stained with saturated uranyl acetate and lead citrate, the sections were observed using TEM.

Effect of Extracts on Spore Germination of Foc TR4

Effect of strain SCA2-4^T extracts on spore germination of Foc TR4 was examined by an optical microscope (Axio Scope A1, Carl ZEISS, Germany) (Chen et al., 2018). Foc TR4 spores were collected using a sterile L-shaped spreader and adjusted to a concentration of 1.0 × 10^5 CFU/mL with sterile distilled water. Ten microliters of extracts and an equal volume of spore suspension were mixed in a cavity glass slide at 28°C for 20 h. Three replications were set for each experiment. One hundred spores in per slide were observed for germination. The germination rate and the inhibition rate of spore germination were calculated according to the following formula: The germination rate = (A or B)/100 × 100% and the inhibition rate of spore germination = (A−B)/A × 100%. A and B were

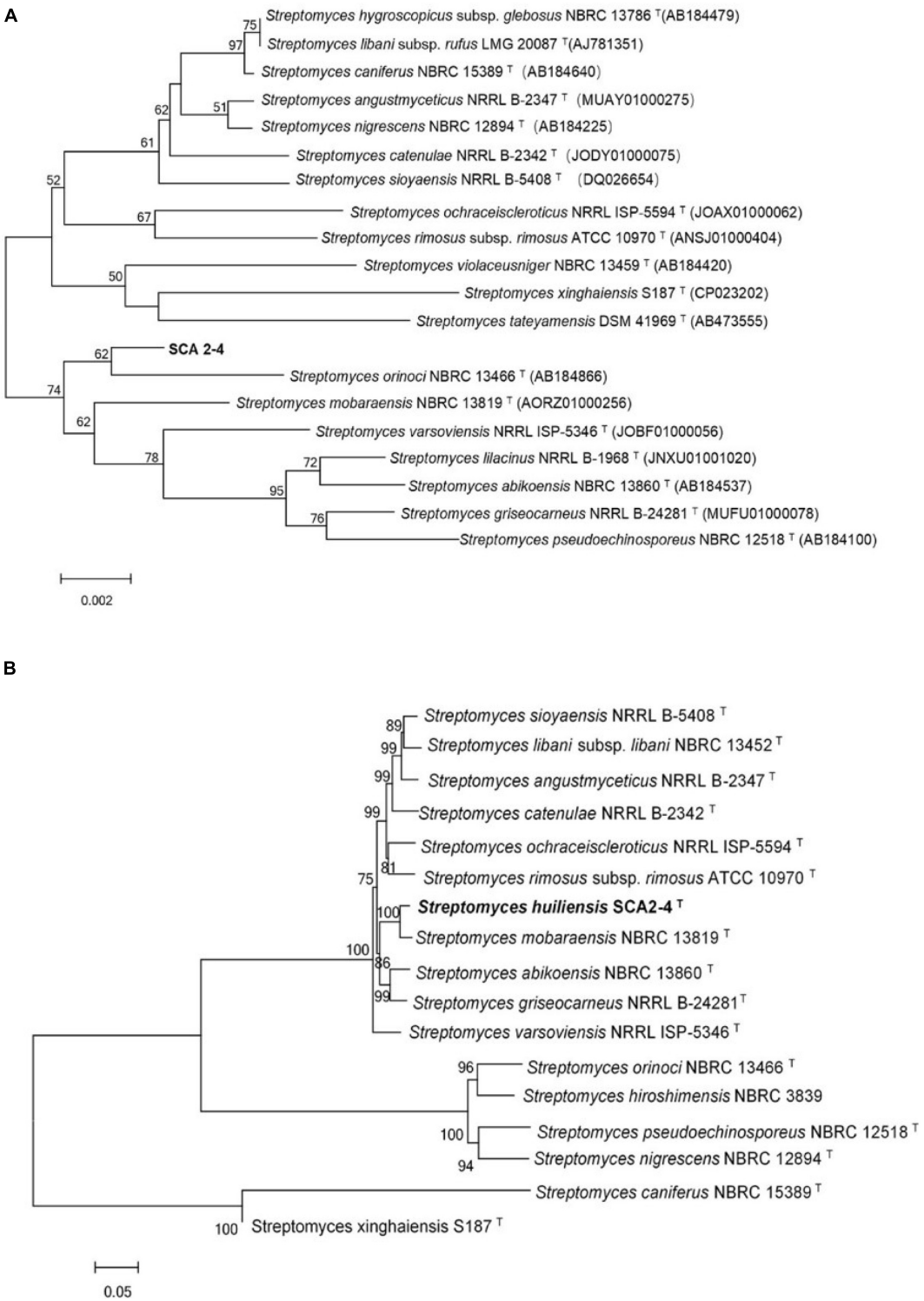

FIGURE 2 | Phylogenetic trees of strain SCA2-4^T based on 16S *rRNA* and house-keeping genes. Bootstrap percentages (based on 1000 replications) were shown at branching points. Bar, 0.002 or 0.05 substitutions per nucleotide position. **(A)** Construction of phylogenetic tree based on the complete 16S *rRNA* sequences using the Neighbor-Joining method. Accession numbers of the selected genes were listed in brackets. **(B)** Construction of phylogenetic tree based on concatenated five house-keeping genes (*atpD*, *gyrB*, *recA*, *rpoB,* and *trpB*) using the Neighbor-Joining method. Strain names and accession numbers were provided in **Supplementary Table 1**.

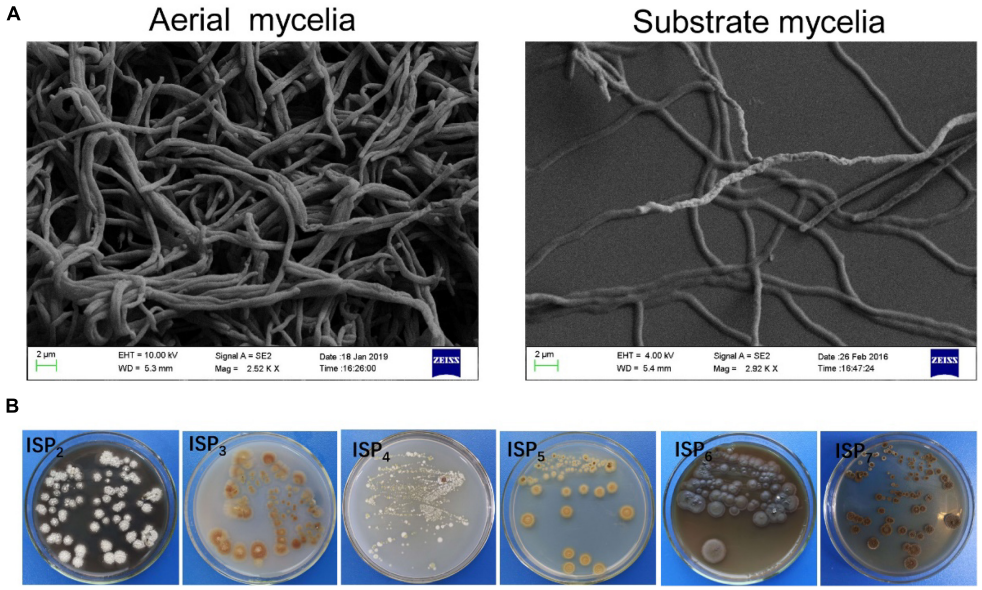

FIGURE 3 | Mycelial and morphological characteristics of SCA2-4^T. **(A)** Aerial and substrate mycelia were detected on the YE agar medium at 28°C for 21 days using the scanning electron microscope. **(B)** Cultural characteristics of strain 2-4^T on six ISP media.

TABLE 1 | Comparison of growth characteristics between strain SCA2-4^T and closely related strains on six standard ISP media.

Medium	Aerial mycelium color			substrate mycelium color			Soluble pigment			Growth		
	1	2	3	1	2	3	1	2	3	1	2	3
Trytone-yeast extract agar (ISP2 or YE)	Gray white	White	None	Dark brown	Pastel yellow	Broom yellow	Brown	None	None	Good	Good	Good
Oatmeal agar (ISP3)	Reddish brown	White	None	Light yellow	Beige	Yellow	None	None	None	Good	Good	Good
Inorganic salts–starch agar (ISP4)	Light yellow	White	None	Light yellow	Colorless	Yellow	None	None	None	Good	Good	Good
Glycerol–asparagine agar (ISP5)	Earthy yellow	White	None	Gold	Beige	Curry	None	None	None	Good	Good	Good
Peptone–yeast extract iron agar (ISP6)	None	None	None	Iron gray	Brown red	Yellow	Brown	None	None	Good	Good	Good
Tyrosine agar (ISP7)	None	White	None	Dark brown	Brown	Yellow	Light brown	Brown	None	Good	Good	Good

SCA2-4^T; 2: Streptomyces mobaraensis NBRC 13819^T; 3: Streptomyces orinoci NBRC 13466^T. The data of Streptomyces mobaraensis NBRC 13819^T and Streptomyces orinoci NBRC 13466^T came from Streptomyces mobaraensis IPCR 16-22 | Type strain | DSM 40847, ATCC 29032, JCM 4168, KCC S-0168 | BacDiveID:16163 (dsmz.de) and Streptomyces orinoci 1882 | Type strain | DSM 40571, ATCC 23202, CBS 767.72, IFO 13466, IPV 1901, ISP 5571, JCM 4546, JCM 4807, NBRC 13466, NRRL B-3379, RIA 1427 | BacDiveID:16172 (dsmz.de).

the number of germinated spores in the control and treatment groups, respectively.

RESULTS AND DISCUSSION

Isolation and Antifungal Activity Assay of Actinobacteria

Forty-eight actinobacteria were isolated using the SCA medium from soil sample of the dry hot valley. Antagonistic activities against Foc TR4 were screened using a conventional spot inoculation method. Fourteen strains exhibited antifungal activities against Foc TR4. Strain SCA2-4^T had a high antifungal activity and was selected for the following study. We further assessed its antifungal activities against other phytopathogenic fungi such as Foc 1, *C. fallax* and *C. lunata* (**Figure 1**). Compared with the growth diameter (85.00 mm ± 0.00) in the control group, the inhibitory zones of strain SCA2-4^T against Foc TR4, Foc 1, *C. fallax*, and *C. lunata* were 53.17 mm ± 2.84, 37.83 mm ± 0.29, 58.83 mm ± 2.02, and 52.83 mm ± 1.26, respectively. The percentages of mycelial inhibition were 62.55, 44.51, 69.21, and 62.15%, respectively.

Phylogenetic and Genomic Analyses of Strain SCA2-4^T

Because 16S *rRNA* had a high resolving ability for relatedness between different organisms on the genus level

TABLE 2 | Morphological, physiological and biochemical characteristics of strain SCA2-4^T and two standard strains.

Characteristics	Strain 1	Strain 2	Strain 3
Morphology	Branched substrate and aerial mycelium, which could not differentiate into spore chains	Umbellate monoverticillate morphology, cylindrical spores with smooth surface	Branched vegetative mycelium, straight spore filaments, cylindrical spores with smooth surface
Physiological			
Temperature range for growth (?)	1745℃ (optimum 28 C)	>45℃	>50℃
PH range for growth	PH5-8 (optimum pH 7.0)	N	N
NaCl tolerance for growth (%)	<6%	≤5%	≤2.5%
Biochemical			
Urease production	−	+	−
Tween 20	−	N	N
Tween 80	+	N	N
Degradation of cellulose	−	N	N
Melanoid pigment	+	−	+
Tyrosinase production	+	+	−
Starch hydrolysis	−	+	−
H_2S production	−	−	+
Gelatin liquefaction	+	−	−
Nitrate reduction	+	+	−
Growth on sole carbon sources (1.0%, w/v)			
L-Arabinose	+	−	±
Cellulose	−	−	±
D-fructose	+	−	±
D-glucose	+	+	±
D-mannitol	−	−	±
Inositol	+	−	±
D-raffinose	+	−	±
L-rhamnose	+	−	±
Sucrose	+	−	±
D-xylose	−	−	±

Strain 1: SCA2-4^T; Strain 2: Streptomyces mobaraensis NBRC 13819^T; Strain 3: Streptomyces orinoci NBRC 13466^T. The data of Streptomyces mobaraensis NBRC 13819^T and Streptomyces orinoci NBRC 13466^T came from Streptomyces mobaraensis IPCR 16-22 | Type strain | DSM 40847, ATCC 29032, JCM 4168, KCC S-0168 | BacDiveID:16163 (dsmz.de) and Streptomyces orinoci 1882 | Type strain | DSM 40571, ATCC 23202, CBS 767.72, IFO 13466, IPV 1901, ISP 5571, JCM 4546, JCM 4807, NBRC 13466, NRRL B-3379, RIA 1427 | BacDiveID:16172 (dsmz.de). +: positive; −: negative; ±: Positive is more than negative. N: No data.

(Stackebrandt and Goebel, 1994), these sequences were first used to identify the genus of strain SCA2-4^T. A complete gene sequence of 16S *rRNA* (1523 bp, Genbank accession number MW547058) was selected from the sequenced genome of strain SCA2-4^T. By aligned with the different databases, the strain belonged to a member of the genus *Streptomyces*. The 16S *rRNA* sequence of strain SCA2-4^T shared 99.17% of similarity with *Streptomyces mobaraensis* NBRC 13819^T. However, the phylogenetic trees constructed by the Neighbor-joining method showed that strain SCA2-4^T fell into a subclade with *S. orinoci* NBRC 13466^T (98.89% of similarity) with 54% of bootstrap value (**Figure 2A**). The taxonomic status of subclade was supported by the maximum-parsimony tree with 25% of low bootstrap value, but was not supported by the maximum-likelihood tree. The low bootstrap values generated by different algorithms indicated that strain SCA2-4^T was not distinguished from closely related species using 16S *rRNA* genes. Likewise, the previous study also showed that 16S *rRNA* genes lacked sufficient resolution for closely related species due to its multiple copies and conservative feature in the single genome (Martens et al., 2008).

In order to further determine the phylogenetic status of strain SCA2-4^T, the multilocus sequence analysis (MLSA) was performed using the sequences of *atpD*, *gyrB*, *recA*, *rpoB,* and *trpB* genes. The MLSA was considered as an alternative method for refining the *Streptomyces* systematics due to its efficiency of inter- and intra-species resolution and reproducibility (Rong and Huang, 2010). The Neighbor-joining tree based on MLSA demonstrated that strain SCA2-4^T formed a distinct clade with *S. mobaraensis* NBRC 13819^T with 100% of bootstrap value (**Figure 2B**). The taxonomic status of subclade was well supported by trees constructed by other two algorithms. These five protein-coding genes were also selected to identify *Streptomyces* (Rong et al., 2010; Huang et al., 2019). Rong and Huang (2012) found high correlation between the five-gene MLSA and the DNA-DNA hybridization in *Streptomyces*. The five-gene nucleotide sequence distance above 0.007 could be

TABLE 3 | Chemotaxonomic characteristics of strain SCA2-4^T.

Characteristic	SCA2-4^T
Major menaquinones (%)	
MK-9(H_2)	7.0
MK-9(H_4)	40.0
MK-9(H_6)	44.0
MK-9(H_8)	9.0
Major fatty acids (>0.5%)	
Saturated	
$C_{14:0}$	0.74
$C_{15:0}$	-
$C_{16:0}$	5.1
Antesio-$C_{15:0}$	35.01
Antesio-$C_{17:0}$	4.27
Iso-$C_{13:0}$	0.64
Iso-$C_{14:0}$	1.57
Iso-$C_{15:0}$	28.01
Iso-$C_{16:0}$	3.01
Iso-$C_{17:0}$	2.64
Unsaturated	
Iso-$C_{16:1}$ H	1.67
$C_{16:1}\omega7c$	11.03
$C_{16:0}$ 9 methyl	1.31
Antesio-$C_{17:1}$ C	1.09
Major polar lipids	DPG, PL_1, PE

DPG, diphosphatidylglycerol; PL_1, unidentified phospholipids; PE, phosphatidylethanolamine.

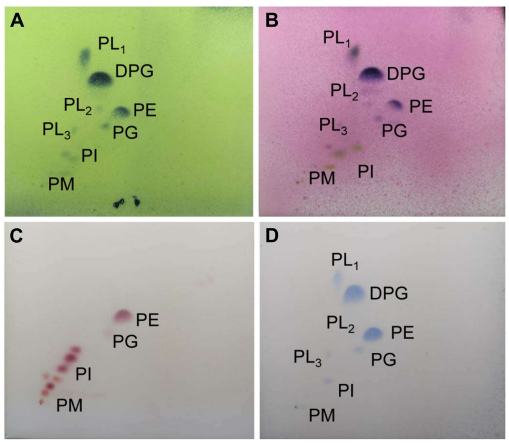

FIGURE 4 | The phospholipid profile of strain SCA2-4 ^{T} sprayed with phosphomolybdic acid **(A)**, a-naphthol **(B)**, ninhydrin **(C)**, and phosphate **(D)**. The horizontal and vertical directions were developed using the chloroform-methanol-water (65:25:4) (v/v) and the chloroform-methanol-acetic acid-water (80:12:15:4) (v/v), respectively. DPG, diphosphatidylglycerol; PE, phosphatidylethanolamine; PL1-3, unidentified phospholipids; PG, phosphatidylglycerol; PI, Phosphatidylinositol; PIM, phosphatidylinositolmannoside.

considered as an independent species. Our results showed the distance of MLSA between strain SCA2-4^T and other selected strains ranged from 0.024 to1.020 (**Supplementary Table 2**), suggesting that strain SCA2-4^T might be a novel species.

Although the conventional DNA-DNA hybridization was often used to clarify the species of strains, the technique was time-consuming, labor-intensive and low reproducible (Stackebrandt and Goebel, 1994; Goris et al., 2007). Average nucleotide identity (ANI) was a robust and sensitive means to compare genetic relatedness among strains by the alignment of genome sequences (Konstantinidis and Tiedje, 2005; Goris et al., 2007). However, the limited availability of strain whole-genome sequences restricted the use of ANI in taxonomic purposes. Based on the above results, we selected two standard strains (*S. orinoci* NBRC 13466^T, = NRRL B-3379^T, GenBank Accession No. NZ_PHNC00000000.1 and *S. mobaraensis* NBRC 13819^T, = DSM 40847, GenBank Accession No. NZ_VOKX00000000.1) to further identify the species of strain SCA2-4^T. We compared with strain SCA2-4^T genome (DDBJ/ENA/GenBank Accession No. JAIQLH000000000) and two standard strain genomes. ANI values were 80.44 and 90.76%, respectively, which were below the threshold value of 95–96% for distinguishing a novel species (Richter and Rossello-Mora, 2009; Chun et al., 2018). Thus, strain SCA2-4^T was identified as a novel species of the genus *Streptomyces*.

Phenotypic Characteristics

Strain SCA2-4^T was an aerobic and Gram-positive bacterium. SEM analysis revealed that the strain produced well-developed and branched substrate and aerial mycelium that could not differentiate into spore chains (**Figure 3A**). It could grow well on ISP2, ISP3 and ISP6 media, followed by ISP4, ISP5 and ISP7 media. Aerial hypha demonstrated gray white, reddish brown, and earthy yellow colors on ISP2 and ISP4 media, respectively. None of aerial mycelia was produced on other two media. The hyphal substrate colors on ISP2-7 media were dark brown, light yellow, light yellow, gold, iron gray, and dark brown, respectively. Strain SCA2-4^T produced brown or light brown soluble pigment on different media except for ISP3-5 (**Figure 3B**). These morphological and cultural characteristics were consistent with those of the genus *Streptomyces*. By contrast, two standard strains selected grew well on all ISP media. Their cultural characteristics were compared in **Table 1**.

In addition, strain SCA2-4^T could grow at pH from 5.0 to 8.0 (optimum pH 7.0), temperature from 17–45°C (optimum 28°C) and NaCl from 0 to 6% (w/v). It could degrade Tween 80, tyrosine, gelatin and nitrate, but not resolve urea, Tween 20, starch and cellulose. Strain SCA2-4^T produced melanoid pigment, but not H_2S. It could utilize carbon sources such as L-Arabinose, D-fructose, D-glucose, inositol, D-raffinose, L-rhamnose, and sucrose, but not Cellulose, D-mannitol and D-xylose (**Table 2**). In addition, strain SCA2-4^T used L-phenylalanine, ammonium sulfate, L-hydroxyproline, L (+)-cysteine, histidine, glycine, valine, and ammonium oxalate as sole nitrogen sources, but not ammonium acetate, ammonium nitrate, ammonium molybdate tetrahydrate, L-arginine and glutamate. The

FIGURE 5 | Genome information and function annotation of strain SCA2-4^T. **(A)** Circular map of strain SCA2-4^T genome. From outside to center, ring 1 was the mark of genome size. Rings 2 and 3 represented CDS on forward/reverse strand. Different colors indicated the functional category of CDS. Ring 4 was tRNA and rRNA. Ring 5 showed the G + C content. The outward red part indicated that the GC content of this region was higher than the average GC content of the whole genome. The inward blue part indicated that the GC content of this region was lower than the average GC content of the whole genome, followed by G + C skew in ring 6. **(B)** The COG annotation of strain SCA2-4^T genome. **(C)** The KEGG pathway annotation of strain SCA2-4^T genome.

TABLE 4 | Genome information of strain SCA2-4^T.

Items	Chromosome characteristics	% of total[a]
Chromosome size (bp)	7681513	100
DNA coding region (bp)	6448287	83.95
GC content (bp)	5621792	73.19
RNA genes[b]	70	–
Protein-coding genes	7137	100
Genes assigned to COG	5165	72.37
Genes assigned to KEGG	2442	34.22
Genes assigned to GO	4350	60.95
CRISPR repeat	114	1.6

[a] *The total was based on either the size of the genome in base pairs or the total number of proteins encoding genes in the annotated genome.*
[b] *RNA genes also included one rRNAs and 69 tRNAs.*

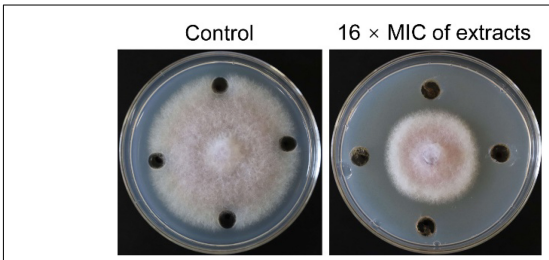

FIGURE 6 | Inhibition assay of strain SCA2-4^T extracts on the mycelial growth of Foc TR4. 10% of DMSO treatment was used as control.

strain was sensitive to rifampicin, but resistant to ampicillin, chloramphenicol, streptomycin, penicillin-G, gentamicin, nystatin, tetracycline, neomycin sulfate and kanamycin sulfate (**Supplementary Table 3**).

Chemotaxonomic Characteristics

By analysis, the predominant menaquinones of strain SCA2-4^T were MK-9(H_4) (40.0%) and MK-9(H_6) (44.0%). MK-9(H_2) (7.0%), and MK-9(H_4) (9.0%) were minor components. The composition of fatty acids included Antesio-$C_{15:0}$ (35.01%), Iso-$C_{15:0}$ (28.01%) and $C_{16:1}\omega7c$ (11.03%) (**Table 3**). The major polar lipids consisted of diphosphatidylglycerol, unidentified phospholipid, and phosphatidylethanolamine. We also identified phosphatidylglycerol, two unidentified lipids, phosphatidylinositol and phosphatidylinositol mannoside (**Figure 4**). The chemotaxonomic characteristics of strain SCA2-4^T were consistent with those of the genus *Streptomyces*.

Bioinformatic Analysis

Strain SCA2-4^T genome was sequenced and contained 7681513 bp. The genome with 73.19% of GC content included

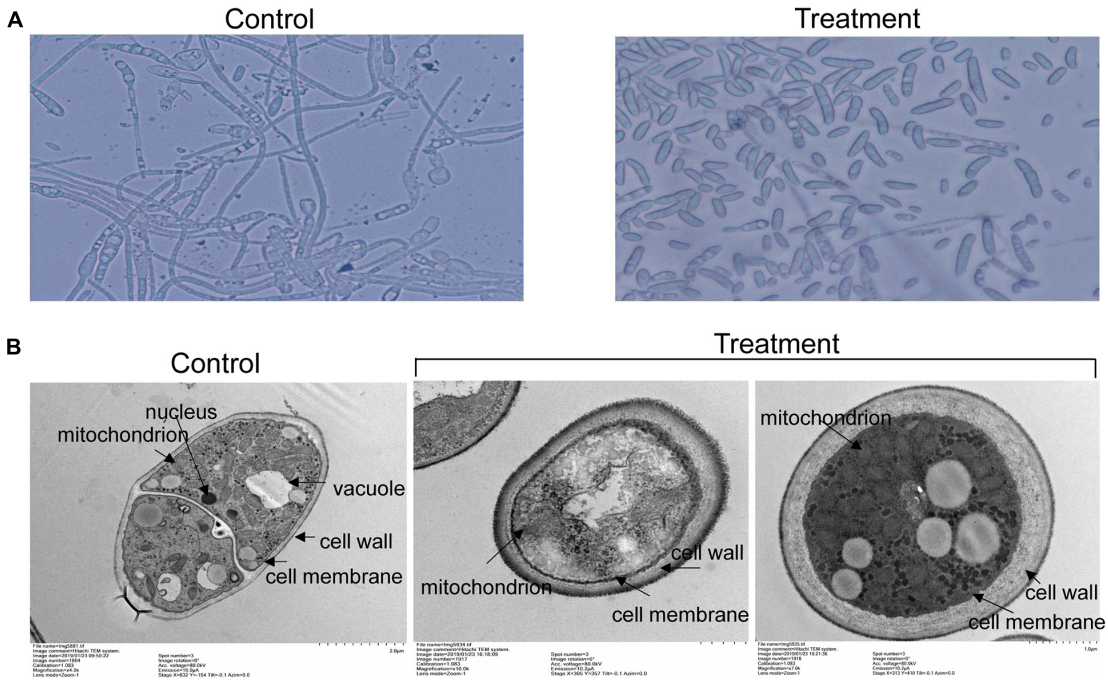

FIGURE 7 | Effects of strain SCA2-4^T extracts on spore germination and cell structure of Foc TR4. 10% of DMSO treatment was used as control. **(A)** Measurement of spore germination after treated with 16 × MIC of strain SCA2-4^T extracts. **(B)** Cell structure of Foc TR4 treated with 16 × MIC of strain SCA2-4^T extracts was detected using the transmission electron microscopy.

one *rRNA* gene, sixty-nine tRNA genes and 7137 coding sequences (CDS) (**Figure 5A** and **Table 4**). By annotation, 73.41, 34.22, and 60.95% of CDS were assigned to COG, KEGG, and GO, respectively (**Table 4**). In the COG categories, 34.26, 17.58, and 14.28% of genes participated in metabolism, information storage and processing as well as cellular processes and signaling, respectively. Significantly, 33.88% of COG genes were unknown function (**Figure 5B** and **Supplementary Table 4**). These coding sequences were responsible for different function profiles in the KEGG pathways (**Figure 5C**). By analysis of antiSMASH software, fifty-one gene clusters related to the secondary metabolite biosynthesis were identified in genome sequences of strain SCA2-4^T (**Supplementary Table 5**). They included nine PKS I gene clusters, eight terpene gene clusters, five NRPS gene clusters, four PKS III gene clusters, three other gene clusters, two lasso peptide gene clusters, two PKS II gene clusters, two siderophore gene clusters, two otherks gene clusters, two lantipeptide gene clusters, one PKS III-siderophore gene cluster, one fused gene cluster, one arylpolyene gene cluster, one lantipeptide-lasso peptide gene cluster, one lantipeptide-NRPS gene cluster, one ladderane gene cluster, one indole gene cluster, one PKS III-terpene gene cluster, one terpene-NRPS gene cluster, one bacteriocin gene cluster, one PKS I-NRPS gene cluster and one thiopeptide gene cluster (**Supplementary Table 6**). The gene and chemical structures of sixteen secondary metabolites with more than 70% of sequence similarity were listed in **Supplementary Figure 1**.

Genome analysis further revealed that ten gene clusters were involved in the biosynthesis of antimicrobial metabolites, including naringenin (Salehi et al., 2019), piericidin A1 (Engl et al., 2018), simocyclinone (Schimana et al., 2000), granaticin (Snipes et al., 1979), medermycin (Takano et al., 1976), cyclothiazomycin b1 (Mizuhara et al., 2011), cyclothiazomycin C (Cox et al., 2014), caboxamycin (Hohmann et al., 2009), rhizomide A-C (Wang et al., 2018), and alkylresorcinol (Dey et al., 2013). Among them, gene clusters encoding naringenin, simocyclinone, cyclothiazomycin C and alkylresorcinol showed 100% of similarity with the known genes. Thirteen gene clusters might participate in the biosynthesis of anticancer agents including naringenin, aranciamycin, AT2433 (Singh et al., 2015), rebeccamycin (Bush et al., 1987), staurosporine (Nakano and Omura, 2009), K-252a (Nakano and Omura, 2009), cladoniamide (Loosley et al., 2013), oviedomycin (Lombó et al., 2004), landomycin (Henkel et al., 1990), simocyclinone, granaticin, medermycin, and caboxamycin.

Notably, one gene cluster was responsible for in the biosynthesis of siderophore bacillibactin. Siderophores had a competition ability for ferric iron (Fe^{3+}) by the receptors of the siderophore-producing strains (Sheng et al., 2020). They played an important role in enhancing plant resistance and reducing pathogen infection (Gu et al., 2020). Sheng et al. (2020) reported that *Brevibacillus brevis* GZDF3 had strong antifungal activity against *Candida albicans* by producing siderophores. The previous study showed that

Streptomyces S96 lacked antagonistic activity against Foc TR4 by adding an excess ferric iron (Cao et al., 2005). The role of siderophore bacillibactin in antifungal activity of strain SCA2-4^T against plant pathogenic fungi including Foc TR4 needs further study. In addition, several unmatched gene clusters were also found in the genome of strain SCA2-4^T, which might participate in the biosynthesis of some key secondary metabolites.

Description of *Streptomyces huiliensis* sp. nov.

Streptomyces huiliensis (hui.li.en'sis. N.L. masc. adj. *huiliensis* of Huili, a county in China, referring to the place where the type strain was first isolated). The strain was Gram-positive, aerobic and non-motile. It formed branched substrate and aerial mycelia and could grow good on all of ISP agars. Aerial mycelia with gray white, reddish brown, light yellow and earthy yellow were formed on ISP2-4, but not aerial mycelia were detected on ISP6 and ISP7. Substrate mycelia were dark brown on ISP2, light yellow on ISP3-4, gold on ISP5, iron gray and dark brown on ISP6 and ISP7. Brown soluble pigments were produced on ISP2, but not on ISP3-4. Melanin was produced on ISP6 or ISP. The strain could grow at 17–45°C (optimum 28°C), pH 5–8 (optimum pH 7) and 0–6% (w/v) NaCl. It could degrade Tween 80, tyrosine, gelatin and nitrate, but not urea, Tween 20, starch and cellulose. The strain did not produce H_2S. It utilized L-Arabinose, D-fructose, D-glucose, inositol, D-raffinose, L-rhamnose and sucrose as sole carbon sources, but not Cellulose, D-mannitol and D-xylose. It could also use L-phenylalanine, ammonium sulfate, L-hydroxyproline, L (+)-cysteine, histidine, glycine, valine and ammonium oxalate as sole nitrogen sources, but not ammonium acetate, ammonium nitrate, ammonium molybdate tetrahydrate, L-arginine and glutamate. strain SCA2-4^T was resistant to ampicillin, chloramphenicol, streptomycin, Penicillin-G, gentamicin, nystatin, tetracycline, neomycin sulfate and kanamycin sulfate, but sensitive to rifampicin.

MK-9(H_4) (40.0%) and MK-9(H_6) (44.0%) were found as the major menaquinones of the strain. The major fatty acids were composed of Antesio-$C_{15:0}$ (35.01%), Iso-$C_{15:0}$ (28.01%) and $C_{16:1}\omega7c$ (11.03%). The major polar lipids consisted of diphosphatidylglycerol, one unidentified phospholipid, and phosphatidylethanolamine.

Strain SCA2-4^T (= GDMCC 4.215^T) was isolated from the soil sample collected from rhizosphere of *O. stricta* in a dry hot valley of the Huili County, Sichuan Province, China. The 16S *rRNA* gene sequence was submitted into GenBank with accession number MW547058. This Whole Genome Shotgun project of the strain has been deposited at DDBJ/ENA/GenBank under the accession JAIQLH000000000. The version described in this paper is version JAIQLH010000000. The genome was 7681513 bp with 73.19% of GC content.

Antifungal Activity and MIC of Extracts Against Foc TR4

In order to determine whether the secondary metabolites of strain SCA2-4^T had antifungal activity or not, extracts were isolated with ethyl acetate. Minimum inhibitory concentration (MIC) of extracts ranged from 100 to 0.781 μg/mL against Foc TR4. Two standard antibiotics cycloheximide and nystatin used as positive controls. The results displayed that MIC of extracts was 6.25 μg/mL and MIC values of two standard antibiotics cycloheximide and nystatin were 1.563 and 6.25 μg/mL, respectively. The results indicated that secondary metabolites of strain 2-4^T had a strong inhibitory activity on Foc TR4 (**Figure 6**). Inhibition zone and mycelial inhibition rate reached 31.83 mm ± 2.36 and 42.47% (**Supplementary Table 7**), respectively.

Effect of Extracts on Spore Germination and Cell Structure of Foc TR4

To further analyze antifungal mechanism of strain SCA2-4^T extracts, inhibition activity of extracts on spore germination of Foc TR4 was investigated (**Figure 7A**). The results showed that spore germination of Foc TR4 was obviously inhibited by extracts of strain SCA2-4^T. Compared with 94.33 ± 2.08% of spore germination rate in the control, the inhibition rate was 89.08% in the treatment group. In addition, cell ultrastructure of Foc TR4 was detected using TEM after treatment. By contrast, cells of Foc TR4 mycelia treated with 10% of DMSO kept an intact and discernible structure of cell membrane with the uniform cytochylema. All organelles such as mitochondria, nuclei and vacuoles had normal morphological characteristics (**Figure 7B**). However, fungal cell wall and cytoplasmic membrane treated with 16 × MIC of extracts became irregular and thickened. Many organelles such as nuclei and vacuoles were broken. Mitochondrial structures were disrupted, suggesting that extracts caused serious damage to cell structure of strain SCA2-4^T extracts.

CONCLUSION

An actinobacterial strain SCA2-4^T was isolated from the rhizospheric soil of *O. stricta* in a dry hot valley and selected for its excellent antifungal activity against *Foc* TR4. Strain SCA2-4^T was identified as a novel species of the genus *Streptomyces* in the light of genotype and phenotype data. The strain was proposed as *Streptomyces huiliensis* sp. nov. The whole genome analysis showed that strain SCA2-4^T contained 51 putative biosynthetic gene clusters. Especially, ten gene clusters were involved in the biosynthesis of antimicrobial metabolites. The strain also exhibited high antifungal activity against pathogens of other banana fungal diseases such as Foc 1, *C. fallax,* and *C. lunata.* Extracts of strain SCA2-4^T seriously destroyed fungal cell structure of Foc TR4, inhibited the mycelial growth and spore germination. MIC was 6.25 μg/mL against Foc TR4. These results implied that this strain could be a promising candidate for biological control of banana *Fusarium* wilt.

DATA AVAILABILITY STATEMENT

The datasets presented in this study can be found in online repositories. The names of the repository/repositories and accession number(s) can be found in the article/ **Supplementary Material**.

AUTHOR CONTRIBUTIONS

DQ, LiZ, DZ, LZ, JX, and WW developed the ideas and designed the experimental plans. WW and JX supervised the research and provided the fund support. DQ, LiZ, DZ, MZ, and YW performed experiments. DQ, WW, and JX provided the materials. DQ, LZ, and WW analyzed the data and prepared the manuscript. All authors contributed to the article and approved the submitted version.

FUNDING

This work was supported by the National Key Research and Development Program of China (2020YFD1000104), the National Natural Science Foundation of China (31770476 and 32072504), the Natural Science Foundation of Hainan (2019RC293 and 320CXTD441), and the China Agriculture Research System (CARS-31).

ACKNOWLEDGMENTS

We thank Xiaolong Huang and Zhufeng Gao for providing your help to this work.

SUPPLEMENTARY MATERIAL

The Supplementary Material for this article can be found online at: https://www.frontiersin.org/articles/10.3389/fmicb.2021.722661/full#supplementary-material

Supplementary Figure 1 | Genome-wide analysis of strain SCA2-4^T for gene clusters of the biosynthesis of secondary metabolites by the online antiSMASH v4.2.0 software.

Supplementary Table 1 | Allele sequence accession numbers of the *Streptomyces* used for the present study.

Supplementary Table 2 | MLSA distance values for selected strains in this study.

Supplementary Table 3 | Nitrogen-source utilization and antibiotic sensitivity of strain SCA2-4^T.

Supplementary Table 4 | Functional cluster of orthologous genes (COG) classification of predicted genes in strain SCA2-4^T.

Supplementary Table 5 | Biosynthetic gene clusters of secondary metabolite of strain SCA2-4^T on the online antiSMASH v 6.0.1.

Supplementary Table 6 | Cluster number and gene number shown in different cluster types of strain SCA2-4^T.

Supplementary Table 7 | Inhibitory activity and MIC of extracts of strain SCA2-4^T against Foc TR4.

REFERENCES

Aghighi, S., Shahidi Bonjar, G. H., Saadoun, I., Rawashdeh, R., and Batayneh, S. (2004). First report of antifungal spectra of activity of Iranian actinomycetes strains against *Alternaria solani*, *Alternaria alternata*, *Fusarium solani*, *Phytophthora megasperma*, *Verticillium dahliae* and *Saccharomyces cerevisiae*. *Asian J. Plant Sci.* 3, 463–471. doi: 10.3923/ajps.2004.463.471

Ahmad, M. S., Elgendy, A. O., Ahmed, R. R., Hassan, H. M., Elkabbany, H. M., and Merdash, A. G. (2017). Exploring the antimicrobial and antitumor potentials of *Streptomyces* sp. AGM12-1 isolated from Egyptian soil. *Front. Microbiol.* 8:438. doi: 10.3389/fmicb.2017.00438

Altschul, S. F., Gish, W., Miller, W., Myers, E. W., and Lipman, D. J. (1990). Basic local alignment search tool. *J. Mol. Biol.* 215, 403–410. doi: 10.1016/S0022-2836(05)80360-2

Bérdy, J. (2005). Bioactive microbial metabolites. *J. Antibiot.* 58, 1–26. doi: 10.1038/ja.2005.1

Brady, C., Cleenwerck, I., Venter, S., Vancanneyt, M., Swings, J., and Coutinho, T. (2008). Phylogeny and identification of *Pantoea* species associated with plants, humans and the natural environment based on multilocus sequence analysis (MLSA). *Syst. Appl. Microbiol.* 31, 447–460. doi: 10.1016/j.syapm.2008.09.004

Bush, J. A., Long, B. H., Catino, J. J., and Bradner, W. T. (1987). Production and biological activity of rebeccamycin, a novel antitumor agent. *J. Antibiot.* 40, 668–678. doi: 10.7164/antibiotics.40.668

Cao, L., Qiu, Z., Dai, X., Tan, H., Lin, Y., and Zhou, S. (2004). Isolation of endophytic actinomycetes from roots and leaves of banana (*Musa acuminata*) plants and their activities against *Fusarium oxysporum* f. sp. cubense. *World J. Microb. Biotechnol.* 20, 501–504. doi: 10.1023/B:WIBI.0000040406.30495.48

Cao, L., Qiu, Z., You, J., Tan, H., and Zhou, S. (2005). Isolation and characterization of endophytic *Streptomycete antagonists* of *Fusarium* wilt pathogen from surface-sterilized banana roots. *FEMS Microbiol. Lett.* 247, 147–152. doi: 10.1016/j.femsle.2005.05.006

Chen, Y. F., Zhou, D. B., Qi, D. F., Gao, Z. F., Xie, J. H., and Luo, Y. P. (2018). Growth promotion and disease suppression ability of a *Streptomyces* sp. CB-75 from banana rhizosphere soil. *Front. Microbiol.* 8:2704. doi: 10.3389/fmicb.2017.02704

Chun, J., Oren, A., Ventosa, A., Christensen, H., Arahal, D. R., Da, C. M., et al. (2018). Proposed minimal standards for the use of genome data for the taxonomy of prokaryotes. *Int. J. Syst. Evol. Micr.* 68, 461–466. doi: 10.1099/ijsem.0.002516

Cox, C. L., Tietz, J. I., Sokolowski, K., Melby, J. O., Doroghazi, J. R., and Mitchell, D. A. (2014). Nucleophilic 1,4-additions for natural product discovery. *ACS Chem. Biol.* 9, 2014–2022. doi: 10.1021/cb500324n

Delcher, A. L., Bratke, K. A., Powers, E. C., and Salzberg, S. L. (2007). Identifying bacterial genes and endosymbiont DNA with Glimmer. *Bioinformatics* 23, 673–679. doi: 10.1093/bioinformatics/btm009

Dey, E. S., Ahmadi-Afzadi, M., Nybom, H., and Tahir, I. (2013). Alkylresorcinols isolated from rye bran by supercritical fluid of carbon dioxide and suspended in a food-grade emulsion show activity against *Penicillium expansum* on apples. *Arch. Phytopathol. Plant Prot.* 46, 105–119. doi: 10.1080/03235408.2012.73471

Engl, T., Kroiss, J., Kai, M., Nechitaylo, T. Y., Svato, A., and Kaltenpoth, M. (2018). Evolutionary stability of antibiotic protection in a defensive symbiosis. *Proc. Natl. Acad. Sci. U.S.A.* 115, E2020–E2029. doi: 10.1073/pnas.1719797115

Felsenstein, J. (1981). Evolutionary trees from DNA sequences: a maximum likelihood approach. *J. Mol. Evol.* 17, 368–376. doi: 10.1007/BF01734359

Felsenstein, J. (1985). Confidence limits on phylogenies: an approach using the bootstrap. *Evolution* 39, 783–791. doi: 10.1111/j.1558-5646.1985.tb00420.x

Fitch, W. M. (1971). Toward defining the course of evolution: minimum change for a specific tree topology. *Syst. Biol.* 20, 406–416. doi: 10.1093/sysbio/20.4.406

Getha, K., Vikineswary, S., Wong, W. H., Seki, T., Ward, A., and Goodfellow, M. (2005). Evaluation of *Streptomyces* sp. strain g10 for suppression of fusarium

wilt and rhizosphere colonization in pot-grown banana plantlets. *J. Ind. Microbiol. Biotechnol.* 32, 24–32. doi: 10.1007/s10295-004-0199-5

Goris, J., Konstantinidis, K. T., Klappenbach, J. A., Coenye, T., and Tiedje, J. M. (2007). DNA-DNA hybridization values and their relationship to whole-genome sequence similarities. *Int. J. Syst. Evol. Microbiol.* 57, 81–91. doi: 10.1099/ijs.0.64483-0

Gu, S., Yang, T., Shao, Z., Wang, T., and Pommier, T. (2020). Siderophore-mediated interactions determine the disease suppressiveness of microbial consortia. *mSystems* 5, e811–e819. doi: 10.1128/mSystems.00811-19

Guo, Y. P., Zheng, W., Rong, X. Y., and Huang, Y. (2008). A multilocus phylogeny of the *Streptomyces griseus* 16s rRNA gene clade: use of multilocus sequence analysis for *Streptomycete systematics*. *Int. J. Syst. Evol. Microbiol.* 58, 149–159. doi: 10.1099/ijs.0.65224-0

Henkel, T., Rohr, J., Beale, J. M., and Schwenen, L. (1990). Landomycins, new angucycline antibiotics from *Streptomyces* sp. I. structural studies on landomycins A-D. *J. Antibiot.* 43, 492–503. doi: 10.7164/antibiotics.43.492

Hohmann, C., Schneider, K., Bruntner, C., Irran, E., Nicholson, G., Bull, A. T., et al. (2009). Caboxamycin, a new antibiotic of the benzoxazole family produced by the deep-sea strain *Streptomyces* sp. NTK 937. *J. Antibiot.* 62, 99–104. doi: 10.1038/ja.2008.24

Huang, X. L., Kong, F. D., Zhou, S. Q., Huang, D. Y., Zheng, J. P., and Zhu, W. M. (2019). *Streptomyces tirandamycinicus* sp. nov. a novel marine sponge-derived actinobacterium with antibacterial potential against *Streptococcus agalactiae*. *Front. Microbiol.* 10:482. doi: 10.3389/fmicb.2019.00482

Jing, T., Zhou, D. B., Zhang, M. Y., Yun, T. Y., Qi, D. F., Wei, Y. Z., et al. (2020). Newly isolated *Streptomyces* sp. JBS5-6 as a potential biocontrol agent to control banana fusarium wilt: genome sequencing and secondary metabolite cluster profiles. *Front. Microbiol.* 11:602591. doi: 10.3389/fmicb.2020.602591

Kai, B., Thomas, W., Chevrette, M. G., Lu, X., Schwalen, C. J., Kautsar, S. A., et al. (2017). Antismash 4.0-improvements in chemistry prediction and gene cluster boundary identification. *Nucleic Acids Res.* 45, W36–W41. doi: 10.1093/nar/gkx319

Kelly, K. L. (1958). Centroid notations for the revised ISCC-NBC color name blocks. *J. Res. Nat. Bur. Stand.* 61:427.

Kimura, M. (1980). A simple method for estimating evolutionary rates of base substitutions through comparative studies of nucleotide sequences. *J. Mol. Evol.* 16, 111–120. doi: 10.1007/BF01731581

Komagata, K., and Suzuki, K.-I. (1987). Lipid and cell-wall analysis in bacterial systematics. *Methods Microbiol.* 19, 161–207.

Konstantinidis, K. T., and Tiedje, J. M. (2005). Genomic insights that advance the species definition for prokaryotes. *Proc. Natl. Acad. Sci. U.S.A.* 102, 2567–2572. doi: 10.1073/pnas.0409727102

Kumar, S., Stecher, G., and Tamura, K. (2016). MEGA7: molecular evolutionary genetics analysis version 7.0 for bigger datasets. *Mol. Biol. Evol.* 33, 1870–1874. doi: 10.1093/molbev/msw054

Kumar, V., Naik, B., Gusain, O., and Bisht, G. S. (2014). An actinomycete isolate from solitary wasp mud nest having strong antibacterial activity and kills the *Candida* cells due to the shrinkage and the cytosolic loss. *Front. Microbiol.* 5:446. doi: 10.3389/fmicb.2014.00446

Kuster, E., and Williams, S. T. (1964). Selection of media for isolation of *Streptomycetes*. *Nature* 202, 928–929. doi: 10.1038/202928a0

Lombó, F., Braña, A. F., Salas, J. A., and Méndez, C. (2004). Genetic organization of the biosynthetic gene cluster for the antitumor angucycline oviedomycin in *Streptomyces antibioticus* ATCC 11891. *Chembiochem* 5, 1181–1187. doi: 10.1002/cbic.200400073

Loosley, B. C., Andersen, R. J., and Dake, G. R. (2013). Total synthesis of cladoniamide G. *Org. Lett.* 15, 1152–1154. doi: 10.1021/ol400055v

Luo, R., Liu, B., Xie, Y., Li, Z., and Liu, Y. (2012). SOAPdenovo2: an empirically improved memory-efficient short-read de novo assembler. *GigaScience* 1:18. doi: 10.1186/2047-217X-1-18

Martens, M., Dawyndt, P., Coopman, R., Gillis, M., Vos, P. D., and Willems, A. (2008). Advantages of multilocus sequence analysis for taxonomic studies: a case study using 10 housekeeping genes in the genus ensifer (including former sinorhizobium). *Int. J. Syst. Evol. Micrrbiol.* 58, 200–214. doi: 10.1099/ijs.0.65392-0

Minnikin, D., Collins, M., and Goodfellow, M. (1979). Fatty acid and polar lipid composition in the classification of Cellulomonas, Oerskovia and related taxa. *J. Appl. Bacteriol.* 47, 87–95. doi: 10.1111/j.1365-2672.1979.tb01172.x

Mizuhara, N., Kuroda, M., Ogita, A., Tanaka, T., Usuki, Y., and Fujita, K. I. (2011). Antifungal thiopeptide cyclothiazomycin B1 exhibits growth inhibition accompanying morphological changes via binding to fungal cell wall chitin. *Bioorgan. Med. Chem.* 19, 5300–5310. doi: 10.1016/j.bmc.2011.08.010

Mohandas, S., and Ravishankar, K. V. (2016). *Banana: Genomics and Transgenic Approaches for Genetic Improvement*. Singapore: Springer, 211–226.

Nakano, H., and Omura, S. (2009). Chemical biology of natural indolocarbazole products: 30 years since the discovery of staurosporine. *J. Antibiot.* 62, 17–26. doi: 10.1038/ja.2008.4

Nogueira, J. H. C., GoncAlez, E., Galleti, S. R., Facanali, R., Marques, M., and Felício, J. D. (2010). Ageratum conyzoides essential oil as aflatoxin suppressor of aspergillus flavus. *Int. J. Food Microbiol.* 137, 55–60. doi: 10.1016/j.ijfoodmicro.2009.10.017

Ploetz, R. C. (2015). Fusarium wilt of banana. *Phytopathology* 105, 1512–1521. doi: 10.1094/phyto-04-15-0101-rvw

Qi, D. F., Zou, L. P., Zou, D. B., Chen, Y. F., Gao, Z. F., Feng, R. J., et al. (2019). Taxonomy and broad-spectrum antifungal activity of *Streptomyces* sp. SCA3-4 isolated from rhizosphere soil of *Opuntia stricta*. *Front. Microbiol.* 10:1390. doi: 10.3389/fmicb.2019.01390

Richter, M., and Rossello-Mora, R. (2009). Shifting the genomic gold standard for the prokaryotic species definition. *Proc. Natl. Acad. Sci. U.S.A.* 106, 19126–19131. doi: 10.1073/pnas.0906412106

Rong, X. Y., and Huang, Y. (2010). Taxonomic evaluation of the *Streptomyces griseus* clade using multilocus sequence analysis and DNA-DNA hybridization, with proposalto combine 29 species and three subspecies as 11 genomic species. *Int. J. Syst. Evol. Microbiol.* 60, 696–703. doi: 10.1099/ijs.0.012419-0

Rong, X. Y., and Huang, Y. (2012). Taxonomic evaluation of the *Streptomyces hygroscopicus* clade using multilocus sequence analysis and DNA-DNA hybridization, validating the MSLA scheme for systematics of the whole genus. *Syst. Appl. Microbiol.* 35, 7–18. doi: 10.1016/j.syapm.2011.10.004

Rong, X. Y., Liu, N., Ruan, J. S., and Huang, Y. (2010). Multilocus sequence analysis of *Streptomyces griseus* isolates delineating intraspecific diversity in terms of both taxonomy and biosynthetic potential. *Antonie Van Leeuwenhoek* 98:237. doi: 10.1007/s10482-010-9447-z

Saitou, N., and Nei, M. (1987). The neighbor-joining method: a new method for reconstructing phylogenetic trees. *Mol. Biol. Evol.* 4, 406–425. doi: 10.1093/oxfordjournals.molbev.a040454

Salehi, B., Fokou, P., Sharifi-Rad, M., Zucca, P., Pezzani, R., Martins, N., et al. (2019). The therapeutic potential of naringenin: a review of clinical trials. *Pharmaceuticals* 12:11. doi: 10.3390/ph12010011

Sasser, M. (1990). *Identification of Bacteria by Gas Chromatography of Cellular Fatty Acids*. Technical Note 101. Newark, DE: MIDI Inc.

Schimana, J., Fiedler, H. P., Groth, I., Suessmuth, R., Beil, W., Walker, M., et al. (2000). Simocyclinones, novel cytostatic angucyclinone antibiotics produced by *Streptomyces antibioticus* Tü 6040. I. taxonomy, fermentation, isolation and biological activities. *J. Antibiot.* 53, 779–787. doi: 10.7164/antibiotics.53.779

Sheng, M. M., Jia, H. K., Zhang, G. Y., Zeng, L. N., Zhang, T. T., Long, Y. H., et al. (2020). Siderophore production by rhizosphere biological control bacteria *Brevibacillus brevis* GZDF3 of Pinellia ternata and its antifungal effects on *Candida albicans*. *J. Microbiol. Biotechnol.* 30, 689–699. doi: 10.4014/jmb.1910.10066

Shirling, E. B., and Gottlieb, D. (1966). Methods for characterization of *Streptomyces* species. *Int. J. Syst. Evol. Micr.* 16, 313–340. doi: 10.1099/00207713-16-3-313

Singh, S., Kim, Y., Wang, F., Bigelow, L., Endres, M., Kharel, M. K., et al. (2015). Structural characterization of Atms13, a putative sugar aminotransferase involved in indolocarbazole AT2433 aminopentose biosynthesis. *Proteins* 83, 1547–1554. doi: 10.1002/prot.24844

Snipes, C. E., Chang, C. J., and Floss, H. G. (1979). Biosynthesis of the antibiotic granaticin. *J. Am. Chem. Soc.* 101, 701–706. doi: 10.1021/ja00497a036

Stackebrandt, E., and Goebel, B. M. (1994). Taxonomic note: a place for DNA-DNA reassociation and 16S rRNA sequence analysis in the present species definition in bacteriology. *Int. J. Syst. Bacteriol.* 44, 846–849. doi: 10.1099/00207713-44-4-846

Takano, S., Hasuda, K., Ito, A., Koide, Y., Ishii, F., Haneda, I., et al. (1976). A new antibiotic, medermycin. *J. Antibiot.* 29, 765–768. doi: 10.7164/antibiotics.29.765

Tepe, B., Daferera, D., Sokmen, A., Sokmen, M., and Polissiou, M. (2005). Antimicrobial and antioxidant activities of the essential oil and various extracts of *Salvia tomentosa* Miller (Lamiaceae). *Food Chem.* 90, 333–340. doi: 10.1016/j.foodchem.2003.09.013

Wang, X., Zhou, H. B., Chen, H. N., Jing, X. S., Zheng, W. T., Li, R. J., et al. (2018). Discovery of recombinases enables genome mining of cryptic biosynthetic gene clusters in *Burkholderiales* species. *Proc. Natl. Acad. Sci. U.S.A.* 115, E4255–E4263. doi: 10.1073/pnas.1720941115

Wang, X. N., Radwan, M. M., Taráwneh, A. H., Gao, J. T., Wedge, D. E., Rosa, L. H., et al. (2013). Antifungal activity against plant pathogens of metabolites from the endophytic fungus *Cladosporium cladosporioides*. *J. Agric. Food Chem.* 61, 4551–4555. doi: 10.1021/jf400212y

Watve, M. G., Tickoo, R., Jog, M. M., and Bhole, B. D. (2001). How many antibiotics are produced by the genus *Streptomyces*? *Arch Microbiol.* 176, 386–390. doi: 10.1007/s002030100345

Williams, S. T., Goodfellow, M., Alderson, G., Wellington, E. M. H., Sneath, P. H. A., and Sackin, M. J. (1983). Numerical classification of *Streptomyces* and related genera. *J. Gen. Microbiol.* 129, 1743–1813. doi: 10.1099/00221287-129-6-1743

Yoon, S. H., Ha, S. M., Kwon, S., Lim, J., Kim, Y., Seo, H., et al. (2017a). Introducing ezbiocloud: a taxonomically united database of 16S rRNA and whole genome assemblies. *Int. J. Syst. Evol. Microbiol.* 67, 1613–1617. doi: 10.1099/ijsem.0.001755

Yoon, S. H., Ha, S. M., Lim, J., Kwon, S., and Chun, J. (2017b). A large-scale evaluation of algorithms to calculate average nucleotide identity. *Antonie Van Leeuwenhoek* 110, 1281–1286. doi: 10.1007/s10482-017-0844-4

Conflict of Interest: The authors declare that the research was conducted in the absence of any commercial or financial relationships that could be construed as a potential conflict of interest.

Publisher's Note: All claims expressed in this article are solely those of the authors and do not necessarily represent those of their affiliated organizations, or those of the publisher, the editors and the reviewers. Any product that may be evaluated in this article, or claim that may be made by its manufacturer, is not guaranteed or endorsed by the publisher.

Advantages of publishing in Frontiers

OPEN ACCESS
Articles are free to read for greatest visibility and readership

FAST PUBLICATION
Around 90 days from submission to decision

HIGH QUALITY PEER-REVIEW
Rigorous, collaborative, and constructive peer-review

TRANSPARENT PEER-REVIEW
Editors and reviewers acknowledged by name on published articles

Frontiers
Avenue du Tribunal-Fédéral 34
1005 Lausanne | Switzerland

Visit us: www.frontiersin.org
Contact us: frontiersin.org/about/contact

REPRODUCIBILITY OF RESEARCH
Support open data and methods to enhance research reproducibility

DIGITAL PUBLISHING
Articles designed for optimal readership across devices

FOLLOW US
@frontiersin

IMPACT METRICS
Advanced article metrics track visibility across digital media

EXTENSIVE PROMOTION
Marketing and promotion of impactful research

LOOP RESEARCH NETWORK
Our network increases your article's readership